PHD

The design of control systems for diesel engines

Howard, D.

Award date:
1987

Awarding institution:
University of Bath

THE DESIGN OF CONTROL SYSTEMS FOR DIESEL ENGINES

submitted by D. Howard
for the degree of Ph.d
of the University of Bath
1987

ProQuest LLC
789 East Eisenhower Parkway
P.O. Box 1346
Ann Arbor, MI 48106-1346

SUMMARY

This thesis reports on the development of control systems for two novel Diesel drives: a variable geometry turbocharged Diesel engine; and the Differential Compound Engine. Both projects deal with multi-variable systems which ideally the driver should be able to operate by the adjustment of a single control parameter. The remaining parameters require some form of automatic control, preferably giving optimum performance. The research has included:-

i) The design and construction of Diesel test facilities.
ii) Theoretical and experimental studies to determine appropriate control strategies.
iii) The development and testing of prototype control systems.

The first part of the thesis contains general material relating to Diesels, control system design, and engine testing. This includes the methods and equipment adopted for engine performance testing, general principles of Diesel control system design, development computers and actuation.

The second part of the thesis covers the variable geometry turbocharging work under the headings steady-state performance optimisation and transient control. The first aims to minimise fuel consumption and improve the Diesel's torque characteristics. The second aims to improve turbocharger response and hence engine load acceptance and smoke.

The final part of the thesis covers the Differential Compound Engine work. The principles of Differential Compounding are explained, the design of the latest test facility is described, and the control system development work is reported. The latter includes the implementation of a prototype steady-state controller and the theoretical investigation of transient control strategies.

ACKNOWLEDGEMENTS

I give my thanks and best wishes to all my colleagues who worked with me and gave advice and encouragement during my period at Bath. In particular thanks go to:-

Professor Wallace for his supervision and patience.

Research colleagues who participated in the work, for their enthusiasm and friendship. The majority of this research has been teamwork and could not have been done without them:

Hubert Muller
Elfed Roberts
David Prince
Urban Anderson
Ralf Krause

The laboratory's technicians for their dedication and hard labour:

Anthony Elley
Keith Britton

All those in the School of Engineering who gave practical assistance and advice including:

William Alexander
Ian Marsh
The Instrumentation section
The School's Workshop
The Secretaries in the School Office

Barbara Cole for her typing and support without which the thesis would never have been finished.

CONTENTS

1 INTRODUCTION

1.1 VEHICLE PROPULSION
1.2 TURBOCHARGING THE AUTOMOTIVE DIESEL ENGINE
1.3 COMPOUNDING
1.4 ENGINE AND DRIVELINE CONTROLS
1.5 THE RESEARCH PROGRAM

2 TEST BED DESIGN FOR PERFORMANCE TESTING AND ENGINE CONTROLS DEVELOPMENT

2.1 INTRODUCTION
2.2 MEASUREMENT
2.3 DATA-ACQUISITION AND REDUCTION
2.4 DYNAMOMETRY
2.5 ENVIRONMENTAL CONTROLS

3 ASPECTS OF DIESEL CONTROL SYSTEM DESIGN

3.1 INTRODUCTION
3.2 STEADY-STATE PERFORMANCE OPTIMISATION
3.3 IMPROVING TRANSIENT RESPONSE
3.4 DEVELOPMENT COMPUTERS AND INTERFACING
3.5 ACTUATION

4 THE DEVELOPMENT OF STEADY-STATE CONTROLS FOR A DIESEL WITH VARIABLE GEOMETRY TURBOCHARGER

4.1 INTRODUCTION
4.2 THE CONTROL VARIABLES
4.3 CONTROL SYSTEM DESIGN, IMPLEMENTATION, AND COMMISSIONING
4.4 STEADY-STATE PERFORMANCE WITH CONTROL OVER LTC. FUELLING, TURBINE GEOMETRY, AND INJECTION TIMING

5 TRANSIENT CONTROL WITH VARIABLE GEOMETRY

5.1 INTRODUCTION
5.2 ALTERNATIVE MODES OF VG. CONTROL
5.3 CONSTANT SPEED FUEL STEPS UNDER VG. CONTROL
5.4 VEHICLE ACCELERATION UNDER VG. CONTROL
5.5 DISCUSSION

6 THE DEVELOPMENT OF THE DIFFERENTIAL COMPOUND ENGINE

6.1 INTRODUCTION
6.2 THE PRINCIPLES OF DIFFERENTIAL COMPOUNDING
6.3 DIFFERENTIAL COMPOUND ENGINE PROTOTYPE DEVELOPMENT
6.4 THE LEYLAND 500 DCE TEST FACILITY

7 CONTROL SYSTEM DEVELOPMENT FOR THE DIFFERENTIAL COMPOUND ENGINE

7.1 INTRODUCTION
7.2 IMPLEMENTATION OF A SIMPLE STEADY-STATE CONTROLLER ON THE PERKINS 6.354 PROTOTYPE
7.3 TRANSIENT CONTROL ALGORITHM DESIGN USING A DYNAMIC COMPUTER MODEL

8 DISCUSSION AND CONCLUSIONS

8.1 DIESEL CONTROL SYSTEM DEVELOPMENT
8.2 THE CONTROL OF A VARIABLE GEOMETRY TURBOCHARGED DIESEL ENGINE
8.3 DIFFERENTIAL COMPOUND ENGINE CONTROLS

REFERENCES

APPENDIX 1. SUPERVISORY CONTROL SOFTWARE
APPENDIX 2. DYNAMIC DCE MODEL (DCESIM)

CHAPTER 1

INTRODUCTION

1.1 VEHICLE PROPULSION

1.1.1 POWER-PLANTS
1.1.2 SATISFYING THE VEHICLE TORQUE REQUIREMENTS (TRANSMISSIONS)

1.2 TURBOCHARGING THE AUTOMOTIVE DIESEL ENGINE

1.2.1 INCREASING CHARGE DENSITY
1.2.2 TURBOCHARGING
1.2.3 MATCHING THE TURBOCHARGER AND THE DIESEL ENGINE

1.3 COMPOUNDING

1.3.1 TURBO-COMPOUNDING
1.3.2 COMPOUNDING WITH MECHANICALLY DRIVEN SUPERCHARGERS
1.3.3 INSULATED COMPOUND ENGINES

1.4 ENGINE AND DRIVELINE CONTROLS

1.4.1 SENSORS AND ACTUATORS
1.4.2 AUTOMOTIVE CONTROL APPLICATIONS

1.5 THE RESEARCH PROGRAMME

1.1 VEHICLE PROPULSION

1.1.1 POWER-PLANTS

The vehicle power-plant converts stored energy, usually in the form of fuel, into mechanical energy. Fuel burning machines are classified as either internal or external combustion engines. Internal combustion (i.c.) devices include the reciprocating i.c. engine and the gas turbine. In this case the combustion products are also the working fluid. In an external combustion engine the heat of combustion is transferred to the working fluid by a heat exchanger. The working fluid is usually water which is turned to steam in a boiler, used to drive a steam turbine or reciprocating steam engine, and then passed through a condenser or expelled to atmosphere.

At the present time steam turbine plants are used for electrical power generation and large ship propulsion units. They can burn a wide range of fuels including coal, and do not suffer from the balancing and vibration problems associated with reciprocating machinery. For these large capacity applications their efficiency can compete with the Diesel engine.

For smaller sea-going vessels and other transportation systems some form of i.c. engine is generally used, to reduce complexity, weight, and size. The gas turbine predominates where high specific power is required ie. a high power to weight/size ratio. As a result it has become the most common propulsion unit for civil and military aircraft. In the jet engine the gas turbine drives a compressor which supplies the combustion chamber with air. The aircraft is propelled by the combustion reaction force. In the more efficient turbo-prop engine the turbine drives both the compressor and a propeller which provides the forward drive.

Gas turbine combustion is continuous unlike that of the reciprocating i.c. engine which is cyclic. This means the reciprocating engine can reach much higher maximum combustion temperatures whilst keeping

within metal temperature limits. As a result the latter burns fuel more efficiently. This fact combined with extremely low manufacturing costs has made the piston engine the most widely used powerplant for land transportation.

Reciprocating i.c. engines are split into two categories: spark ignition (petrol); and compression ignition (Diesel). Both types can be designed as four-stroke or two-stroke machines. A full description of these differences and their implications on engine operation and design can be found in ref. 1.

The Diesel engine is more efficient than the petrol, particularly at part load. The major reasons for this are as follows:-

i) The Diesel can operate at higher compression ratios which leads to improved thermal efficiency/combustion. In practice increased friction losses and engine weight offset combustion improvements at ratios higher than about 15:1. The petrol engine is limited to approx. 9:1 to avoid detonation problems.

ii) At part load the petrol engine is governed by throttling the air intake, this is an inefficient process which increases pumping work. The Diesel, on the other hand, is governed by adjusting the amount of fuel injected into the cylinders, no intake throttling is involved.

iii) The Diesel's air-fuel ratio increases with decreasing load, this being the method of governing the engines output. This results in very good part load efficiencies because the excess air available ensures complete combustion.

The Diesel's disadvantages include: lower specific power and hence greater size and weight; higher initial cost as a result of its more rugged construction; and noisier operation. These considerations make the Diesel more appropriate for high usage applications where the savings in fuel costs outweigh the disadvantages. Accordingly almost all haulage, public transport, and off-highway vehicles are Diesel powered. The petrol engine dominates for personal transport and low

usage applications such as garden equipment. The work described in this thesis has been with large automotive Diesels aimed at the former applications.

Automotive Diesels of haulage truck size (typically 8 to 12 litres capacity) are invariably four-stroke devices. The reasons for this are not immediately apparent as the two-stroke has a higher specific power and the differences in fuel consumption are minor. Large marine Diesels are usually two-stroke because cylinder pressures are lower than for the same size and power four-stroke. This is important because structural constraints become a deciding factor in large bore (over 12") engine design (ref. 1).

1.1.2 SATISFYING THE VEHICLE TORQUE REQUIREMENTS (TRANSMISSIONS)

The torque vs. speed curve required from a power-plant and its transmission depends upon the application. For instance a ship's engine must work against a propeller law curve (fig. 1.1a), that is torque increases with the square of speed. Conversely a road vehicle must be capable of acceleration from standstill, hill climbing, and a high maximum speed on the flat. The first two criteria require much higher road torque than the third where rolling friction and aerodynamic drag are the only contributors to tractive resistance (fig. 1.2). These requirements are best met if maximum engine power is available at all road speeds ie. the ideal torque curve is a constant power hyperbola (fig. 1.1b). At low speed high torque is available for acceleration and hill climbing without the vehicle being overpowered at maximum speed.

The steam engine produces the desired torque curve with no need for any additional transmission. This is the case because the working fluid is independent of the combustion process ie. the boiler can operate at maximum output whatever the piston speed. In practice many power-plants cannot be designed to operate in this manner.

The Diesel engine produces a relatively flat torque curve (fig. 1.1c) because the maximum fuel input per revolution depends upon capacity and cylinder pressure limitations. In addition the Diesel is unable to operate down to stall because the combustion process is transient in nature and occurs over a relatively inflexible period. These arguments apply equally to the petrol engine.

The purpose of the transmission is to convert the engine's output into the hyperbolic form required. Traditionally the automotive Diesel has driven through a manually operated multi-ratio gearbox. The minimum speed limitation means that a clutch or fluid coupling is needed to start the vehicle from rest. The combination of Diesel, manual gearbox and clutch gives the vehicle tractive force characteristic shown in fig. 1.3. It can be seen that maximum power is only achieved at a series of fixed vehicle speeds corresponding to maximum engine speed in each gear ratio. As engine speed falls the tractive force curve drops away from the ideal hyperbola. There are three ways to reduce or eliminate this effect:-

i) Increasing the number of ratios in the mechanical box improves the match with the ideal tractive force curve by reducing the engine speed range used in each gear. However the loss of torque during de-clutching limits the number of ratios that can usefully be employed. More ratios also increases driver strain and gearbox cost.

ii) A continuously variable transmission (CVT) allows engine speed to remain constant whatever the vehicle speed. Thus the engine can be run at maximum power throughout the vehicle speed range. The problem with most of these devices is their low efficiency which results in lower maximum power and poorer fuel consumption than with a manual gearbox. However developments in mechanical CVT design may soon lead to the widespread replacement of manual boxes with devices such as the Perbury and Van-Doorne (ref. 2). The Differential Compound Engine (DCE) attempts to produce a similar effect by using a fully

floating epicyclic. The DCE is the subject of research discussed later in this thesis.

iii) Improving the engine's torque characteristic reduces the divergence from the ideal hyperbola that occurs as engine speed drops (fig. 1.3). This can be used to reduce the number of gear-ratios required or to improve vehicle performance with the same number of ratios. One of the major aims of the research reported in this thesis was the improvement of torque back-up and useful speed range using a Variable Geometry Turbocharger.
Torque back-up (%) is defined as:-

(peak torque-max. speed torque)*100/max. speed torque

Useful speed range (rpm) is defined as:-

maximum rpm-peak torque rpm

1.2 TURBOCHARGING THE AUTOMOTIVE DIESEL ENGINE

1.2.1 INCREASING CHARGE DENSITY

The power developed by a naturally aspirated Diesel is proportional to the rate at which fuel can be burnt, which in turn depends upon the engine's air throughput. Air flow can be raised by using: a larger engine capacity; higher engine speeds; or increased air density. The first option results in a larger heavier engine, which therefore reduces the vehicle's carrying capacity and suffers from greater friction losses. The second option is difficult with the direct injection (d.i.) Diesel because of combustion period inflexibility. However a maximum speed of 4500 rpm has been achieved with a 2.5 litre d.i. Diesel (FORD) by using swirl inducing inlet ports. Higher engine speeds also produce greater friction losses. The final option is probably the most beneficial for the d.i. Diesel, power is increased without any change in capacity or speed.

Inlet air density can be increased by raising inlet pressure and lowering inlet temperature (intercooling). The second method is only used when the inlet air has already been compressed and is therefore at a temperature somewhat higher than ambient. Automotive intercoolers use either jacket water or ambient air as the cooling medium, fig. 1.4 shows some alternative arrangements. The most common methods of increasing inlet air pressure are described below:-

1. Mechanical Supercharging

Air is delivered to the engine by a crank-shaft driven compressor. A positive displacement compressor is used because it has similar flow characteristics to the engine when driven through fixed ratio gearing. The engine sees a higher but constant inlet pressure. Hence the torque curve is similar to that of a naturally aspirated engine of larger capacity. The supercharging compressor takes power from the crank-shaft and therefore reduces overall efficiency.

2. Turbocharging

A gas turbine in the exhaust system drives a centrifugal compressor which supplies the engine with air. This method results in better overall efficiencies than mechanical supercharging because exhaust gas energy is used that would otherwise be wasted. Turbocharging is the basis for part of the research reported in this thesis, a general introduction is given in the following sub-sections. References 3 & 4 provide comprehensive coverage of turbocharging theory and practice.

3. Resonant Intake Systems (fig. 1.5)

The use of tuned manifolds can improve engine volumetric efficiency over a limited speed range (ref. 3). The manifolds can be designed to resonate in such a way that, at low engine speeds, a pressure wave arrives at the inlet valve just before it closes. This results in an increase in the mass of air trapped. At high engine speeds the pressure wave is delayed (in terms of crank angle) and volumetric efficiency is reduced (fig. 1.6). This effect can be used to advantage with turbocharged engines where low speed air supply is a problem.

4. The Comprex Pressure Charging System (fig. 1.7)

The Comprex passes energy from exhaust gas to inlet air by utilising pressure waves in a cellular rotor. The rotor is driven by the engine so that the cells are exposed to inlet and exhaust for periods long enough to allow energy transfer at sonic velocity. The exhaust gas moves more slowly than the pressure wave and therefore does not mix with the inlet air. The process is complicated and an excellent description can be found in ref. 4. The major advantages over standard turbocharging are better torque back-up and transient performance. This device has not proved competitive because of its complexity and hence high cost.

1.2.2 TURBOCHARGING

Turbochargers for road vehicles generally consist of a radial inflow exhaust turbine coupled directly to a radial outflow compressor (fig.

1.8). These components are relatively efficient at the massflows and pressure ratios involved and form a compact unit. They are separated by a bearing assembly which supports their connecting drive-shaft and prevents excessive heat transfer between exhaust and inlet. Journal bearings pressure fed with engine lube oil are commonly used.

Compressor performance is described by a pressure ratio vs. massflow map such as the one shown in fig. 1.9. Within the flow range of the compressor, pressure ratio depends mainly upon rotor speed, as would be expected with a momentum transfer device. The flow range is limited by compressor surge at low flow and choke at high flow.

The turbine is usually of fixed geometry and has orifice like flow characteristics ie. massflow increases with pressure ratio until choke is reached (fig. 1.10). The curve shifts with turbine speed because of the centrifugal action of the rotor opposing the gas flow.

The turbine stage can be connected to the engine by three alternative forms of exhaust manifold: constant pressure; pulse; and pulse converter. The choice depends upon the engine rating and the number of cylinders. A highly rated engine is one which operates at high mean effective pressures.

Constant pressure turbocharging involves the use of a large plenum type manifold to damp out the pressure fluctuations caused by exhaust valve opening. This method loses some of the exhaust pulse energy, however the turbine operates more efficiently and reflected pulses do not interfere with the exhaust process. These advantages are more important at high engine loads. At part-load the loss of pulse energy results in higher fuel consumption and poor transient response.

Pulse turbocharging overcomes the part-load and transient disadvantages of the constant pressure method by preserving the exhaust pulse energy. One or more small volume manifolds connect the exhaust valves to either one single entry turbine per manifold or a lesser number of multi-entry turbines. Each manifold collects exhaust

from no more than three cylinders. This prevents the manifold pressure peaks caused by exhaust valve opening from interfering with the scavenging process in other cylinders. With three cylinder groupings valve overlap occurs when exhaust manifold pressure is at a minimum resulting in good scavenging (fig. 1.11). When two cylinder groupings are used the turbine operates at low pressure ratio and hence poor efficiency over a larger proportion of the cycle. Pulse turbocharging is therefore most effective when the number of cylinders is divisable by three.

As ratings increase the peak pressure ratio caused by exhaust blow-down will exceed that at which the radial flow turbine can efficiently operate. Reflected pressure pulses may also interfere with engine scavenging. As a result the constant pressure system becomes more attractive for highly rated engines. It has been suggested (ref. 3) that the constant pressure method becomes superior to the pulse method at boost pressure ratios over 3:1 (2:1 when two cylinder groupings are used). The pulse system is used for almost all turbocharged road vehicles because of their moderate ratings.

Pulse converters are devices which connect two or more pulse manifolds. They are designed to combine and preserve pulse energy without creating undue interference between manifolds. Thus a single entry turbine can be used, operating under steadier flow conditions than those experienced in normal pulse turbocharging. The pulse converter (fig. 1.12) acts as a junction and nozzle, converting pressure to kinetic energy and thus reducing pulse interference. The application of pulse converters has so far been limited to engines with two cylinder groupings. In this case the advantages of steadier flow conditions outweigh the throttling losses.

The mechanical design of the Diesel must be altered to make it suitable for turbocharging. If an unmodified naturally aspirated engine is turbocharged then final compression pressure and hence peak cylinder pressure will be higher. Therefore, if the mechanical limitations are the same, the turbocharged engine must have a lower

compression ratio. In this case final compression pressures are similar to the naturally aspirated engine, but the clearance volume at TDC is greater and so there is more air to burn.

Ideally valve design and timing will also be altered so that engine breathing is optimised with the higher manifold pressures and massflows. Finally the maximum fuelling schedule must be modified to suit the available inlet manifold pressure (boost). In particular a smoke limiting control (aneroid) is necessary to reduce fuelling when boost is too low.

1.2.3 MATCHING THE TURBOCHARGER AND THE DIESEL ENGINE

The free-running turbocharger is inherently stable when connected to the Diesel ie. a natural equilibrium occurs. However, the turbine, compressor, and engine must be matched in terms of pressure ratios, massflows, and efficiencies. Choosing the turbocharger components is a complex task based on empirical data and many simplifying assumptions. Final adjustments are often made as a result of test-bed or road performance.

The design figures for air massflow and boost at maximum (rated) engine power determine an approximate turbine swallowing capacity Turbine pressure ratio is assumed to be a little lower than boost. Given an estimate of swallowing capacity an appropriate turbine stage and turbocharger frame size can be selected. The compressor stage is chosen so that engine air flow requirements are met with the compressor operating at high efficiency. Fig. 1.9 shows engine air flow characteristics superimposed on the compressor map. The match should satisfy the following criteria:-

i) There should be a good surge margin, particularly for pulse turbocharging and large altitude variations (ref. 3). Surge margin is the gap between the engine flow lines and the compressor surge line.

ii) The engine operating range should lie in an area of high compressor efficiency. This is most important between peak torque and rated speed.

The validity of the original assumptions can be checked by using a turbocharger energy balance equation/model to calculate a revised operating point. If this is not close enough to the required design point then the whole procedure is repeated. Turbocharger balance must be achieved with the correct engine output.

If component efficiencies are good, and the compressor map well matched with the engine, then boost will often exceed exhaust manifold pressure. The resulting positive pumping work and good scavenging give low specific fuel consumption (s.f.c.). A far more detailed account of turbocharger matching can be found in ref. 3.

The procedure described above provides a compromise match between the Diesel and a standard turbocharger with fixed geometry components. This match is a compromise because the standard turbo's air flow characteristics are quite different from those required by the engine. Referring to fig. 1.9, it is apparent that on the limiting torque curve (LTC.) boost pressure falls with engine speed. This is incompatible with the requirement for good torque back-up, ideally boost pressure should rise with falling engine speed. Additional low speed boost could be utilised to increase torque back-up within mechanical and thermal constraints. The major constraint on low speed torque is the legal smoke limit, this would be overcome if boost could be maintained.

The two most common approaches to eliminating this mismatch are the exhaust waste-gate and the variable geometry (V.G.) exhaust turbine. The waste-gate is used with an undersized turbine which provides adequate boost at low engine speeds. As speed rises, overboosting is avoided by allowing exhaust gas to bypass the turbine. Boost pressure is held roughly constant once the waste-gate begins to operate. This method is inherantly inefficient because exhaust energy is not fully

utilised. Variable geometry is a potentially more efficient solution which would also allow boost to rise with falling engine speed. The turbine stage incorporates some variable element which alters its swallowing capacity and thus provides a means of controlling the turbocharger output. Variable Geometry Turbocharging is a major part of the research reported in this thesis, and is covered in detail in chapters 4 and 5.

The turbocharger is also transiently mismatched in the sense that its response to sudden changes in fuelling is poor. Although exhaust enthalpy rises rapidly with fuelling the turbo' must accelerate to provide the corresponding boost increase. The delay between fuelling and boost is referred to as turbo-lag. The aneroid fuel control ensures smoke limits are not exceeded, however initial vehicle acceleration is poor and hence drivability suffers. This problem is covered in more detail in Chapter 5.

1.3 COMPOUNDING

The exhaust energy available at high engine power is usually greater than that required by the turbocharger compressor. This is particularly the case when the engine is highly rated (ie. operates at high b.m.e.p.s). Higher overall efficiency can be achieved if the excess exhaust energy is recovered as additional crankshaft power.

The two most likely solutions to this problem are: the application of some form of mechanical expander in the exhaust system; and the use of a Rankine bottoming cycle to extract heat from the exhaust. The latter requires an exhaust to water heat exchanger and the associated secondary water circuit (fig. 1.13). This additional complexity and expense has prevented serious development for automotive applications where cost and installation considerations are paramount. The installation of an expander in the exhaust stream could be a more feasible solution requiring only the expander and a means of transferring its power to the crankshaft.

An engine with an exhaust expander geared to the crankshaft is referred to as a compound engine. This section discusses alternative compound schemes and the associated research and development in progress.

1.3.1 TURBO-COMPOUNDING

Perhaps the most obvious form of compound engine is one where the turbocharger is connected to the engine by a fixed ratio gear-train. Any excess turbine power over that required by the compressor would be available at the crankshaft. However, driving the turbocharger with fixed ratio gearing has several disadvantages:-

1. Normal turbocharger running speeds can be up to 100,000 rpm depending on the engine capacity. Therefore with an engine speed of say 2500 a gear ratio of 40 would be required. Such high

ratios would involve considerable expense and high frictional losses.

2. Compressor speed reduces in proportion with engine speed. The resulting variation in boost pressure would be greater than that experienced with a free-floating turbocharger (ref. 3). Low speed torque would suffer as a result even when compared with the turbocharged engine.

3. Compressor speed and hence boost are a function of engine speed only and do not vary with load. Therfore at part load the engine is over boosted and compressor torque will be unnecessarily high. However turbine torque will reduce with load as the exhaust energy falls. At low loads turbine torque will be less than compressor torque and the engine will drive the turbocharger. Poor part load efficiencies will result.

The "Cummins turbo-compound" scheme (fig. 1.14) overcomes these problems by using a normal free-floating turbocharger and an additional power turbine which is connected to the crankshaft by a fixed ratio gear-train. The power turbine is installed after the turbocharger and therefore operates at a lower inlet pressure. Because volume flow is greater through the low pressure (L.P.) power turbine it is larger and runs at a lower rotational speed (approx. 50,000). This reduces the required gear ratio to a more acceptable figure (20). Being free-floating the turbocharger can produce more boost at low speed and is not driven by the engine at part load. In fact the L.P. turbine has the effect of reducing the variation of boost pressure with engine speed (in much the same way as two stage turbocharging).

1.3.2 COMPOUNDING WITH MECHANICALLY DRIVEN SUPERCHARGERS

The "Cummins turbo-compound" and the standard turbocharged Diesel both suffer from reduced boost pressure at low engine speeds and hence poor low speed torque. In addition the turbo-lag phenomenum affects load

acceptance and hence drivability. The traditional mechanically supercharged engine (using a positive displacement compressor) does not suffer from these problems, boost pressure is almost independent of engine speed and load. However the unnecessarily high boost at part load results in poor efficiency. These considerations have led some researchers to investigate the combination of positive displacement supercharging and compounding to recover exhaust energy.

Wurm et al (ref. 5) suggest that, if practical, positive displacement expanders would be more efficient than exhaust turbines and could be used with a supercharged diesel engine. Screw type devices are advocated which would be connected to the crankshaft by fixed ratio gearing. The rotational speeds would be much lower than for turbo-machinery thus reducing gear losses. High overall efficiencies are predicted. However these are based on optimistic component efficiencies. In addition some means of modulating the compressor pressure ratio is necessary to avoid excessive power consumption at part load. Other researchers (ref. 6) have also investigated the theoretical performance of systems incorporating positive displacement expanders but are less optimistic about the potential efficiency improvements. The practical design of the expander would involve the use of advanced ceramic materials and no suitable device is at present available.

The Differential Compound Engine (DCE) as advocated by Prof. F.J. Wallace attempts to combine the best features of the compound schemes already described. A positive displacement screw compressor and a variable geometry exhaust turbine are used. The engine, compressor and drive-shaft are connected by a fully floating epicyclic, the turbine is geared directly to the drive-shaft. This arrangement is used to greatly enhance the torque back-up available and hence reduce the transmission ratios required.

Some of the advantages of the DCE are listed below:-

1. The components used are all based on existing technology. Therefore performance predictions are more reliable and practical implementation straightforward.

2. The compressor pressure ratio is approximately proportional to engine load and therefore excessive compressor power consumption is avoided.

3. Engine boost pressure can be controlled independently whatever the engine speed. Thus inadequate boost is never a problem.

4. The differential gearing provides a torque conversion effect which results in exceptional torque back-up. This additional feature combined with recovery of exhaust gas energy makes the additional expenditure on gear-trains more worthwhile.

The DCE is a major part of the research reported in this thesis, and is covered in detail in chapters 6 and 7.

1.3.3 INSULATED COMPOUND ENGINES

Considerable research and development effort is being directed at producing practical low heat loss (adiabatic) diesels. Reducing heat loss to coolant is expected to give the following gains (ref. 7):-

1. Lower heat loss to coolant and hence increased cylinder work and more exhaust energy available for compounding.

2. The reduction in capacity or total elimination of engine cooling systems. This would in turn result in smaller installation volumes, lower ancillary power consumption, and improved cooling system reliability.

3. Higher combustion temperatures and hence improved combustion and multi-fuel capability.

In practise the energy saved contributes little to cylinder work and simply increases exhaust energy. In fact the effect of lower volumetric efficiency caused by higher cylinder temperature may cancel any gain in cylinder work. It is apparent that the improvements obtained by insulating a naturally aspirated engine are likely to be small if not negative. If a compound engine is insulated the picture is different. Higher supercharging or turbocharging pressures can easily overcome the reduction in volumetric efficiency and the increased exhaust energy can be recovered by the power turbine. In fact the advantages of compounding should be substantially increased if the engine is insulated.

The advantages of insulated compound engines are greatest when high b.m.e.p.s are used. Highly rated uninsulated engines lose considerable heat to coolant which can make cooling system installations large. Insulating overcomes this problem and combined with high ratings results in correspondingly high exhaust enthalpy which is available to drive the power turbine. As a result very high specific powers are possible particularly with respect to installation volume. Because of these considerations the major interest in the insulated compound engine is for military applications such as the tank.

Insulating the diesel engine requires advanced materials technology with comprehensive use of ceramics. Recent work on the practical implementation of insulated turbo-compound diesels is described in references 8 & 9.

1.4 ENGINE AND DRIVELINE CONTROLS

The increasing availability of cheap electronics and computer hardware (the "microprocessor") has brought together the disciplines of design, thermodynamics, and control engineering in automotive research and development. The engine-transmission system is inherently complicated and multi-variable in nature. For instance engine parameters such as fuelling, injection timing, boost pressure, valve timing etc. can usefully be manipulated to improve efficiency, performance, and environmental impact. Traditionally these variables have been fixed with a compromise setting or altered crudely by a mechanical system such as vacuum advance. However the use of computer controls and sophisticated actuation techniques allows more variability. Thus there is greater scope for optimistion of overall performance.

This section provides a brief survey of the automotive applications of control technology. Commercial systems, either already on the market or at the prototype stage, are described. The purpose is to give an overview of the type of technology likely to be commonplace within ten years. The material is covered in two parts: sensors and actuators; and automotive control applications. It should be emphasised that some of the developments described were reported after the work covered in this thesis was complete.

1.4.1 SENSORS AND ACTUATORS

Perhaps the most important aspect of automotive control system development is the design of sensors and actuators. Both must be accurate, reliable, and low cost when manufactured in bulk. These requirements combined with the harsh environment in which they must operate make good design a priority. The following survey of devices is not meant to be comprehensive merely illustrative. The sensors and actuators used for the author's research are described in sections 2.2 and 3.5.

Where possible automotive sensors should take advantage of integrated circuit technology as this lends itself to economic mass production. An example of this is the growing number of monolithic silicon pressure transducers (refs. 10,11,&12) appearing on the market. These are piezo-resistive devices etched onto a single silicon chip which includes the strain-gauged diaphragm and its associated conditioning circuitry (fig. 1.15).

The potential divider is widely used for position and level measurement (float systems). Conductive plastic devices have better wear characteristics and should be simpler to produce than wire-wound dividers. Where velocities are high and continuous cycling occurs displacement is usually measured with inductive or capacitative transducers. Bosch have developed an inductive sensor to measure injector needle movement and hence fuel quantity injected for electronic Diesel control (ref. 13).

Rotational speed is simply measured using toothed wheels (often existing gears) and proximity detectors. The most common detector is the magnetic pick-up which is rugged and unaffected by oil and dirt. The Bosch anti-skid braking system (ABS) uses this type of device to monitor wheel speeds (ref. 14). The bearing manufacturers RHP have designed integral bearing/speed pick-up assemblies (ref. 15).

Air-flow measurement has been used successfully by Bosch as an input to their engine control units (L-Jetronic and Motronic). They use a flap sensor (fig. 1.16) which converts a small part of the air's momentum to deflect the flap against a restoring spring (ref. 16).

Temperature is usually sensed with temperature dependent resistance devices, this technology is well established having long been used to provide dashboard information.

Fuel flow sensors have been used with trip computers to provide the driver with fuel consumption data. However, accuracy is poor (5% at best) and they are not considered suitable for control applications at

present (ref. 17). Sensors are usually of the turbine or positive displacement variety producing a pulse train frequency proportional to flow.

Actuation can be either electrical (battery/alternator driven), engine oil pressure driven, or pneumatic. The latter may use the inlet manifold vacuum, a separate air or vacuum pump, or in the case of commercial vehicles the air-compressor supplying the braking system.

Electrical devices include: high power solenoids such as the Lucas Helenoid; torque motors working against a restoring spring; stepper motors; and DC servo-motors. The last two may be used in conjunction with reduction gearing.

Engine oil driven actuators may be rotary (motors) or linear (cylinders). Solenoid valves are used for on/off control of oil flow to the actuator. An example of this type of device is the variable injection timing mechanism mentioned in ref. 13. A pulse width modulated solenoid valve controls oil pressure to the actuating piston.

Pneumatic actuators are usually of the diaphragm capsule type. Pressure or vacuum can be applied by solenoid operated valves in a similar manner to the oil pressure servo mentioned above.

1.4.2 AUTOMOTIVE CONTROL APPLICATIONS

The majority of engine controls development has been in the petrol engine field, the motivation being emission regulations, fuel economy, and performance. Electronic controls for the Diesel engine have advanced more slowly because of its better emmissions characteristics and already good fuel economy.

The German Bosch company are one of the leaders in automotive control technology and can be considered as a yardstick by which to judge further advances. Their "Jetronic" family of petrol injection

controllers are well known and widely used (ref. 16). There are mechanical and electronic versions both of which measure inlet air-flow and hence meter fuel to give accurate mixture control. More recently these devices are being superceded by the Bosch MOTRONIC family of micro-processor based engine control units (ECU). These units are more powerful in terms of the number and complexity of control functions they can handle. They are also more flexible, re-configuring the control software (algorithms and maps) requires only a simple EPROM change. Some of the features that might be included in an advanced MOTRONIC system, or its equivalent, are:-

1. Spark advance controlled as a function of engine speed and load (2-D map). Using truly optimum settings has a primary effect on performance and efficiency. The speed signal and a reference marker (eg. TDC) are sensed using proximity detectors such as the magnetic pick-up. For a petrol engine load is dependent upon air throughput per revolution. This is measured with either an inlet manifold pressure sensor or an air-flow sensor (Bosch flap device). Inlet air temperature may also be taken into account especially when using a pressure sensor.

2. Dwell angle controlled as a function of speed and battery voltage. This gives the correct ignition energy throughout the speed-load range, which in turn produces smoother running and makes lean burn operation easier.

3. Accurate mixture control by adjusting the fuel quantity injected as a function of air throughput. Fuel quantity is controlled by using solenoid operated injection valves. This feature can be used to minimise fuel consumption under normal driving conditions and provide acceleration and warm-up enrichment. Fuel consumption can be improved by lean burn operation and overrun fuel cut-off at speeds above idle. The latter requires a switch to detect the closed throttle position. The need for acceleration enrichment can be detected by monitoring the rate of change of air-flow. In

the case of warm-up enrichment a coolant temperature sensor provides the necessary information.

4. Exhaust gas recirculation (EGR) control. EGR refers to the mixing of a proportion of the exhaust with the engine's air supply. The purpose is to lower emissions and thus keep within government regulations. EGR control can be open or closed-loop. In the first case a pre-determined map of EGR settings vs. speed and load is used. This method is not ideal because a safety margin must be included so that emissions regulations are not exceeded between services or with increased mileage. In the second case a lambda sensor (exhaust oxygen content) is used so that feedback control of EGR is possible. The elimination of any safety margin means less EGR and therefore better performance and fuel economy.

A more detailed description of the Bosch MOTRONIC range of controllers can be found in reference 18.

Carburetted petrol engines can also benefit from electronic controls, an example can be found in ref. 19. In this case the choke plate and main throttle stop are adjusted by a micro-processor based control unit (fig. 1.17). The throttle remains under the direct control of the driver. This system provides: cold start/warm-up adjustments; acceleration enrichment; idle speed control; and fuel cut-off during deceleration. The latter is achieved by moving the throttle stop back until the butterfly is below the idle jet.

As already mentioned progress has been slower with the Diesel engine. However Bosch have been developing electronic Diesel controls in anticipation of stricter emissions regulations and increasing fuel costs (ref. 13). To date they have concentrated on exhaust gas recirculation and fuel injection timing. The engine governor and fuel pump have remained essentially mechanical, except for the solenoid valve which adjusts timing. However they anticipate full electronic fuel governing, similar to that implemented by the author (sub-section 4.2.2), being introduced in the near future. This will provide

control over full load fuelling independent of the fuel system characteristics. Diesel engine control is the subject of this thesis and is fully discussed in later chapters.

The turbocharging system can also benefit from some form of automatic control. The major aim is to overcome the inherant mismatch between turbocharger and engine air-flow characteristics and hence improve the torque curve. In addition fuel consumption and emmissions improvements are possible. The most common approaches to the problem are the waste-gate and the variable geometry (VG) turbine, the latter is still at the development stage.

The most common form of control for these devices is a pneumatic capsule operated by engine boost pressure (fig. 1.18). As boost increases the waste-gate or VG opens and hence regulates boost at a level determined by the capsule spring coefficient. This form of control is rather limited and does not give optimum fuel consumption, although the torque curve is improved. More advanced electronic controls have been investigated by several companies (refs. 20,21,&22) and promise greater utilisation of the mechanisms' potential. The VG controller development undertaken by the author is described in Chapters 4 and 5.

Electronic controls are also employed to manage transmission systems. The Bosch MOTRONIC has been expanded to include advanced control of a 4-speed automatic with lock-up clutch (ref. 23). Complex gear shift programs have been implemented which improve fuel consumption and drivability.

Where sophisticated control can really improve vehicle economy and performance is in the management of continuously variable transmissions (CVT). Reference 24 describes a controller for a Perbury transmission which alters ratio to follow the engine's economy line. The economy line is the locus of minimum fuel consumption with increasing power as plotted on the engine's torque-speed map (fig.

1.19). The Differential Compound Engine is a form of CVT and the development of suitable control systems is discussed in Chapter 7.

Other vehicle sub-systems such as braking, suspension, and steering can benefit from automatic controls. The Bosch anti-skid braking system (ABS) is a commercially successful example of the application of electronic controls (ref. 14). A speed sensor on each wheel detects any speed mismatch (locking) and solenoid valves reduce the brake-line pressure to the appropriate wheels.

Looking further into the future vehicle handling may be improved by intelligent active suspension. Development work on such a system is described in ref. 25. Handling is improved by varying the suspension stiffness to suit the road conditions. Faster cornering is achieved by leaning the vehicle into bends.

1.5 THE RESEARCH PROGRAMME

The author was originally employed by Prof. F.J. Wallace for the purpose of Diesel engine/driveline control system development. Because of the very small research teams involved the author's work has, in fact, covered most aspects of engine testing and test facility construction as well as control system development. This work has included:-

i) The design, construction, and instrumentation of test facilities.
ii) Theoretical and experimental studies to determine appropriate control strategies.
iii) The design, implementation, and testing of prototype control systems.

The work was undertaken as part of two long term projects: Variable Geometry (VG) Turbocharging; and the Differential Compound Engine (DCE). Both projects deal with multi-variable systems which ideally the driver should be able to operate by the adjustment of a single control parameter. The remaining parameters require some form of automatic control, preferably giving optimum performance.

General material which is applicable to both projects is covered in Chapters 2 and 3. The first discusses the general principles of test-bed design along with equipment and methods common to both experimental facilities. The second covers common ground under the heading of control system design for Diesels. This includes general principles, a description of the development computer, and actuation techniques.

The VG turbocharging work is discussed under two headings: steady-state control (Chapter 4); and transient control (Chapter 5). The former is aimed at obtaining an improved engine torque curve and minimising fuel consumption at all speeds and loads. Transient

controls are aimed at minimising the turbo' lag phenomenum which results in poor response and smoke.

The DCE research is covered by the following two chapters. Chapter 6 contains: a general introduction to Differential compounding; a history of prototype development; and a description of the latest prototype test facility design. Chapter 7 reports the DCE control system development to date. This includes the practical implementation of a steady-state controller and theoretical studies to determine suitable transient control algorithms.

The final chapter is a general discussion of the work and its implications. The results of the research are summarised, the commercial potential discussed, and suggestions made for further research to follow that reported.

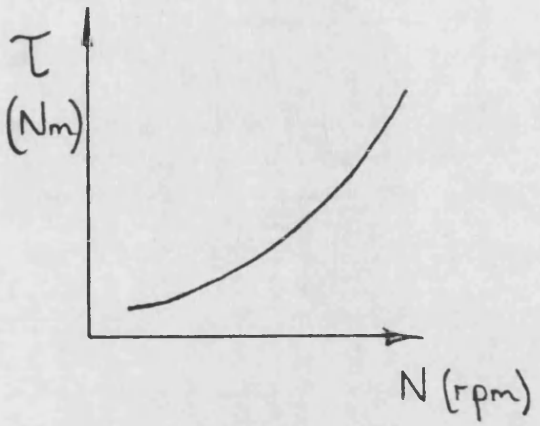

a) propellor law torque curve

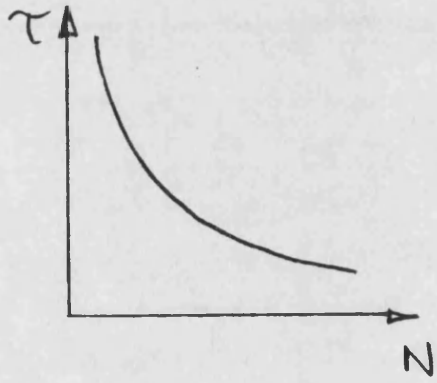

b) constant power torque curve

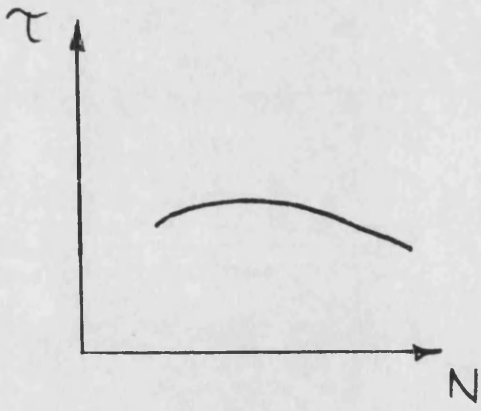

c) typical diesel torque curve

FIG. 1.1 TORQUE VS. SPEED CURVES

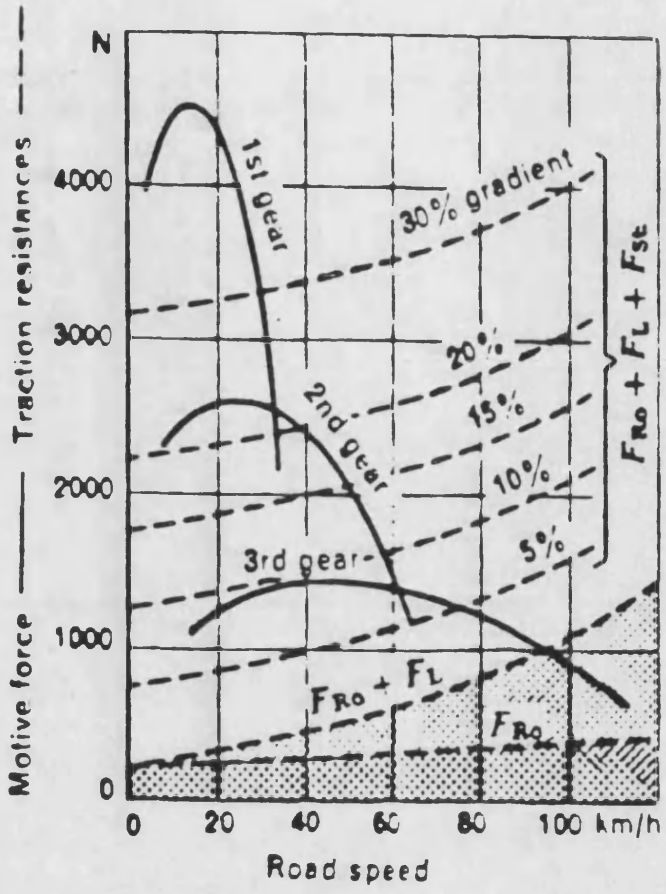

F_{Ro} rolling resistance

F_L aerodynamic drag

F_{St} climbing resistance

FIG. 1.2 VEHICLE TRACTIVE RESISTANCE

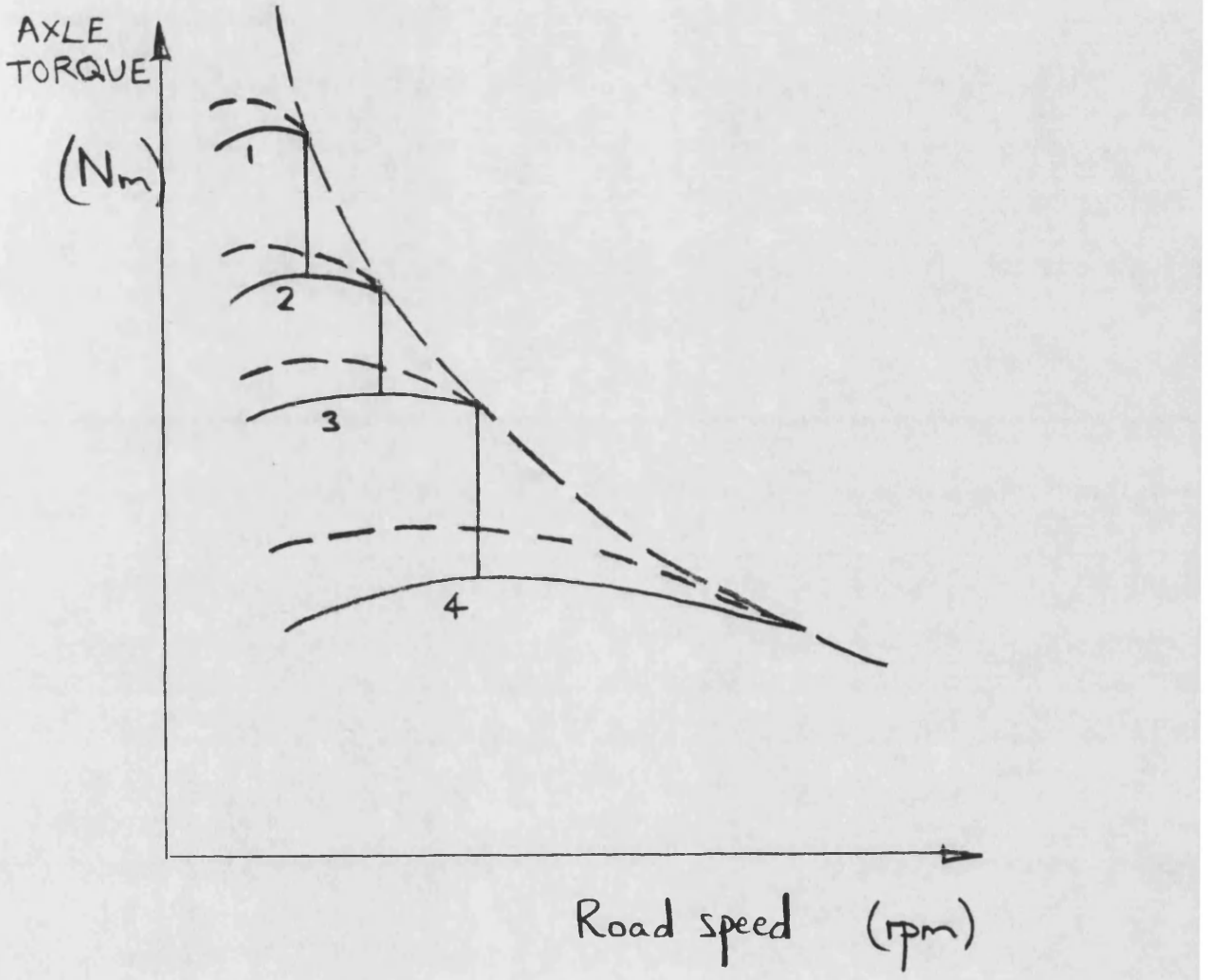

FIG.1.3 MOTIVE FORCE USING A MANUAL MULTI-RATIO GEARBOX

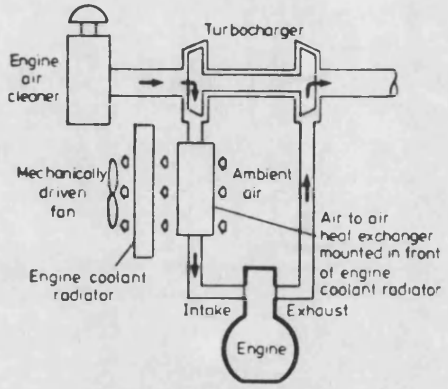

a) Mechanical fan drive air-to-air intercooling system

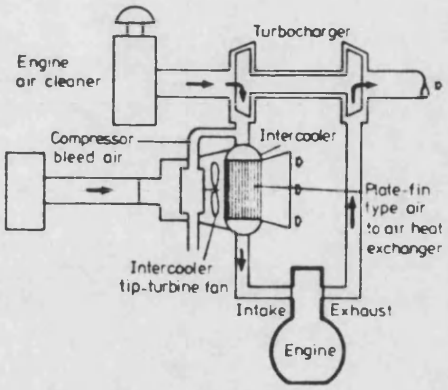

b) Air-to-air tip turbine fan intercooling system

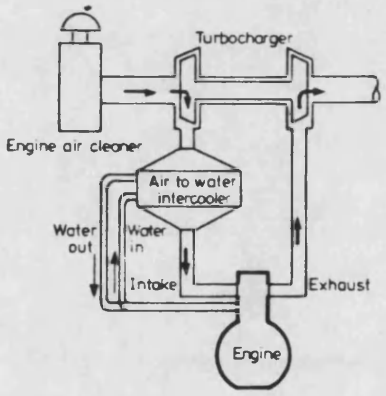

c) Air-to-water intercooling system (using engine cooling system)

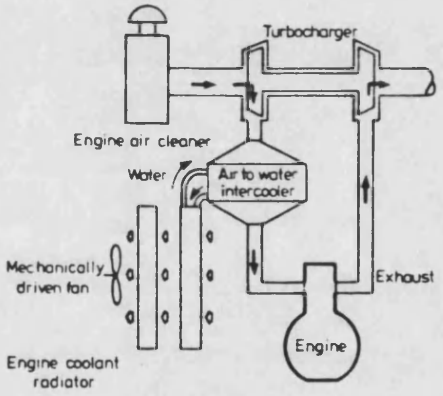

d) Air-to-water intercooling system (using closed water cooling system)

FIG. 1.4 INTERCOOLING SYSTEMS

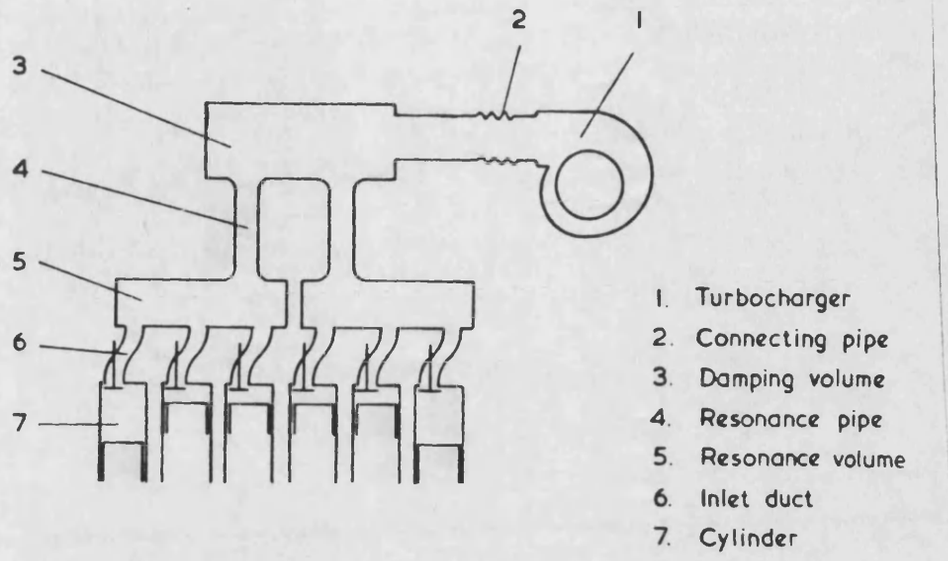

FIG 1.5 RESONANT INTAKE SYSTEM

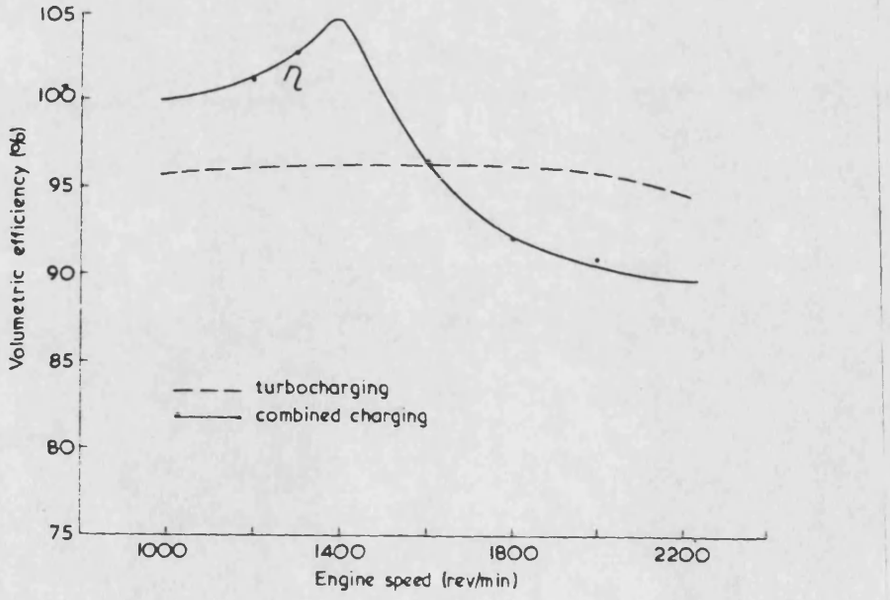

FIG. 1.6 VOLUMETRIC EFFICIENCY USING A RESONANT INTAKE SYSTEM

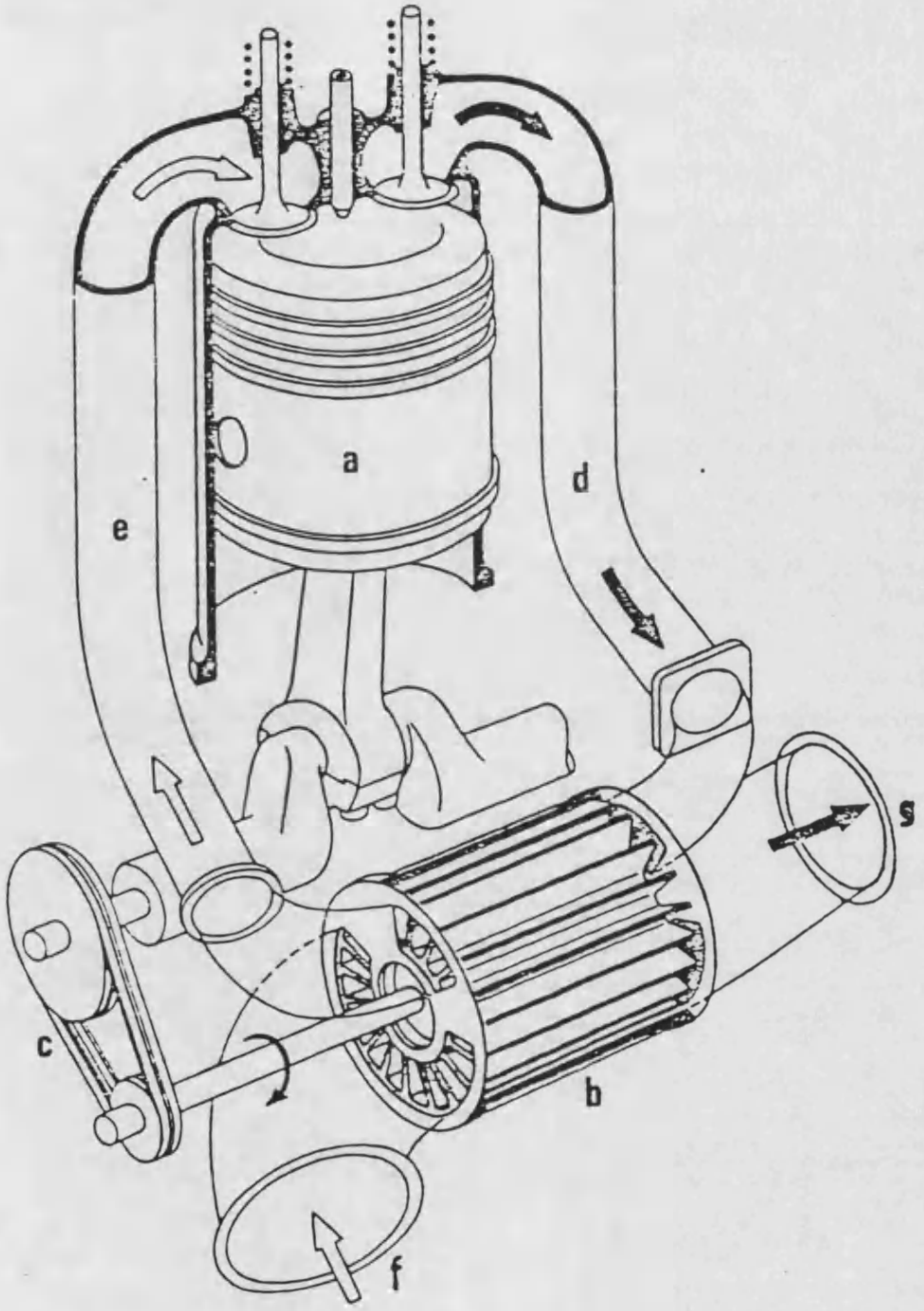

COMPREX: Pressure -wave Machine

as a super-charger

a: Engine
b: Cell-wheel
c: Belt drive
d: High-pressure gas
e: High-pressure air
f: Low-pressure air
g: Low-pressure gas

FIG. 1.7

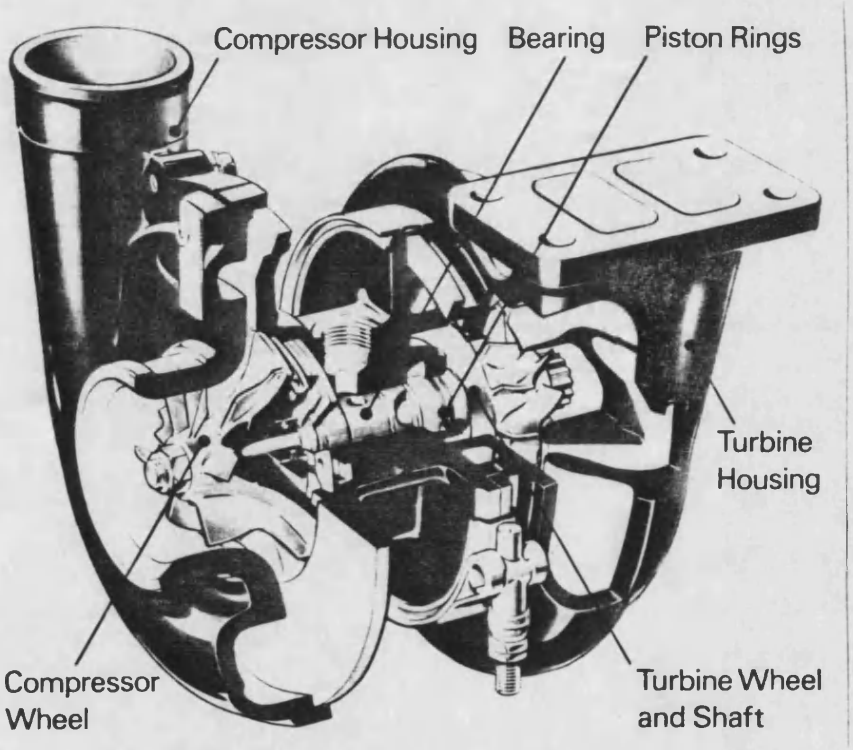

FIG. 1.8 SECTIONAL VIEW OF TURBOCHARGER

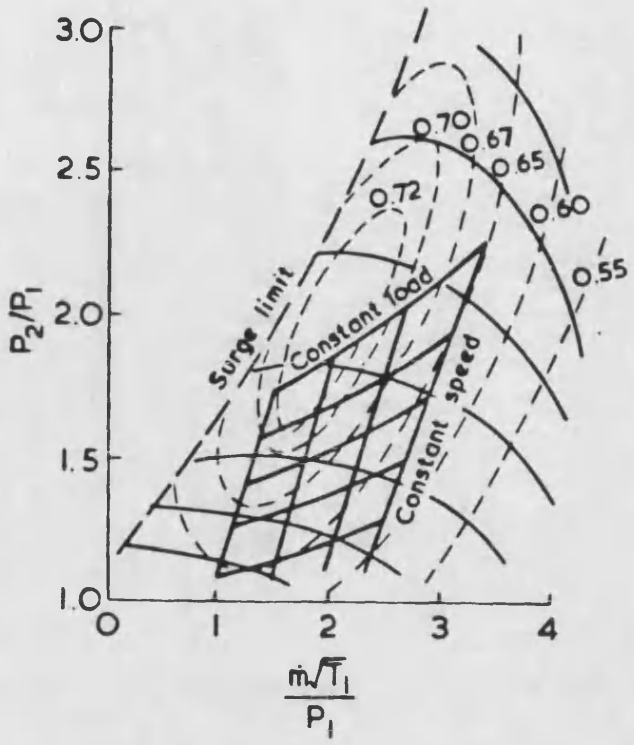

FIG. 1.9 COMPRESSOR MAP WITH ENGINE AIR-FLOW CHARACTERISTICS

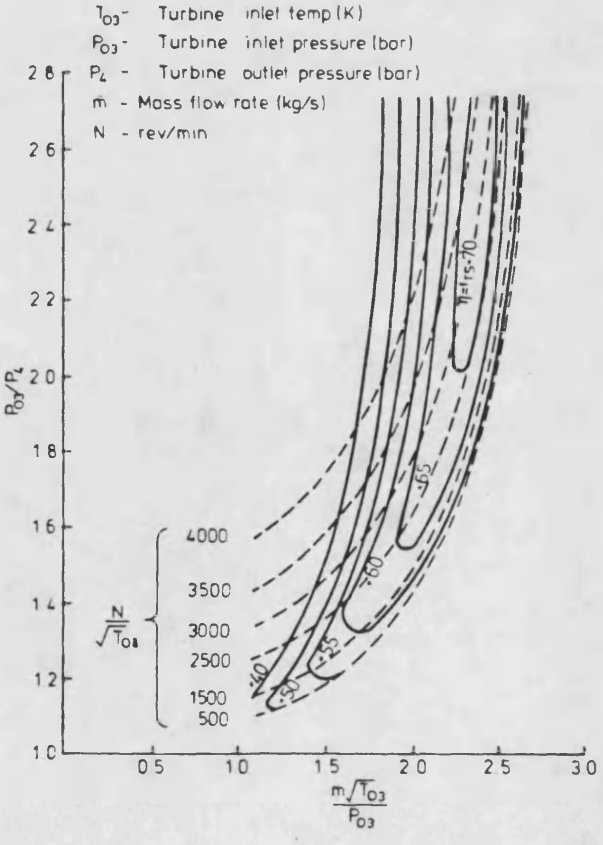

FIG. 1.10 TURBINE MAP

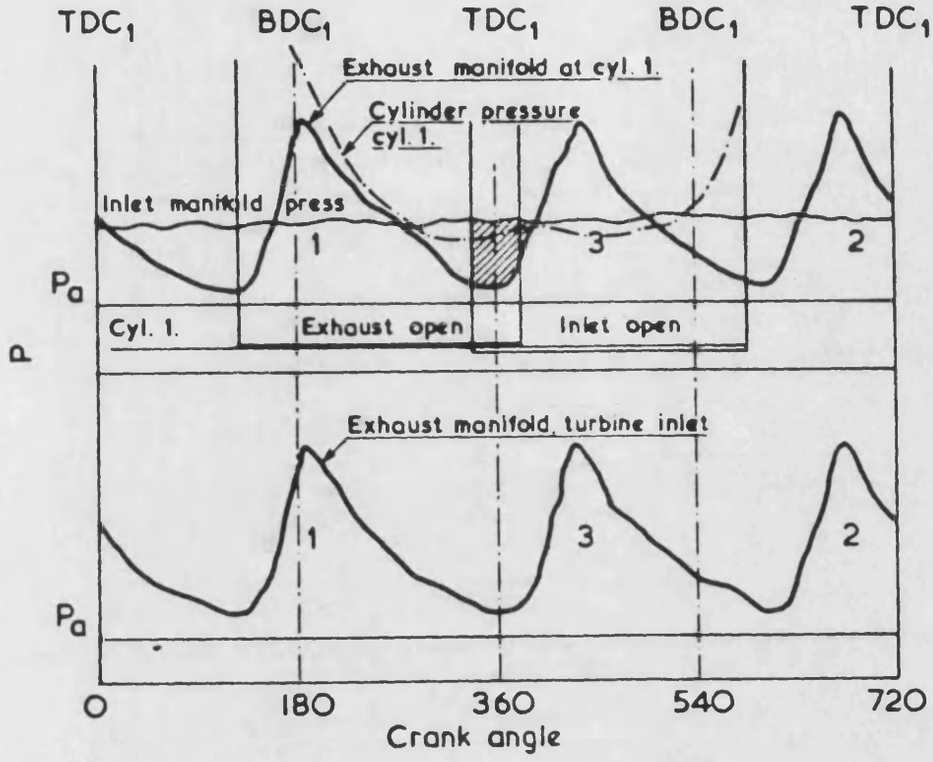

FIG. 1.11 EXHAUST PRESSURE IN 3-CYLINDER PULSE MANIFOLD

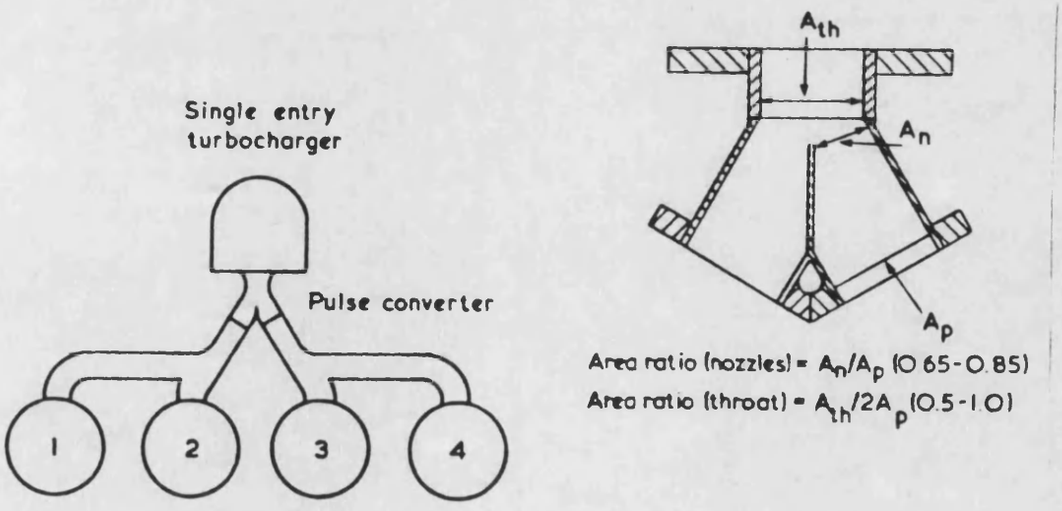

FIG. 1.12 PULSE CONVERTER

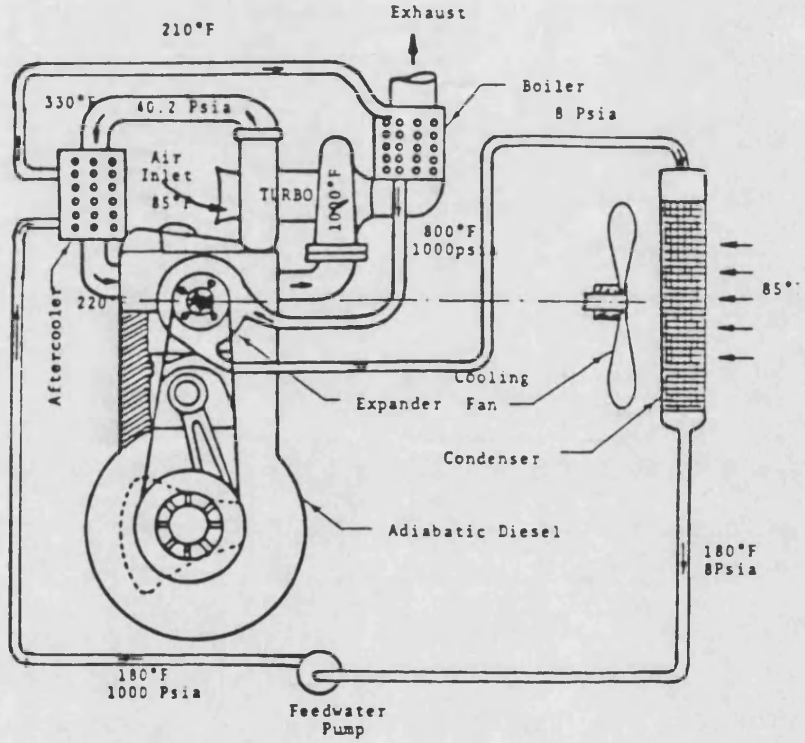

FIG 1.13 RANKINE BOTTOMING CYCLE TO EXTRACT ENERGY FROM THE EXHAUST GAS

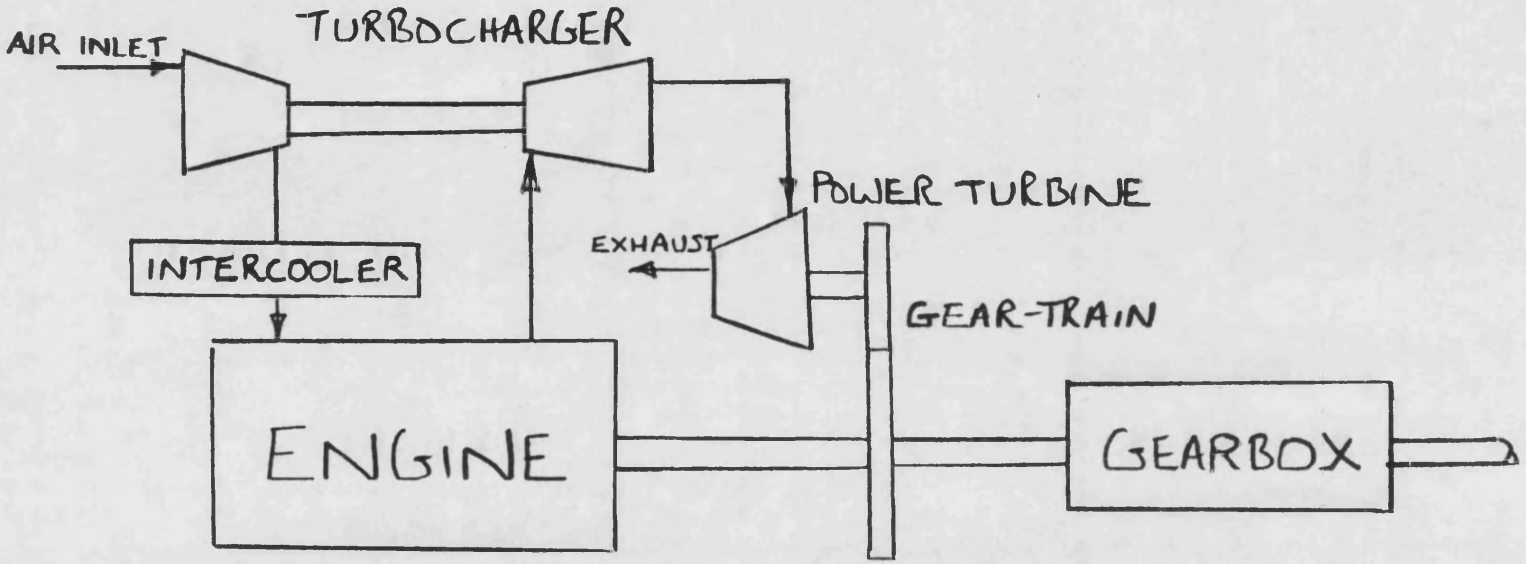

FIG. 1.14 CUMMINS TURBO-COMPOUND

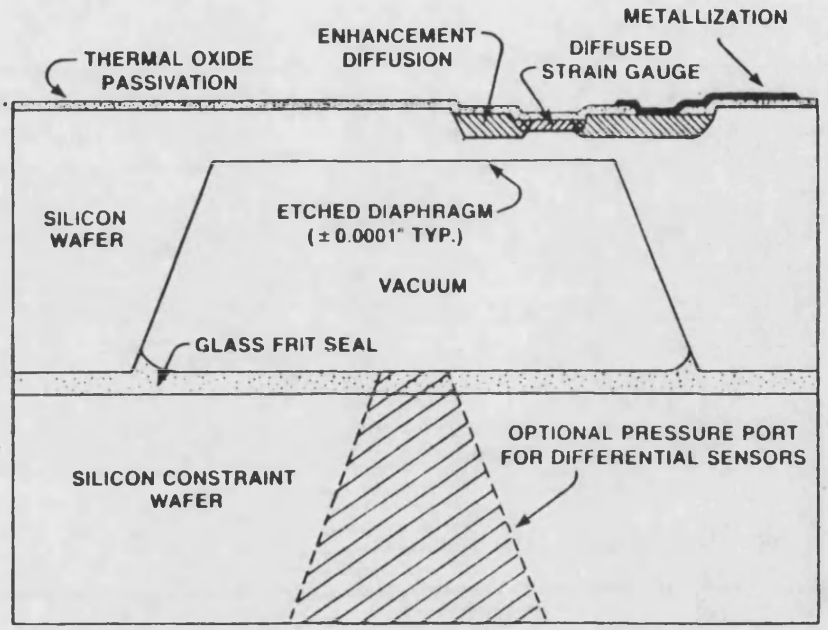

FIG 1.15 MOTOROLA INTEGRATED PRESSURE SENSOR

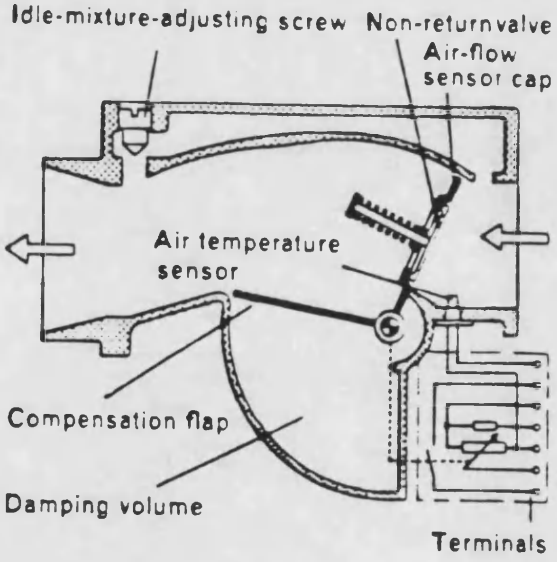

FIG. 1.16 BOSCH AIR-FLOW SENSOR

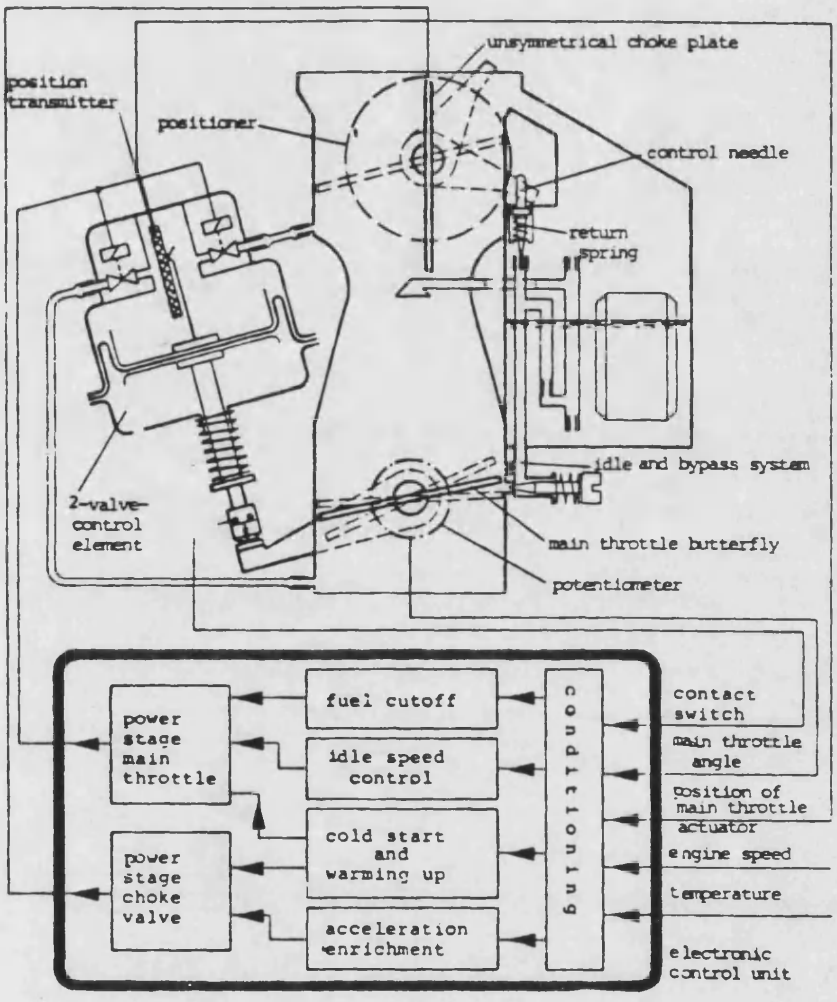

FIG 1.17 MICRO-PROCESSOR CONTROLLED CARBURETTOR

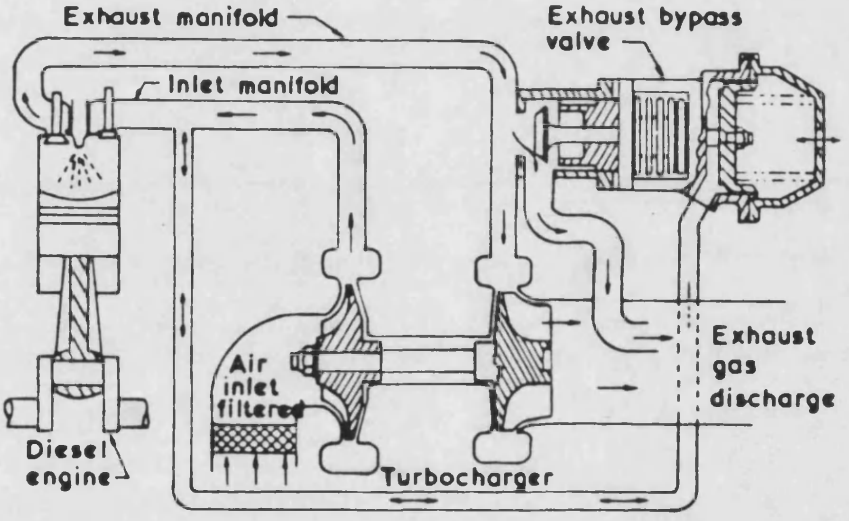

FIG 1.18 EXHAUST WASTE-GATE

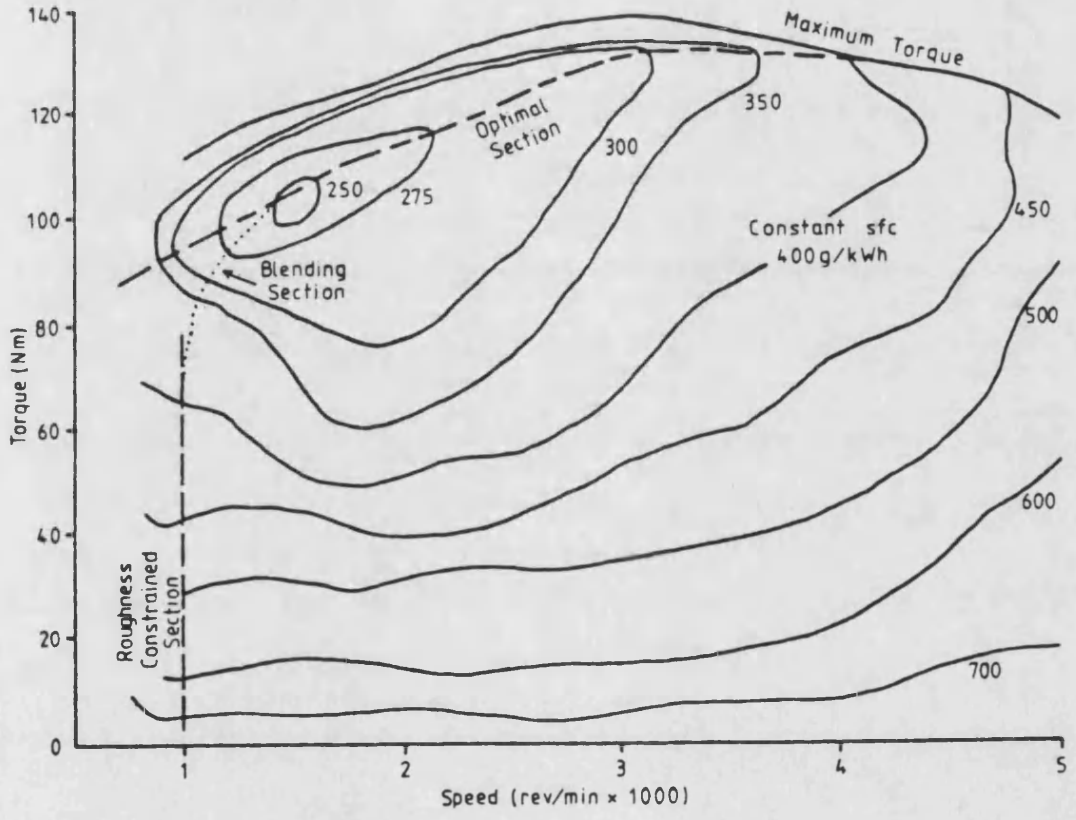

FIG. 1.19 ENGINE ECONOMY LINE

CHAPTER 2

TEST BED DESIGN FOR PERFORMANCE TESTING AND ENGINE CONTROLS DEVELOPMENT

2.1 INTRODUCTION

2.2 MEASUREMENT

- 2.2.1 THE MEASUREMENT SYSTEM
- 2.2.2 ENVIRONMENTAL CONSIDERATIONS
- 2.2.3 SPEED MEASUREMENT
- 2.2.4 TORQUE MEASUREMENT
- 2.2.5 PRESSURE MEASUREMENT
- 2.2.6 TEMPERATURE MEASUREMENT
- 2.2.7 FUEL MASSFLOW MEASUREMENT
- 2.2.8 GAS FLOW MEASUREMENT
- 2.2.9 DISPLACEMENT MEASUREMENT
- 2.2.10 SMOKE MEASUREMENT
- 2.2.11 SIGNAL CONDITIONING

2.3 DATA-ACQUISITION AND REDUCTION

- 2.3.1 STEADY-STATE DATA REDUCTION
- 2.3.2 TRANSIENT DATA-ACQUISITION

2.4 DYNAMOMETRY

- 2.4.1 THE HYDROSTATIC LOADING PUMP
- 2.4.2 THE LOADING VALVES
- 2.4.3 BOOST SUPPLY
- 2.4.4 COOLING AND FILTRATION
- 2.4.5 DYNAMOMETER CONTROLS

2.5 ENVIRONMENTAL CONTROLS

2.5.1 AMBIENT CONDITIONS

2.5.2 FUEL CONDITIONS

2.5.3 INLET AND EXHAUST RESTRICTION

2.5.4 ENERGY DISSIPATION THROUGH HEAT TRANSFER

2.1 INTRODUCTION

This chapter describes those aspects of test-bed design and procedures that are common to both of the test-facilities built for this work. It can be looked upon as a description of the methods used in the Wolfson engine and transmission laboratory. The aim when building a test-facility is to provide enough control over the tests to produce realistic data and for that data to be comprehensive, useful and accurate. This aim can be sub-divided into the following requirements:-

1. Measurement accuracy and repeatability, which is achieved by using equipment with suitable specifications and following recommended practices.

2. A comprehensive data recording system so that any changes in performance or lack of repeatability can be attributed to the correct sources.

3. Test-bed controls capable of providing realistic engine operation, steady-state and transient. This implies flexible and fast diesel driveline and dynamometer controls.

4. Repeatability of test conditions so that performance from test to test can be compared without environmental changes complicating the picture. This means controlling environmental conditions such as jacket water temperature and air inlet temperature.

5. Comparability with data produced by other test facilities. This is achieved by following recommended practices, as laid down in the appropriate SAE and BS standards on engine testing and measurement.

The equipment and methods used to satisfy these criteria are covered in the following sections on measurement, data-recording, dynamometry and environmental controls.

2.2 MEASUREMENT

This section describes the measurement methods and equipment adopted for both experimental test-rigs. The measurement system as a whole, its matching and specification are considered. Problems caused by the Diesel environment are discussed. Measurement methods are described under the following headings:-

1. Speed
2. Torque
3. Pressure
4. Temperature
5. Fuel mass flow
6. Gas flow
7. Displacement
8. Smoke

And finally signal conditioning techniques are described.

2.2.1 THE MEASUREMENT SYSTEM

A measurement system is an interconnection of the devices shown in fig. 2.1. The transducer converts the measured phenomenum into a signal, usually electrical, which then moves in the direction of the arrows. The function of the transmitter is to convert the transducer output into a form capable of being transmitted through the channel, usually a cable. The signal conditioning then prepares the signal for display or recording, The separate blocks are not always clearly defined, for example, the transmitter is often an integral part of the transducer. A manometer is an example of an instrument which combines all of these functions.

The elements of a measuring system need to be correctly matched if it is to provide accurate results. If the signal is in the form of a voltage then the signal conditioning must have an impedance much greater than that of the transducer and channel, so that the signal level is maintained.

An alternative approach, used where cable runs are long, is to use a current transmitter. The signal is transmitted as a current rather than a voltage, this ensure that signal level is maintained. This method requires a power supply to the transmitter. In the laboratory environment where cable runs are short a transmitter is often unnecessary, the transducer output being suitable for transmission in its original form.

The performance specification of a measurement system can be described under two headings:-

A. Static Performance

Static performance is defined by the following parameters:-

Accuracy --

The difference between the indicated reading and the true value of the measured variable as represented by a "standard" instrument. This is usually checked by producing a calibration curve. Readings are taken moving up through the measuring range and then back down through the range to include any hysteresis or backlash. The absolute accuracy of an instrument does not usually take account of drift as defined below.

Accuracy is often quoted as a percentage of full-scale, in which case it is important to use the full range of the device to maintain accuracy.

Range --

The range or span of an instrument refers to the limits between which it will measure. It is important to use equipment with the correct range to maintain accuracy and linearity.

Sensitivity --

The change in transducer output for a unit change of the measured variable. Higher sensitivity means a better signal to noise ratio. Sensitivity is sometimes quoted as mV/V, this refers to the full-scale millivolts output per volt of transducer excitation.

Drift --

The shift in calibration caused by some parameter other than the measured variable eg. temperature or time. The drift with temperature is usually referred to as the temperature coefficient (% per deg.C)

Resolution --

The smallest change in output the measurement system can register. Resolution should not be confused with accuracy and is often a smaller percentage of full-scale to take full advantage of the available accuracy.

Linearity --

The percentage deviation of the calibration curve from its straight line fit. If the device is supposed to be linear this is often included in the accuracy figure. Linerisation is incorporated in the signal conditioning when a transducer has a known, repeatable non-linear characteristic.

Repeatability --

The ability of a measurement system to reproduce previously taken readings under the same conditions. This parameter can be quoted as a percentage of full-scale.

B Dynamic Performance

The dynamic performance of a measurement system is usually described by its frequency response, a typical example is shown in fig. 2.2. The frequency range over which the response remains flat, within a specified tolerance (usually 3dB), is referred to as the instrument's bandwidth. The required bandwidth is determined by the frequency spectrum of the input signal.

The overall response of a measurement system is made up of the individual component responses, each of which must have an adequate bandwidth. Transducer response can be affected by installation, for example, any dead volume between a presssure transducer diaphragm and the pipe or manifold will have a resonant frequency, which should be an order of magnitude greater than any measured frequencies.

2.2.2 ENVIRONMENTAL CONSIDERATIONS

The Diesel environment makes sensor survival and reliability an important consideration. Some of the more important environmental effects are described below:-

Temperature

Many areas on the Diesel call for high temperature sensors and leads. Sensors can be cooled and PTFE insulated leads used. Wrapping sensors and leads in crumpled aluminium foil reflects radiation and provides an air gap to minimise conduction from the foil.

Transducer temperature coefficients are critical where the transducer operates over a wide temperature range; an accurate calibration at room temperature is then meaningless.

Vibration

Transducers fitted with rugged, positively retained connectors are preferable to those with flying leads. However, in the majority of cases there is no choice if cost is to be kept low. Looping flying leads and tying to the transducer body moves the fatigue point. Should fatigure occur a length of lead is left intact and a repair can be effected.

Oil

Where oil ingress is likely a transducer which will operate immersed in oil must be chosen or a protective case employed. Optical and slip-ring devices are especially prone to oil contamination.

Soot

Deposits of soot can cause sensor drift and block tappings, regular cleaning and re-calibration may be necessary.

Chemical action

This can be avoided by ensuring sensors are made of suitable materials, the use of stainless steel sheathed thermocouples is one example.

2.2.3 SPEED MEASUREMENT

Rotational speed measurements are made with inductive pick-offs wherever possible as they are low cost, reliable and simple to install. Where the performance of the inductive pick-off is inadequate other devices such as the optical encoder and the tacho-generator are used.

1. The inductive (magnetic) pick-off consists of a small coil and magnet assembly which is positioned close to passing ferrous

teeth. As the teeth move past the pick-off the change in permeability, and hence field, induces a voltage. The result is a pulse train, the frequency of which is proportional to speed.

Engine speed is measured using flywheel teeth, turbo-charger speed using compressor blades. Because the compressor wheel is made of an aluminium alloy the change in permeability is small and the pulse train can distort as speed changes. This makes it difficult for the frequency to voltage (F-V) converter (section 2.2.11) to trigger properly throughout the speed range. Where a gear wheel is not available a dedicated toothed wheel is fitted to a convenient coupling

The inductive pick-off is not affected by oil and dirt as an optical device would be, however, it can be damaged by overheating and vibration may cause cable fatigue.

2. The optical encoder gives a greater number of pulses per revolution than is normally practical with an inductive pick-off. This is useful if cylinder conditions are to be displayed against crank-angle.

   Frequency response of both the inductive pick-off and the encoder is determined by the number of pulses per revolution and the frequency to voltage converter time constant (section 2.2.11).

   Coupling encoders to the crank-shaft has proved difficult: If the coupling is too stiff it tends to fatigue or damage the encoder unless alignment is perfect; if it is too soft torsional oscillation causes spurious pulses resulting in an unreliable signal.

3. Tacho-generators produce a DC voltage proportional to speed. They are used when a good frequency response over a wide speed range is required, in particular for critical control loops such as dynamometer speed control. They are affected adversely by oil

ingress, and where this is likely are fitted with oil seals and a splash proof cover.

2.2.4 TORQUE MEASUREMENT

Two methods of torque measurement are used: in-line torque transducers and load cells. A load cell can only be used if one of the coupled components is mounted on trunnion bearings and restrained from rotating by the load cell.

1. In-line torque transducers are the only method of measuring torque between components which are both rigidly fixed. They are coupled between the two components using a ½ gear coupling at each end, thus acting as a prop-shaft which takes up any mis-alignment. This ensures the torque-meter is not subjected to bending stresses. Two types are used; slip ring devices and inductively coupled devices. Both devices are based on strain gauged shafts, only the method of transmitting the excitation and signal differs.

   The slip-ring devices are less expensive but will not operate at high speeds because of brush bounce, and are adversely affected by oil mist which can settle on brushes and slip-rings.

   The inductively coupled type passes the high frequency bridge excitation, typically 8 KHz for the "Vibrometer type", through two transformer coils one stationary the other rotating with the strain gauged shaft. The output from the strain gauge bridge is returned in a similar manner. This type will operate at higher speeds and is generally more reliable. However, cost can be prohibitive, partly because special conditioning must be purchased with the device.

2. Load-cells are used with trunnion bearing dynomometers, they measure the force on a torque arm restraining the dynomometer from rotating. Advantages include low cost and more compact test-bed

layout. However, long term accuracy is affected by vibration induced trunnion bearing wear which occurs at the point where the weight is supported. This localised wear results in stiction causing a dead-band around zero torque. Vibration is also readily transmitted to the load cell and results in a noisy signal and eventual damage. Isolation from the Diesel engine greatly reduces these problems.

2.2.5 PRESSURE MEASUREMENT

Wherever possible steady-state pressure measurements are taken using water and mercury manometers to reduce costs. Static pressure tappings are made to the recommendations in ref. 26. On the exhaust side the tappings are 1/16" dia. to reduce the frequency with which they become blocked by soot. Several tappings are used in any one measuring plane and commoned together, this reduces errors caused by uneven flow profiles.

Pressure transducers are used for dynamic measurements or where the range is outside that easily covered by a mercury manometer. Manifold, plenum and pipe pressures are measured with strain-gauge types and cylinder pressure with piezo-electric devices. Water cooling is often required.

1 Strain gauge devices are usually based on a diaphragm which either has gauges bonded directly to it or is connected to a cantilever beam system which is itself strain-gauged. There are two major groupings: bonded metal strain gauge and semi-conductor strain gauge devices. The second group are becoming more widely used for general purpose applications as they are based on a bridge of piezo-resistors diffused into a silicon chip and can, therefore, be mass-produced at low cost. The semi-conductor type can be designed to cover a wide frequency range, however, temperature limits and fluid compatibility must be established before choosing a sensor.

2 Piezo-electric pressure transducers are used for cylinder pressure measurement as they have a very good frequency response and will withstand the pressures and temperatures within the cylinder. They are dynamic devices based on charge movement within a quartz crystal and will not measure statically. Becauce of this calibration can be problematic. Increasing the time-constant of the charge-amplifier allows static calibration with a dead weight tester. If this facility is not available pressure steps can be provided by a system which allows compressed gas to be rapidly expelled to atmosphere.

Pressure transducer installation can critically affect frequency response, any cavity in front of the diaphragm will act as a Helmholtz resonator. Sensitivity will increase rapidly as the resonant frequency is approached and will lead to major errors.

A fuller survey of pressure transducers can be found in ref. 27.

2.2.6 TEMPERATURE MEASUREMENT

For the majority of temperature measurements the School of Engineering has standardised on the Chromel-Alumel (K-type) thermocouple. Of the base metal types this category has the widest temp. range (up to 1100 deg.C) and adequate accuracy (approx. ±1%). Standardising avoids several differing conditioning requirements and accidental mis-matching of equipment.

Mineral insulated thermo-couples are used wherever survivability is important; they are mechanically tough and can be bent to aid installation. The correct choice of metal sheath avoids chemical attach.

Thermocouples have a poor dynamic response which is inversely proportional to their diameter. Typically a sheathed thermocouple, 1/16" diameter, would have a time constant of the order of 5 seconds

(ref. 28). By its very nature this figure is highly approximate depending on heat transfer coefficients.

A thermocouple shield is employed when the total temperature of a flowing gas is required, or where radiation might be a source of error (in exhaust pipework). These are designed to the recommendations in ref. 26.

2.2.7 FUEL MASS FLOW MEASUREMENTS (fig. 2.3)

Steady-state fuel consumption readings are made with a fuel weigh-gear consisting of a set of scales and an electronic system which records time and revolutions. The scales have a beaker of fuel on one side and weights on the other. An opto-switch detects the scales tipping towards the side holding the weights, which starts or stops a timer-counter. Revolutions are sensed by a TDC detector or similar device, the pulses from which are fed to a counter.

Referring to fig. 2.3, engine fuelling is switched from the day-tank to the beaker to measure fuel consumption. Fuel is consumed from the beaker until the scales tip over activating the counters, a suitable weight is then removed from the scales allowing them to move back to their original position. When a mass of fuel equal to the weight removed has been consumed, the scales again tip over stopping the counters. The operator can now record the time and revolutions over which the known mass of fuel was consumed. The weight removed should always be enough to give at least a 100 second consumption period so that changes in the dynamics of the scales are negligible.

Transient fuel consumption measurements have, in the past, been made with a turbine flow meter. However, pulsations in the fuel line can cause problems. An alternative method is to record fuel rack position and fuel pump speed (half engine speed), and then use a steady-state fuel pump calibration to estimate fuel flow.

When a continuous steady-state reading is required (for fuel consumption optimisation) a gear type positive displacement flowmeter is used. This type of device is unsuitable for transient measurement because output frequency is too low.

2.2.8 GAS FLOW MEASUREMENT

Gas mass flow is measured using a pressure drop device such as an orifice plate or nozzle. These devices are manufactured and installed to the recommendations in refs. 29-30. The flow through the orifice must be fully developed and without pulsations. A suitable length of straight pipe or a straightening device ensures a fully developed flow profile. Where the engine causes significant flow pulsations a plenum is installed between the orifice and the engine to smooth the measured flow.

The mass flow is calculated from the pressure difference across the orifice, upstream gas density, orifice geometry and correction factors which are often incorporated in a single discharge coefficient C_D. To avoid the need to correct for gas compressibility the pressure difference is kept below 10" water gauge.

For steady-state measurements an inclined manometer is used to measure differential pressure. If transient gas flow measurements are required a differential pressure transducer provides the necessary response and an electrical output for recording purposes. If accidental overpressure is possible the transducer must have a large overpressure capacity as any restriction in the ducting is likely to result in pressures well over the range of the transducer (10" WG).

2.2.9 DISPLACEMENT MEASUREMENT

Various position signals are useful both for performance testing and as feedback in control loops. Some examples include: fuel rack position, turbine geometry, static timing (where a variable timing device is fitted) and injector needle lift. The two sensors most

commonly used for general displacement measurement are the resistive potentiometer and the LVDT (linear variable differential transformer). Needle lift sensors are of the simple inductive type as they need only a single coaxial cable, which is kept as short as possible. This allows a high frequency response and reduces noise coupling through the cable.

1 The resistive potentiometer (fig. 2.4a) produces a voltage proportional to the position of the slider so long as the output is buffered (ie has high impedance) and the supply voltage is constant. They can be wire-wound, conductive plastic or a hybrid (wire-wound plastic coated). The hybrid combines the advantages of the conductive plastic type (hardwearing, low noise and infinite resolution) with the lower temperature coefficient of the wire-wound type. The temperature coefficient is only important if the track varies in temperature along its length, otherwise the resistance change is the same throughout the track and no error is generated.

Frequency response depends on the slider maintaining good contact with the track, and is normally specified as maximum slider velocity. Conditioning is simple, no amplification being necessary. However, an accurate stable supply voltage is required.

2 The LVDT is used where survivability is important, it can be designed to work at high temperatures, pressures and be immersed. It has no components in mechanical contact and hence does not wear. Advantages include infinite resolution, frictionless movement, and good frequency response. As a "rule of thumb" the LVDT can be used for dynamic measurements up to 0.1 x supply frequency.

The principle of operation is shown in fig. 2.4b, the outer body is a transformer with a primary and two secondary windings. The secondary windings are connected back to back so that with the

core centralised the secondary e.m.f.s cancel. If the core moves in either direction one secondary e.m.f. will increase while the other decreases resulting in an output, the polarity is dependent on which side of centre the core is.

The LVDT requires more complex conditioning than the resistive potentiometer as the AC signal requires amplification and de-modulation (section 2.2.11). So called DC-DC LVDTs with built in conditioning are available, however, they are more expensive and a failure means replacing the whole unit. The frequency response of DC-DC devices should be checked as their in-built conditioning may be crude.

2.2.10 SMOKE MEASUREMENT

Two methods of smoke measurement are employed, one a manual steady-state method, the other an electronic system capable of dynamic measurement. Both methods provide a measure of opacity, but give no break-down of exhaust composition.

Opacity is a useful measure of how much smoke is being produced and provides a fuelling limit at low engine speed (BS Au 141a specifies a smoke limit of 10% opacity or 3.5 Bosch units). Opacity is also a measure of how well the fuel injected is being burnt and as such can be used in development work to determine if improvements have been made. In the work described in this thesis the transient opacity meter was particularly useful in giving a measure of boost pressure (ie turbo-charger) response, a poor response leads to a larger transient puff of smoke.

1 The Bosch "spot" smokemeter is a manually operated steady-state device which sucks a fixed volume of exhaust gas through a filter paper. A special nozzle is installed in the exhaust stack which is connected to the sampler only when taking the sample. The filter paper is removed from the sampler and a photo-electric evaluation unit produces a reading based on the light reflected

from the filter paper (fig. 2.5). Ref. 31 describes the correct installation and operating procedures for this device.

2 The transient opacity meter was constructed in house for the research described in this thesis and is based on a design similar to the "Berkeley Celesco" (ref. 32). The device fits in the exhaust stack and is of the same diameter, taking the full exhaust gas flow. A light source and a photo-electric light detector are positioned opposite each other so that light pulses can be transmitted through the exhaust gas (fig. 2.6). The loss in transmission as a result of smoke is converted into either an opacity or smoke density reading which is displayed digitally by the electronics. Analogue signals are also available for dynamic display on an oscilloscope or input to a data-acquisition system.

Compressed air is blown across the lenses to prevent soot deposition, and a water cooling system protects the light source and detector from overheating. Both of these protective devices must be operating whether measurements are being taken or not.

Bosch units are the standard way of expressing smoke levels both for industry and standards organisations. Fig. 2.7 is a calibration of opacity readings versus Bosch units with the opacity meter installed on the V.G. turbo-charging test facility (Leyland TL11). Any change of installation should involve re-calibration.

2.2.11 SIGNAL CONDITIONING

The signal produced by the transducer is transmitted though the cable and then prepared for display or recording by the signal conditioning. The signal may be low level requiring amplification, it may be DC, AC or digital (a pulse train for example) requiring demodulation or conversion to a suitable form. Finally the signal may have picked up a noise component and require filtering.

The standard forms of conditioning used on both test-rigs are described below along with the methods used to minimise and eliminate signal noise.

1 DC signal conditioning

The standard conditioning card for low level DC signals is an in house design based on a monolithic differential instrumentation amplifier (the AD521 or the ED5-C). This device provides a programmable fixed gain and high common-mode noise rejection. The gain of the AD521 is given by the ratio of two resistors (R_m/R_g) and is chosen to suit the sensitivity of the transducer. An op-amp (741) configured as a variable amplifier is used for fine adjustment of the output.

For high level DC signals an op-amp (741) configured as a differential amplifier is used instead of an AD521.

2 AC signal conditioning

Transducers requiring AC excitation, such as the LVDT, are used with "Sangamo" AC carrier amplifier cards. These cards are amplitude modulated (a.m.) systems comprising an oscillator, demodulator and DC amplifier with gain and zero controls. The facility for ±100% offset is provided to allow a uni-polar output.

3 Pulse train conditioning (F-V conversion)

The standard frequency to voltage (F-V) conversion card is an in house design based on an "Ancom" F-V module. The pulses, usually from a magnetic pick off or encoder, are first squared up by a fast comparator. The comparator has an adjustable trigger level to enable it to be matched to the pick-off producing the pulse train. The Ancom module then converts the squared up pulse train to an analogue voltage. It achieves this by shaping the pulses, that is fixing their height and width, and then integrating the pulse train.

The integrator discharges between the pulses and hence the higher the frequency the higher the mean integrator output must be for charge and discharge to balance (see fig. 2.8). The integrator time constant is set by the values of an external resistor and capacitor (R_g & C_{rip}). The choice of time constant is a trade off between output ripple and frequency response, reducing output ripple is at the expense of overall response.

4 Thermocouple conditioning

For manual recording of steady-state temperatures commercially available digital displays with multi-way switches are used. These displays incorporate linearisation and auto-cold junction.

Where an electrical signal is required, for input to a computer or to activate a safety trip, a card is designed using commercial modules for amplification, linearisation and auto-cold junction.

5 Signal noise

Several precautions are taken to protect against unwanted signal noise:-

The signal ground is not earthed at the transducer, both lines return to the conditioning where the first stage is a differential amplifier. This method of connection avoids ground loops and any common-mode noise is rejected by the differential amplifier.

Shielded cables are used between transducer and conditioning to minimise capacitative coupling.

High quality connectors with positive retention are used so that cable/connector movement does not create noise.

Signal high and low always follow the same route so that any electromagnetic interference is induced in both and cancels out.

Ideally a twisted pair should be used, however, this is not always possible.

Known sources of noise are either shielded or cables are routed to avoid the source.

These measures can only protect against external interference. Unwanted transducer noise must be eliminated by filtering the signal. Luckily most noise is at higher frequencies than the required bandwidth and a low pass filter can be used. Often a simple RC low pass filter will suffice. However, if the cut-off frequency needs to be close to the required signal bandwidth a sharper cut-off is necessary, and an active circuit such as a 2nd order Butterworth filter is used.

2.3 DATA-ACQUISITION AND REDUCTION

During testing the measured variables need to be recorded, and afterwards processed and plotted as required. Because of the number of variables involved in steady-state tests, it would be too costly to interface them all to a computer, hence readings are entered manually into a data-reduction and plotting program on a portable Commodore PET computer. Transient tests necessitate on-line recording of engine variables because readings are required at intervals of between 10-1000m sec, in this case a PET computer with suitable analogue interfacing is used to capture the data, process it and plot as required.

2.3.1 STEADY-STATE DATA REDUCTION

These programs are specific to their particular experimental rigs, so detailed descriptions are not appropriate here. For program listings, date reduction formulae, input and output variables etc. see the relevant program users guide. The following description refers to desired program features rather then those actually available.

The user enters one-off data for the test-run such as data-file name, date, barometric pressure and relevant comments. The first test-point is then set up. After allowing at least ten minutes for conditions to settle, data is entered through the keyboard and displayed on the VDU. When the user has entered all the data for this test-point, he or she confirms the data on the screen and edits if necessary. The program then applies conversion factors to the data and calculates relevant performance criteria such as efficiency, air fuel ratio etc. The reduced data is stored on disc and the next test-point is set-up. After the series of test-points has been completed, and any final comments have been added, the reduced data for all the test-points is tabulated on the printer.

All comments, as well as the reduced data, are both stored on disc and printed out. The data stored includes all variables in their original

measured form except where the original value can be obtained by a reverse calculation not involving another measured variable. This ensures the actual data entered is available or can be reliably calculated. The DCE data reduction program also produces standardised graphs using a HP intelligent plotter.

2.3.2 TRANSIENT DATA-ACQUISITION

A general purpose data-acquisition program is used for transient testing. Originally this program was written in FORTRAN on a DEC PDP/8E. The machine was connected to all the various laboratories in the School of Engineering by land-lines and a multiplexor. This arrangement was highly inconvenient and the length of the lines caused noise and frequency response problems. The present improved system uses a portable PET computer, and is written in BASIC and machine code.

The block diagram in fig. 2.9 shows the hardware arrangement. The PET computer is based on a 6502 microprocessor which communicates with peripherals, via an IEEE bus, and analogue interface cards, via an extension of its own internal bus (I/O is memory mapped). A ribbon cable connects the 6502 bus to a card frame containing an 8 channel ADC module and 2 DAC modules. The IEEE bus allows the PET to communicate with a dual floppy disc drive, a printer, and a HP intelligent plotter. The plotter is an RS232 serial device and is connected to the IEEE bus through a dedicated interface box. The ADC and DAC modules operate on principles similar to those described in section 3.4.3.

The data-acquisition software consists of three distinct parts:-

A. A machine code initialisation routine which sets up the I/O hardware, that is the VIA (versatile interface adaptor) chips which control the ADC and DACs. The VIA chips also contain the timer-counters used to control the sample interval. In addition

the routine sets up various BASIC text pointers before running the BASIC master program.

B. A BASIC master program which communicates with the user and implements his commands by calling appropriate subroutines.

C. A machine code subroutine, called from the BASIC program, which executes the transient. This routine handles all the time critical actions, it runs the ADC and DACs accessing memory to read and store the appropriate data. It also controls the timing of the transient.

The BASIC program is menu driven and offers the user five options:-

1. ADC calibration --
   Calibration data for the ADC channels is stored on disc as a "calibration" file. This option allows the user to create a new file or modify an old one.

2. DAC ramp creation --
   A "ramp" data file contains DAC calibration data and the DAC schedules to be output during the transient. This option allows the user to create or modify a "ramp" data file.

3. Engine control --
   This option runs a transient. It first sets up the data defining the transient by reading the appropriate calibration and ramp files. Then the machine code subroutine executes the transient, after which the ADC calibration factors are applied, and the data stored on disc along with information entered by the operator.

4. Hardcopy plot --
   This option produces a full set of curves for a transient along with comments on a single A4 sheet.

5 Quick view --

This option rapidly plots a single variable on an A4 sheet, and is intended to give the operator a means of assessing a transient quickly without waiting for a complete hardcopy plot.

Transient data tabulation on the printer is performed by a separate BASIC program which also includes some data analysis, this program is specific to the series of tests being undertaken.

The BASIC software was written by the author's research colleague, U.Anderson, and is described in greater detail in reference 33.

The machine code subroutine which runs the transient has two control variables: the sample interval in milliseconds; and the number of samples or sample count. They are set by the user through the BASIC program. The maximum sample rate is 500 Hz, the maximum number of samples being 256 per channel.

A timer-counter is loaded with the sample interval and proceeds to count down. The 8 ADC channels are sampled, each sample consisting of a dummy conversion to allow the multiplexor to settle and the actual conversion. The ADC data is stored in a reserved area of memory. Data is then accessed from a second reserved area and output to the 2 DAC channels. The sample count is then decremented and if equal to zero the routine ends. If not the routine waits for the sample interval to end (counter timeout) and then repeats the procedure for the next sample.

ADC and DAC data is stored in two reserved areas at the top of memory. Two pointers locate the data blocks for the present sample and are reset to point to the following data blocks after the 8 ADC and 2 DAC channels have been serviced.

Both BASIC and machine code listings can be found in ref. 33.

2.4 DYNAMOMETRY

The test rigs used for this work both incorporate hydrostatic dynamometers. Load dissipation was the only requirement, motoring facilities or energy recovery (regeneration) are not included. The hydraulic components making up a simple loading system are shown in fig. 2.10 in the form of a hydraulic circuit diagram. The circuit consists of a main loop which dissipates the Diesel-drive's power output and a make-up system which maintains the correct inlet pressure to the loading pump.

The main loop consists of the hydrostatic loading pump which is driven by the Diesel engine, a pressure relief valve, filter and oil cooler. The pump is a positive displacement device, neglecting viscous friction effects, torque is proportional to displacement and pressure. The relief valve (loading valve) controls the pressure output of the pump and hence the load torque, at the same time it converts the pressure energy of the pump's output into heat which is dissipated through the oil cooler. A full flow filter is included in the loop to prevent any oil contamination damaging the pump.

The make-up system or "boost supply" provides a make-up flow which compensates for internal pump leakage and hence maintains the correct loading pump inlet pressure. Internal pump leakage goes back to the tank and is then returned to the main loop by a gear pump. The latter is driven either mechanically by the main pump or by a separate electric motor.

The individual components and their influence on dynamometer performance are discussed in the following sections.

2.4.1 THE HYDROSTATIC LOADING PUMP

The pumps employed on both test-rigs are of the axial piston type. Referring to fig. 2.11, the cylinder block is rotated by the drive shaft resulting in a reciprocating movement of the pistons as they are

pushed against the angled swash-plate. On the suction stroke the pistons are held against the swash plate by the make-up or "boost" pressure at the inlet port. This pressure also ensures adequate lubrication of the moving parts, in particular the slipper pads on the swash plate. The valve plate connects the cylinders on the suction stroke to the inlet port and those on the delivery stroke to the outlet port.

The displacement per revolution is determined by the swash plate angle and is one method of controlling torque, the other method is to control the delivery pressure using the loading valve, this gives a faster response.

A typical pump operating envelope is shown in fig. 2.12, the upper torque limit is determined by the maximum delivery pressure, usually 350 BAR. Although reducing swash angle does allow some increase in maximum speed, it does not result in a constant power envelope. For any Diesel driveline where torque rises as speed decreases the pump "corner power" will be much greater then the Diesel's rated power. One solution to this problem is to use a gearbox with several ratios to cover the speed range.

A dynamometer system based on a multi-ratio box is unsuitable for transients covering a wide speed range. However, this type of system can be used for steady-state testing and constant speed transients. The DCE dynamometer design incorporates a splitter box, with two ratios, driving two pumps. This compromise design allows speed transients over either the entire speed range up to approx. 60% of maximum (stall) torque or over the lower 60% of the speed range up to maximum torque. A detailed discussion of the DCE design can be found in section 6.4.1.

2.4.2 THE LOADING VALVES

Pump delivery pressure and hence torque is controlled by the main pressure relief valve which is fitted in series with the pump in the

main loop. Abex Denison (R4V series) pilot operated relief valves are used on both test-rigs. Referring to fig. 2.13 the pump delivery enters port A, pressure drops through the valve cartridge, and the flow leaves through port B. The main poppet is designed to lift and pass flow when the pilot pressure behind it is less than the pressure at A. The poppet lift, and hence pressure drop through the valve, depends on the magnitude of the pressure differential across the poppet. Pilot pressure is controlled by a pilot stage connected to port X. Any pilot flow results in a drop through the orifice and hence a pressure differential across the main poppet.

Dynamic performance of the R4V is limited by the rate at which the poppet can open and close, which in turn depends on the response and flow capacity of the pilot stage, and the volume behind the main poppet.

The pilot stage chosen depends upon the dynamic response required. Abex Denison (SE03) solenoid operated pressure control valves have been the usual choice. However, their response and flow capacity is thought to be a limitation on the overall response of the dynamometer. The Fluid Power Group within the School of Engineering is investigating alternative pilot stages, including "moog" type servo-valves which have a very good response for a wide range of flow capacities. The SE03 valve (fig. 2.13) controls pilot pressure by forcing the flapper down onto the orifice. Inlet pressure is proportional to solenoid force which is proportional to solenoid current. The SE03 valve inlet is connected to port X of the main relief valve, the outlet is connected to the tank.

2.4.3 BOOST SUPPLY (MAKE-UP) (fig. 2.10)

The boost supply ensures that pump inlet pressure is maintained within the limits recommended by the manufacturer. A gear pump is connected through a relief valve, which regulates pressure, and two check-valves to both sides of the pump. Should the pressure at either port drop below the boost pressure a check-valve will open and allow a make-up

flow through. The relief valve diverts the excess flow from the gear pump back to the tank.

The gear pump flow capacity is also the throughput of the tank and thus determines the tank size. The oil requires several minutes in the tank for de-aeration purposes. The gear pump delivery must always be greater than the sum of: pump leakage, pilot flow to tank and swash-servo consumption. If the main loading pump is likely to run at low speeds a mechanically driven boost pump may prove inadequate and an electrically driven pump should be used

2.4.4 COOLING AND FILTRATION

Both dynamometer systems include a full flow filter in the main loop to prevent any contamination continuously circulating through the pump leading to its eventual destruction. The boost supply is also filtered as it leaves the tank. Filters are fitted with 10 μm nominal rated elements.

Coolers are generally of the shell and tube variety, with the hydraulic oil on the shell side and the cooling water, drawn from the cooling pond, flowing through the tubes. They are piped up so that the two media flow in opposite directions through the cooler i.e. counter flow.

2.4.5 DYNAMOMETER CONTROLS

Dynamometer control is achieved by supplying the appropriate current to the SE03 solenoid pilot valve, which in turn determines line pressure and hence torque. The two basic modes of control are torque and speed, both implemented with analogue loops receiving their feedback signals from a torque and speed transducer respectively.

The torque control loop is necessary because of the non-linear relationship between SE03 valve current and torque and to eliminate

the inherent drift associated with open-loop control. A P+I algorithm is incorporated to ensure zero steady-state error.

Speed control is implemented by closing an outer speed feedback loop around the torque control loop. Again a P+I algorithm is included to give zero steady-state error. Fuel rack feed-forward is sometimes used to improve the speed loop dynamics, this has the effect of anticipating any speed error resulting from a rapid change in fuelling.

A useful load characteristic is one which produces rising torque with increasing speed. This is usually referred to as a "windage" characteristic, although the relationship may not be parabolic. This characteristic results in a very safe, drivable test-engine and is therefore preferred for most steady-state testing. Two methods of producing this rising torque characteristic have been used, one sets valve current proportional to speed, the other sets torque demand proportional to speed. The former is open-loop and therefore lacks repeatability, especially with changes in oil temperature.

The speed and torque controls can be used with purpose designed electronics or computer software to provide any load-speed characteristic within the capabilities of the hydraulic hardware. An example of this is described in section 5.4.1 which deals with vehicle inertia simulation.

2.5 ENVIRONMENTAL CONTROLS

Three areas of test-bed control can be identified: operational controls, safety controls and environmental controls designed to ensure test repeatability. Operational controls are the subject of this thesis excepting load control which is described in the previous section. Safety controls are described in ref. 34 for the TL11 and ref. 35 for the Differential Compound Engine (DCE). This section deals with environmental controls.

Environmental controls are designed to regulate those parameters which affect Diesel performance and would otherwise lead to a lack of repeatability between tests conducted at different times. Three criteria are useful in the design and setting-up of environmental controls:-

1. Repeatability, that is the ability to repeat a test at a later time and produce the same results. To achieve this the previous test conditions are recorded and where possible controls are used to reproduce those conditions.

2. Realistic test conditions are important if the data is to reflect the performance of the diesel drive in a real vehicle.

3. Comparability with experimental work done by other organisations. This is more likely to be the case if test conditions are regulated at the levels recommended by the appropriate standards (ref. 36) or at the levels used by the organisation supplying results for comparison.

Those test conditions which most affect performance can be split into the following groups: ambient conditions; fuel conditions; inlet and exhaust restriction; and energy loss through heat transfer. The following sections cover each group in turn, the effects on performance and methods of control are discussed.

2.5.1 AMBIENT CONDITIONS

Ambient atmospheric conditions are described by barometric pressure, temperature and humidity all of which have an effect on Diesel performance. Pressure and temperature alter the inlet air density, this has a direct effect on the air flow through a naturally aspirated engine. However, if the engine is turbo-charged or compounded, changes in turbo-machinery performance complicate the situation. Turbine and compressor powers can be expressed as:

$$\text{turbine power} = \dot{m}_T . T_3 . c_{p(ex)} [1-(P_4/P_3)^{\theta_{ex}}] . eff_T$$

$$\text{compressor power} = \dot{m}_C . T_1 . c_{p(air)} [(P_2/P_1)^{\theta_{air}}-1]/eff_C$$

$\theta = (\gamma-1)/\gamma$
$\gamma = c_p/c_v$
c_p & c_v = specific heats
T = temperature
$\dot{m}$ = massflow
P = pressure
eff = efficiency
$_T$ = turbine
$_C$ = compressor
$_1$ = compressor inlet conditions
$_2$ = compressor outlet conditions (inlet manifold)
$_3$ = turbine inlet conditions (exhaust manifold)
$_4$ = turbine outlet conditions
$_{ex}$ = exhaust properties
$_{air}$ = air properties

A rise in inlet temperature T_1 will increase the compressor power requirement as well as reducing the charge density, thus the detrimental effect of inlet temperature changes is amplified when the engine is supercharged. A drop in atmospheric pressure, P_1 and P_4, increases the turbine expansion ratio and hence power output. The compressor uses the extra power to increase its pressure ratio and hence to offset the effect of reduced inlet pressure on overall performance.

The variation in ambient conditions at the University is typically as follows:-

Atmospheric temperature	270-305 deg.K	(12%)

Barometric pressure	955-1005 mBar	(5%)
Vapour pressure (humidity)	2-25 mBar	(2% of barometric)

Formulae are available to correct power and fuel compensation for ambient variations, they are based on empirical performance correlations for existing standard Diesel engines. The research work undertaken involves two non-standard Diesel-drives which makes the use of correction formulae inadvisable because of their empirical nature. Controlling ambient conditions where possible and recording variations where not is considered to be the appropriate solution.

Turbo-machinery components reduce the effect of barometric pressure variations, which would, in any event, be difficult to control. Variations are recorded but no correction is applied to brake power or SFC.

Humidity changes have a negligible effect on performance (ref. 16). Correction formulae use dry barometric pressure ($P_{dry}=P_{atm}-P_{vap}$), typically vapour pressure changes are less than 2% of P_{atm}, this confirms that humidity has only a small effect on performance. Humidity is recorded for completeness but this is probably unnecessary.

Taking into account the amplification a compressor has on ambient temperature effects it is apparent that air inlet temperature should be controlled. Control can be achieved by using either an electrical heater or engine coolant to raise the temperature of the incoming air. The latter method uses a thermostatic control valve to feed engine coolant to a water to air heat exchanger. The air temperature is controlled to 25 deg.C as this is the standard adopted by the SAE (ref. 36), when ambient exceeds this figure testing must be abandoned, however, this is rarely the case.

2.5.2 FUEL CONDITIONS

Fuel related factors which influence performance include specific gravity, fuel temperature and the head at the inlet to the lift pump.

The net calorific value of diesel fuel can vary over a range of approximately 1% primarily as a function of specific gravity. This is periodically measured especially after a new delivery of fuel.

Fuel temperature affects viscosity and hence the fuel injection process. Reference 36 recommends maintaining the fuel temperature, at the inlet to the injection pump, at 37.8 ±5 deg.C. This is achieved by installing a fuel cooler in the fuel circuit (fig 2.14). No thermostatic control is required for these wide limits.

A change in head as seen by the lift pump can affect engine performance, to ensure a constant head the fuel from the day tank is fed through a float chamber at the same height as the fuel-weigh gear.

2.5.3 INLET AND EXHAUST RESTRICTION

The depression at the air inlet and the back pressure at the exhaust outlet are determined by two butterfly valves. Restriction is usually set so that the pressures are those quoted by the manufacturer at the rated condition ie. the air filter and exhaust system of a real vehicle are simulated.

2.5.4 ENERGY DISSIPATION THROUGH HEAT TRANSFER

Heat transfer from the Diesel occurs through heat exchangers and by radiation and convection to the surroundings. Heat rejection to the surroundings is the minor part, approx. 10% (ref. 16), and is relatively repeatable because test-cell temperature variations are minimised by the extraction and air heating systems. The majority of heat rejection, approx. 30%, occurs through the engine oil and water coolers and hence repeatable operation is important.

The cold water supply to heat exchangers is taken from a cooling pond located outside the laboratory, the temperature of which fluctuates with ambient conditions, typically between 0 and 20 deg.C. Where repeatability is critical thermostatic controls are used to compensate for these fluctuations.

Engine coolant temperature is controlled by the standard engine thermostat. If this is not capable of keeping water temperature within the limits specified by the SAE (ref. 36), ±5 deg.C of nominal thermostat setting, an additional thermostatic control is installed on the cold water supply to the coolant heat exchanger

The engine oil cooler operates normally ie. connected into the engine coolant circuit. This ensures repeatability so long as engine water temperature is repeatable.

The DCE incorporates an intercooler to increase charge density and hence improve performance. Repeatability is achieved by thermostatic control of the water supply to the intercooler. Inlet manifold air temperature can thus be regulated at a realistic level irrespective of water temperature.

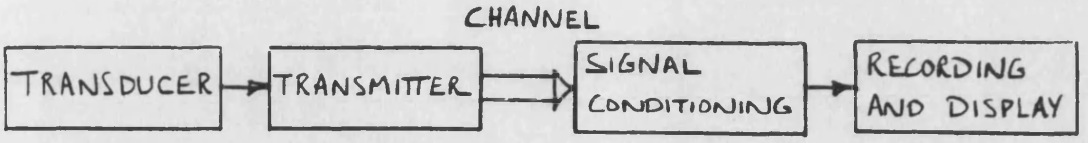

FIG. 2.1 THE MEASUREMENT SYSTEM

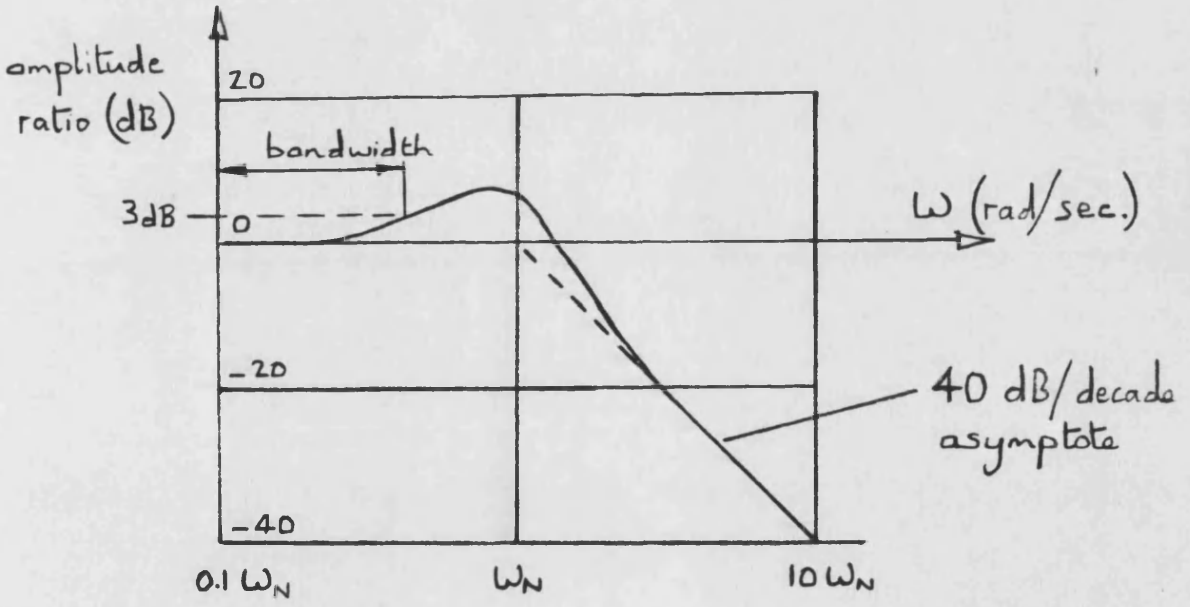

FIG. 2.2 BODE PLOT FOR 2ND ORDER MEASUREMENT SYSTEM

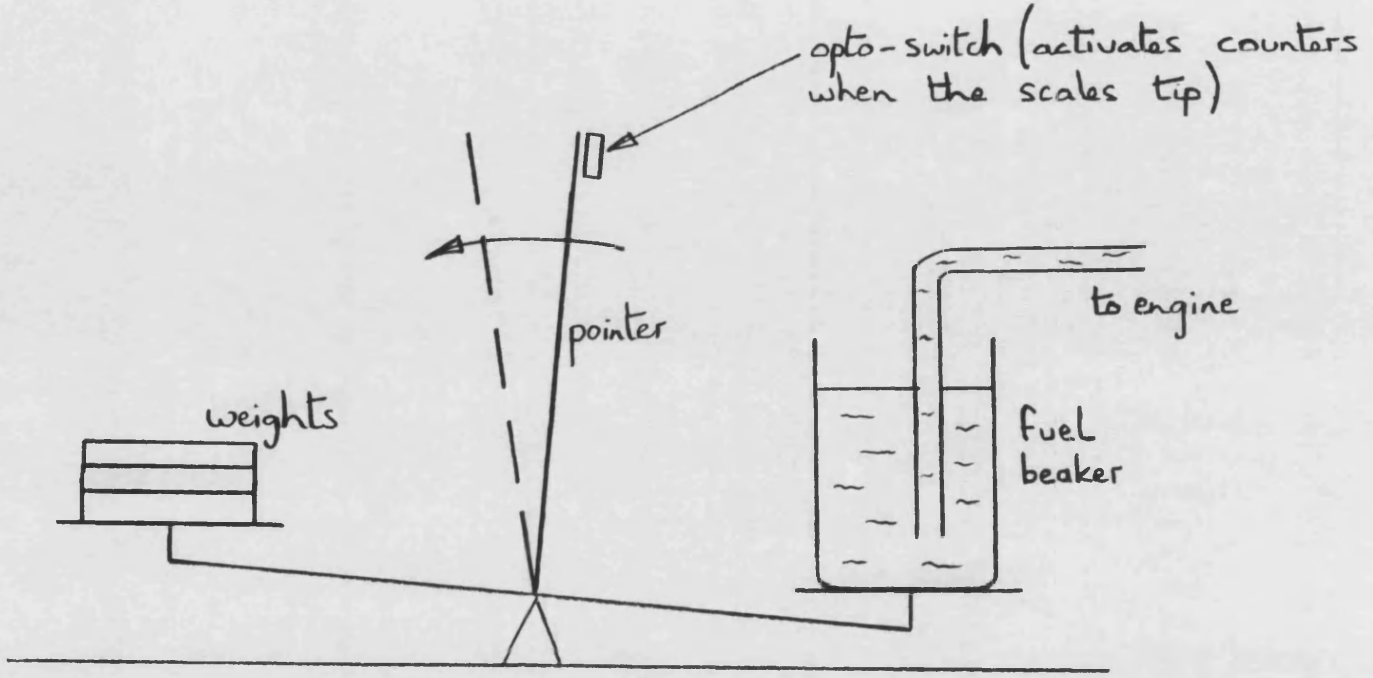

FIG. 2.3 FUEL WEIGH GEAR SCALES

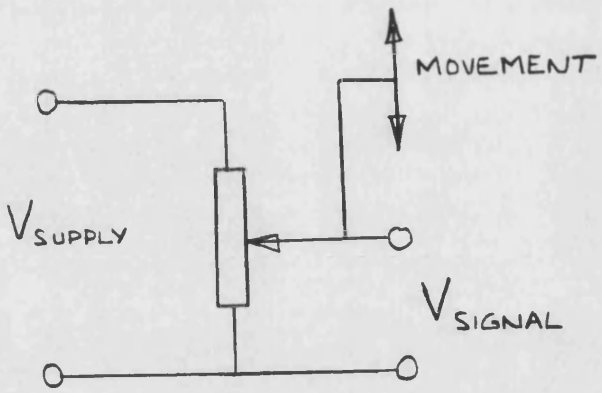

a) resistive potentiometer

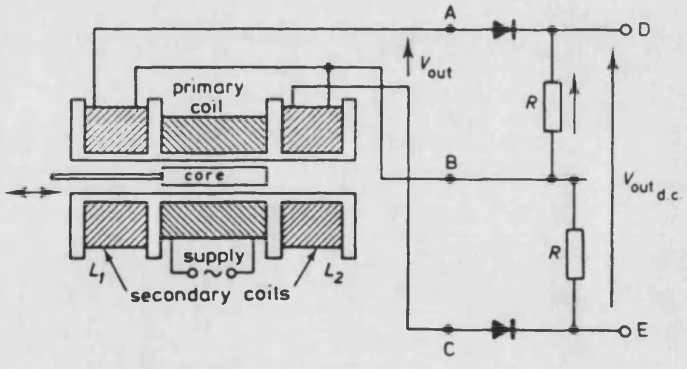

b) LVDT

FIG. 2.4 DISPLACEMENT MEASUREMENT

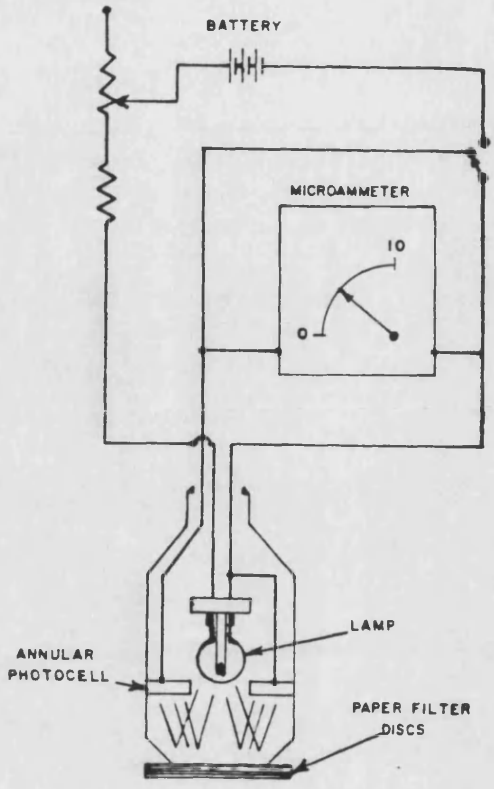

FIG. 2.5 BOSCH SMOKE METER

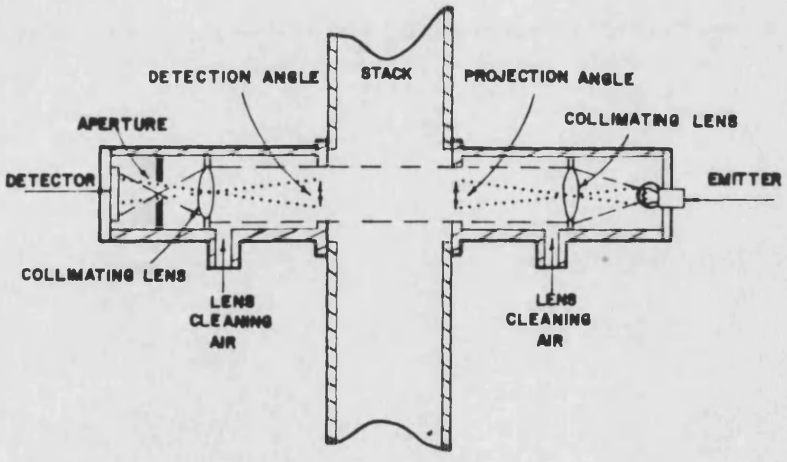

FIG. 2.6 IN-LINE OPACIMETER

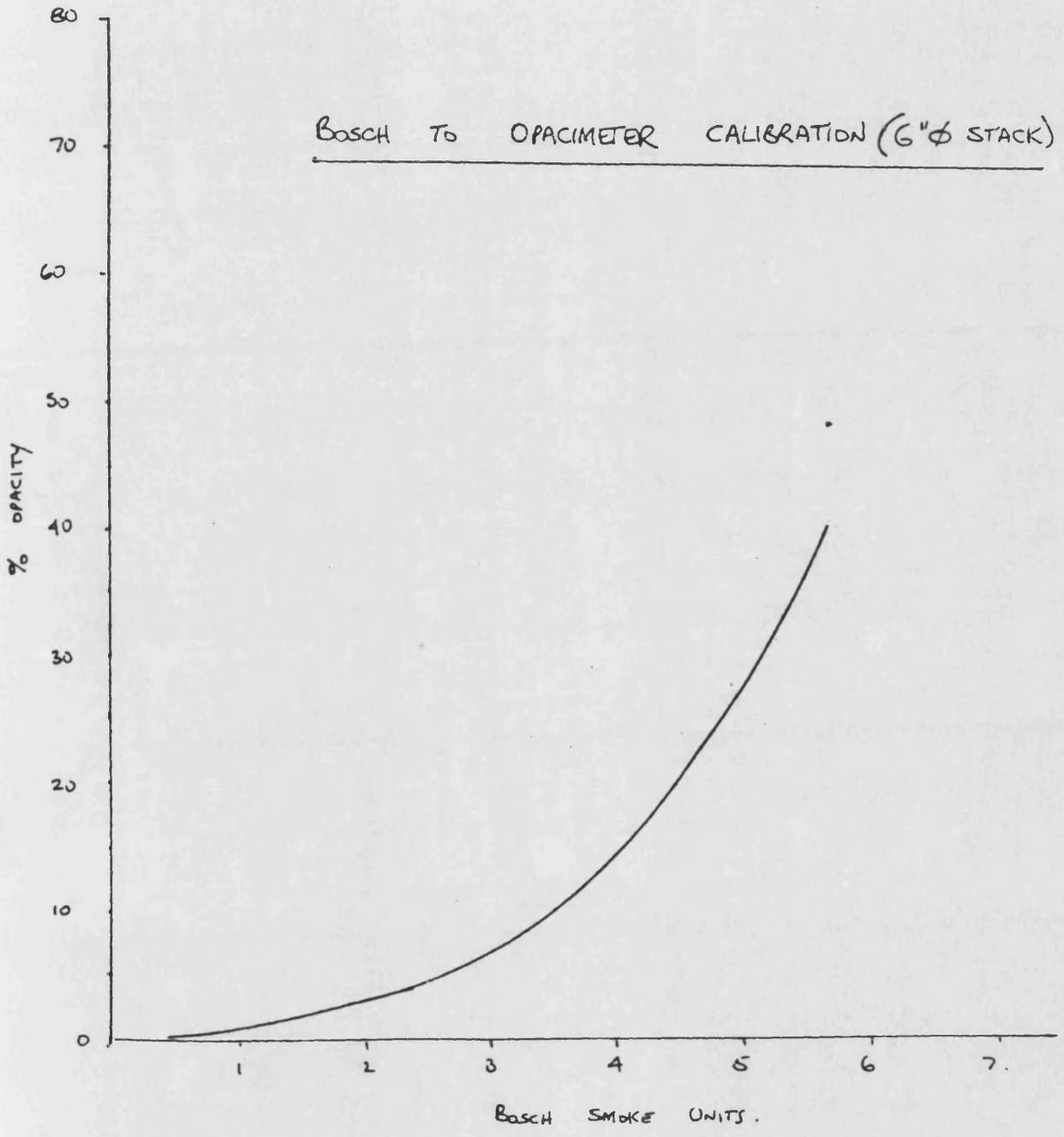

FIG. 2.7 OPACITY VS. BOSCH UNITS

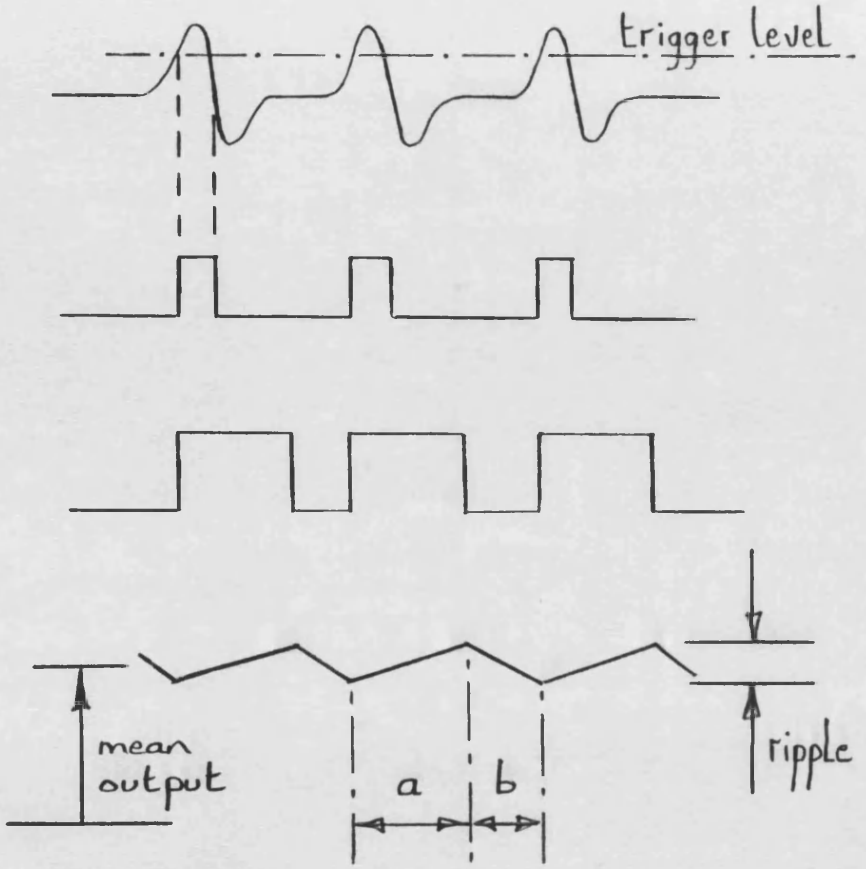

PULSE TRAIN FROM MAG. PICK-OFF

SQUARED UP PULSES FROM COMPARATOR

PULSES OF FIXED HEIGHT AND WIDTH

INTEGRATOR OUTPUT

a = charge period

b = dis-charge period

FIG. 2.8 F-V CONVERSION PRINCIPLE

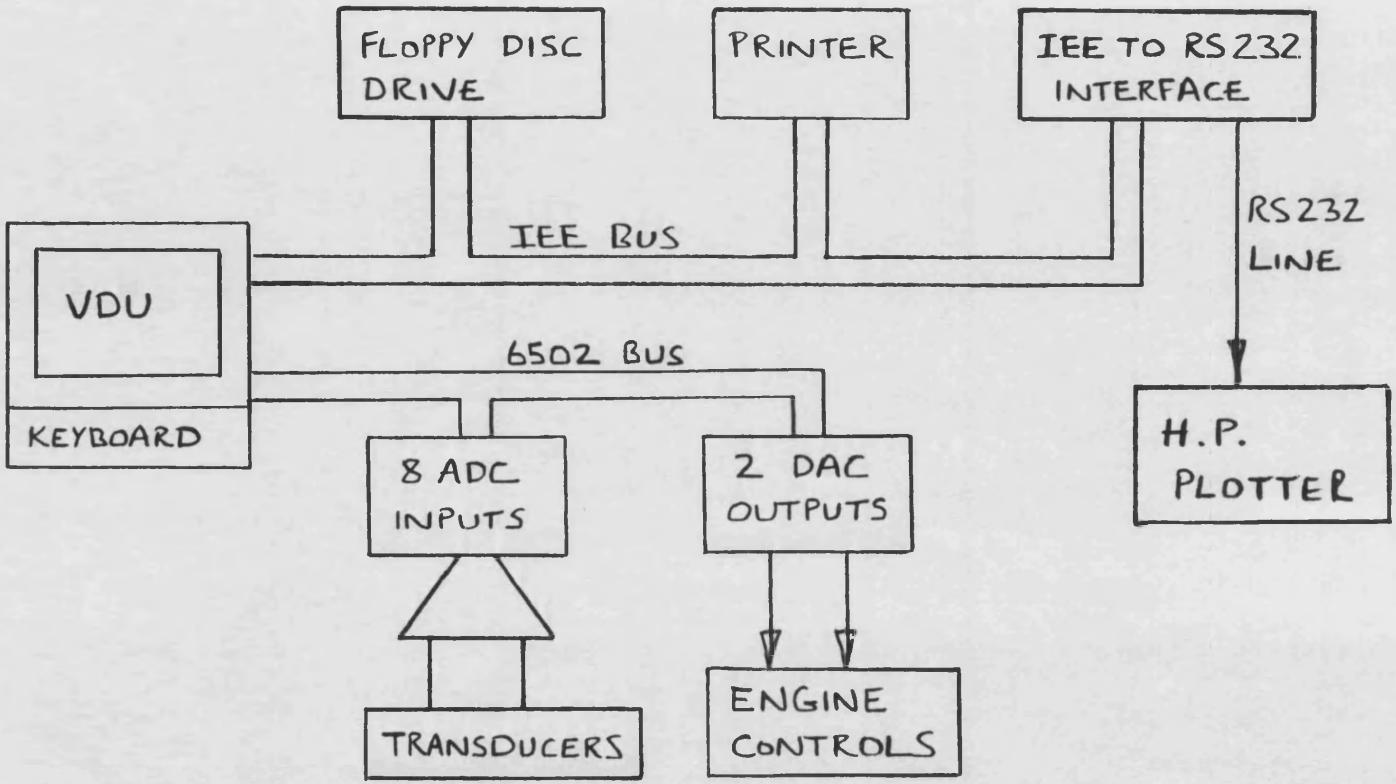

FIG. 2.9 COMMODORE PET BASED DATA-ACQUISITION SYSTEM

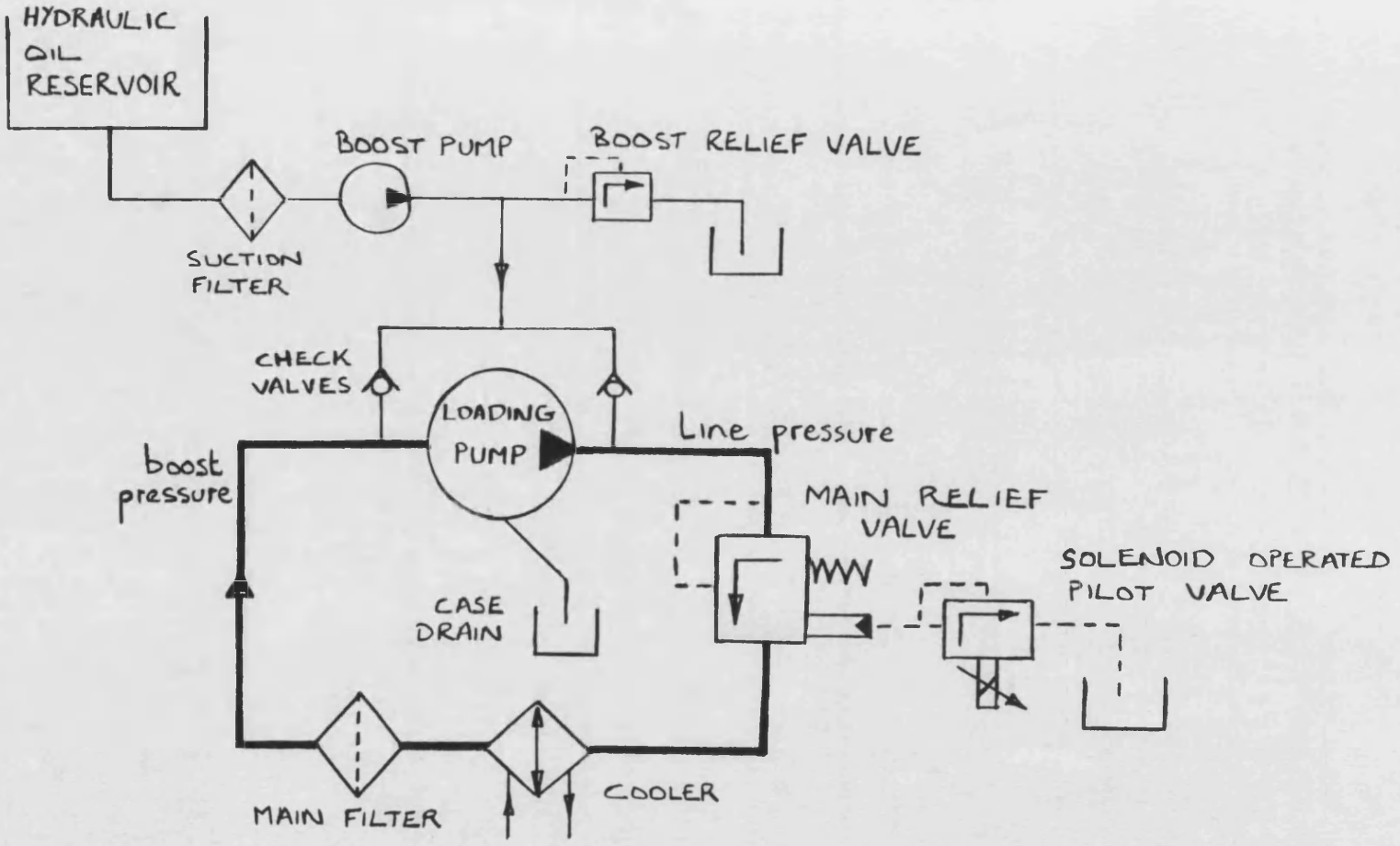

FIG. 2.10 DYNAMOMETER HYDRAULIC CIRCUIT

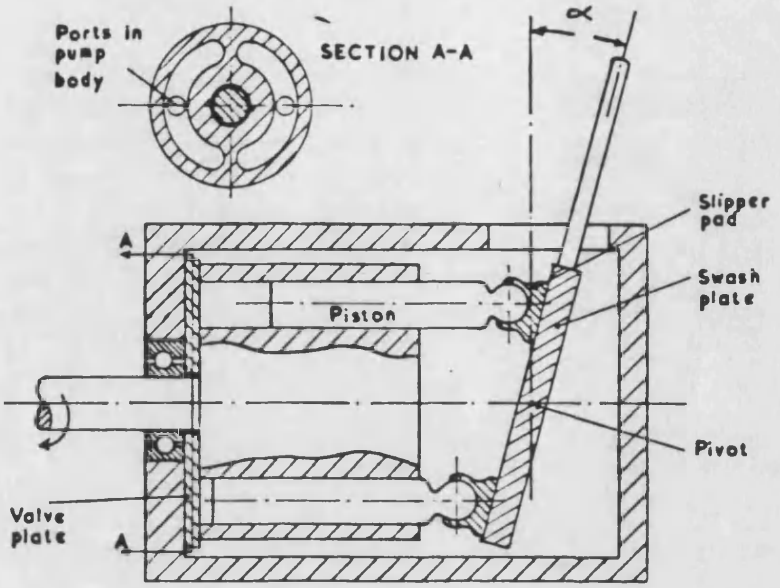

FIG. 2.11 HYDROSTATIC PUMP

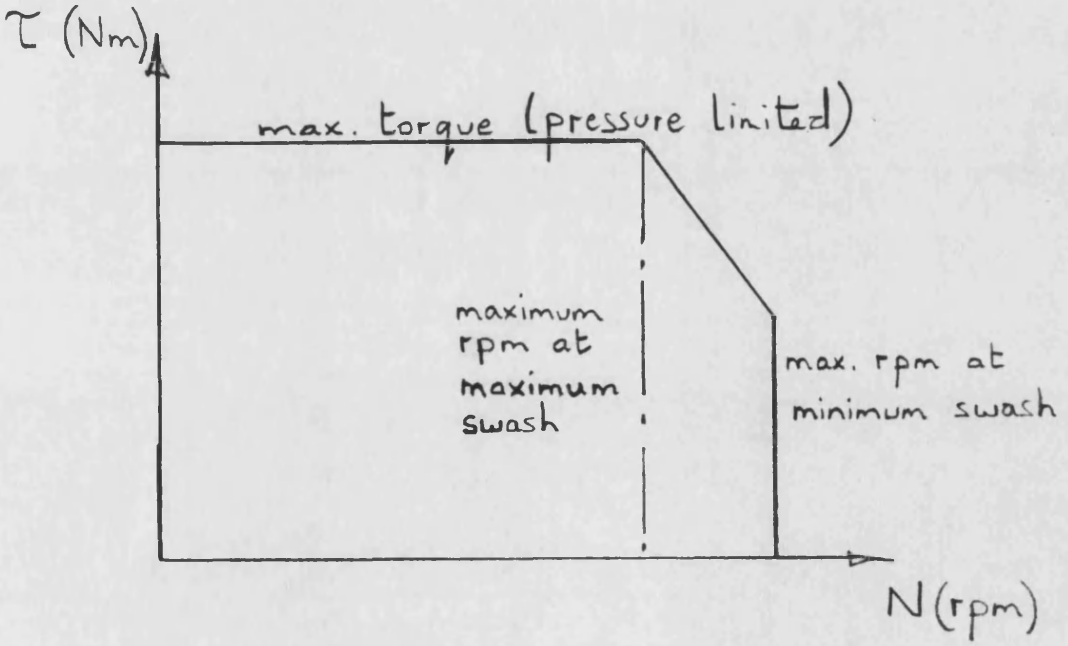

FIG. 2.12 TYPICAL PUMP OPERATING ENVELOPE

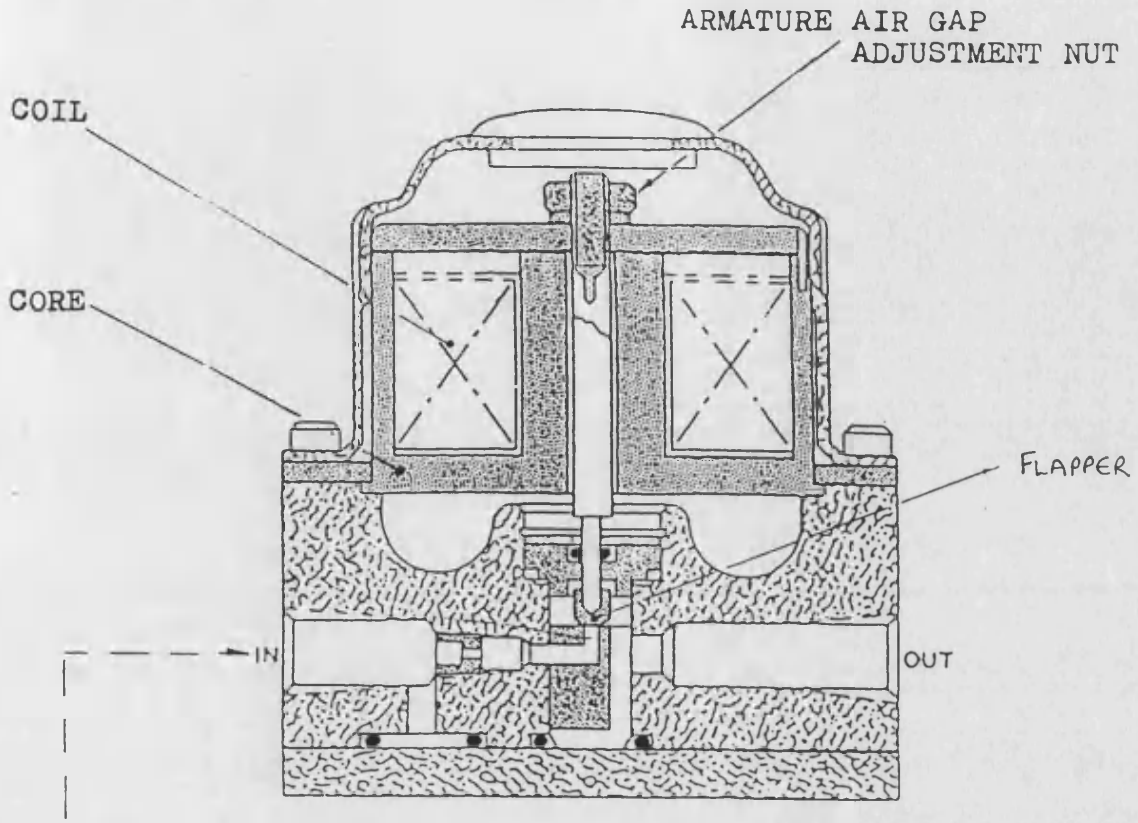

PILOT STAGE (ABEX DENISON SE03)

EXTERNAL
CONNECTION
LINE

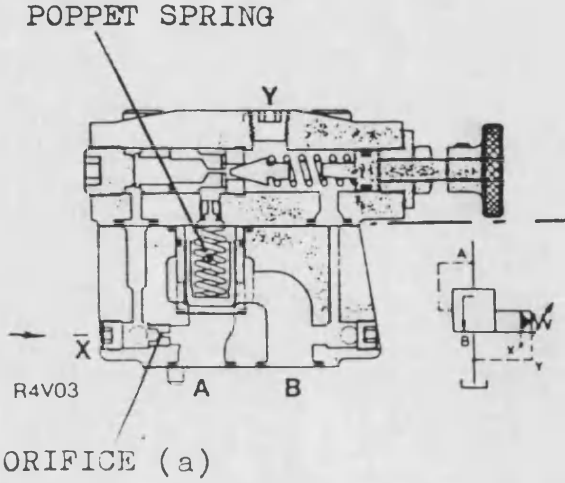

MECHANICAL
SAFETY RELIEF

MAIN
BODY

A-INLET
(UPSTREAM
PRESSURE)
B-OUTLET
(DOWNSTREAM
PRESSURE)

MAINSTAGE (ABEX DENISON)
(R4V10 SIMILAR DESIGN)

FIG. 2.13 PRESSURE CONTROL VALVE ASSEMBLY
(TWO STAGE)

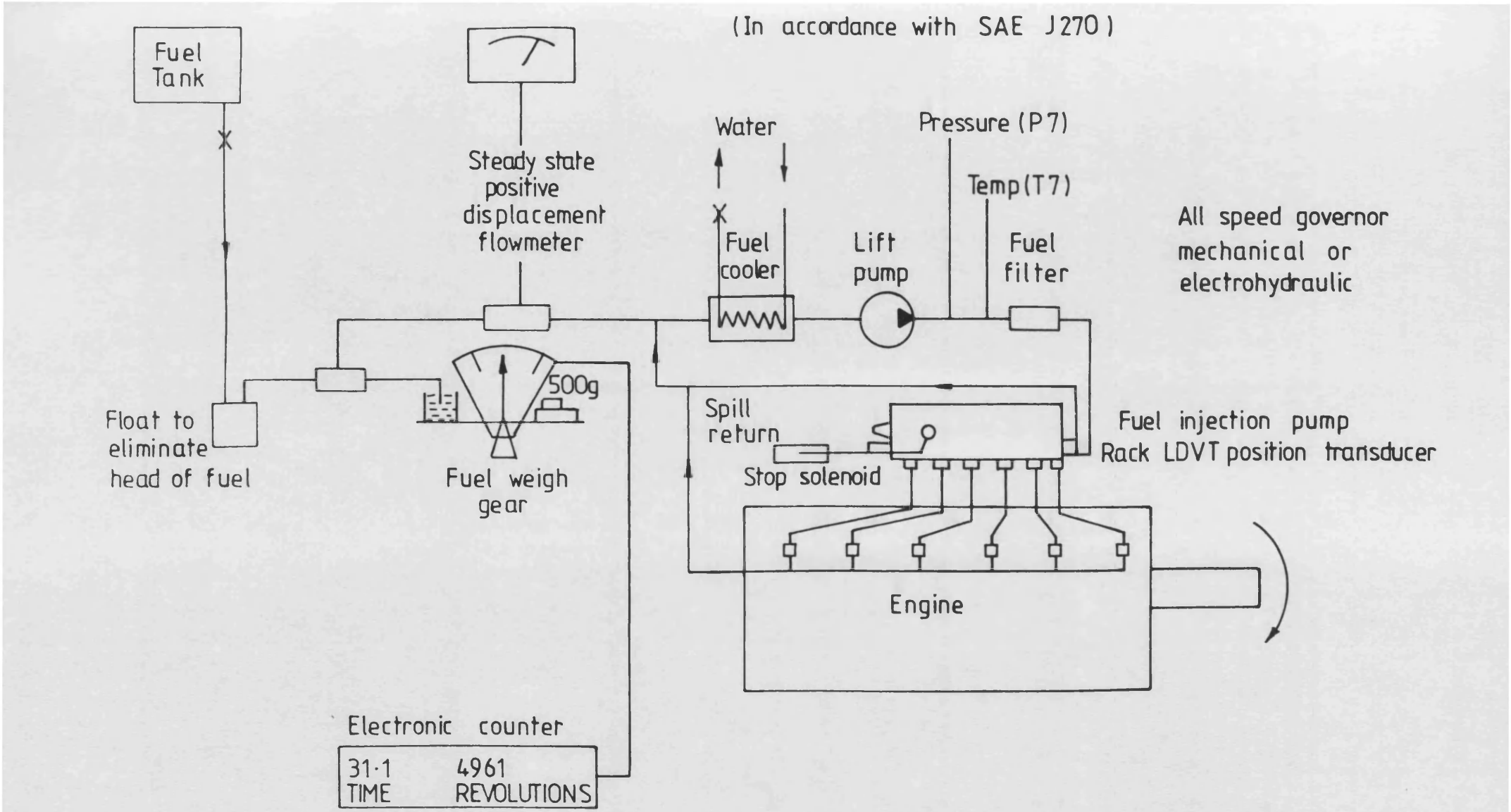

FIG. 2.14 FUEL SUPPLY ARRANGEMENTS

CHAPTER 3

ASPECTS OF DIESEL CONTROL SYSTEM DESIGN

3.1 INTRODUCTION

3.2 STEADY-STATE PERFORMANCE OPTIMISATION

3.2.1 PRE-RECORDED OPTIMUM SCHEDULES
3.2.2 TEST BED DETERMINATION OF THE OPTIMUM SCHEDULES
3.2.3 SELF OPTIMISING SYSTEMS

3.3 IMPROVING TRANSIENT RESPONSE

3.3.1 CONTROL ALGORITHM DESIGN
3.3.2 ADAPTIVE CONTROL ALGORITHMS
3.3.3 MULTI-VARIABLE CONTROLLERS
3.3.4 CONTROLLER IMPLEMENTATION

3.4 DEVELOPMENT COMPUTERS AND INTERFACING

3.4.1 HARDWARE AND PERIPHERALS
3.4.2 SOFTWARE
3.4.3 ANALOGUE INTERFACING

3.5 ACTUATION

3.5.1 ELECTROHYDRAULIC SERVO-SYSTEMS
3.5.2 ELECTROHYDRAULIC SERVO-VALVES

3.1 INTRODUCTION

Diesel driveline control systems must satisfy three, often conflicting, criteria:-

1. Optimum steady-state performance in terms of: the available torque curve; fuel consumption; and environmental effects.

2. Rapid response to changes in driver demand and road conditions.

3. Drivability, which can be thought of as minimising the demands on the driver. This requirement is obviously related, at least in part, to the need for rapid response.

These criteria are all well defined except for drivability which is a qualitative parameter. However, for the purposes of this work the following assumptions are used to define drivability:-

a. A change in driver or road demand should result in a rapid change in developed torque. However, torque rise should not be faster than driver response as this leads to "jerky" operation.

b. Torque changes should be smooth and predictable without unexpected discontinuities in rate of change, or overshoot.

c. There should be no delay between a change in demand and torque beginning to rise, as this requires unnecessary driver anticipation.

d. The engine torque curve should be such as to eliminate the need for excessively frequent gear changes.

A generalised picture of a Diesel control system, consisting of four blocks, is shown in fig. 3.1. Sensors and actuators interface with the Diesel, monitoring operating variables and adjusting control inputs respectively. Supervisory control manages the Diesel-driveline, that

is it monitors conditions and determines appropriate control demands. Control loops then follow these demands by means of feedback signals and actuator commands.

Steady-state performance optimisation is usually the function of the supervisory block. However, transient or dynamic control may be the function of both the supervisory and control loop blocks. The distinction between these two blocks is not always obvious, so this chapter deals with control algorithms (strategies) under headings of steady-state optimisation and transient performance (sections 2 & 3).

Except for simple feedback loops, experimental control algorithms have been implemented on the development computer described in section 4. Actuation methods are discussed in the final section. Sensors have already been dealt with in Chapter 2, and are, therefore, not discussed in this Chapter.

3.2 STEADY-STATE PERFORMANCE OPTIMISATION

One function of a Diesel driveline control system is to provide optimum steady-state performance. This can be summarised as: minimising fuel consumption; maximising the torque and speed range available within mechanical design constraints; and minimising environmental effects such as noise and emissions.

Three approaches to optimising Diesel performance can be identified:-

1. The use of pre-recorded optimum schedules for the available control parameters.

2. A self-optimising system which "homes in" on minimum SFC. whilst the vehicle is operating.

3. Some combination of the above where schedules provide limits and/or initial conditions for a self-optimising algorithm.

All these approaches have been discussed in great detail in refs. 37 & 38.

3.2.1 PRE-RECORDED OPTIMUM SCHEDULES

This method involves monitoring the driveline's operating conditions and using these to access appropriate control demands from optimum schedules. The first stage in the design of such a system is the choice of monitored and controlled variables. The steady-state operating point of the drive-line is determined by 'n' independent variables where 'n' is the number of degrees of freedom of the drive. These include the control parameters and external influences such as road and atmospheric conditions.

The system may have further degrees of freedom under dynamic conditions, but this is not important for SFC optimisation as during rapid transients response is the major control criterion. Slow

transients can be regarded as a series of steady-state conditions, acceleration in higher gears is an example of a slow transient.

The monitored variables are usually the external influences and a demand from the driver for vehicle speed or torque. However, the monitored variables are not a fixed set, any set can be used provided that, along with the control variables, they are all independent and unambiguously define the driveline operating point. The control parameters may act directly on the drive such as fuel-rod and turbine nozzle position or indirectly through feedback loops such as speed or pressure demands.

The choice of monitored and controlled variables is not only a theoretical decision, the commercial consequences must also be considered. The feasibility of manufacturing economical and reliable sensors is a major factor. In particular torque, fuel flow, and cylinder pressure measurement all present practical difficulties which could rule out a commercial system. Conversely manifold pressure, temperature, speed and position all lend themselves to simple and, if produced in quantity, economic measurement.

Engine-transmission output torque is particularly difficult to measure. However, if all other external effects are monitored, including road speed and driver demand, output torque becomes a dependent variable. It is, therefore, not required by the control system. In the case of the Diesel engine, fuel rod position is a good measure of developed torque, although this is not always the case dynamically when air-fuel ratios may be very low.

Pre-recorded schedules are the basis of the control development work described in this thesis. The development of self-optimising controllers would have reduced the time available for studying transient control algorithms aimed at response and drivability.

3.2.2 TEST-BED DETERMINATION OF THE OPTIMUM SCHEDULES

Pre-recorded schedules are determined in a two stage process. The first stage is to determine the level of interaction between the control parameters. If interaction is high optimisation must be an iterative process. Interaction must be tested at selected points throughout the operating map of the driveline. The second stage is the optimisation procedure itself.

The optimum control settings must be determined for each point in a grid covering the entire operating map. The spacing of these points depends on the rate of change of the control settings. Neglecting atmospheric conditions the operating map is usually defined by two variables representing load and speed. In the case of the Diesel engine, fuel rack position and engine speed can be used to define the operating point. Fuel rack position is a more practical measure of load than engine torque because of the difficulties associated with measuring the latter. When an all-speed governor is used fuel rack position is proportional to the difference between demanded and actual speed, which may be easier to monitor than fuel rack directly.

Where the degree of interaction between the control variables is low, each parameter can be varied in turn to establish its optimum setting, this need only be done once. The full range should be covered in case there is more than one SFC 'minimum'. One approach is to move the control element in coarse steps to determine the approximate setting giving minimum SFC, and then to home in on the optimum value from there.

If the degree of interaction is high the above procedure must be repeated until the optimum settings converge. For example, if three parameters A, B and C are being optimised the procedure must be repeated in the order ABCABCABC etc until the optimum values no longer change.

3.2.3 SELF-OPTIMISING SYSTEMS

A self-optimising system monitors the fuel input, power output, and hence efficiency of the Diesel-drive whilst continually adjusting the control parameters. In this way the system converges upon an optimum condition. Such a device must converge rapidly so that the drive does, in fact, operate at near minimum SFC at all times.

The optimising algorithm must execute rapidly and converge over a small number of iterations. A simple algorithm may be better than a complex one with a long execution time. An example of a simple algorithm using a single performance criterion (SFC) and operating on one control parameter is described by the following equation:-

$$C_{n+1} = C_n - F[(SFC_n - SFC_{n-1})/(C_n - C_{n-1})]$$

where:-

C = control setting
SFC = specific fuel consumption
n = iteration number
F = optimisation function

The control setting (C) is adjusted by a function of the rate of change of SFC with respect to C. Under steady state conditions this form of equation may perform well. However, changes in SFC caused by influences other than C will result in incorrect adjustment of C. This will occur during transient operation when SFC alters because of changes in other operating conditions. Similar problems occur with multiple control parameters, the improvement in performance must be related to the correct parameter.

To detect improvements in SFC as a result of a single parameter the effects of all other major parameters must be known or else they must remain constant. If control parameters take effect at markedly different rates this may reduce the problems associated with

distinquishing their individual influence. For example a change in fuel injection timing will have an effect after a single engine cycle whereas turbine goemetry may take up to one second to produce a decrease in SFC.

A sophisticated self-optimising system monitoring multiple performance criteria and adjusting multiple control variables would require a very complex algorithm, probably using statistical methods, to relate performance changes to control parameter adjustments. In the case of a Diesel-driveline for automotive applications, the algorithm must execute extremely quickly so that its accuracy is only affected during rapid transients where SFC is probably of less interest than response.

From this discussion it is apparent that a fully self-optimising system presents many problems and may only function satisfactorily under long established steady-state conditions. One solution to this problem is a hybrid system which is based on stored schedules but incorporates an algorithm to update these schedules on-line. The execution speed of the optimising algorithm is less critical because the schedules ensure sensible transient operation. The control parameters are only adjusted under well established steady-state conditions. In this ways the schedules are gradually updated.

The purpose of the hybrid system is to compensate for differences between supposedly identical drives and for changes in performance with time ie. component wear or maladjustment. However, it is important that if maladjustment is compensated for the control system should indicate this, so that the vehicle can be serviced.

3.3 IMPROVING TRANSIENT PERFORMANCE

The dynamic performance of a Diesel-driveline should ensure rapid response to changes in driver demand or road conditions, whilst maintaining drivability. In general good response is not obtained by moving through a series of optimum SFC points during a transient. A dynamic controller, to improve response, must be incorporated with steady-state optimisation. The dynamic controller modifies control demands, under transient conditions, to enhance response and drivability. Under steady-state conditions the dynamic controller must have no effect, control demands being the optimum values stored in schedules.

Dynamic control is achieved by the incorporation of suitable feedback loops. An error signal (demand minus feedback) can be thought of as a transient measure, that is an indication of divergence from an optimum steady-state condition. The precise form of the dynamic control loops depends on the Diesel driveline in question. However, several general arrangements can be identified:-

1. The control loops which regulate steady-state conditions provide suitable dynamic control without the need for additional loops. This is the case when good response is achieved by ensuring rapid updating of the steady-state optimum settings.

   An example of this is the use of boost pressure as a control variable for the VG turbo-charged Diesel engine. The major limitation on transient performance is turbo-charger lag. This can be partly overcome by a boost pressure feedback loop, which will over-restrict during a transient in an attempt to raise boost as quickly as fuelling. This is discussed in more detail in Chapters 4 and 5.

2. Additional loops or algorithms are added for their transient effect alone. In this case it is important that they have no effect under steady-state conditions.

3. Dynamic controls are "switched-in" during transient operation. This is necessary when the desired algorithm adversely affects steady-state operation if it is allowed to operate continuously.

The following sub-sections discuss dynamic control algorithm design and implementation, particularly with respect to Diesel drivelines.

3.3.1 CONTROL ALGORITHM DESIGN

The feedback loops making up the dynamic controller, and in many cases also regulating steady-state conditions, require careful design. The objectives are:-

a. accurate control
b. rapid response to changes in demand
c. stable operation under all conditions
d. integrity, that is safe failure modes

Although closing a feedback loop around a control parameter usually improves perforance, stability problems can result. To achieve the performance specification with sufficient stability may require the inclusion of compensation, either in the forward path or feedback path (fig. 3.2).

Well established methods exist for the design of single input-single output (SIO) control loops (ref. 39). These techniques include several graphical methods which have the advantage of providing qualitative as well as quantitative information, in particular, the Bode diagram and Nyquist plot in the frequency domain and the Root locus plot in the s-plane. Although these methods assume a linear system, they will often produce adequate designs even when the system includes non-linearities, which is usually the case. This is because many systems act in a linear fashion for small changes in state.

SIO design techniques generally rely on a description of the open loop system in either the time domain, frequency domain or the s-plane.

This description is referred to as the open loop transfer function (OLTF) and is obtained by either measurement or mathematical modelling of the system. This approach avoids measurement of the closed loop transfer function (CLTF), which may well be unstable before appropriate compensation algorithms are designed. Measurement of the OLTF is referred to as system identification. Methods include:-

1. Frequency response analysis (FRA) using specialised FRA equipment (ref. 40)

2. Transient measurement such as step and ramp responses using an oscilloscope.

3. Statistical measurement such as cross correlation between input and output. White noise or a pseudo random binary sequence (PRBS) are used as the system input. Ref. 41 discusses the use of the PRBS method.

When system identification is difficult and/or a full design study is not thought to be necessary, general purpose algorithms can be used. These algorithms are tuned on-line to give acceptable control. A common form of general purpose forward path compensation is the PID algorithm. This provides proportional, integral and derivative action (fig. 3.3).

The Diesel drives studied in this research are non-linear multi-variable systems, non-linear in that inherent system gains depend on operating conditions, multi-variable in the sense that output variables depend on more than one input or control variable. The following two sub-sections discuss the problems resulting from these effects and possible solutions. The final sub-section discusses control algorithm implementation.

3.3.2 ADAPTIVE CONTROL ALGORITHMS

The Diesel engine and its associated turbo-machinery behave in a linear fashion for small changes about one operating point. However, the inherent system gains, which describe this linear behaviour, vary considerably with large changes of operating point. This means that a controller can be designed assuming a linear plant, but fixed controller gains will not give good performance under all conditions. In fact, instability may occur under some conditions whilst at others response is very stable but sluggish. The most effective solution is to make the controller adaptive, that is capable of adjusting its own gains to give the desired performance specification.

The general form of the adaptive control algorithm is based on the linear small perturbation behaviour of the Diesel-drive. However, the controller gains are adjusted to compensate for changes in operating point.

The controller gains can be stored in schedules, in much the same way as optimum SFC control parameters, alternatively they may be determined on-line by a self-tuning algorithm (ref. 42).

Self-tuning controllers determine system gains on-line and hence calculate appropriate controller gains. Control loop performance depends on the overall gains, system and controller, so any change in system gains will result in a corresponding adjustment of the controller gains. The basic principle is shown in fig. 3.4, the identifier monitors system input and output to determine system gains. These gains are then used to calculate appropriate controller gains.

The identifier is of the general form shown in fig. 3.5, a system model is used to estimate the output at the next time step (assuming a digital controller). The error between actual and estimated output is used to update the assumed system gains.

Controller gain calculation may be based on closed loop pole assignment or optimal control. The pole assignment approach calculates controller gains to give the desired closed loop poles and hence dynamic behaviour. The optimal control approach minimises some statistical performance measure such as the mean square error between desired and actual output. In fact, system identification and controller design may not be distinguishable as two separate processes because of algorithm simplification.

3.3.3 MULTI-VARIABLE CONTROLLERS

Diesel drive-lines are complex multi-variable systems with multiple inputs and outputs. There is invariably some cross-coupling, that is any one output is related to several inputs. If one particular input-output pair are closely related and interaction with other variables is low, a single input-output (SIO) control loop will provide adequate control. However, a high level of cross-coupling may create stability or controllability problems if simple SIO loops are used.

There is a large area of control theory devoted to the study of multi-variable systems and the design of suitable controllers (refs. 43&44). These techniques are based on matrix representations of the simultaneous equations describing the plant. Two forms of model are commonly used, input-output models and state-space models (fig. 3.6).

Input-output models use a matrix equivalent of the SIO transfer function, each element of the matrix is a transfer function relating one output to one input:-

$$\begin{bmatrix} y_1(s) \\ y_2(s) \end{bmatrix} = \begin{bmatrix} g_{11}(s) & g_{12}(s) \\ g_{21}(s) & g_{22}(s) \end{bmatrix} \begin{bmatrix} u_1(s) \\ u_2(s) \end{bmatrix}$$

in symbolic form:-

$\underline{y}(s) = G(s).\underline{u}(s)$ where: $\underline{y}$ is the output vector
$\underline{u}$ is the input vector
G is the transfer function matrix

The elements of G(s) may be of any order and represent the response of a single output to a single input when all other inputs are zero.

State-space models use an auxiliary set of "state-variables" which fully describe the system's dynamic state without recourse to initial conditions. This is done by using a model based on first-order differential equations only (an nth order equation can be broken down into n 1st order equations). The resulting matrix equations take the following form:-

$$\begin{bmatrix}\dot{x}_1\\ \dot{x}_2\end{bmatrix} = \begin{bmatrix}a_{11} & a_{12}\\ a_{21} & a_{22}\end{bmatrix}\begin{bmatrix}x_1\\ x_2\end{bmatrix} + \begin{bmatrix}b_{11} & b_{12}\\ b_{21} & b_{22}\end{bmatrix}\begin{bmatrix}u_1\\ u_2\end{bmatrix}$$

$$\begin{bmatrix}y_1\\ y_2\end{bmatrix} = \begin{bmatrix}c_{11} & c_{12}\\ c_{21} & c_{22}\end{bmatrix}\begin{bmatrix}x_1\\ x_2\end{bmatrix}$$

in symbolic form:-

$$\dot{\underline{x}} = A.\underline{x} + B.\underline{u}$$
$$\underline{y} = C\underline{x}$$

where: $\underline{y}$ is the output vector
$\underline{u}$ is the input vector
$\underline{x}$ is the state vector
A is the coefficient matrix
B is the input matrix
C is the output matrix

Multi-variable frequency response methods are based on the input-output type model (transfer function matrix). Rosenbrock (ref. 44) has extended the Nyquist technique to multi-variable controller design. This method aims to determine a compensation matrix K(s) which renders the system diagonally dominant ie. the product K(s).G(s) is a diagonally dominant matrix. Diagonal dominance means low interaction and hence the system can be controlled by a set of SIO feedback loops. The purpose is to make the control problem manageable rather than produce optimum controller performance. A typical controller implementation is shown in fig. 3.7.

State-space methods lead to a more generalised multiple feedback approach. The output vector $\underline{y}$ is multiplied by a feedback matrix K and summed with a demand vector $\underline{u}_1$ to give the original input vector $\underline{u}$ (fig. 3.8). Methods exist whereby the system's poles, which determine its dynamics, can be altered to desired values by the appropriate choice of K (ref. 43)

Although the theory is well established the practical implementation of true multi-variable controllers has been limited. There are several reasons for this:-

1. Multi-variable controllers are complex and hence difficult, if not impossible, to tune manually on line. Tuning on line is necessary when the system dynamics are not accurately known. SIO loops can be designed from approximate system models and tuned to match the actual plant. In fact, some SIO algorithms, such as the PID controller, are general purpose and can be tuned to suit most simple feedback loops.

2. The integrity of multi-variable controllers can be problematical, that is it can be difficult to guarantee safe failure modes. Because of the cross-coupling inherent in a multi-variable controller, failure of a single feedback or control signal can cause loss of control over several parameters. It may also be difficult to predict the exact effect of such a failure. Using separate SIO loops a failure will only affect one control parameter, and in a predictable manner. In fact, a safe failure mode can usually be designed in.

3. Cross-coupling problems can often be dealt with by compromises or modifications in the design of separate SIO loops. When two highly interactive loops cause problems this can often be solved by reducing the gain (response) of one loop. The other loop then dominates dynamic effects. This is only possible when it is acceptable for the "slugged" control parameter to deviate under transient conditions. Alternatively changes in the choice of

control and feedback variables can sometimes solve cross-coupling problems.

3.3.4 CONTROLLER IMPLEMENTATION

Control algorithms may be implemented with either analogue circuitry or software in a digital system. The choice is usually determined by the complexity of the algorithms. Simple feedback loops are well suited to analogue design, whereas scheduling, self-tuning, or similarly complex algorithms are invariably implemented digitally.

Digital controllers add another dimension to the design problem in that the system is no longer continuous. A digital controller samples feedback signals and increments control signals at discrete intervals. This form of control is known as Direct Digital Control (D.D.C.). Stability and performance criteria depend on the sample period "T" as well as the system dynamics. As sample rates increase the digital system's stability and performance improves, approaching that of the equivalent analogue system. Sample data theory uses the z-transform rather than the s-transform, an introduction to which can be found in ref. 39.

In the case of the Diesel engine the major control element, fuel rod position, is itself sampled at firing frequency. This being the case there is little to be gained by running a digital system at a faster rate. In fact, it is probably wise to run the controller at firing frequency to avoid aliasing with variations over the Diesel cycle.

The writer has used a mixture of analogue and digital controls, the advantages of this are twofold: Simple loops can be kept external to the computer and hence execution times kept low; basic manual control of the experimental rigs is possible without the computer being involved.

For this work prototype digital controllers have been implemented using the development computer described in the next section (with the

exception of one simple "PET" based system). Analogue control loop implementation was accomplished with appropriate OP-AMP circuitry. For a guide to OP-AMP circuit design see ref. 45.

3.4 DEVELOPMENT COMPUTERS AND INTERFACING

The control system development work described in this thesis was aimed at establishing suitable algorithms with subsequent testing of those algorithms experimentally. The development of prototype controller hardware suitable for installation in a vehicle was not part of the brief. Hence the requirements on the development computer are only those associated with ease of software development and modification, algorithm execution times, and interfacing with the experimental rig. The software requirements can be summarised as follows:-

1. To enable different control algorithms, some complex, to be tested without making programming time a limitation.
2. Algorithms should be easily modified during development.
3. Software should be readable and well documented so that future work is not hindered.
4. Execution speed should be high enough for dynamic control loop implementation.

These objectives can, to a large extent, be met by ensuring that the hardware and compilers allow the maximum use of high level languages whilst maintaining acceptable execution speed.

The required execution speed is a function of the sample period for the dynamic controller. Steady-state optimisation can be implemented at a lower frequency consistent with drivability and SFC considerations. As discussed in the previous section the highest sample frequency ever required is likely to be engine firing frequency, as fuel rack position is sampled at this rate by the fuel pump. Assuming a maximum speed of 3000 rpm, the firing frequency for a six cylinder Diesel would be 150 Hz. Hence if a control loop algorithm were to iterate at this frequency it would have to run in less then 6.66 msec.

To achieve this level of performance with a high level language it was considered necessary to use a computer system with the following attributes:-

1. 16 bit architecture and hardware floating-point arithmetic to provide fast machine code execution.
2. An efficient high level language compiler so that the above mentioned hardware speed is used to good effect by the compiler.
3. Simple and fast communication between the high level language and interface hardware (or the machine code routines which run the hardware).

As well as these execution speed related factors the software environment must include a proven and flexible operating system to simplify software development. This means a powerful editor to reduce coding effort, informative compilers and linkers to aid software debugging, and a wide range of useful utilities. In short the facilities expected of a powerful mini-computer.

The system hardware should include the following minimum requirements:-

1. VDU and keyboard for programmer communication.
2 Some mass storage media, the minimum requirement being a floppy disc drive. Tape systems are too slow for sensible access times.
3. A printer to provide software and data listings.
4. If the system is to be used for data-acquisition as well as control a plotter is recommended to eliminate manual graph plotting.
5. Analogue interface hardware for controlling and monitoring the Diesel driveline. All the necessary interface cards should be available off the shelf from the computer manufacturer. In-house interface design is wasteful in time and money.

A DEC LSI 11/23 system was chosen as the most cost effective means of providing the above requirements at the time. A brief description of the system follows.

3.4.1 HARDWARE AND PERIPHERALS

The LSI 11/23 utilises large scale integration (LSI) technology, to provide a micro-computer member of the well known PDP-11 range of computers. The result is a machine with mini-computer power, which executes PDP-11 software, at micro-computer prices.

The 16 bit processor board includes hardware floating point arithmetic and a memory management unit which allows the use of up to 256 K bytes of memory (the system actually has 160K bytes of RAM). A disc interface card links the bus to an RX02 dual floppy disc drive. A multi-function card provides two RS232 serial lines and the bootstrap ROM, which pulls the operating system into main memory on power-up. One serial line is used for the VDU and keyboard communication, the other line is available for connection to either a printer (DOLPHIN) or a plotter (HP.7470A)

3.4.2 SOFTWARE

The RT11 single user operating system is used, providing all the facilities mentioned earlier. The FORTRAN IV compiler produces code which utilises the floating point hardware thus providing rapid algorithm execution. A comprehensive library of system subroutines allows most hardware functions to be controlled from a FORTRAN program. Where machine code is necessary it is a simple matter to write a FORTRAN callable routine, an example is the A/D conversion routine which controls the ADC card.

The operating system is stored on the disc in drive 0, applications software on the disc in drive 1.

3.4.3 ANALOGUE INTERFACING (ref. 46)

Two analogue interface boards are provided, an 8 channel ADC board and a 4 channel DAC board. Both boards are connected via ribbon cable to a connection box which provides a BNC connector for each individual channel. Facilities for filtering the incoming analogue signals are provided within the box, at present no filtering is applied.

The analogue input board has a single 12 bit A/D convertor which uses the successive approximation method. The 8 channels are multiplexed into a "sample and hold" before conversion takes place. Fig. 3.9 is a block diagram showing the general arrangement. Conversions can be started by the program, by a real-time clock, or other external trigger. End of conversion is either detected by software polling or by an interrupt request. The module is set up for a unipolar input range of 0V to +10V which corresponds to an output of 0 to 4095 (all 12 bits set).

The analogue output board has 4 separate 12 bit DAC channels. Their output voltages are proportional to the 12 bit integers in their respective holding registers EXCLUSIVE-ORED with HEX FFF (ie. 0 corresponds to 10V, 4095 corresponds to 0V). In the control programs the required output voltage is multiplied by 409.5 and EXCLUSIVE-ORED before being poked to the DAC. The fourth DAC channel has a secondary purpose, the least significant 4 bits in the holding register are taken to the output connector, they provide 4 digital control signals ie. ON-OFF control.

The ADC module is controlled by a FORTRAN callable machine code routine written by the user. The DAC registers are loaded using the system subroutine IPOKE.

3.5 ACTUATION

The control system development discussed in this thesis involves automatic adjustment of various engine and drive-line parameters such as: fuel-rod position, turbine geometry, bypass valve opening, static injection timing and CVT ratio. The majority of these parameters require linear or rotary movement, when rotary movement is required it is invariably over less than 90 deg. and can therefore be achieved with a linear actuator and lever arm where this is advantageous. The actuator requirements can be summarised as follows:-

1. The actuation time for maximum travel should be an order of magnitude less then the engine/driveline response times. The dominant time constants are those associated with engine and turbo-machinery acceleration and are typically between 0.5 and 1.5 seconds. Hence an actuator travel time of less than 0.1 sec would be desirable to avoid adversely affecting response and controllability.

2. Actuators must be mounted on the engine and/or turbo-machinery, and will therefore be subjected to space and weight constraints. In particular actuators should be light to minimise fatigue failures as a result of vibration.

3. Actuator position should accurately follow a voltage demand signal. This implies the need for a means of actuator position control, preferably with a linear characteristic as feedback loops may be closed around the actuator controls. This requirement is necessary to provide repeatability for performance testing and control implementation. In practice an accurate position indication is only available if a transducer is fitted or the actuator is a digital device such as a stepper motor. Most open-loop mechanisms lack repeatability because of variations in actuation force.

Every application should be considered separately as there is no single actuator type which satisfies all operating criteria. However, general comparisons can be made between the three broad categories of electric, pneumatic, and hydraulic actuation.

One of the most important criteria is the torque (or force) to inertia ratio, a large ratio means the actuator can be smaller and lighter thus minimising installation problems. A large torque to inertia ratio also gives rapid acceleration and hence superior response, when the actuator is a major contributor to total inertia. Hydraulic actuation provides the highest torque to inertia ratios because the only limitations are the mechanical ones on maximum pressure. Electrical machines are limited by the heating effect of armature current, and magnetic saturation. Pneumatic actuation is limited by the low pressures achievable with commercial compressors.

Dynamic response is generally superior with hydraulic actuation, there is no inherent lag involved in increasing oil pressure as there is with pneumatics because of air compressibility. This advantage only holds if the servo-valve controlling oil flow or pressure has a rapid response. Electrical machines have an inherent lag as a result of their inductance resisting rapid changes in current.

The performance advantages of hydraulic over electro-mechanical actuation are summarised by fig. 3.10 which shows that hydraulic control is generally used where power levels are high and/or good dynamic performance is necessary.

The major advantage of electrical actuation is that power conversion is unnecessary. With hydraulics and pneumatics a pump or compressor and appropriate filtration is needed. A hydraulic servo-pack also needs a reservoir, and the actuators require return as well as supply lines. Pneumatics can exhaust to atmosphere, are cleaner and low in cost.

Electro-hydraulic actuation was chosen for the work described here to guarantee dynamic performance at least an order of magnitude faster than the controlled systems. Because the Diesel test rigs are stationary the servo-pack and reservoir can be located wherever is most convenient. Electro-hydraulic equipment and expertise is available in-house from the Fluid Power Group, reducing cost and providing design advice.

The following sub-sections describe the design of electro-hydraulic servo-systems and the components used.

3.5.1 ELECTRO-HYDRAULIC SERVO-SYSTEMS

There are two common forms of hydraulic servo-control: servo-valve control and servo-pump control (figs. 3.11 a & b)

Servo-valve control operates with a constant pressure supply, the flow to the motor or jack being controlled by the valve. Several servo-valves can be operated from the same servo-supply. Dynamic performance and accuracy are significantly better using servo-valve control than with alternative means of hydraulic control. For optimum performance the servo-valve should be located as close as possible to the actuator. The servo-valve controls flow by throttling and hence efficiency is poor because of the friction losses involved.

Servo-pump control is used where the flows are too large for a servo-valve and/or a higher efficiency is required. Motor or actuator movement is controlled by altering the displacement of a pump which is hydraulically connected to the load. A separate pump is used for each load. Zero displacement results in no flow and hence no load movement, varying displacement in either direction pumps fluid to one port or the other of the actuator. The work of the pump is primarily associated with load movement and hence efficiency is high. Dynamic performance is limited by swash-plate (displacement) response and fluid compressibility in the lines between the pump and load.

The control elements involved in this work alter Diesel operating characteristics but do not in themselves transmit power. The requirement is for positioning devices with relatively low actuation forces. As dynamic performance and simplicity are of importance whereas efficiency is not, servo-valve control is used. One servo-pack supplies all the actuators on a test rig. The servo-pack is driven independently as the actuators can be thought of as auxiliaries and their power consumption therefore not taken from the Diesel output. The arrangement of constant pressure supply, servo-valves and actuators is shown in fig. 3.12. The constant pressure supply may be either a pressure compensated (variable displacement) pump, or a fixed displacement pump with an accumulator and relief valve.

The individual position control loops (fig. 3.13) consist of a servo-valve and filter, hydraulic jack, position feedback transducer and position control electronics. The control electronics (fig. 3.14) implement a summing point and proportional gain, the resulting error signal is converted to a current to drive the servo-valve. Servo-valve flow is proportional to current and results in a jack velocity, the direction of movement depending on the polarity of the driving current. Position feedback is necessary as in open loop mode this set-up produces a velocity, not a position. The jack is only stationary when the error signal and hence valve flow is zero, therefore, this simple proportional loop results in zero steady-state error

3.5.2 ELECTRO-HYDRAULIC SERVO-VALVES

The servo-valves are usually two-stage devices to reduce the required drive current, a typical device is shown in fig. 3.15. The first stage consists of a flapper operated by an electric force motor, this produces a differential pressure proportional to input current. This first stage is in effect a hydraulic pre-amplifier, the differential pressure moves the second stage which is a 3 land spool valve. As the spool moves the effective orifice size between the supply ports and

the output ports increases, passing more flow for a constant pressure drop through the valve.

Typical performance characteristics are shown in fig. 3.16. For a given valve pressure drop flow is essentially linear with valve current (fig a). The load pressure vs. flow characteristics are of the parabolic form typical of flow through an orifice (fig b). Below the 90 deg. phase lag point the servo-valve frequency response can be approximated by a second-order transfer function with a damping ratio between 0.5 and 0.7 (fig c).

Servo-valve selection was simplified by assuming that dynamic performance would be adequate using any correctly sized valve from the stock available within the School. Because of the low actuation forces and the mechanical limitations on minimum cylinder diameter, load pressure was invariably much less than supply pressure:-

$P_L << P_s$ $\quad$ P_L = load pressure
P_s = supply pressure

Hence:-

$Q_L \simeq Q_{NL}$ $\quad$ Q_L = required load flow
Q_{NL} = no load flow

Servo-valve flow capacities are defined at 1000 psi valve pressure drop, this is the so called rated-flow. At no load the entire supply pressure drops across the valve hence the rated flow Q_R is given by:-

$$Q_R = Q_{NL}.\mathrm{sqrt}(1000/P_s) \simeq Q_L.\mathrm{sqrt}(1000/P_s)$$

The required load flow Q_L is obtained from the maximum required actuator slew rate. Over-estimating servo-valve flow capacity reduces accuracy/linearity because in practice the valve only operates over part of its range.

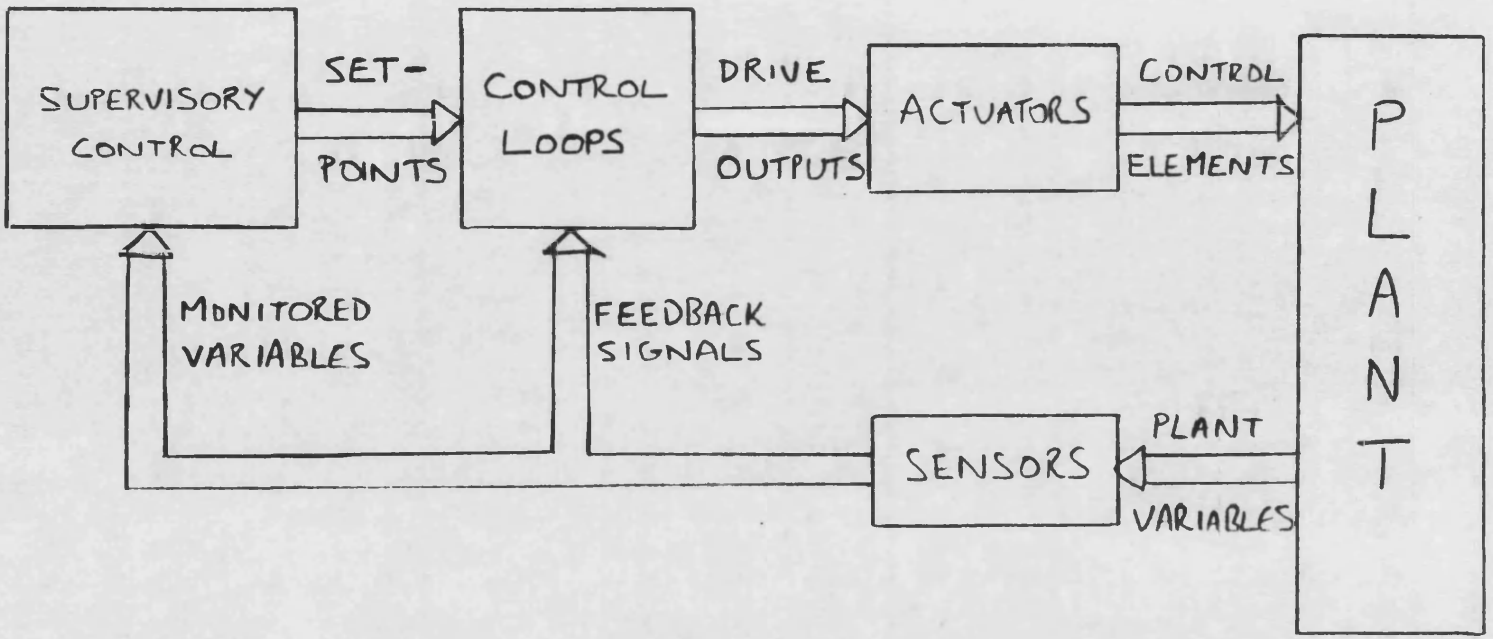

FIG. 3.1 GENERALISED VIEW OF A CONTROL SYSTEM

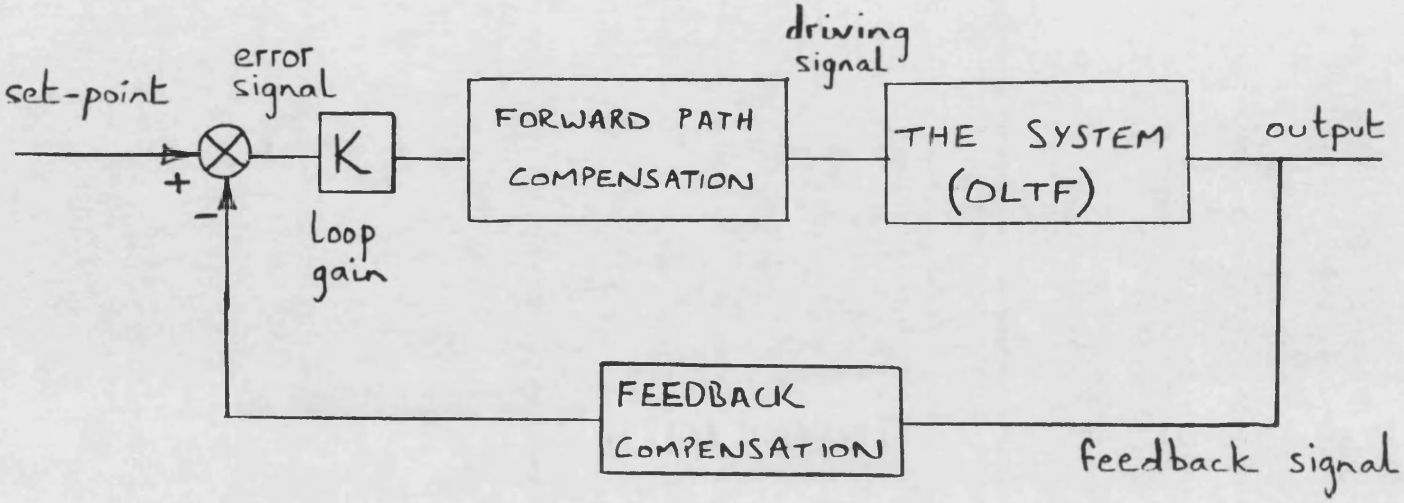

FIG. 3.2 CONTROL LOOP COMPENSATION

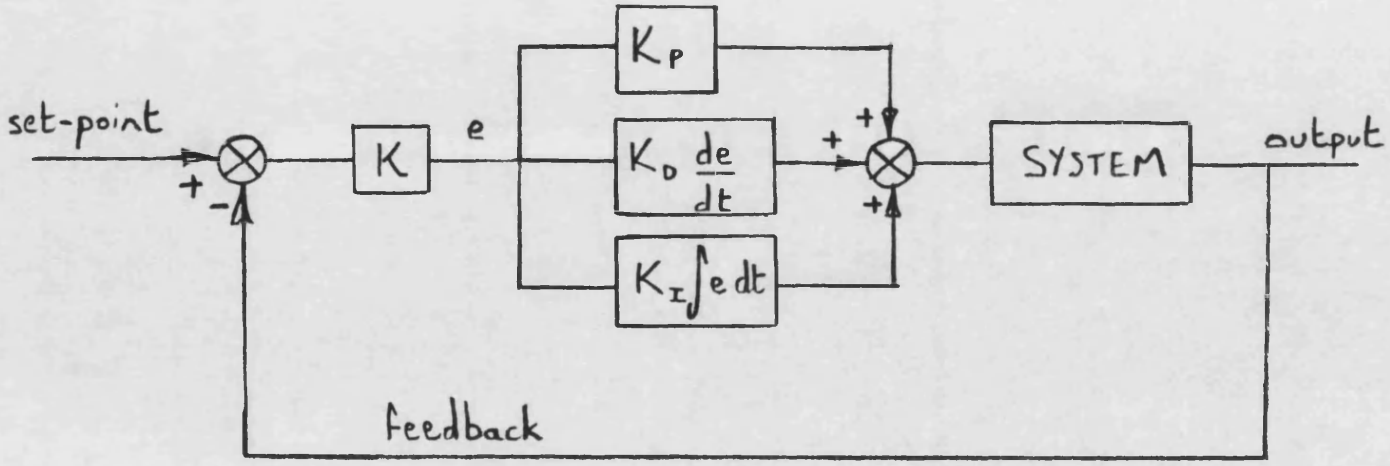

FIG. 3.3 3-TERM (P.I.D.) CONTROLLER

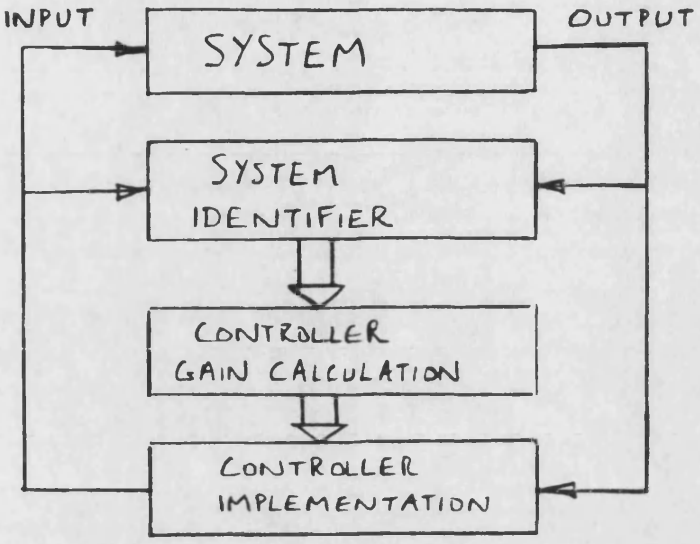

FIG. 3.4 SELF-TUNING CONTROLLER

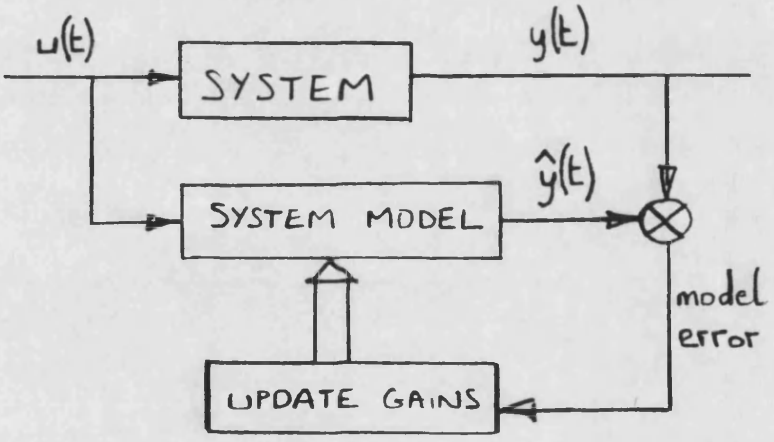

FIG. 3.5 SYSTEM IDENTIFIER

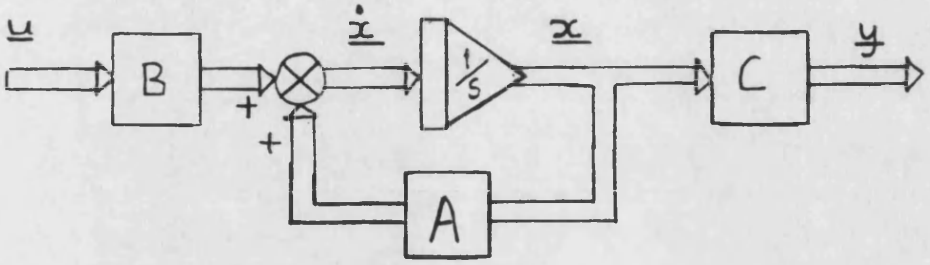

b) STATE – SPACE MODEL

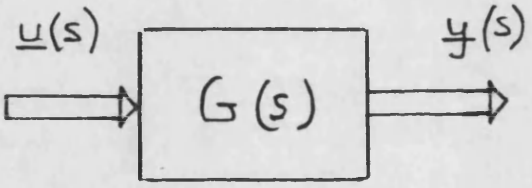

a) INPUT – OUTPUT MODEL
(TRANSFER FUNCTION MATRIX)

FIG. 3.6 MULTI-VARIABLE SYSTEM MODELS

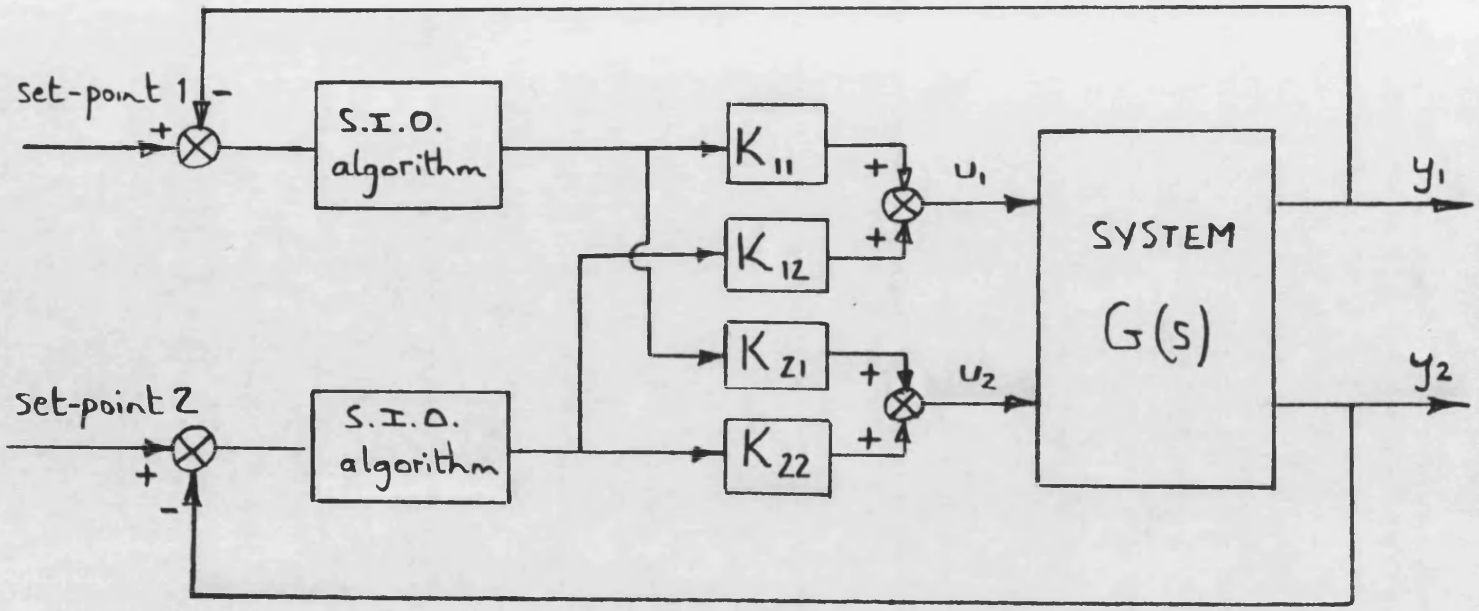

NOTE :- K is shown as a scalar matrix however it's elements could be s-functions

FIG. 3.7 MULTI-VARIABLE COMPENSATION TO GIVE DIAGONAL DOMINANCE

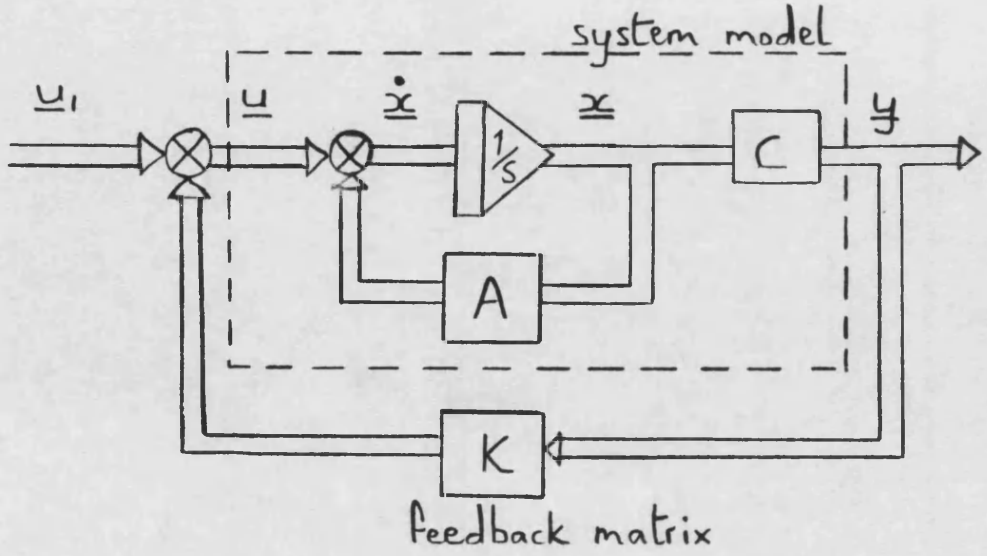

FIG. 3.8 MULTI-VARIABLE FEEDBACK AROUND A STATE-SPACE MODEL

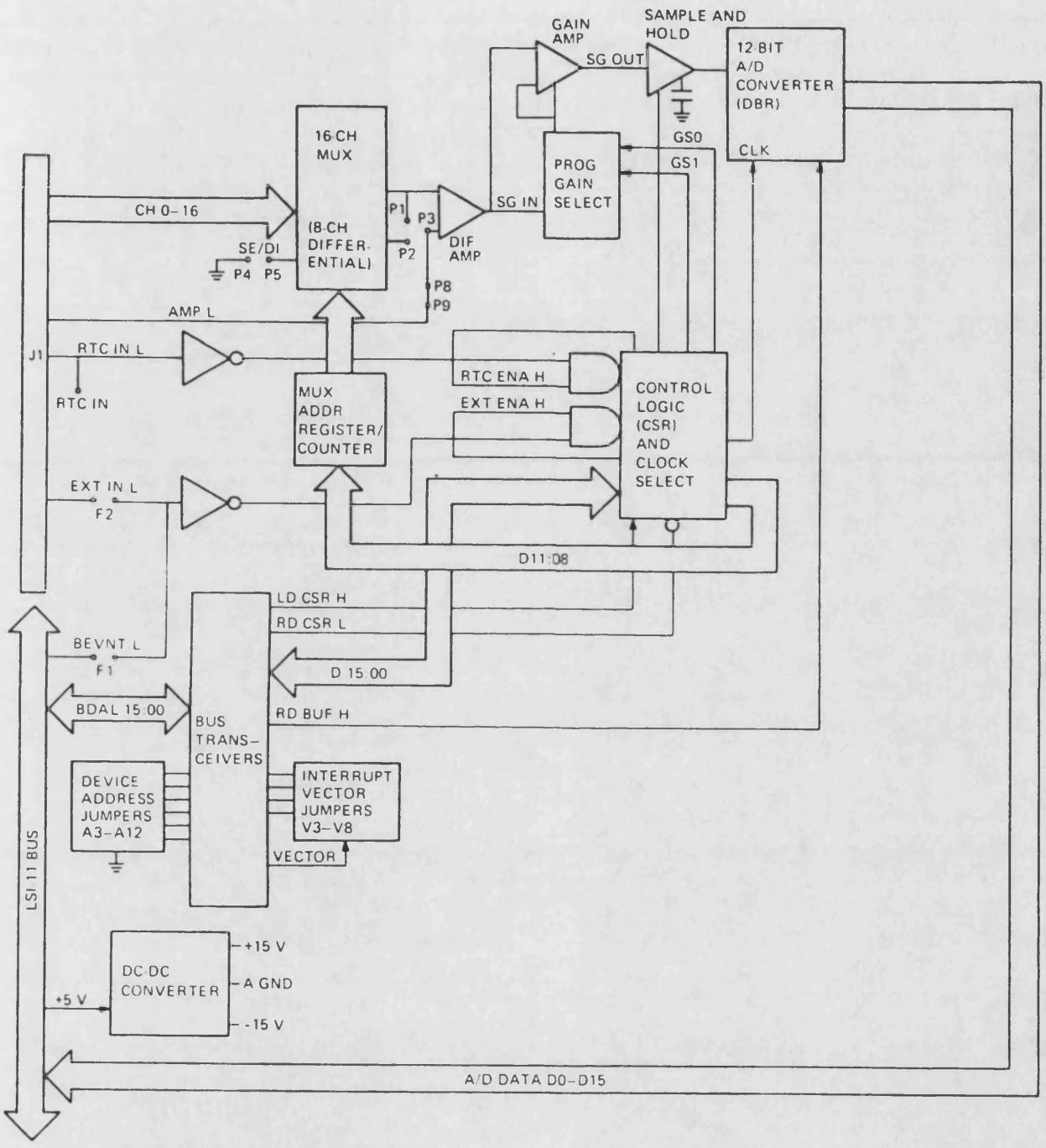

FIG. 3.9 ANALOG TO DIGITAL CONVERTER — BLOCK DIAGRAM

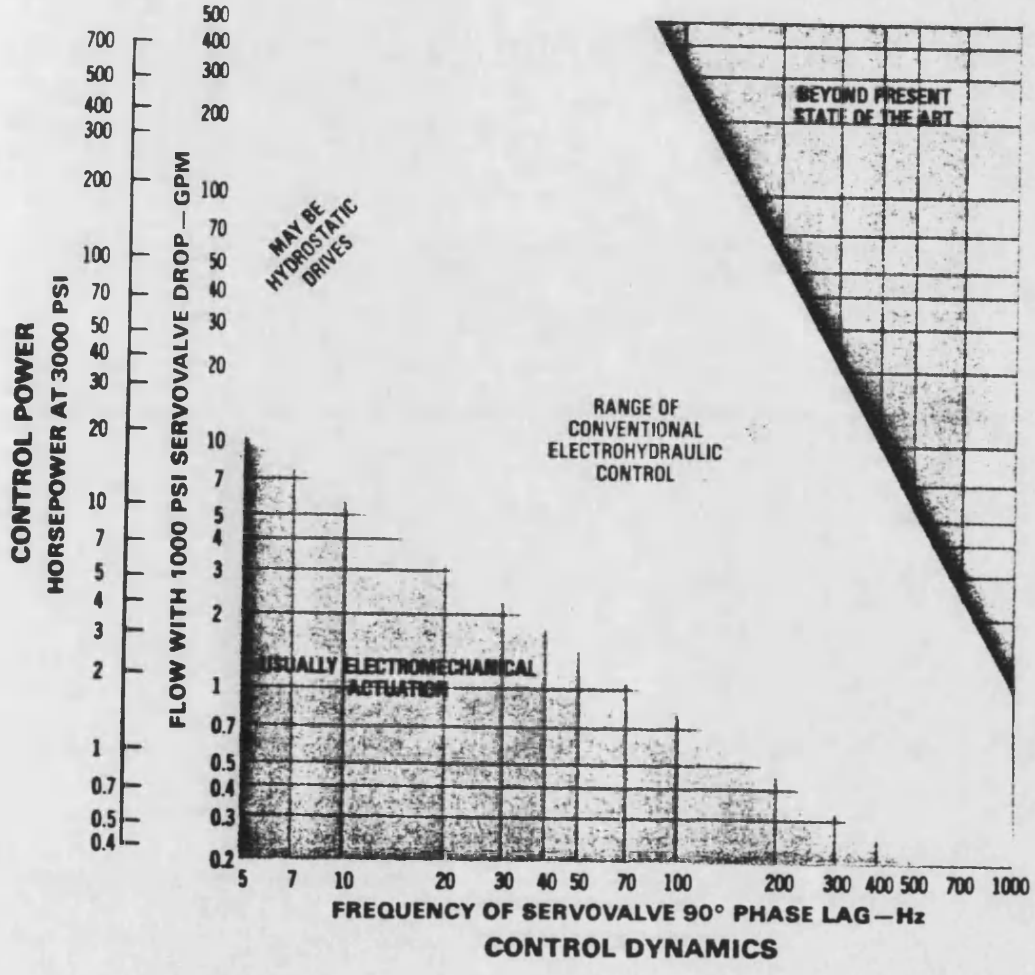

FIG. 3.10 HYDRAULIC VS. ELECTRO-MECHANICAL ACTUATION PERFORMANCE

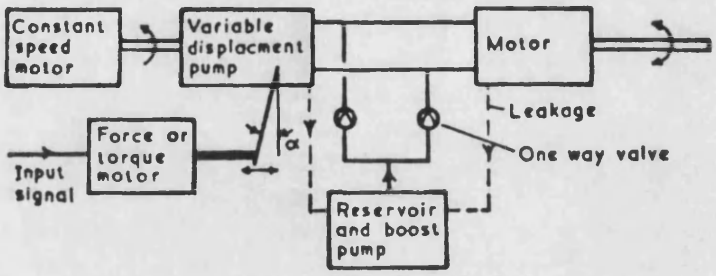

b) pump control

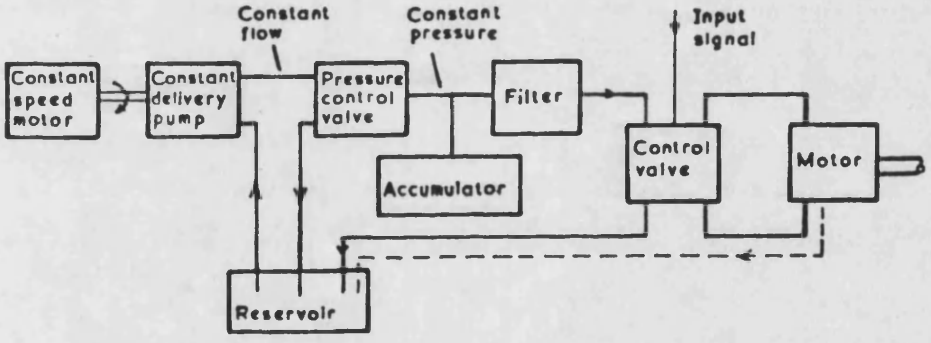

a) valve control

FIG. 3.11 SERVO-VALVE AND SERVO-PUMP CONTROL

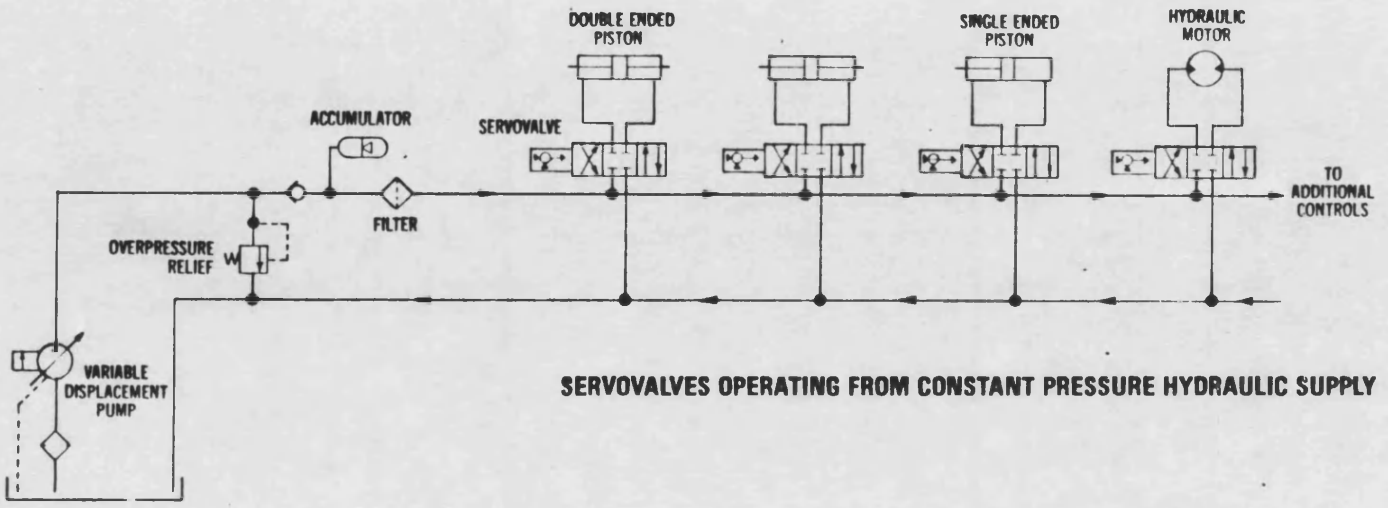

FIG. 3.12 SERVO-SYSTEM ARRANGEMENT

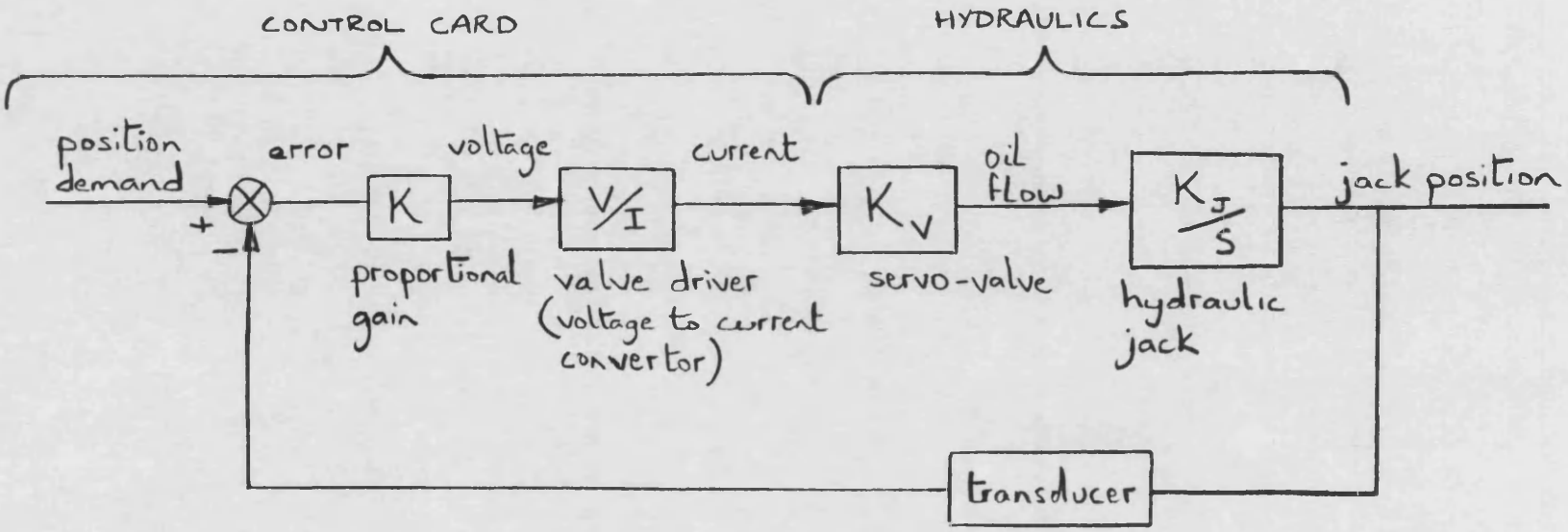

FIG. 3.13 ELECTRO-HYDRAULIC POSITION CONTROL LOOP

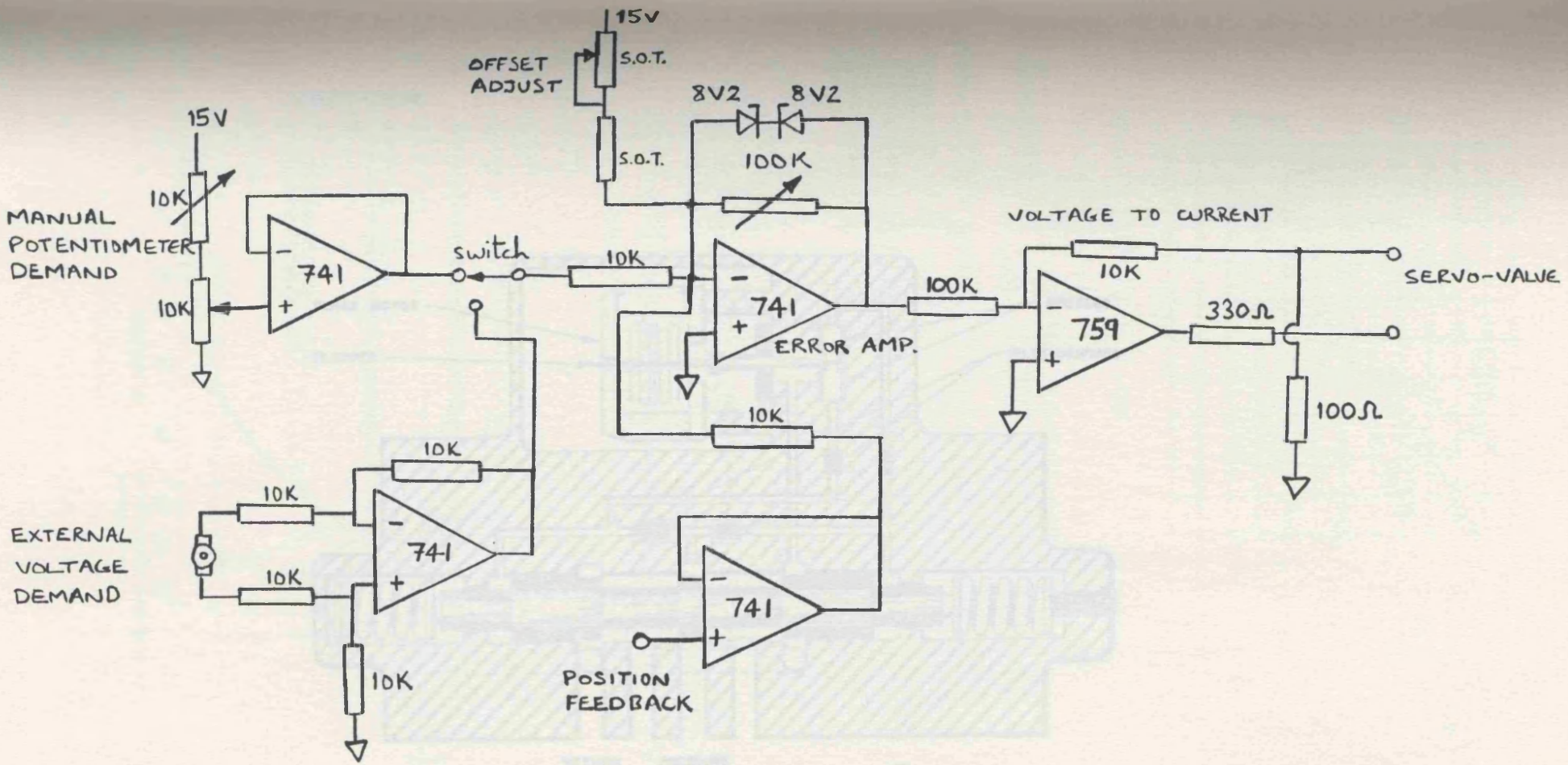

FIG. 3.14 POSITION CONTROL CIRCUIT

(component values are only typical)

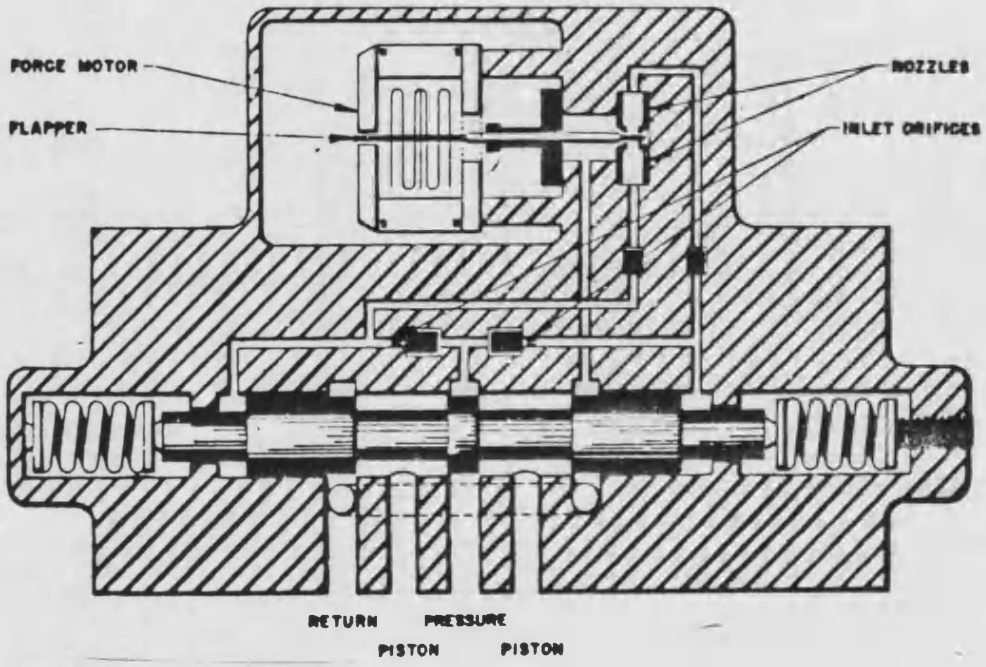

FIG. 3.15 ELECTRO-HYDRAULIC SERVO-VALVE

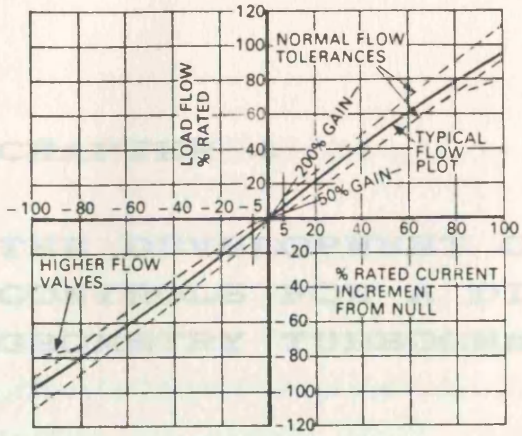

a) Flow vs. current (constant valve pressure drop)

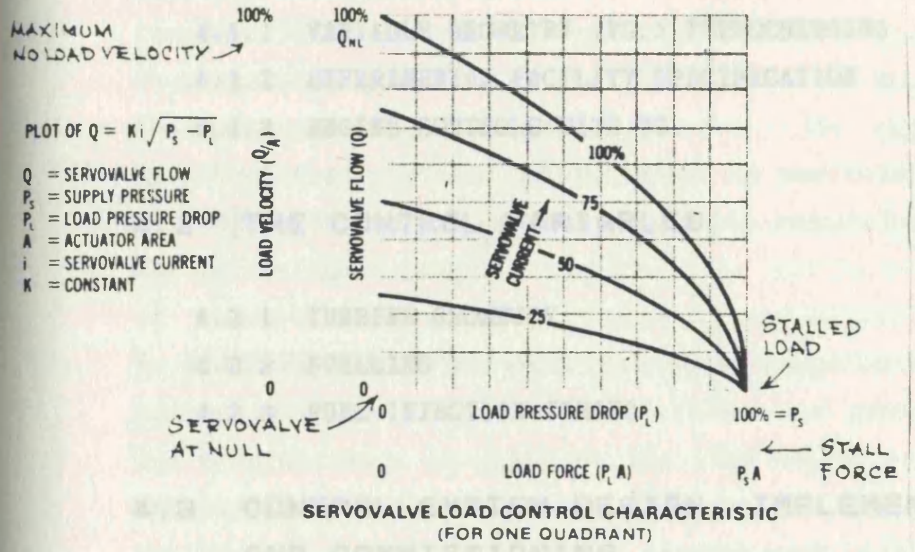

SERVOVALVE LOAD CONTROL CHARACTERISTIC
(FOR ONE QUADRANT)

b) Flow vs. pressure characteristics

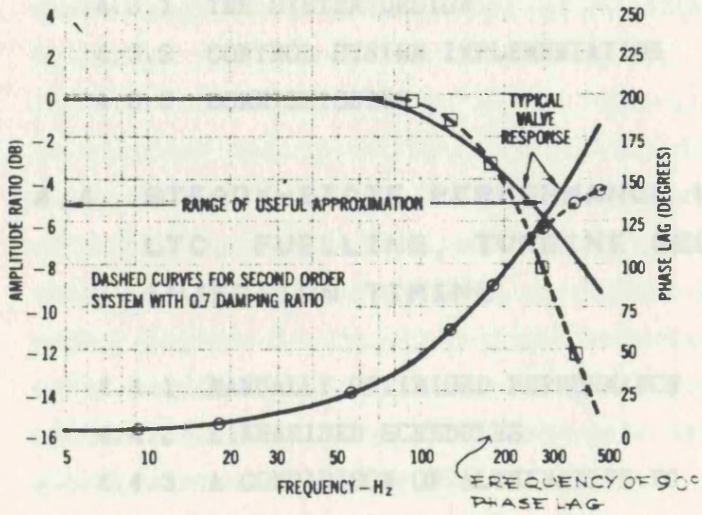

c) Frequency response

FIG. 3.16 SERVO-VALVE PERFORMANCE CHARACTERISTICS

CHAPTER 4

THE DEVELOPMENT OF STEADY-STATE CONTROLS FOR A DIESEL WITH VARIABLE GEOMETRY TURBOCHARGER

4.1 INTRODUCTION

4.1.1 VARIABLE GEOMETRY (VG.) TURBOCHARGING

4.1.2 EXPERIMENTAL FACILITY SPECIFICATION

4.1.3 ENGINE CONTROLS WITH VG.

4.2 THE CONTROL VARIABLES

4.2.1 TURBINE GEOMETRY

4.2.2 FUELLING

4.2.3 FUEL INJECTION TIMING

4.3 CONTROL SYSTEM DESIGN, IMPLEMENTATION, AND COMMISSIONING

4.3.1 THE SYSTEM DESIGN

4.3.2 CONTROL SYSTEM IMPLEMENTATION

4.3.3 COMMISSIONING

4.4 STEADY-STATE PERFORMANCE WITH CONTROL OVER LTC, FUELLING, TURBINE GEOMETRY, AND INJECTION TIMING

4.4.1 MANUALLY OPTIMISED PERFORMANCE

4.4.2 LINEARISED SCHEDULES

4.4.3 A COMPARISON OF ALTERNATIVE VG. SCHEDULES

4.4.4 CONCLUSIONS

4.1 INTRODUCTION

4.1.1 VARIABLE GEOMETRY (VG.) TURBO-CHARGING

On the limiting torque curve (LTC.) a standard turbocharger operates effectively over only part of the Diesel engine speed range. This is because the turbine stage's behaviour approximates to that of an orifice of fixed dimensions. An increase in engine speed and hence massflow results in an increase in pressure (expansion) ratio. The increase in turbine power resulting from this produces a similar rise in compressor pressure ratio, given that the massflows are nominally the same ($m_T=m_C+m_F$, $m_F<<m_C$). However, the engine requires a wide massflow range without large changes in manifold pressures, otherwise the engine's cylinder pressure capacity cannot be fully utilised over the entire speed range.

In truck applications, where the speed range is relatively small, the narrow massflow range of the turbine has generally been accepted. The turbine stage is sized so that the engine is not over-boosted at the rated condition. At low speeds the boost is inadequate and fuelling is reduced, by a boost control unit on the governor, to avoid excessive smoke. The corresponding drop in torque means the useful speed range is less than that of a naturally aspirated engine (fig. 4.1).

To increase the operating range of the turbocharger a means must be found either to control the massflow through the turbine, or alter its effective orifice size, and hence control expansion ratio. One solution already used on small automotive Diesels and high performance petrol engines is the waste-gated turbocharger (fig. 1.18). In these cases engine speed varies too much to accept the narrow range of a standard turbocharger. The waste-gate is operated by boost pressure acting against a diaphragm and spring. As boost increases a valve opens bypassing exhaust gas around the turbine. In this way overboosting at high speeds is avoided. A small turbine is used, capable of providing adequate boost at low speed. The disadvantage of

the system is its inefficiency. The "wasted" exhaust energy (lower turbine massflow) mean a higher exhaust back-pressure is needed to drive the turbocharger. This is reflected in higher engine pumping losses. If the turbine's effective orifice size can be increased then all the exhaust gas can pass through the turbine reducing the back-pressure required for the same turbocharger power. This solution is referred to as variable turbine geometry.

Although variable geometry (VG.), in the form of rotating nozzle blades, has been used in larger turbines for some time, a commercially viable system for automotive application has yet to be developed. Variable geometry manipulates pressure ratio by varying the effective orifice size of the turbine, that is its swallowing capacity (fig. 4.2). In this case exhaust energy is not wasted, turbocharger power is limited by reducing expansion ratio and hence engine pumping work. In practice the potential of such a device can only be realized if turbine efficiency can be maintained with the incorporation of the VG. mechanism.

A VG. turbocharger is an attractive proposition for large truck Diesels where the waste-gated turbocharger is too inefficient, but improved torque back-up and a wider speed range would be desirable. In this case the requirement is for a simple and cheap, but also efficient device. Although efficient, the traditional swivelling nozzles are too complex to manufacture at low cost. Several alternative methods of varying turbine swallowing capacity have been investigated by researchers in this field (refs. 21,47&48). The approach adopted at Bath was to adjust the volute exit area by moving an annular nozzle ring axially across the rotor inlet. Development work sponsored by Holset Engineering Limited (refs. 49&50) was sufficiently promising for the company to produce their own prototypes based on the initial work at Bath.

The project reported here was initiated to do engine test-work and control system development aimed at:-

(i) Determining the best Holset prototype.

(ii) Examining the performance improvements, steady-state and transient, available with that device.

(iii) Implementing a prototype control system to demonstrate that the improvements can be achieved in a real installation.

The project was sponsored by Holset Engineering, Leyland Vehicles, Dowty Fuel Systems and the D.O.I., the companies' interests being turbocharging, truck Diesels and controls respectively. The research was undertaken by the author and a co-researcher, Dr E.W. Roberts, under the supervision of Prof. Wallace. Dr Roberts was responsible for determining the best prototype, and steady-state performance optimisation with that prototype. The author's work included control system design, implementation, and testing, and experimental investigations to determine suitable transient control strategies.

The steady-state test work and a comprehensive experimental rig description are included in ref. 51. A brief rig specification is given in the following subsection to provide the reader with a quick reference. The following two chapters report the work in a condensed form concentrating on the control system aspects and the transient control investigations

4.1.2 EXPERIMENTAL FACILITY SPECIFICATION

Engine

Leyland TL11 turbocharged direct injection Diesel engine
cylinders: 6
displacement: 11 litres
rated power: 190 KW @ 2100 rpm (standard)
static injection timing: 22 deg. BTDC (standard without timing device)
compression ratio: 15.75:1

Turbocharger

Standard: HOLSET H2B-8081C-L25A3 nozzleless twin entry turbine.
Variable Geometry: HOLSET H2C-8625N-Z31U3 (Mk IIb) nozzled single entry turbine, with variable nozzle area.

Fuel injection equipment

CAV MAJORMEC in-line fuel pump (P5476)
standard governor: CS servo-governor fitted with boost (aneroid) control unit.
electronic governor: hydraulic jack operating directly on the fuel rack (subsection 4.2.2)

Dynamometer

Hydrostatic dynamometer designed and built in-house (see section 2.4)
pump: LUCAS HD2-3000
loading valve: Abex Denison R4V06
pressure control valve: Abex Denison SE03

Instrumentation and controls

A general description of the equipment and methods adopted can be found in chapter 2. Specifications and circuit diagrams can be found in ref. 34.

4.1.3 ENGINE CONTROLS WITH VG.

To use the VG. turbocharger effectively some additional control over fuelling was required. The limiting torque curve (LTC.) fuelling schedule must be adjustable so that the best possible torque curve can be determined. In addition injection timing should be adjustable to avoid cylinder pressure limitations preventing full utilisation of the VG. turbocharger.

With a mechanical governor the fuel control rod (rack) has a fixed mechanical stop, which is set to give the correct rated power at rated speed. The governor will then give the correct fuel curve for the standard engine and turbocharger. This fuel curve is determined by the mechanical characteristics of the pump and governor, and is tailored by the pump manufacturers to suit the standard build. With the VG. fitted it was necessary to adjust the fuel stop (maximum rack limit), at each speed, to maximise torque within operating constraints such as cylinder pressure, turbine inlet temperature, and smoke.

To simplify testing and enable the prototype control system to schedule LTC. fuelling, remote electronic control over the rack limit was considered necessary. Two methods were considered: either electronically controlled adjustment of the rack stop on the mechanical governor; or an electronic governor with the rack limit implemented within the electronics. The latter method was chosen as this has the simplest mechanical construction and the greatest operational flexibility. The entire mechanical governor is replaced by a small hydraulic ram acting directly on the fuel rack. The electronic governor design and the facilities it provides are discussed in subsection 4.2.2.

The work undertaken by Baghery (ref. 50) was limited by cylinder pressure on the LTC. A variable fuel injection timing device was advocated as retarding timing lowers cylinder pressures. This allows fuelling to be increased further, making better use of the boost pressure made available by the VG. turbocharger. In addition to an improved torque curve variable timing also gives better fuel consumption throughout the load-speed map. This is explained by the need for combustion to occur over the optimum part of the cycle. The time delay between start of injection and ignition, commonly known as ignition delay, is to a large extent independent of speed. This means that in terms of crank angle rather than time it will increase with speed. Because of this, injection timing should be advanced with speed. In addition the longer duration of injection associated with increasing fuelling makes timing advance with load a useful facility.

Timing needed to be varied remotely for the same reasons as maximum fuel rack limit: ease of testing; and prototype control system development. Although some fuel-pumps do have variable injection timing, notably the DPA type, no suitable device was available for the Leyland TL11 engine used for this work. A device was constructed in house and is described in subsection 4.2.3.

This chapter deals with steady-state engine control. The three control mechanisms and their associated feedback loops are described in detail in the following section. The control system design and implementation is described in section 4.3. Finally, section 4.4 discusses steady-state performance with alternative control schedules.

Chapter 5 covers transient control, that is using the VG. turbocharger to improve transient characteristics such as boost response, load acceptance and smoke.

4.2 THE CONTROL VARIABLES

4.2.1 TURBINE GEOMETRY

The variable geometry turbocharger was a prototype supplied by HOLSET ENGINEERING. Three versions were tested before the performance was considered suitable for the development work described here, the version finally adopted being the Mk 11b. The performance of the three versions is described in detail in ref. 51.

The Mk 11b turbocharger had a variable turbine inlet area, this was achieved by moving an annular restrictor into the nozzled inlet area. An area turndown of 50% was available which provided a 38% mass flow turndown. The annular restrictor was moved axially by two rods on either side of the bearing housing. Originally these rods were moved by two pneumatic capsules similar to those used on waste-gated turbochargers (supplied by HOLSET). Shop air pressure, controlled by a regulator valve, was supplied to the capsules. The movement of the rods was dependent on the regulator setting, capsule spring constants, any inherent stiction, and pre-turbine pressure.

This open loop double actuator system had the following disadvantages: a lack of repeatability because of changes in stiction and exhaust pressure; restrictor twist when stiction is unbalanced; and slow response because of the limited pressures and flow rates available. To provide fast closed loop control for transient studies, and at the same time implement computer control over the VG. system, it was decided that an electro-hydraulic actuation mechanism should be developed. The advantages of hydraulic over pneumatic or electrical actuation are discussed in section 3.5.

In the mean time the capsules provided manual open loop control over restriction, suitable for steady-state test work only. A miniature high temperature position transducer (Schaevitz 201-01 LVDT) was fitted inside one of the capsule springs, so that manual optimisation could be undertaken while the electro-hydraulic mechanism was under

development. The single transducer gives no indication of restrictor twist, also changes in build or turbine condition may cause repeatability problems. Hence boost pressure was used as the optimised variable, although restriction was recorded.

The electro-hydraulic system was designed to meet the following criteria:-

1. A single hydraulic jack to be used to avoid synchronisation problems.
2. The jack, transducer and servo-valve should be protected against conductive and radiative heat transfer from the turbine casing.
3. Side load on the restrictor rods, which might cause stiction problems, to be negligible.
4. Rod seals to be used to prevent exhaust gas leakage and hence loss of efficiency.
5. The mechanism must not lock-up when rod stiction forces are unbalanced.
6. Minimal backlash in the mechanism.

These requirements led to a design which allows the jack and transducer to be located over the compressor, maximising both distance from the turbine case and installation space. A central lever arm over the bearing housing rotates a torsion bar which transmits the jack movement to two lever arms either side of the bearing housing. The whole lever arrangement rotates in two rose bearings which also support its weight. Misbalanced rod stiction is taken up by twisting of the torsion bar, avoiding jamming of the mechanism. Vertical movement of the lever ends due to lever rotation is taken up by three con-rod type links (motor-cycle cam chain links were employed). Sealing of the rod bushes and cooling is provided by compressed air fed to the small chambers through which the rods enter the turbine back plate. Springs fitted over the restrictor rods take up backlash in the pivots. Seizing due to differential expansion of the hot restrictor as compared to the turbine back-plate was avoided by the

inclusion of crude expansion joints at the rod to restrictor connections.

The hydraulic jack, transducer and servo-valve are configured as the standard position loop described in section 3.5. The servo-valve is mounted remotely from the engine and connected to the jack by flexible hose, thus avoiding temperature and vibration failures.

The analogue controls provide the following facilities:-

a) restriction control
b) inlet manifold pressure (boost) control
c) manual potentiometer settings or external voltage demands for a) and b).
d) a zero restriction button which overrides other facilities.

Boost control was implemented by installing a strain-gauge pressure transducer in the inlet manifold. This provides feedback for an outer loop around the restrictor position loop (fig. 4.3a). A proportional plus integral (P+I) algorithm is used in the forward path of the boost loop to eliminate any steady-state error. This ensures that computer demands are followed exactly. The OP-AMP circuit implementing these control loops is shown fig 4.4.

4.2.2 ENGINE FUELLING (figs 4.5 & 4.6)

To provide the additional facilities required for this work, such as control over the LTC fuelling curve, the CAV CS Governor was replaced by an electronic governor designed especially for the task.

The fuel injection system initially fitted was a CAV MAJORMEC in-line fuel pump with a CS servo governor and boost control unit. The entire governor was removed from the pump and replaced by a hydraulic jack operating directly on the end of the fuel control rod (rack). A position transducer, also mounted directly to the rack, provides feedback for the position loop. Speed feedback is provided by a

magnetic pick-off triggered by the flywheel teeth. The analogue control circuitry is remote from the engine and provides the following facilities:

a) all speed governing
b) direct rack operation
c) a maximum fuel stop, continuously variable whilst the engine is running
d manual potentiometer settings or external voltage demands for a) to c)
e) a stop button which overrides all other facilities

The all speed governing mode is the most convenient and safe method of control, avoiding accidential runaway of engine speed. Direct rack control is provided for those tests where a specific rack schedule is required, notably transient investigations and transfer function analysis work. The maximum rack stop facility is used to tailor the LTC fuel curve either manually or as part of a computer control system. It is also useful as an adjustable safety limit when doing other work.

The control loop block diagram is shown in fig. 4.3c. Speed control is achieved with a simple proportional loop as this behaves in a similar manner to a mechanical governor, that is it has the characteristic droop line. The gain K_1 was adjusted to produce the same droop as the CS governor. When operating in the speed control mode, rack position feedback (the inner loop) is retained as this improves dynamic performance. Response is superior to the mechanical governor because of the fast position loop. A discussion of speed loop performance can be found in subsection 7.2.3. The maximum fuel rack limit is effective whether operating in speed or rack control mode and is implemented by a variable saturation circuit before the position summing point. The OP-AMP circuit implementing these facilities is shown in fig. 4.6

4.2.3 FUEL INJECTION TIMING (figs. 4.7 & 4.8)

Having decided to incorporate variable injection timing it was found that no commercially available system existed which could be fitted to the TL11 engine. A device was designed and manufactured based on variable timing components for a GARDNER 6LXB engine (fig. 4.7). The components were modified to suit an assembly fitting in place of the automotive compressor, that is in-line between the gear-case and fuel pump.

A helically splined shaft is driven from the gear-case end, along which a collar with matching internal splines can be moved by a yoke and lever mechanism. The collar has straight external splines which drive the output shaft and hence the fuel-pump. The bearings and splines are pressure lubricated from the engine oil system. The external operating lever is connected to a hydraulic jack, servo-valve and rotary position transducer configured as the standard position loop described in section 3.5. There is no outer loop, dynamic timing being altered in an open loop fashion (fig. 4.3b).

The range of the device corresponds to a static timing swing of 22 deg. at the crankshaft, and can be set up to cover the required crank angle range by manually adjusting the static timing of the mid point

4.3 CONTROL SYSTEM DESIGN, IMPLEMENTATION AND COMMISSIONING

4.3.1 THE SYSTEM DESIGN (fig. 4.9)

As stated previously the aim of this work was twofold: to determine the benefits attainable from the addition of a variable geometry turbocharger; and to develop a prototype control system, hence proving the feasibility of realising those benefits in a real vehicle. To utilise fully the potential of such a system, variable injection timing and the facility to tailor the LTC fuel curve were included (as explained in 4.1.3). These control variables were to be used to optimise fuel consumption over the entire load-speed map, and to maximise the torque back-up available within cylinder pressure, turbine inlet temperature and smoke limitations.

There are three approaches to the design of a steady-state controller for optimum engine operation: applying pre-determined optimum schedules for the control parameters; on-line optimisation of those parameters; or a combiniation of the previous two methods. The relative advantages of these three systems are discussed in section 3.2. However, for this work the pre-determined schedule approach was adopted as this method can be implemented with simple transducers and hence is more likely to be accepted as a commercial proposition. In particular, on-line optimisation of fuel consumption requires fuel flow and engine torque measurement.

The schedules or look-up tables can be functions of any set of independent variables which unambiguously define the engine's operating conditions. In this case it was decided to neglect ambient conditions for simplicity and only to define the operating point in terms of load and speed. Speed measurement is relatively straightforward and inexpensive. However, torque measurement could be extremely difficult to achieve, at low cost, in a real vehicle installation. Because of this fuel rack position was chosen as the measure of engine load. Rack position determines fuel per shot for a

given pump speed and hence approximates torque. Fig. 4.10 depicts the relationship for the engine and pump used.

The controlled parameters chosen were boost pressure, LTC fuel rack position and static injection timing. Boost pressure was used instead of turbine restriction for the following reasons:-

1. Difficulty was encountered in obtaining repeatable results when setting restriction with the pneumatic capsules. This was thought to be caused by variations in stiction which in turn cause "cocking" of the restrictor. Boost pressure was, therefore, preferred for the purpose of manual optimisation.

2. Similar problems were considered likely with a commercial system, long term repeatability would be particularly affected by the build up of soot and mechanical wear.

3. The use of an absolute pressure transducer would result in a control system which can compensate for changes in atmospheric pressure (altitude) within turbocharger limitations.

4. Boost pressure feedback allows control loop algorithms to be incorporated which enhance turbocharger transient behaviour. This is discussed in chapter 5.

The resulting control system design is shown in fig. 4.9. Boost pressure and injection timing are functions of speed and rack position. LTC fuelling is a function of speed only. These schedules are implemented on the development computer described in section 3.4. The three control outputs are connected to the analogue control loops described in section 4.2 (fig. 4.3). Boost and timing are control loop set-points, LTC fuelling sets the governor's adjustable maximum rack limit. A commercial system may well incorporate the loops in software, however, it was convenient when testing to have the facilities provided by the analogue controllers without the necessity of running the computer system.

4.3.2 CONTROL SYSTEM IMPLEMENTATION

The control scheme described in the previous section is implemented by a computer program running on the development machine (LSI-11/23). Engine speed and fuel rack signals are fed to 2 ADC channels, from which the program then calculates control demands for static timing, boost pressure, and maximum rack limit. These demands are output via 3 DAC channels to the appropriate analogue control loop set-points. The control loops and their control mechanisms are described in section 4.2.

The control program can be regarded as having four distinct parts:-

1. Program initialisation
2. Bumpless transfer from manual to computer control
3. The set-point scheduling loop.
4. Bumpless return from computer to manual control.

The first section of the program initialises variables and common blocks, reads in control schedule data, sets up the VDU display and calculates the atmospheric pressure adjustment. The control schedule data is read from a data-file on disc and converted from engineering units to DAC units ie. integer numbers suitable for outputting to DAC channels. The converted data is stored in 1-D and 2-D arrays. The VDU display is then initialised and the barometer reading entered by the operator so that the atmospheric pressure adjustment can be calculated.

The operator is led through the bumpless transfer procedure with a series of instructions displayed on the VDU. The engine is started under manual control and the control parameters are then adjusted to the settings requested by the program, before switching to computer control. The manual/external switches on the analogue controls are used to transfer control

The program then enters the main scheduling loop which continuously updates the optimum set-points output to the analogue loops. This program loop consists of: ADC conversion using a machine code routine; set-point calculation; DAC output using the IPOKE routine; and an exit request check (ie. has the space bar been pressed).

Set-point calculations are all undertaken in ADC and DAC units to increase execution speed, conversion from engineering units is avoided and integer arithmetic can be utilised to a large extent. The optimum schedules are representated by either equations, fitting the relationships required, or arrays of discrete values. If arrays are used then specially written "fast" integer interpolation functions are called to pull values from them. These functions require normalised array indices, as inputs, to reduce the code needed.

If the space-bar is pressed the scheduling loop is left and the exit routine run. This routine is the reverse of the bumpless transfer procedure, and returns the system to manual control.

Further details along with program listings can be found in Appendix 1.

4.3.3 COMMISSIONING

The analogue loops were implemented and tuned independently prior to program commissioning. Tuning was an intuitive process using step inputs and an oscilloscope display of feedback response. The aim is usually to minimise rise time whilst maintaining stability and acceptable overshoot. Figure 4.11 shows three typical responses: a sluggish response due to low proportional gain; a large overshoot and oscillation due to high gain; and a well tuned response with correct gain. When a proportional and integral (P+I) algorithm is used the integral component is zeroed to obtain an initial proportional setting. Using this as a starting point a balance between initial rise time and final integrator settling time is struck by adjusting integral and proportional settings, whilst maintaining stability.

The three position loops (VG, rack & timing) and the governor speed loop proved to be straightforward so far as tuning was concerned. However, the boost pressure loop (fig. 4.12) proved more difficult because of the inherently variable nature of the turbocharger transfer function, the gain K_T varying with exhaust enthalpy. The maximum value of loop gain K_L consistent with stable operation was determined for a range of load-speed combinations. Figure 4.13 shows the approximate relationship between loop gain, torque and speed. Ideally an adaptive controller (see subsection 3.3.2) should be adopted in these circumstances to adjust K_L. However, a compromise gain was set, low enough to give stable operation over the whole load-speed map.

The response to steps in boost demand was measured, with the compromise gain setting. Surprisingly the response was no worse than with the ideal gain, over most of the map. This is attributed to the restrictor hitting its end stops for any sigificant error in pressure, and hence removing any beneficial effect from setting a higher gain.

The combination of supervisory control program and analogue control loops appeared to function as expected at part load. However, at high load the previously stable boost pressure loop became oscillatory. This was found to be due to an oscillating rack position which in turn led to the computer demanding an oscillating boost pressure. This effect was only present with all-speed governing, not under direct rack operation (the equivalent of two-speed governing).

Figure 4.14 attempts to explain the phenomenon in terms of the effect of boost pressure (restriction) on engine efficiency. Assume an increase in boost (restriction) causes an increase in efficiency, and hence an increase in speed using the windage load characteristic. The increase in speed then causes the governor to pull back the fuel rack, which results in reduced boost demand (restriction) from the computer. This has the effect of closing an unwanted feedback loop around the supposedly open loop scheduling system. At high loads the gain between boost and efficiency is greatest and leads to instability.

One conclusion which may be drawn from this problem is that fuelling and restriction are sufficiently interactive to warrant the adoption of a multi-variable approach to Diesel engine governing (see section 3.3.3). A multi-variable governor operating on rack and restriction is shown in fig. 4.15. The cross-coupling between inputs and outputs is represented by the dotted lines. A pre-compensator de-couples the two loops by cancelling the effect of the engine's inherent cross-coupling. Once de-coupled, the two loops can be tuned independently and the type of problem discussed above should be eliminated. Multi-variable governor development is the subject of a research project using the same experimental facility (ref. 52).

4.4 STEADY-STATE PERFORMANCE WITH CONTROL OVER LTC, FUELLING, TURBINE GEOMETRY AND INJECTION TIMING

4.4.1 MANUALLY OPTIMISED PERFORMANCE

The optimum schedules, which are the basis of the steady-state control system, were determined by manual testing (ref. 51). The electro-hydraulic governor and timing device had been commissioned for these tests. However, the VG. turbine restrictor was still under pneumatic operation prior to the implementation of the electro-hydraulic lever mechanism. As mentioned in 4.2.1, it was considered that boost pressure would be a more appropriate and repeatable variable for optimisation than restriction. Nevertheless one of the pneumatic capsules incorporated a position transducer so that restriction could be recorded.

Restriction and injection timing were used to minimise SFC at discrete points forming a grid covering the load-speed map. There was little interaction between restriction and timing, therefore minimising SFC was a simple two stage process (first optimise timing and then restriction). On the limiting torque curve (LTC), restriction, timing and fuelling were adjusted to maximise torque within the following operating constraints:-

peak cylinder pressure - 1850 psi
turbine inlet temp. (T.I.T.) - 700 deg.C
exhaust smoke shade - 3.5 Bosch units

Changes in efficiency were detected by operating the fuel controls in "all-speed" governing mode, and the dynomometer in "constant torque" mode. Any improvement in efficiency results in an increase in speed and a reduction in fuel rack position because of the governor droop characteristic. In control loop terms an increase in efficiency results in a higher speed loop gain, and hence smaller error (droop) for the same torque output.

The results of this work are presented in two groupings:-

1. LTC performance
2. Load-speed maps

Load is described by either torque or fuel rack postion, whichever is most appropriate. Rack is essentially a measure of torque as it controls the fuel per shot. However, this relationship is not entirely independent of speed nor is it linear, hence the maps are distorted when rack replaces torque. Base performance refers to standard turbocharger build and injection timing (22 deg. BTDC static).

1. LTC performance

The compressor map, fig. 4.16, is wide enough for the increased range of the turbocharger. However, peak-torque has moved away from the most efficient part of the map implying the need for a re-match. With a VG turbocharger pressure ratio increases from rated to peak torque. Hence the rated condition should be matched at a lower point, relative to the high efficiency islands, than with a standard turbocharger.

Comparison of the VG and base LTC operating lines shows that the VG turbocharger supplies a lower boost at rated conditions. This is a result of the larger swallowing capacity of the VG turbine when fully open. The maximum speed to which the engine was tested was increased from 2100 to 2300 rpm to take advantage of the larger turbine swallowing capacity. This was justified by the fact that SFC at 2300 rpm was the same as that previously only obtainable up to 2100 rpm with the base turbocharger. This was partly due to the introduction of variable injection timing which allowed timing to be advanced with speed.

Figures 4.17-4.18 show optimised engine performance on the LTC compared with the base performance. The restrictor was fully open down to 1800 rpm and was then gradually closed until, at 1400 rpm,

maximum restriction (50%) was required. Over the control range (1800-1400rpm) manifold pressures increase producing a rising torque curve, with air-fuel ratio constant at approximately 22.5. The VG torque curve is well above the base and the SFC curves should be compared bearing this in mind.

The following table describes the improvements in the torque curve (over base) as a result of optimisation

PERFORMANCE CRITERIA	BASE	OPTIMISED VG AND VT
RATED POWER	191 KW @ 2100 rpm	191 KW @ 2300 rpm
PEAK TORQUE	1057 Nm @ 1300	1155 Nm @ 1360
TORQUE BACK-UP	21%	46% (119% increase)
USEFUL SPEED RANGE	800 rpm	940 rpm (17½% increase)

2. Load-speed maps

The consumption loops for the base and optimised engines are shown in figs. 4.19 & 4.20 respectively. It is immediately apparent that the loops have increased in size, in particular the 210 gm/KW.hr island has increased in area by 61%. The improvement is mainly in the low and mid speed range as this is where the base turbocharger produces inadequate boost and where timing changes are most important. Standard timing is near optimum between peak torque and rated speed, ie. at higher speeds.

Although the low SFC islands cover a larger area they do not reach as low a minimum as the base. However, this only affects a small area of the map. This higher value of minimum SFC is thought to be due to lower turbocharger efficiency with the VG arrangement.

The timing map (fig. 4.21) is shown plotted against engine speed and fuel rack position as this is the form required by the control system. At high load, approaching the LTC, timing was used to keep within cylinder pressure and smoke limits. Above peak torque it is retarded

to reduce cylinder pressure, below peak torque it is advanced to limit smoke.

At part load timing was adjusted to give minimum SFC, the general trend being to advance timing with both speed and load. However, there are unexpected speed dependent 'kinks' which are considered to be a result of the experimental procedure. At part load the SFC vs. timing relationship is fairly flat around the optima. Hence with no other variable to optimise, such as noise, large variations may occur. The map was covered by moving from LTC to minimum load at each speed, a set of points at one speed constituting a test. No conscious effort was made to take account of any pattern in the results, so anomalies were more likely to occur between speeds especially if tests were undertaken on different days.

Because of these observations and the relative insensitivity of SFC to small changes in timing it seemed reasonable to smooth the timing map (fig. 4.22). However, further optimisation work to eliminate the anomalies would be appropriate if this work is considered worth pursuing commercially.

Restriction and boost pressure maps are shown in figs. 4.23 & 4.24. Because of the problems associated with the pneumatic actuation (see section 4.2.1.) the restriction map has less significance and requires smoothing. A smoothed restriction map is shown superimposed on the boost map in fig. 4.24 to indicate the approximate control range. Outside the control range of the restrictor boost increases with engine speed and torque (exhaust enthalpy). Inside the control range torque becomes the major determinant of boost. If boost is plotted against rack position and speed (fig. 4.25), it is virtually independent of speed within the control range.

4.4.2 LINEARISED SCHEDULES

A series of tests were conducted using linearised schedules which, in a commercial design, could be implemented by simple analogue circuitry. The aim was to assess the loss in performance due to schedule simplification. The linearised schedules can be represented by simple equations, which for the purpose of these tests are implemented on the development computer.

The simplified timing schedule is a linearisation, by eye, of the schedule determined under manual optimisation. Figs. 4.22 and 4.26 show respectively the original and linearised timing maps together with the equation for the linearised map. Both maps are functions of engine speed and fuel rack position.

The simplified boost schedule is derived from the map obtained by manual optimisation (fig. 4.25). It can be seen that within the control range of the turbocharger, boost pressure is a function of rack position only. Fig. 4.27 is obtained by plotting boost against rack within the control range (at approx. 1400 rpm). A straight line fit of the higher points is used because it is only at higher torques that the VG produces optimum boost. At low torques the restrictor is fully open and boost cannot be reduced further.

A linear relationship between fuel rack and boost makes sense because it implies improved SFC results from attempting to maintain constant air-fuel ratio.

The performance with simplified schedules is discussed in two parts: LTC performance and Load-speed maps

A. LTC performance (figs. 4.28-29)

The operating constraints defining the LTC were the same as for manual optimisation. The torque and hence power curves (fig. 4.28) are slightly lower than those obtained from manual optimisation (fig.

4.17), this was thought to be because the simplified timing schedule does not retard to offset cylinder pressure or advance to limit smoke. The LTC consumption curve is flatter particularly at low speed, the following factors explain this improvement:-

1. The simplified timing schedule is derived from the entire map and hence approximates optimum settings for minimum SFC. However, during manual optimisation timing was used to maximise torque rather then minimise SFC on the LTC. This effect is very marked below 1200 rpm where timing was advanced to limit smoke rather than retarded for best SFC.
2. Below 900 rpm torque drops away more steeply than in the fully optimised scheme thus improving air-fuel ratio.
3. The restrictor opens more gradually over a wider speed range (1300-1900 rpm) which has the effect of smoothing the manifold pressure curves.

B **Load-speed maps** (figs. 4.30 & 4.31)

The consumption loops are still larger than those of the base engine. However, they have been pushed higher than the manually optimised loops resulting in poorer low load efficiency. Comparing the boost and restriction maps (figs. 4.24 & 4.31), it is apparent that the restrictor closes at higher torques resulting in lower boost levels generally. This explains the reduced low load efficiencies. The implication is that the linear boost relationship has either too shallow a slope, or should have been left in the form of a curve.

If a simple linear system is considered of commercial interest then these linear schedules should be adjusted to obtain the optimum slopes and intercepts. However, this would involve substantial test work and was not considered appropriate at this stage of the work.

4.4.3 A COMPARISON OF ALTERNATIVE VG SCHEDULES

A series of tests, comparing alternative VG schedules, has been undertaken. The purpose was to obtain fuel consumption loops, which together with the transient performance characteristics described in the next chapter, provide a basis for an overall assessment of these alternative schedules. Three schedules are compared:-

1. Optimum boost pressure (or restriction) - the restrictor is adjusted to give the boost pressure previously determined by manual optimisation (fig. 4.32).

2. Speed VG schedule - restriction is a function of engine speed only, and is optimum on the LTC ie. the same as the previous schedule on the LTC (fig. 4.33).

3. Boost capsule type schedule - restriction is a linear function of boost pressure ie. similar operation to a waste-gate. Restriction is 50% at and below 600 mmHg. gauge pressure, 0% at and above 700 mmHg. (fig. 4.34).

All three sets of consumption loops were undertaken with timing following the smoothed version of the manually determined optimum map (fig. 4.22).

The purpose of these tests was two-fold: to compare the three alternative VG schedules and to assess the role of timing in SFC improvement. If the alternative strategies show little difference at part load, then any part load improvement over base performance (std. turbo', std. timing) can be assumed to be mainly due to timing.

The original manually optimised SFC loops (fig. 4.20) differ so much from the new set (fig. 4.32), created for this comparative study, that it is not considered advisable to compare these with the original base results either. Unfortunately, no time was available for a new base performance test.

The differences between the original and the new optimum loops are probably due to a combination of the following factors:-

1. The original timing map was far from smooth.
2. Test conditions and engine performance will differ with time. The original manual tests took account of all parameters, including ambient conditions, in much the same way as a self-optimising system would. There was a gap of two years between the original and the present tests which obviously leaves something to be desired, especially as the optimum schedules are recorded as a function of two variables only (speed and load).
3. The turbocharger build had changed, electro-hydraulic replaced pneumatic actuation.
4. The tester had changed and the original tester was no longer available for consultation on methods.

However, the results are considered useful for comparison purposes as they were all conducted within a period of 8 weeks, by the same tester.

Performance comparisons

Three SFC maps are presented with their corresponding VG. schedules superimposed (figs 4.32-4.34).

The optimum boost schedule (fig. 4.32) produces the best fuel consumption loops as expected. In particular at part-load, low to medium speed, SFC is appreciably lower than with the other two schedules. The speed schedule (fig. 4.33) gives the same restriction, and hence SFC, at high speeds (>1750 rpm) and on the LTC. The capsule type schedule results in 50% restriction over most of the map. Therefore low speed (<1300 rpm) SFC is the same as that obtained with the speed schedule. This schedule produces the worst results at medium to high speeds because excess restriction is applied.

Surprisingly, the capsule type schedule produces similar LTC performance to the other two schedules (ie. optimum LTC restriction). This implies that the boost vs. restriction schedule chosen was a very good match. The break points (600 and 700 mmHg) were chosen to give a torque curve close to that possible with the other schedules.

4.4.4 CONCLUSIONS

Both LTC and part-load performance have been improved using a VG turbocharger and variable timing device. The use of a timing device to limit cylinder pressure (retarding injection) results in a higher torque back-up than would be obtainable with a VG turbocharger alone. Manual optimisation produced the following improvements over the base performance (std. turbo', std. timing):-

1. Torque back up was increased by 119% to 46% (from 21%).
2. The useful speed range has been increased by 17½% to 940 rpm (from 800 rpm).
3. The LTC fuel consumption curve is flatter than the base curve, particularly at high speeds, allowing an increase in maximum speed to 2300rpm (from 2100rpm) without an SFC penalty.
4. The consumption loops have increased in size, in particular the 210gm/KW.hr island has increased in area by 61%.

The consumption loop improvements are concentrated in the low to medium speed range for two reasons. Firstly, standard timing (22 deg. BTDC, 7 volts) is closer to the optimum between peak torque and rated speed. Hence variable timing has the greatest effect at lower speeds where standard timing is too advanced. Secondly, the turbocharger match is such that its control range is only used to advantage in the low to medium speed range.

The restriction map (fig. 4.24) shows that a larger VG turn-down ratio could be usefully employed. In particular a larger turbine stage, which could be opened still further, would allow the control range to include higher speeds. The requirement, therefore, is for a mass flow

turn-down greater than the 38% provided by the prototype unit. Increasing turn-down may prove difficult as turbine efficiency must remain high to profit from VG. Any loss of turbine performance detracts from the benefits of turn-down.

The simplified (linearised) schedules resulted in disappointing part load SFC. This was attributed to the restriction map (fig. 4.31) being pushed higher with respect to load than the optimum map. This in turn pushed the SFC loops (fig. 4.30) higher increasing low load consumption.

To assess fully the use of simplified schedules the best slope or form of curve should be determined experimentally. This is only suggested if a commercial prototype is being considered, and linear schedules reduce cost considerably. If a micro-processor based controller is chosen, 2-D interpolation from the original optimum maps presents no problems assuming the input signals of speed and rack are available.

A comparison of three alternative VG schedules confirmed that restriction, as well as injection timing, affects part-load efficiencies. Maintaining optimum boost pressure levels, as a function of speed and load, gives significantly better fuel consumption than the alternative compromise strategies (figs. 4.32-4.34). LTC performance is similar whichever strategy is chosen. However, transient comparisons must also be taken into account when choosing a control strategy. This is discussed at greater length in the following chapter on transient performance.

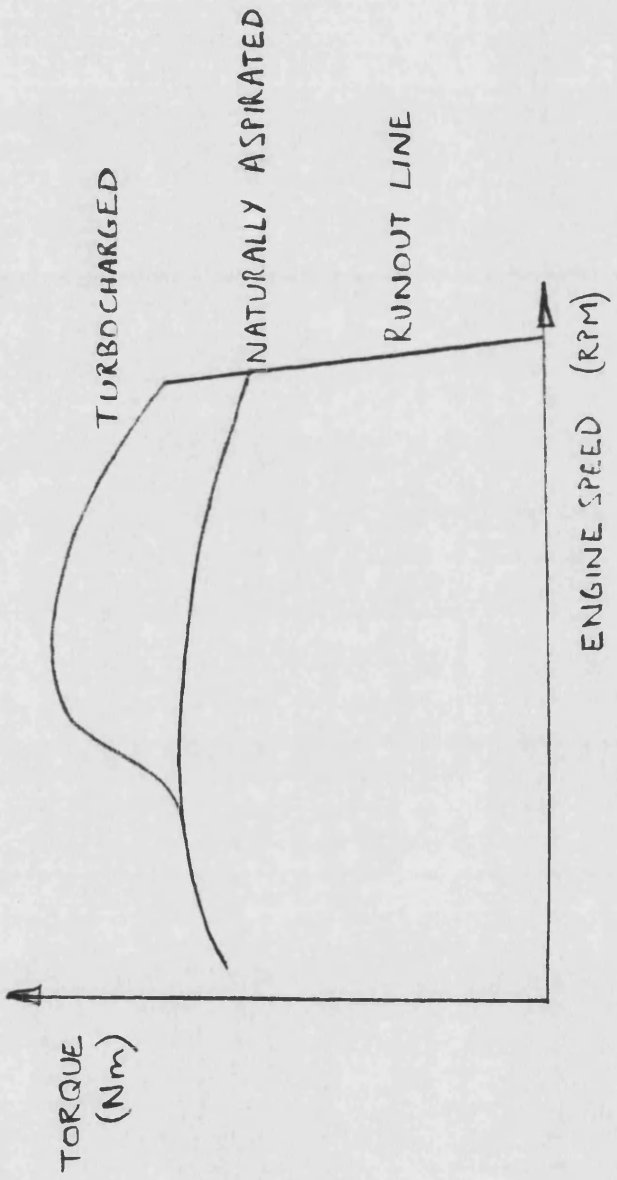

FIG 4.1 TORQUE CURVES FOR NATURALLY ASPIRATED AND TURBOCHARGED DIESEL ENGINES

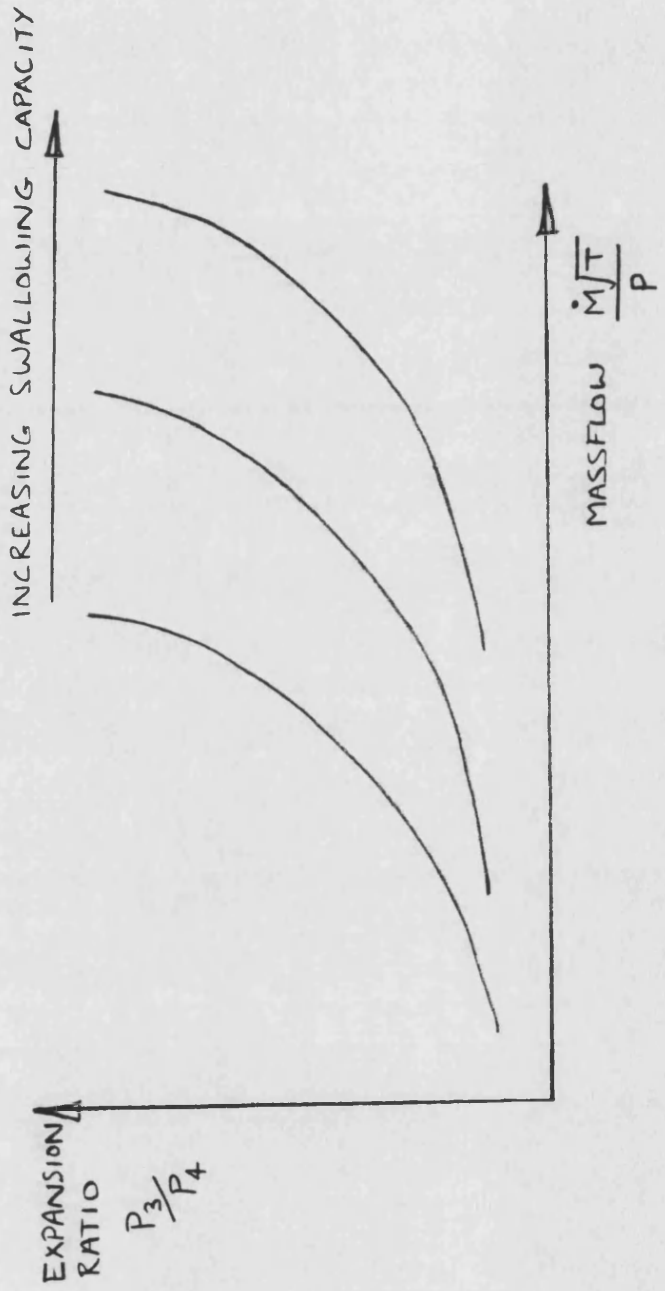

FIG. 4.2 VARIABLE TURBINE SWALLOWING CAPACITY

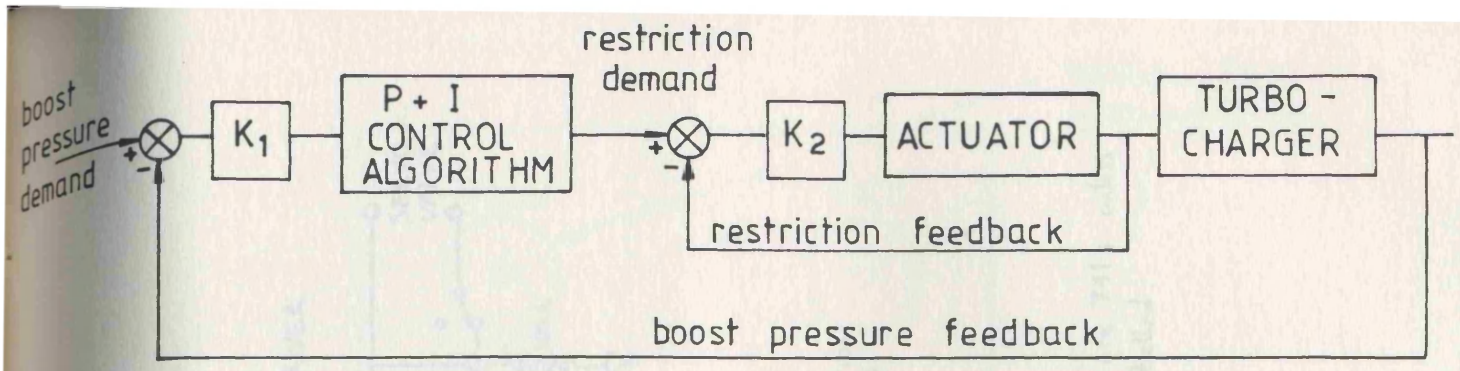

(a) TURBINE RESTRICTION CONTROL

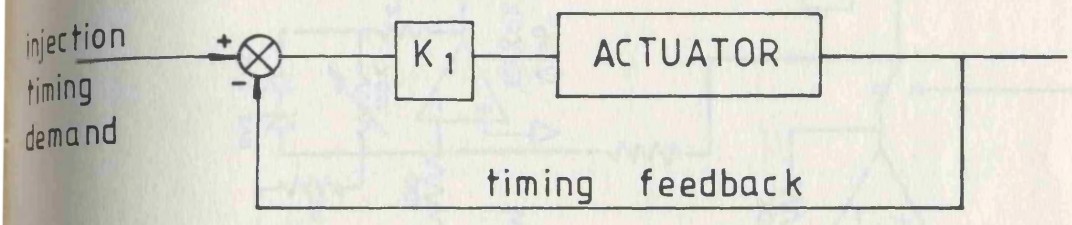

(b) INJECTION TIMING CONTROL

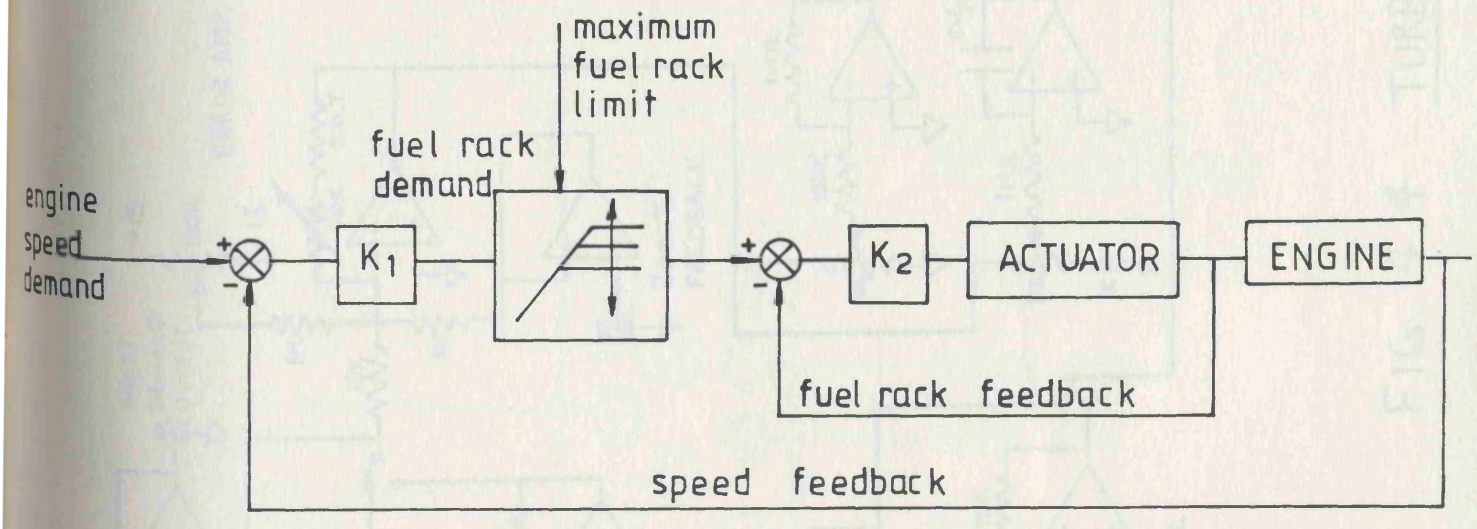

(c) FUEL PUMP CONTROL

NOTE: All demands can be either by manual adjustment (potentiometer setting) or by external voltage inputs (computer generated if required)

FIG. 4.3 CONTROL LOOPS

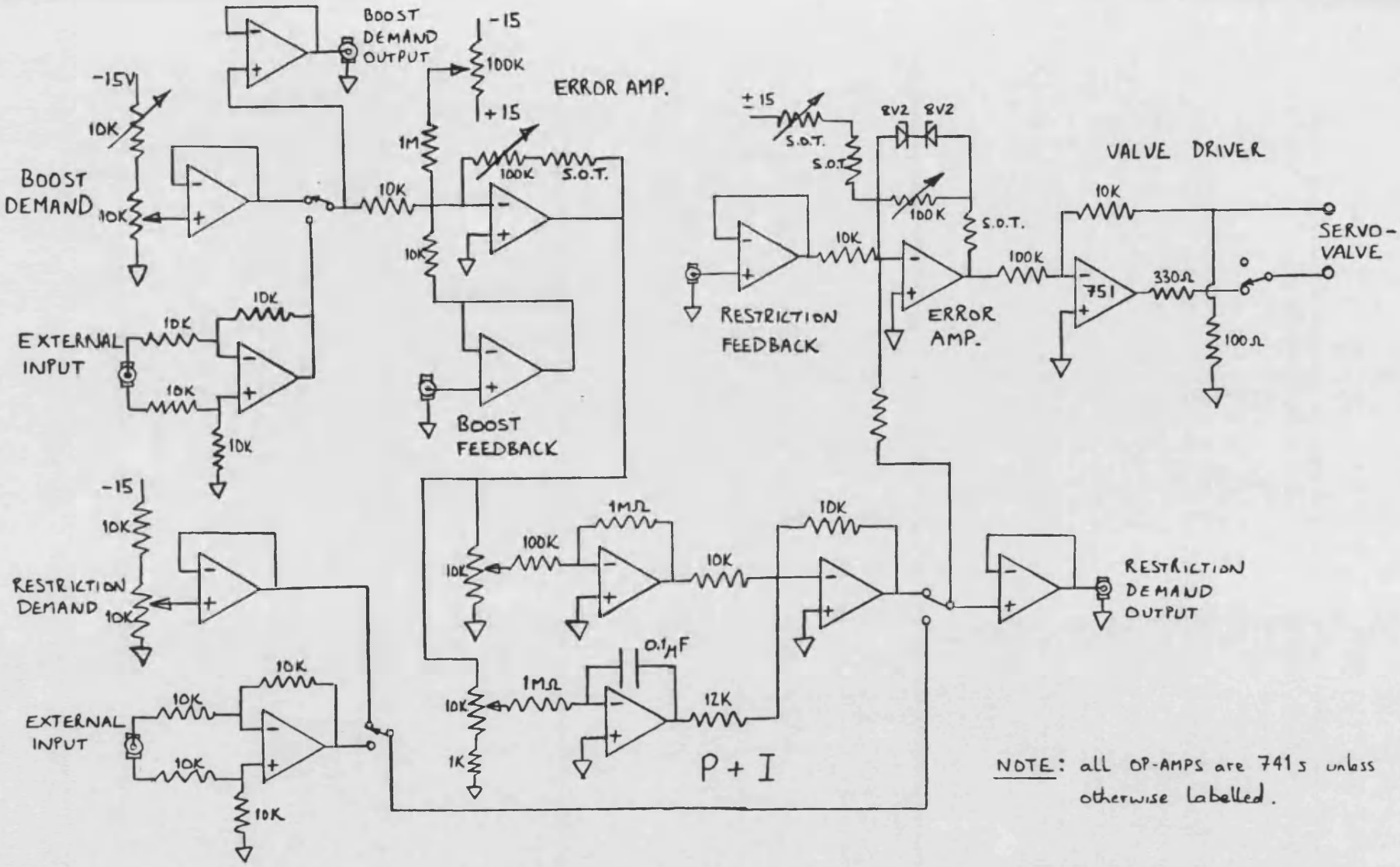

FIG. 4.4 TURBOCHARGER CONTROLS

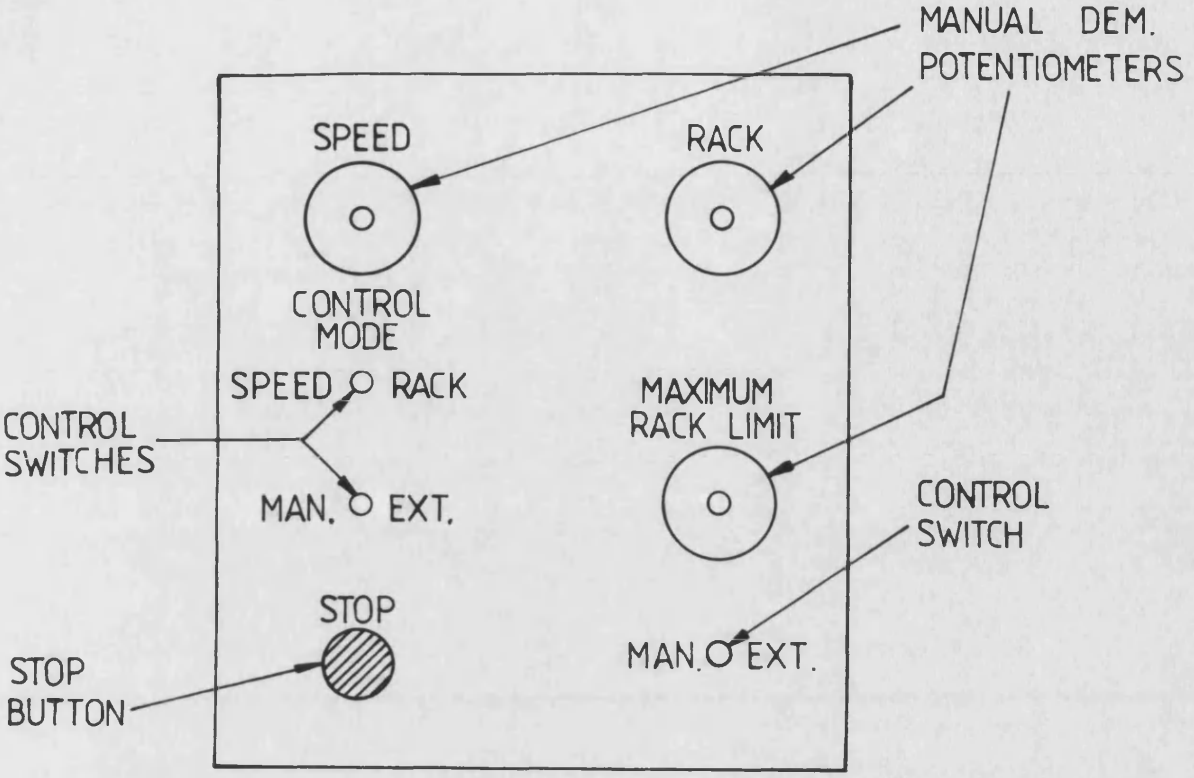

(a) LAYOUT OF FRONT PANEL

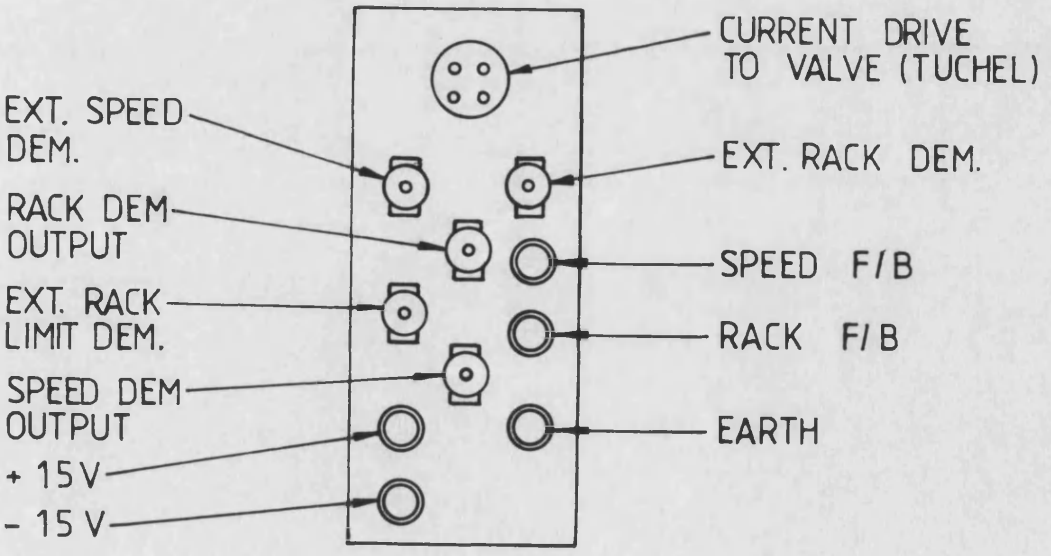

(b) LAYOUT OF BACK MODULE

FIG. 4.5 ELECTRONIC GOVERNOR DESIGN

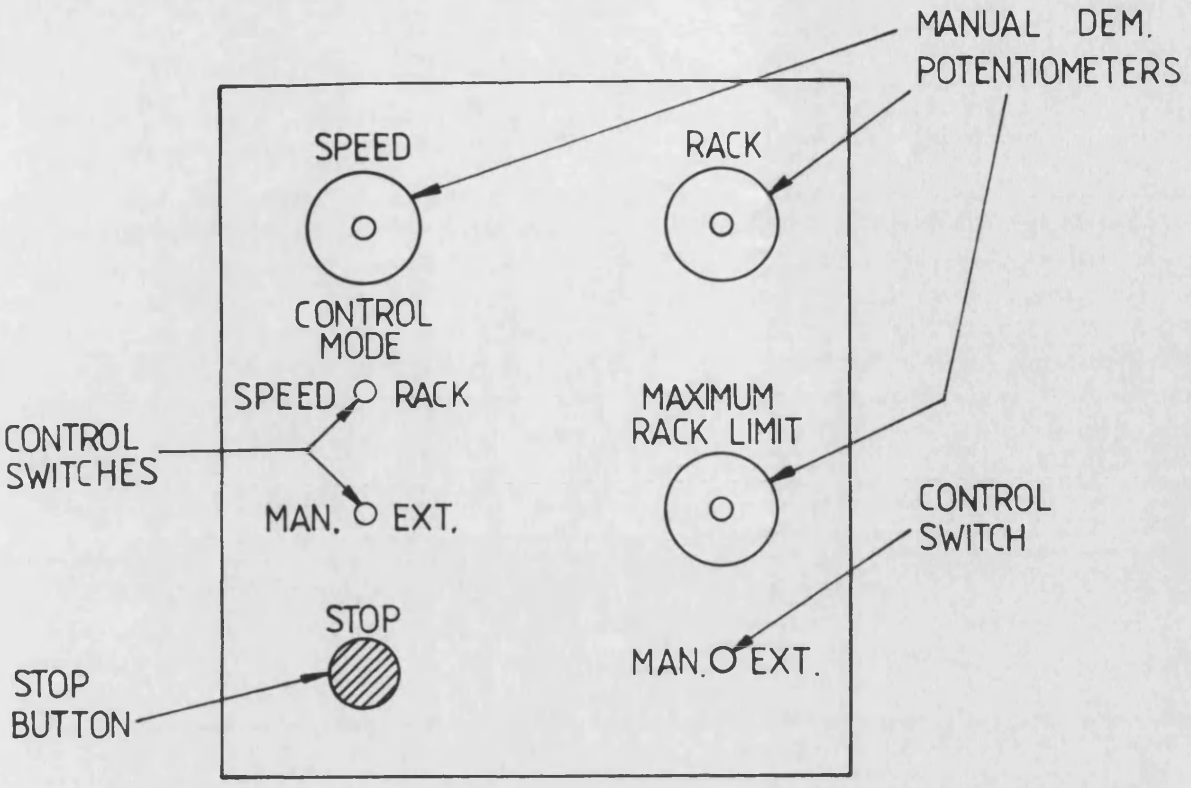

(a) LAYOUT OF FRONT PANEL

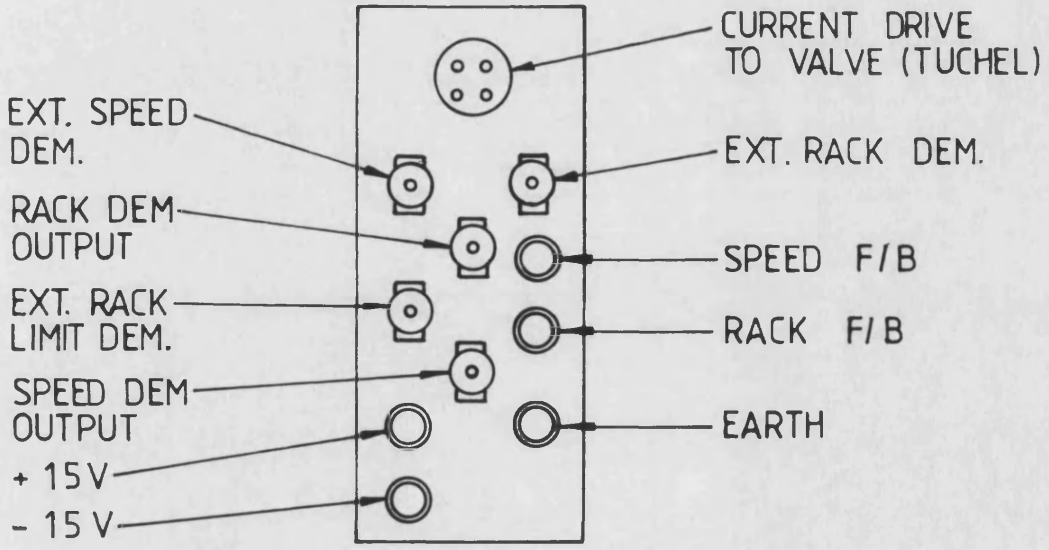

(b) LAYOUT OF BACK MODULE

FIG. 4.5 ELECTRONIC GOVERNOR DESIGN

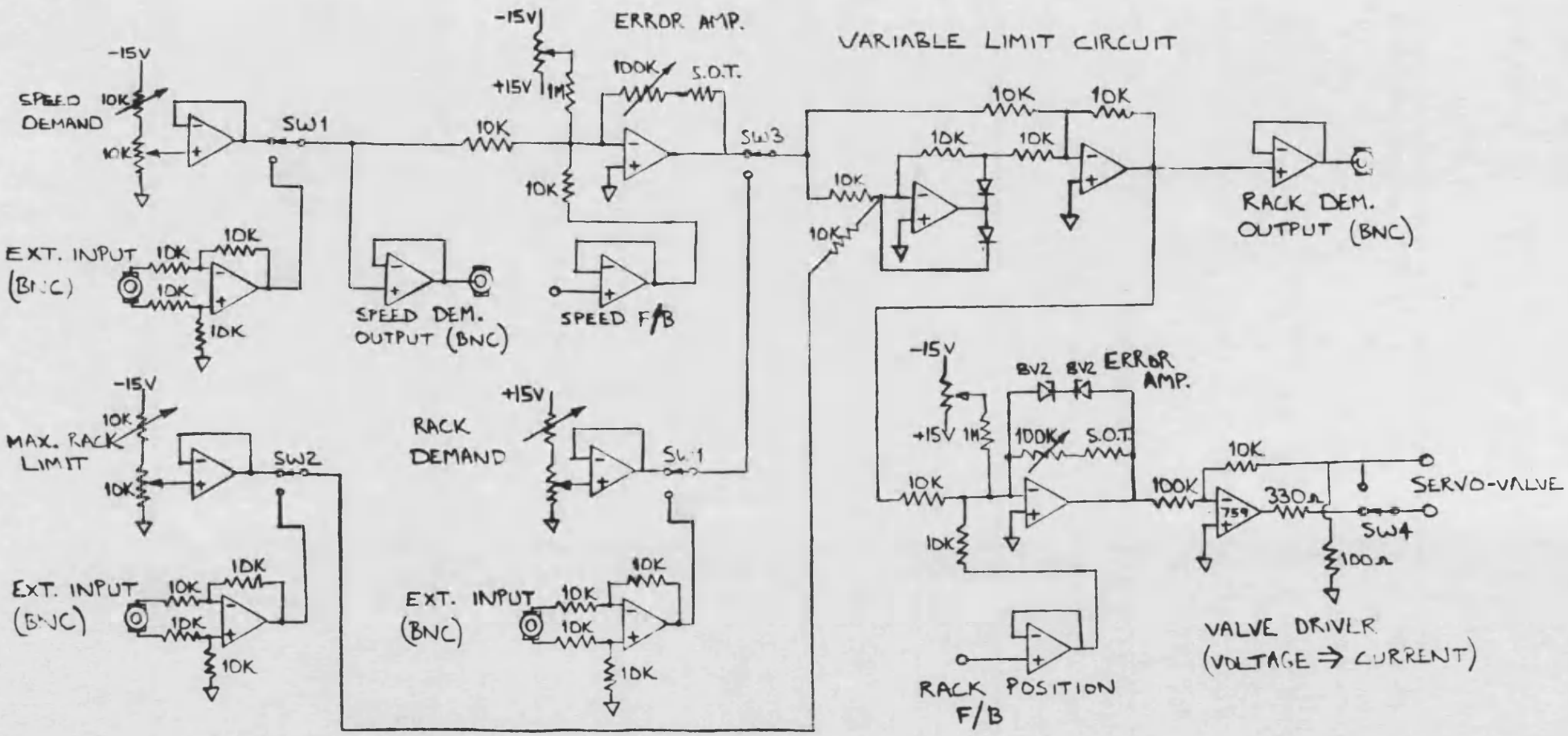

FIG. 4.6 ELECTRONIC GOVERNOR CIRCUIT DESIGN

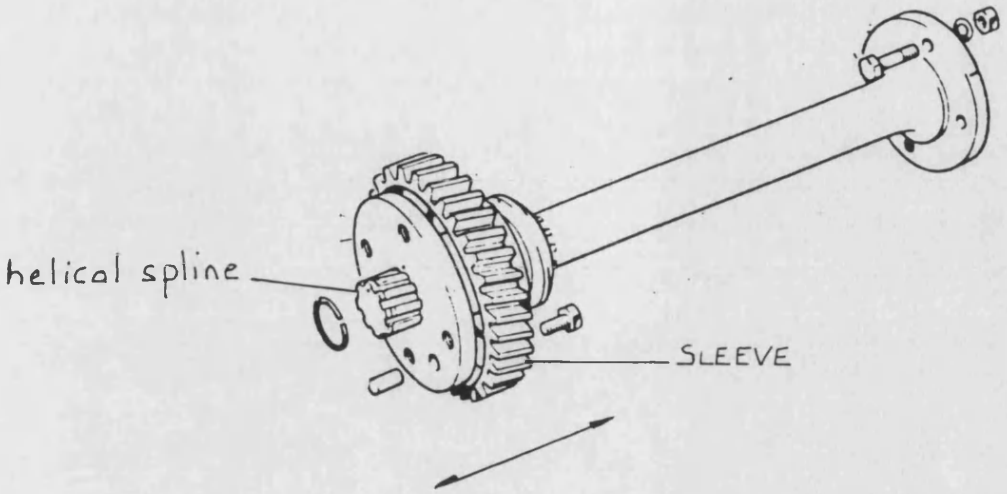

(a) TIMING GEARS

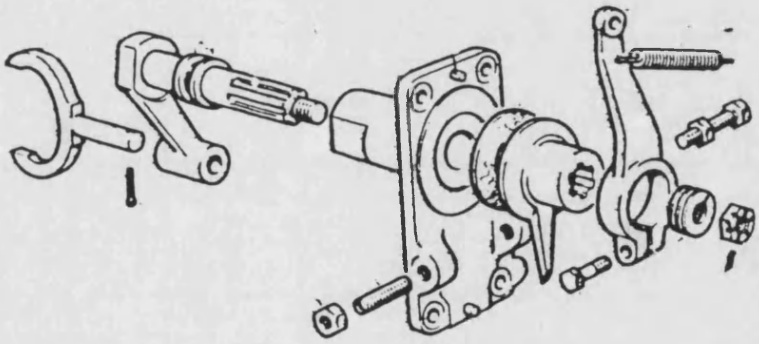

(b) ACTUATING LEVER

FIG. 4.7 GARDNER VARIABLE TIMING PARTS

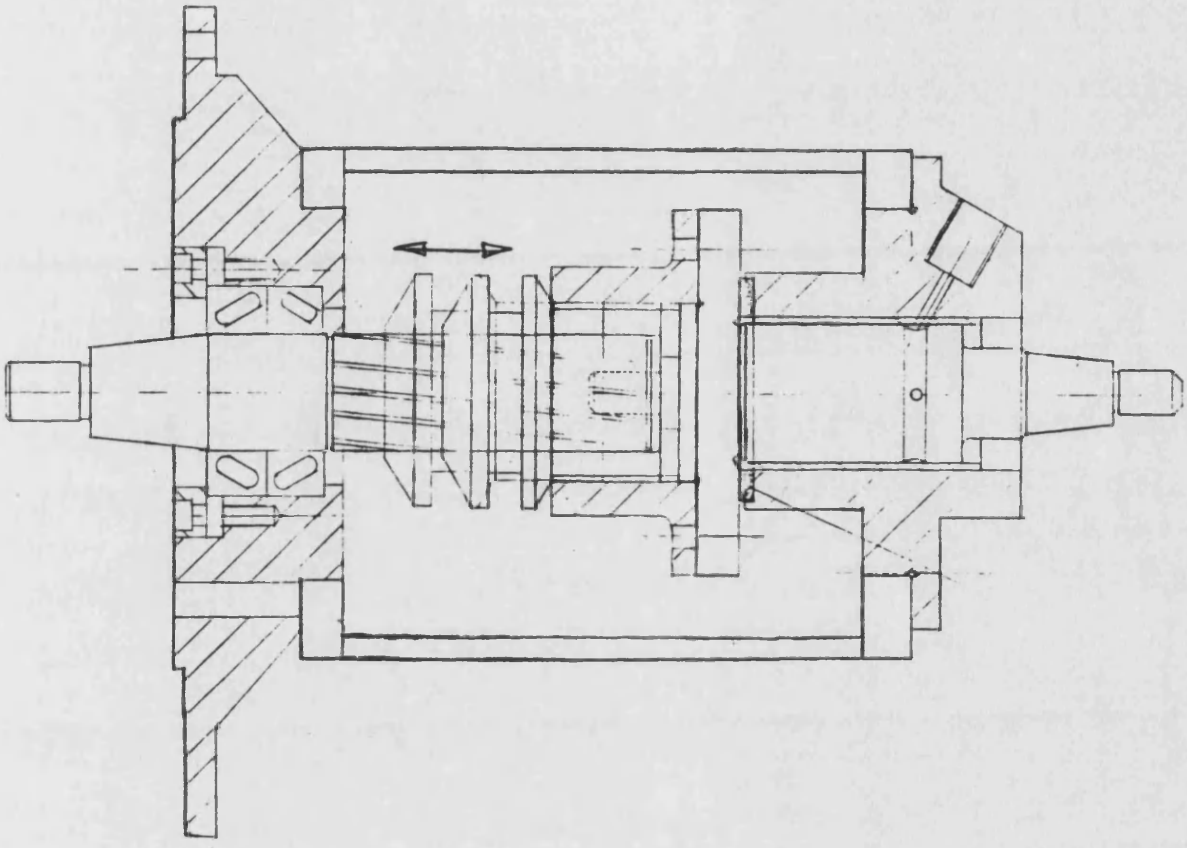

FIG. 4.8 VARIABLE TIMING DEVICE

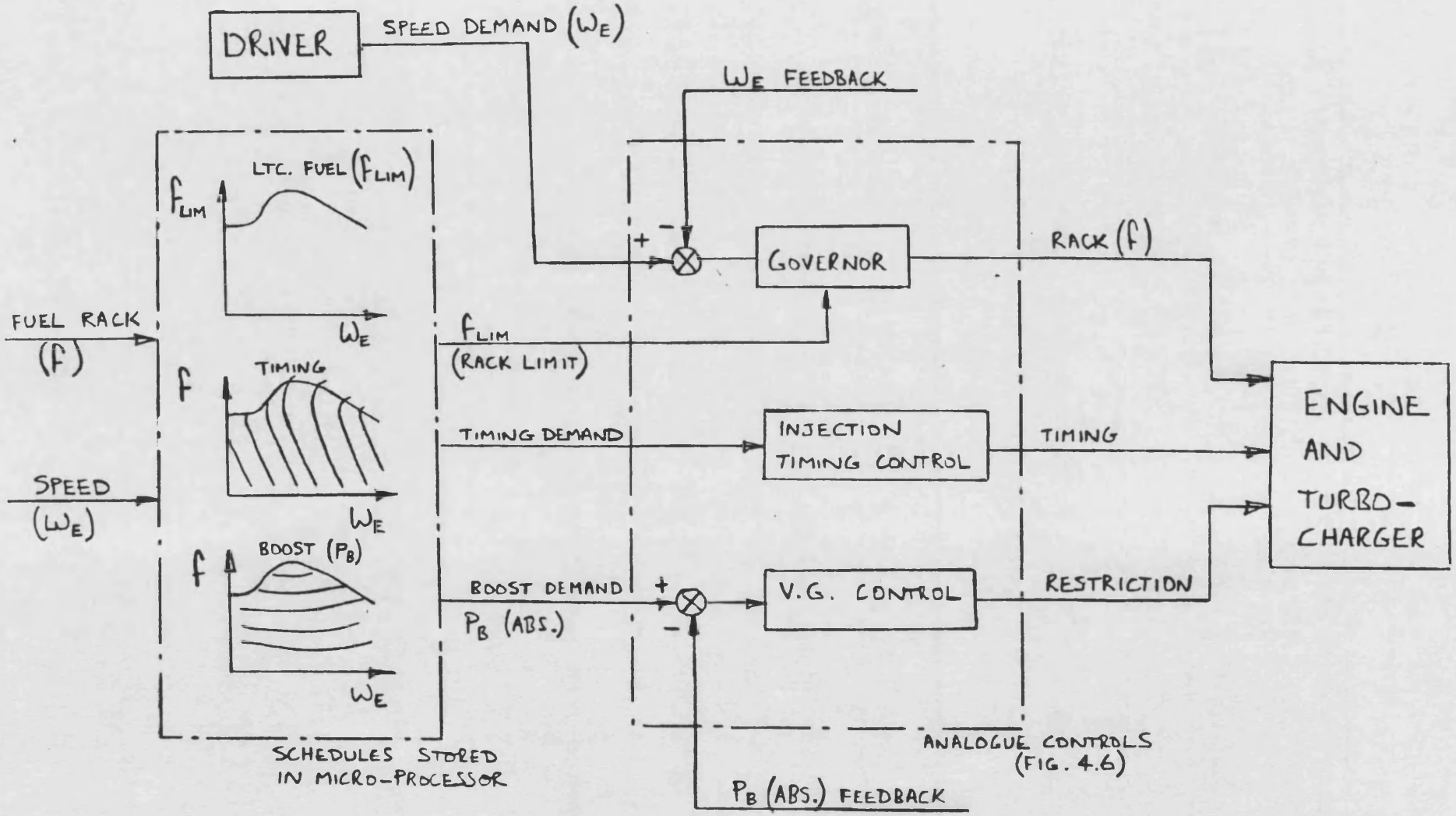

FIG. 4.9 STEADY-STATE CONTROL SYSTEM

Date ..... Graph .....

Engine LEYLAND TL11 ENGINE—11.1L DISPLACEMENT

Drawn By .....

Title CALIBRATION OF MAJORMEC PUMP WITH ELECTRONIC GOVERNOR

Power Curve Rating—190 kW at 2100 rev/min

Holset / Leyland / Dowty / DoI Contract

Test No.	Timing	Amb'nt °C	Barometer mm Hg.

FUEL MASSFLOW VS. RACK AND SPEED

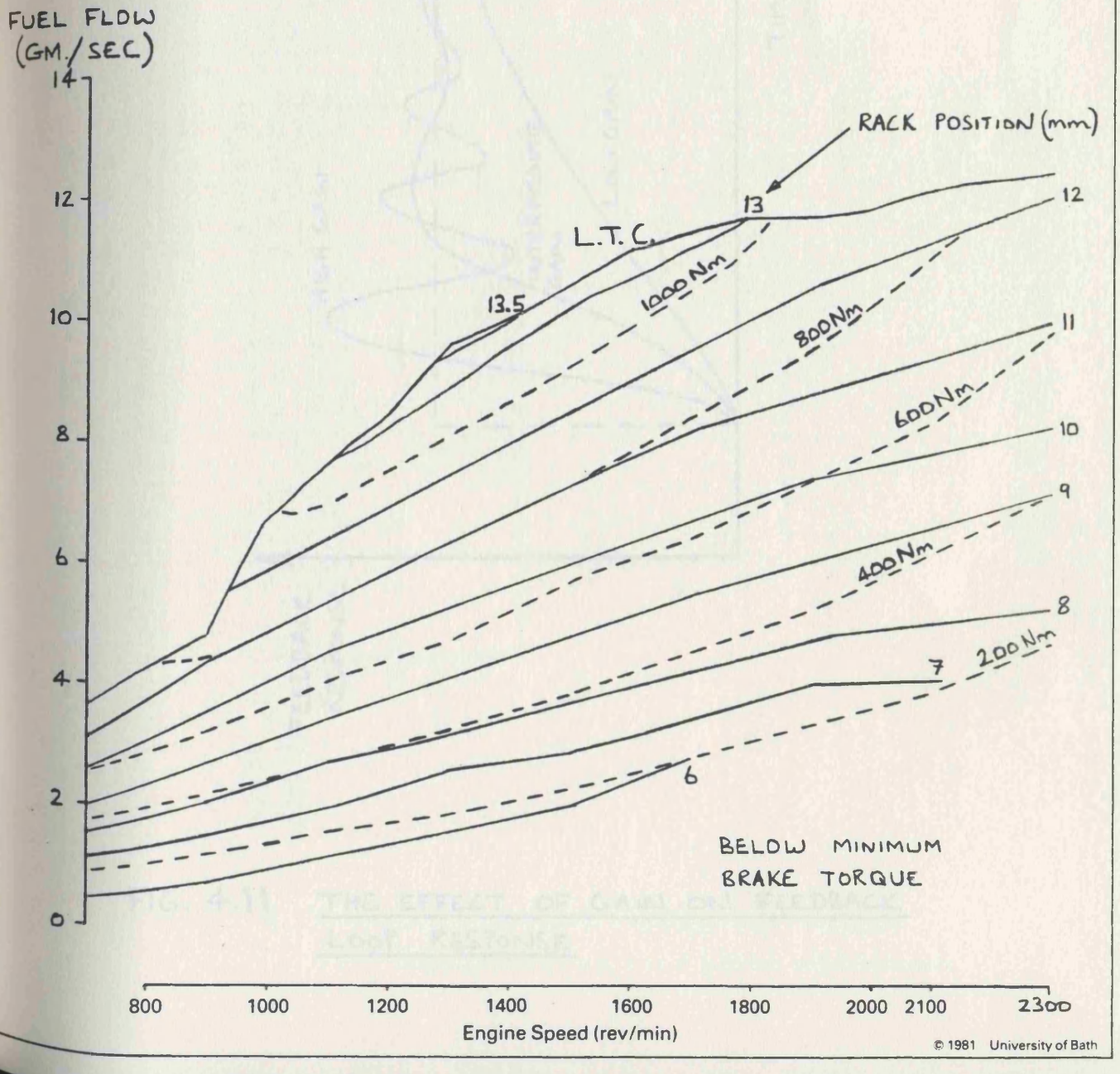

FIG. 4.10

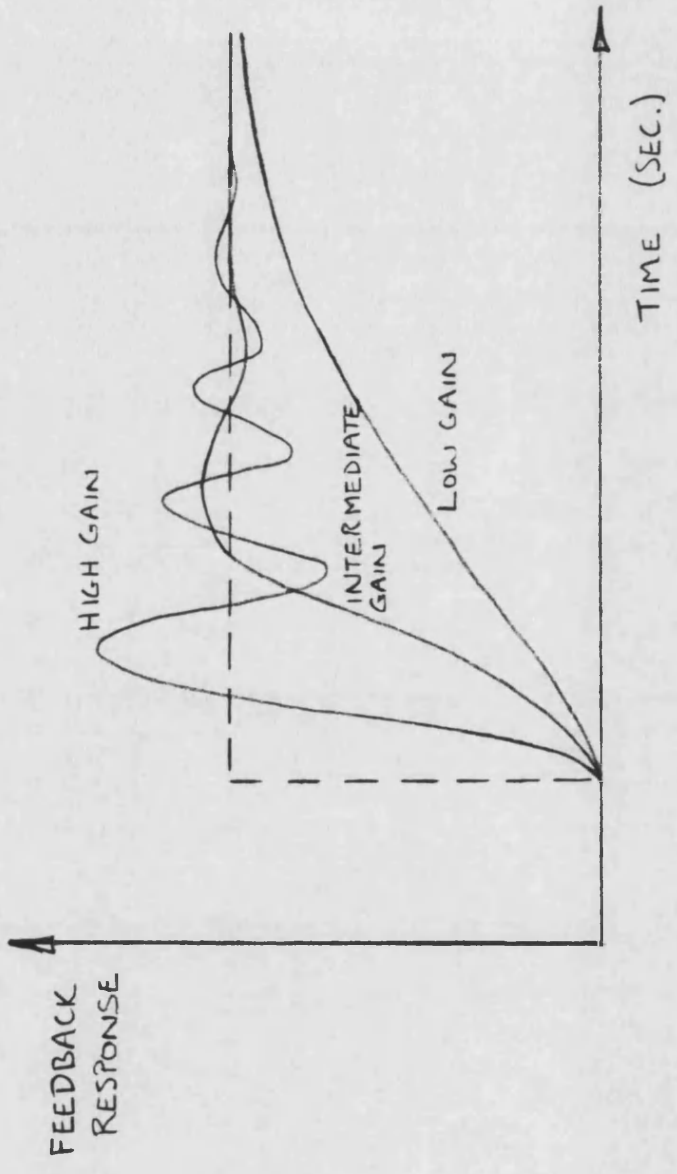

FIG. 4.11 THE EFFECT OF GAIN ON FEEDBACK LOOP RESPONSE

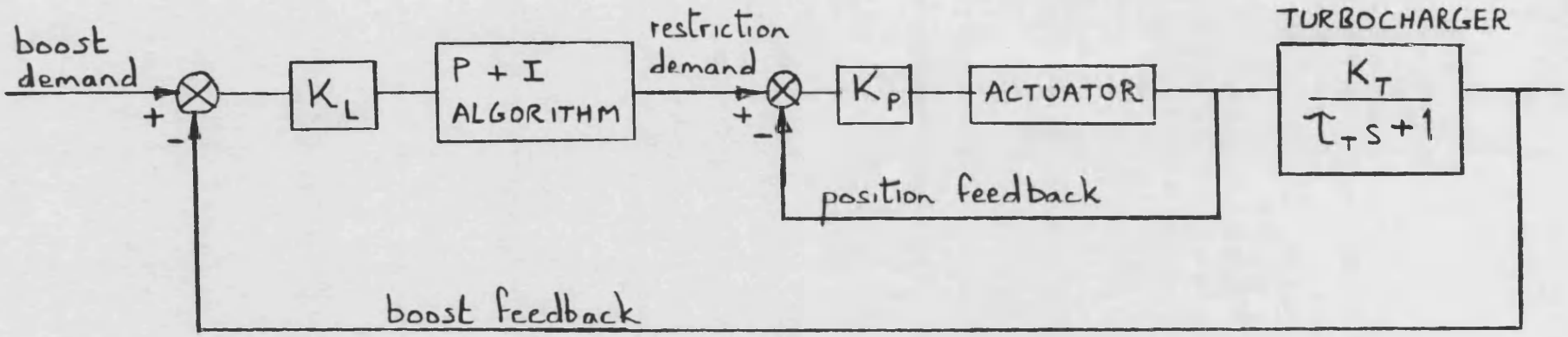

K_L — adjustable boost loop gain

K_P — adjustable position loop gain

K_T — inherant turbo' gain (dependant upon exhaust enthalpy)

τ_T — turbo' time constant (a function of inertia)

FIG. 4.12 BOOST PRESSURE FEEDBACK LOOP

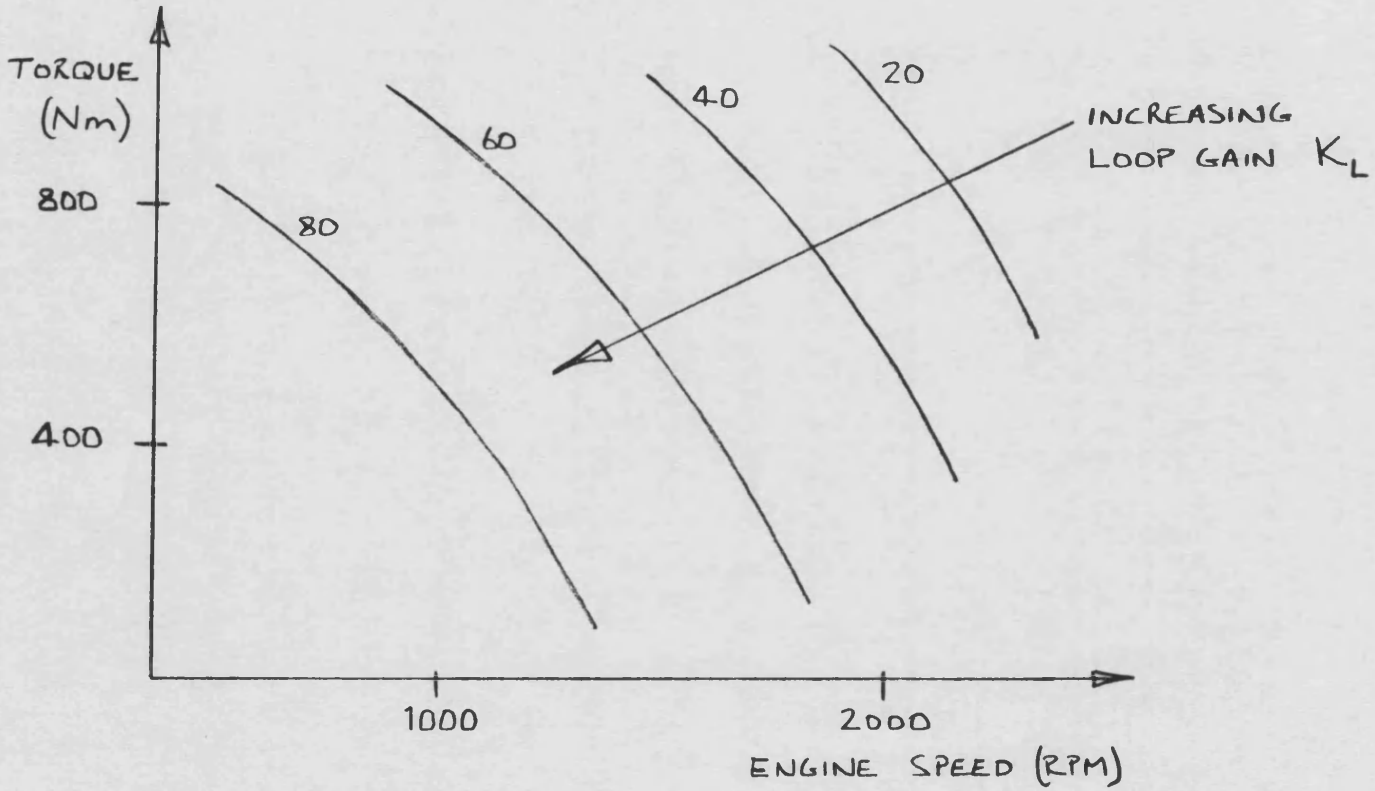

FIG. 4.13 LOOP GAIN VS. SPEED AND TORQUE CONSISTENT WITH STABLE OPERATION

NOTE: this is a sketch indicating the form of relationship only

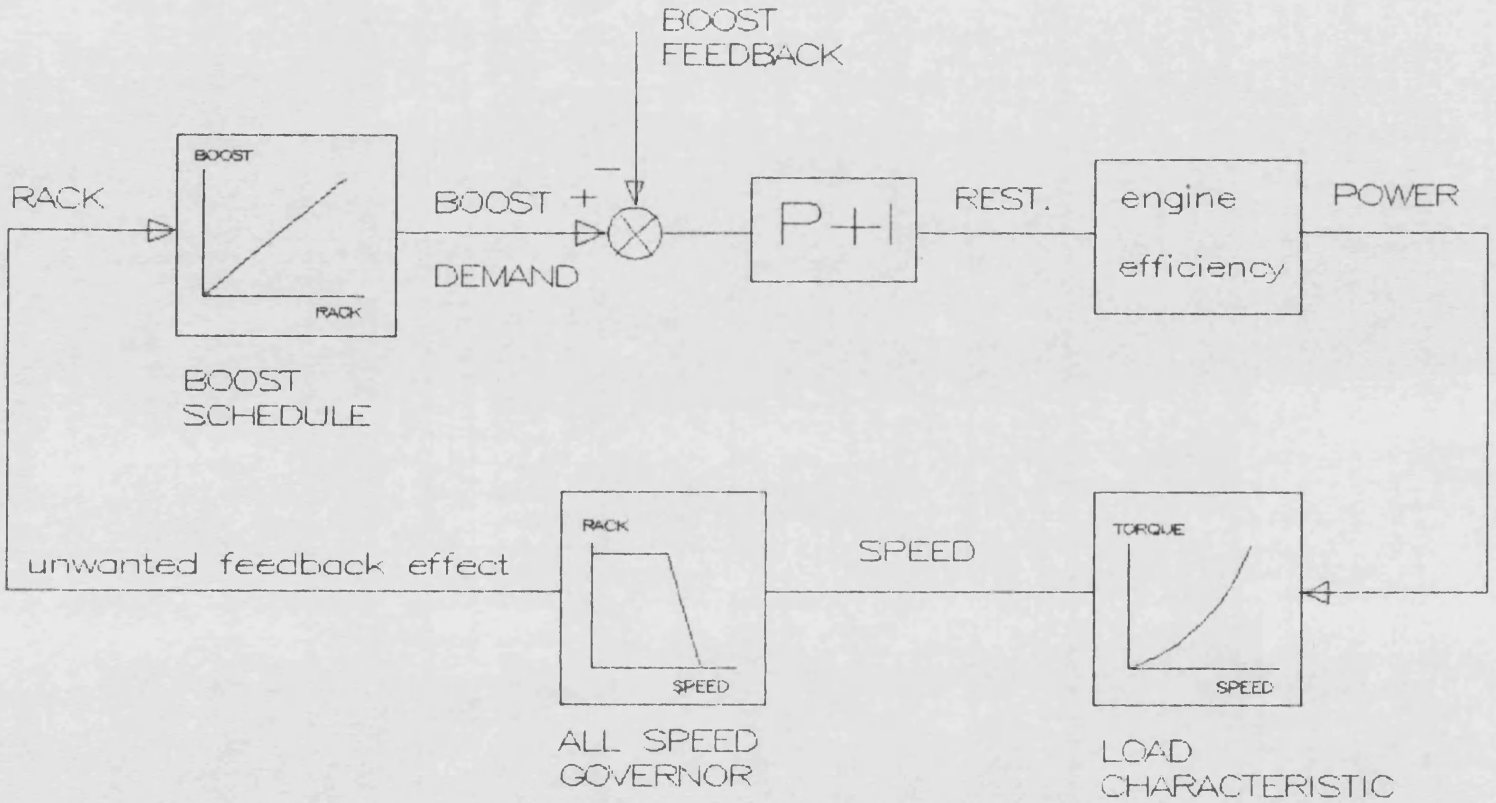

FIG. 4.14 The effect of all speed governing on the computer scheduling of boost pressure

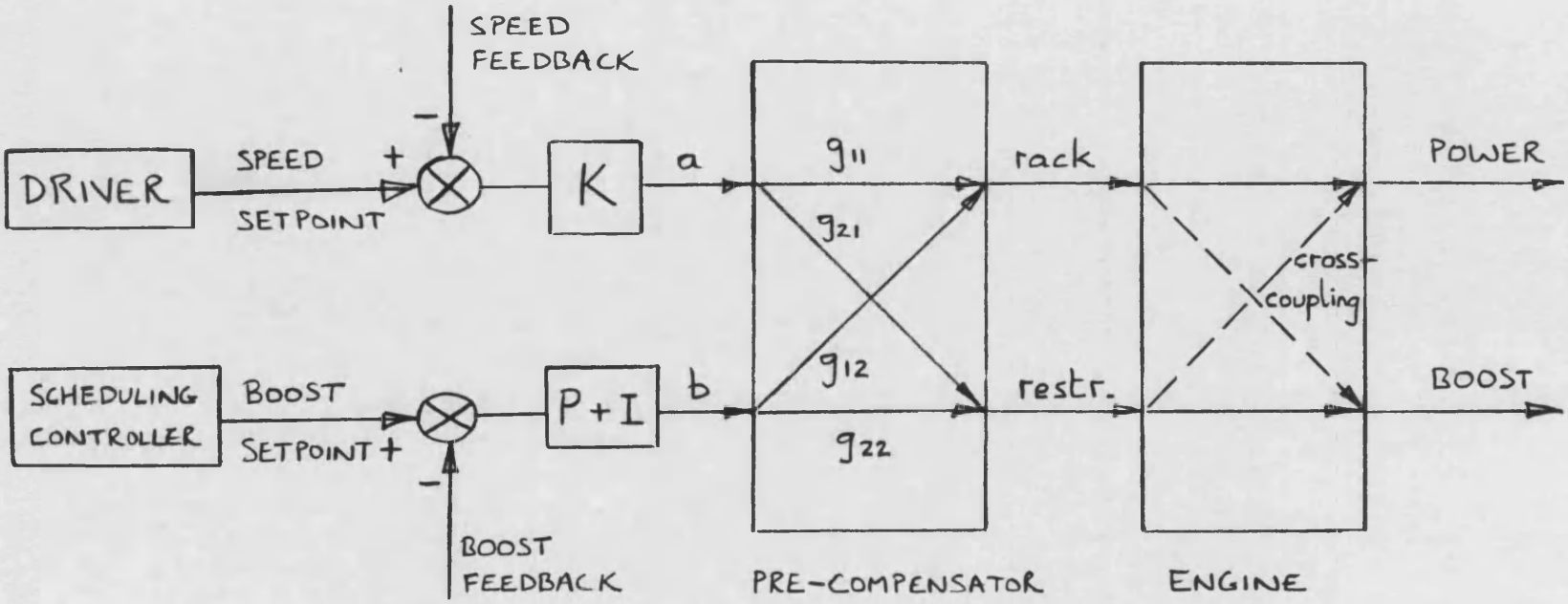

$$\begin{pmatrix} \text{rack} \\ \text{restr.} \end{pmatrix} = \begin{pmatrix} g_{11} & g_{12} \\ g_{21} & g_{22} \end{pmatrix} \begin{pmatrix} a \\ b \end{pmatrix}$$

FIG. 4.15 ENGINE CONTROL WITH A MULTI-VARIABLE PRE-COMPENSATOR

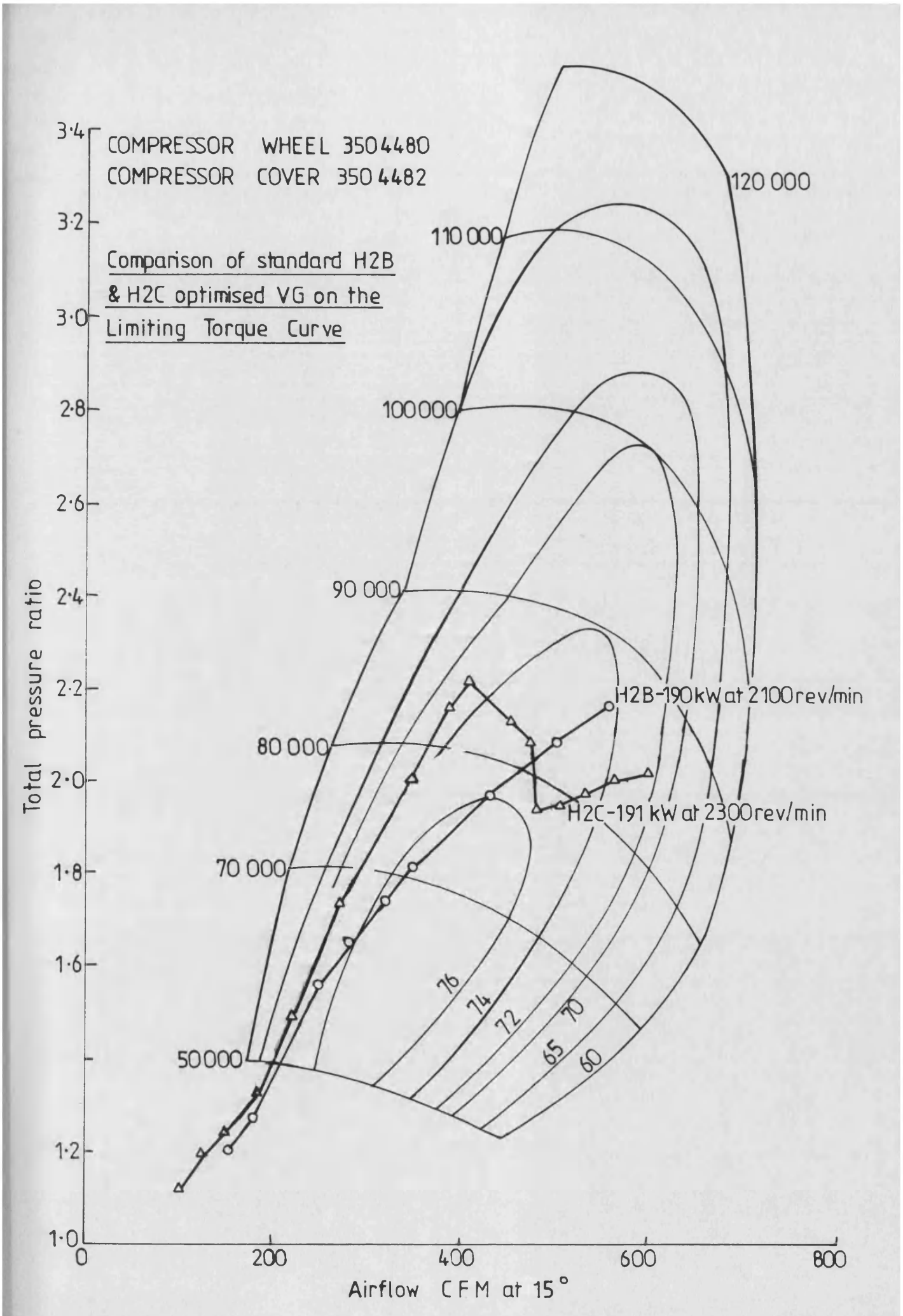

FIG. 4.16 COMPRESSOR MAP

Date..... Graph.....

Engine LEYLAND TL11 ENGINE—11.1L DISPLACEMENT Drawn By .....

Title LTC. PERFORMANCE — BASE & MANUALLY OPTIMISED

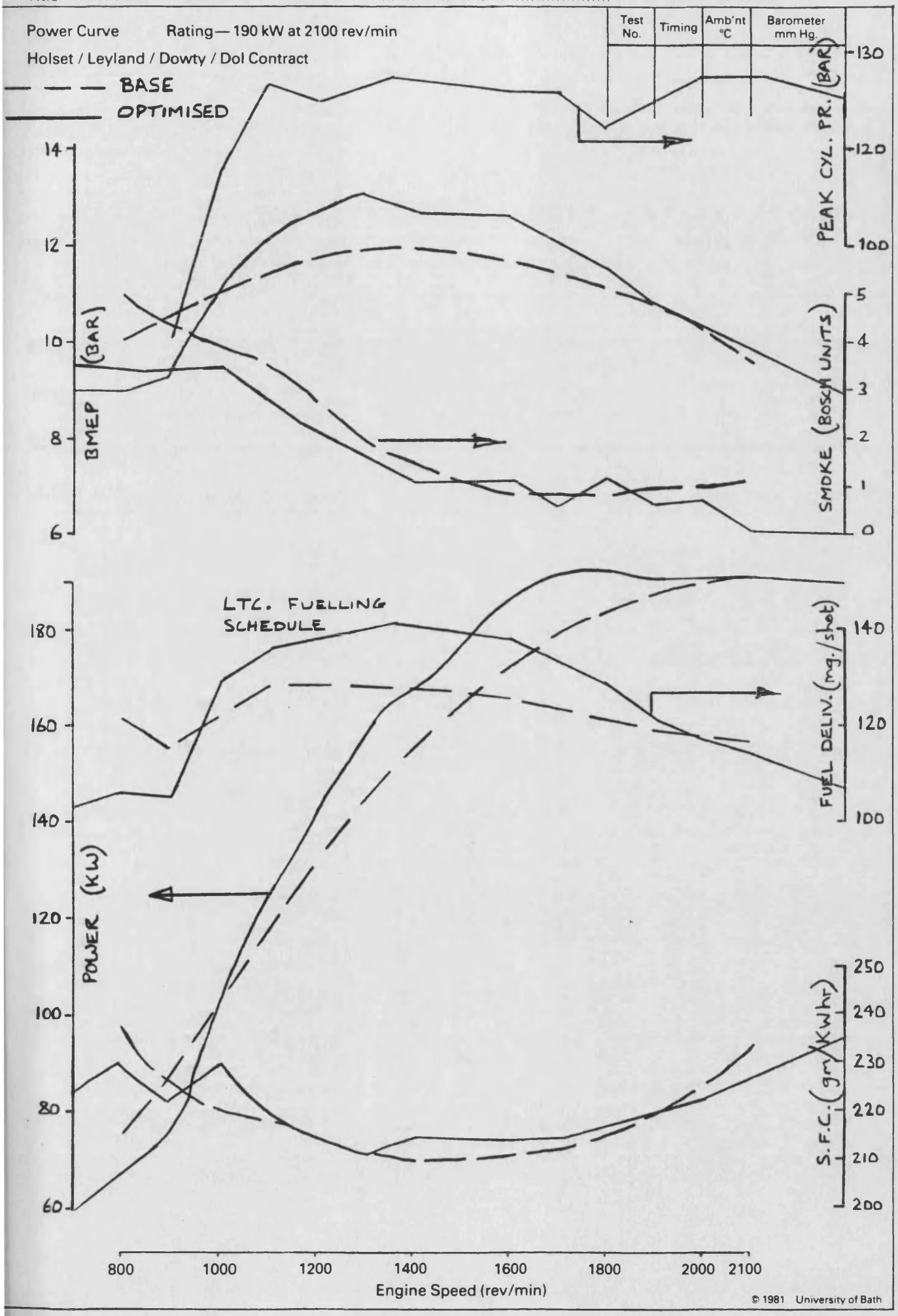

FIG 4.17

Date ..... Graph .....

Engine LEYLAND TL11 ENGINE—11.1L DISPLACEMENT

Drawn By .....

Title LTC. PERFORMANCE — BASE + MANUALLY OPTIMISED

Power Curve Rating—190 kW at 2100 rev/min

Holset / Leyland / Dowty / DoI Contract

— — — BASE

——— OPTIMISED

Test No.	Timing	Amb'nt °C	Barometer mm Hg.

NB. 10V ≙ 22° SWING

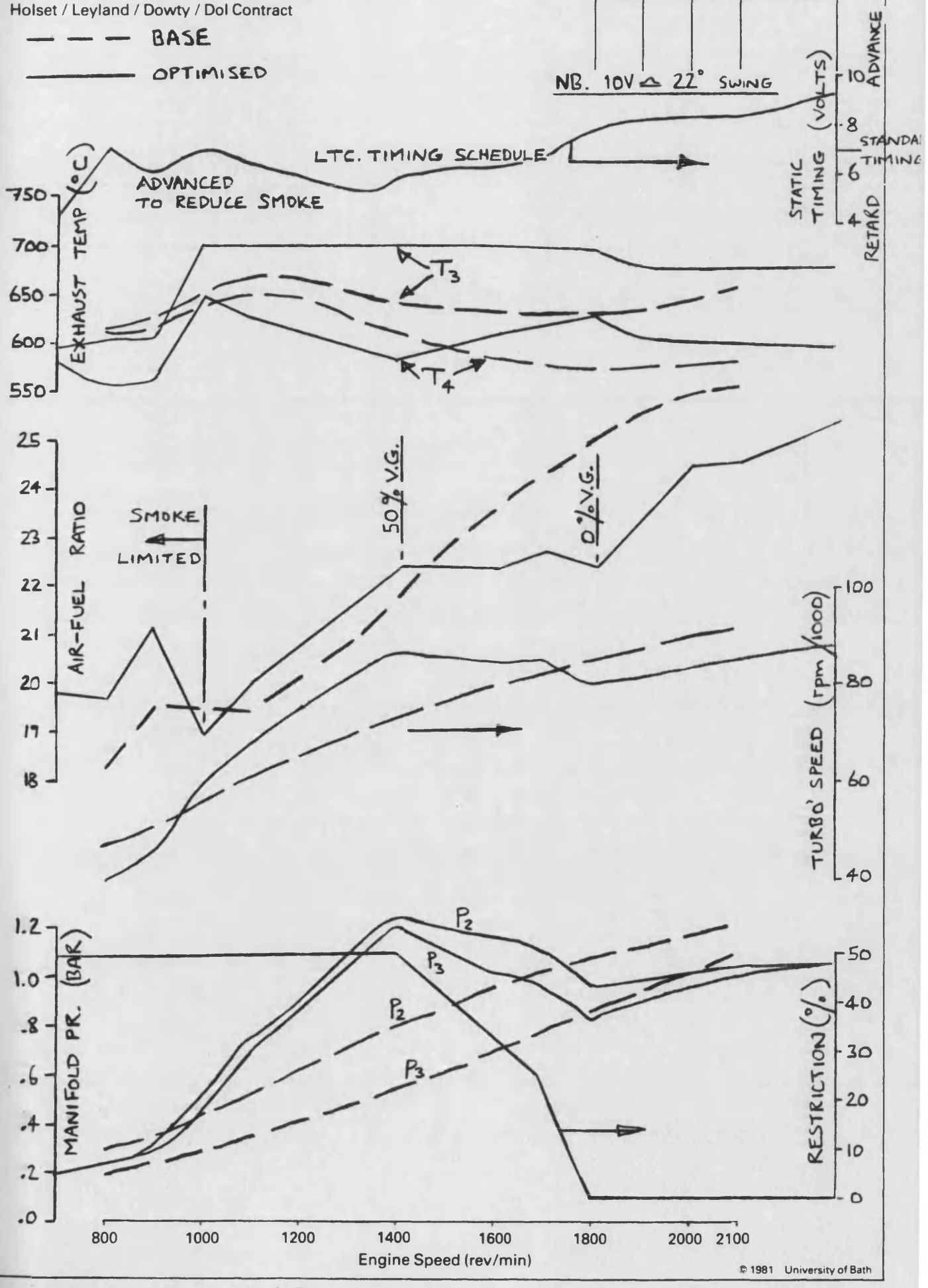

FIG 4.18

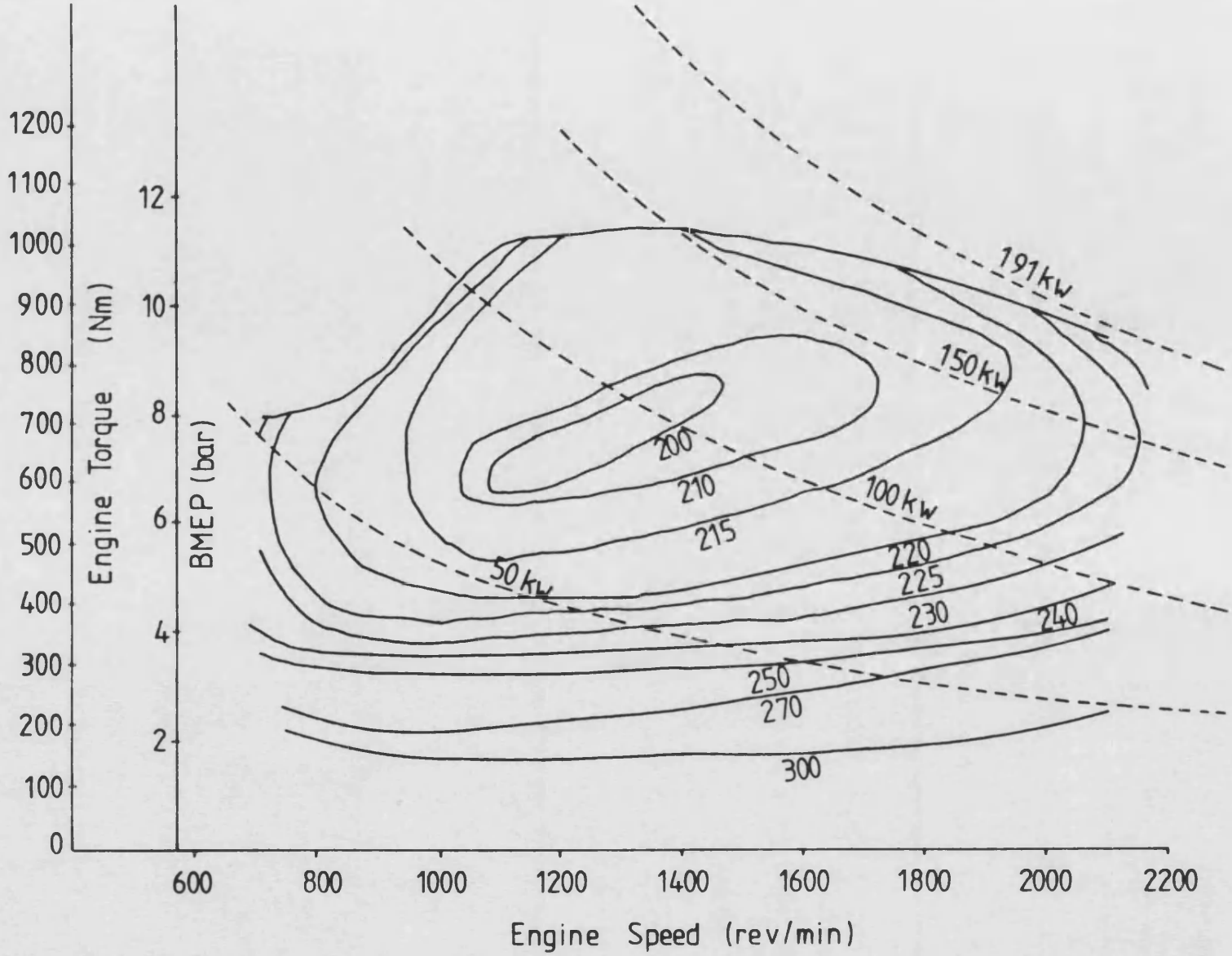

FIG. 4.19 BASELINE ENGINE PERFORMANCE MAP

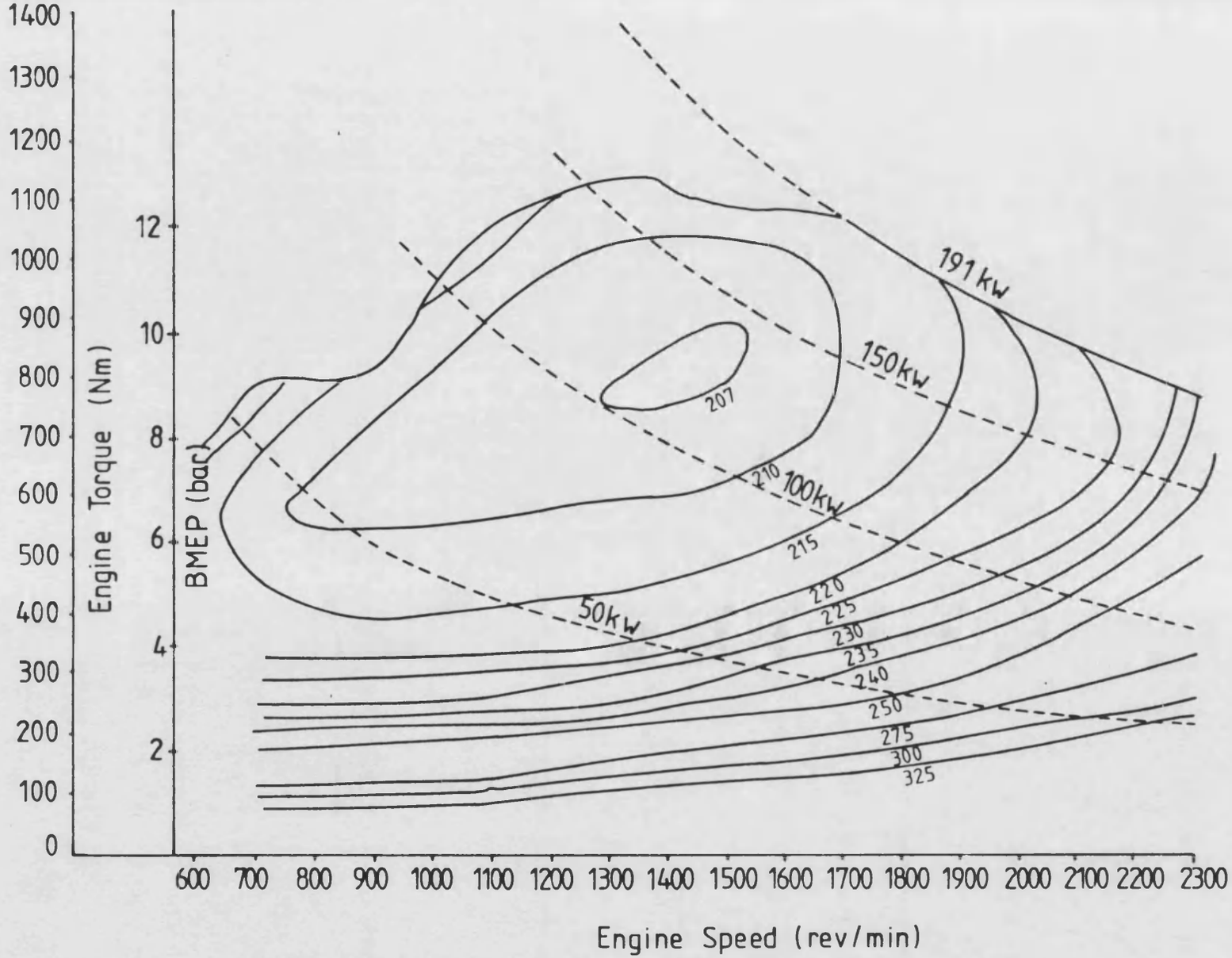

FIG. 4.20 STEADY STATE OPTIMIZATION
(FULLY OPTIMIZED SYSTEM)

Date 12.5.83 Graph

Engine LEYLAND TL11 ENGINE—11.1L DISPLACEMENT Drawn By. D. HOWARD

Title TIMING (ANALOGUE VOLTAGE) VS. SPEED & RACK

Constant Speed Curve at 2100 rev/min

Holset / Leyland / Dowty / DoI Contract

Test No.	Timing	Amb'nt °C	Barometer Ins. Hg.
	VARIABLE	22	

STEADY-STATE OPTIMISATION

TIMING — ANALOGUE VOLTAGE

0—10V ≈ 22° TIMING SWING AT THE FLYWHEEL

ADVANCE WITH LOAD & SPEED FOR MIN. SFC. AT PART LOAD.

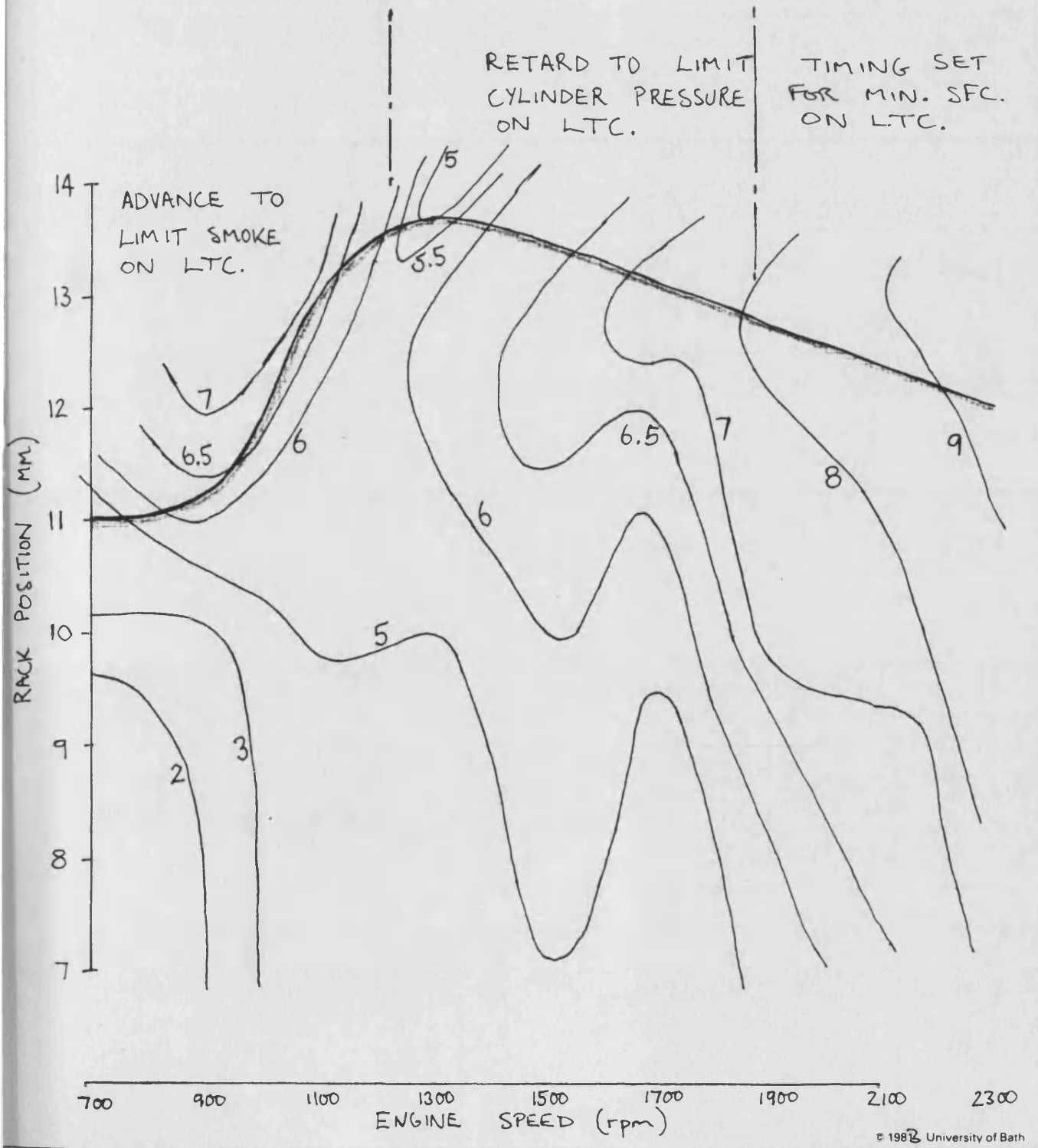

FIG 4.21

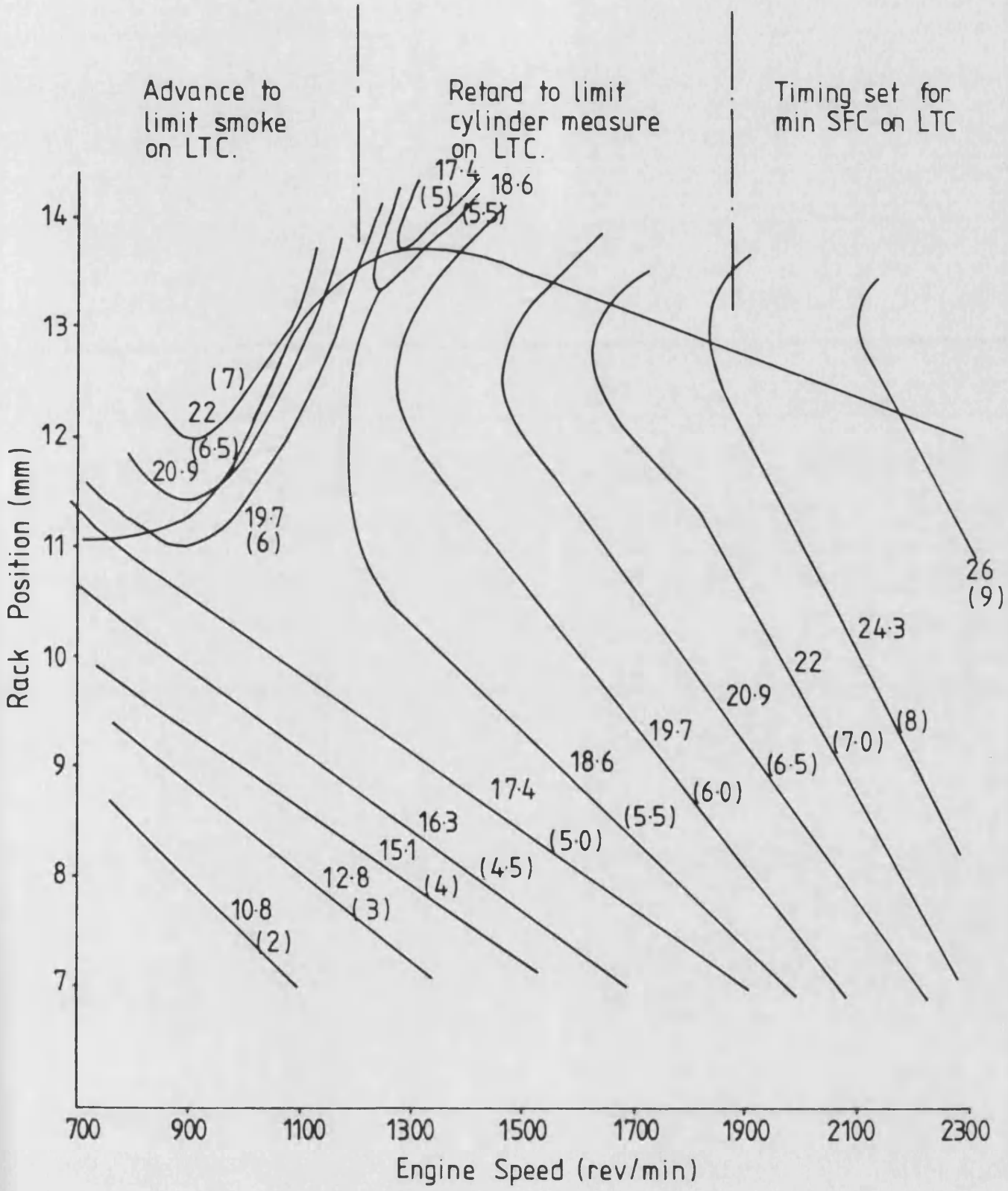

FIG. 4.22 STEADY STATE OPTIMIZATION
STATIC INJECTION TIMING SCHEDULE

Engine LEYLAND TL11 ENGINE—11.1L DISPLACEMENT Drawn By. Z W Koberlein

Title TURBINE INLET RESTRICTION (%) AS A FUNCTION OF ENGINE SPEED & LOAD — OPTIMISED

STEADY STATE OPTIMISATION

Holset / Leyland / Dowty / DoI Contract

Test No.	Timing	Amb'nt °C	Barometer Ins. Hg.
	VARIABLE (22)	22	

191 kW @ 2300 rev/min. 46% TORQUE BACK UP @

1155 Nm @ 1350 rev/min. 59% OF RATED SPEED.

HOLSET H2C B625 Z31U11 TURBOCHARGER WITH A SINGLE ENTRY NOZZLED VARIABLE AREA TURBINE STAGE. CENTRE MOUNTED TO AN UNEQUAL AREA DIVIDED MANIFOLD (6 cylinder) WITH SIAMESED PORTS.

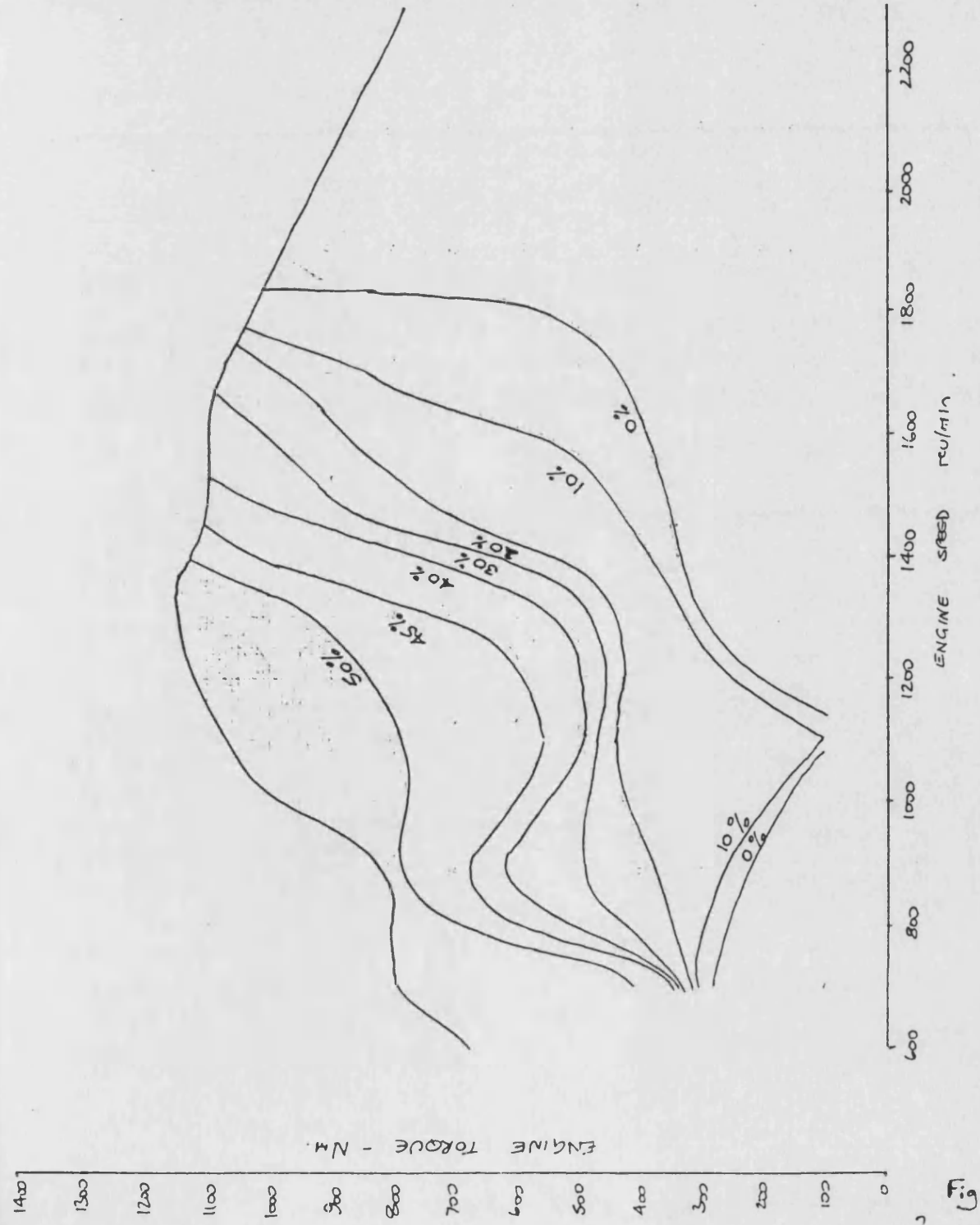

Fig 10

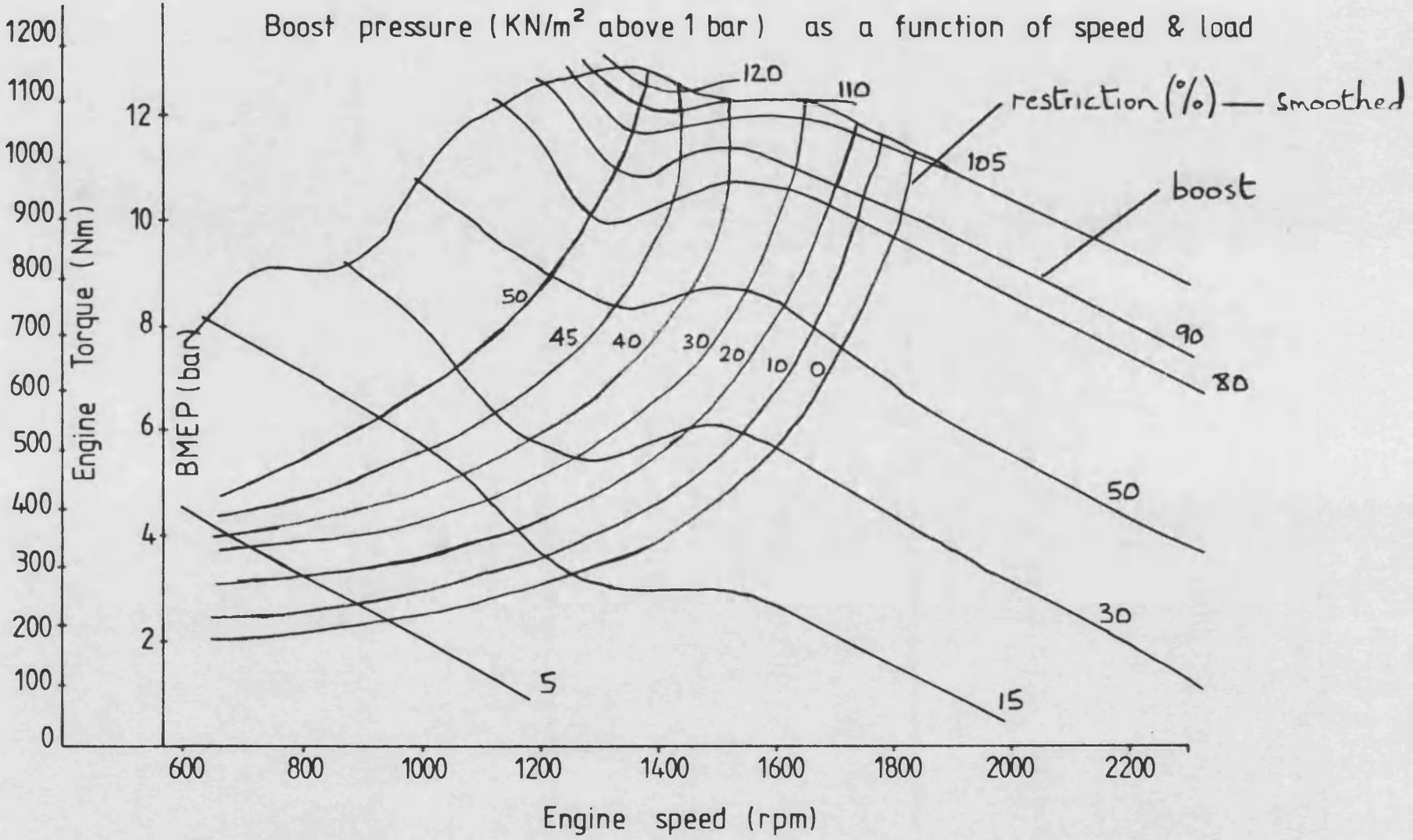

FIG. 4.24 STEADY STATE OPTIMIZATION:- LINES OF CONSTANT BOOST

Engine LEYLAND TL11 ENGINE—11.1L DISPLACEMENT

Date [illegible] Graph

Drawn By D. HOWARD

Title BOOST PRESSURE (STATIC – 750 MMHG) VS. SPEED & RACK

Constant Speed Curve at 2100 rev/min

Holset / Leyland / Dowty / DoI Contract

Test No.	Timing	Amb'nt °C	Barometer Ins. Hg.
	VARIABLE	22	

STEADY-STATE OPTIMISATION

BOOST PRESSURE ABOVE 750 MMHG

'STATIC' MMHG

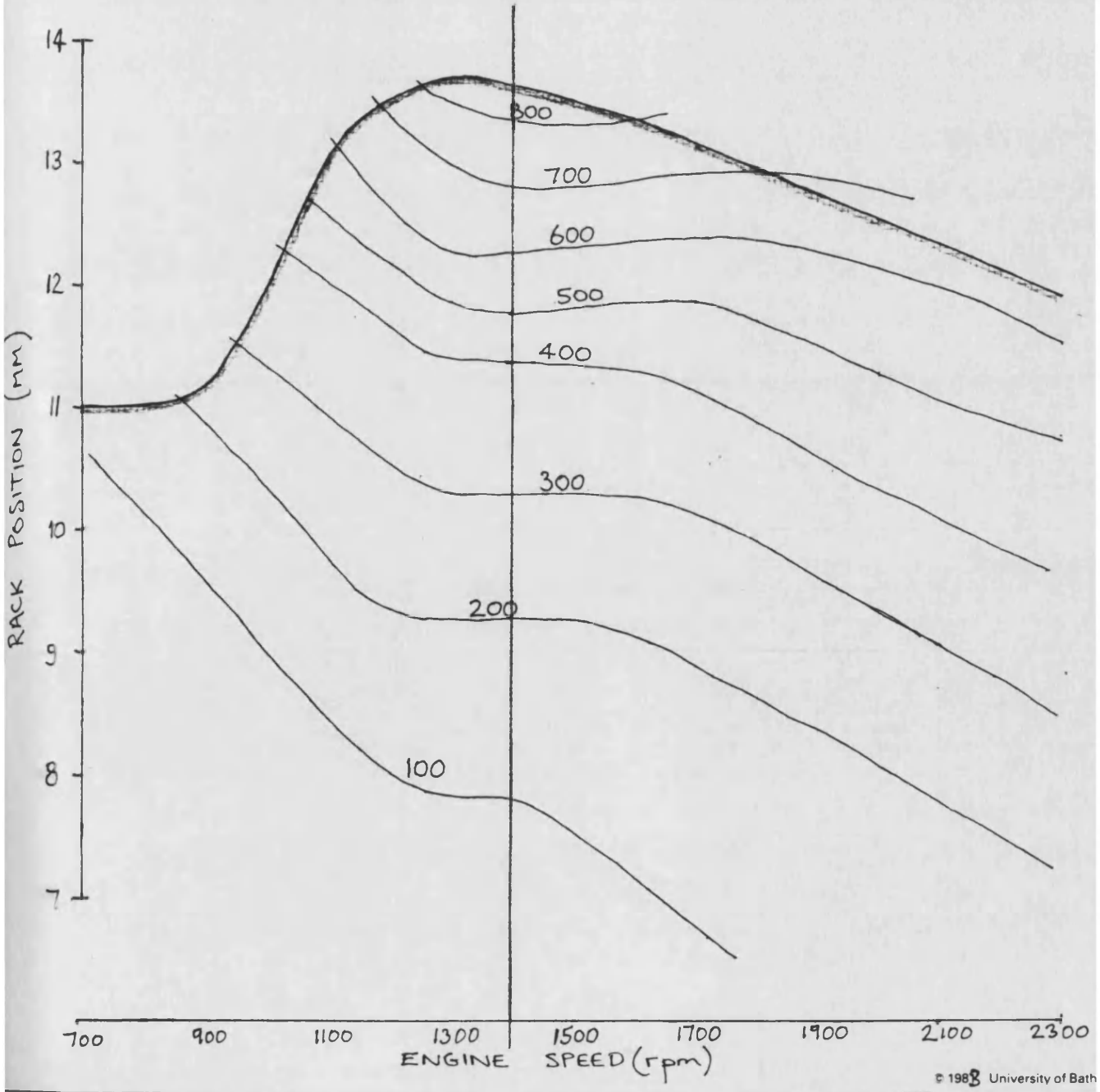

Equation: Timing = 1/250 (rev/min - 500) + 1/3·125 (rack - 5)

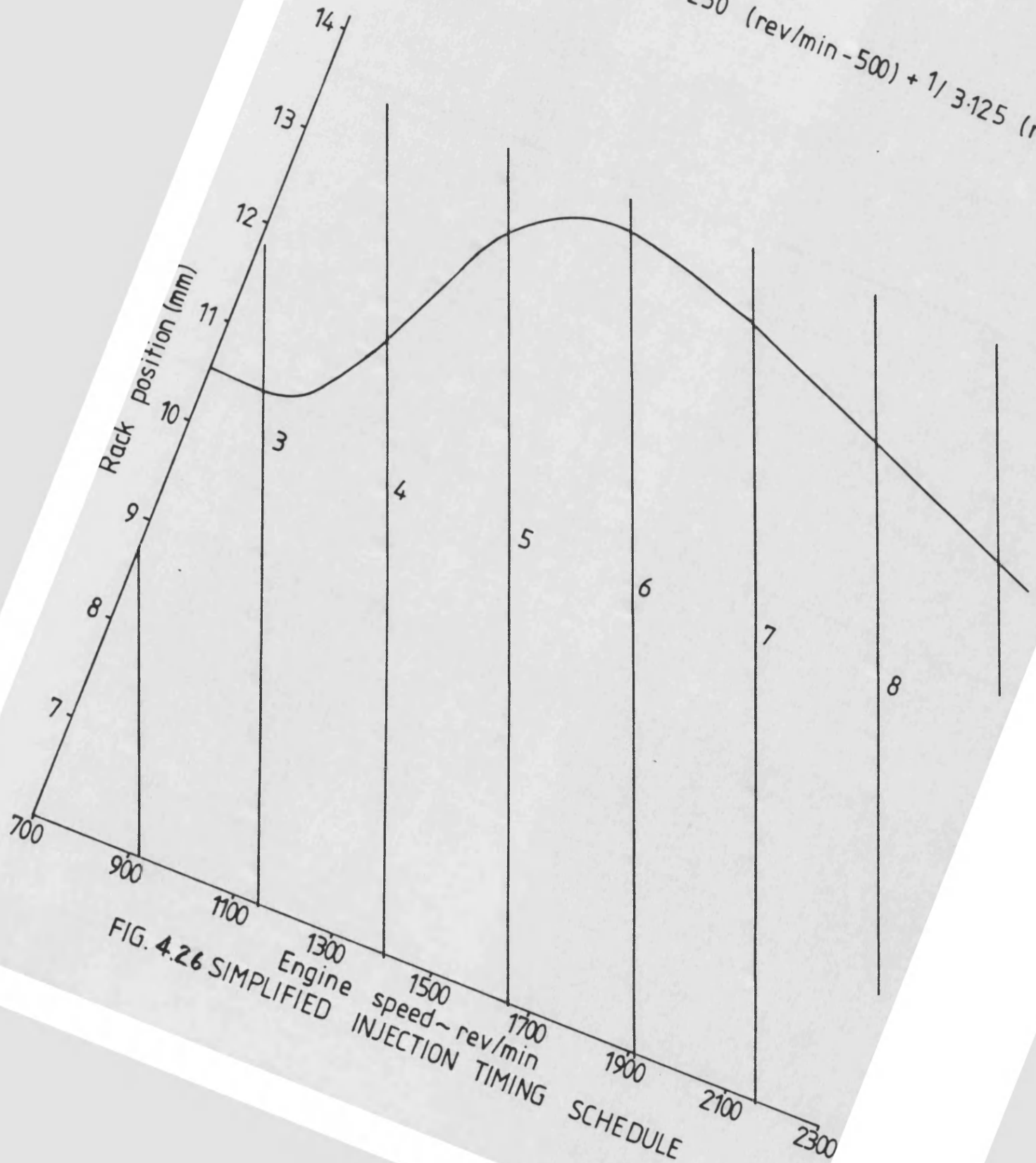

FIG. 4.26 SIMPLIFIED INJECTION TIMING SCHEDULE

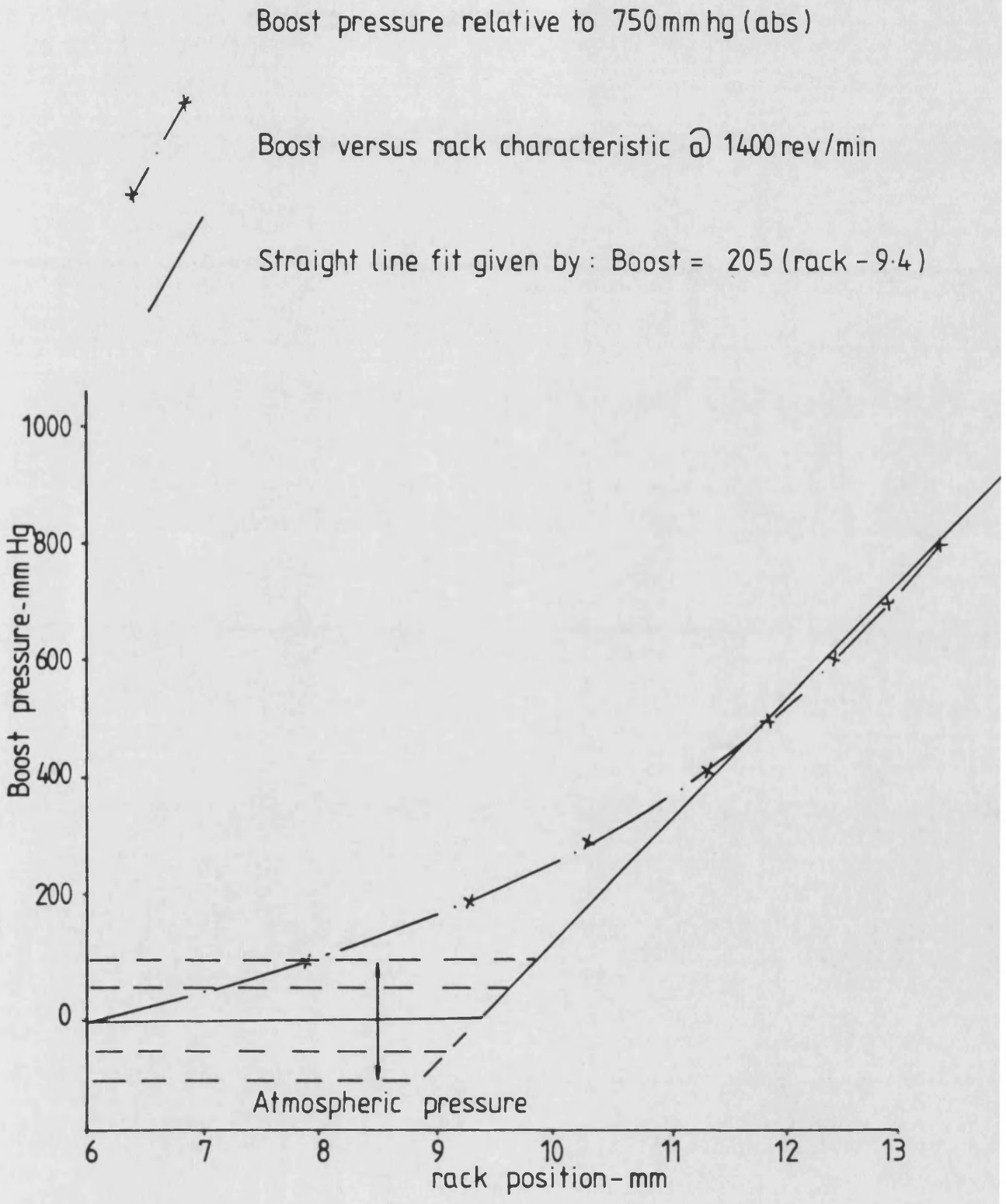

FIG.4.27 SIMPLIFIED BOOST CONTROL SCHEDULE

Engine LEYLAND TL11—7962756 Project No. DH

Title LTC. PERFORMANCE — LINEARISED SCHEDULES

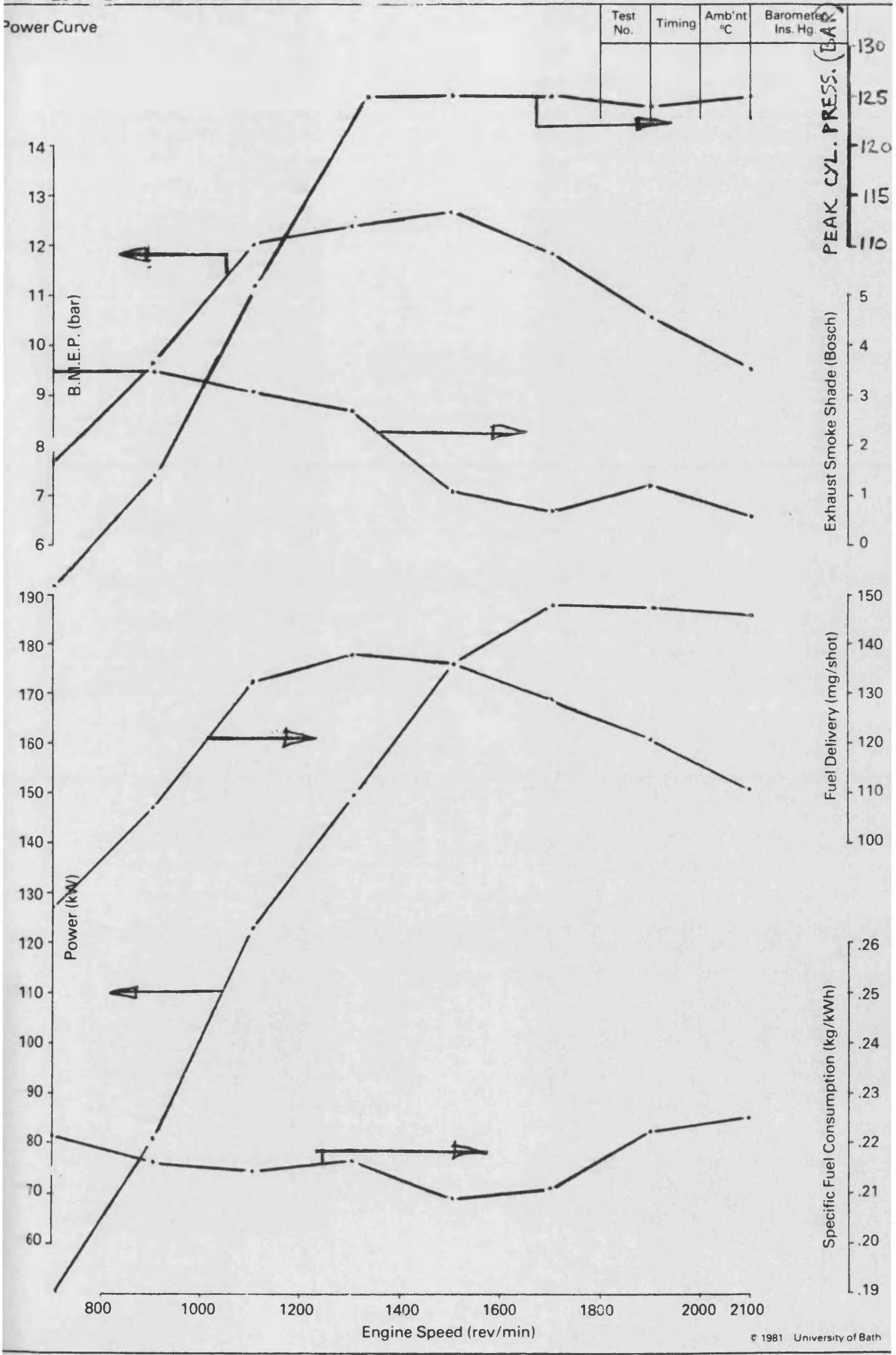

FIG 4.28

Date 10.10.83 Graph .....

Engine LEYLAND TL11—7962756 ~~Project No~~ DH.

Title LTC. PERFORMANCE — LINEARISED SCHEDULES

Power Curve

Test No.	Timing	Amb'nt °C	Barometer Ins. Hg.

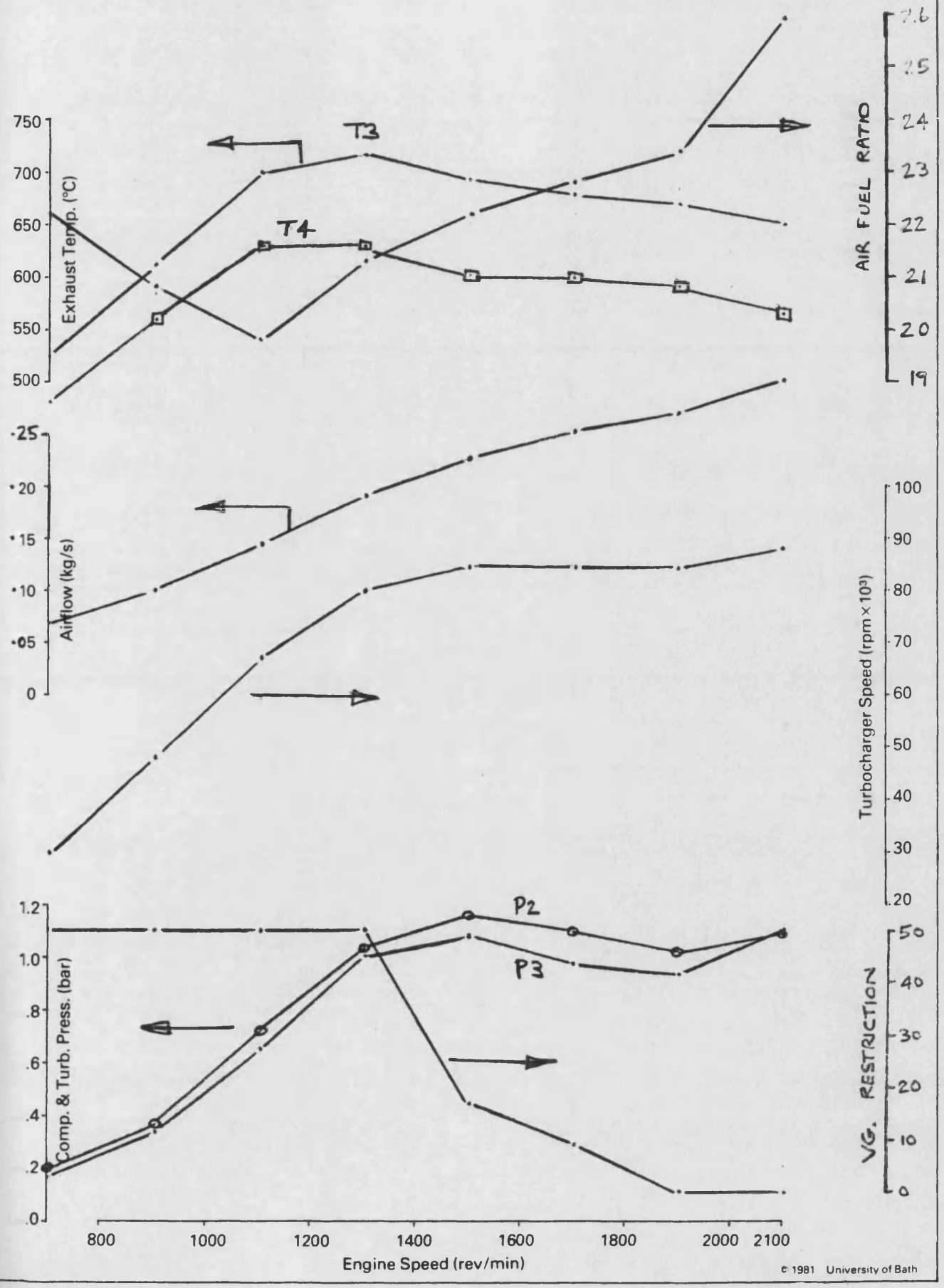

FIG. 4.29

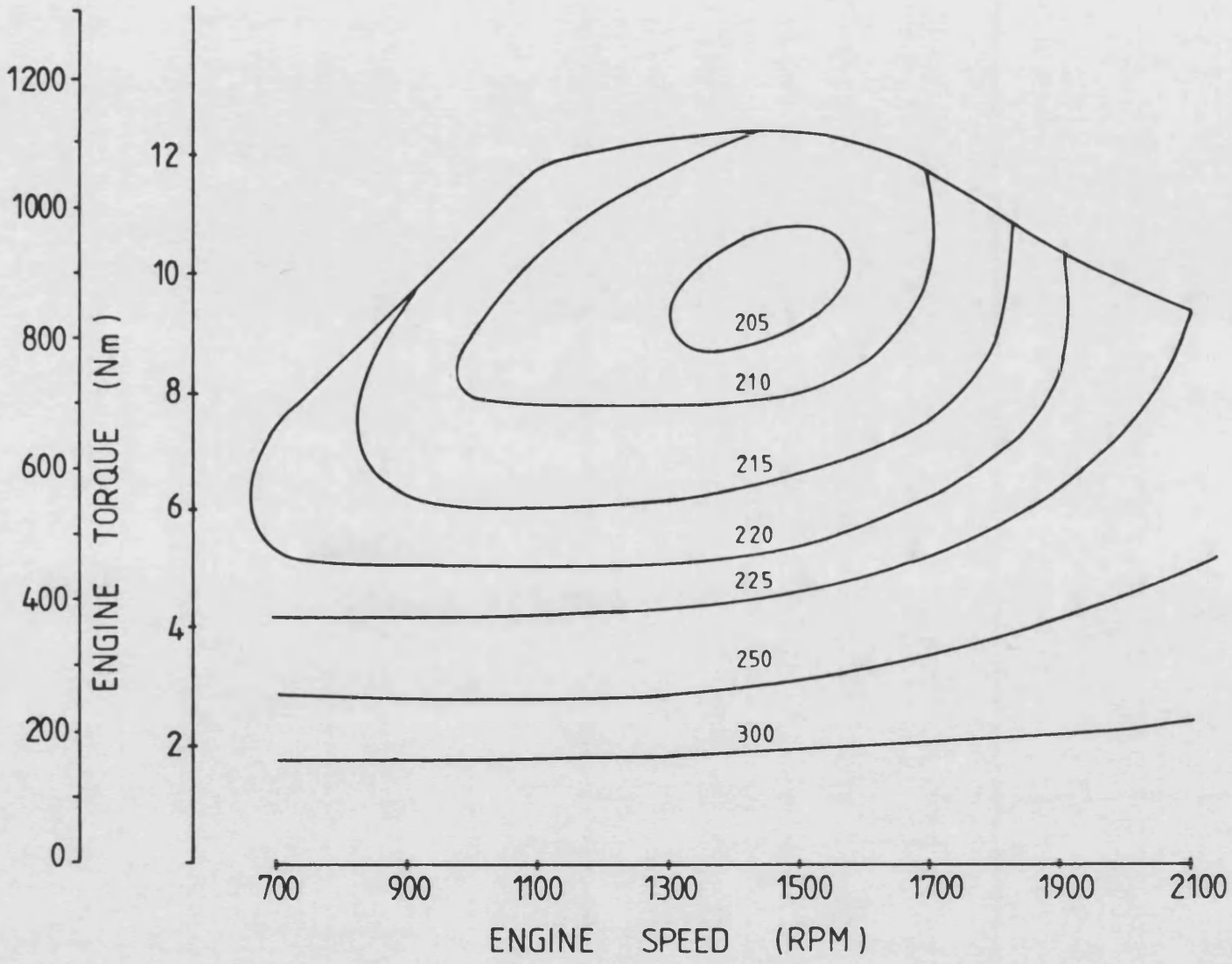

FIG. 4.30 STEADY STATE OPTIMIZATION (SIMPLIFIED SCHEDULE)

Engine LEYLAND TL11 ENGINE—11.1L DISPLACEMENT

Drawn By DtI

Title 150 - BOOST CURVES UNDER COMPUTER CONTROL

Test No.	Timing	Amb'nt °C	Barometer Ins. Hg.

Holset / Leyland / Dowty / DoI Contract

STATIC BOOST OVER 750 MMHG ABS.

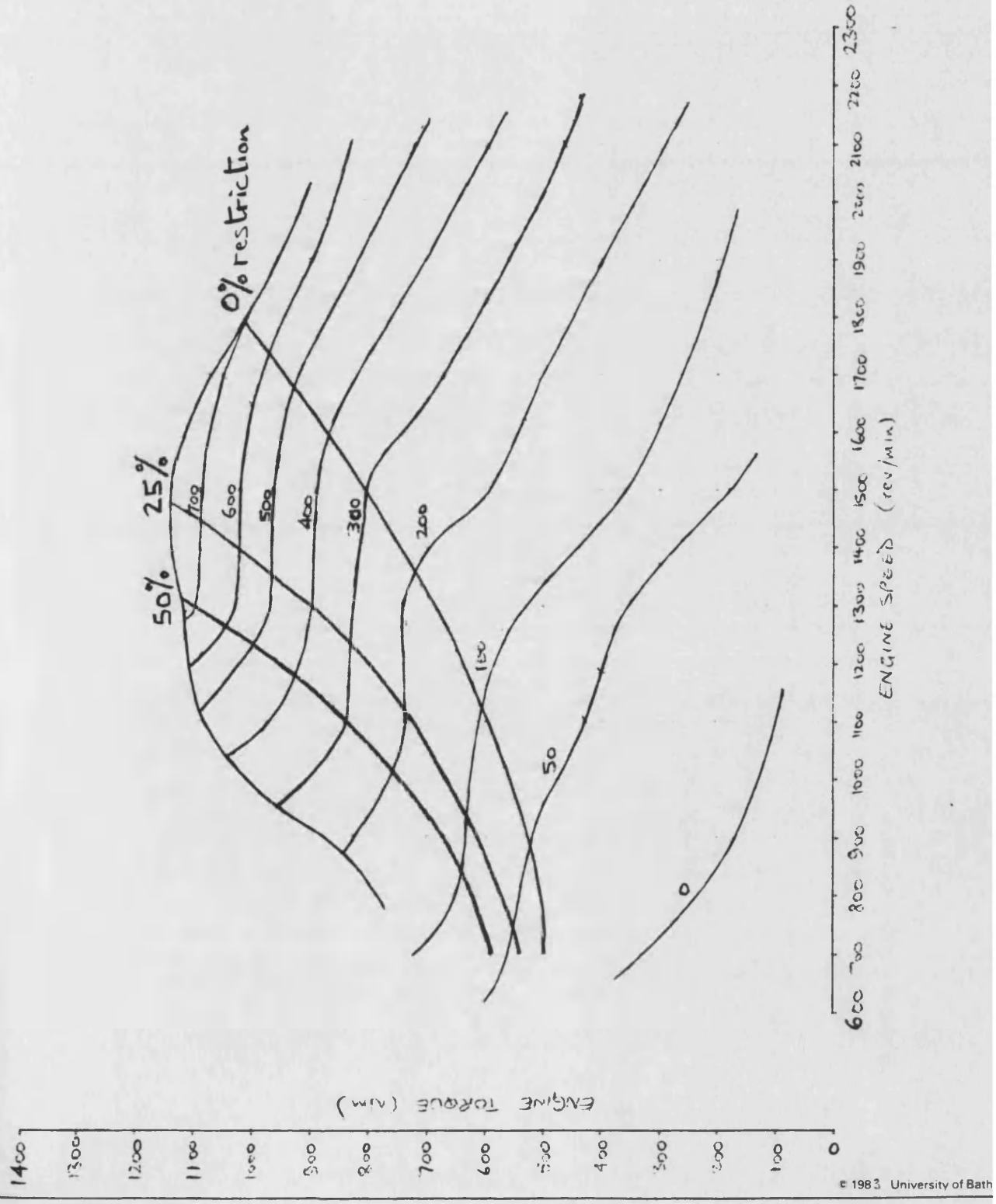

Engine LEYLAND TL11 ENGINE—11.1L DISPLACEMENT

Date ..... Graph .....

Drawn By ..... DH .....

Title SFC. OPTIMUM BOOST SCHEDULE

Power Curve Rating—190 kW at 2100 rev/min

Holset / Leyland / Dowty / DoI Contract

Test No.	Timing	Amb'nt °C	Barometer mm Hg.
	OPT.		

SFC. GM/KW.HR

BOOST PR. IS A FUNCTION OF SPEED & TORQUE

(SMOOTHED OPTIMUMS)

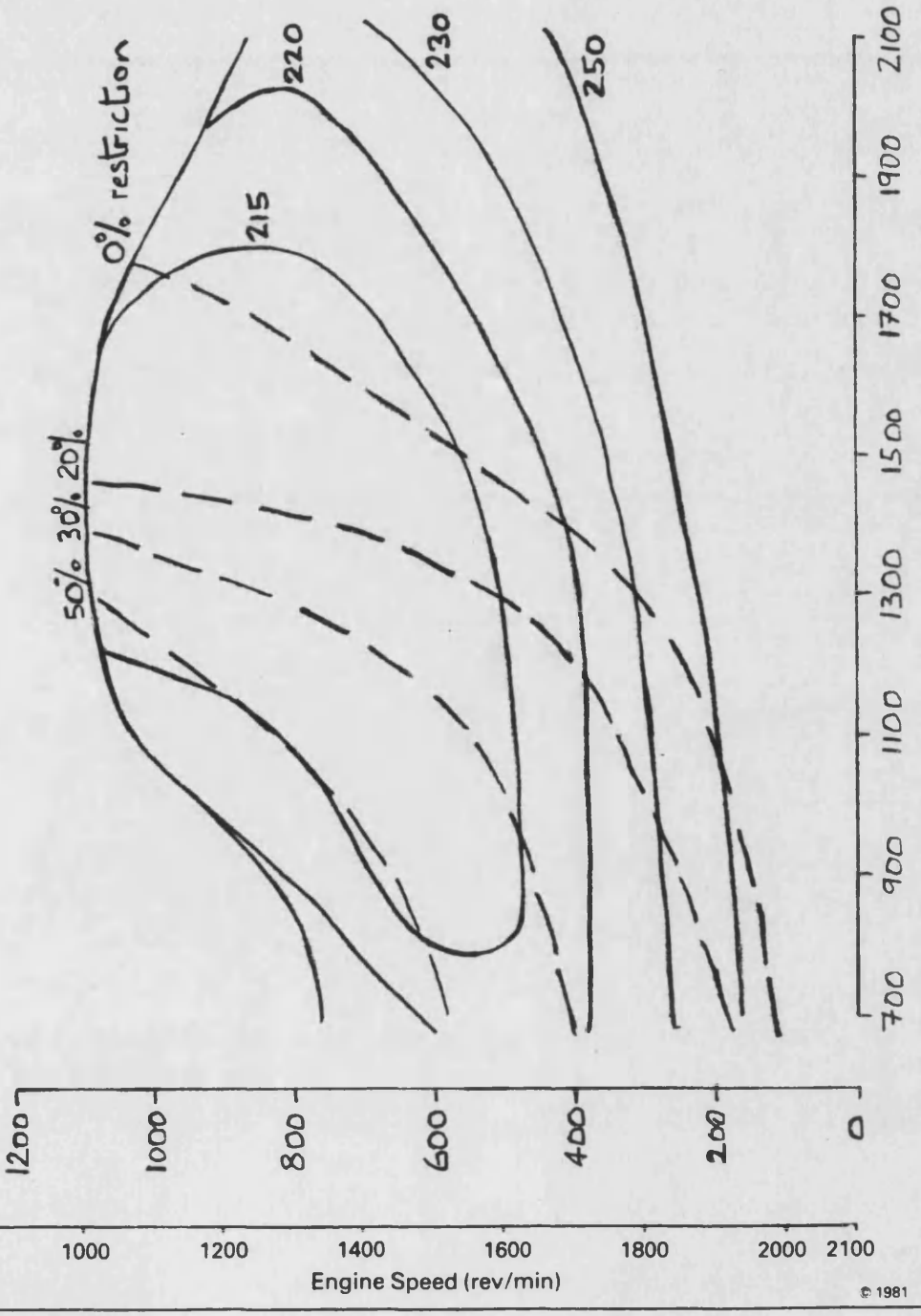

FIG. 4.32

Engine LEYLAND TL11 ENGINE—11.1L DISPLACEMENT
Title SFC. SPEED SCHEDULE

Date ..... Graph .....
Drawn By DH.

Power Curve Rating—190 kW at 2100 rev/min
Holset / Leyland / Dowty / DoI Contract

Test No.	Timing	Amb'nt °C	Barometer mm Hg.
	OPT.		

SFC. GM/KW.HR

RESTRICTION IS A FUNCTION OF SPEED

OPTIMUM ON LTC.

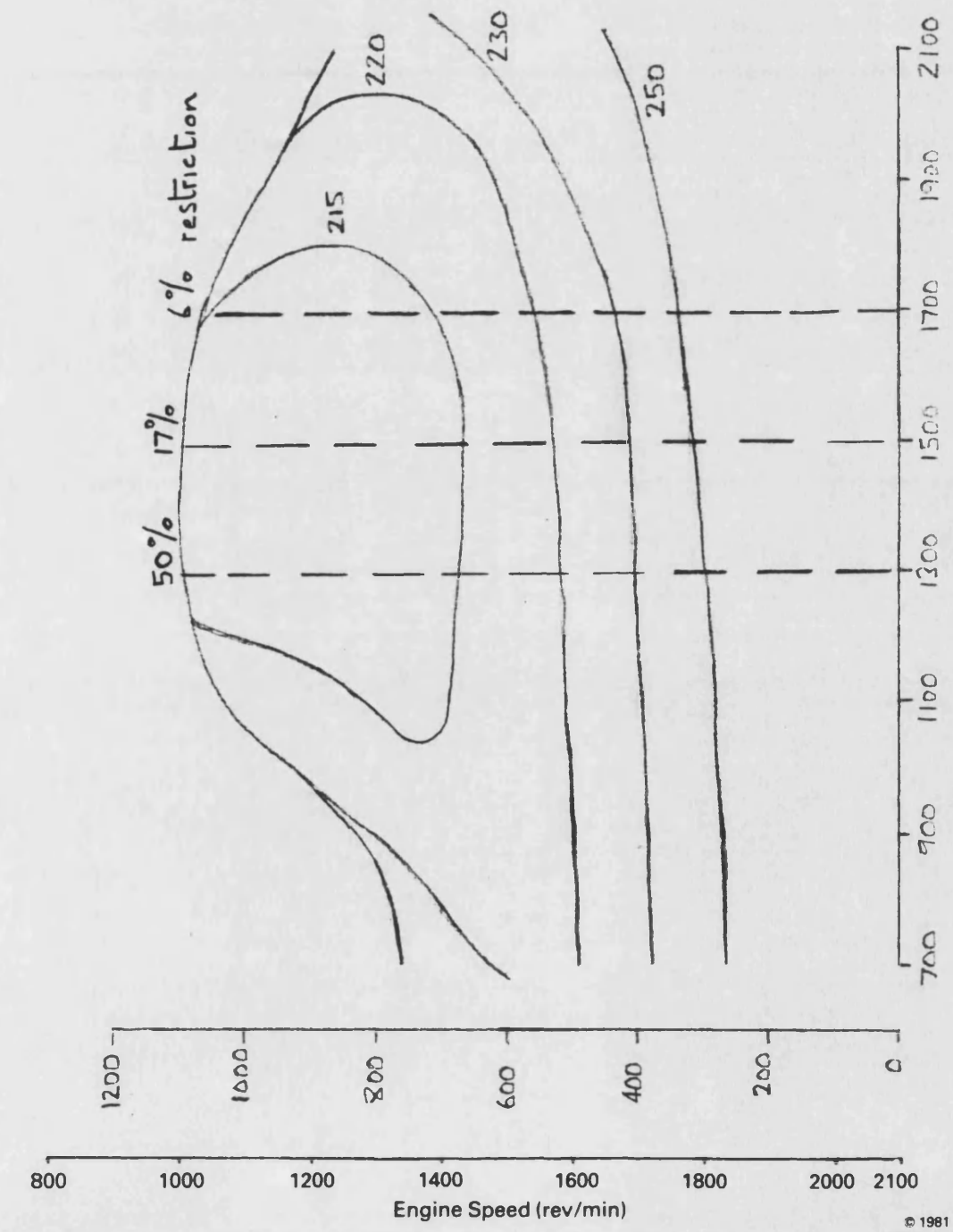

FIG. 4.33

Date ..... Graph .....

Engine LEYLAND TL11 ENGINE—11.1L DISPLACEMENT Drawn By DH

Title SFC. CAPSULE TYPE SCHEDULE

Power Curve Rating—190 kW at 2100 rev/min

Holset / Leyland / Dowty / DoI Contract

SFC. GM / KW.HR.

Test No.	Timing	Amb'nt °C	Barometer mm Hg.
	OPT.		

RESTRICTION IS A LINEAR FUNCTION OF BOOST

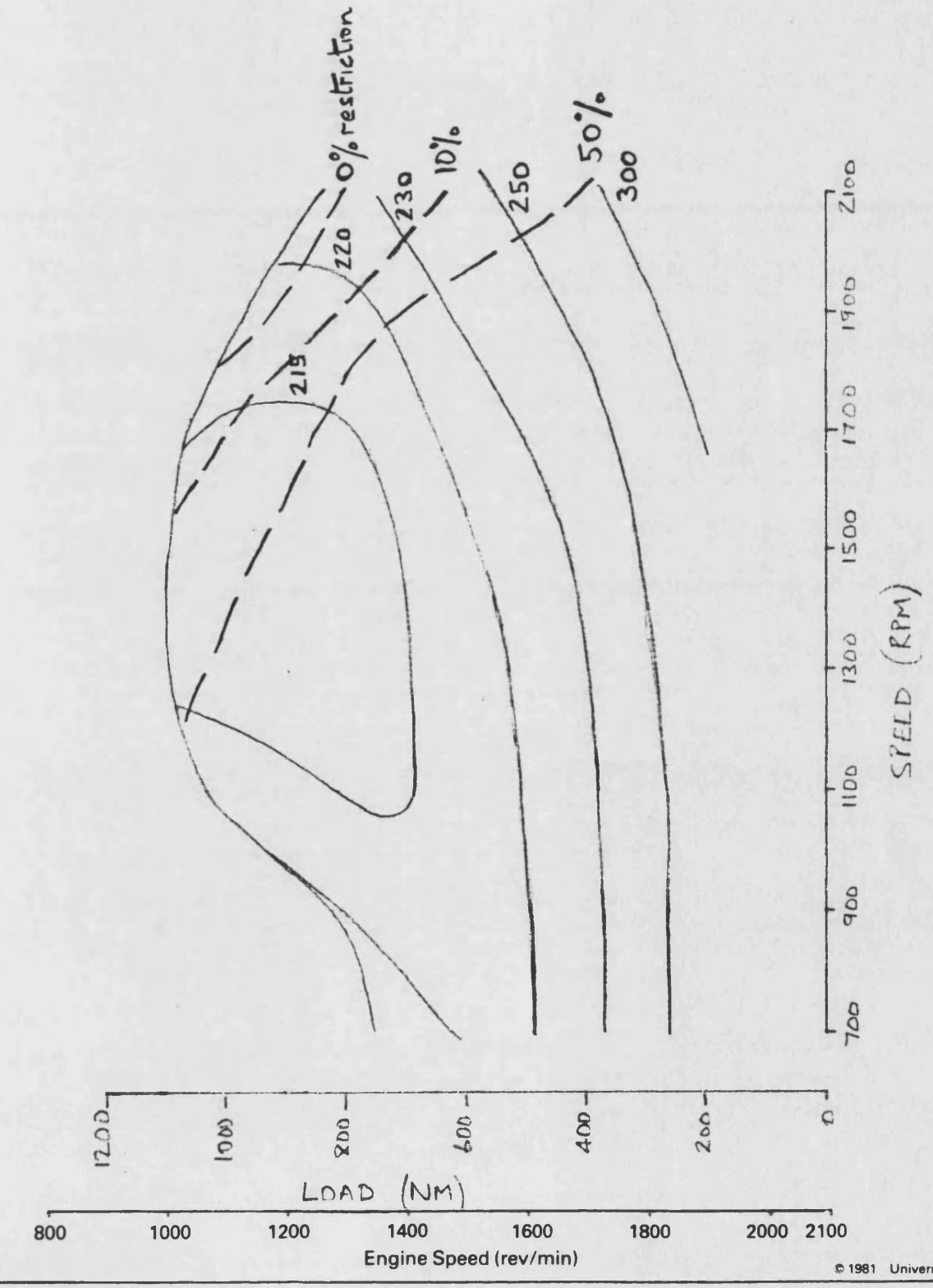

FIG. 4.34

CHAPTER 5

TRANSIENT CONTROL WITH VARIABLE GEOMETRY

5.1 INTRODUCTION

5.2 ALTERNATIVE MODES OF VG. CONTROL

5.2.1 BOOST PRESSURE SCHEDULING
5.2.2 RESTRICTION VS. ENGINE SPEED SCHEDULING
5.2.3 RESTRICTION VS. SPEED AND LOAD SCHEDULING

5.3 CONSTANT SPEED FUEL STEPS UNDER VG. CONTROL

5.3.1 EXPERIMENTAL RESULTS
5.3.2 CONCLUSIONS

5.4 VEHICLE ACCELERATION UNDER VG. CONTROL

5.4.1 REAL-TIME VEHICLE SIMULATION
5.4.2 ACCELERATION TEST PROCEDURE
5.4.3 EXPERIMENTAL RESULTS
5.4.4 CONCLUSIONS

5.5 DISCUSSION

5.1 INTRODUCTION

Diesel engine transient performance (torque response to changes in fuelling) is a function of fuel supply and air supply dynamics. Fuel supply dynamics consist of a simple time delay between a change in fuel control rod position and increased fuel injected. The delay is equal to or less than the reciprocal of firing frequency ie. the time to the next injection. From a vehicle response point of view this delay is negligible and is not discernible to the driver.

Air supply dynamics depend on the type of Diesel (naturally aspirated, supercharged, turbocharged etc). The naturally aspirated Diesel has an air supply dependent only on atmospheric conditions, air intake drop, and volumetric efficiency. In this case there is no major change in air supply associated with a fuel increase and hence no dynamic effect. The naturally aspirated Diesel engine therefore responds immediately to changes in fuelling. Vehicle response is purely a function of: vehicle mass; road conditions; gear-change times; and the number of ratio changes required, which depends on the engine torque curve (see section 1.1.2). Supercharged engines are similar in that air supply does not change with fuelling but only with speed, and hence response to fuelling changes is immediate.

With a turbocharged Diesel, air supply varies with fuelling as a result of the changes in exhaust enthalpy. Although enthalpy change follows fuelling immediately, there is a first-order lag in the turbocharger speed and hence boost pressure response because of turbocharger inertia. This lag has a time constant of between 0.5 and 1.5 seconds (figs. 5.6-5.17).

There are also first order lags associated with the filling of the manifolds. However, they are negligible in comparison with turbocharger lag. Frequency response tests undertaken on the author's experimental facility suggest that the inlet manifold has a time constant of approximately 30 msec ie. a 5Hz break point (ref. 52). The exhaust manifolds have far less effect because of their smaller

volume. However, this would not be the case with a constant pressure turbocharging system (ref. 3) because of the large manifold volumes associated with pulse damping.

Turbocharger lag causes a delay in torque response and excessive smoke. Both are a result of poor air-fuel ratio due to low boost pressure. In commercial road vehicles an aneroid control (diaphragm operated by boost pressure) reduces fuelling when boost pressure is too low. This avoids excessive smoke which is illegal, but reduces torque response and hence drivability still further. The aim of the transient control investigations described in this chapter is to reduce turbocharger lag and hence improve drivability without increased smoke.

Two types of transient have been investigated: constant speed fuel steps and simulated vehicle acceleration tests. The constant speed test is a pure test of torque response and simplifies analysis because engine speed is fixed. However, a vehicle only experiences this type of transient in high gears where vehicle acceleration times are long compared to turbocharger lag. In lower gears significant engine acceleration occurs during the turbocharger lag period, which alters both torque response and smoke. For this reason the series of acceleration tests was undertaken.

Transient response is recorded by the data-acquisition system described in section 2.3, which reads in transient parameters such as smoke, speed, torque, manifold pressures, fuel rack position, restrictor position and turbocharger speed. Smoke is probably the most useful parameter because it is a measure of combustion quality, which both torque response and SFC are a function of. The area under the smoke trace (opacity integrated w.r.t. time) is used as this gives a measure of the total particulate emission over the transient. Integrated smoke is most useful as a measure of turbocharger lag if the aneroid fuel control is disabled. Then fuelling is identical for the alternative control strategies being tested and the smoke trace is more pronounced.

Both modes of transient were run with several alternative VG. control strategies. The strategies tested are described in the next section. The experimental methodology and results are discussed in the following two sections. In the final section conclusions are drawn and other aspects of transient vehicle control discussed.

5.2 ALTERNATIVE MODES OF VG. CONTROL

Transient tests have been conducted using three alternative restriction control strategies and zero-restriction, which is used as a reference for comparison purposes. Zero-restriction refers to the fully open position and gives a greater swallowing capacity than the standard turbocharger fitted to the TL11 engine. This means the fully open response should be slower than with the standard turbocharger.

The strategies are implemented using the LSI-11/23 development computer (see section 3.4) and the engine's analogue controls. A program similar to that described in section 4.3.2 implements the control demand schedules. Bumpless transfer was not considered necessary as the restrictor mechanism can be safely stepped without causing unduly harsh operation. Depending on the form of schedule used, the DAC outputs are fed to the appropriate analogue loop external demands.

5.2.1 BOOST PRESSURE SCHEDULING

This control mode uses the boost pressure feedback loop described in section 4.2.1. The demand is scheduled by the control computer (LSI-11/23). The 2-D boost pressure schedule giving optimum steady-state SFC is shown in fig. 4.25. However, as explained in section 4.4.1, within the restrictor control range boost pressure is a function of rack position only. Boost only rises with speed when the restrictor has hit its stops (ie. 0% and 50% restriction). Hence to save digitising effort a simple 1-D schedule was used (fig. 5.1) representing boost vs. rack in the control range. In practice the restrictor will hit the stops in precisely the same way, thus producing the original 2-D boost map.

For the constant speed tests all that was required was a boost demand step corresponding to the fuel rack step used. This was implemented by simply switching rack and boost demand simultaneously, the computer system was not required for scheduling.

The important features of a boost scheduling system are that it gives optimum steady-state SFC. combined with over-restriction during transients. Over-restriction results from the inherent feedback effect of the boost pressure control loop. During the transient actual boost is lower than demanded boost and the result is increased restriction. As the boost rises restriction will gradually drop to its new steady-state value (fig. 5.2).

5.2.2 RESTRICTION VS. ENGINE SPEED SCHEDULING (fig. 5.3)

In this case the VG. controls are used in restriction mode, that is using the inner position loop only. Restriction demand is scheduled by the control computer as a function of speed only. This schedule gives optimum SFC. on the limiting torque curve (LTC), as it is derived from the optimum LTC performance described in section 4.4. However, at part load the same restriction is applied as for full load. This results in unnecessary exhaust back pressure and hence a fuel consumption penalty at part load.

The reason for maintaining LTC. restriction at part load is to enhance transient performance. The turbocharger is kept spinning so that initial boost pressure is higher before a transient than it would be with the restrictor opened to its optimum SFC. position. What this schedule will not do is temporarily over restrict to improve response as does the boost control loop.

For the constant speed tests all that was required was to hold restriction constant at the appropriate LTC. setting.

5.2.3 RESTRICTION VS. SPEED AND LOAD SCHEDULING (fig. 5.4)

The control computer again outputs a restriction demand to the restrictor position control loop. Restriction is a function of speed and torque and, being derived from the optimum performance described in section 4.4, gives optimum SFC throughout the engine operating map.

For the constant speed tests restriction was switched from its part load setting to LTC. restriction in unison with the fuel step. The computer was not required for scheduling.

Although this schedule produces optimum SFC under steady-state conditions it was not expected to perform well transiently for two reasons:

1 The initial boost before a transient is low because the restrictor is open at part load to avoid adverse exhaust back-pressure. The speed schedule is a compromise to provide more initial boost.

2 Restriction moves through a series of steady-state optimum values during the transient rather than temporarily over restricting to raise boost pressure more rapidly. The boost control loop overcomes this because of its inherent feedback effect.

5.3 CONSTANT SPEED FUEL STEPS UNDER VG. CONTROL

Once the electrohydraulic VG. actuator mechanism (section 4.2.1) had been commissioned a true investigation of transient VG. control could be carried out. Previously the manually operated pneumatic capsules had only allowed fixed restriction transients to be undertaken. The electrohydraulic mechanism was designed to ensure restrictor actuation time had a negligible effect on overall transient response, the transition from zero to full restriction taking under 0.1 sec.

The transients consisted of a fuel step at constant speed, which was achieved by using the dynamometer in its speed control mode. Four modes of VG. control were tested at four different engine speeds. Referring to figure 5.5, tests were undertaken at 800, 1200, 1600 and 1800 rpm, the following control schedules were tested at each speed if appropriate:-

1. **Zero restriction.**
   The VG. turbine is kept fully open throughout the transient. This test provides a baseline for comparison purposes.

2. **LTC restriction, prior to and throughout the transient.**
   This corresponds to the control strategy shown by fig. 5.3 where restriction is a function of engine speed only and is optimum on the LTC. It should be noted that this strategy does not give minimum SFC at part load as it is a compromise aimed at improving transient performance.

3. **A restriction step occurring simultaneously with the fuel step.**
   This corresponds to the optimum restriction schedule (fig. 5.4) which gives minimum SFC throughout the load-speed map. Restriction is stepped from its initial part load setting to optimum LTC. restriction.

4. **A boost pressure demand step occurring simultaneously with the fuel step.**
   This corresponds to the optimum boost schedule (fig. 4.25) which is an alternative means of establishing minimum SFC over the entire load-speed map. Boost control is implemented by the feedback loop described in section 4.2.1.

By inspection of the schedules (fig. 5.5) it is apparent that four of the tests are redundant, producing the same restrictor movement as another test at the same speed. At 1800 rpm schedules 2 and 3 leave the restrictor fully open. At 800 and 1200 rpm boost control (schedule 4) will fully close the restrictor (50%) producing the same results as schedule 3.

The fuel, restrictor and boost steps were implemented by switching the controls from manual to external demands, the manual settings being the initial low load conditions and the external inputs determining the final high load conditions. The dynamometer speed demand was held constant at the appropriate test speed.

5.3.1 EXPERIMENTAL RESULTS (figs 5.6-5.17)

1800 rpm

Only two transients were recorded at 1800rpm: zero restriction which corresponds to schedules 1,2 and 3 (fig. 5.6); and boost control, schedule 4 (fig. 5.7). The effect of boost control is to close the restrictor initially so that boost rises rapidly towards the level required (demanded) for the increased fuelling. As boost error reduces the restrictor opens until it is again fully open.

As would be expected boost and turbocharger speed rise more rapidly with boost control resulting in a smaller smoke puff (integrated smoke). Because the aneroid fuel control was disabled there is little difference in torque response (load acceptance). However if fuel was reduced to keep within legal smoke limits the engine with zero

restriction would receive less fuel and hence develop less torque during the transient.

1600 rpm

At 1600 rpm all four transient strategies were tested. As expected the fully open case (fig. 5.8) produced the largest smoke puff. The three remaining tests produced ambiguous results.

The restriction step from 0 to 34% (fig. 5.10) resulted in a faster turbocharger response and correspondingly lower integrated smoke than a fixed (optimum on the LTC.) restriction of 34% (fig. 5.9). This should never be the case as setting LTC. restriction prior to the transient implies a higher initial turbocharger speed. This should therefore produce better results than stepping to LTC. restriction at the start of the transient.

Comparing the restriction step (fig. 5.10) with the boost control strategy (fig. 5.11) again gives ambiguous results. Boost control results in a step to 50% restriction which is maintained for over 3 seconds. Turbocharger speed and boost rise considerably faster. However, the difference between the integrated smoke values is negligible.

1200 rpm

At 1200 rpm restriction schedules 1 to 3 were tested. In this case boost pressure control is equivalent to the restriction step (0-50%). As expected turbocharger speed and boost pressure started at a higher initial value when restriction was set to 50% prior to the transient (fig. 5.13). This resulted in the lowest integrated smoke reading. With a restriction step from 0 to 50% (fig. 5.14) boost and turbocharger speed only catch up with the fixed (LTC.) restriction case after 3 seconds. The fully open case (fig. 5.12) gives the worst response with very high smoke readings as would be expected.

800 rpm

The results at 800 rpm show minor differences, the only point of interest being the higher initial turbocharger speed for the fixed (LTC.) restriction case (fig. 5.16). This led to a lower smoke level in the first half second. However, integrated smoke over the whole transient showed negligible differences between the schedules tested.

5.3.2 CONCLUSIONS

The results obtained from this series of constant speed fuel steps were considered unsatisfactory for two reasons. Firstly, the ambiguous nature of the results at 1600 rpm suggests that each test should have been repeated several times to provide a measure of repeatability, and hence show up any measurement problems. Secondly, some of the smoke traces show secondary puffs which could not be explained and hence made the smoke readings suspect.

Rather than repeat these tests it was considered more useful to continue with the acceleration tests described in the next section paying more attention to these problems.

Despite the above reservations about the test results some useful conclusions can be drawn:-

1. As expected, leaving the restrictor fully open produces the slowest turbocharger response in terms of speed and boost. This results in the highest smoke emission as determined by integrating the opacity signal.

2. At engine speeds exceeding 1800 rpm boost control was the only control mode tested which resulted in any restriction during the transient. Therefore, at higher speeds boost control resulted in minimum smoke.

3. At lower speeds, setting LTC. restriction prior to the transient led to a higher initial turbocharger speed and hence boost pressure. At 1200 rpm this produced lower smoke levels than a step to LTC. restriction. However, the tests at 1600 rpm contradict this result and cannot be explained.

5.4 VEHICLE ACCELERATION UNDER VG. CONTROL

Having concluded the series of constant speed fuel steps described in the previous section, the question was raised as to whether that method of testing was, after all, the most informative. It was suggested that during acceleration in low gears the turbocharged Diesel does not reach the limiting torque curve before the next gear change is necessary. This is attributed to the fact that engine and turbocharger acceleration both occur over a similar period and hence the engine never has enough air to produce limiting torque. In the higher gears the vehicle inertia prevents a large change in engine speed before the turbocharger has accelerated, and so the transient more closely resembles a constant speed fuel step.

The type of path the engine takes through the torque-speed map is shown in fig. 5.18. The period of interest is the first 3 to 5 seconds when turbo' lag effects are visible. In the higher gears this approximates to a constant speed fuel step, in the lower gears the engine may reach governor runout in less than five seconds.

It was decided that a series of engine acceleration tests should be undertaken to provide a more realistic appraisal of the alternative VG. control strategies. This work was completed with the assistance of the author's research colleague, Mr U. Anderson.

Two approaches to undertaking simulated vehicle acceleration tests were considered:-

1. Simulating vehicle inertia, wind resistance and rolling resistance and hence generating the appropriate dynamometer control signals. Such a simulation must operate in real-time ie. 1 second of simulation time is 1 second of real-time.

2. Using torque and speed data obtained from a real vehicle to schedule the dynamometer controls and hence follow the same

transient path across the torque-speed map. This could be done using the data-acquisition computer.

The transient path will vary depending on the turbocharger's transient performance and so the second method introduces errors when turbocharger geometry is different from that of the original test vehicle. In addition to this, it was shown that rolling road data is very difficult to interpret in terms of crankshaft torque because of the compliances in the rolling road and vehicle drive-train (ref. 33). These considerations led to the adoption of the vehicle simulation approach.

The following sections describe: the method of vehicle simulation; the procedure adopted for the acceleration tests; the test results; and the conclusions drawn from those results.

5.4.1 REAL-TIME VEHICLE SIMULATION

The engine is the only element of the vehicle on the test-bed. For acceleration tests the tractive resistance of the remainder of the driveline, the vehicle, and the road must be simulated by the dynamometer.

Tractive resistance can be split into acceleration dependent (inertia), speed dependent, and speed independent torque. Speed dependent terms include viscous friction in the gearbox and back-axle and aerodynamic drag. Speed independent terms include rolling friction and gradient.

It is the lowest gears that are of greatest interest as they produce transients furthest removed from a constant speed fuel step. This greatly simplifies the model as the speed related loads are negligible because of the low vehicle speed. For example, in the second gear of the 5-speed box on which the simulator is based the torque at the crankshaft due to aerodynamic drag does not exceed 3 Nm.

Thus the simulator requirements reduce to inertia simulation with a fixed road load (ie. speed independent load). Inertia torque is given by:-

$$\tau = I.\dot{\omega}$$

or:- $$\omega = \frac{1}{I}.\int \tau \, dt \quad (5.1)$$

τ = torque (Nm)

I = inertia ($kg.m^2$)

ω = angular speed (rad/sec)

Using the first equation, the dynamometer torque demand could be calculated from a differentiated engine speed signal. Alternatively a torque signal can be integrated to provide dynamometer speed demand. The second method was chosen because differentiation tends to amplify signal noise whereas an integrator will filter out unwanted noise giving a less troublesome solution.

Referring to fig. 5.19, the constant road load is subtracted from developed torque (measured) to give acceleration torque. This is then divided by inertia I to give acceleration, which is then integrated to provide a dynamometer speed demand signal. The speed demand due to acceleration is added to an initial speed demand and compared with the speed feedback to control the dynamometer. Speed is controlled with the standard control loop described in section 2.4.5.

The inertia simulator is implemented with the operational amplifier (op-amp) circuit shown in fig. 5.20. Two potentiometers on the front panel set road load (Nm/200) and inertia (see table below for settings). A switch determines which inertia range is in operation. Measured torque and road load both go through buffer amplifiers before being subtracted and fed to the integrator. The output from the integrator is then scaled to suit the dynamometer speed controls.

The integrator gain is equal to 1/RC, R is either 3.3 MΩ or 300 KΩ depending on the inertia range, C is 4.7 μF. A "reset" switch is included to discharge the integrators capacitor and zero the output.

The integrator obeys the equation:-

$$V_{out} = (1/RC).\int V_{in}dt$$

where: $V_{in} = (\tau/tqcal)\times(11-s)/11$
$V_{out} = N/spcal = (\omega.60)/(2\pi.spcal)$
tqcal = torque calibration = 100 Nm/volt
spcal = speed calibration = 250 rpm/volt
s = inertia potentiometer setting = 0 to 10

therefore
$$\omega = \frac{2\pi.spcal.(11-s)}{RC.60.tqcal.11}\int \tau\, dt \qquad (5.2)$$

combining equations 5.1 and 5.2 gives:

$$RC = \frac{I.2\pi.spcal.(11-s)}{60.tqcal.11} \qquad (5.3)$$

Total vehicle inertia (I), excepting the engine and referred to the crankshaft, was calculated using the following equation:

$$I = I_G + I_P/R_G^2 + (I_A+10.I_W+I_V)/(R_G.R_A)^2 \qquad (5.4)$$

Typical inertia data was obtained from Saab-Scania (ref. 33), a 32 tonne truck with a 5 speed box and 10 wheels was assumed.

I_G = gearbox inertia (ratio dependant)

gear	kg.m²
1	0.2
2	0.3
3	0.4
4	0.5
5	0.6

I_P = propellor shaft inertia = 5.3 kg.m²
I_A = axle inertia = 3.5 "
I_W = wheel inertia = 14 "
I_V = vehicle inertia = mr^2 = 8000 "
m = vehicle mass = 32000 kg
r = wheel radius = 0.5 m
R_G = gearbox ratio (see following table)
R_A = back axle ratio = 3.7

Values of total inertia were calculated for each gear of the 5 speed box, which has a typical ratio range (9:1). The following table lists

the inertias and their respective potentiometer and switch settings (determined by using equation 5.3).

gear	ratio	total inertia ($kg.m^2$)	inertia pot. setting	inertia switch setting
1	9.00	7.59	3.19	LOW
2	5.64	19.00	7.89	LOW
3	2.89	72.40	2.00	HIGH
4	1.74	199.00	7.73	HIGH
5	1.00	600.00	9.92	HIGH

5.4.2 ACCELERATION TEST PROCEDURE

Because of the poor results produced by the constant-speed fuel step tests it was considered important to repeat each transient several times to avoid false readings. The smoke traces again contained secondary puffs which were not repeatable, all other measurements showed good repeatability between tests. On investigation this problem was found to be a result of idling between tests. When the engine was run at medium speed and load, prior to conducting the test, smoke readings were repeatable and no secondary puffs were evident.

The most likely cause of this is oil leakage from the turbocharger bearings to the compressor housing at low boost pressures. The oil collects in the inlet manifold and is blown through during the transient. Apparently some oil leakage when idling is normal for turbocharged Diesel engines.

Two computer systems were used to run the acceleration tests. The VG. mechanism and maximum fuel limit were controlled by the laboratory's DEC LSI-11/23 microcomputer running the FORTRAN program TL11VG. This program implements the control schedules described in section 5.2, a listing can be found in ref. 33. The 'PET' data-acquisition system described in section 2.3 scheduled the fuel governor and recorded 8 channels of data during the transient.

The transient consisted of a fuel step from an initial condition of 1000 rpm and 300 Nm. The engine was allowed to accelerate under maximum fuelling to 2000 rpm with inertia simulation in operation. This was achieved by setting up the data-acquisition system to output a governor demand step, ensuring that the runout line was above 2000 rpm.

The maximum fuel rack limit was set to 6.3 volts (maximum rack at approx. 1800 rpm) except for two tests where an aneroid fuel control (smoke limiter) was simulated by the LSI-11/23 microcomputer. The latter reduced maximum rack linearly with boost from 6.3 volts at 0.5 Bar gauge to an adjustable value at 0.0 Bar gauge. Above 0.5 Bar max. rack was held at 6.3 volts. The reduction (in mm) at 0.0 Bar is entered at the keyboard and for these tests was 2mm (Scania data, ref. 33).

The test procedure adopted was as follows:-

1. Run the engine at medium load and speed (600Nm, 1600rpm) for 3 minutes to avoid smoke problems. The governor is switched to manual control, the dynamometer in torque mode.

2. Switch the dynamometer to speed mode with the inertia simulator disabled ("reset" switch closed). NB. The actual speed must be less than the demand when switching to speed mode.

3. Move the engine to the initial condition (1000rpm, 300Nm, governor demand=4.1 volts)

4. Prepare the data-acquisition system for the transient, the DAC should be outputting 4.1 volts to the external governor demand. Switch the governor to external control.

5. Switch the inertia simulator on with road load set to 1.5 (300 Nm).

6. Instruct the 'PET' to run the transient as soon as boost has settled. If the transient is delayed repeat the test sequence to remove oil from the inlet manifold.

7. Repeat each test 5 times to assess the scatter of results.

5.4.3 EXPERIMENTAL RESULTS

The four control strategies described in section 5.2 were each tested in first and second gear, five identical tests were performed for each combination. An example of the data-acquisition system output for each strategy and gear combination is shown in figs. 5.21-5.30. A full set of output plots for all the repeat tests can be found in ref. 33. The following table lists the tests undertaken and the appropriate figure numbers.

VG. schedule (α=restriction)	gear	maximum rack	figure
boost schedule	1	constant @ 6.3	5.21
α=fn(speed)	1	"	5.22
α=fn(speed,torque)	1	"	5.23
α=zero	1	"	5.24
α=zero	1	smoke limited	5.25
boost schedule	2	constant @ 6.3	5.26
α=fn(speed)	2	"	5.27
α=fn(speed,torque)	2	"	5.28
α=zero	2	"	5.29
α=zero	2	smoke limited	5.30

Fuel rack was operated in the smoke limited mode for two tests to demonstrate the resulting drop in acceleration. However, the full set of tests were run with fixed fuel rack position (maximum at 1800 rpm). Fixed fuelling resulted in more smoke and hence larger differences between control strategies, this made interpretation of the results easier.

It can be seen from the figures that the governor demand step results in a fuel step, as required. Maximum fuelling is maintained to over 2000 rpm where governor runout prevents engine overspeed. The fuel

step causes a rapid rise in developed torque which in turn produces a ramp output from the inertia simulator card. This ramp is the engine acceleration due to that increase in torque.

The dynamometer response is not instantaneous and hence a small speed excursion from the desired ramp is evident at the beginning of the transient. In a real vehicle transmission wind-up would cause some excursion so this was not considered a major problem. The initial torque overshoot is a result of the dynamometer correcting for the speed excursion, one would expect true developed torque to rise smoothly with turbocharger speed.

The turbocharger accelerates under the influence of increased fuelling and the VG. control schedule. This results in manifold pressures rising and hence smoke reducing from its initially high value. Although the alternative control strategies could be assessed by studying figs. 5.21-5.30, comparison is easier if the important transient parameters are quantified.

Three parameters were used to compare the different control strategies: integrated smoke, total fuel consumed, and acceleration time. These values were calculated for an engine speed increase of 1000 rpm (nominally 1000-2000 rpm), by the auxiliary printout program INT (ref. 33) running on the 'PET'. This data is presented for both first and second gear as plots of:

a) smoke vs. acceleration time (figs. 5.31 & 5.34)
b) fuel vs. acceleration time (figs. 5.32 & 5.35)
c) fuel vs. smoke (figs. 5.33 & 5.36)

First gear results

In first gear the difference in acceleration time between the best and worst restriction schedules is only 8% (fig. 5.31). Similarly the difference in total fuel consumed is only 10% (fig. 5.32). If the zero restriction case, which is included for comparison only, is ignored these differences become 4% and 5% respectively. Integrated

smoke, however, varies by as much as 65% (fig. 5.31) so this is considered to be by far the best indicator of transient performance.

Turbocharger speed and hence boost pressure rise most rapidly and reach the highest levels under boost control (fig. 5.21). This is because boost pressure does not reach that demanded and hence the restrictor remains closed throughout the transient. Integrated smoke, however, is no less than that obtained with the speed schedule (fig. 5.22) which opens the restrictor as the engine accelerates. This is attributed to poorer scavenging with boost control as a result of the adverse pressure gradient across the engine.

The torque-speed schedule (fig. 5.23) gives higher integrated smoke because restriction is only 20% before the transient and hence the initial turbocharger speed is lower. Both the boost pressure and speed schedules start the transient with 50% restriction and therefore a higher initial boost pressure.

As expected zero-restriction (fig. 5.24) produces the slowest turbocharger response and leads to correspondingly high smoke levels. With smoke limited fuelling (fig. 5.25) the acceleration time increases by 12%, total fuel consumption drops by 7% and integrated smoke by 55% (figs. 5.31 & 5.32).

Second gear results

From a control strategy comparison point of view the second gear results (figs. 5.34-5.36) are similar to those obtained in first gear. However the high exhaust back pressure produced by boost pressure control is more pronounced (fig. 5.26). Again this appears to nullify any boost pressure advantage over the speed schedule, resulting in very similar values for integrated smoke. There may be a case for using exhaust pressure as the control variable. However a high temperature pressure sensor would be required which would increase the cost of a commercial system.

5.4.4 CONCLUSIONS

In conclusion either boost control or the speed schedule will give the best transient performance in terms of minimising integrated smoke. The differences between the two are minimal so far as integrated smoke, fuel consumed and acceleration time are concerned. However, boost pressure control does result in a more rapid turbocharger response, presumably at the expense of efficient scavenging.

Boost scheduling results in optimum part load and LTC fuel consumption whereas the speed restriction schedule is a compromise which is only optimum on the LTC. For a fair comparison to be made the respective steady-state consumption loops must be taken into account along with the relative complexities of the two schemes.

5.5 DISCUSSION

Of the control strategies tested boost pressure control and the compromise restriction vs. speed schedule gave the best turbocharger response. In addition the steady-state comparisons discussed in section 4.4.3 confirmed the superior SFC given by a true optimum schedule such as boost vs. speed and load. The implication is that a boost pressure control loop driven by an optimum schedule (fig. 4.25 or 5.1) is the best solution for both steady-state and transient performance.

Under most conditions the boost capsule type schedule (fig. 4.34) will give the best transient performance because initially the VG. is almost always fully closed. This schedule has not been tested transiently because SFC. was much worse than with other schedules. This was thought to preclude its use with any system designed to improve fuel consumption as well as transient performance.

Both modes of transient test were considered useful. The acceleration tests simulate engine/turbocharger response in lower gears when engine acceleration has an effect on turbocharger lag. The constant speed tests provide a basic worst case reference, which is similar to a fuel step in a high gear when vehicle inertia prevents rapid engine acceleration.

During the course of the constant speed tests a problem with the smoke traces was identified. The traces lacked repeatability and often contained unexplained secondary smoke 'puffs'. This turned out to be a result of oil collecting in the inlet-manifold whilst idling between tests. The solution was to run the engine at medium load and speed prior to each test, hence blowing the excess oil through the engine.

The work described in this chapter has concentrated on minimising turbocharger lag with variable geometry. However, improvements in vehicle response and drivability can be achieved using other features of the engine control system developed in this research.

During vehicle speed transients temporary over fuelling and boosting together with changes in timing can increase torque above that developed under normal steady-state conditions. Retarding timing reduces peak cylinder pressure but increases SFC. Under transient conditions this may be an acceptable method of raising limiting torque temporarily. The degree to which these methods may be used depends on the mechanical design of the engine and the way in which reliability is assessed.

Another important use of VG. during vehicle acceleration may be to keep the turbocharger spinning during gear-changes. Rather than reducing boost demand with fuelling during the gear-change, boost would be maintained in anticipation of clutch engagement in the new gear. A switch detecting clutch depression could be used to determine a gear-change situation.

Fuelling and VG. are interactive in the sense that they each have an effect on both boost pressure and engine speed. Because of this, a multi-variable engine controller may give better engine response than two separate single input-single output (SIO) control loops. This approach is mentioned in sections 3.3.3 and 4.3.3. Ref. 52 describes some multi-variable work undertaken using the same experimental facility.

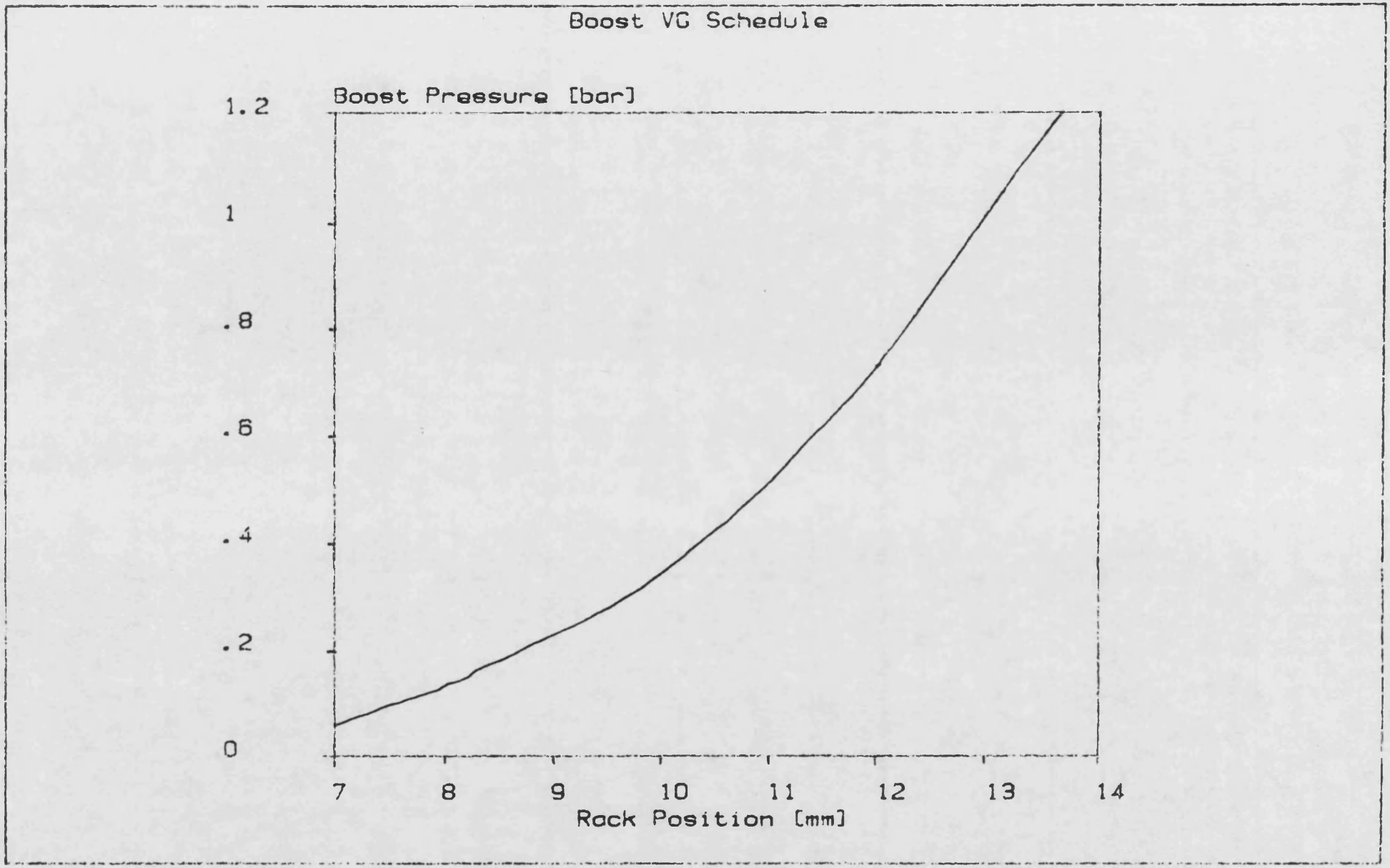

Figure 5.1 Variable Geometry Schedule

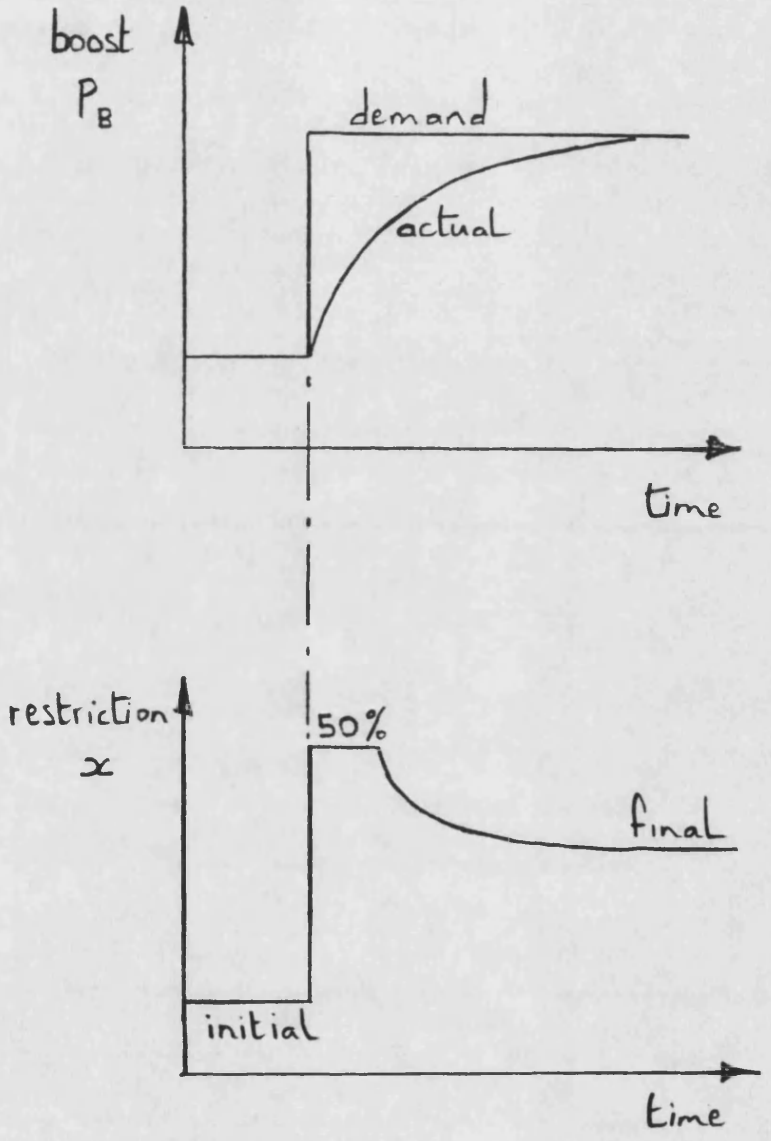

FIG. 5.2 OVER RESTRICTION DURING A TRANSIENT USING A BOOST FEEDBACK LOOP.

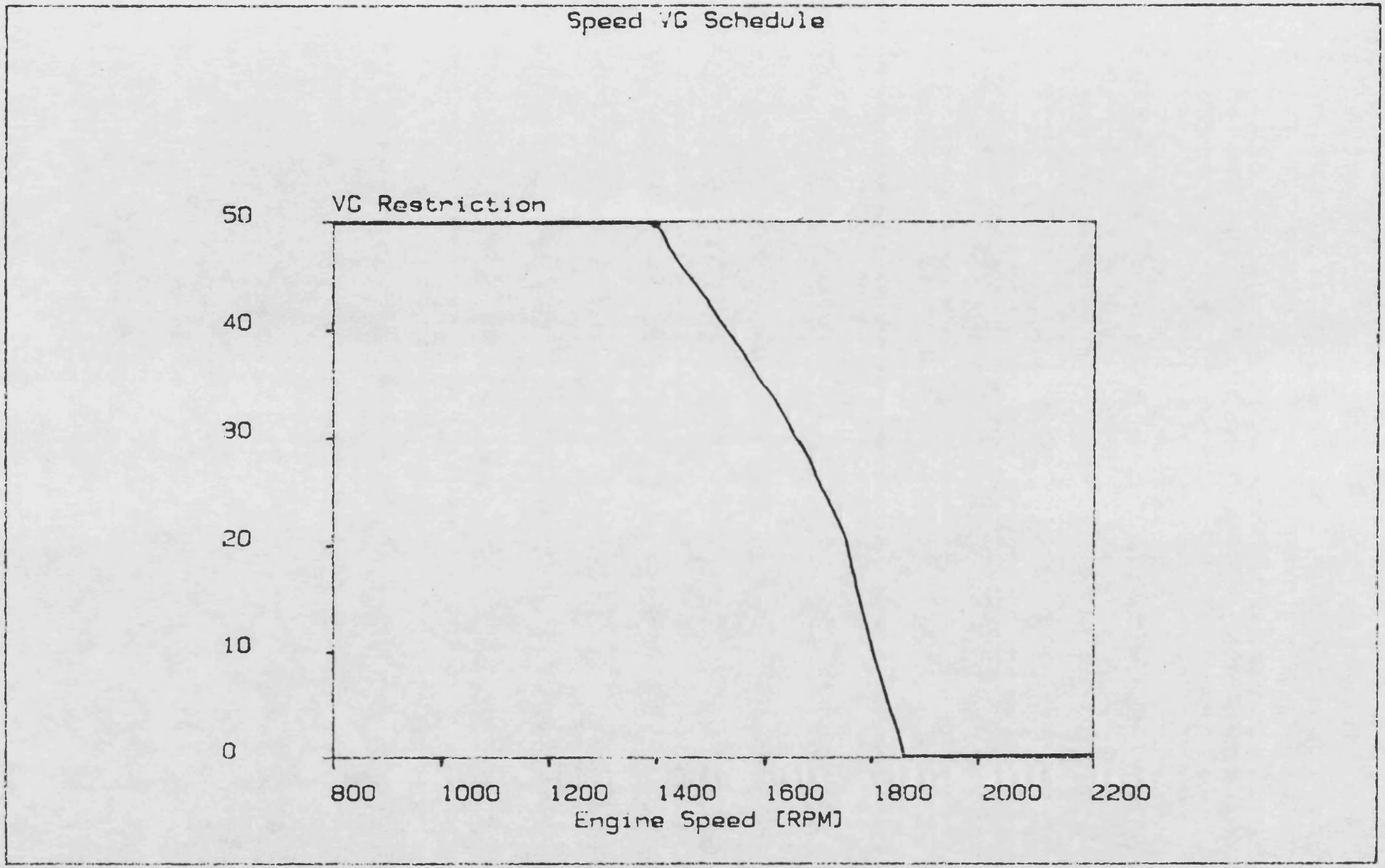

Figure 5.3 a) Variable Geometry Schedule

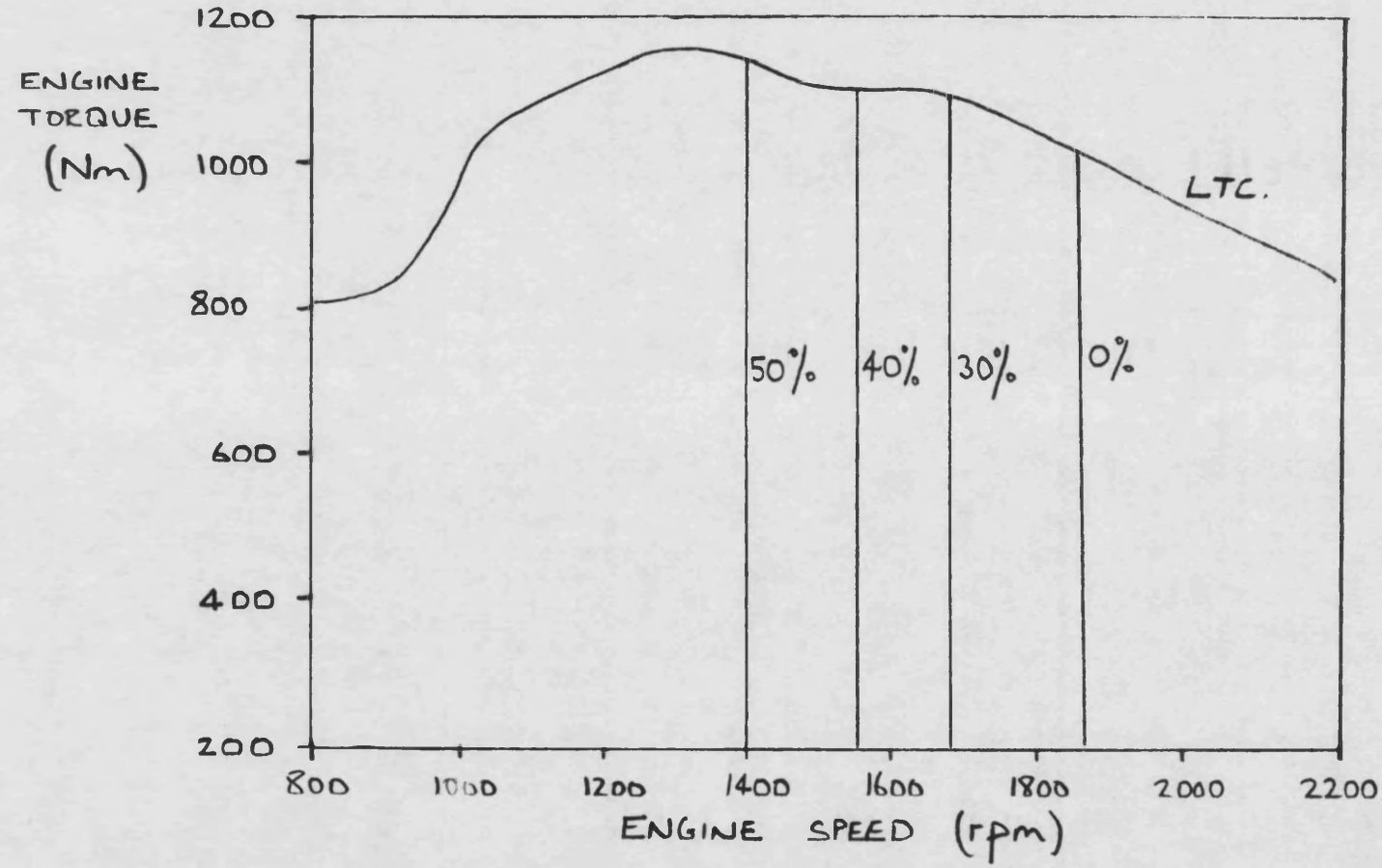

FIG. 5.3 b) V.G. RESTRICTION VS. SPEED SCHEDULE

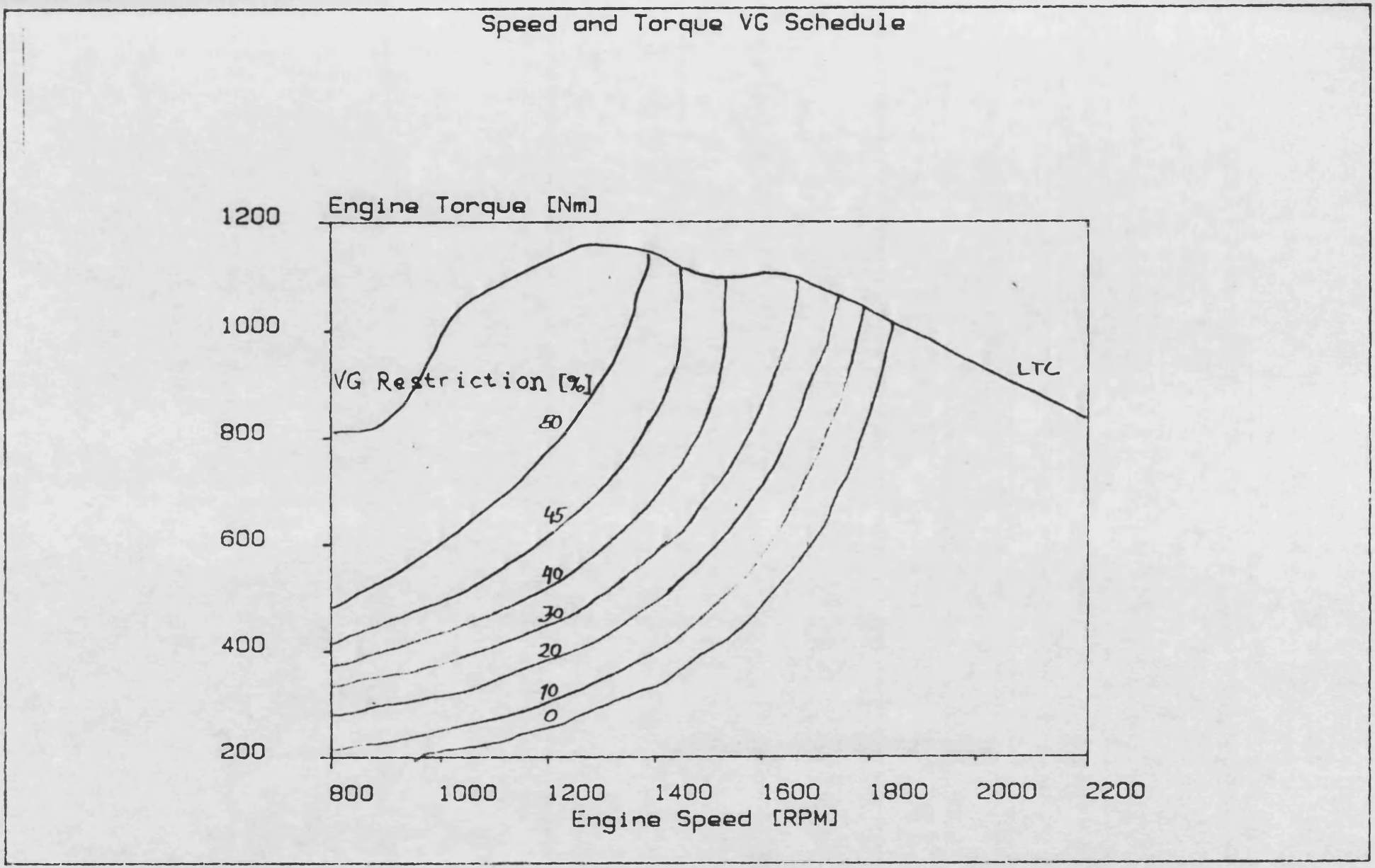

Figure 5.4 Variable Geometry Schedule

TURBINE CONTROL SCHEDULE	ENGINE SPEED - rev/min 800	1200	1600	1800
Fully open (0%)	0%	0%	0%	0%
Fixed (LTC) Restriction	50%	50%	34%	As above
Restriction Schedule	0 - 50%	0 - 50%	0 - 34%	As above
Boost Demand Schedule	As above	As above	0 – 1.08 BAR	0 – 0.8 bar

FIG 5.5 TRANSIENT TEST PROGRAMME

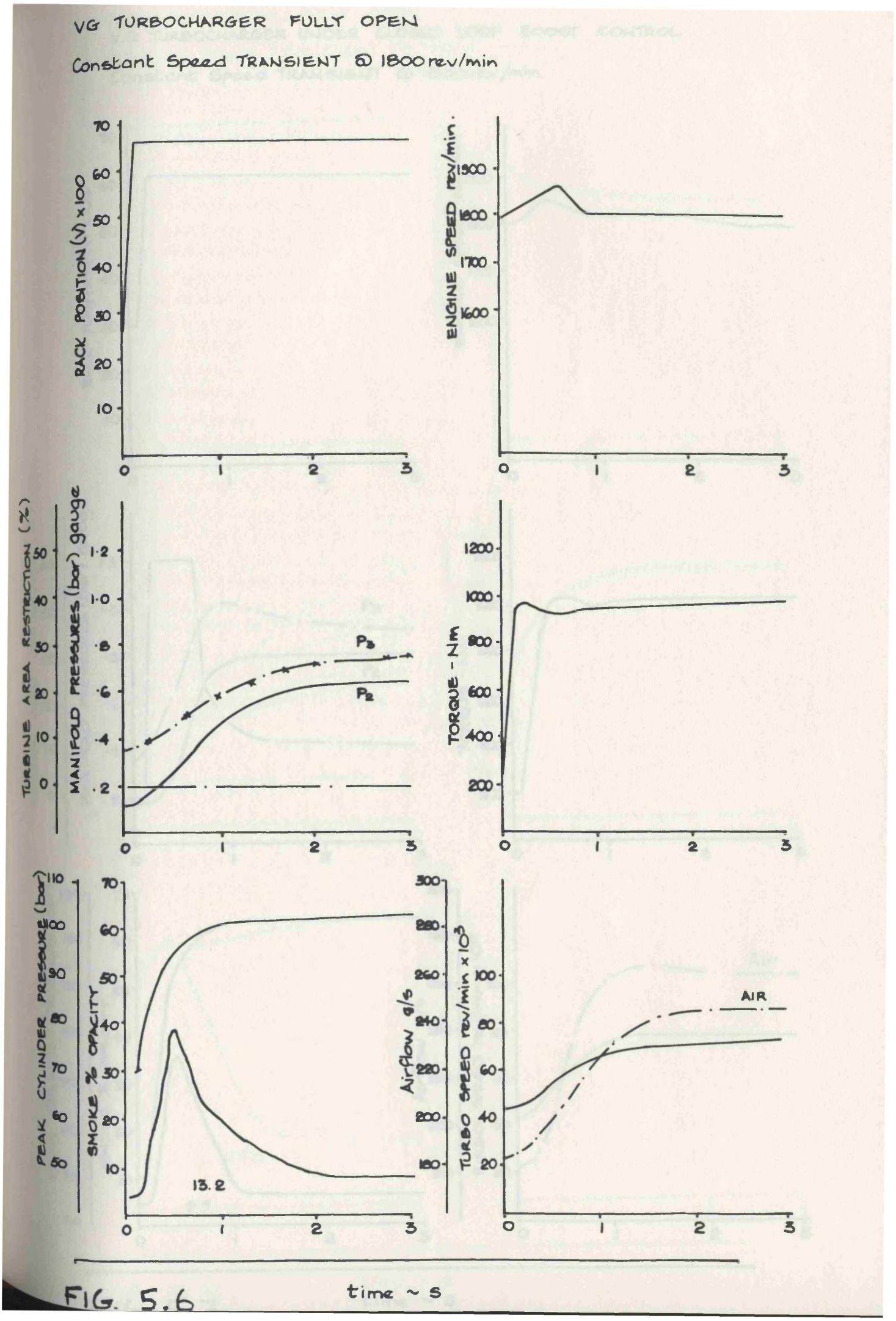
VG TURBOCHARGER FULLY OPEN
Constant Speed TRANSIENT @ 1800 rev/min
RACK POSITION (V) x 100
ENGINE SPEED rev/min.
TURBINE AREA RESTRICTION (%)
MANIFOLD PRESSURES (bar) gauge
P3
P2
TORQUE - Nm
PEAK CYLINDER PRESSURE (bar)
SMOKE % OPACITY
13.2
Airflow g/s
TURBO SPEED rev/min x 10³
AIR
time ~ s

FIG. 5.6

V.G. TURBOCHARGER UNDER CLOSED LOOP BOOST CONTROL

Constant Speed TRANSIENT @ 1800 rev/min

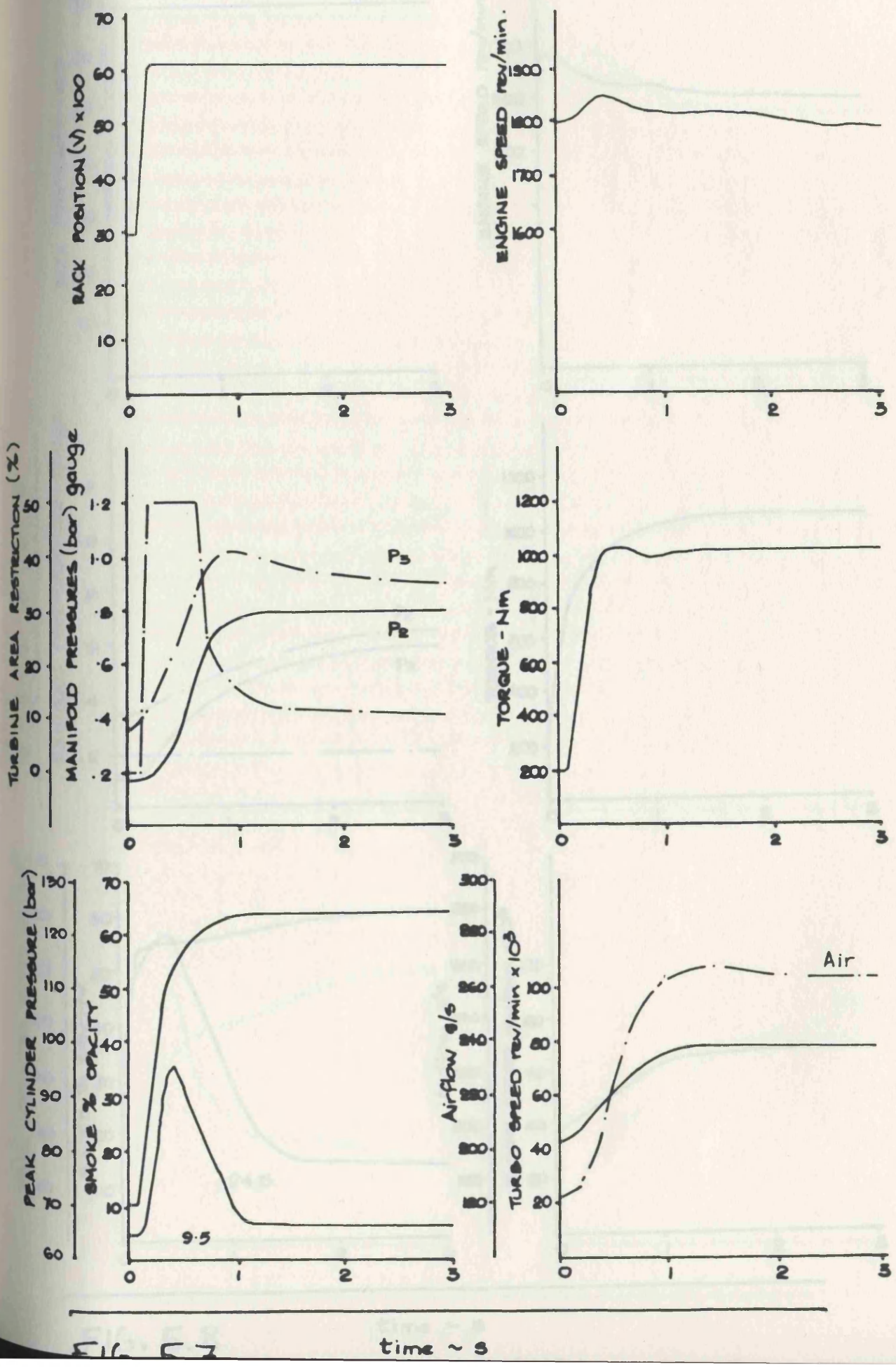

Fig. 5.7

VG TURBOCHARGER FULLY OPEN

Constant Speed TRANSIENT @ 1600 rev/min

Fig. 5.8

VG TURBOCHARGER 34% RESTRICTED

Constant Speed TRANSIENT @ 1600 rev/min

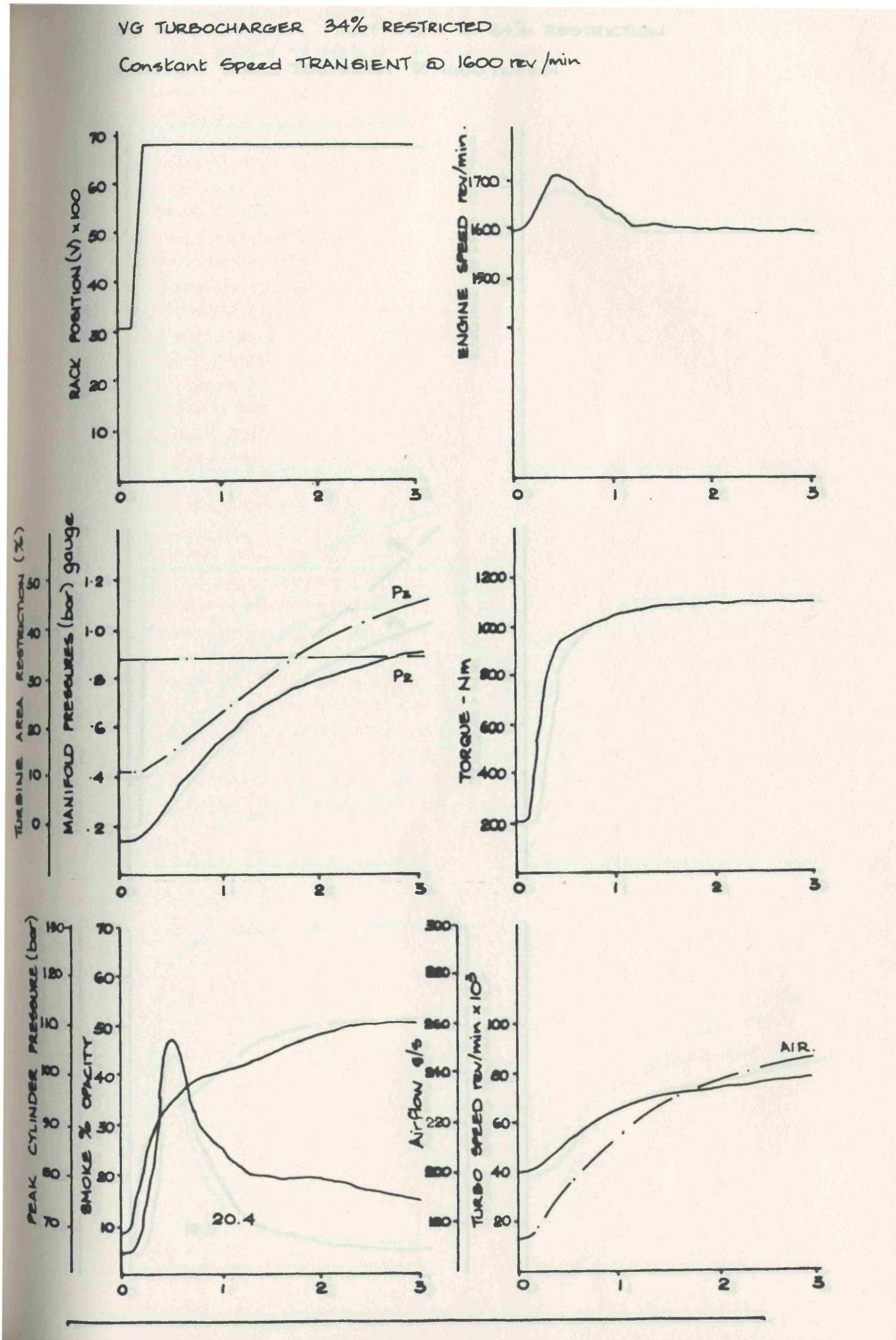

FIG 5.9

VG TURBOCHARGER FULLY OPEN TO 34% RESTRICTION

Constant Speed TRANSIENT @ 1600 rev/min

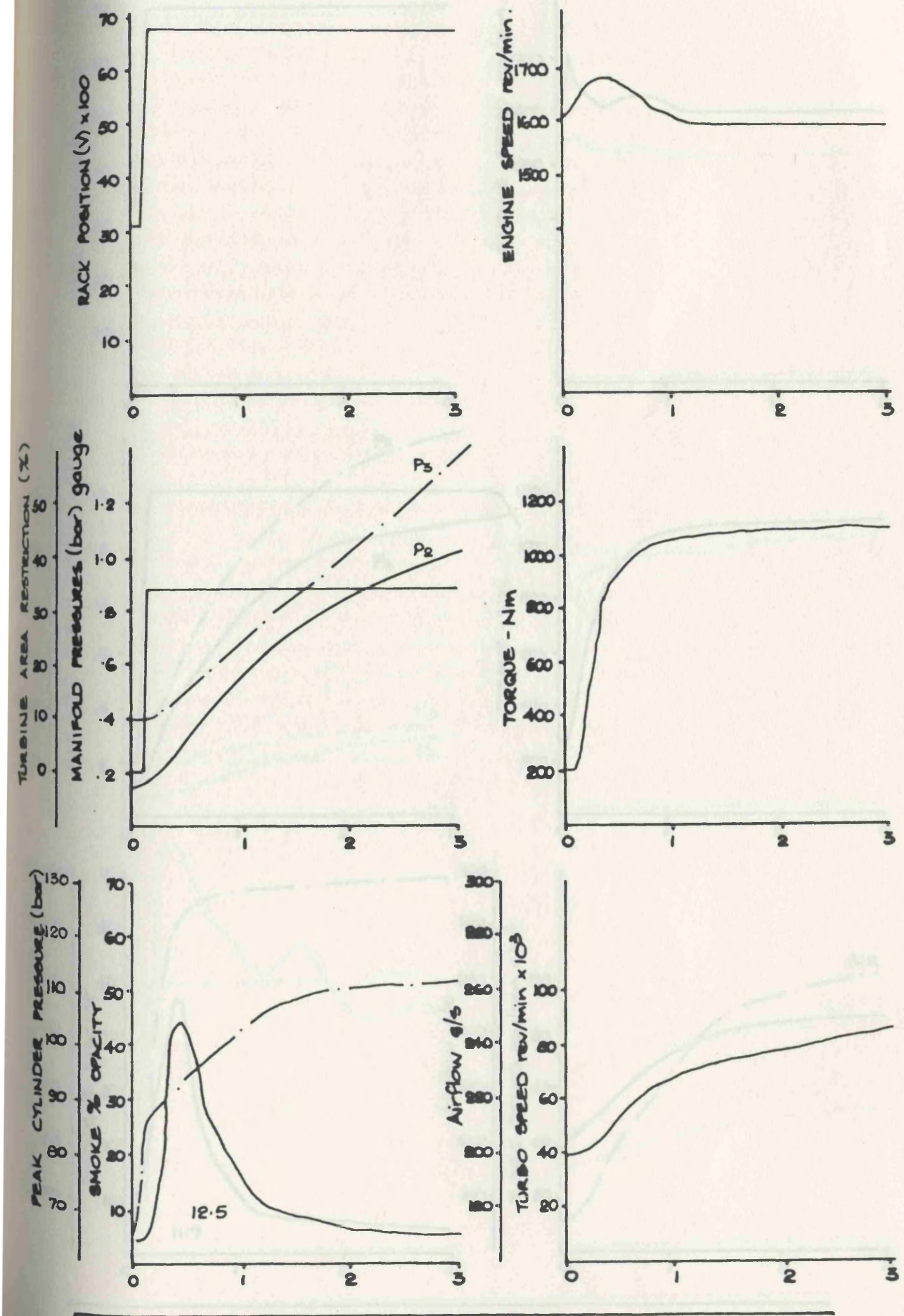

FIG. 5.10

VG TURBOCHARGER UNDER CLOSED LOOP BOOST CONTROL

Constant Speed TRANSIENT @ 1600 rev/min

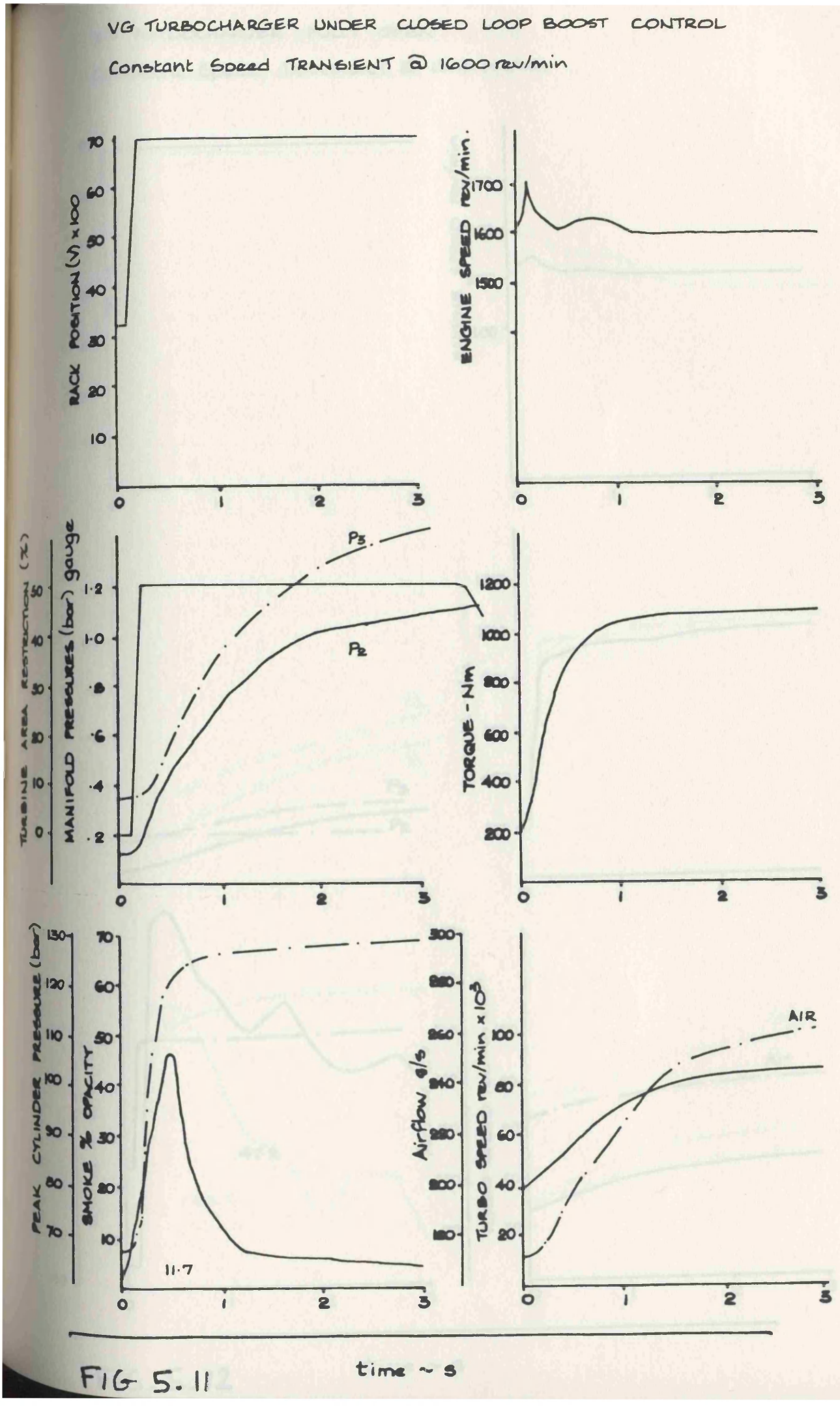

FIG 5.11

VG TURBOCHARGER FULLY OPEN

Constant Speed TRANSIENT @ 1200 rev/min

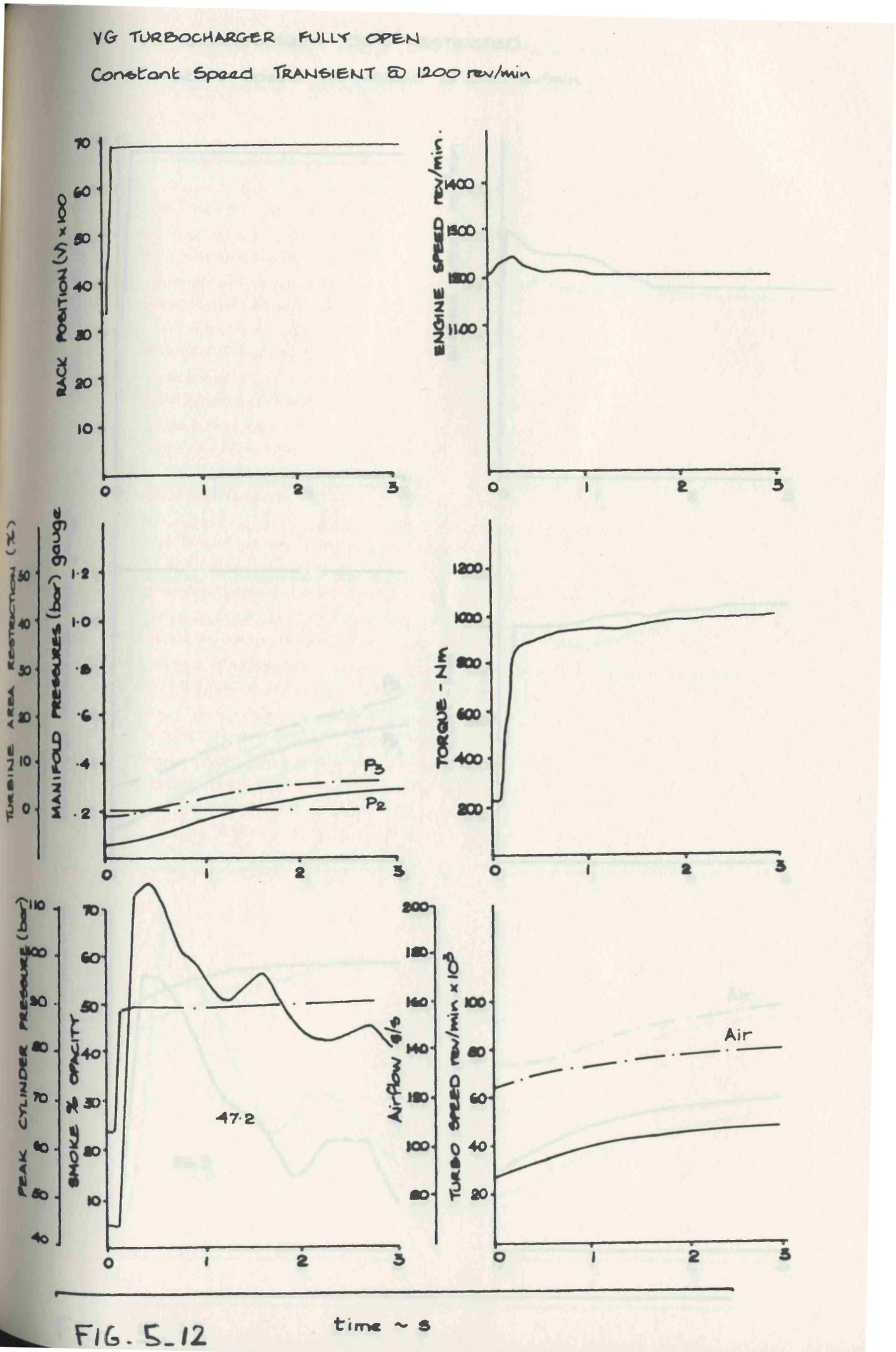

FIG. 5_12

VG TURBOCHARGER 50% RESTRICTED

Constant Speed TRANSIENT @ 1200 rev/min

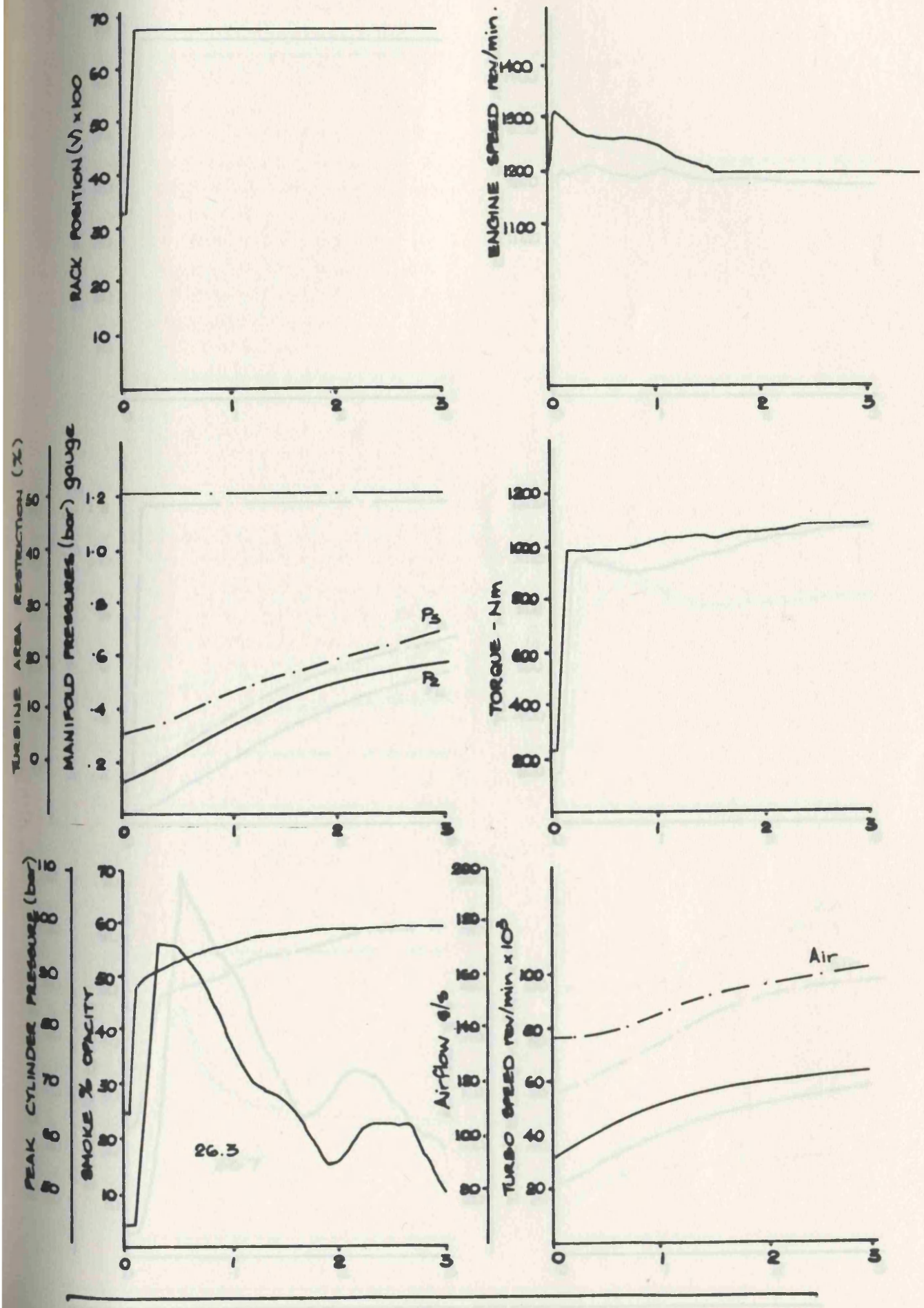

FIG. 5.13

VG TURBOCHARGER FULLY OPEN TO 50% RESTRICTED

Constant Speed TRANSIENT @ 1200 rev/min

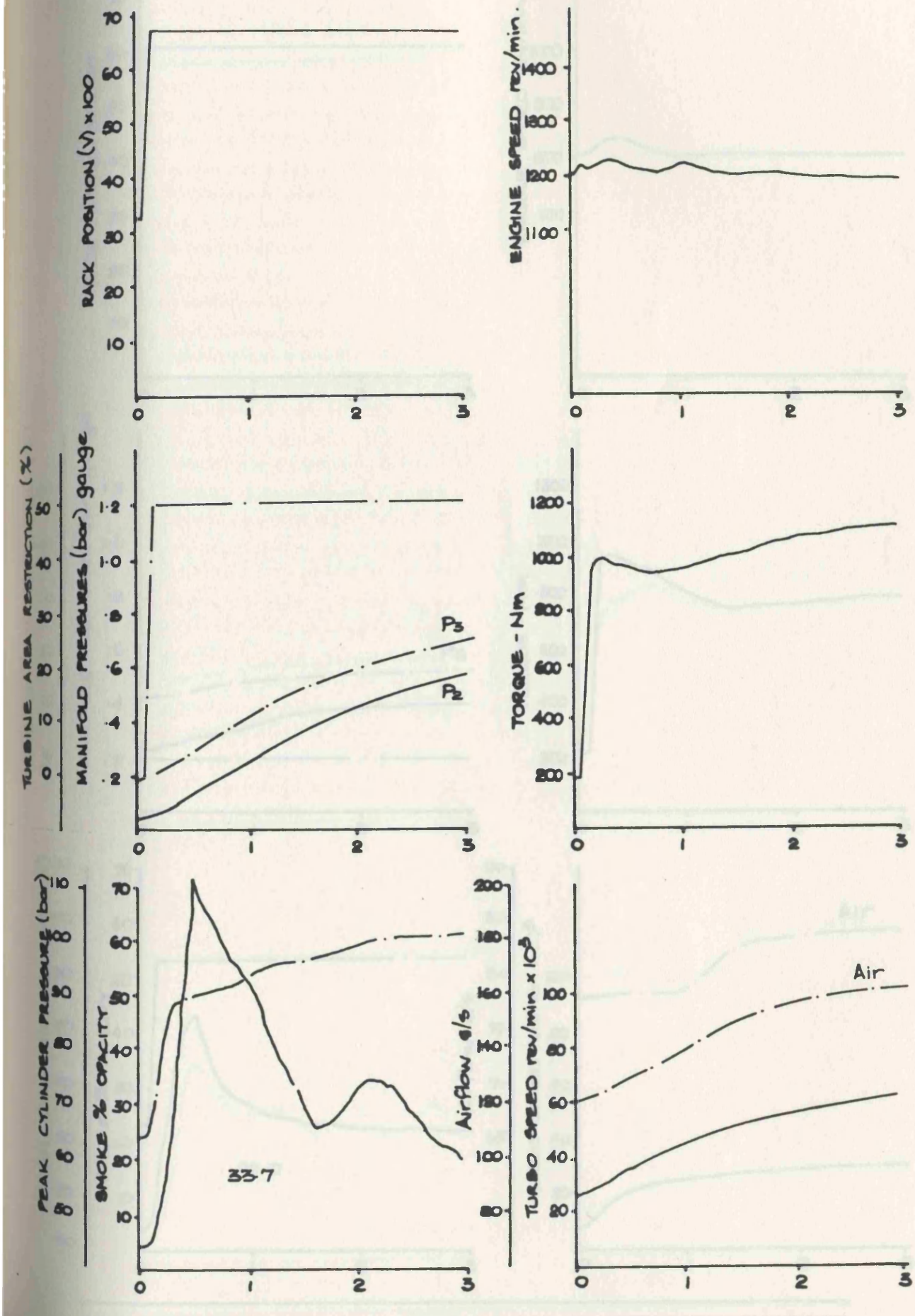

FIG 5.14

VG TURBOCHARGER FULLY OPEN

Constant Speed TRANSIENT @ 800 rev/min

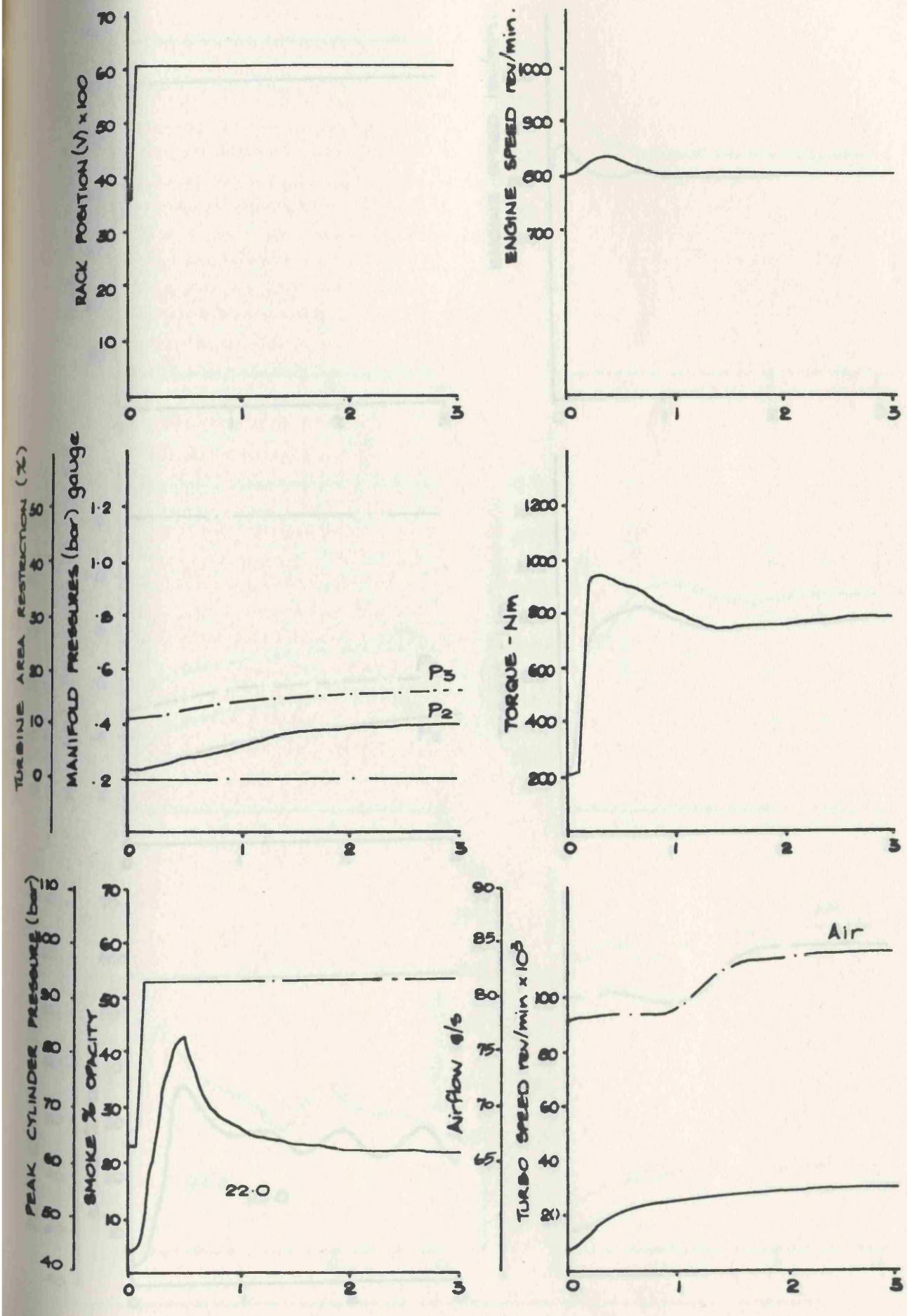

FIG. 5.15

VG TURBOCHARGER FULLY RESTRICTED

Constant Speed TRANSIENT @ 800 rev/min

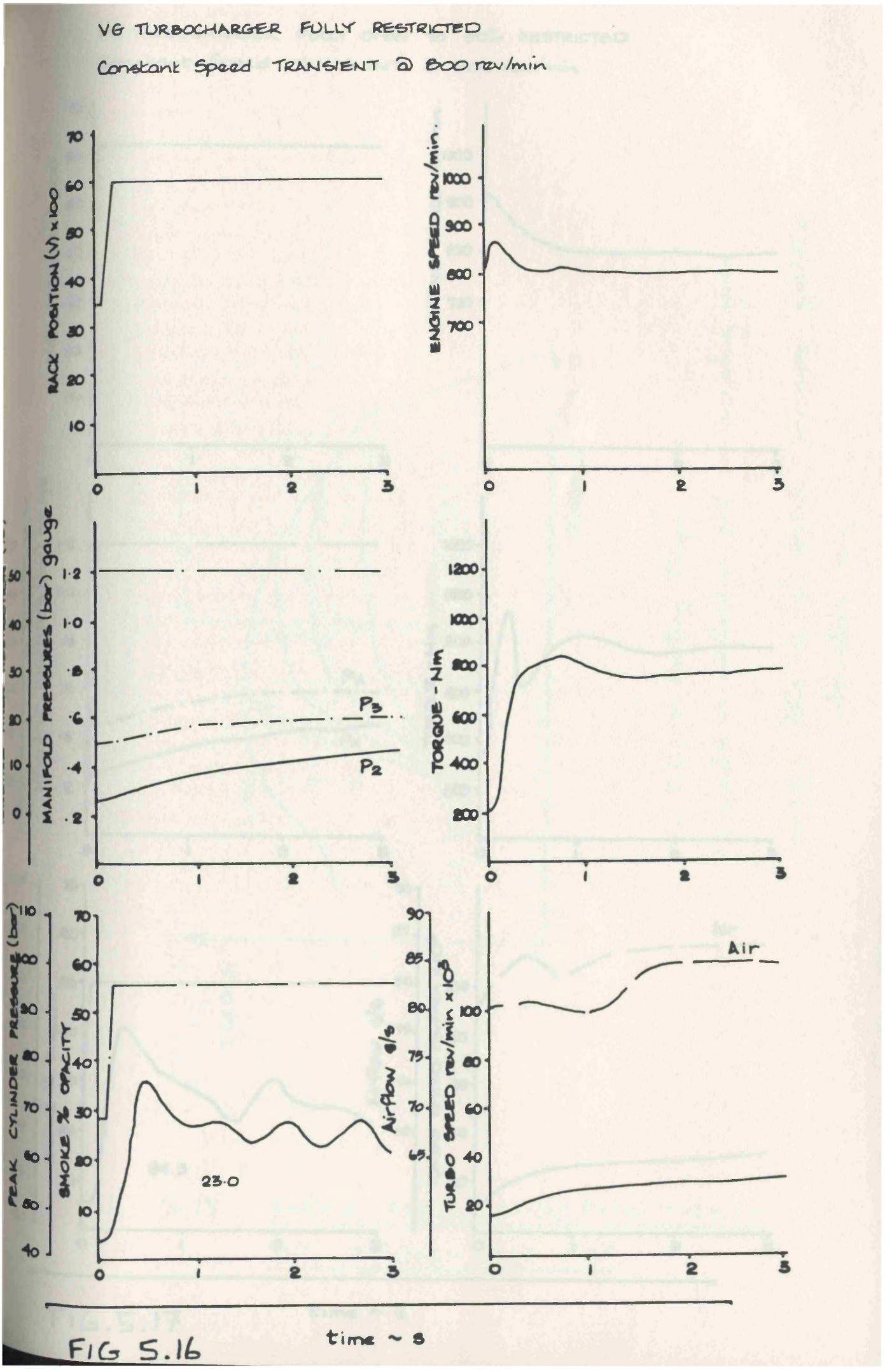

FIG 5.16

VG TURBOCHARGER FULLY OPEN TO 50% RESTRICTED
Constant Speed TRANSIENT @ 800 rev/min

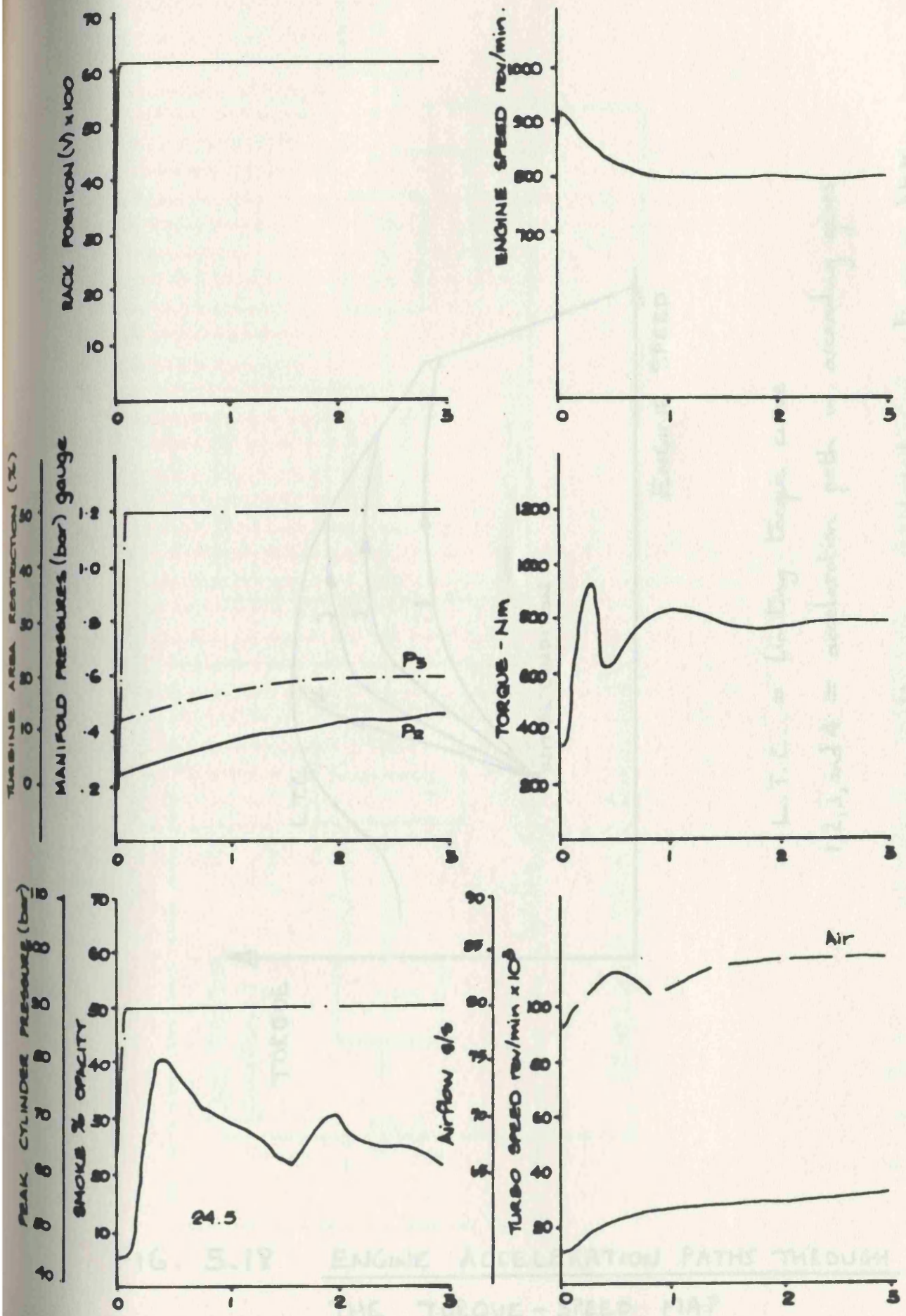

FIG. 5.17

FIG. 5.18 ENGINE ACCELERATION PATHS THROUGH THE TORQUE - SPEED MAP

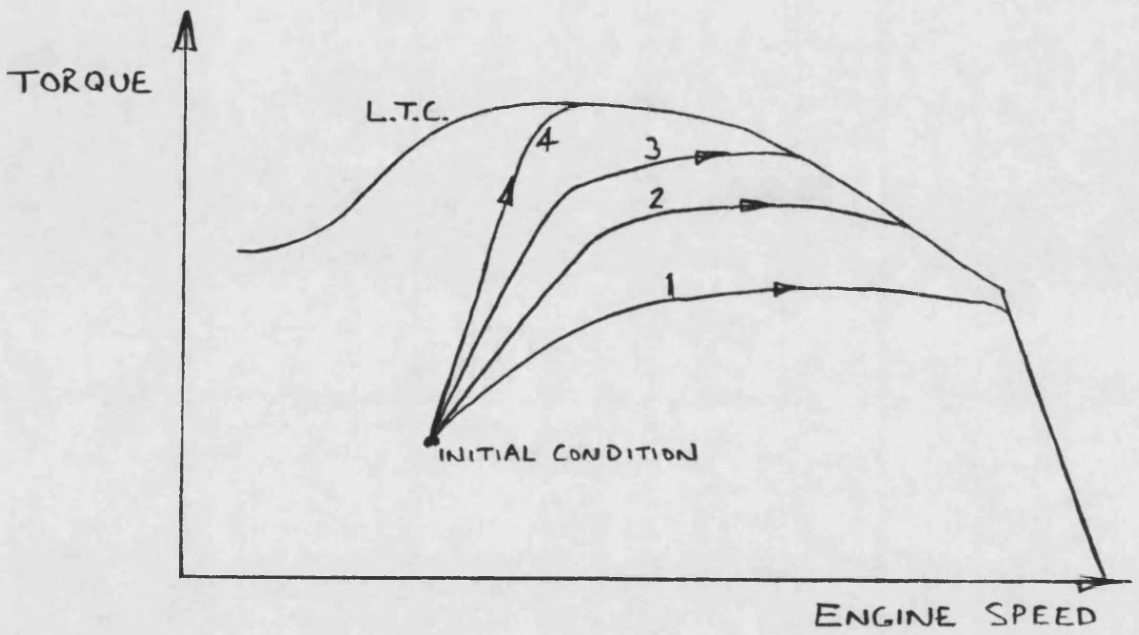

L.T.C. = Limiting torque curve

1, 2, 3, and 4 = acceleration path in ascending gears

NOTE:- this is a sketch providing qualitative information only.

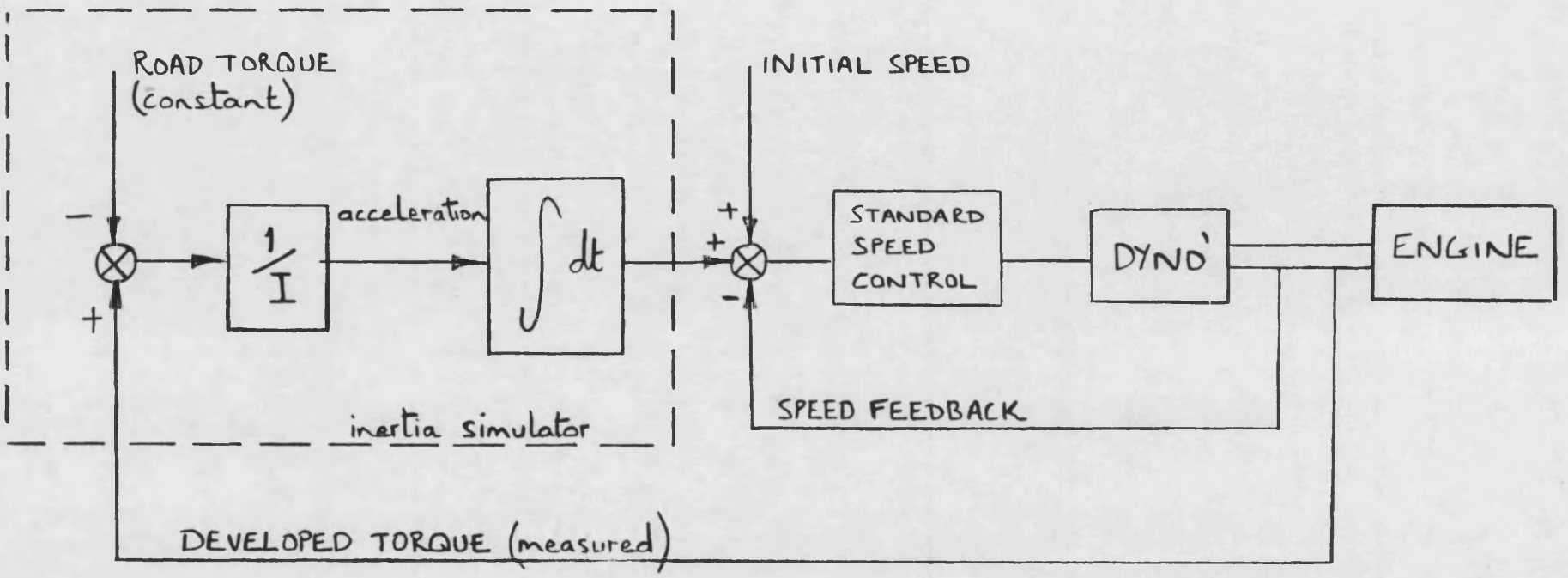

FIG 5.19 VEHICLE INERTIA SIMULATOR BLOCK DIAGRAM

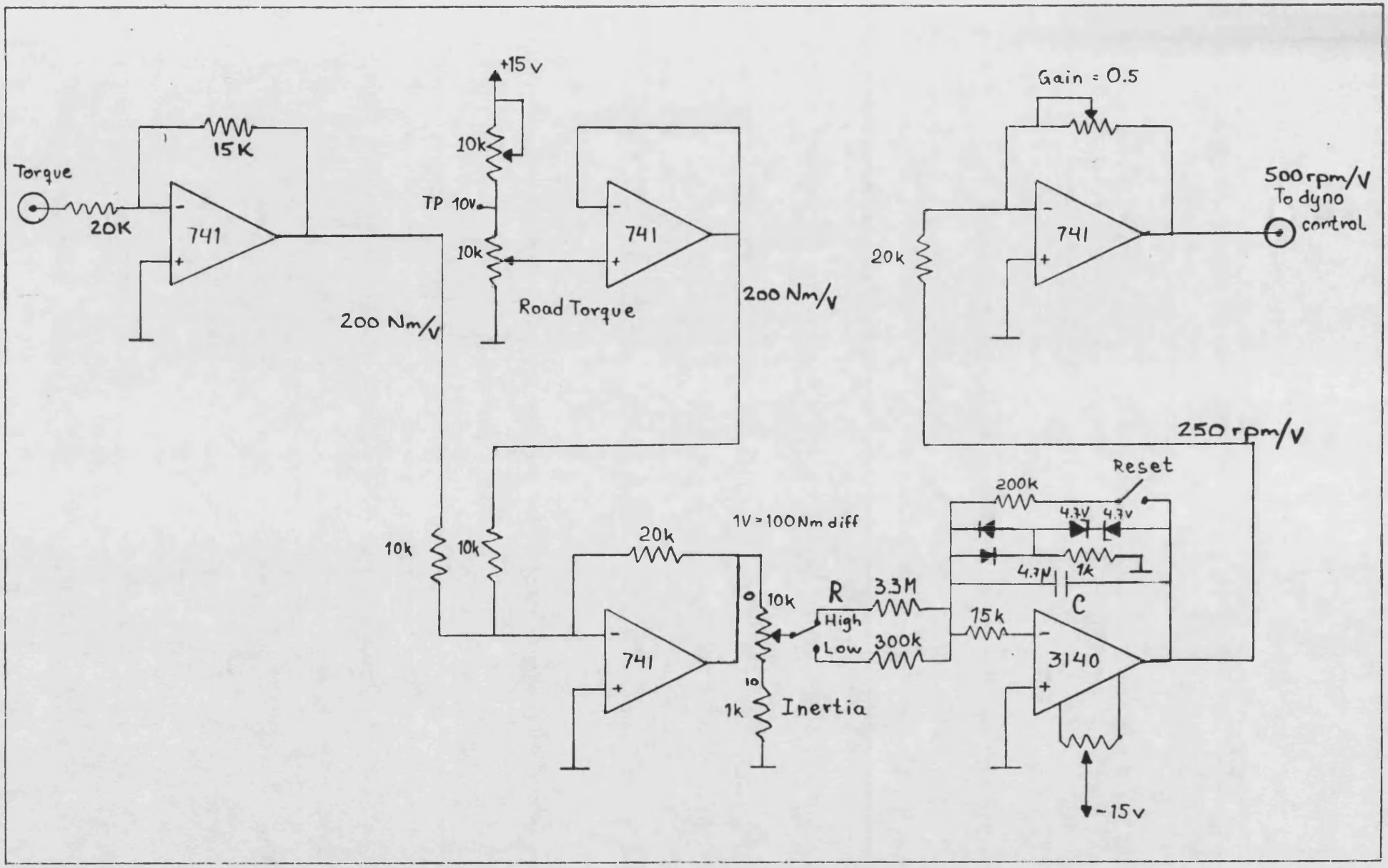

Figure 5.20 Inertia Simulator Circuit Diagram

FIG. 5.21

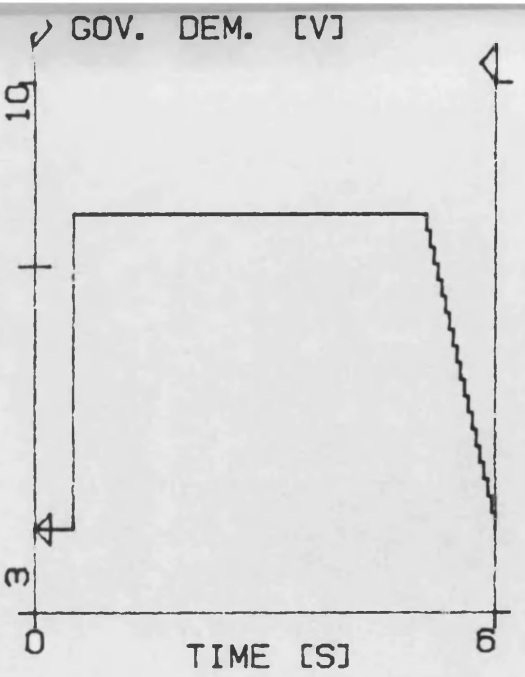

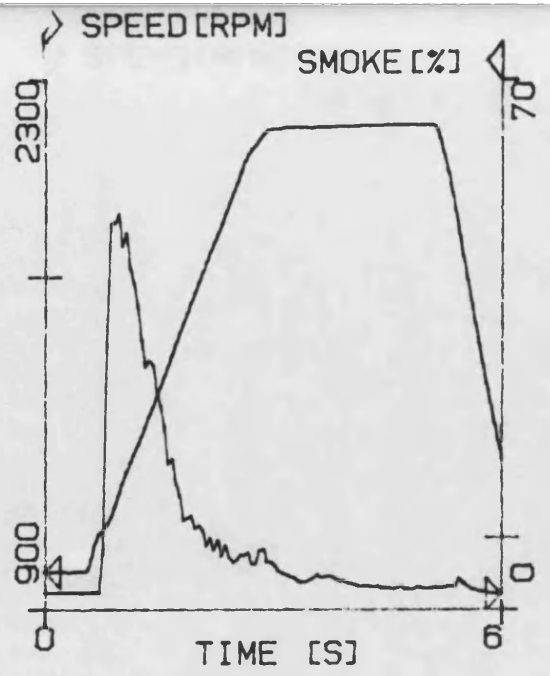

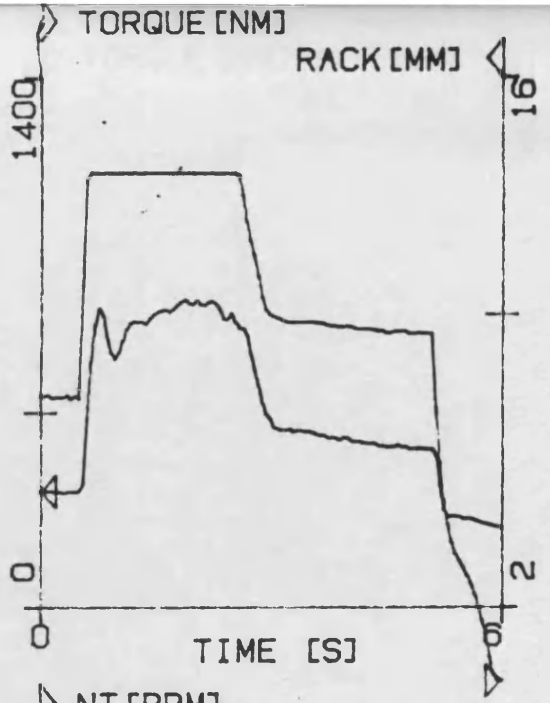

COMMENTS:
1000-2000 TRANSIENT
MAX RACK 6.3
1ST GEAR
BOOST VG SCHEDULE
.
.
.

RAM R1004002
CAL C1004001
DAT D1009102

AMBIENT TEMP: 26.1 C
PRESSURE : 996 MBAR
SIGN : UA
TIME : 152118

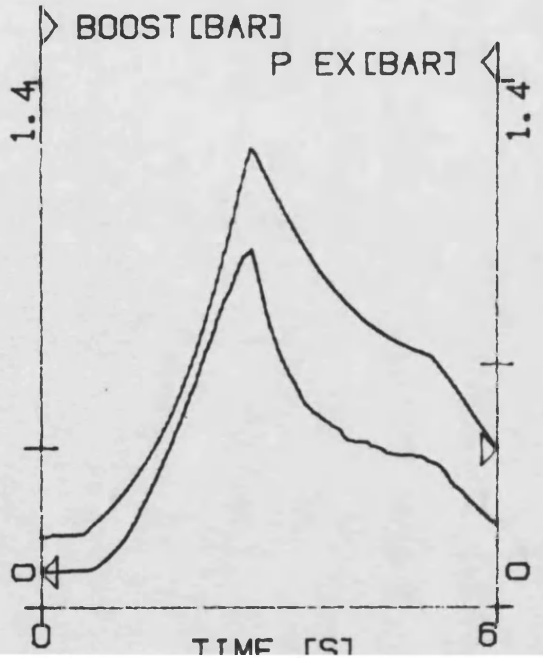

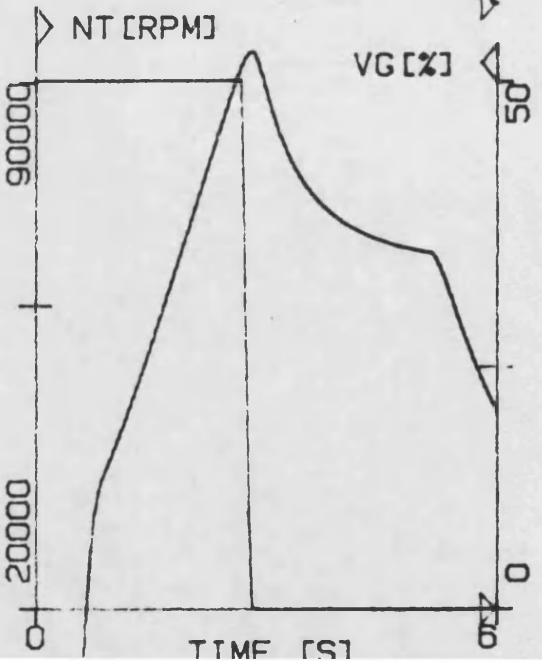

FIG. 5.22

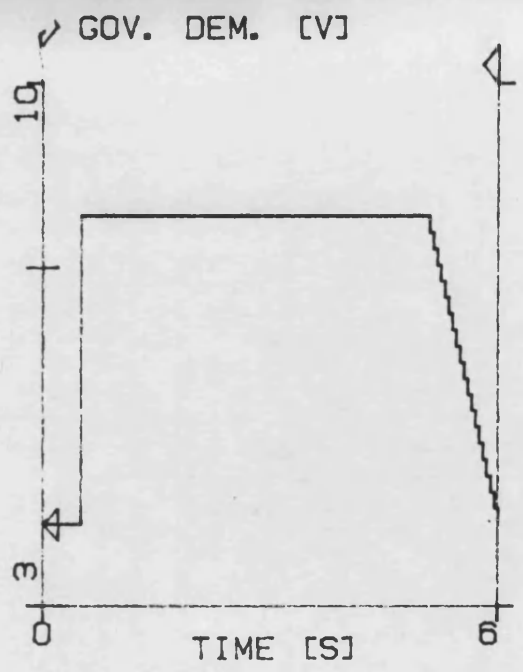

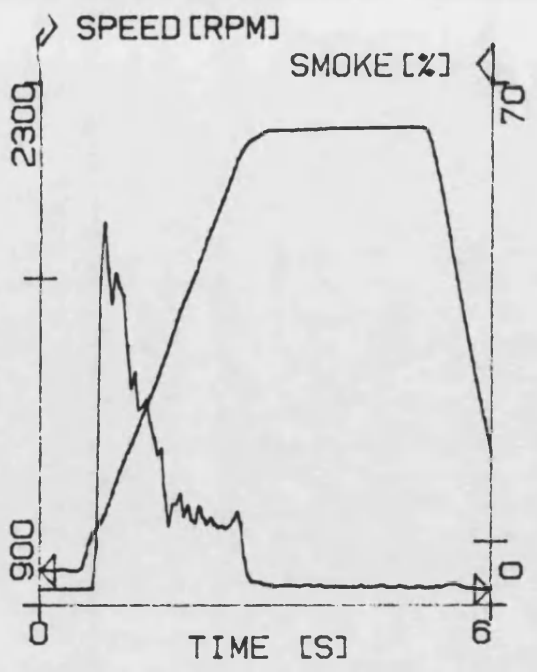

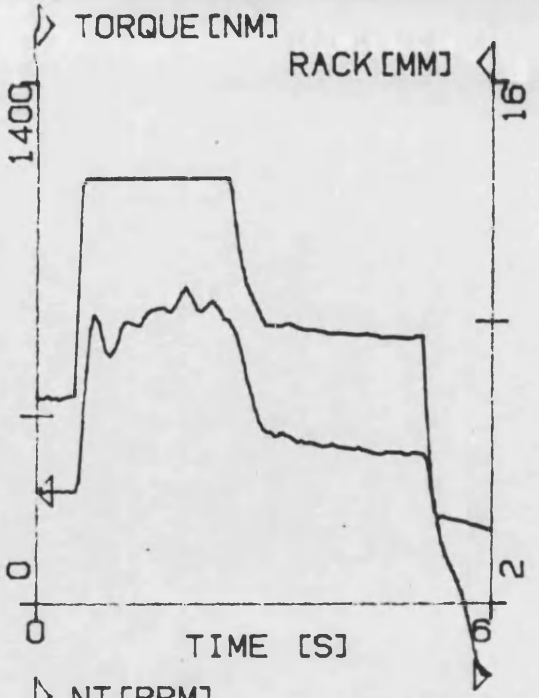

COMMENTS:
1000-2000 TRANSIENT
MAX RACK 6.3
1ST GEAR
SPEED VG SCHEDULE
.
.
.

RAM R1004002
CAL C1004001
DAT D1010202

AMBIENT TEMP: 24.7 C
PRESSURE : 997 MBAR
SIGN : UA
TIME : 114528
DATE : 841010

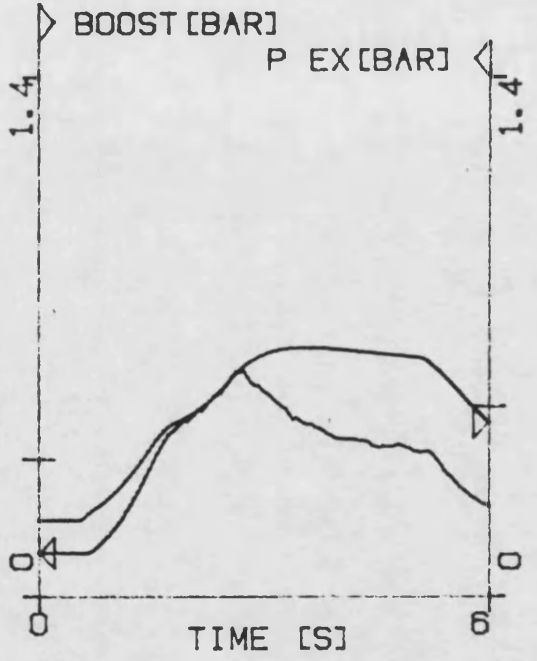

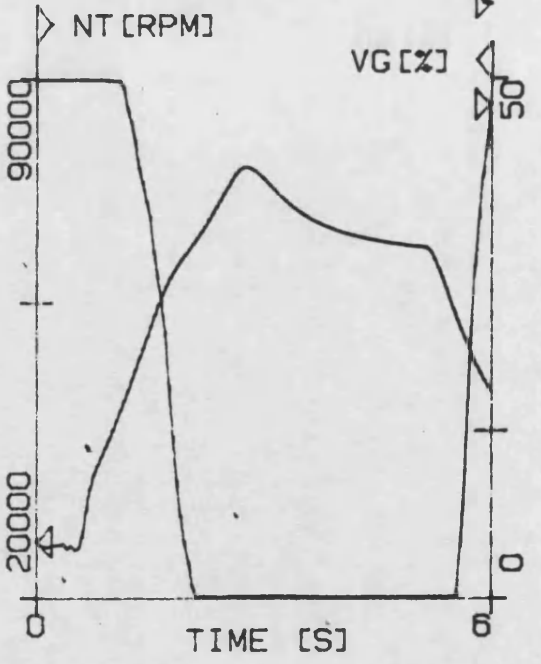

FIG. 5.23

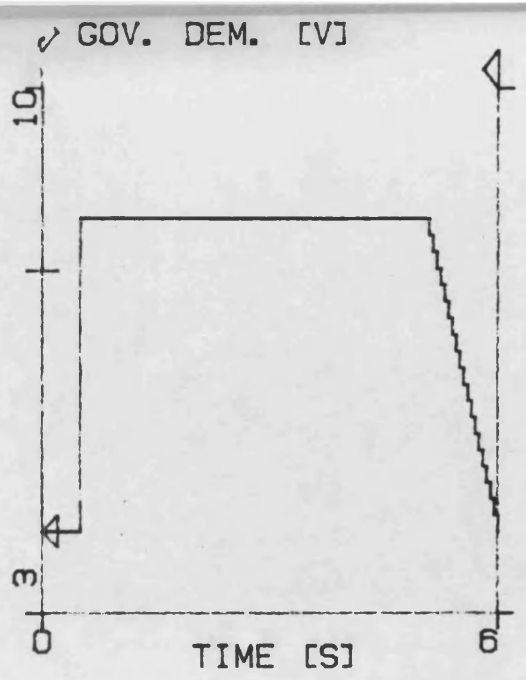

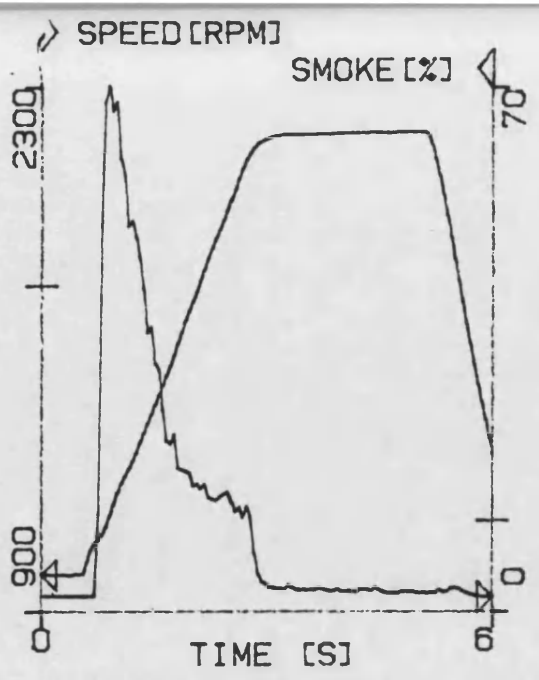

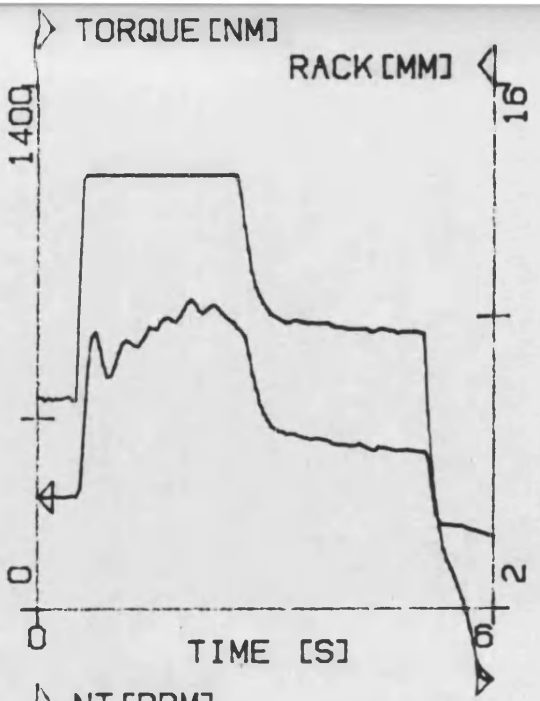

COMMENTS:
1000-2000 TRANSIENT
MAX RACK 6.3
1ST GEAR
SPEED+TORQUE VG SCHEDULE
.
.
.
RAM R1004002
CAL C1004001
DAT 1010304

AMBIENT TEMP: 27.3 C
PRESSURE : 996 MBAR
SIGN : UA
TIME : 150538
DATE : 841010

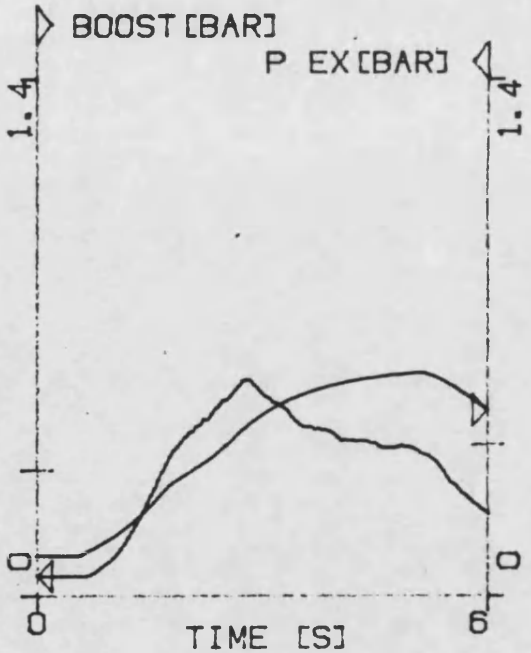

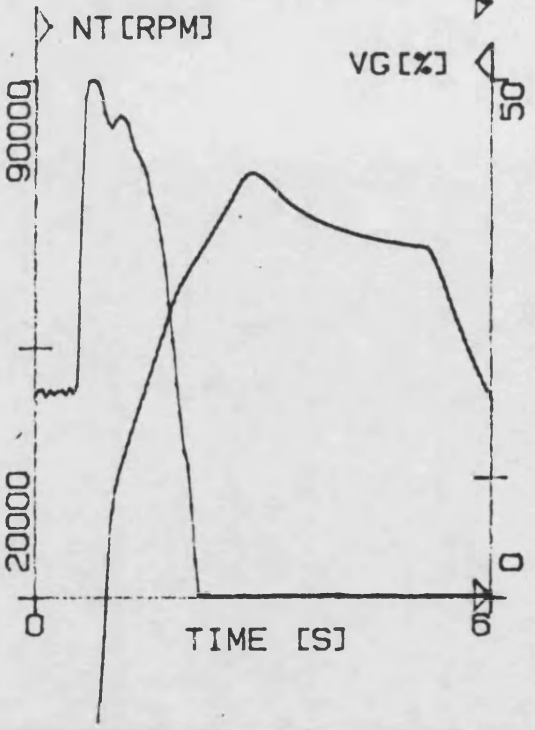

FIG. 5.24

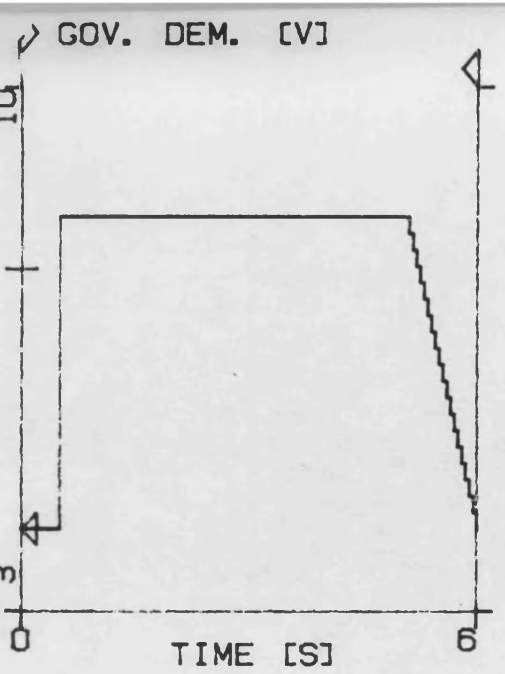

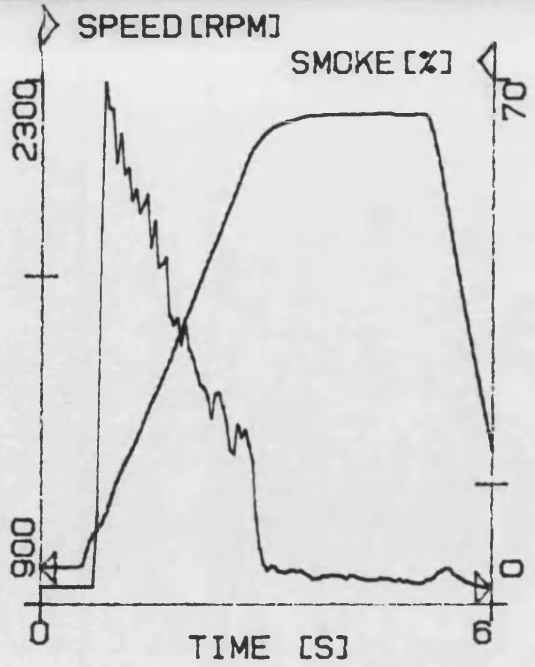

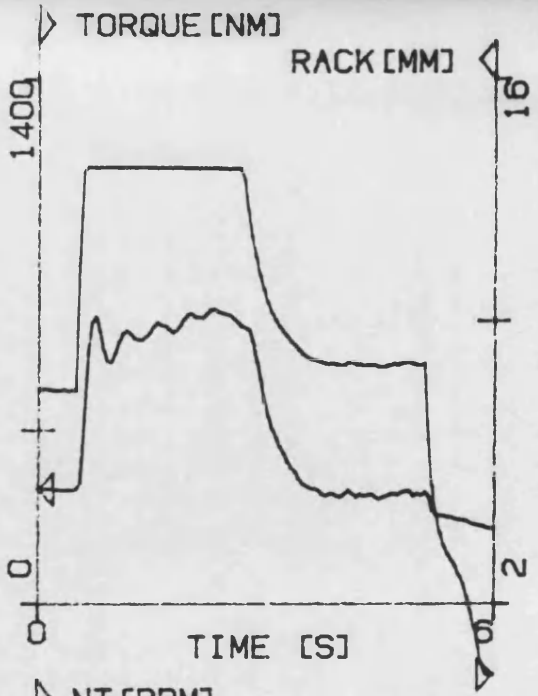

COMMENTS:
1000-2000 TRANSIENT
MAX RACK 6.3
1ST GEAR
ZERO RESTRICTION
.
.
.
RAM R1004002
CAL C1004001
DAT D1010403

AMBIENT TEMP: 26.6 C
PRESSURE : 996 MBAR
SIGN : UA
TIME : 161331
DATE : 841010

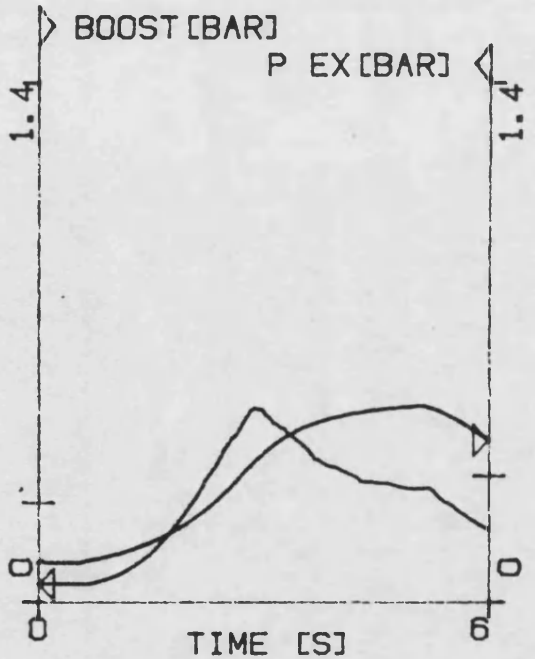

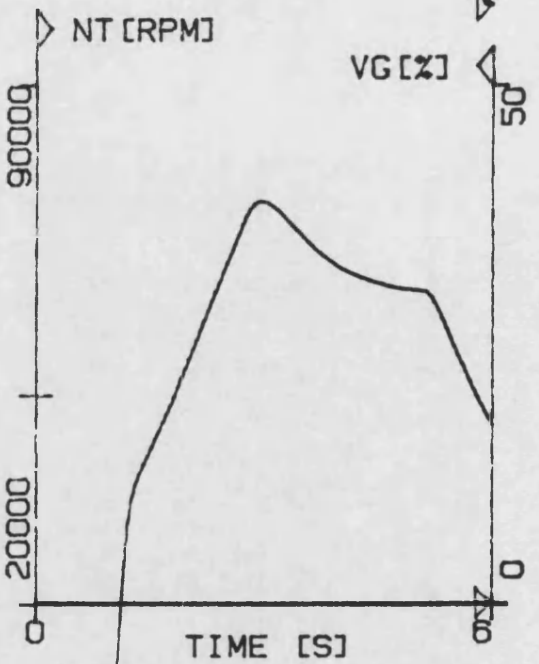

FIG 5.25

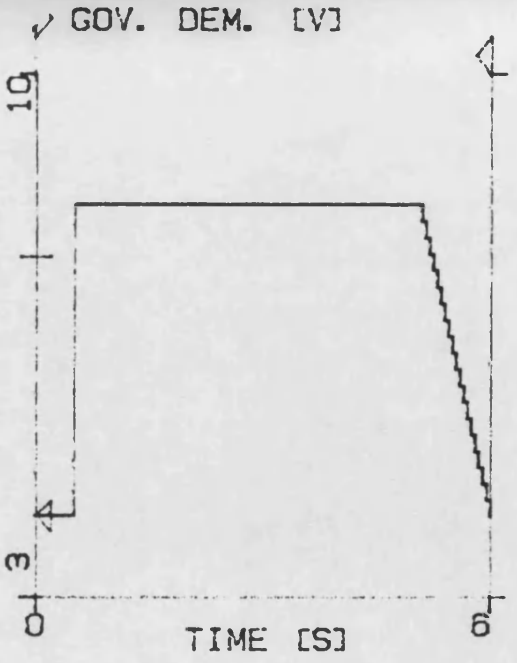

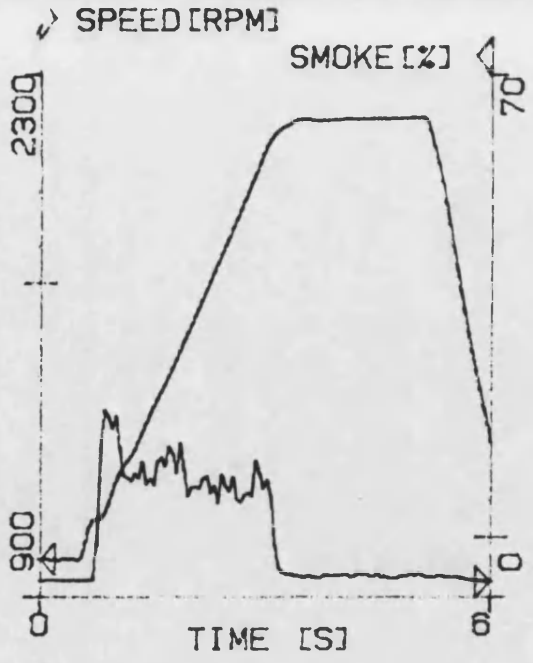

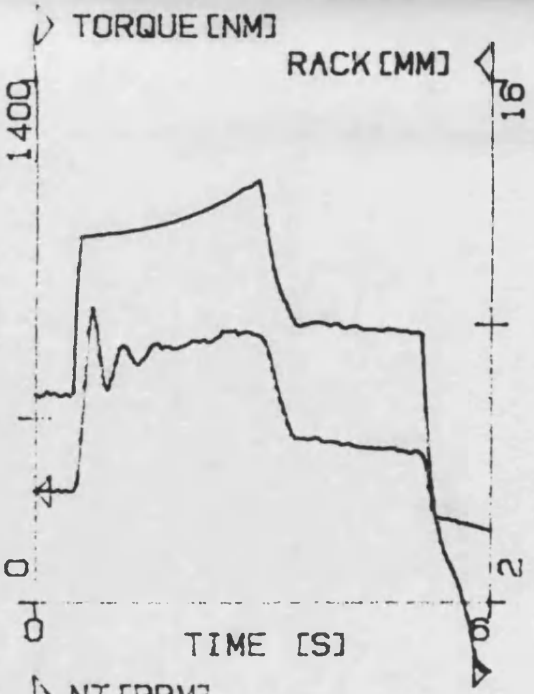

COMMENTS:
1000-2000 TRANSIENT
MAX RACK SCHEDULE 1
1ST GEAR
ZERO RESTRICTION
.
.
.

RAM R1004002
CAL C1004001
DAT D1011902

AMBIENT TEMP: 25.6 C
PRESSURE : 997 MBAR
SIGN : UA
TIME : 173435
DATE : 841011

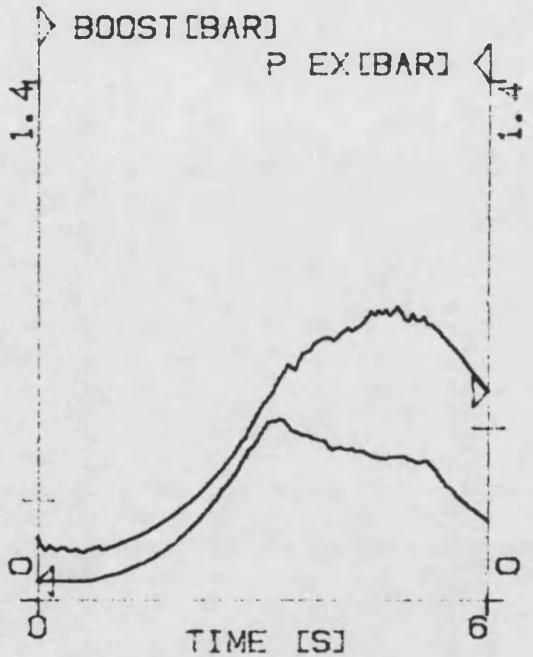

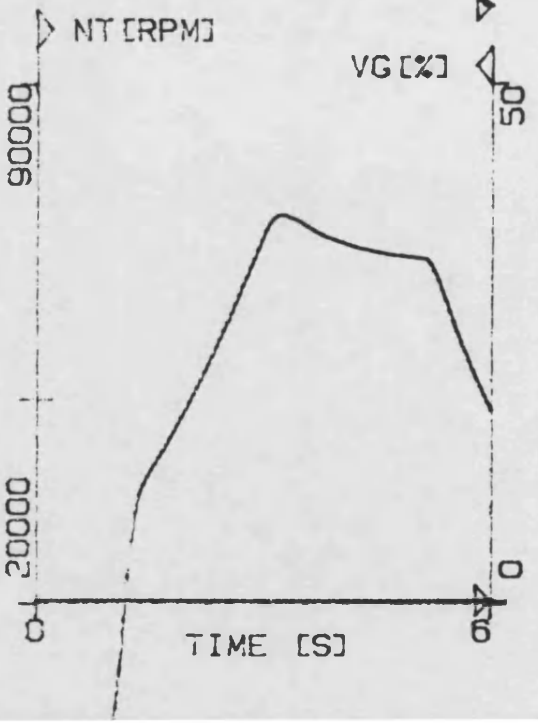

FIG. 5.26

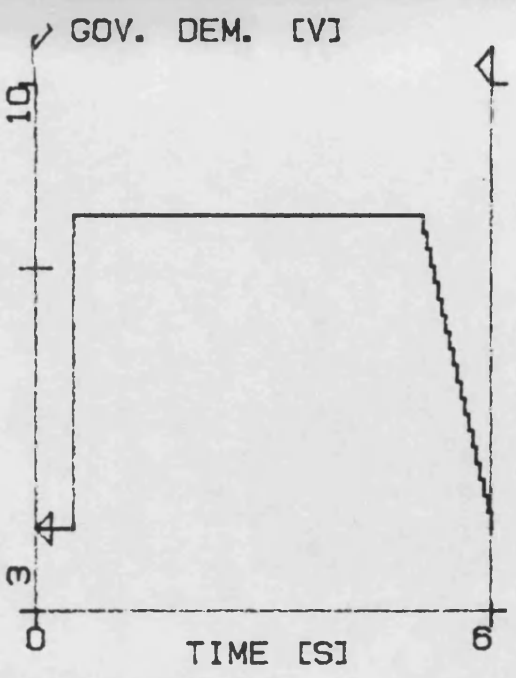

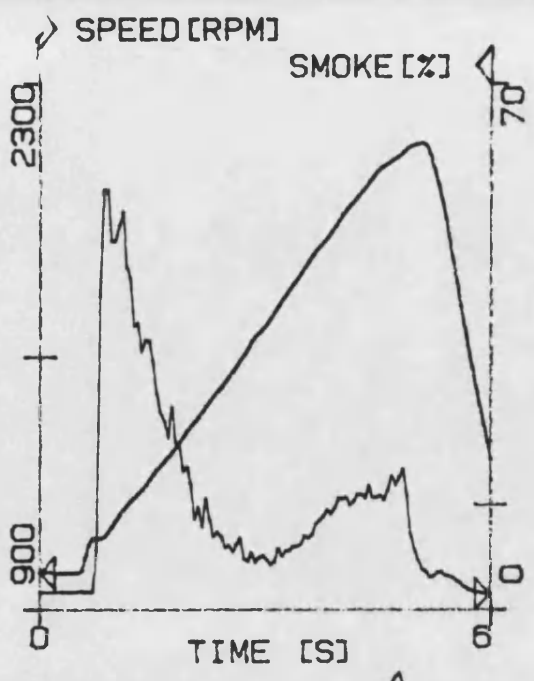

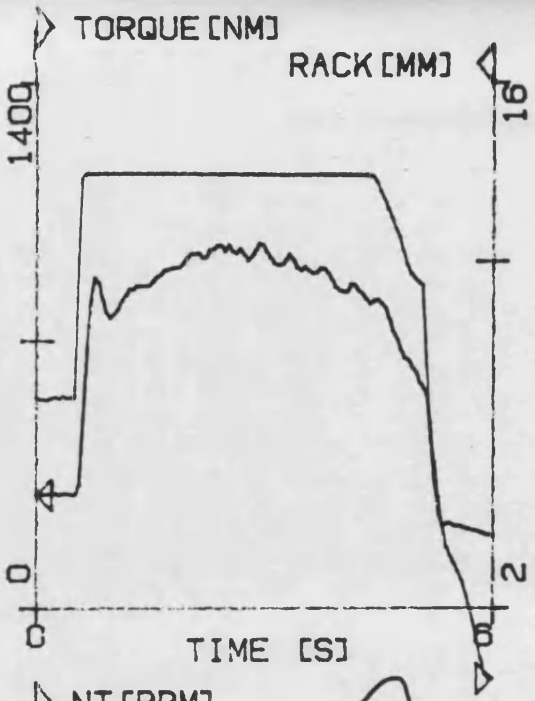

COMMENTS:
1000-2000 TRANSIENT
MAX RACK 6.3
2ND GEAR
BOOST VG SCHEDULE
.
.
.

RAM R1004002
CAL C1004001
DAT D1010111

AMBIENT TEMP: 24.8 C
PRESSURE : 996 MBAR
SIGN : UA
TIME : 174844
DATE : 841010

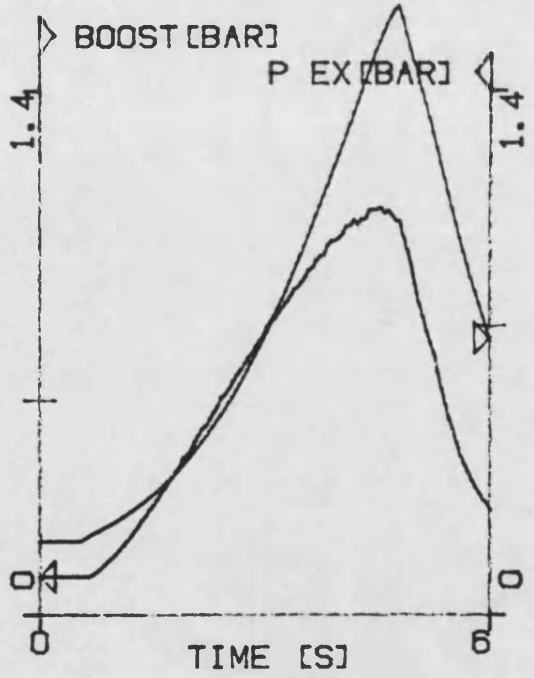

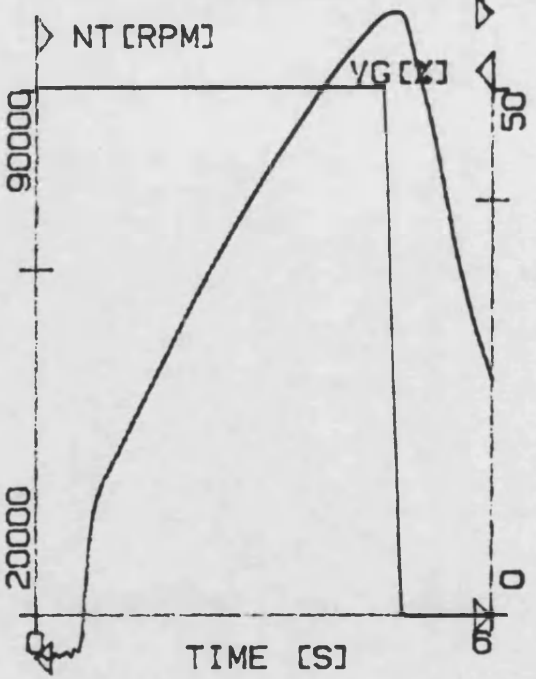

FIG 5.27

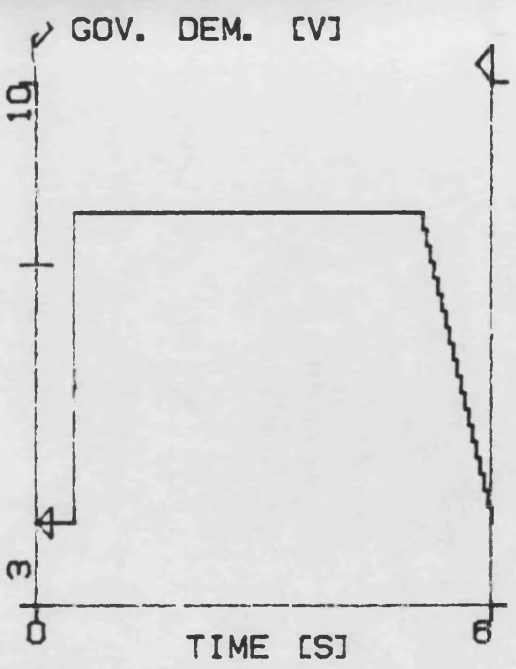

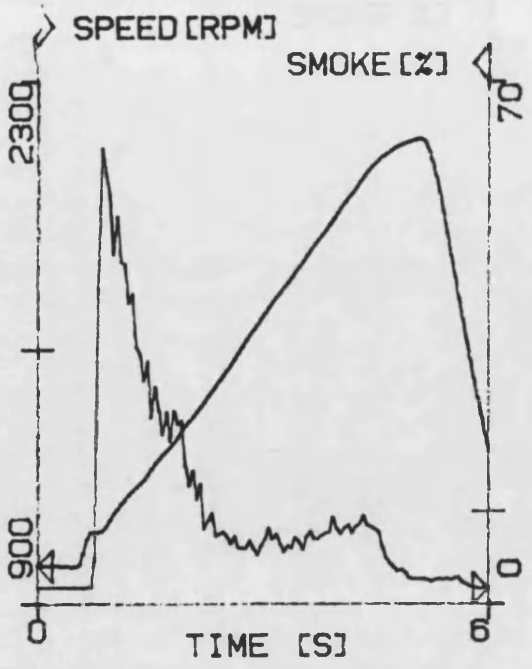

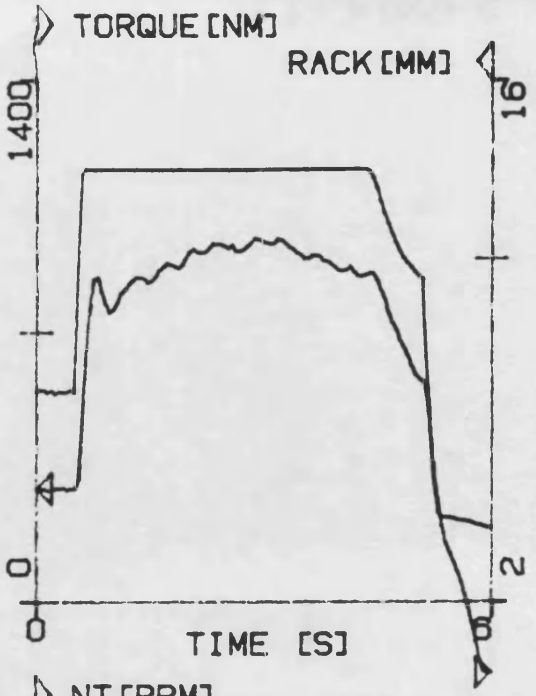

COMMENTS:
1000-2000 TRANSIENT
MAX RACK 6.3
2ND GEAR
SPEED VG SCHEDULE
.
.
.

RAM R1004002
CAL C1004001
DAT D1010212

AMBIENT TEMP: 25.3 C
PRESSURE : 996 MBAR
SIGN : UA
TIME : 180149
DATE : 841010

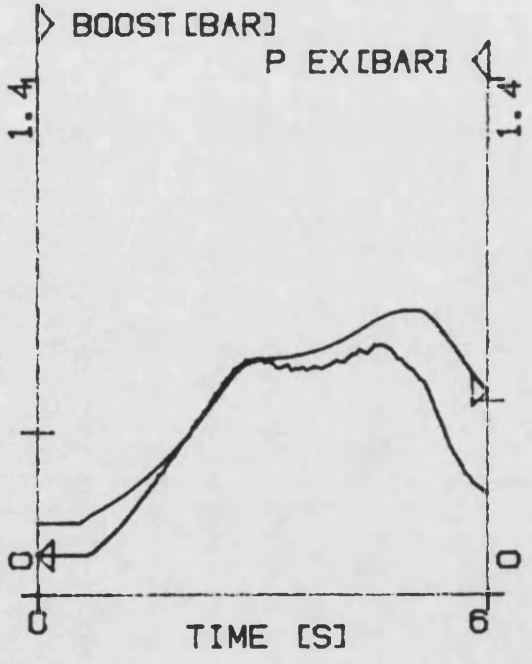

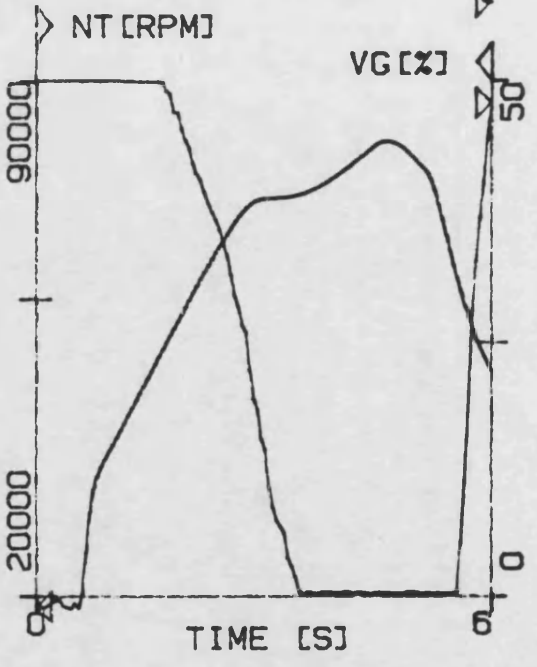

FIG 5.28

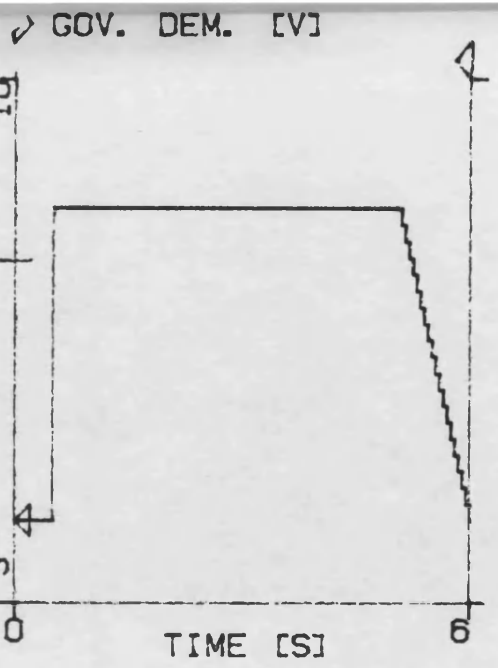

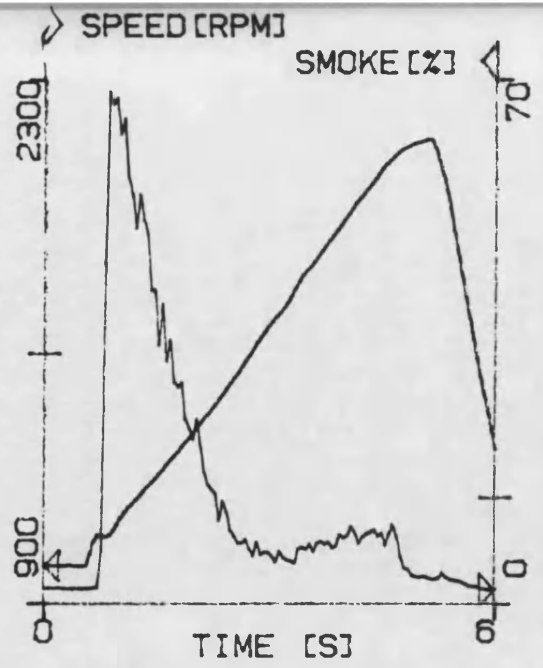

COMMENTS:
1000-2000 TRANSIENT
MAX RACK 6.3
2ND GEAR
SPEED+TORQUE VG SCHEDULE
.
.
.

RAM R1004002
CAL C1004001
DAT D1010312

AMBIENT TEMP: 25.3 C
PRESSURE : 996 MBAR
SIGN : UA
TIME : 182804
DATE : 841010

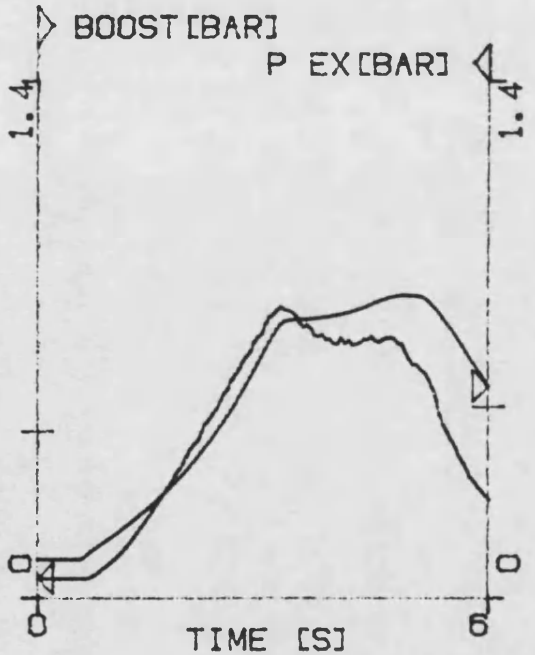

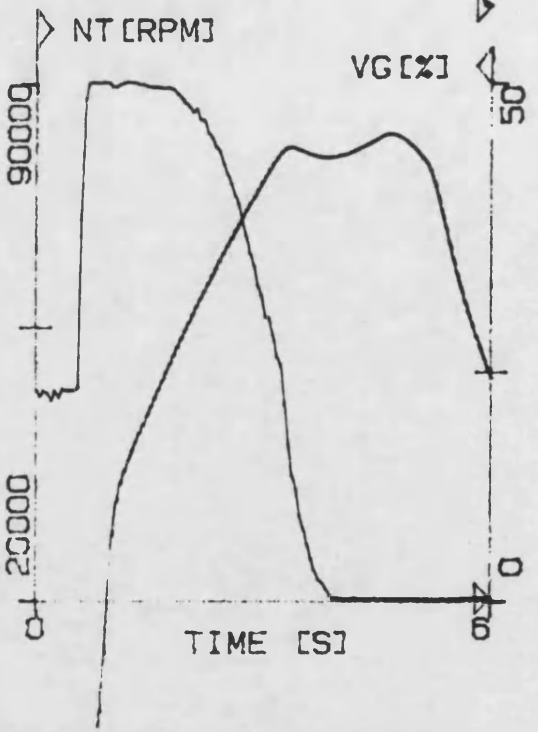

Fig 5.29

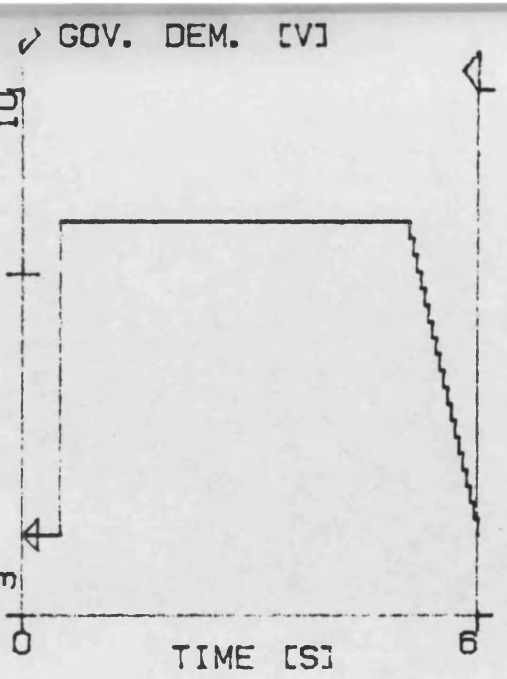

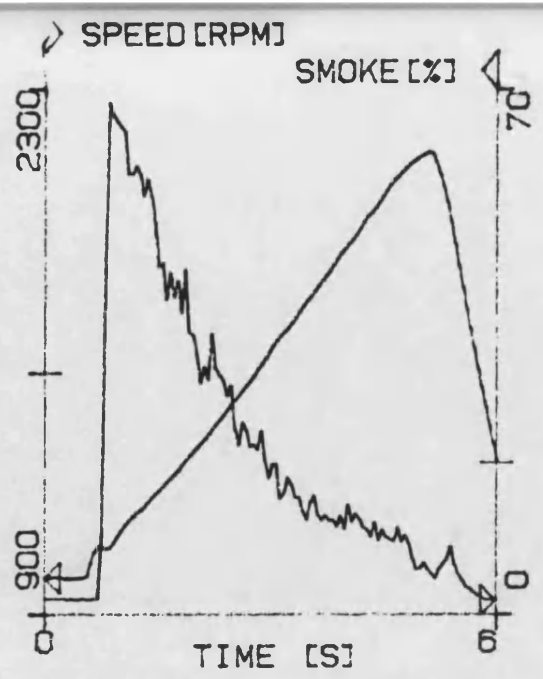

COMMENTS:
1000-2000 TRANSIENT
MAX RACK 6.3
2ND GEAR
ZERO RESTRICTION
.
.
.
RAM R1004002
CAL C1004001
DAT D1010411

AMBIENT TEMP: 24.5 C
PRESSURE : 996 MBAR
SIGN : UA
TIME : 185410
DATE : 841010

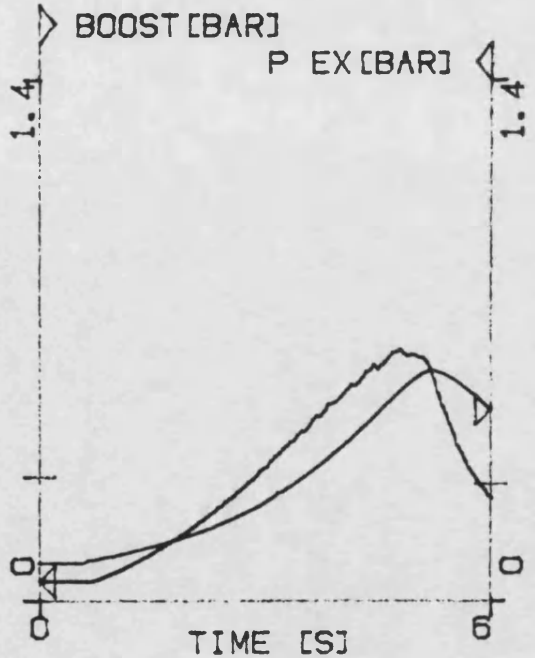

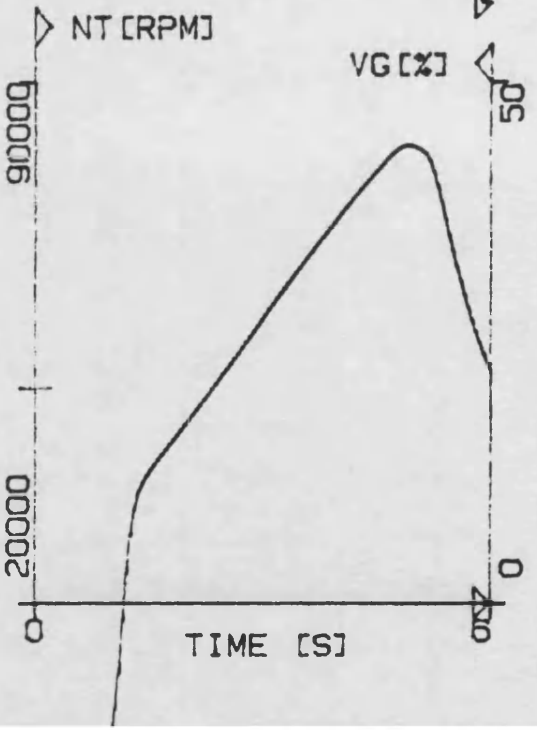

Fig. 5.30

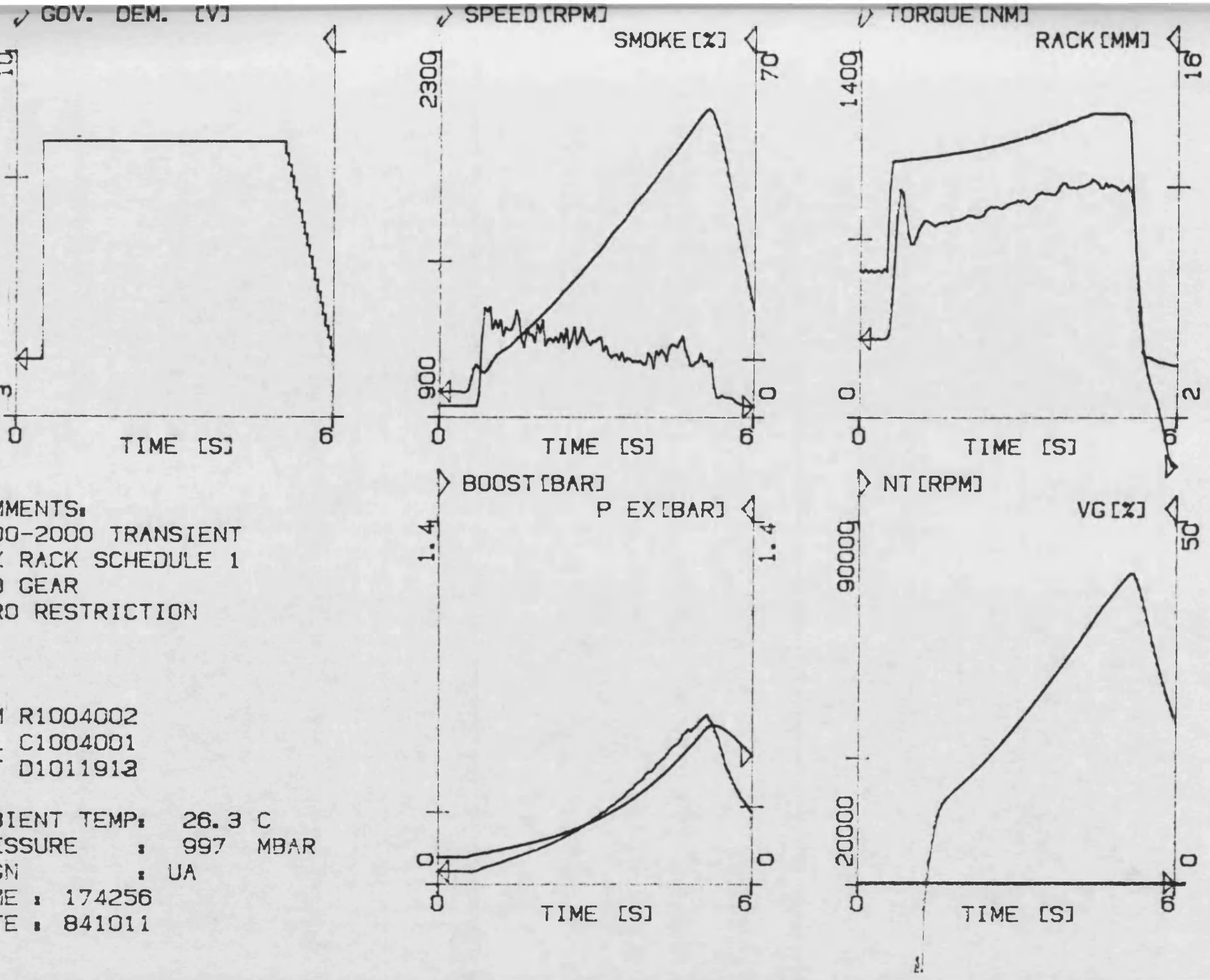

COMMENTS:
1000-2000 TRANSIENT
MAX RACK SCHEDULE 1
2ND GEAR
ZERO RESTRICTION
.
.
.
RAM R1004002
CAL C1004001
DAT D1011913

AMBIENT TEMP: 26.3 C
PRESSURE : 997 MBAR
SIGN : UA
TIME : 174256
DATE : 841011

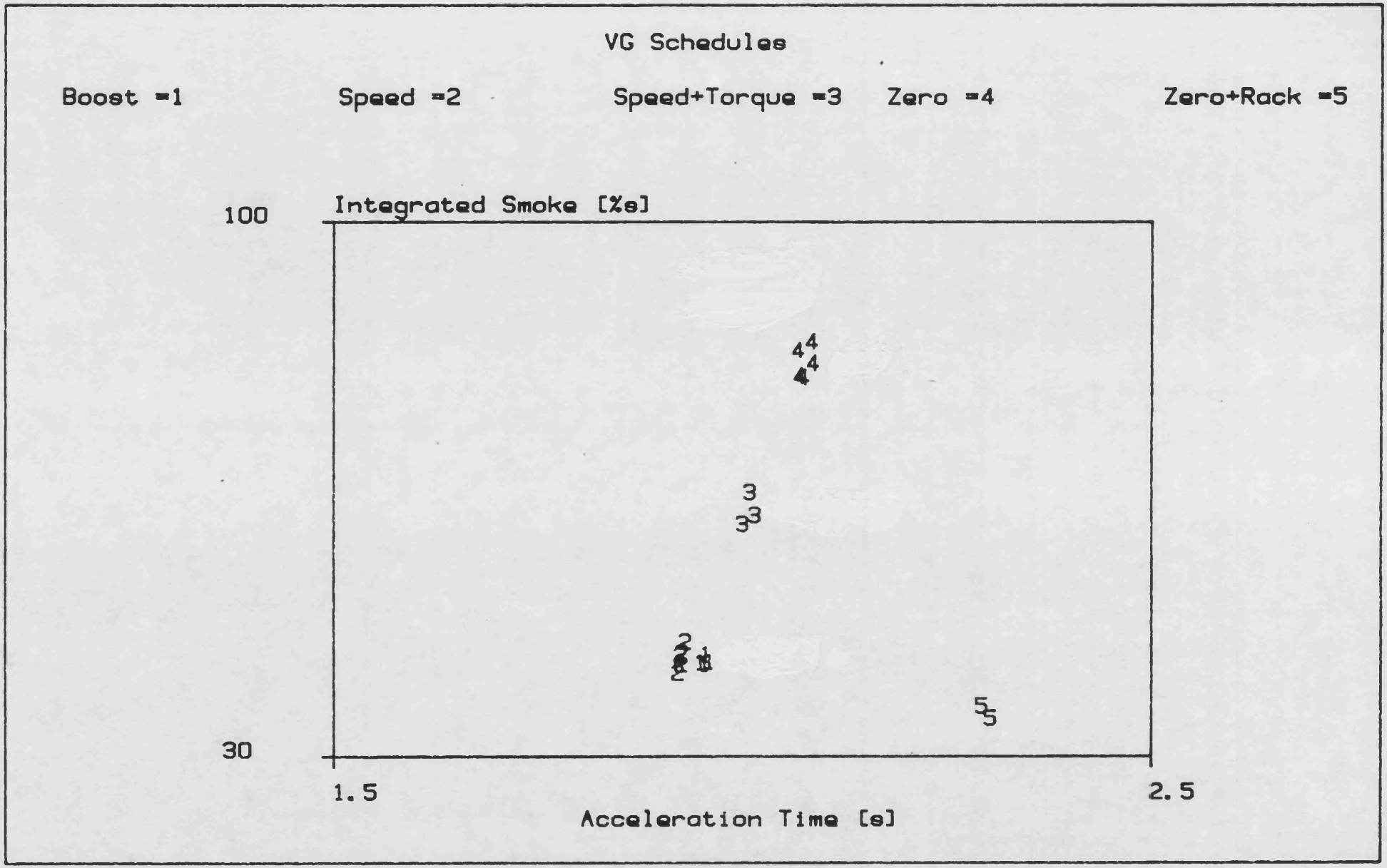

Figure 5.31 Smoke vs. Time 1st Gear

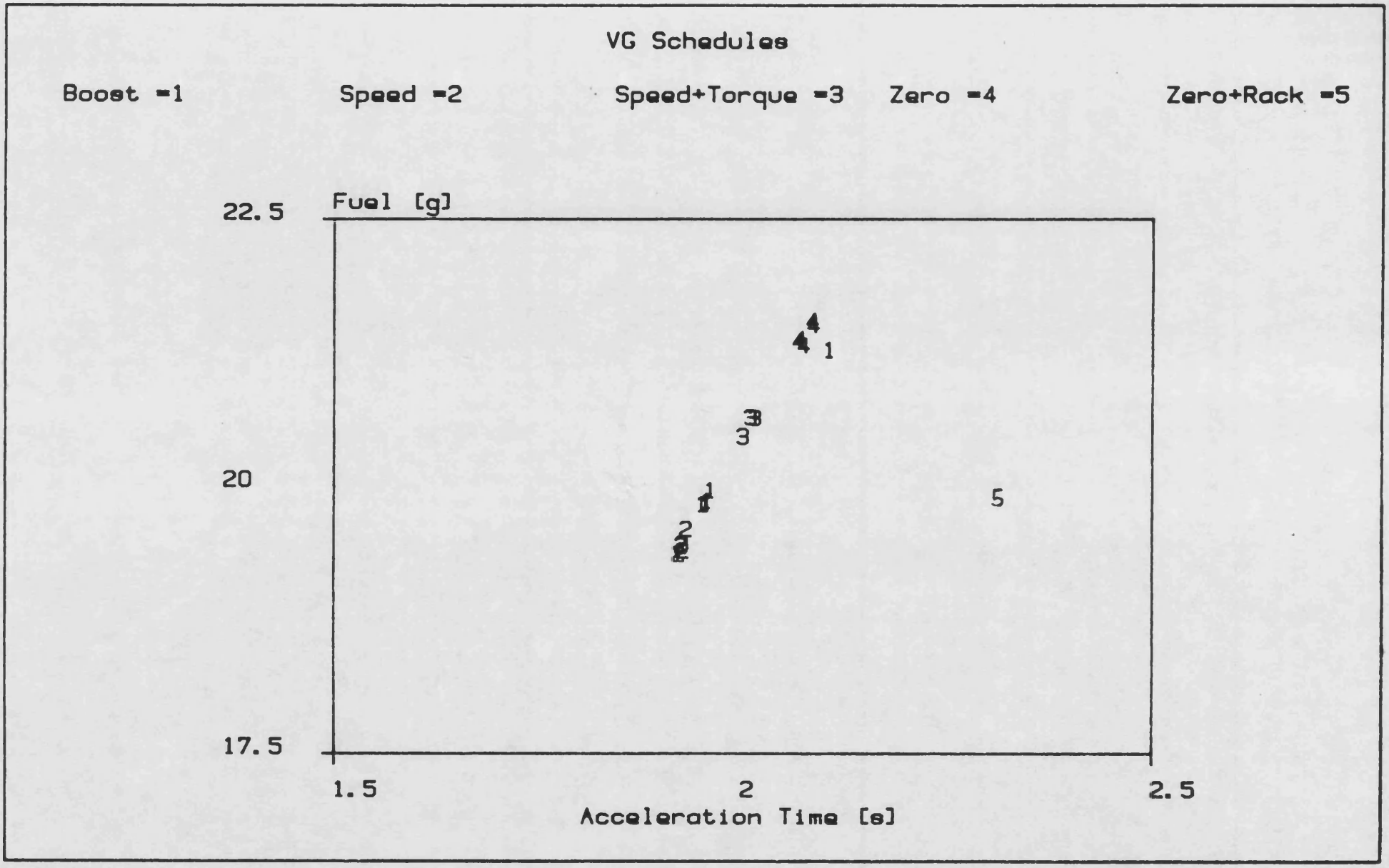

Figure 5.32 Fuel vs. Time 1st Gear

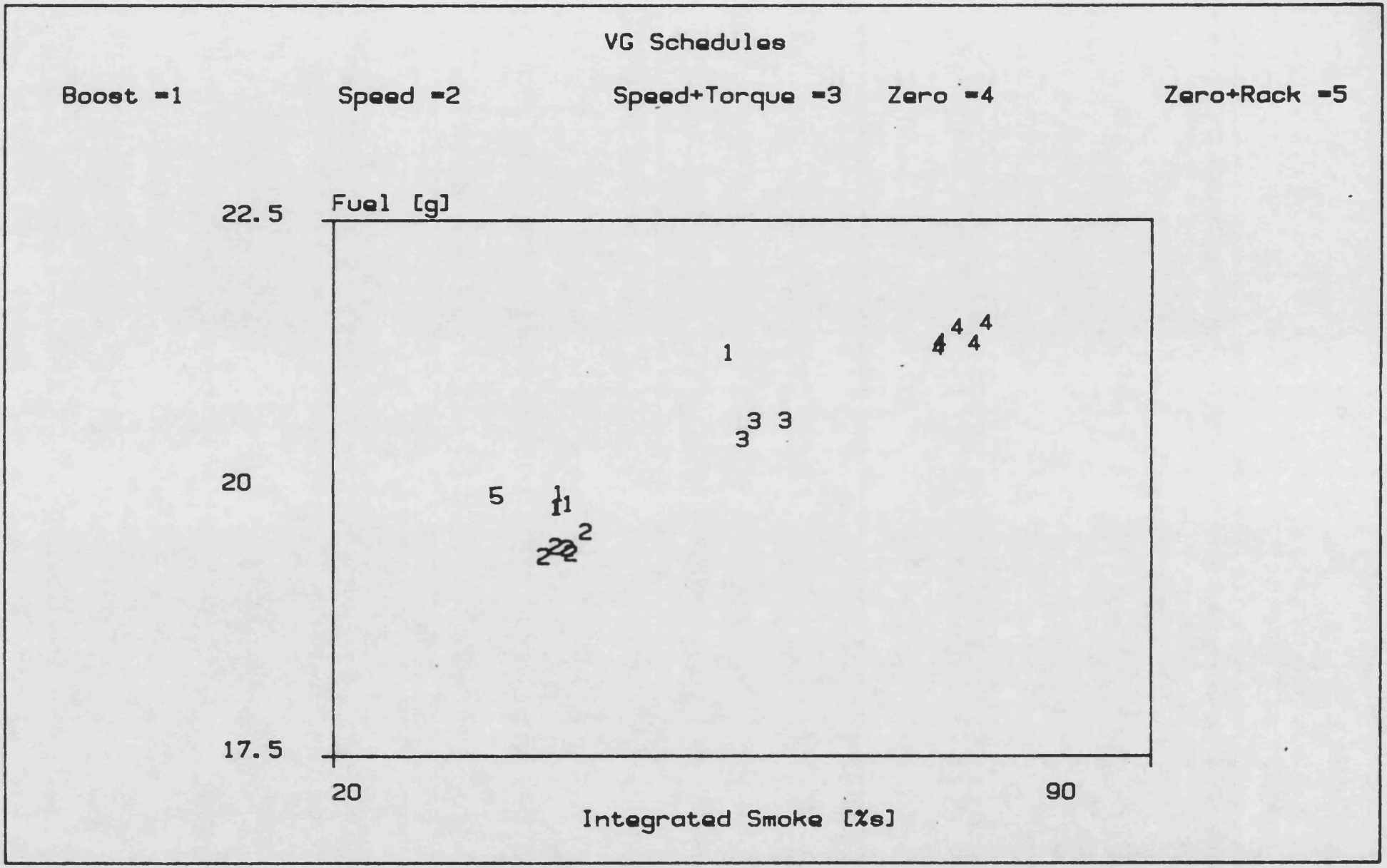

Figure 5.33 Fuel vs. Smoke 1st Gear

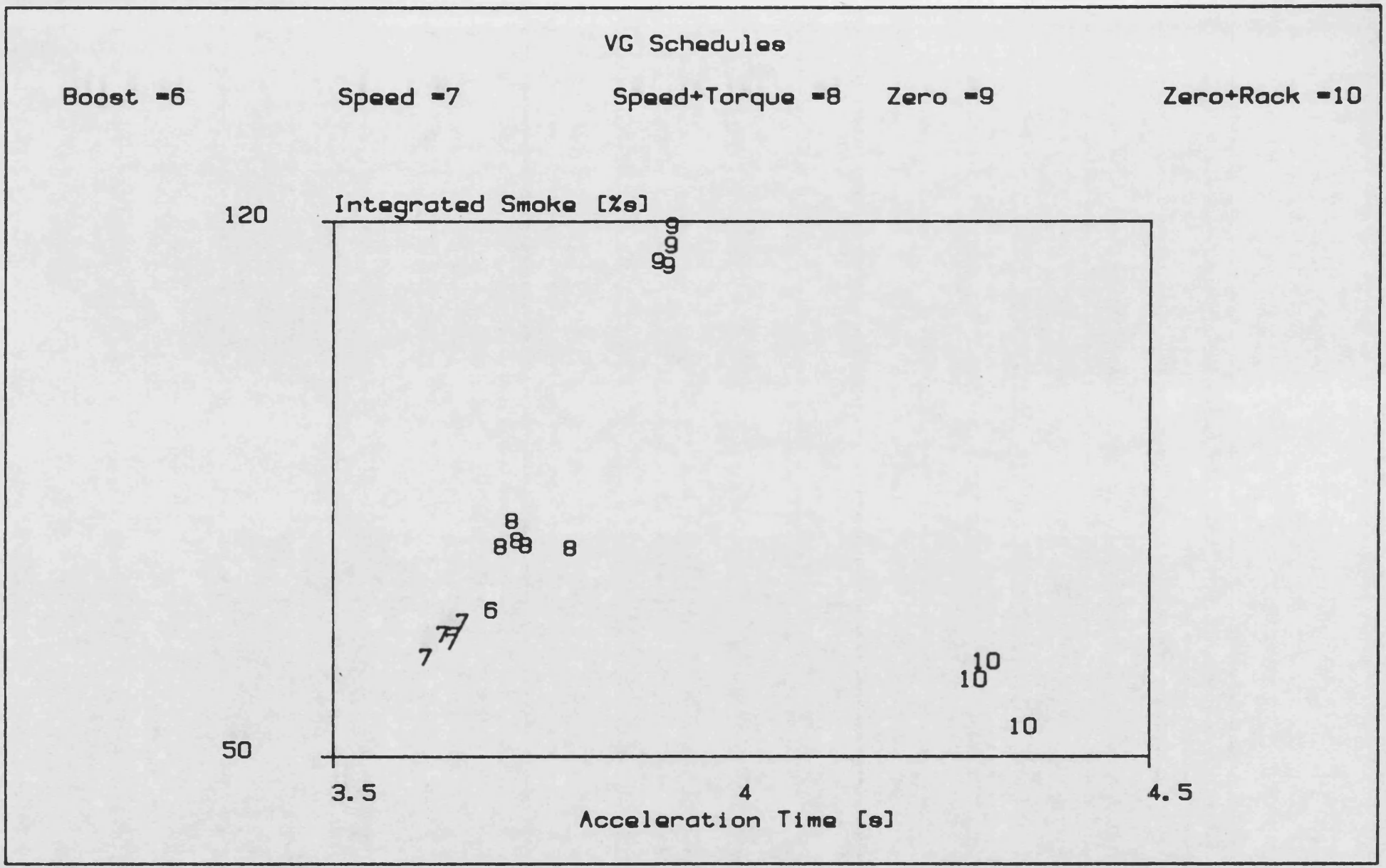

Figure 5.34 Smoke vs. Time 2nd Gear

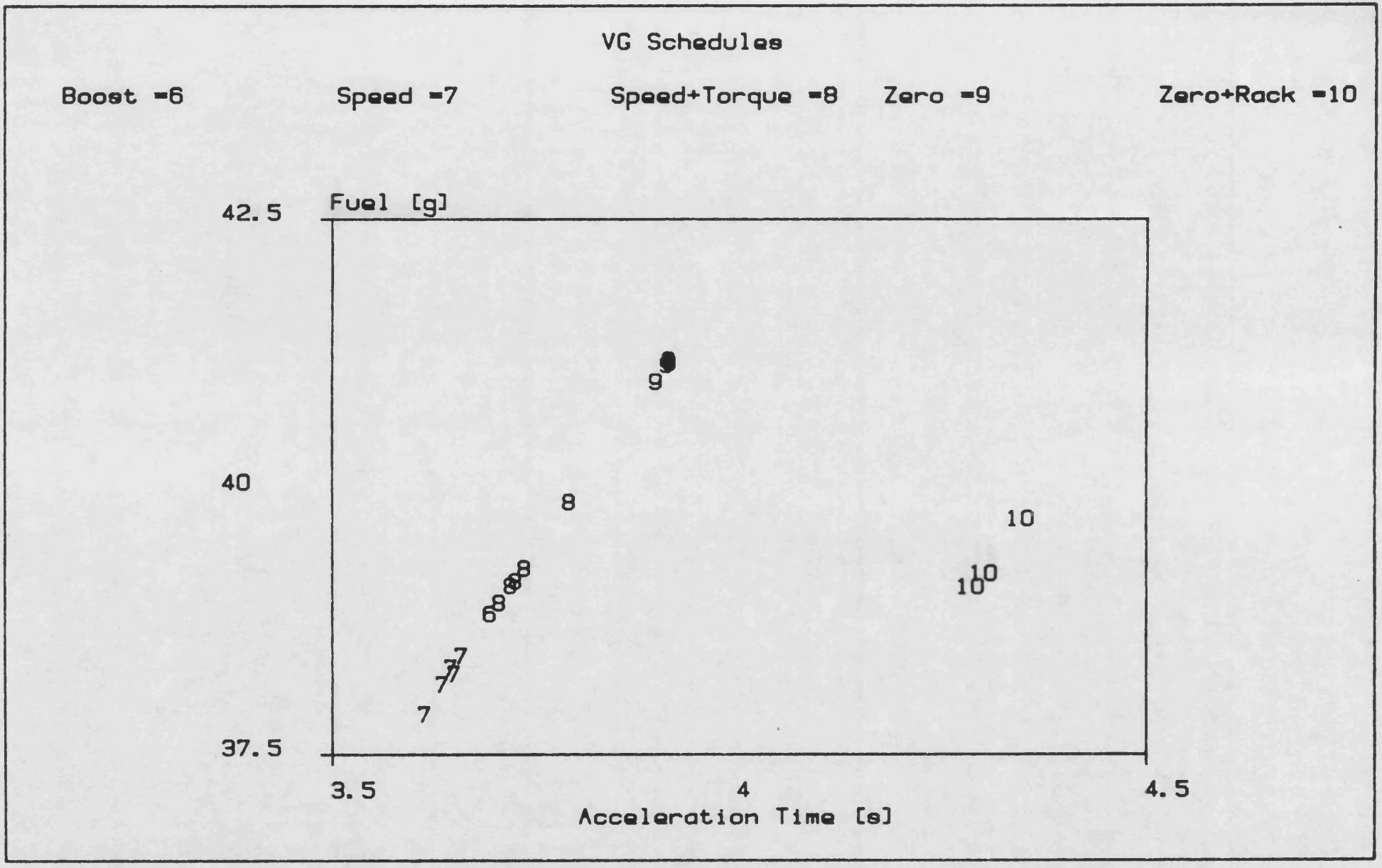

Figure 5.35 Fuel vs. Time 2nd Gear

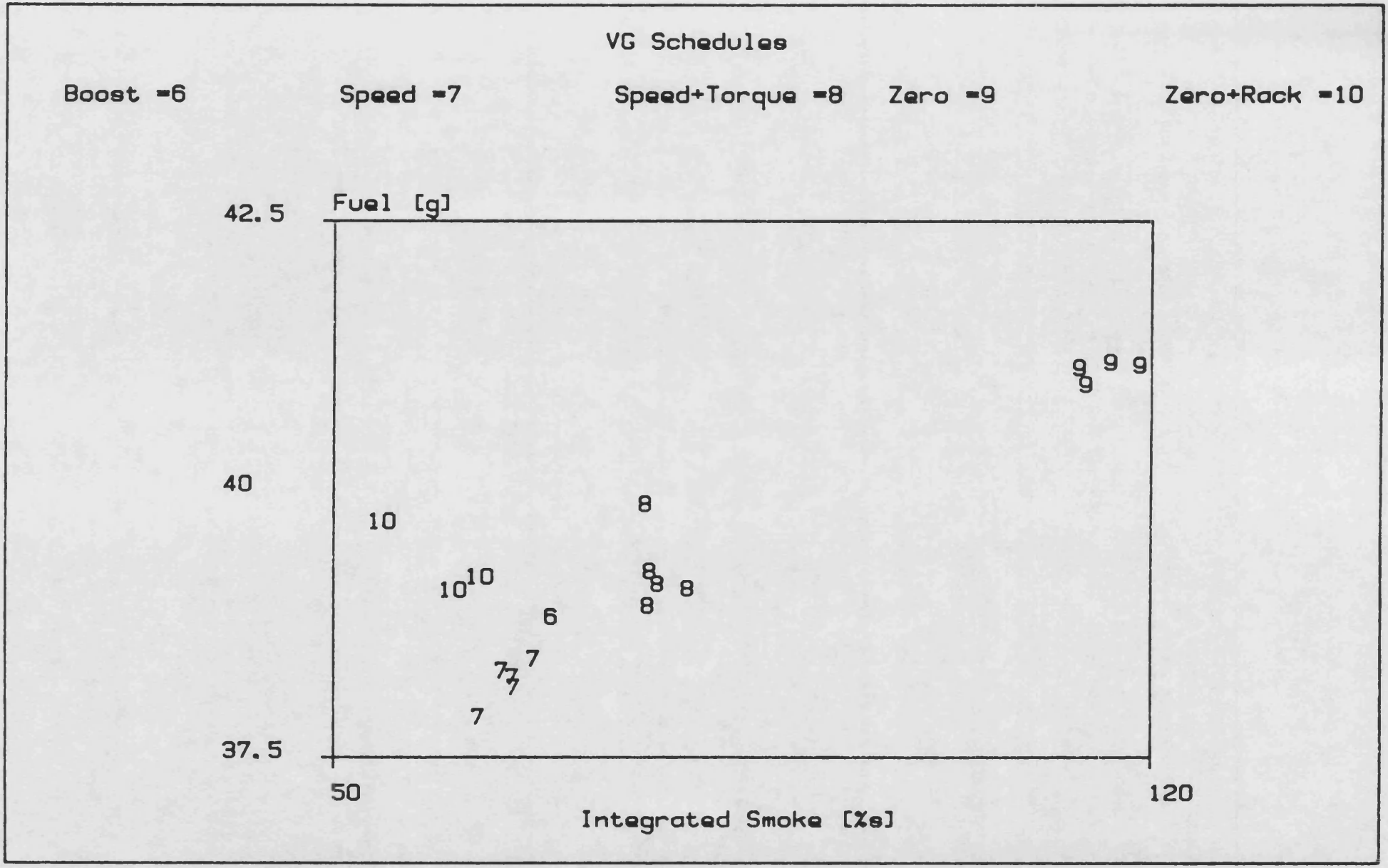

Figure 5.36 Fuel vs. Smoke 2nd Gear

CHAPTER 6

THE DEVELOPMENT OF THE DIFFERENTIAL COMPOUND ENGINE

6.1 INTRODUCTION

6.2 THE PRINCIPLES OF DIFFERENTIAL COMPOUNDING

6.2.1 EPICYCLIC GEARING
6.2.2 DIFFERENTIAL SUPERCHARGING
6.2.3 THE DIFFERENTIAL COMPOUND ENGINE

6.3 DIFFERENTIAL COMPOUND ENGINE PROTOTYPE DEVELOPMENT

6.3.1 THE TWO-STROKE VERSION WITH FIXED GEOMETRY POWER AND AUXILIARY TURBINES
6.3.2 THE PERKINS 6.354 FOUR STROKE VERSION WITH A SINGLE VARIABLE GEOMETRY POWER TURBINE
6.3.3 THE LEYLAND 500 VERSION WITH VARIABLE GEOMETRY POWER TURBINE AND TURBINE CVT

6.4 THE LEYLAND 500 DCE TEST FACILITY

6.4.1 THE DYNAMOMETER DESIGN
6.4.2 INSTRUMENTATION
6.4.3 TEST-BED CONTROLS
6.4.4 TEST-BED LAYOUT, COMPONENT SUPPORT, AND COUPLING
6.4.5 AIR AND EXHAUST SYSTEMS
6.4.6 SERVICES

6.1 INTRODUCTION

The Differential compound engine (DCE) was originally proposed by F.J. Wallace (ref. 53) in 1962. At that time compounding did not attract the commercial attention it now does, because of much lower fuel costs. The DCE was in general ahead of its time and as a result has only been developed under the direction of Prof. Wallace, who has continued to pursue the idea over the past twenty-four years. Only one test-bed proto-type has been in existence during this period, however it has gone through several stages of development involving layout and component changes. The author's involvement has been in the development of DCE control systems and the design and build of the new Leyland 500 based DCE test facility.

The control system development work has been undertaken with the two most recent versions of the experimental proto-type (Perkins 6.354 and Leyland 500) and is described in Chapter 7. Transient control algorithms were developed with the aid of a dynamic computer model to avoid potentially hazardous test work on the proto-type.

This chapter describes the development of the DCE concept and the design of the latest proto-type test facility.

6.2 THE PRINCIPLES OF DIFFERENTIAL COMPOUNDING

As discussed in Chapter 1 the ideal torque-speed curve at the vehicle prop-shaft is a constant power hyperbola ie. maximum engine power should be available at all vehicle speeds. The purpose of the transmission is to provide as close an approximation to this as possible. Because maximum engine power invariably occurs at one speed (usually the top of the operating range) the aim is to allow engine speed to remain constant whilst output speed drops. One way of doing this is to drive through a fully floating epicyclic or equivalent differential gearing. An epicyclic has three shafts through which power can be transmitted, one is driven by the engine, another drives the prop-shaft, leaving the third requiring a source or consumer of power. The ideas explained below are based on the third member driving a supercharging air compressor.

6.2.1 EPICYCLIC GEARING

To understand the principles behind differential compounding it is first necessary to have a knowledge of the equations governing the behaviour of a loss-free fully floating epicyclic (fig. 6.1a). Loss terms need only be included for accurate modelling purposes and otherwise only serve to confuse.

A. Loss free torque equations

Under equilibrium conditions (ie. steady-state running) the sum of the moments on the planets and the planet carrier will be zero, otherwise acceleration would occur. The following equations can be derived from the force diagram (fig. 6.1b):-

Notation:-

τ = torque
F = force
r = gear radius
t = no. gear teeth
v = tooth velocity
ω = angular velocity

$_{ann}$ = annulus
$_{sun}$ = sun
$_{pc}$ = planet carrier

$$\tau_{ann} = F.r_{ann}$$

$$\tau_{sun} = F.r_{sun}$$

$$\tau_{pc} = -2F.(r_{ann}+r_{sun})/2$$

defining the epicyclic gear ratio as:

$$R = r_{ann}/r_{sun} = t_{ann}/t_{sun}$$

then $$\tau_{ann} = \tau_{sun}.R = -\tau_{pc}.R/(R+1) \qquad \text{eq. 6.1}$$

If the planet and carrier inertias are neglected these equations apply under dynamic (acceleration) conditions. The important point to note is that the three epicyclic torques are directly proportional to one another.

B. Speed equations

Referring to the velocity diagram in fig. 6.1c, the planet axis will have a velocity which is the average of the velocities where the planet meets annulus and sun:-

$$v_{pc} = (v_{ann}+v_{sun})/2$$

$$\omega_{pc}(r_{ann}+r_{sun})/2 = (\omega_{ann}.r_{ann}+\omega_{sun}.r_{sun})/2$$

$$\omega_{pc}(R+1) = \omega_{ann}.R+\omega_{sun} \qquad \text{eq. 6.2}$$

Although this equation should be used for numerical calculation the velocity diagram upon which it is based gives, in the author's opinion, the best qualitative picture of the speed relationship. The important point to note is that there are no fixed ratios between the three members of the epicyclic, any one speed is a function of the other two.

6.2.2 DIFFERENTIAL SUPERCHARGING

Differential supercharging is achieved by connecting the three members of an epicyclic to the diesel engine, the vehicle drive-shaft, and a supercharger. These connections can be chosen so that reducing drive-shaft speed ($N_{D/S}$), at fixed engine speed (N_E), results in increased supercharger speed (N_C). This principle has been applied to both the Differential compound engine (DCE), and a Differentially supercharged diesel engine (DDE) developed by Perkins in the 1960s (ref. 54).

The DDE proto-type is shown in fig. 6.2, the engine drives the planet-carrier, the annulus is connected to the drive-shaft, and the sun to the supercharger. Referring to the limiting torque curve (fig. 6.3a), and the epicyclic velocity diagram (fig. 6.3b), it can be seen that $N_{D/S}$, N_E, and N_C all decrease together. However N_E is reduced by a smaller factor than $N_{D/S}$, so the corresponding reduction in N_C is less again. Both the engine and supercharger are positive displacement machines and hence air-volume flow is proportional to their speed. The result is rising boost pressure because engine and compressor massflow must balance. Increasing boost produces a rise in engine b.m.e.p. (torque) from 9.7 Bar at 2800 rpm to 17.6 Bar at 1350 rpm. The resulting torque back-up produced at the epicyclic output (annulus) is 80% at 40% of maximum output speed, which is much better than that produced by a turbo-charged diesel. This improvement is a result of the large rise in b.m.e.p. and the wider speed range of the epicyclic output over that of the engine. In the proto-type vehicle the epicyclic output was followed by a torque convertor and a 2-speed gearbox which produced the tractive effort curve shown in fig. 6.4.

The DDE is limited by the maximum b.m.e.p. compatible with a long engine life and reliability. It is also limited by the need to pass the total supercharger output through the engine. These two limitations force engine speed down as torque rises, which as previously mentioned is not the ideal situation. The concept of the DCE as envisaged by Wallace allows some of the compressor air-flow to bypass the engine. The energy put into the bypass air by the

compressor is recovered by a turbine which is geared into the output shaft. In principle engine speed can now be held at its maximum throughout the epicyclic output speed range. Compressor speed will increase producing a higher bypass flow as output shaft speed decreases. Without losses such a system would produce the constant power hyperbola required. In practice the design of an efficient unit requires the combination of differential supercharging with recovery of exhaust gas energy. The following sub-section discusses the practical implementation of such a system.

6.2.3 THE DIFFERENTIAL COMPOUND ENGINE

The proto-type DCE (fig. 6.5) differs from the DDE in the arrangement of the epicyclic, however, this is arbitrary and does not change the differential supercharging effect. The engine drives the annulus, the planet-carrier is connected to the output shaft, and the sun to the compressor. The velocity diagram for this arrangement is shown in fig. 6.6, the principle of operation is unchanged, although the sun rotation is now reversed. As explained previously a bypass pipe is incorporated allowing compressor massflow to exceed engine massflow as ouput shaft speed drops.

The DCE recovers energy from the exhaust gas and bypassed compressor airflow, by using them to drive at least one radial inflow turbine. It has been shown that the method of coupling the turbine to the system affects the compressor overspeed ratio (ref. 53). The overspeed ratio is related to epicyclic powers thus:-

$$n_c = P_{ann}/P_{sun}$$

$$n_c = \frac{N_{sun} \text{ at zero } N_{pc} \text{ and rated } N_{ann}}{N_{sun} \text{ at rated } N_{pc} \text{ and rated } N_{ann}}$$

P_{sun}=sun power
P_{ann}=annulus power

It is apparent from this that P_{ann} (input power) should be as low as possible to minimise the compressor overspeed ratio. This is important for a practical installation where the compressor speed range is usually a limitation. From this observation it follows that

the turbine should not drive through the epicyclic (ie. be geared to the engine crank-shaft), but should drive directly into the output shaft with suitable step-up gearing.

To obtain the optimum limiting torque curve (LTC) it is necessary to run the engine at maximum power, and hence maximum speed, at all output-shaft speeds. This results in a compressor speed range of typically 3 to 1 from stall to maximum output speed. Over this wide speed range the compressor must provide constant boost pressure so that the engine remains at its rated (maximum) power. A centrifugal unit produces rising boost with speed (fig. 6.7a) and is therefore inappropriate. Conversely a positive displacement device has no fixed relationship between speed and pressure ratio (fig. 6.7b), flow is proportional to speed and the pressure ratio is determined by the downstream restriction.

As well as its ability to work at constant pressure ratio over a wide speed range, the positive displacement compressor is well suited to the epicyclic's inherent torque balance. Under steady-state conditions pressure ratio is proportional to sun torque and hence engine torque. Engine torque is itself roughly proportional to fuel per shot. Proportionality between fuel per shot and boost pressure implies efficient engine operation at all loads as air-fuel ratio can be held close to its optimum.

To maintain constant pressure ratio over the wide air massflow range requires a variable restriction (swallowing capacity) downstream of the compressor. The solution adopted for the more recent proto-types was to use a turbine with variable geometry nozzles. By adjusting nozzle angle swallowing capacity and hence boost pressure can be set.

To summarise the ideal DCE limiting torque curve is produced by running the engine at rated power at all output speeds. At maximum output speed, engine and compressor massflow balance and there is no bypass flow. As output speed drops compressor speed and hence massflow increase. The additional massflow bypasses the engine, its

energy being recovered by the turbine which also recovers exhaust gas energy. Engine boost pressure is held at the rated level by gradually opening the turbine nozzles (increasing swallowing capacity) as massflow increases.

6.3 DIFFERENTIAL COMPOUND ENGINE PROTOTYPE DEVELOPMENT

The DCE has progressed through several stages of prototype development leading to the latest build utilising a Leyland 500 fixed head engine. Progress has been gradual over a period of approximately twenty years as a result of sporadic funding. However, more realistic funding has now become available from the S.E.R.C. because of increased commercial and defence interest in high output compound schemes. This section describes the stages of development which led up to the present design. Although changes were gradual three specific builds are discussed, in chronological order, which demonstrate the major design changes.

6.3.1 THE TWO-STROKE VERSION WITH FIXED GEOMETRY POWER AND AUXILIARY TURBINES

The original prototype (fig. 6.8) was powered by a highly rated opposed piston two-stroke engine (Rootes TS3). Two turbines were used both of fixed geometry: a power turbine to recover exhaust energy; and an auxiliary stall turbine to recover bypass air energy. Both were geared into the output shaft, the power turbine directly, and the stall turbine through a clutch arrangement. The twin screw compressors were driven by the sun through splitter gearing. A two-stoke engine was chosen for two reasons:

i) Its orifice type flow characteristic allows large airflows without excessive pressure drop across the engine. This was particularly important for this build as engine airflow varied considerably because of the fixed geometry turbines.

ii) It has high power to weight and power to size ratios.

Air flow through the engine was limited by the swallowing capacity of the fixed geometry power turbine. As output speed reduced on the limiting torque curve (LTC), airflow and hence turbine pressure ratio

increased. To avoid excessive b.m.e.p.s as stall was approached the bypass valve was opened and the stall turbine engaged to recover energy from the bypass air. The stall turbine gear ratio was higher than that of the power turbine so that it would operate efficiently near stall. This proto-type suffered from several disadvantages:-

i) The two-stroke was not capable of the high ratings required. In particular piston reliability was poor even with additional piston cooling and b.m.e.p. was limited to 160 psi (ref. 55).

ii) The use of two turbines and a clutch mechanism resulted in a bulky and complex arrangement.

iii) Opening the bypass and clutching in the auxiliary turbine at low speeds makes smooth operation difficult and increases control system complexity.

6.3.2 THE PERKINS 6.354 FOUR STROKE VERSION WITH A SINGLE VARIABLE GEOMETRY POWER TURBINE

Because of the low ratings achieved with the two-stroke it was thought a more highly rated four-stoke could have a similar power to weight ratio without the same reliability problems. This led to the replacement of the TS3 with the Perkins 6.354 four-stroke diesel. A variable geometry power turbine was introduced replacing both of the fixed geometry devices used in the previous design (fig. 6.5). Any bypass flow mixes with the exhaust before passing through the turbine. The gearbox and screw compressors remained unchanged.

Because of the four-stroke's positive displacement nature large changes in airflow create unacceptable pressure drops across the engine. For this reason the bypass is kept open throughout the DCE speed and load range ensuring similar inlet and exhaust pressures. As explained in section 6.2 the V.G. turbine allows pressure ratio to be controlled despite the positive displacement nature of the engine and compressor. Hence engine b.m.e.p. can be controlled at levels

compatible with reliability constaints. This proto-type was less complex, more reliable, and allowed continuous smooth operation. However, the efficiencies were well below the theoretical predictions, the suspected causes being:-

i) High parasitic losses in the epicyclic and its associated geartrains. This was thought to be due to the gearbox design which is of the type used for high reliability marine rather than automotive applications. Accurate figures for geartrain losses were not available and hence no efficiency corrections could be made.

ii) The relatively low efficiency of the twin screw compressors which was attributed to their old design and high rotational speed.

iii) Operation at very low output-shaft and hence turbine speeds resulted in poor turbine efficiencies as stall was approached. This reduces stall torque as well as overall efficiency.

6.3.3 THE LEYLAND 500 VERSION WITH VARIABLE GEOMETRY POWER TURBINE AND TURBINE CVT

The latest proto-type (fig. 6.9) was constructed in an attempt to achieve experimentally the DCE's true performance potential in terms of efficiency and torque back-up. This involved eliminating the suspected causes of low efficiency mentioned above and demonstrating that the high ratings inherent in the DCE concept are not unreasonable. The basic layout is the same as the Perkins 6.354 proto-type, the only additional features being a turbine CVT and a lock-up torque converter in the output drive.

The Perkins 6.354 has been replaced by the larger Leyland 520 fitted with low compression ratio pistons (12.8:1) because of the high supercharging pressures. This engine has an integral block and head being designed for high b.m.e.p.s. Experimental work at Leyland and

Imperial college has shown it to be capable of operating at over 20 bar b.m.e.p. The higher power output of the engine results in higher system torques and air massflows.

The torque converter operates over the bottom 20% of the output speed range and is locked at higher speeds. It serves two purposes: to avoid running at zero turbine speed and hence low efficiency; and to produce a final torque-backup high enough to eliminate the need for any additional ratio change gearbox. The torque converter is not included in the experimental test-rig because it would increase the dynamometer torque requirement by a factor of approx. 4. The performance of the remainder of the proto-type can be tested between 20% and 100% of maximum output speed to prove the DCE concept. Being proprietary devices the performance of torque converters is well documented.

The turbine CVT was introduced to improve efficiency and stall torque by allowing the turbine to run near to its design speed at all output speeds. The Napier V.G. turbine has been retained as its capacity is more than enough despite the increased flow rates.

The twin Godfrey screw compressors have been replaced by a single more efficient Compair unit which rotates at lower speed. It is an ex-proto-type unit used by Compair for development work. Although more efficient the lower operating speeds mean the compressor is considerably larger which might not be acceptable in a commercial application. The lower step-up ratio from the sun and the elimination of the splitter gearing also reduces gear losses.

Ideally a specialist vehicle geartrain manufacturer should have been commissioned to design and produce a new gearset, the aim being to reduce gear losses to the levels now possible with the latest technology. However sufficient funding was not available for this major expenditure as well as the rest of the proto-type build. The original gearbox has been modified to provide the correct step-up to the new compressor and reduce losses as far as economically possible.

The redundant auxiliary turbine drive was removed and the dimensions of the turbine step-up gearing reduced to minimise windage losses. The original step-up gearing was sized to transmit the combined power and auxiliary turbine torques. The higher engine and turbine powers driving the gearset should make the losses a smaller percentage of total power and hence improve overall efficiency.

The predicted performance of the new proto-type is described in ref. 56, and summarised by fig. 6.10

6.4 THE LEYLAND 500 DCE TEST FACILITY

The author acted as project leader for the design and build of the latest prototype test facility. This involved specifying the facilities required including their basic design, and the supervision of the detail design and construction work. The bulk of the detail design and equipment procurement was carried out by the author and his research colleague Mr D. Prince.

The proto-type design has been discussed in the previous section, the purpose of this section is to describe the test-bed design. The intention is to give an overview of the design criteria adopted and the resulting hardware, detailed equipment specifications can be found in refs. 35 & 57. General principles of test-bed design and descriptions of standard equipment are covered in Chapter 2.

A decision on the type of turbine CVT to be purchased has not yet been made because of the high cost of commercially available devices. Because of this the initial proto-type build has a fixed turbine gear ratio. This is not a great problem if a computer model of the DCE can be accurately matched to the experimental results and data is available on CVT performance.

6.4.1 THE DYNAMOMETER DESIGN

The allocation for dynamometry was set very low (£5000) ruling out any commercial dynamometer package. Hydrostatic dynamometers have been built in house by the Fluid Power Centre at relatively low cost, the same approach was adopted for the DCE. A general description of the construction and operation of hydrostatic dynamometers can be found in section 2.4. The predicted torque curve for the new proto-type approximates to a constant power hyperbola. However, a hydrostatic pump has a box shaped envelope. This means the corner power of a single unit capable of loading the DCE would be equal to stall torque * maximum speed ie. 970 KW. Three alternative methods of matching

hydrostatic pumps to the DCE torque curve are described below (fig. 6.11) :-

i) Use a single pump with a corner power of 970 KW. Such a pump would be prohibitively expensive and low speed, therefore requiring a step-up gearbox.

ii) Use a number of smaller pumps having a total corner power of 970 KW. Again this solution would be expensive and require a multi-way splitter box.

iii) Use a smaller capacity pump with a speed change box. In this case the gearbox would be expensive, and even with a 400KW pump would require three ratios to cover the operating map. This solution would limit transient work to constant speed tests.

The method finally adopted was a compromise based on options ii and iii. Two existing Sundstrand SPV25 pumps having a total corner power of approx. 500KW are driven through a two way splitter box. Two ratios cover the majority of the operating map, the envelopes covered are shown in fig. 6.12. To minimise cost a fixed ratio splitter box was purchased with a second set of gears for the low speed envelope. This limits flexibility as the box must be stripped and re-assembled to test in the low speed high torque corner of the map. The following description of the dynamometer system is meant as a brief summary only, further information can be found in section 2.4 and ref. 57.

It was considered advisable to keep the hydraulic circuit (fig. 6.13) completely separate from the laboratory's common hydraulic system. This avoids cross contamination from the other test-cells and down time due to hydraulic failures and/or modifications elsewhere in the laboratory.

The pumps are loaded by two Abex Denison R4V pressure relief valves, which were chosen in preference to a single MIDI cartridge. The R4V flow capacities are a closer match with the pumps and the combined

displacement of the two spools is less than that of the single MIDI spool. The effect of spool displacement on dynamometer dynamic performance is discussed in section 2.4.

The pilot stage will initially be a single Abex SE03 solenoid pressure control valve. A mechanical pilot is also used to set a safety limit on system pressure. One of the R4V relief valves has its pilot orifice replaced with a blanking plug, otherwise the SE03 would have to pass twice its normal flow unnecessarily. The SE03 and the safety pilot are mounted on the other R4V manifold block which contains the pilot orifice. This minimises flow path lengths and hence any resultant dynamic effects. If the dynamometer response proves to be limited by the flow capacity of the SE03 an alternative will be tried, possibly a flow control servo-valve used in a pressure feedback loop.

An independent electrically driven boost supply is used to ensure satisfactory boost at low output speeds. The original mechanically driven boost pumps were removed to avoid excessive flow around the boost cicuit. This would require a much larger tank for de-aeration purposes. One of the redundant boost pump drives is used to provide a tacho-drive, the other is blanked off. Both replacement assemblies have the necessary tappings for boost supply and drain connections.

The controls provided are similar to those described in section 2.4. The tacho-generator was fitted to provide a "fast" speed feedback signal which would operate satisfactorily over the wide output speed range of the DCE. Torque feedback is provided by the in-line torque transducer (Vibrometer).

6.4.2 INSTRUMENTATION

The methods described in Chapter 2 have been adhered to for the majority of measurements on the new prototype. To reduce total cost electrical sensors have only been used where transient measurement is a requirement. This applies mainly to pressure and flow where the U-tube manometer provides an economic means of steady-state measurement.

Turbine and compressor torques are not measured because of the difficulty of installing suitable devices without increasing the length and complexity of the experimental rig. In addition expensive high speed in-line devices would have been required.

The measurements taken and their associated sensors are described in detail in ref. 35. The purpose of the reading is defined as falling in one or more of the following categories:-

1. Steady-state performance readings which are taken manually and entered into the data-reduction system (see section 2.3).

2. Transient performance measurements which are available as electrical signals with appropriate bandwidth. These can be recorded by the data-aquisition system described in section 2.3, displayed on an oscilloscope, or used as feedback signals in a control scheme.

3. Safety and diagnostic measurements which are intended to provide additional information useful for trouble-shooting.

6.4.3 TEST-BED CONTROLS

Test-bed controls are grouped under four main headings:-

A. "Dynamometer Controls" which have already been dealt with in sections 2.4.5 and 6.4.1.

B. "The Monitoring and Automatic Shutdown system". The design of this system is described in ref. 35.

C. "Environmental Controls" which are intended to ensure test repeatability. The principles and methods usually adopted have been described in section 2.5.

D. "Operational Controls" which act on the proto-types primary operating parameters: fuel rack position; fuel injection timing; turbine nozzle angle; and bypass valve opening. The mechanisms and their associated controls are described below.

The Engine Fuel Governor

The fuel pump has been converted to electro-hydraulic operation and an electronic governor implemented. The design is very similar to that described in section 4.2.2, the major difference being the additional facility of fuel flow control.

Fuel flow control is provided as a tool for steady-state optimisation. For example the adjustment of nozzle angle for maximum efficiency involves running at constant fuel flow (ie. constant power in) and constant output torque. Optimum nozzle angle is then determined by maximising ouput speed and hence power out. Flow control is implemented by putting fuel flow feedback around the rack position loop (fig. 6.14). A P+I algorithm is included to ensure fuel flow remains fixed while optimising parameters which change engine speed. With a simple proportional loop the droop would vary with engine speed because rack position must decrease with increasing engine speed for flow to remain constant.

For this facility to be a useful optimisation tool the fuel flow sensor must produce repeatable results. Good linearity is not important unless it affects loop behaviour. In addition the feedback signal must have a reasonable bandwidth to ensure loop stability. Initially a transient flow meter developed in-house (fig. 6.15) will

be tried. An electric motor drives a positive displacement pump which supplies the engine with fuel. The flow signal is derived from pump speed. The pressure after the pump is regulated by putting a pressure feedback loop around the motor speed controller. Under transient conditions the motor accelerates rapidly in response to pressure errors, in this way a good bandwidth is achieved.

Fuel Injection Timing

Variable injection timing was implemented by the method originally developed for the variable geometry turbocharging work (section 4.2.3). The design was modified for the Leyland 500 by reducing the overall length and altering the coupling arrangements at each end.

Turbine Nozzle Angle

The turbine was the same device as previously used on earlier prototypes, a Napier CO-45 inward radial flow machine fitted with variable nozzles. The principle of operation is shown in fig. 6.16, each individual nozzle blade is pivoted and connected by a pivot arm and spring to the actuating ring. The ring bore runs on a set of rollers, the ring being rotated by a lever arm which is driven by a hydraulic jack. The jack is part of a standard electo-hydraulic position loop as described in section 3.5.1. The implementation of additional feedback loops around nozzle angle is discussed in the next chapter as this is related to overall controller design.

Bypass Valve Opening

The bypass area is controlled with a commercially available butterfly-valve. A butterfly-valve has two advantages over alternative devices: when open it offers a low resistance to flow; and secondly flow forces are balanced so that actuation force should be independent of flow and fairly low. Electro-hydraulic actuation has not initially been fitted because theoretical work to date suggests the bypass will be left wide open under both steady-state and transient operation. However, should this prove to be false remote control over bypass opening will be implemented for ease of testing and control development work.

6.4.4 TEST-BED LAYOUT, COMPONENT SUPPORT, AND COUPLING

The layout of the DCE test facility is governed by the epicyclic gearbox shaft centres. The gearbox is also the widest component and is positioned to provide gangways on both sides of the test-cell, one wider than the other for equipment movement.

The shaft centres are not on the same centre line or at the same height (fig. 6.17), in particular the output-shaft is much higher and offset to one side of the engine input shaft. This makes it very difficult to construct a single vibration isolated bedframe for the entire rig. A frame able to support all the components at widely differing heights and stiff enough to avoid torsional flexing or bending would be bulky and expensive. The alternative adopted was to construct separate bedframes for each component. Except for the engine all components were solidly bolted to the floor with no vibration isolation. This guarantees rigidity under load thus avoiding the flexing possible with a single isolated bedframe and preserving shaft alignments.

Being a reciprocating machine the engine must be isolated on rubber mounts to protect the floor from vibration damage. Hence the engine prop-shaft has to accept relatively large mis-alignments as a result of torsional movement on the mountings and vibration. Similarly all

other connections with the engine must be flexible and all components on the engine able to withstand vibration. Conversely the remainder of the rig, like the floor, is isolated from engine vibration. The correct choice of engine mountings minimises vibration at normal running speeds by reducing the natural frequency of the engine and its support so that it is only excited during start-up.

Torsional resonance through the gearbox can also be excited by the reciprocating nature of the Diesel engine. Calculations showed that this might cause problems eventually leading to shaft/gear fatigue (ref. 58). The resonant frequency was reduced below normal running speeds by installation of a torsionally soft coupling (HOLSET).

Flange mounted components such as the turbine and hydraulic pumps are coupled rigidly with splined shafts and collars. The remaining connections are of the prop-shaft type to allow for some mis-alignment. The engine and output prop-shafts include in-line torque transducers which may be affected by bending stresses. Where possible half gear-couplings are used as the flexible elements because they do not rely on elastic strain and hence create minimal bending stresses. The compressor couplings are of the flexring type (AUTOFLEX) as these could be supplied with the required maximum speed capability.

The dynamometer splitter box could not fit alongside the compressor and so had to be installed behind it. To minimise output prop-shaft length the compressor prop-shaft was kept as short as possible. However the required length was still approximately twice that of the output torque transducer, so an extension was necessary.

The previous prototype had a large drum brake installed in the output-shaft as a safety device. The shaft was therefore split and supported midway by a pedestal bearing (plummer block). However, an output brake is inappropriate for the new prototype. It could not be applied at engine speeds of more than approx. 1200 rpm without causing compressor overspeed. In addition it would have to resist very high

torques. Compressor reversal is prevented by a compressor brake activated by the Monitoring and Shutdown system.

The removal of the heavy drum brake suggested a single unsupported shaft might be feasible, whirling calculations confirmed this. The torque transducer and extension must be an interference fit so that whirling is not induced by free play between the two. The torque transducer can be damaged by pressing or shrinking a hot component onto it so a mechanical compression coupling (ETP bush) was used.

A similar method was used to provide an extension to the engine torque transducer, and hence increase the prop-shaft length. This was necessary to avoid excessive angular mis-alignment of the flexible couplings as a result of engine movement on its rubber mounts during start-up.

The component support and coupling requirements described above resulted in the final layout shown in fig. 6.17. The overall height was kept as low as possible so that the dynamometer would still be reasonably accessible. It was necessary to leave enough space below the epicyclic gearbox for its lube oil tank as the oil return is by gravity only.

6.4.5 AIR AND EXHAUST SYSTEMS

The air and exhaust pipework had to fit in with the layout described in the previous sub-section. The unrealistic positioning of the compressor made it impossible to keep pipework volumes down to a realistic size without seriously affecting pipe losses. For this reason low but realistic losses were the governing parameter rather than volumes.

The original exhaust manifold was replaced with a plenum type manifold to ensure a constant rather than pulsed turbine inlet pressure. The reasons for this change are as follows:-

i) The layout of the proto-type would make exhaust pulse utilisation extremely difficult. The turbine is some distance (1m) from the exhaust manifold and the frictional losses in small bore pipe-work would be excessive.

ii) A pulse preserving manifold would require very careful design to avoid pulse interference between cylinders. A successful design would probably involve the use of a complex computer model. This was thought to be beyond the scope of a simple pipe-work design exercise

iii) Constant pressure turbocharging can be superior to pulse turbocharging at high engine ratings (see section 1.2). It has been suggested that for a six cylinder engine the cross-over point where constant pressure becomes superior to pulse turbocharging is at a pressure ratio of approx. 3:1. The DCE is not a standard turbocharged engine, however, the turbine expansion ratio can be as high as 4:1. It is therefore considered likely that a constant pressure system will result in higher overall efficiencies.

Computer simulation was used to define a suitable plenum volume (ref. 59), which was given as 5 litres, this reduces pulsations to less than 5% of manifold pressure. The new manifold exit is at one end to suit the pipework layout.

The old intercooler was grossly oversized which made pipework layout unnecessarily complicated and bulky. A more realistically sized replacement was purchased which therefore also produces a more realistic pressure loss across it.

The maximum predicted compressor flow was 52 Kg/min (ref. 56). In contrast engine and bypass flows never exceed 28 Kg/min. From a pipe diameter point of view it is therefore advantageous to separate engine and bypass flow as close to the compressor as possible. Similarly they should be recombined as close to the turbine as possible. This

was achieved by using two plenum/junction chambers, one at the compressor exit and the other at the turbine entry.

Because of the DCE's layout and overall dimensions, bends and fittings are the major cause of losses rather than total pipe length. To minimise the number of bends required the layout in fig. 6.18 was adopted. Unfortunately the compressor outlet must face down, this orientation is determined by lube oil drains, the lube oil being gravity drained. The intercooler is positioned so that it provides a necessary reversal in flow direction rather than increasing the number of bends required. Four additional bends were required and long sweeps were used to minimise losses. This layout was also convenient in terms of pipework support and accessibility.

Gas flow measurement was a secondary requirement, and it was decided that this should not unduly affect pipe-work layout. Total compressor airflow is measured by an orifice plate at the air-intake. By positioning the orifice at the intake the long straight upstream pipe-run that is normally required can be eliminated (orifice theory is available for flow from a large volume to a pipe). Engine airflow is also measured with an orifice plate. Engine flow was chosen rather than bypass flow because a longer straight pipe-run was available without altering the layout. Compressor pulsations may affect the accuracy of the engine airflow measurement. However, it was not possible to fit in a compressor plenum large enough to damp out pulsations completely.

The orifice plate design calculations dictated minimum pipe-bores of 7 and 4 inches for the air intake and the pipe-run from compressor to intercooler respectively. The turbine exhaust is 6 inches diameter to suit the turbine exit and the transient smoke-meter. The remaining pipe-work is 3 inches diameter to keep the loss in any single run to around 0.05 Bar. Simulation results (ref. 59) predict a loss in overall DCE efficiency of approx. 0.6% as a result of a maximum intercooler drop of 0.26 Bar (at rated) and a 0.05 Bar drop in the four other flow paths. In fact the estimated drop through the

intercooler and pipe-run to the compressor plenum does not exceed 0.13 Bar (0.1 across the intercooler). The bypass produces an estimated loss of 0.06 Bar at stall, the remaining runs contribute negligible losses in comparison.

Bypass control and engine air shut-off are both implemented with bought-in 3 inch butterfly valves suitable for the pressure and temperature after the compressor. Butterfly valves present a low resistance to flow and are balanced, which reduces actuation forces. As recommended in section 2.5 the inlet and exhaust stack incorporate simple sheet steel butterfly valves to set inlet and exhaust restriction. The inlet also includes a panel air filter to protect the compressor without creating an excessive depression. Inlet air-heating is to be included at a later stage.

6.4.6 SERVICES

This sub-section gives a brief summary of the services supplying such items as lubrication oil, cooling water, compressed air etc. Some of these are general laboratory facilities, others were installed specifically for the DCE test facility. Engine services such as fuel supply, engine coolant, and engine oil cooling are described in the relevant parts of Chapter 2.

Two lube-oil systems were constructed to supply the turbine bearings, the two gearboxes, and the screw compressor. One feeds the gearboxes and the turbine which can all run with the same lube-oil, the other feeds the compressor which uses a different specification oil. Both systems are pressure fed and gravity drained. The gearbox/turbine supply uses a vortex pump with a throttled bypass to set the supply pressure, an oil to water cooler is included to dissipate the heat generated by gearbox losses. The compressor supply uses a gear-pump sized to provide approximately the correct flow, a relief valve sets the supply pressure. The small amount of heat rejected to the compressor oil is dissipated by the oil tank. The pumps are both electrically driven so that the measured DCE performance does not

include ancillaries. Both oil tanks are sized for an oil change time of approx. two minutes, this allows sufficient time for de-aeration. The "Monitoring and Shutdown System" checks oil pressures, temperatures and tank levels.

A constant pressure hydraulic servo-supply is provided to drive servo-controls such as the nozzle, fuel-rack, and injection timing actuators. The supply consists of an electrically driven swash-plate type pump, relief valve, accumulator, and filter. Individual controls are preceded by filters where flow control servo-valves are used as they are very susceptible to contamination. Servo-controls are discussed in more detail in section 3.5.

The three oil supplies mentioned above and the dynamometer boost supply can be switched on and off by contactors within the test-cell. However there is also a single remote switch outside the cell which turns all four supplies off. This was provided so that in the event of oil spillage or fire within the test-cell all oil supplies can be stopped.

Compressed air is needed for turbine cooling, transient smoke-meter lens protection, and manual purging of the Bosch smoke-meter probe. Air filters and regulators have been installed to satisfy these requirements. The air is supplied by the laboratories own compressor and air drier, which services all three test-cells.

A cooling water supply for heat exchangers is provided by an external cooling pond and a single large pump supplying all three test-cells. Strainers are installed in each test-cell to prevent debris blocking coolers, valves, and pipe-work. Thermostatic valves are installed to control cooling water flow when the temperature of the cooled medium can affect test repeatability (see section 2.5) or control loop stability (dynomometer oil temp. for example).

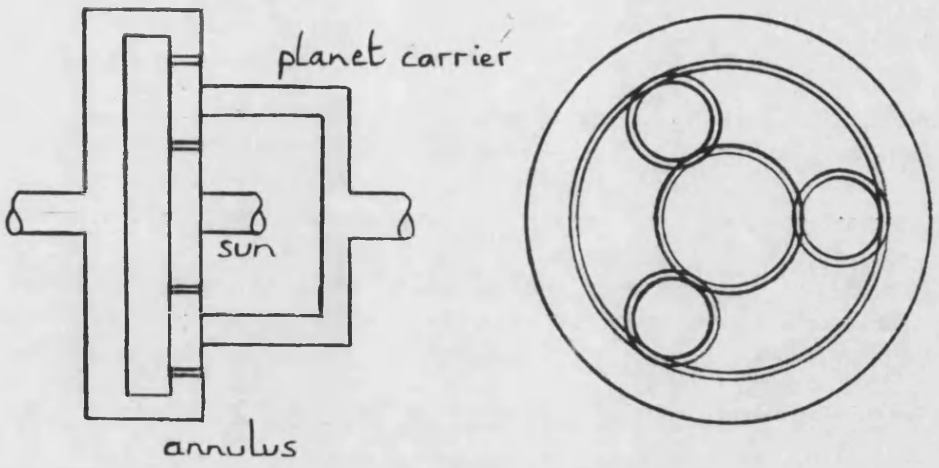

a) epicyclic gearing

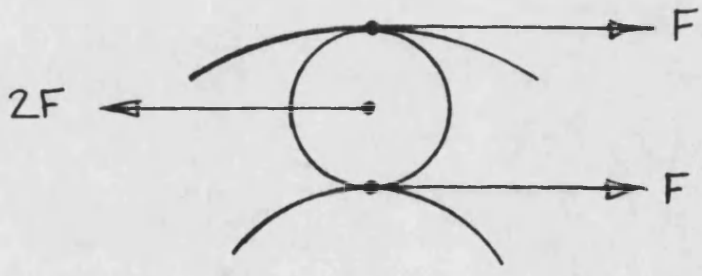

b) force diagram

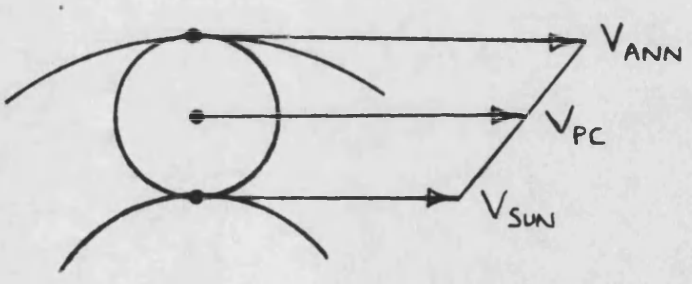

c) velocity diagram

FIG. 6.1 THE FULLY FLOATING EPICYCLIC

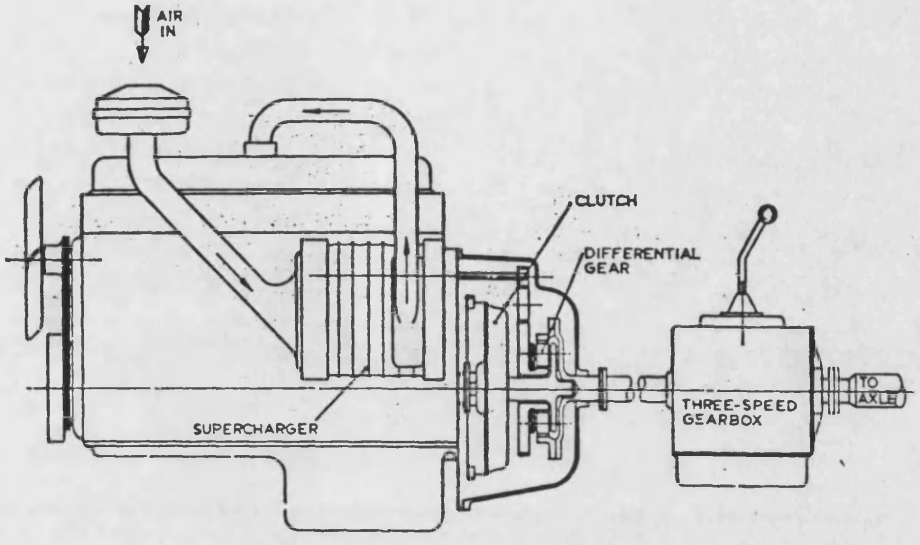

Simple differential supercharging arrangement

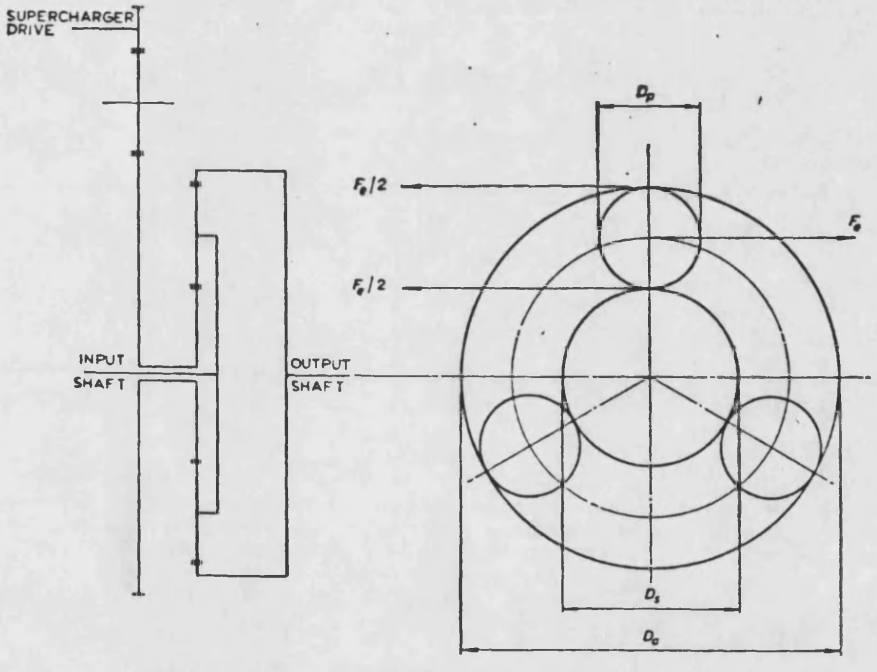

Differential gear arrangement

FIG. 6.2 THE DIFFERENTIALLY SUPERCHARGED DIESEL ENGINE (D.D.E.)

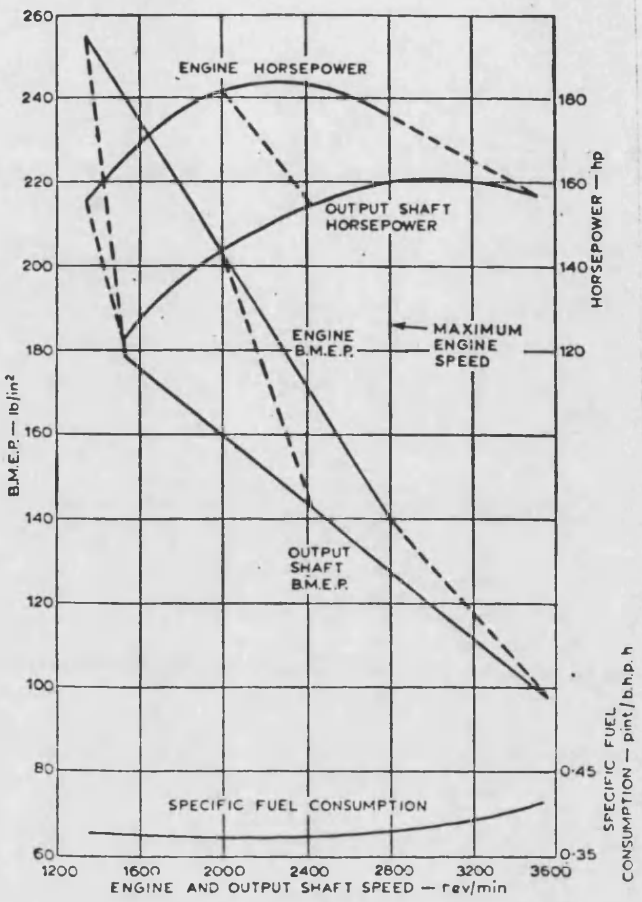

a) DDE torque curve performance

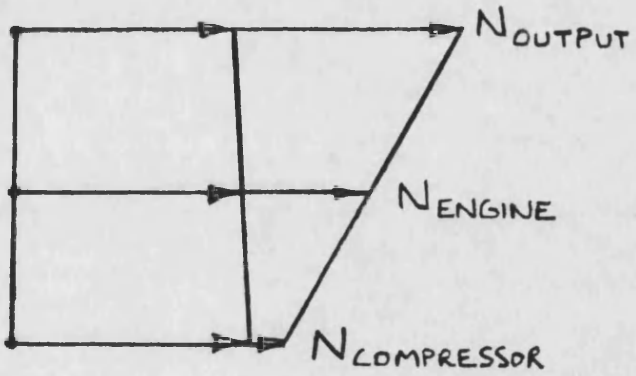

b) DDE velocity diagram

FIG. 6.3 DDE OPERATING CHARACTERISTICS

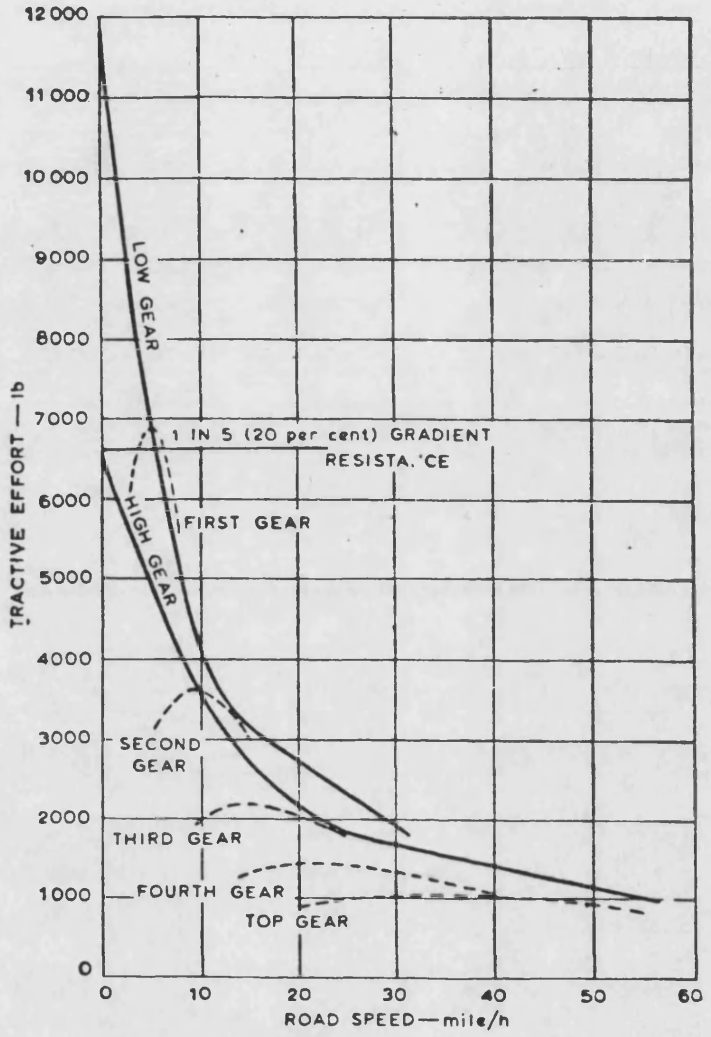

——— Differential engine.
- - - - - Conventional engine/transmission.

Calculated performance comparison between turbocharged 6·354 and 6·354 DD engine in a truck of 31 400 lb gross weight. Vehicle details: frontal area 65 ft² (air resistance 0·14 (mile/h)²); rolling resistance 12 lb/1000 lb; axle ratio, 7·17/1 for DD engine and 5·95/1 for turbocharged engine; gear ratios for turbocharged engine 1·0, 1·47, 2·24, 3·78 and 7·08; gear efficiency, turbocharged, 90 per cent direct gear, 85 per cent indirect; DD engine, 90 per cent low gear, 95 per cent high.

FIG. 6.4 D.D.E. TRACTIVE EFFORT

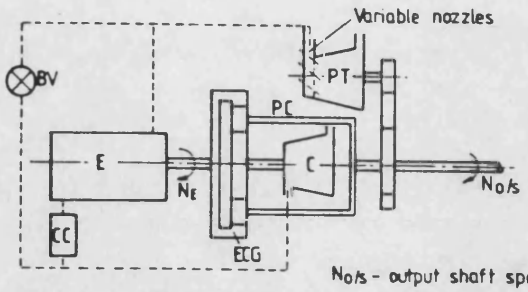

BV - bypass valve
CC - charge cooler
C - compressor
E - engine

$N_{o/s}$ - output shaft speed
ECG - epicyclic gearbox
PC - planet carrier
PT - power turbine
N_E - engine speed

FIG. 6.5 THE DIFFERENTIAL COMPOUND ENGINE

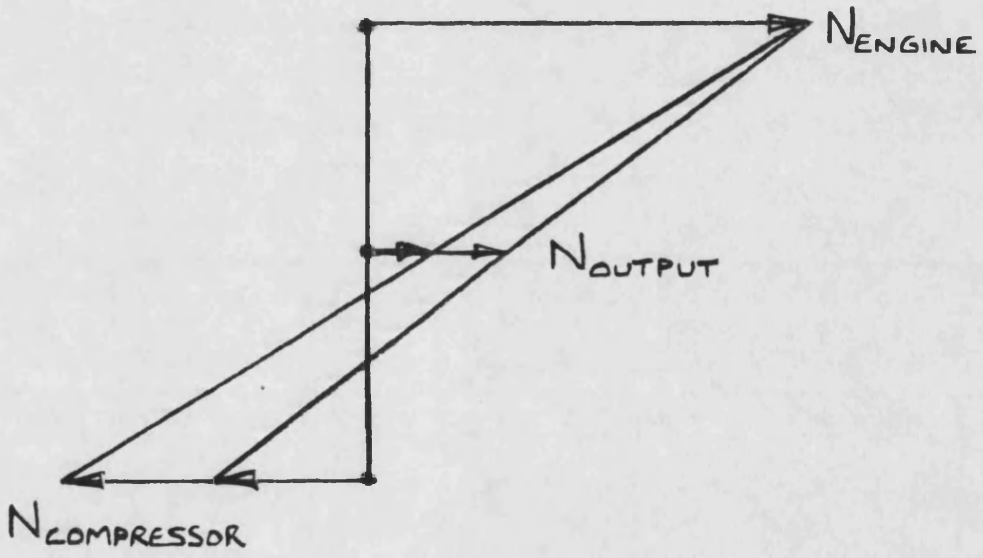

FIG 6.6 DCE VELOCITY DIAGRAM

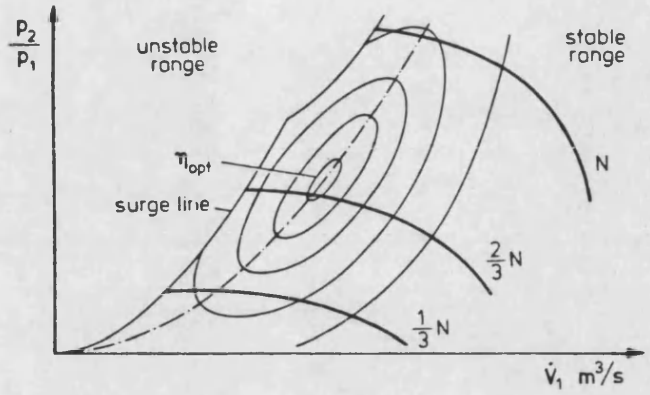

a) centrifugal compressor

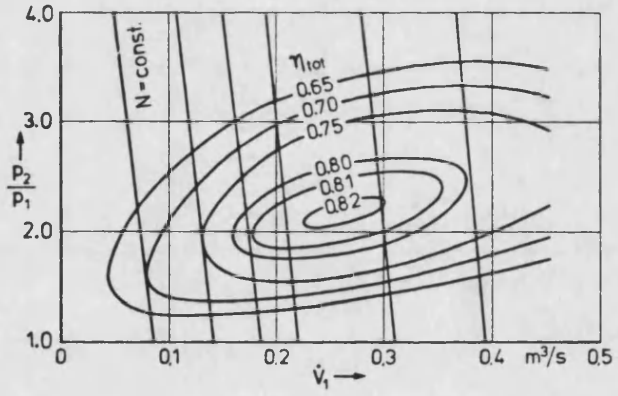

b) positive displacement compressor

FIG. 6.7 COMPRESSOR CHARACTERISTICS

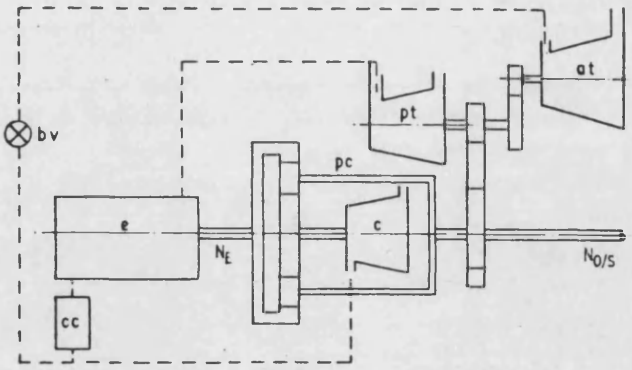

FIG. 6.8 THE 2-STROKE VERSION WITH POWER AND AUXILIARY TURBINES

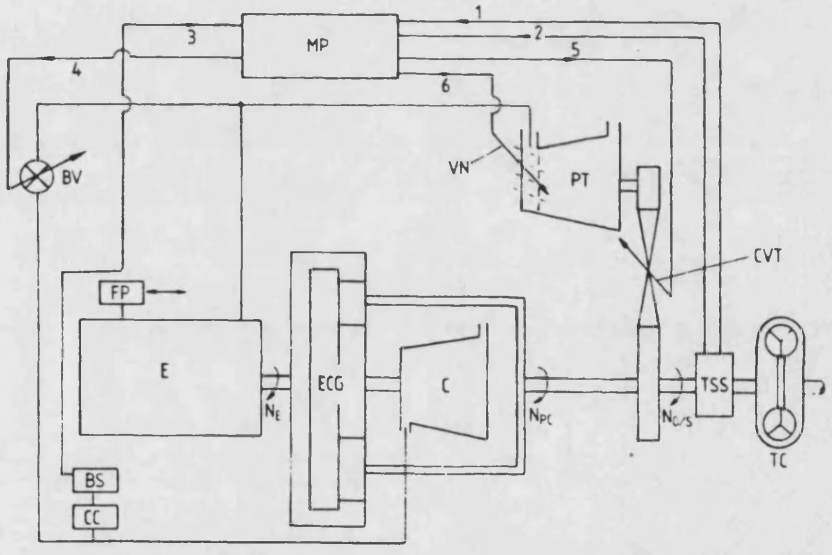

DCE layout: final version
BV bypass valve; BS boost sensor; C compressor; CC charge cooler; E semi-adiabatic engine; ECG epicyclic gear train; FP fuel pump; PT power turbine; TC torque converter; VN variable turbine nozzles; TSS output torque and speed sensor; N_E engine speed; $N_{o's}$ output shaft speed; N_{pc} planet carrier speed; MP micropressor;
Input signals: 1 torque transducer; 2 speed transducer; 3 boost transducer
Output signals: 4 bypass valve control; 5 CVT control; 6 nozzle control

FIG. 6.9 THE LEYLAND 500 VERSION WITH V.G. POWER TURBINE AND TURBINE CVT.

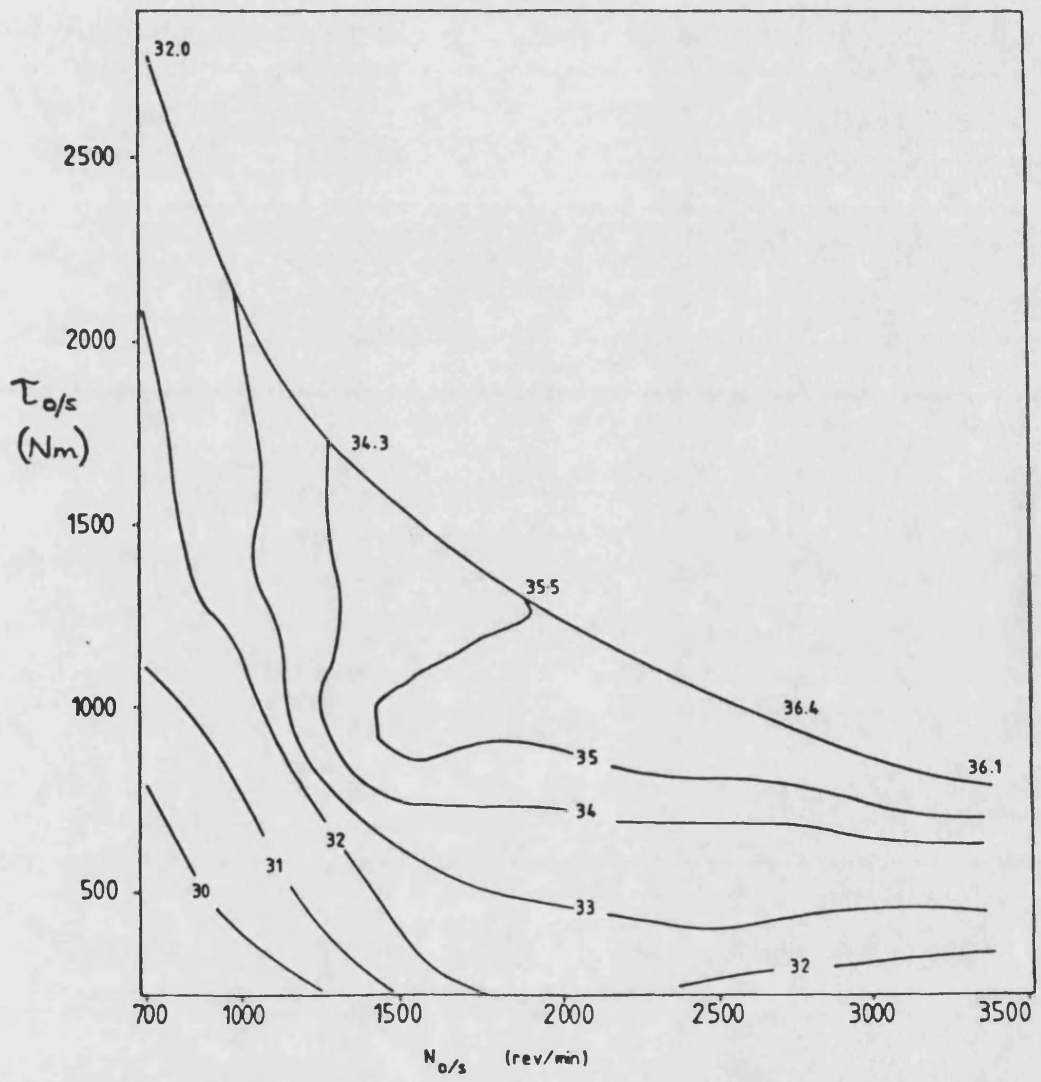

FIG. 6.10 LEYLAND 500 VERSION PERFORMANCE (PREDICTED)

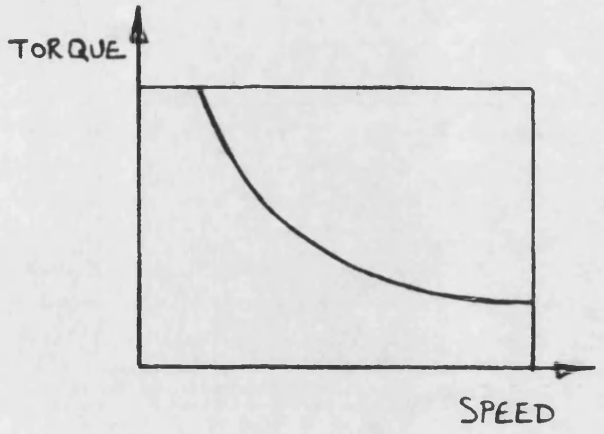

a) 1 pump with very high corner power

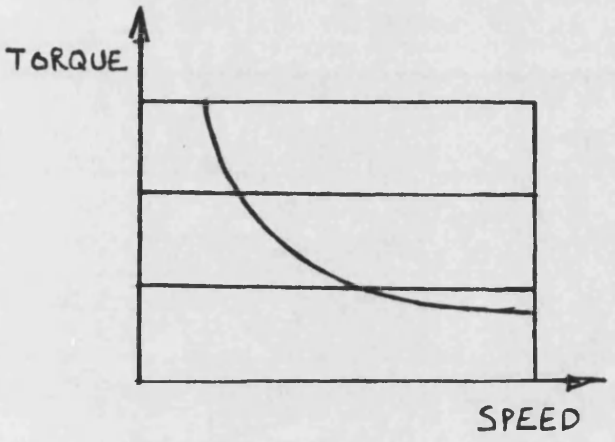

b) multiple pumps and a splitter box

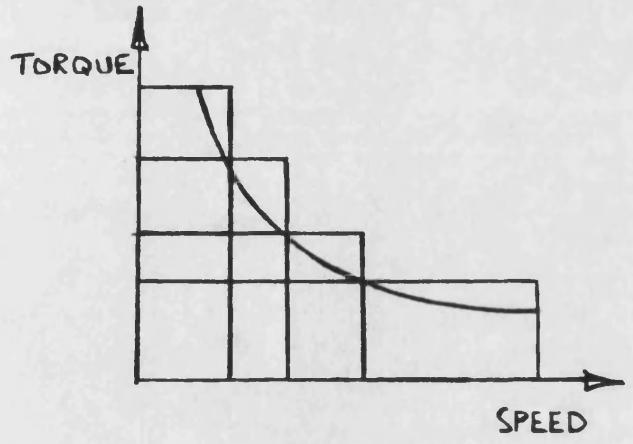

c) 1 pump and a multi-ratio gearbox

FIG 6.11 ALTERNATIVE DCE DYNOMOMETER SCHEMES

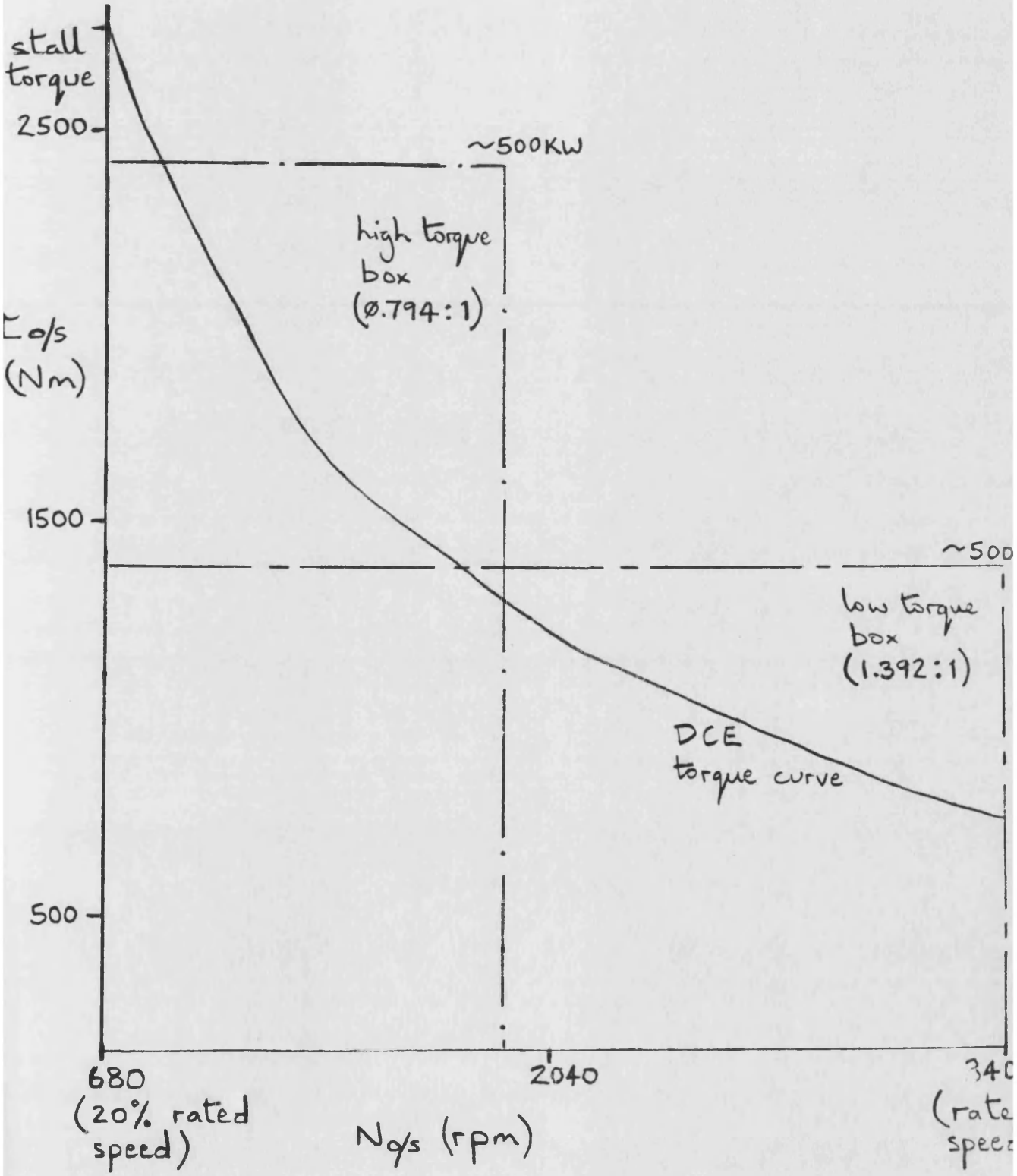

FIG. 6.12 DCE DYNAMOMETER OPERATING ENVELOPES

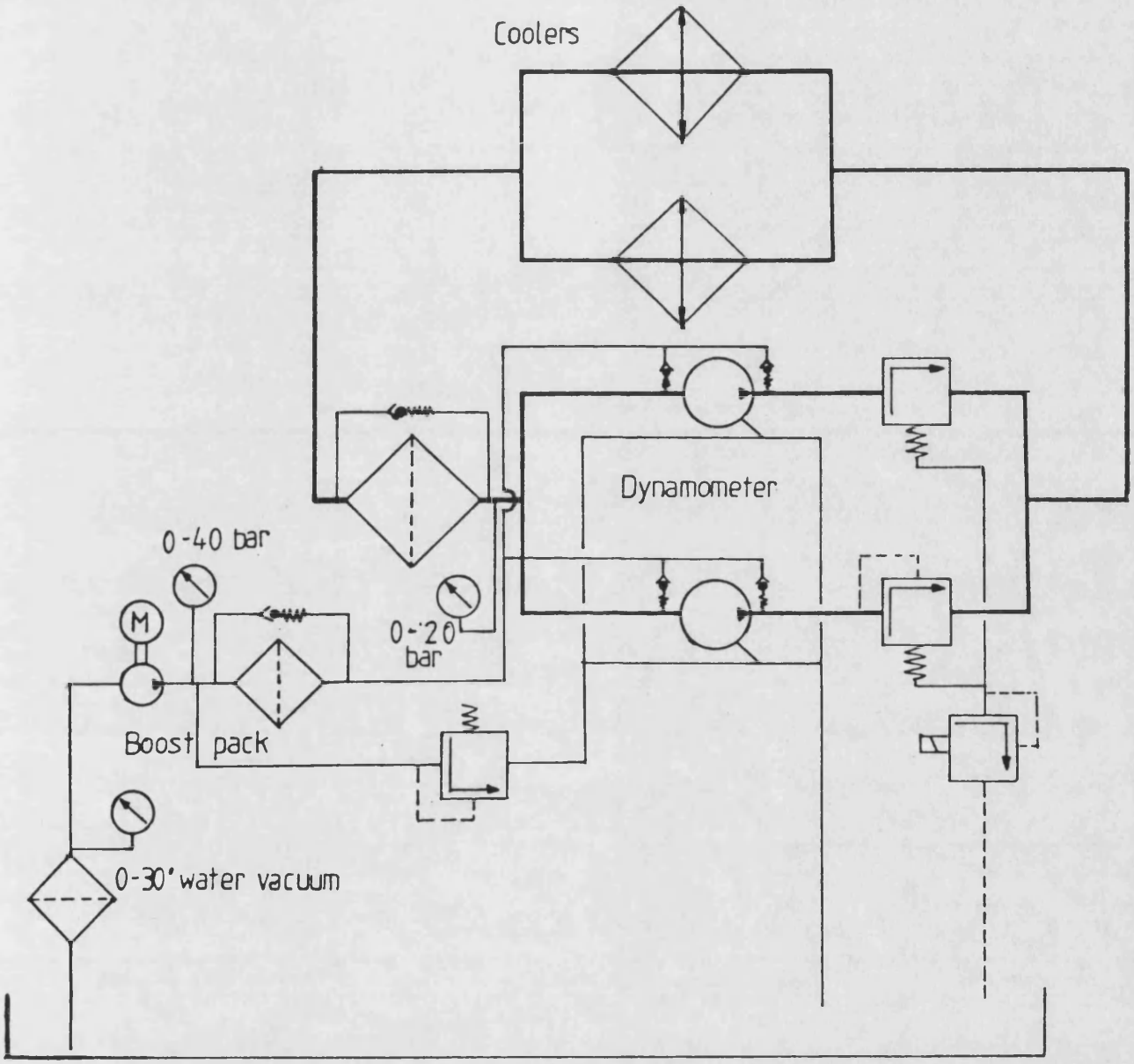

FIG. 6.13 DYNOMOMETER HYDRAULIC CIRCUIT

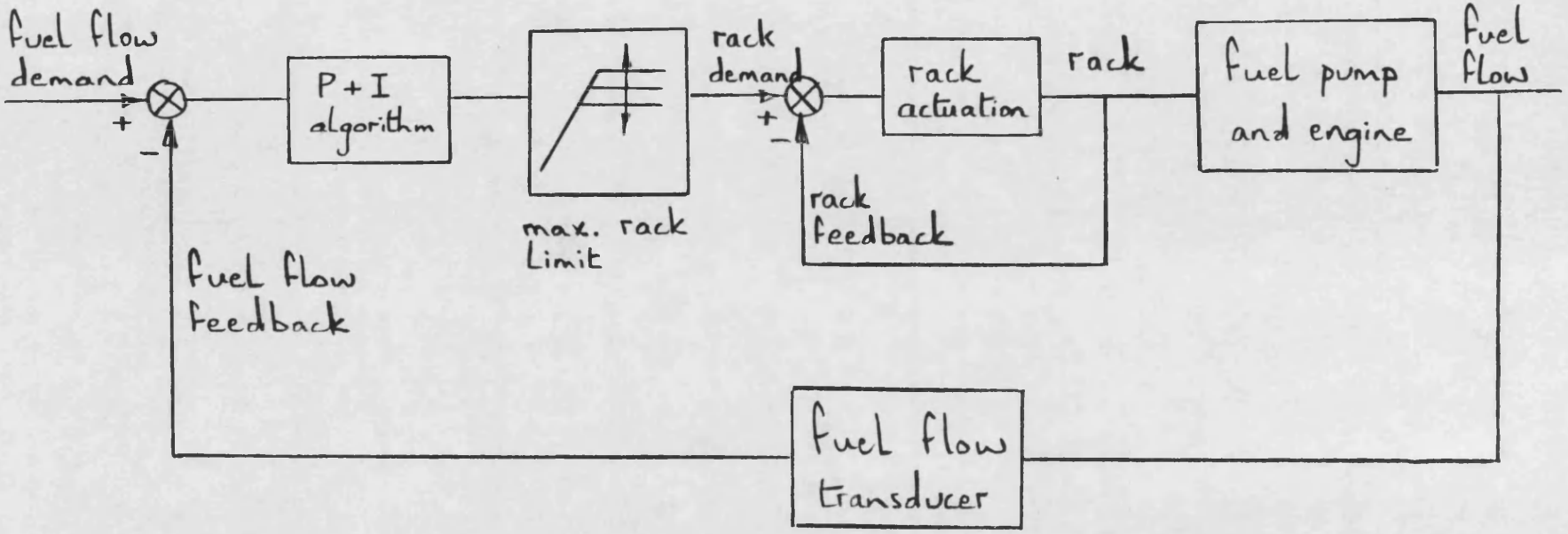

FIG. 6.14 FUEL FLOW CONTROL

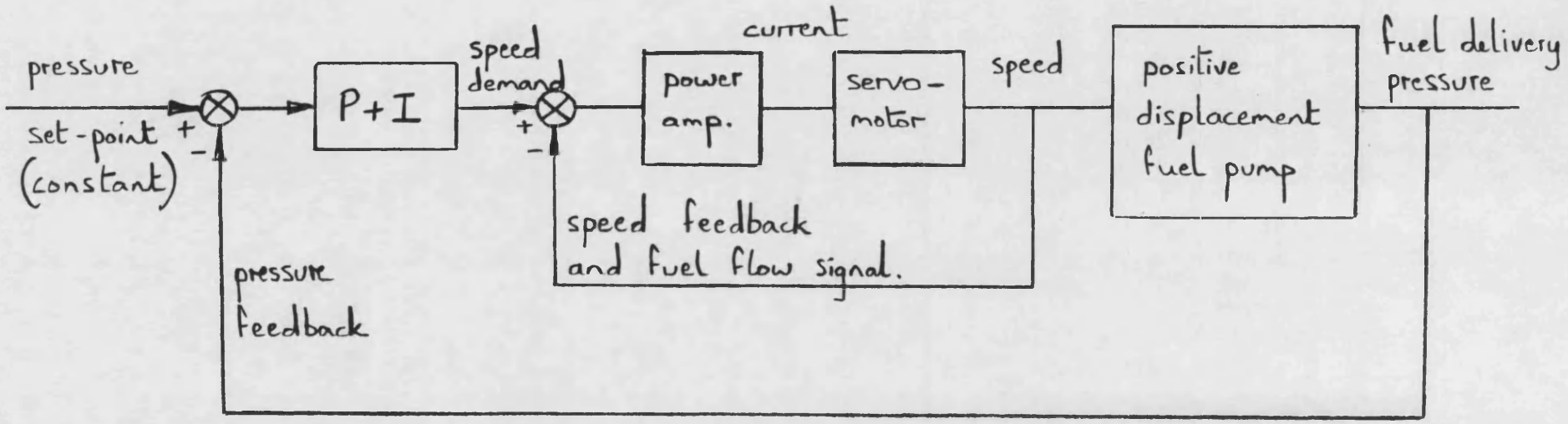

FIG. 6.15 TRANSIENT FUEL FLOW TRANSDUCER

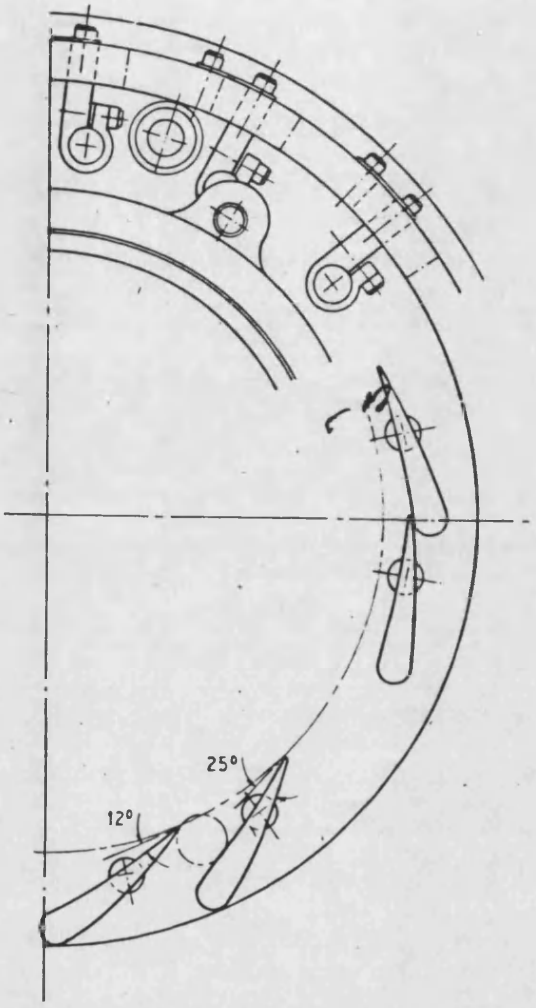

FIG. 6.16 VARIABLE NOZZLE ANGLE ARRANGEMENT

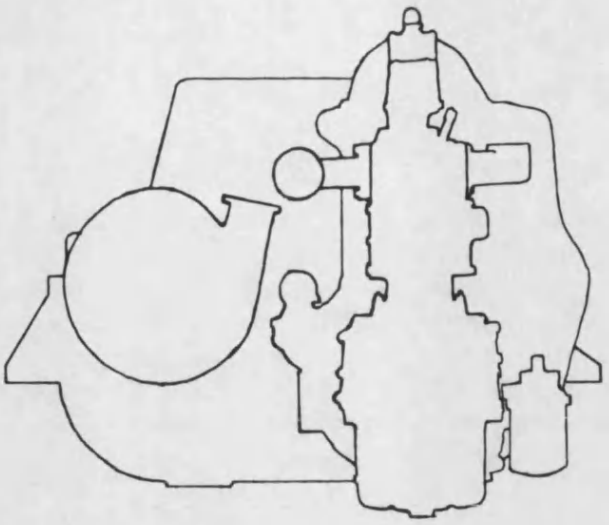

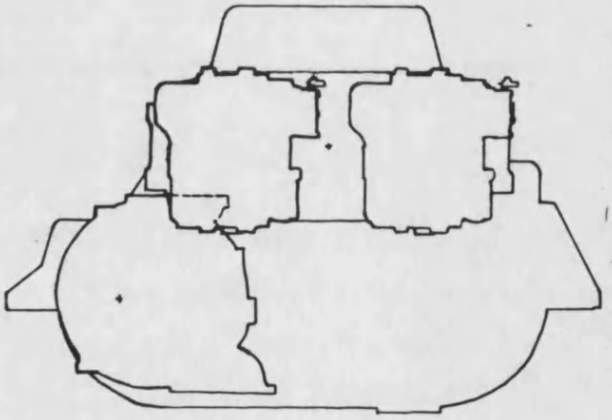

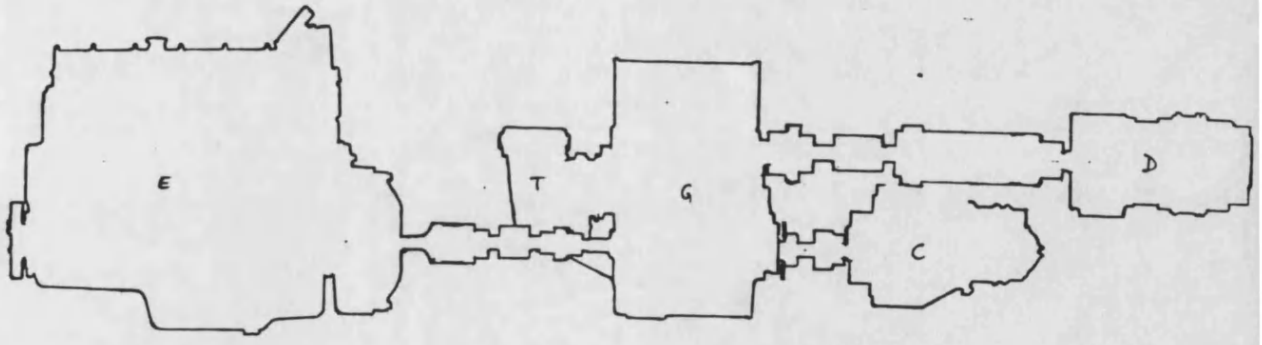

FIG. 6.17 D. C. E. LAYOUT

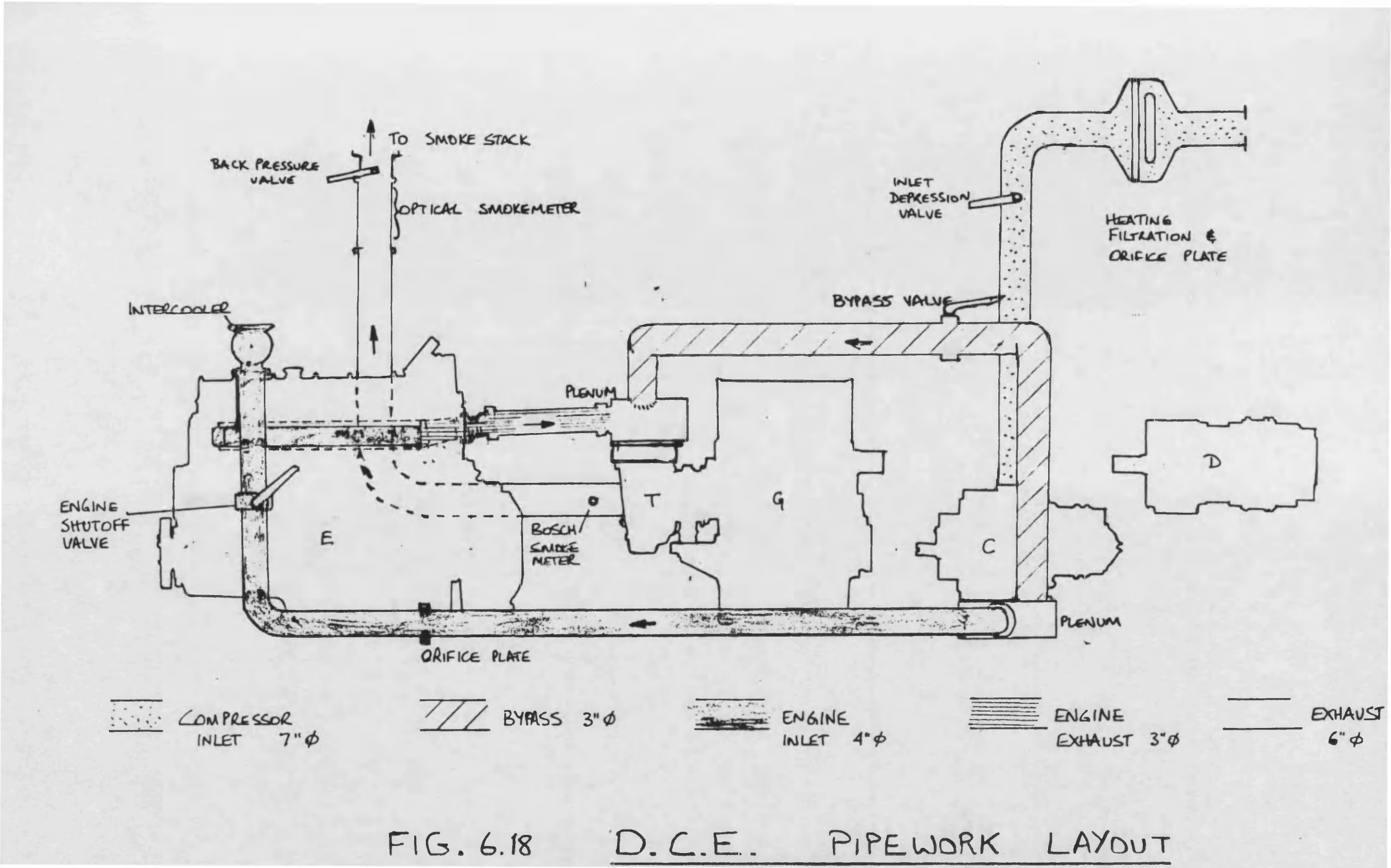

FIG. 6.18 D.C.E. PIPEWORK LAYOUT

CHAPTER 7

CONTROL SYSTEM DEVELOPMENT FOR THE DIFFERENTIAL COMPOUND ENGINE

7.1 INTRODUCTION

7.2 IMPLEMENTATION OF A SIMPLE STEADY-STATE CONTROLLER ON THE PERKINS 6.354 PROTOTYPE

7.2.1 CONTROL SYSTEM DESIGN PROPOSALS
7.2.2 BOOST PRESSURE CONTROL
7.2.3 ENGINE SPEED CONTROL
7.2.4 COMPUTER SCHEDULING
7.2.5 CONCLUSIONS

7.3 TRANSIENT CONTROL ALGORITHM DESIGN USING A DYNAMIC COMPUTER MODEL

7.3.1 THE BASE RESPONSE
7.3.2 TRANSIENT CONTROL SCHEME A
7.3.3 TRANSIENT CONTROL SCHEME B
7.3.4 TRANSIENT CONTROL SCHEME C
7.3.5 TRANSIENT CONTROL SCHEME D
7.3.6 DISCUSSION

7.1 INTRODUCTION

The DCE is a multi-variable Diesel Driveline with two primary control elements, that are fundamental to its operation, and several secondary controls to improve performance. This means that some form of automatic controller is necessary to relieve the driver of the burden of control as well as to optimise performance. For a normal Diesel the fuel control rod (rack) is the primary control element and all others serve only to improve performance and economy. Both rack and turbine nozzle angle are fundamental to the operation of the DCE. The following discussion describes their effect. The principles of DCE operation have already been covered in detail in section 6.2.

Under equilibrium conditions (steady-state) fuel rack position is roughly proportional to fuel per revolution (FPREV) and therefore sets an engine torque. This in turn determines compressor torque and thus boost pressure. Alternatively if engine speed feedback is introduced (ie. an all-speed governor is implemented) then rack is adjusted to regulate speed. This in turn determines compressor speed (for a given output speed) and therefore air massflow.

Nozzle angle establishes the position of the turbine's pressure vs. massflow characteristic (swallowing curve) with respect to the massflow axis (fig 4.3). The major effect of this depends upon the fuel control mode. If rack and hence boost are controlled then nozzle angle governs turbine massflow and thus engine/compressor speed. If engine speed and therefore massflow are controlled then nozzle angle determines turbine pressure ratio (boost) and thus torque.

To summarise, the steady-state control functions of the rack and nozzles are interchangeable and together they establish epicyclic speed and torque levels. This in turn determines air massflow and boost. Other variables such as fuel injection timing and turbine CVT ratio can alter efficiency and therefore increase output power. However they are not essential for basic control.

Under non-equilibrium (transient) conditions the above reasoning is no longer valid. If fuelling is smoke limited then instantaneous rack position determines the engine's developed torque. For a given output speed, developed torque is split between engine/compressor acceleration and epicyclic load torque. The latter is proportional to compressor torque and hence boost pressure. The rate of change of boost is determined by turbine massflow and therefore nozzle angle (turbine swallowing capacity).

If volume dynamics are negligible then nozzle angle will control instantaneous boost and therefore the split of compressor torque between acceleration and boost. Higher boost during a transient will leave less torque available for engine and compressor acceleration.

Under steady-state conditions the control elements should be adjusted to give optimum performance in terms of: torque back-up, efficiency, and environmental impact. One approach is to use stored control demand schedules. These schedules must be functions of a set of independent variables which unambiguously define the DCE's operating point.

Section 7.2 discusses the design and implementation of a simple steady-state control system for the Perkins 6.354 prototype. A microprocessor stores an optimum boost pressure schedule which is output via a DAC channel to a boost pressure feedback loop. The driver controls engine speed with another feedback loop (all-speed governor). The root-locus method was used to analyse alternative feedback loop configurations, the resulting designs were implemented with analogue electronics.

Under transient conditions the control requirements are rather different, response and drivability are primary concerns. To improve these characteristics a special transient algorithm is used which overrides the steady-state control schedules. The design of such algorithms has been investigated using a dynamic computer model of

the DCE, this work is discussed in section 7.3. A description of the computer model can be found in Appendix 2.

7.2 IMPLEMENTATION OF A SIMPLE STEADY-STATE CONTROLLER ON THE PERKINS 6.354 PROTOTYPE

7.2.1 CONTROL SYSTEM DESIGN PROPOSALS

This section describes the implementation of a micro-processor based controller to run the DCE at optimum efficiency throughout its operating map. The research was undertaken with the old PERKINS 6.354 prototype (refer to section 6.3). Experimental optimisation of the prototype's control parameters had already been carried out, with the objective of minimising fuel consumption (refs. 60,61). The resulting 3-D control surfaces are shown in fig. 7.1, the control variables being functions of output speed and torque (ambient conditions are neglected). These surfaces can be discretised and held as 2-D arrays, the array indices being output speed and torque.

The DCE has three operating controls: fuelling; turbine nozzle angle; and bypass valve setting. Optimum S.F.C. results from keeping the bypass fully open, which reduces the optimising controls to two. The driver and/or scheduling controller may set these indirectly via feedback loop demands. For instance an engine speed (N_E) governor is used which adjusts fuelling automatically to give the demanded speed. This was considered a safer approach than acting on fuelling directly which would be more likely to result in over-speeding under certain failure conditions. It was decided that the scheduled variables which optimise S.F.C. should not be subject to mechanical drift caused by such things as wear, mal-adjustment, soot build up etc. For this reason boost pressure (P_B) control was implemented by putting a feedback loop around nozzle angle.

A micro-processor based controller (fig. 7.2) was proposed in ref. 61 to run the DCE on the optimum surfaces. Output speed ($N_{O/S}$) and torque ($\tau_{O/S}$) along with the driver's output speed demand ($N_{O/S(dem)}$) are read via A/D converters. A scheduling program then pulls demands for engine speed and boost pressure from 2-D arrays containing the optimum surfaces previously mentioned. The demands are output to

their respective feedback loops via D/A converters. It was suggested that $N_{o/s\langle dem\rangle}$ and $\tau_{o/s}$ be used as the array indices. Because of error accumulation $N_{o/s}$ would not follow $N_{o/s\langle dem\rangle}$ exactly, the micro' would eliminate any error by adjusting $N_{E\langle dem\rangle}$. This defeats the object of the controller because the system moves off the optimum N_E surface. There is in fact no requirement to match $N_{o/s}$ and $N_{o/s\langle dem\rangle}$ exactly so long as the DCE operates at maximum efficiency. The following discussion explains the actions that will keep the system on the optimum surfaces.

When operating the experimental prototype or studying the DCE's theoretical behaviour it is apparent that only three of the four variables used above ($N_{o/s}, \tau_{o/s}, N_E, P_B$) are required to determine the steady-state operating condition. The fourth then becomes another dependent variable. For example with fixed $\tau_{o/s}$, N_E, and P_B the DCE will converge on one output speed only (neglecting changes in ambient conditions). This implies that so long as the three independent variables constitute an "optimum set" maximum efficiency will result when steady-state conditions are reached.

The controller previously mentioned would work if no attempt was made to exactly match $N_{o/s}$ and $N_{o/s\langle dem\rangle}$ by adjusting N_E. The $N_{o/s}$ input to the micro' is therefore eliminated from the scheme. In this case the "optimum set" is N_E, P_B, and $\tau_{o/s}$. $N_{o/s\langle dem\rangle}$ is the means by which the driver selects his desired operating condition and does not have to equal $N_{o/s}$.

If the accuracy with which the scheduled variables follow their demands is critical an integral component must be included in the control loop algorithms to ensure zero steady-state error. The importance of this was investigated and is discussed in the following sub-section, the conclusion was that an integral component was necessary.

A more useful result of the "optimum set" principle becomes apparent if the three independent variables chosen are P_B, $N_{o/s}$, and $\tau_{o/s}$.

The resulting control scheme is shown in fig. 7.3, the driver provides the engine speed demand and the micro' schedules the boost demand. Only one control surface is required the second becomes redundant, in addition only the boost feedback loop need incorporate an integral component to eliminate steady-state error. Engine speed was chosen as the drivers control for the following reasons:-

i) Under optimum steady-state conditions N_E behaves like a power demand ie. output speed and torque rise with engine speed (see fig. 7.1).

ii) The micro-processor scheduled variable is more likely to fail. A loss of nozzle control, especially if they fail open, is fairly safe and predictable. Conversely loss of engine speed control could be disastrous.

iii) The vehicle can limp home under manual control with the nozzles wide open.

This alternative design simplifies the scheduling software and eliminates the need for an integral component in the engine speed loop. The following sub-sections describe the implementation of a prototype controller based on these observations. The analogue controls described in the following two sub-sections were implemented with op-amp circuitry similar to that described in section 4.2.

7.2.2 BOOST PRESSURE CONTROL

Boost pressure is controlled by adjustment of turbine nozzle angle, the swivelling nozzle arrangement is described in sub-section 6.4.3. The lever actuator is driven by an electro-hydraulic positioning loop similar to that described in section 3.5. Several alternative boost control configurations were considered. To assess their likely behaviour a root-locus analysis was undertaken.

The root-locus method was used because it can give a qualitative assessment of feedback loop dynamics when accurate system data is not available (ie. system gains and time constants). The following explanation is only intended as a guide to root-locus interpretation, a full description of the technique can be found in ref. 39.

The poles and zeros of the open loop transfer function (OLTF) are plotted on the s-plane. The loci of the closed loop pole positions, with increasing loop gain, can then be drawn by following the rules in ref. 39. The loci begin at the open loop poles where loop gain is zero and end at the zeros where gain is infinite. When there are more open loop poles than zeros the loci converge on asymptotes drawn to the aforementioned rules. The loci are always symmetrical about the real axis because the complex poles come in conjugate pairs.

The loci are shown as bold lines (to distinguish them from axes) with arrows indicating the direction of increasing loop gain. The asymptotes are shown as dotted lines.

Numerical values for the open loop poles and zeros are not necessary so long as their relative positions are realistic. This is enough to provide a qualitative assessment of dynamic behaviour.

Figure 7.4 gives a simplified guide to the effect of loci position on loop dynamics. The further the closed loop poles (loci) are to the left the faster the system dynamics ie. faster exponential decay. Positive poles result in instability, that is an exponential rise. Poles with an imaginary component produce oscillatory behaviour, the frequency of oscillation increases with the imaginary component.

The electro-hydraulic positioner consists of a servo-valve governing the oil flow to a hydraulic cylinder. A position sensor is attached to provide a feedback signal. The servo-valve produces an oil flow and hence jack velocity proportional to valve current. The dynamics of the valve and jack are assumed to include velocity and acceleration (inertial) effects, the transfer function is therefore first order:-

$$\frac{V}{I} = \frac{K_v}{(1+\tau_v . s)} \qquad (7.1)$$

K_v=servo-valve gain
τ_v=servo-valve time constant
V=jack velocity
I=valve current

Referring to fig. 7.5, the open loop transfer function (OLTF) relating jack position X to error signal E is of the form:-

$$G(s) = \frac{X}{E} = \frac{K_{ACT}}{(1+\tau_v . s)s} \qquad (7.2) \qquad K_{ACT}=K_{ERR} \times K_v$$

Hence the closed loop transfer function (CLTF) is given by:-

$$\frac{X}{X_{dem}} = \frac{G}{G+1} = \frac{K_{ACT}/\tau_v}{s^2+s/\tau_v+K_{ACT}/\tau_v} \qquad (7.3)$$

The root locus in fig. 7.6 shows the position of the open loop poles and the locus of the corresponding closed loop poles with increasing gain. It can be seen that as gain is increased response improves but the loop becomes oscillatory. This is the typical behaviour of a second order system. There is no steady-state position error because any error results in a jack velocity.

The gas dynamics of the DCE are represented in a simplified manner by fig. 7.7. Volume V represents the inlet and exhaust manifolds, the intercooler, the bypass, and other interconnecting pipework between the compressor and turbine. The cumulative flow into the volume is given by:-

$$Q = Q_C - Q_T = K_1 . \omega_c - K_2 . \alpha_n . (P_B)^{1/2} \qquad (7.4)$$

Q_C=compressor flow
Q_T=turbine flow
ω_c=compressor speed
α_n=nozzle angle
P_B=boost pressure
K_1, K_2=linear gains

where the turbine is approximated to a variable orifice. Boost pressure P_B in the volume varies with the integral of Q.

Q_C and the time variant coefficient $K_2.(P_B)^{1/2}$ are assumed constant for dynamic purposes (root locus analysis) as they change slowly in comparison with α_n and hence Q_T. Therefore the volume dynamics can be represented simply by:-

$$P_B = (Q_C - K_T.\alpha_n).K_{vol}/s. \qquad (7.5)$$

K_T=turbine gain
$=K_2.(P_B)^{1/2}$
K_{vol}=volume gain

By combining position loop and volume dynamics the effect of boost pressure feedback can be analysed, three alternative schemes are discussed (figs. 7.8 and 7.9):-

1. Boost feedback, with a simple proportional gain, and no inner position feedback loop (fig. 7.8 without α_n feedback).

$$OLTF = \frac{K_B}{(1+\tau_v.s)s^2} \qquad (7.6)$$

K_B=combined boost loop gain
$= K_{ERR}.K_{ACT}.K_T.K_{vol}$

2. Boost feedback, with a simple proportional gain, and the inner position loop retained (fig. 7.8 with α_n feedback).

$$OLTF = \frac{K_B/\tau_v}{s^2+s/\tau_v+K_{ACT}/\tau_v}.\frac{1}{s} \qquad (7.7)$$

3. Boost feedback, with proportional plus integral (P+I) compensation, and an inner position loop (fig. 7.9).

$$OLTF = \frac{\tau_I.s+1}{\tau_I.s}.\frac{K_B/\tau_v}{s^2+s/\tau_v+K_{ACT}/\tau_v}.\frac{1}{s} \qquad (7.8)$$

τ_I=integrator time constant

Scheme 2 produces a positive steady-state boost error (droop). This is the case because a positive error signal is necessary to give any nozzle position other than zero (fully open). If necesssary this can be overcome by using one of the other two schemes. Without the inner loop (scheme 1) any error results in a jack velocity and hence the error signal is driven to zero. Similarly the integrator in the P+I algorithm (scheme 3) ramps until the error signal is zero. The P+I algorithm supplies a driving signal which is the sum of two

components: one proportional to the error signal; and the other proportional to the time integral of the error signal.

The root-locus plots for the three schemes are shown in the following figures:-

figure 7.10 scheme 1
figure 7.11 scheme 2 with low inner loop gain (over damped)
figure 7.12 scheme 2 with high inner loop gain (under damped)
figure 7.13 scheme 3

Proportional boost control with no inner position feedback loop (scheme 1) would be unstable because the loci are to the right of the origin. It is therefore totally unsuitable and should not be considered.

Proportional boost control with the inner loop included (scheme 2) should have good dynamic performance because the loci are well to the left of the origin. However this scheme suffers from a steady-state boost error (droop) which increases with nozzle angle. Adjusting inner loop gain has little effect close to critical damping (see figs. 7.11 and 7.12), the loci of the dominant (slow) closed loop poles are not significantly altered. This is due to the position loop dynamics being relatively fast ie. well to the left of the dominant loci.

Adding P+I compensation (scheme 3) eliminates any boost error but reduces dynamic performance (the locus moves closer to the origin). This is the usual penalty of introducing an integral component.

Initially scheme 2 (proportional control) was implemented, the gains K_{ACT} and K_{ERR} were the only adjustments necessary to tune the loop. It was found that inner loop gain K_{ACT} had to be adjusted to eliminate excessive vibration of the nozzle ring; too high a gain allowed the actuator to follow signal noise created by inlet manifold pressure pulsations. The boost loop gain K_{ERR} was adjusted to give good response to changes in demand without overly harsh operation.

Under normal operating conditions the steady-state error (droop) varied between -6% and -10%. This could be partly overcome by supplying a corrected boost demand which assumes a droop of 8%, the error would then be within ±2%. To assess the effect of this some overall efficiency measurements were made with boost pressure set at, above, and below the optimum. Normally an error of 2% had little effect on efficiency, however there were extreme cases where the efficiency dropped by 3% (eg. 29% to 26%) which is clearly unacceptable.

As a result it was decided the P+I algorithm should be included (fig. 7.9) to eliminate the boost droop. Using this type of algorithm ensures the error signal is driven to zero, leaving transducer inaccuracy as the only source of error. The adjustment of the proportional and integral gains was a compromise between dynamic performance (less integral, more proportional) and rapid elimination of the boost droop (more integral, less proportional).

Although dynamic performance is reduced by incorporating the P+I algorithm this was not so important for what was a slow steady-state controller anyway. When transient algorithms are incorporated (see section 7.3) boost dynamics may be more critical. Figure 7.14 shows a means of using a simple proportional loop (better dynamics) without incurring large steady-state errors. The scheduling computer outputs the approximate nozzle angle setting as well as a boost pressure demand. The boost feedback loop then serves as a fine tuning mechanism, overcoming mechanical drift such as soot build up. In addition the boost loop provides transient over restriction when manifolds and pipe-work are being filled.

7.2.3 ENGINE SPEED CONTROL

The PERKINS proto-type had a DPA distributor type fuel pump rather than the in-line type used on the latest Leyland 500 based proto-type. However an electro-hydraulic governor similar to that described in section 6.4.3 had been implemented with a small hydraulic jack acting on the metering valve arm.

In the proposed control scheme the engine speed demand is set by the driver. Because he automatically adjusts his demand to suit the road conditions there is no need to eliminate any steady-state speed error (governor droop). In fact the characteristic runout line (fig. 7.15) created by mechanical governor droop gives smooth operation because fuelling does not increase suddenly at the demand speed. Hence speed is controlled with a simple proportional loop (fig. 7.16), which behaves in a similar manner to a mechanical governor so long as the inner position loop is retained. Without the inner loop there would be no speed runout because any error signal results in a metering valve velocity. The following analysis shows that the inner loop also improves governor response.

The torque developed by the engine is assumed to be proportional to fuel per shot and hence metering valve position. Engine dynamics can therefore be represented by the following equation:-

$$\tau_E = K_{mv} \cdot x_{mv} = \tau_L + I \cdot \dot{\omega} + D \cdot \omega \qquad (7.9)$$

τ_E=developed torque
τ_L=load torque
ω=engine speed
x_{mv}=metering valve position
I=lumped inertia term
D=lumped viscous drag term
K_{mv}=metering valve gain

Actuator dynamics have already been discussed in the previous sub-section. Combining engine and actuator dynamics results in the speed control block diagram shown in fig. 7.16, the optional inner position loop is dotted.

The open loop transfer functions are:-

1. Without the inner position loop

$$OLTF = \frac{K_{speed}}{(1+\tau_v . s)s} \cdot \frac{1}{1+\tau_{ENG} . s} \qquad (7.10)$$

K_{speed}=combined loop gain
$= K_{ERR} . K_{ACT} . K_{mv} . K_{ENG}$
K_{ENG}=engine gain
$=1/D$
τ_{ENG}=engine time constant
$=I/D$

2. With the inner position loop

$$OLTF = \frac{K_{speed}/\tau_v}{s^2+s/\tau_v+K_{ACT}/\tau_v} \cdot \frac{1}{1+\tau_{ENG} . s} \qquad (7.11)$$

The root-locus plots in figs. 7.17 and 7.18 show the effect of the inner loop on dynamics. The locus moves closer to the origin when the inner loop is omitted, this means poorer governor response. Hence the inner loop should be included to give smooth engine operation due to the characteristic runout line, and good dynamic response.

7.2.4 COMPUTER SCHEDULING

The computer scheduling of boost demand was implemented using a Commodore PET micro-computer. The hardware configuration was the same as that used for transient data-acquisition (see section 2.3.2). Two of the ADC channels were used to read output speed and torque, one DAC was used to output the analogue boost pressure demand.

The scheduling software was written in BASIC and calls machine-code subroutines to run the ADC and DAC. Optimum boost and engine speed maps were digitised and are stored as DATA statements. The DATA statements are READ into 2-D arrays, the array indices being output speed and torque. The engine speed array is used only to provide a comparison with the actual engine speed achieved ie. a measure of the accuracy and/or repeatability of the optimum maps. The boost pressure map is used to schedule the output to the analogue boost control loop.

After initialising interface hardware, optimum arrays, and the VDU display, the program enters the scheduling loop. This loop continuously updates boost pressure demand by executing the following procedure:-

1. Read ADC channels for output speed and torque.

2. Limit speed and torque values to those covered by the optimum maps.

3. Pull optimum boost demand from array using a 2-D interpolation method similar to that described in Appendix 1.

4. Step the boost demand output by the DAC one increment towards the optimum. The increment (step size) is defined by the operator through the keyboard.

5. Wait until the end of the update period before continuing. The update period is defined by the operator together with the boost step size to set a boost demand slewing rate.

6. Unless the "jump out key" is pressed restart the scheduling loop.

If the operator presses the "jump out key" the scheduling loop is halted and he can alter or request an update of the parameters displayed on the screen, which are:-

i)	Boost step size	---	set by the operator
ii)	update period	---	set by the operator
iii)	DAC boost demand	---	updated by the computer
iv)	predicted engine speed	---	updated by the computer
v)	ADC readings	---	updated by the computer

When the "restart key" is pressed the scheduling loop is re-started. The displayed values are not updated whilst the scheduling loop is running because this reduces execution speed dramatically.

The scheduling loop (compiled version) executes in approx. 0.1 sec., which is a relatively slow update rate. As a result the boost step size was limited to 0.05 Bar to avoid excessively harsh movement of the turbine nozzle assembly. As expected boost pressure followed the computer scheduled demand very accurately under steady-state conditions. Because of the P+I algorithm included in the boost feedback loop the only sources of error are pressure transducer and DAC inaccuracies (<1%).

The slow update rate combined with the step size limitation results in a lag between any rapid changes in operator demand (N_E) and boost pressure changes. The implication is that, even if no additional transient algorithms are added to the program, execution speed is too slow. The program should be written in machine code or run on a faster machine. Since this work was done the development computer (LSI-11/23) described in section 3.4 has been purchased and will be used for future proto-type systems. This machine has been used to implement a similar scheduling system on the V.G. turbocharger test engine, the execution speed is over ten times faster.

Program listings have not been provided as the PET is not recommended for future control development work. The LSI-11/23 software described in Appendix 1 implements a similar scheduling system.

7.2.5 CONCLUSIONS

A micro-processor based steady-state controller (fig. 7.3) has been implemented on the old PERKINS 6.354 proto-type. The system schedules a boost pressure control loop to keep the DCE running at peak efficiency. The driver uses an engine speed governor as his output power control.

A previous proposal to schedule both boost and engine speed has been shown to be over complicated and prone to error. The proposal was based on a misconception that both parameters require scheduling to maximise efficiency.

Boost pressure was scheduled as a function of output speed and torque. This was the case simply because the optimum boost map had already been defined in this form. In practice fuel rack position would be a more commercially viable measure of load. A simple low cost position sensor could be mass produced using existing measurement technology.

The analogue feedback loops controlling boost and engine speed were designed using the root-locus technique. Accurate time constant data was not required to provide the qualitative information needed to decide upon the best feedback loop configurations. The loop gains were determined by on-line tuning during commissioning.

The dynamic performance of both control loops has been shown to benefit from the inclusion of an inner position (rack or nozzle angle) feedback loop. It was found necessary to incorporate a P+I algorithm in the boost control loop to ensure the scheduled demand was followed exactly. A significant loss of overall efficiency can otherwise result (up to 3% in extreme cases).

The scheduling software was too slow to follow rapid changes in driver demand, thus demonstrating the need for a more powerful computer for this sort of development work.

7.3 TRANSIENT CONTROL ALGORITHM DESIGN USING A DYNAMIC COMPUTER MODEL

This section describes a theoretical investigation into the design of transient control algorithms for the Differential Compound Engine (DCE). Section 3.3 discusses the design of transient algorithms in a generalised manner without reference to a particular engine/ driveline. As the DCE is a complex multi-variable driveline there is considerable scope for maximising response and improving drivability. The transient algorithms explored where all aimed at achieving the following design goals:-

i) Rapid response to changes in power/torque demand.
ii) Good drivability in terms of initial response ie. no time lag and smooth predictable characteristics (see section 3.1).
iii) The transient algorithm should be part of an overall control scheme which produces optimum performance under steady-state conditions.

The DCE is a complex non-linear system and therefore does not lend itself to analytical design methods based on linear theory. Given a particular feedback loop the comparison of alternative compensation algorithms is possible by making linear approximations (section 7.2). However, the design of a transient controller involves the correct choice of control and feedback variables and the configuration of suitable control loops. The only method available for this is the application of control experience combined with a knowledge of the DCE's dynamic behaviour to produce an intuitive design.

Controller designs must be tested either on the experimental prototype or with a dynamic computer model of the DCE. The latter method was chosen as it saves the time and expense incurred by controller implementation and testing. In addition potentially hazardous transient tests are avoided and steady-state testing of the prototype can continue unhindered. Many alternative control algorithms can be tried with only simple modifications to the dynamic model.

Although a dynamic model was already available (DCETRAN) the author decided to write his own simplified model for the following reasons:-

i) Whilst modifying DCETRAN to model the military version of the DCE (ref. 62) the author discovered numerous mistakes, redundant and untidy coding, and a total lack of explanatory comments. This did not encourage a trust in the program's accuracy and logic.

ii) For comparative control studies, rather than accurate simulation, there is no need for detailed thermodynamic modelling. All that is required is a reasonable model of the dynamics and principal non-linearities inherent in the DCE. This will then give stability/response behaviour similar to that of the DCE itself.

iii) With a simple program it is relatively easy to have a conceptual grasp of the model as a whole. This is not the case with a complicated thermodynamic model.

iv) A simple model is easier to modify and debug, needs fewer parameters to define the particular DCE build, and is more efficient in its use of computer power. Rapid modification is important if many different control algorithms are to be tried. Faster execution speed is particularly useful if long vehicle transients or frequency response tests are simulated.

This new program (DCESIM) is described in detail in Appendix 2.

Four alternative transient control schemes (A,B,C,&D) have been modelled along with a base response for comparison purposes. They were compared by simulating the response to a fuel step at constant output speed (stall=500rpm) representing an increase in output of approx. 220%. This was chosen because it involves large changes in boost pressure, engine speed, and output torque. For each scheme the control gains were varied to establish their effect and obtain a typical response for discussion.

Transient control schemes A, B, and C are described by figs. 7.19-7.21. A set of typical responses along with the base response are shown in figs. 7.22-7.27.

Scheme D (fig. 7.28) was simulated with 3 different values for the gain K2 as this has a major effect on the action of the algorithm. The corresponding responses along with the base response are shown in figs. 7.29-7.34.

Because a fuel step at constant output speed was simulated, the variables which are shown as functions (array interpolations) of rack and speed are simply stepped to their new values in unison with the fuel step. The remainder of the control algorithm is programmed into the dynamic DCE model.

NOTE: Precise details of the transients including any control system parameters used can be found in the transient response printouts in Appendix 2. A printout is included for the base response and each of the control schemes modelled.

The following sub-sections discuss the design and performance of the transient control algorithms investigated. The algorithms are described in order of conception so that an insight into the design process might be obtained. The final sub-section draws conclusions and makes suggestions for further work.

7.3.1 THE BASE RESPONSE

Before attempting to design a transient algorithm the effect of a simple step in both fuelling and nozzle angle was simulated. This provides a basis for assessing further improvements in response. Nozzle angle was stepped to its final optimum steady-state position in unison with the fuel step. This effect would be produced by a simple steady-state controller which adjusts nozzle angle as a function of output speed and fuel rack position [NOTE: rack position approximates

to fuel per revolution (FPREV) which is the parameter used for this simulation work].

The fuel step at stall, described above, was simulated. Referring to figs. 7.22-7.27, the immediate opening of the nozzles causes boost pressure to drop slightly initially, after which it only rises at the same rate as compressor speed [NOTE: the compressor speed response is not shown because at constant output speed it corresponds to the engine response]. This low boost early in the transient causes air-fuel ratio (AFR) limiting fuel reduction (the bottom limit for AFR being 20). As a result the initial torque rise is non-existent, output torque only rises as engine speed and hence boost increase. The driver gets no initial response to his change in torque demand, this is clearly unacceptable from a drivability point of view.

7.3.2 TRANSIENT CONTROL SCHEME A (fig. 7.19)

Perhaps the most obvious way of avoiding AFR limiting fuel reduction is to use the nozzles to rapidly increase boost pressure and hence hold AFR above 20. A boost control scheme similar to that advocated in section 7.2 (fig. 7.3) will have this effect. If the inputs to the scheduling computer were output speed and FPREV then a boost demand step would be produced in unison with the fuel step. The boost loop would then reduce nozzle angle to rapidly raise boost to the new steady-state optimum demanded.

The scheme simulated is slightly different to that described in section 7.2, the following discussion explains why.

Two alternative approaches to driver (fuel) control have been suggested (section 7.1): either the driver controls an engine governor and hence engine and compressor speed; or he has direct control of rack position (FPREV) and hence engine and compressor torque.

In the first case the major effect of a nozzle angle change is to alter the pressure ratio across the turbine and thus torque levels in

the epicyclic. Hence a boost loop can be used to schedule steady-state pressure ratio and provide the transient effect suggested above ie. the scheme proposed in section 7.2 can be used with FPREV replacing output torque as an input.

In the second case the major effect of a nozzle angle change is to alter the massflow through the turbine and thus engine and compressor speed. FPREV is the major determinant of engine (compressor) torque and hence boost pressure (see discussion in section 7.1). As boost pressure is not primarily a function of nozzle angle, a steady-state boost control loop (section 7.2) would not be appropriate and may not function at all.

However, under dynamic conditions the first effect of a nozzle angle adjustment is a pressure change which then causes engine/compressor acceleration or deceleration until pressure ratio again matches compressor torque. Therefore a transient boost loop combined with steady-state nozzle angle scheduling should give the transient properties of boost control with stable and accurate steady-state operation (fig. 7.19). Under steady-state conditions boost is dependent upon FPREV, and nozzle angle follows a steady-state optimum setting. Dynamically the transient boost loop attempts to raise boost rapidly to its new steady-state value.

The overall effect of the two options is similar, however, the latter option was simulated as it avoids the need to incorporate the P+I algorithm. The integrator can reduce feedback loop stability and also requires increased use of numerical integration.

As before a fuel step at stall was simulated. Referring to figs. 7.22-7.27, boost pressure rises rapidly to 3.3 Bar absolute which corresponds to an AFR of 25. This results in a good initial output torque rise from 1000 to 2000 Nm. Drivability and smoke would be greatly improved as compared with the base response. However, torque then rises more slowly and only reaches 2800 Nm after 3 seconds as compared with 3200Nm for the base.

The long rise time for the second phase of torque increase was attributed to the high initial boost pressure leaving little compressor torque available for acceleration. This results in a slower rise in engine/compressor speed, massflow and hence turbine torque.

It is apparent from this response that inertias rather than volumes dominate the dynamics of the DCE. The final torque rise time is governed by engine and compressor acceleration not rate of boost pressure rise which is very rapid indeed.

It should be noted that the combined volume of 10 litres for manifolds and pipework is an estimate for a commercial DCE build. The experimental prototype has a larger combined volume because its length is extended by coupling and torque measurement requirements.

7.3.3 TRANSIENT CONTROL SCHEME B (fig. 7.20)

The poor final rise time of scheme A led to the idea of using a reduced boost pressure demand during the transient. This would leave a larger proportion of compressor torque available for acceleration. However, boost should be high enough to avoid AFR limiting fuel reduction as this results in low initial torque. After the transient, nozzle angle and boost should revert to their optimum steady-state values.

Scheme B does this by using engine speed error as a transient measure. The speed error is the difference between the steady-state optimum and actual engine speed. Whilst an error exists (ie. the engine is accelerating) a transient boost control loop is switched in. The transient boost demand is a function of FPREV and gives an AFR just above 20, thus avoiding fuel reduction and increasing engine/compressor acceleration.

The boost loop subtracts a transient adjustment from the normal steady-state nozzle angle setting. When engine speed reaches the

required level (within 50rpm of the new steady-state condition) the transient adjustment is switched out. This allows boost and AFR to rise to their steady-state optimums.

Referring to figs. 7.22-7.27, in this case engine/compressor acceleration is the same as the base response for the first second and is then better, the steady-state speed being reached in approx. 1.5 seconds. Boost immediately rises to 2.7 Bar absolute giving an AFR of 21 which avoids any fuel reduction. Output torque has a correspondingly rapid initial rise to 1800Nm followed by a slower ramp up to 2700Nm after 1.5 seconds. At this point torque has fallen slightly below that of the base because boost is still being held artificially low which reduces turbine torque. At this stage the transient boost control is switched out and nozzle angle steps to its steady-state value. This results in a rapid rise in boost and hence output torque to its final value of 3200Nm.

Although this response is a large improvement over that of scheme A torque still drops slightly below that of the base between 1.0 and 1.5 seconds. In addition the final step to 3200Nm could produce unpredictable (jerky) operation in a vehicle installation.

7.3.4 TRANSIENT CONTROL SCHEME C (fig 7.21)

Scheme B produced a final step in torque at the end of the transient which is obviously unacceptable from a drivability point of view. To overcome this the switch was replaced with a variable gain dependent on the speed error (transient measure). This reduces the effect of transient boost control gradually as engine speed approaches its final steady-state value.

For simplicity the boost loop gain (K_1) is proportional to the engine speed error. A non-linear relationship may produce better results but the exact form of equation would have to be determined by considerable empirical investigation. The switch in scheme B can be thought of as

a non-linear gain equation, demonstrating that schemes B and C are of the same general form.

By referring to figs. 7.22-7.27, it can be seen that the resulting torque response follows a path which eliminates the final step produced by scheme B. The initial torque rise is similar to scheme B, but after the first second output torque follows much the same path as the base response. Good initial torque without loss of torque later in the transient is achieved by avoiding AFR limiting fuel reduction. This allows engine acceleration to match that of the base despite higher initial boost pressure.

This response has the advantages of:-

i) A rapid initial torque rise with no AFR limiting fuel reduction.
ii) No significant loss in torque later in the transient, as compared with the base
iii) A smooth and predictable torque rise, with no final step in torque at the end of the transient.

7.3.5 TRANSIENT CONTROL SCHEME D (fig 7.28)

If an engine speed governor is used a combined boost pressure loop is a possibility, that is one which controls both steady-state and transient boost. To control transient boost pressure in a similar way to scheme C, the boost demand must be adjusted as a function of engine speed error (the transient measure). Scheme D does this by subtracting a transient boost reduction from the optimum steady-state demand. The boost reduction is calculated to give an AFR reduction proportional to speed error. The boost demand is not allowed to fall below that which would give an AFR of 21, this should avoid unnecessary fuel reduction.

The combined boost pressure demand is fed to a boost control loop which satisfies both steady-state and transient requirements. For

optimum steady-state running actual boost must closely follow the demand. This is achieved by: either incorporating a P+I algorithm; or adding an optimum steady-state offset to nozzle angle (fig. 7.14). The latter has a similar effect to a P+I algorithm in the sense that the required nozzle angle is set at zero boost error. However, mechanical changes due to wear, soot etc. could result in error accumulation although this would be much less than with a simple nozzle scheduling system. The offset approach was adopted as this simplifies the changes to DCESIM and avoids the deterioration of loop dynamics associated with the P+I algorithm.

Whereas schemes A,B, and C use a single boost demand throughout the transient, this arrangement varies demand with speed error. As a result the gain (K2) between AFR reduction and speed error has a major effect on the action of the algorithm. A series of gains were tried to give an idea of the limitations on DCE transient response improvement. Three representative responses are shown in figs. 7.29-7.34.

The highest gain (K2=0.1) produces similar behaviour to scheme B, with a loss of mid-transient torque and a step to the final steady-state value after approx. 1.5 seconds. The ramp in torque up to 1.25 seconds corresponds to a constant boost demand which if followed exactly would give an AFR of 21. In fact AFR ramps from 20 to 22 as the boost error changes. The final torque rise after 1.25 seconds corresponds to boost demand increasing with reducing engine speed error.

An intermediate gain (K2=0.02) gives a response similar to scheme C, with no loss in mid-transient torque and the final torque rise matching that of the base. Again the initial ramp in torque corresponds to constant boost demand. After 0.55 seconds boost demand begins to increase with reducing speed error.

The lowest gain (K2=0.01) results in a similar response to scheme A, higher initial and mid-transient torque but a longer final rise time

than the base. In this case boost demand is increasing from the beginning of the transient.

To summarise these responses demonstrate that:-

i) Further improvements in initial and mid-transient torque, over scheme C (D with intermediate gain), are at the expense of a longer final rise time than the base.

ii) A more rapid final rise time is at the expense of mid-transient torque as in the case of scheme B (D with a high gain).

7.3.6 DISCUSSION

A dynamic computer model has been used in the design of transient control algorithms for the DCE. Four alternative control schemes have been simulated along with a base response representing a controller with no transient algorithm. Control algorithm performance was assessed by simulating a fuel step at stall (output speed = 500rpm).

The baseline response is the result of nozzle angle stepping to its final steady-state value in unison with the fuel step. There is no initial response to the change in fuelling, output torque only rises as the engine and compressor accelerate. This is due to AFR limiting fuel reduction, AFR was not allowed to drop below 20. This is not acceptable from a drivability point of view requiring considerable operator anticipation.

Scheme A (fig. 7.19) produced a high initial torque because of the generous steady-state boost demand used during the transient. However, this was at the expense of engine/compressor acceleration and results in lower torque later in the transient (a long final rise time). This highlights the way in which compressor torque is split between boost and acceleration, one is increased at the expense of the other.

It should be noted that boost rose almost instantaneously in response to nozzle movement. This demonstrates that volume dynamics are negligible, the DCE's dynamics being dominated by engine, compressor and gear inertias. Because of this there is no advantage to be gained from transient closure of the bypass valve. In fact such closure would reduce transient turbine pressure ratio and hence turbine torque.

Scheme B (fig. 7.20) uses a transient boost demand which holds AFR in the lower twenties until engine speed is within 50 rpm of its steady-state value. This produces an initial torque rise almost as good as scheme A's. Engine speed rises as rapidly as the base despite the higher initial boost. However mid-transient torque dips below the base because boost is then artificially low. The transient boost loop is switched out after 1.5 seconds and torque rises rapidly to its final steady-state value. This final step in torque would result in unpredictable operation in a vehicle.

Scheme C (fig. 7.21) attempts to overcome the disadvantages of scheme B by replacing the switch with a variable boost loop gain. The gain is proportional to the engine speed error so that it gradually reduces, reaching zero at steady-state. This eliminates both the loss in mid-transient torque and the final torque step.

Scheme D (fig. 7.28) was tried to provide an alternative to scheme C when an engine speed governor is used. In this case boost demand increases with reducing engine speed error, reaching its steady-state value at zero error. Depending on the gain K2 this algorithm has a similar action to each of the previous three schemes. The optimum gain resulted in a similar transient performance to scheme C.

Schemes C and D both satisfy the requirement of an improved initial torque rise without loss of torque later in the transient. Both do this by avoiding AFR (smoke) limiting fuel reduction. However, scheme D can be incorporated with a steady-state boost scheduling system.

This reduces, or with P+I compensation totally eliminates, the long term error accumulation associated with nozzle angle scheduling.

Whichever control scheme is chosen the optimum controller gains will depend on the particular operating conditions. For example, at rated speed the turbine's contribution to output torque is a far smaller percentage than at stall. This means that a higher initial boost could be worthwhile as the turbine torque penalty later in the transient may be small.

Ideally an adaptive system would be required which schedules gains as well as steady-state set-points. Future work may include the comprehensive optimisation of controller gains for all operating conditions. Hopefully gains will only need changing with one parameter, probably output speed.

Similar theoretical studies should be undertaken on the DCE's deceleration characteristics (DCE braking). Control scheme D would increase boost during deceleration thus increasing DCE braking considerably. A maximum limit on boost demand would be necessary to avoid over-pressurising the system.

It would also be a relatively simple matter to add a vehicle/road model to the program. Vehicle acceleration and deceleration characteristics could then be investigated, providing further information about drivability.

The new program (DCESIM) has proved to be a useful control algorithm development tool. Being a simple model it runs quickly and is easy to modify and debug. This means that many different algorithms can be tried with the minimum of effort and time expended. The form of response is represented reasonably accurately because the major non-linear and dynamic characteristics of the DCE are modelled. This means that comparitive studies will be valid, and the relative performance of the algorithms tested should be repeatable experimentally. Although accurate thermodynamic data is not provided,

transient response could be modelled very accurately if experimentally obtained maps were used for the individual components (ie. engine, compressor, and turbine).

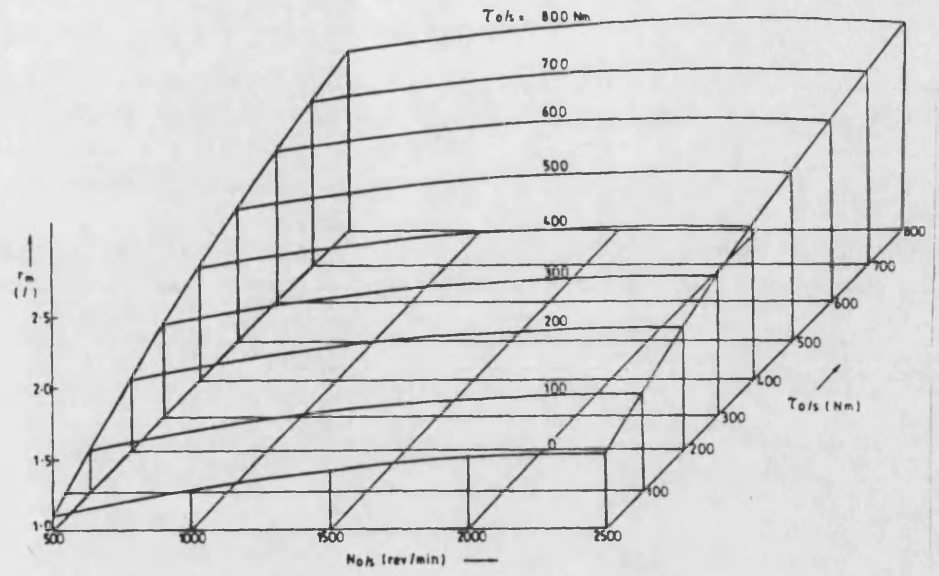

a) boost pressure map

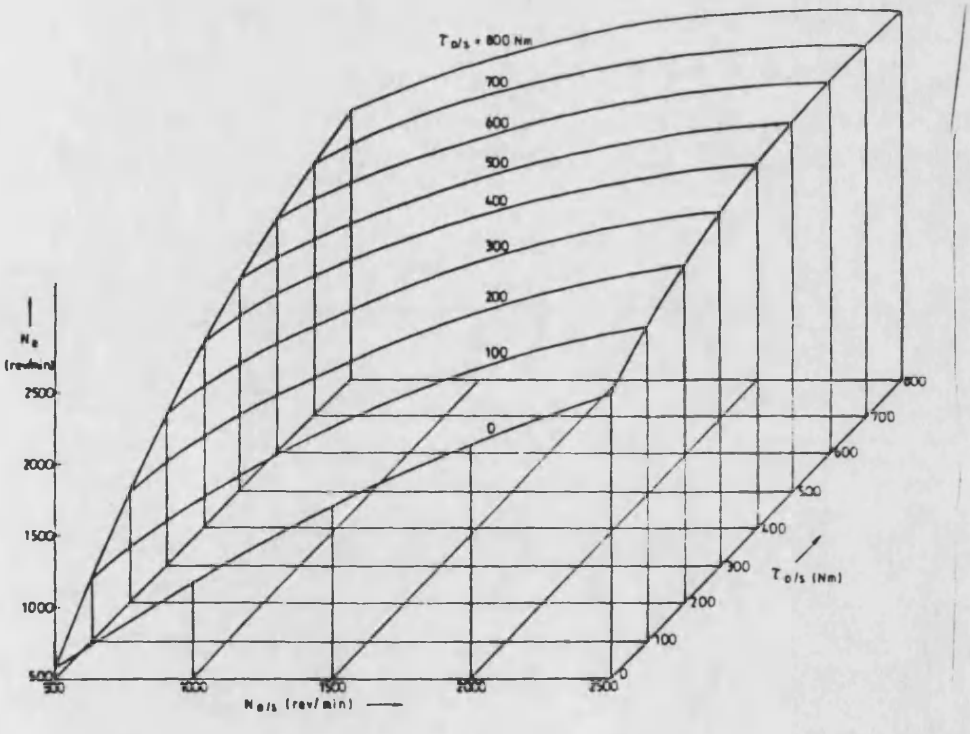

b) engine speed map

FIG 7.1 OPTIMUM CONTROL SURFACES

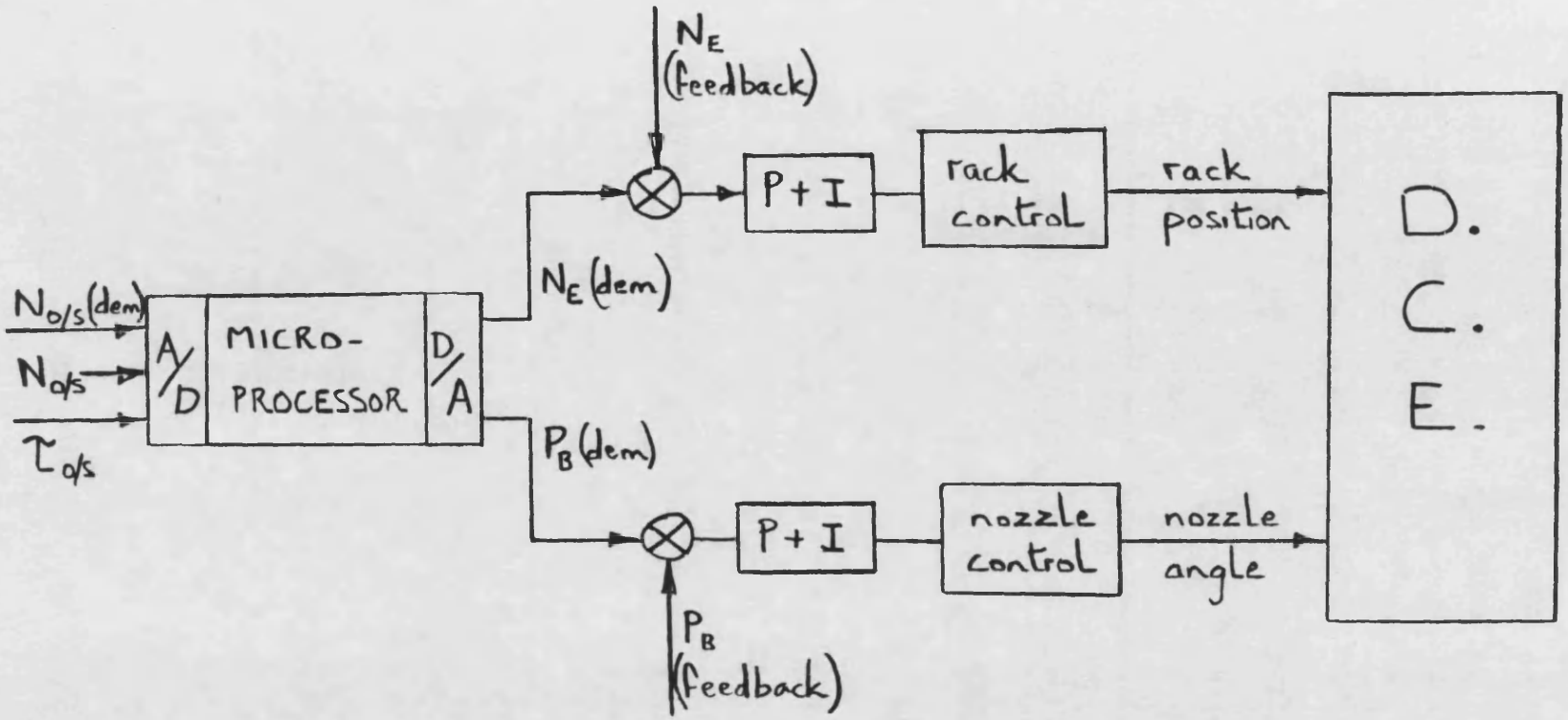

FIG. 7.2 ORIGINAL CONTROL SCHEME PROPOSAL

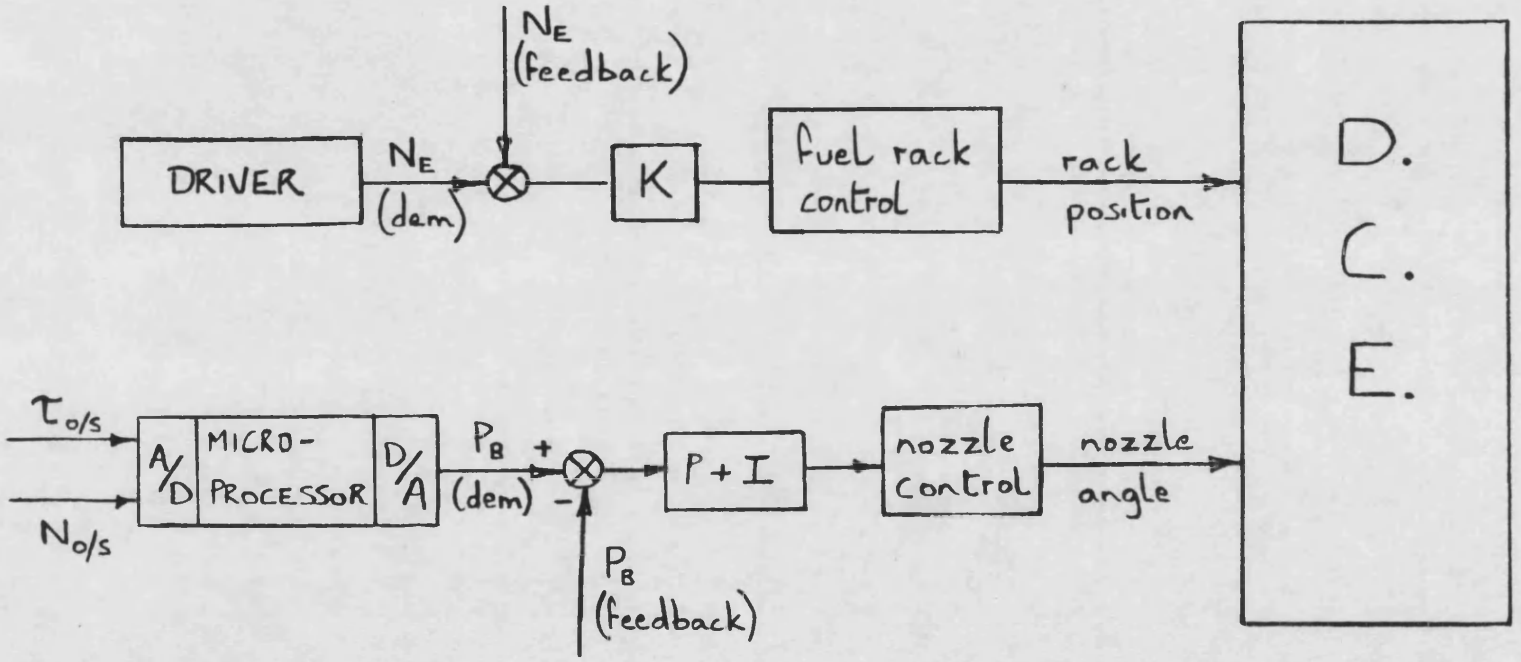

FIG. 7.3 SIMPLIFIED CONTROL SCHEME

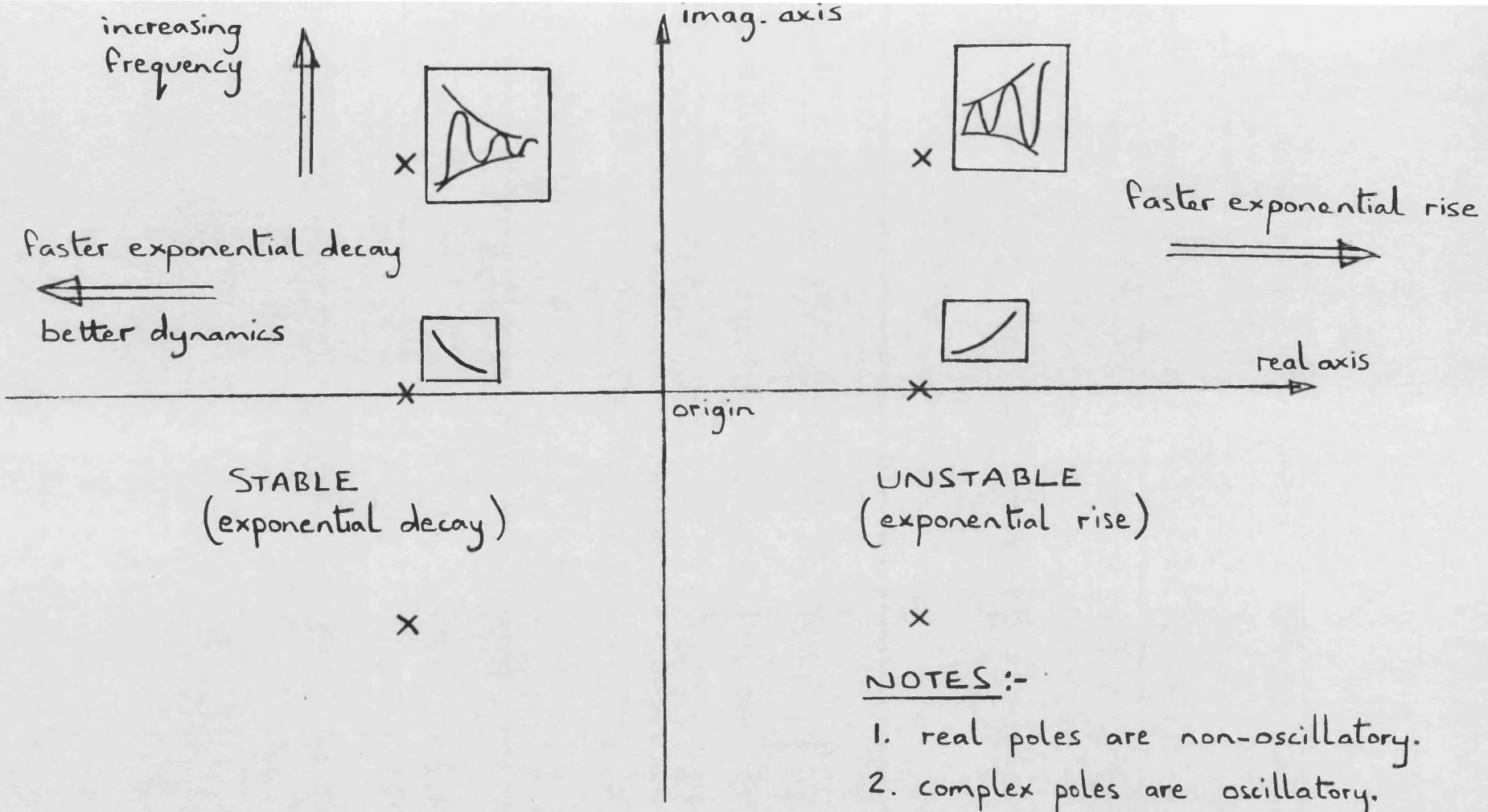

FIG. 7.4 ROOT-LOCUS INTERPRETATION

NOTES:-

1. real poles are non-oscillatory.
2. complex poles are oscillatory.
3. x marks the position of closed loop poles on this diagram. Normally x marks open loop poles.
4. complex poles come in conjugate pairs.

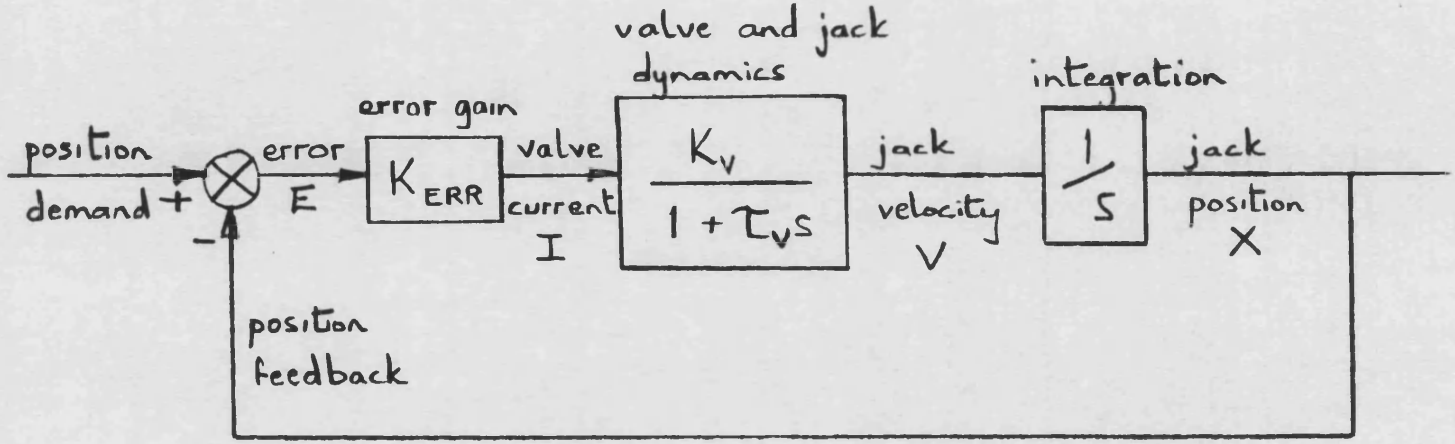

FIG. 7.5 POSITION LOOP DYNAMICS

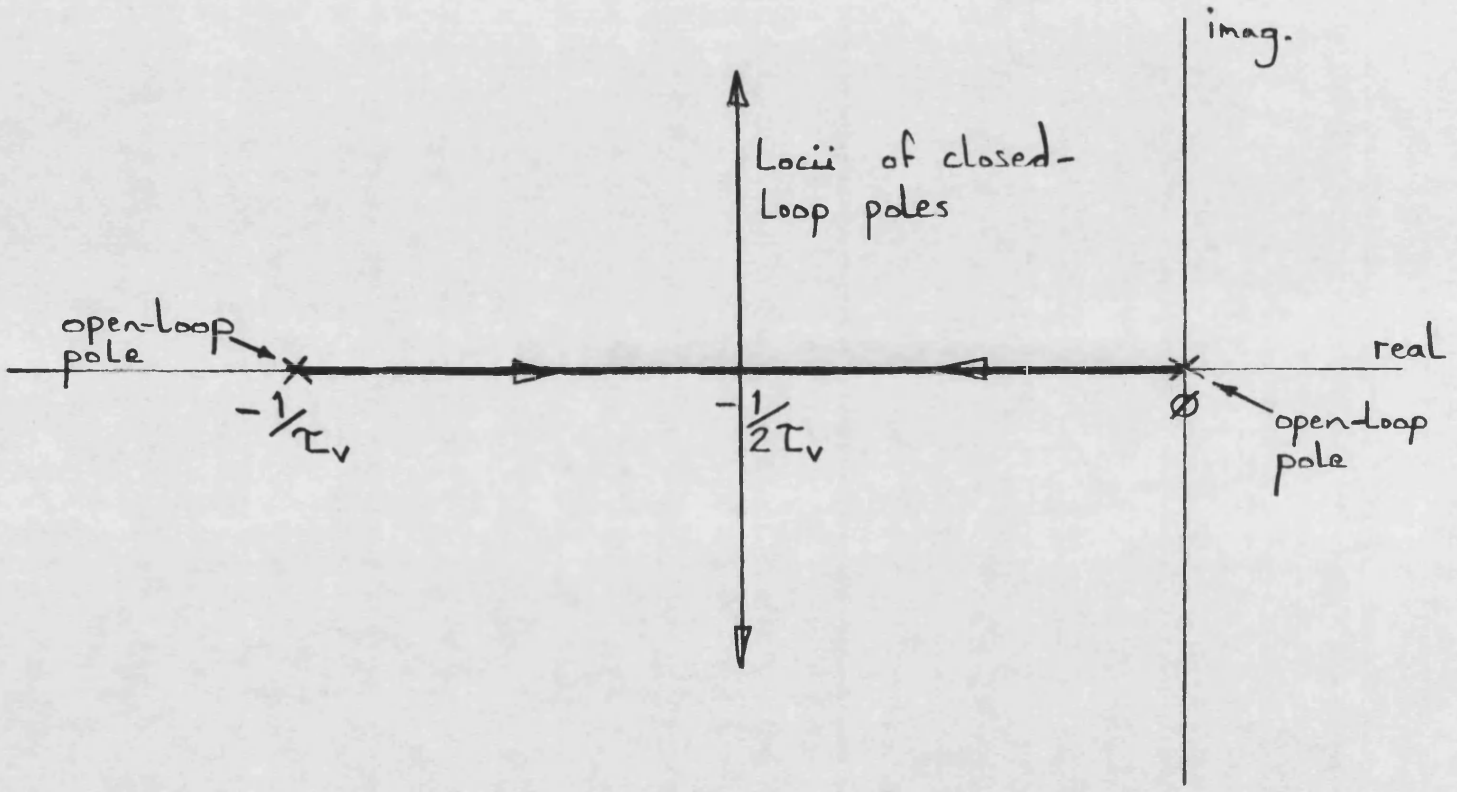

FIG. 7.6 ROOT-LOCUS PLOT FOR POSITION FEEDBACK LOOP DYNAMICS

FIG. 7.7 GAS DYNAMICS OF DCE

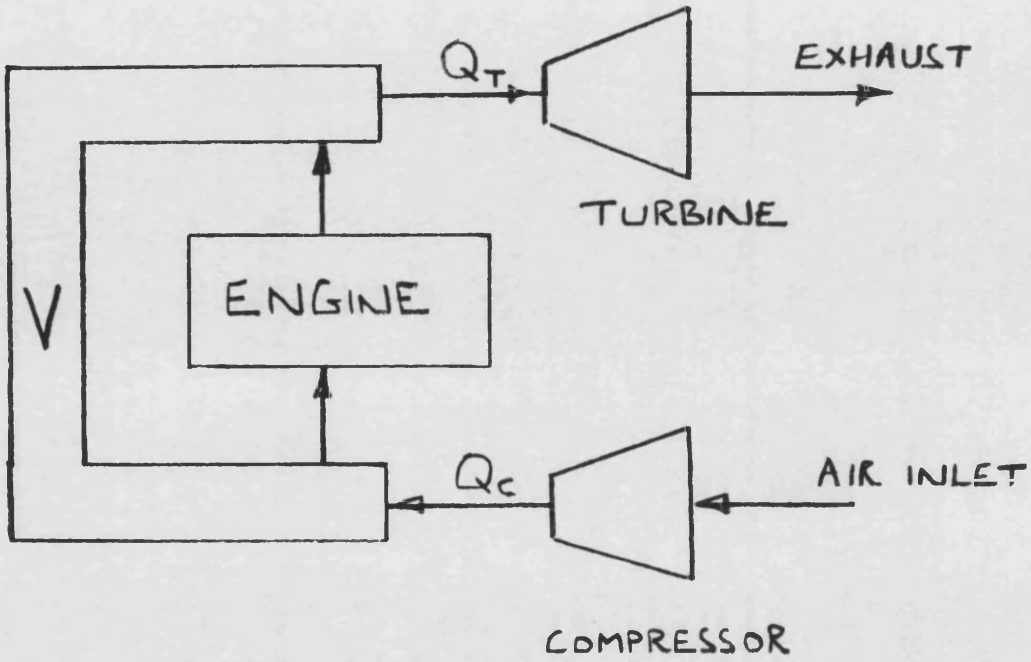

V = COMBINED VOLUME OF MANIFOLDS, INTERCOOLER, BYPASS, AND OTHER INTERCONNECTING PIPE-WORK

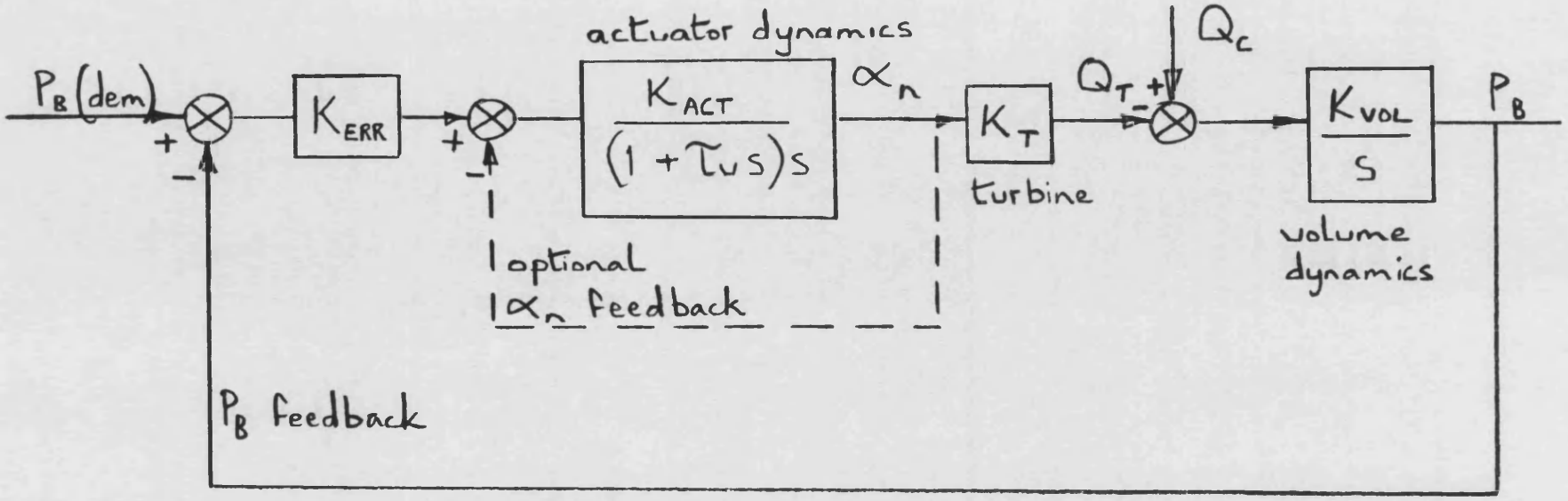

FIG. 7.8 Boost pressure feedback with optional nozzle position feedback

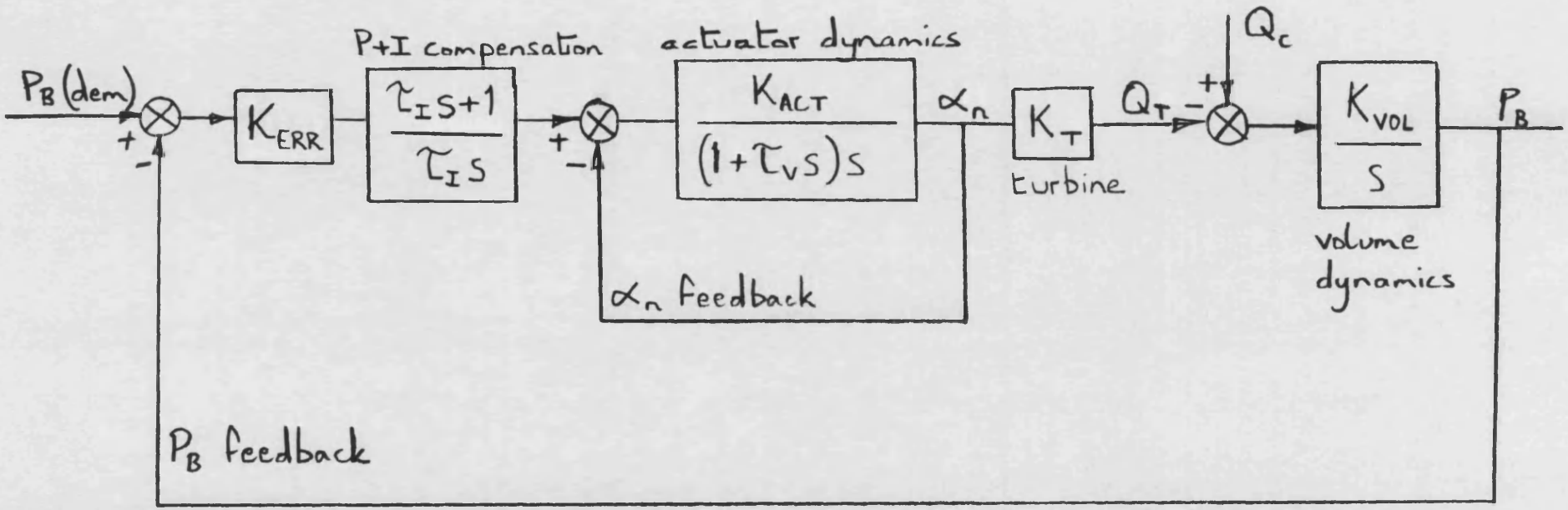

FIG. 7.9 Boost pressure feedback with P+I compensation and nozzle position feedback

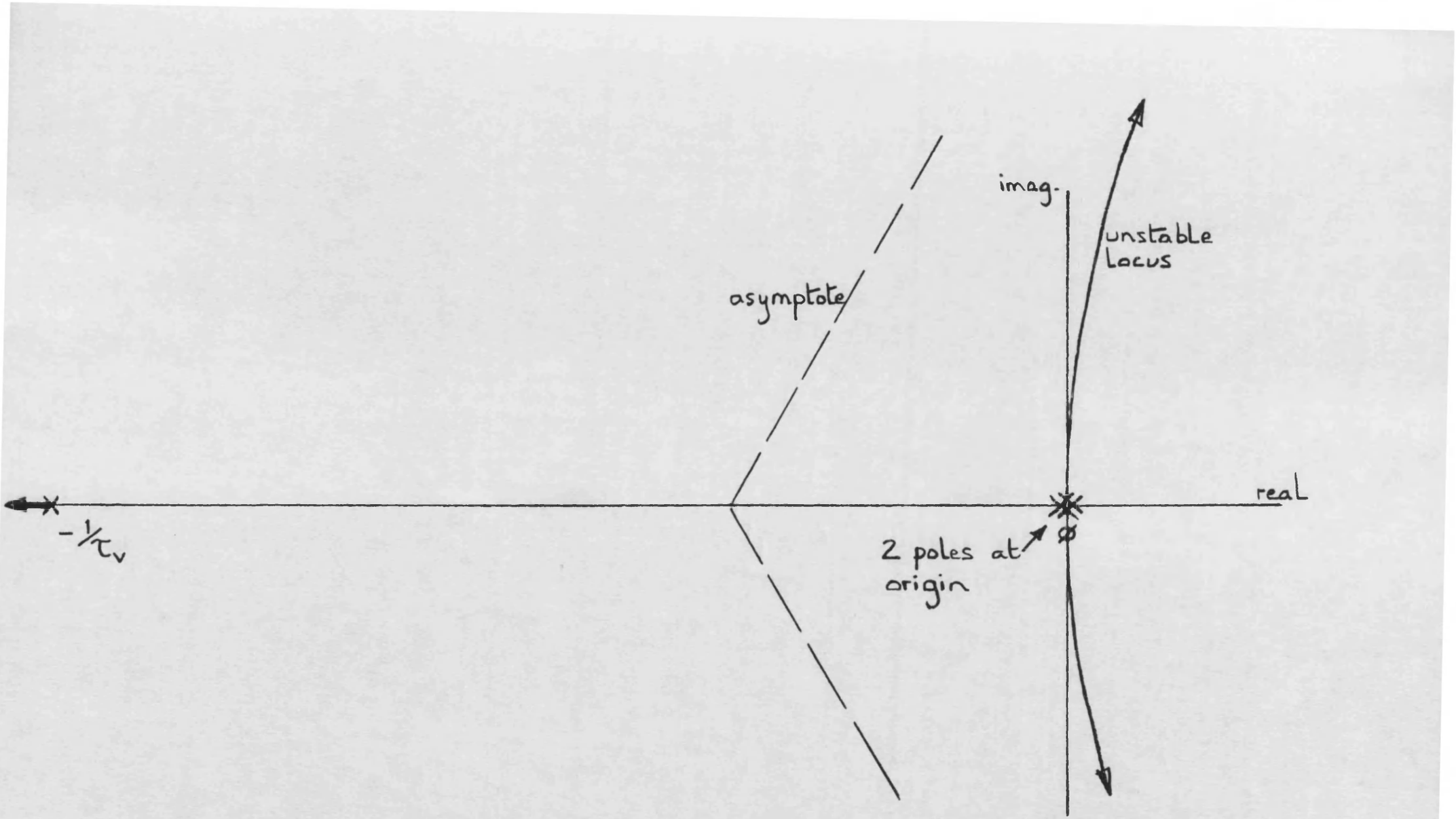

FIG. 7.10 PROPORTIONAL BOOST CONTROL WITHOUT AN INNER POSITION LOOP

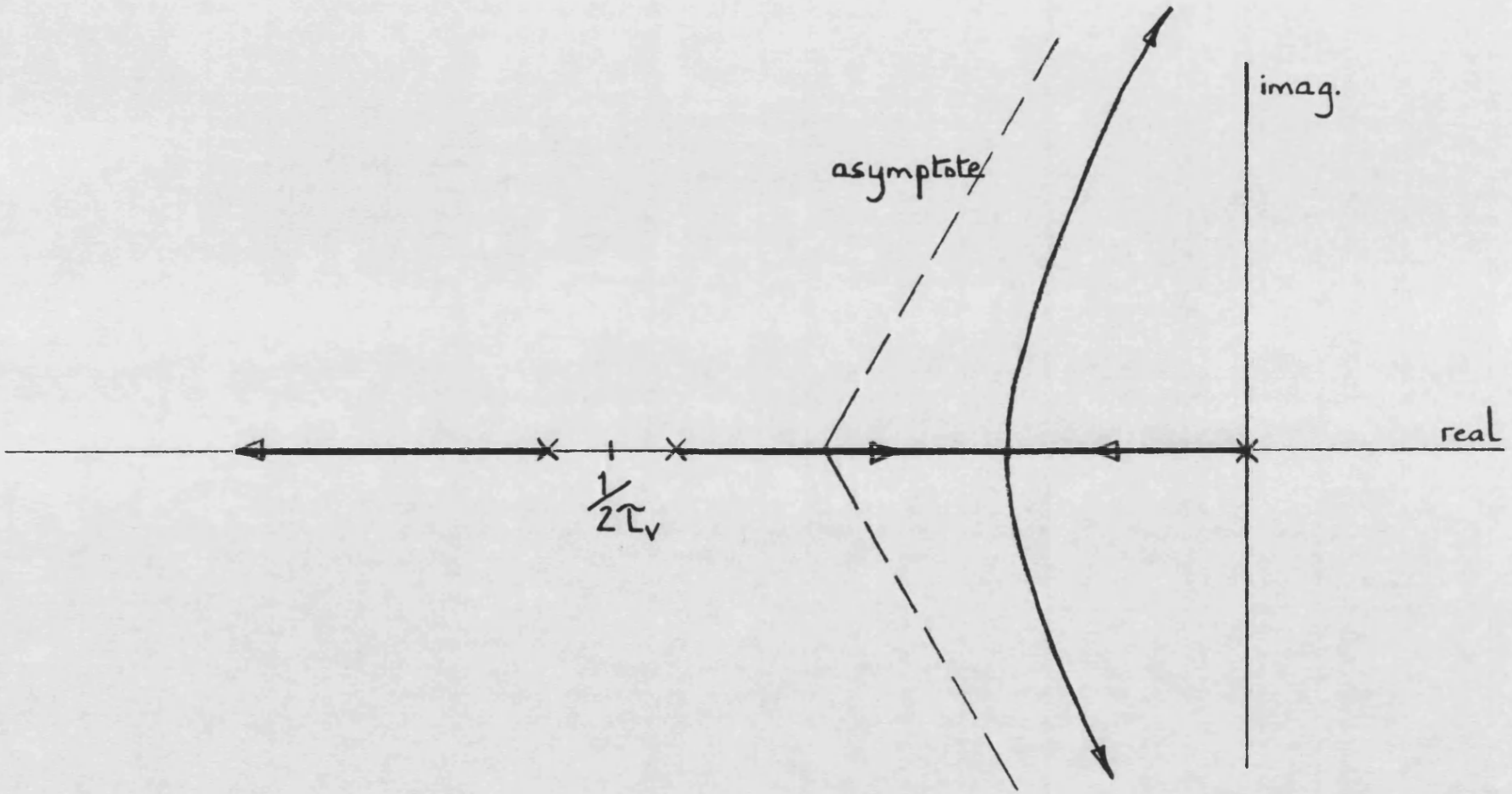

FIG. 7.11 PROPORTIONAL BOOST CONTROL WITH AN INNER POSITION LOOP

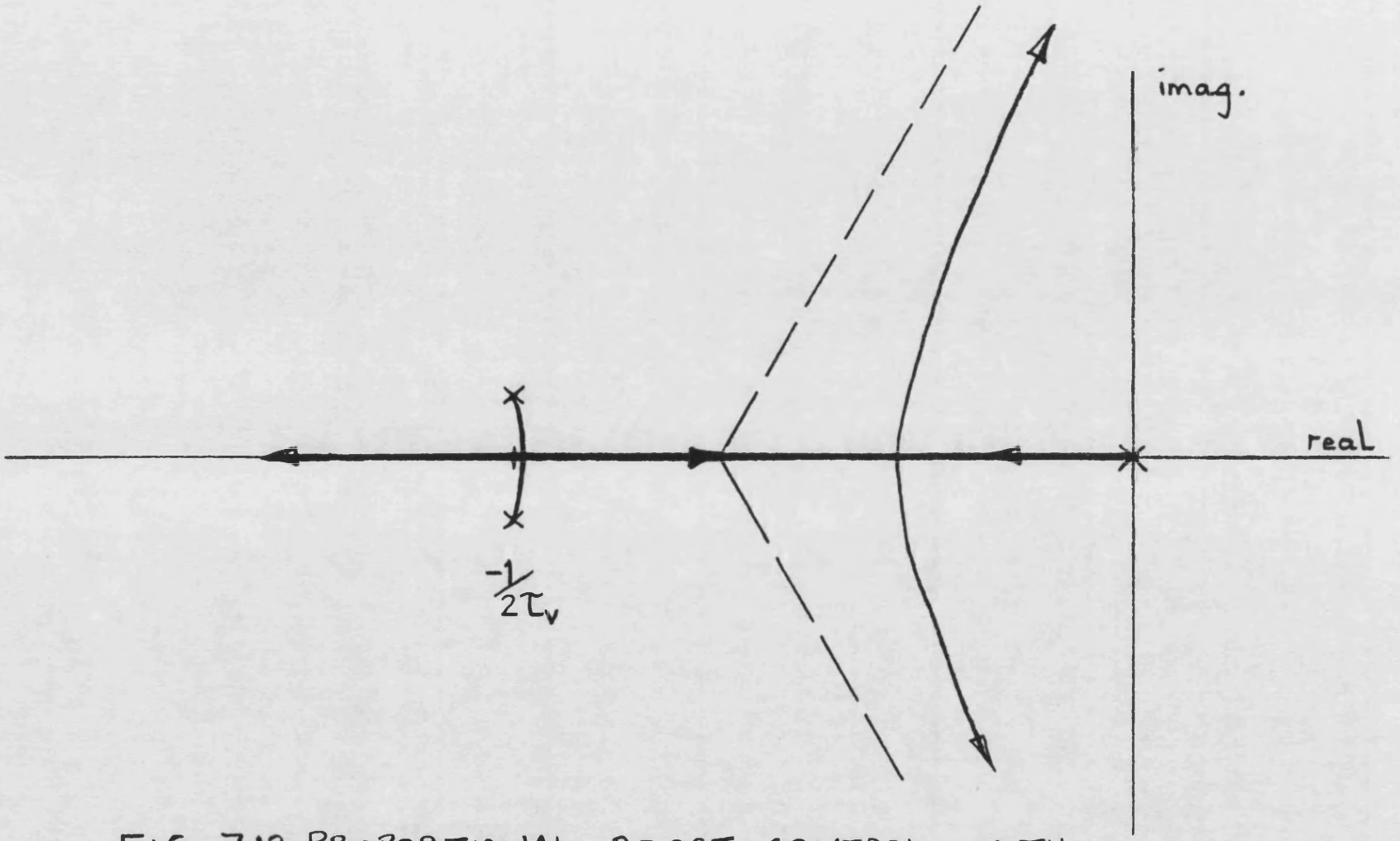

FIG. 7.12 PROPORTIONAL BOOST CONTROL WITH UNDER-DAMPED INNER LOOP

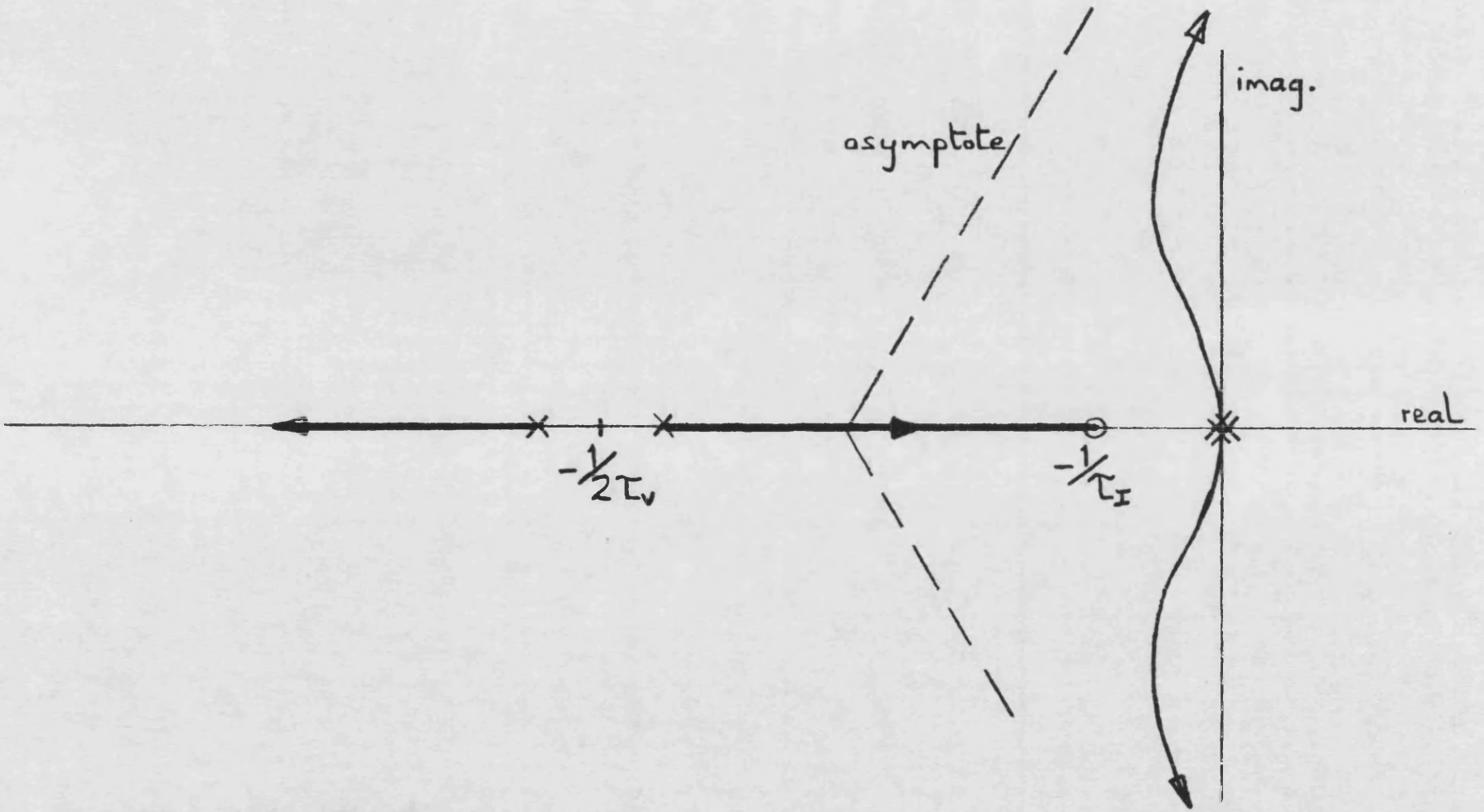

FIG. 7.13 P+I BOOST CONTROL WITH AN INNER POSITION LOOP

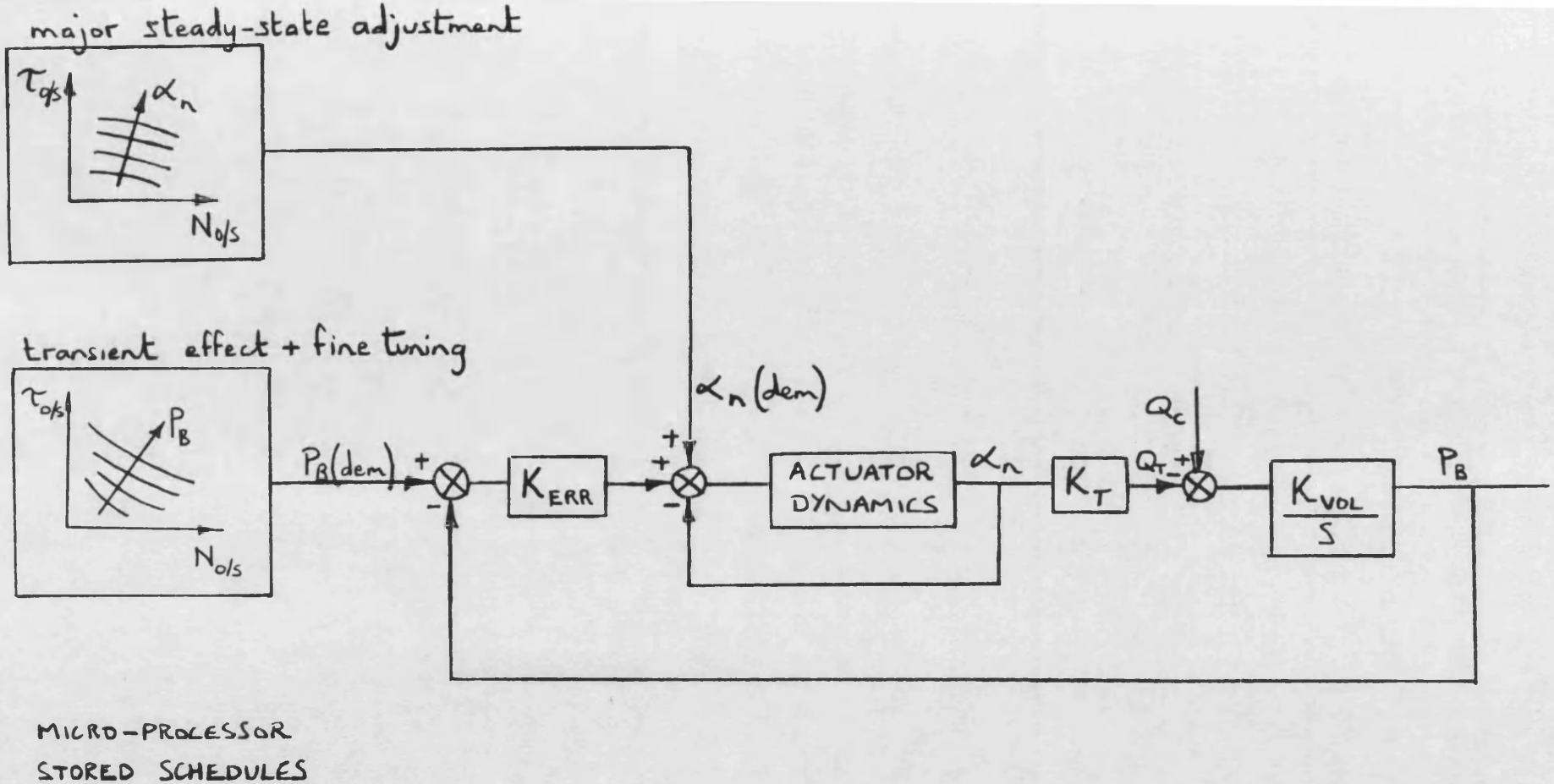

FIG. 7.14 Using a nozzle angle offset in preference to P+I compensation in the boost feedback loop

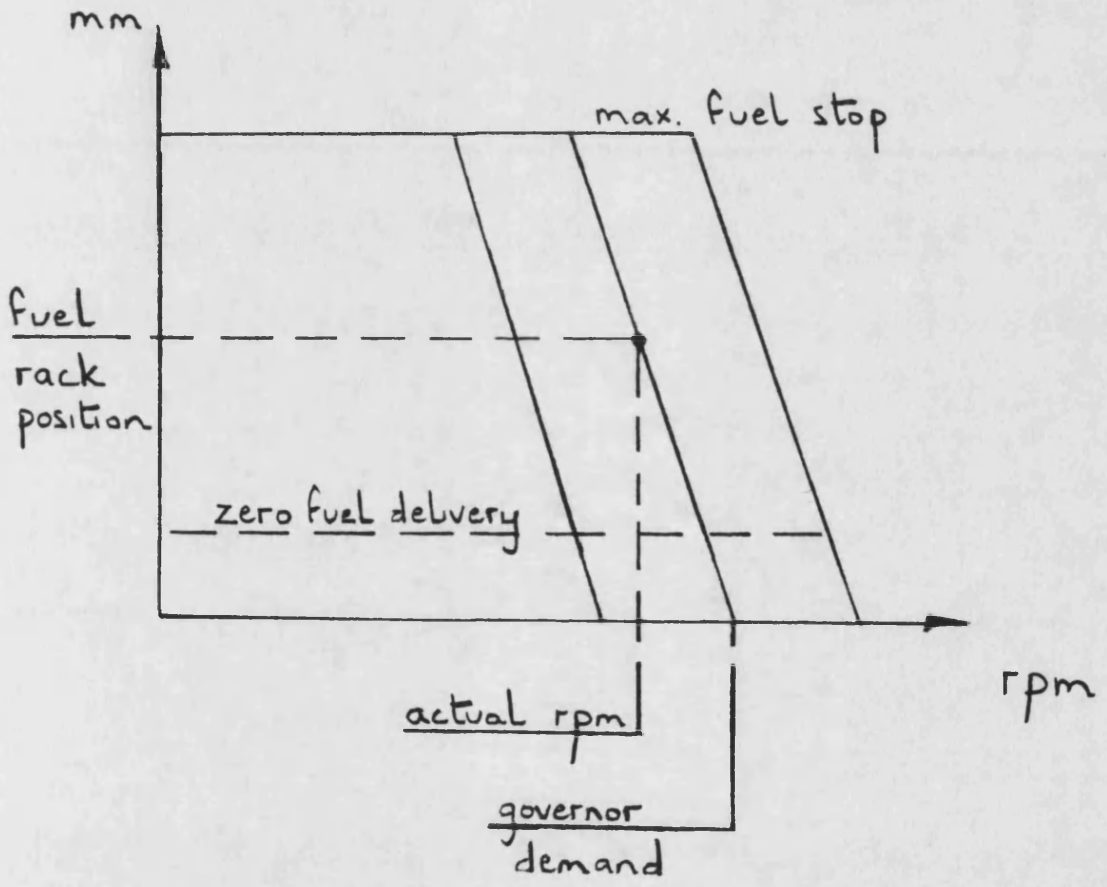

FIG. 7.15 MECHANICAL GOVERNOR CHARACTERISTIC

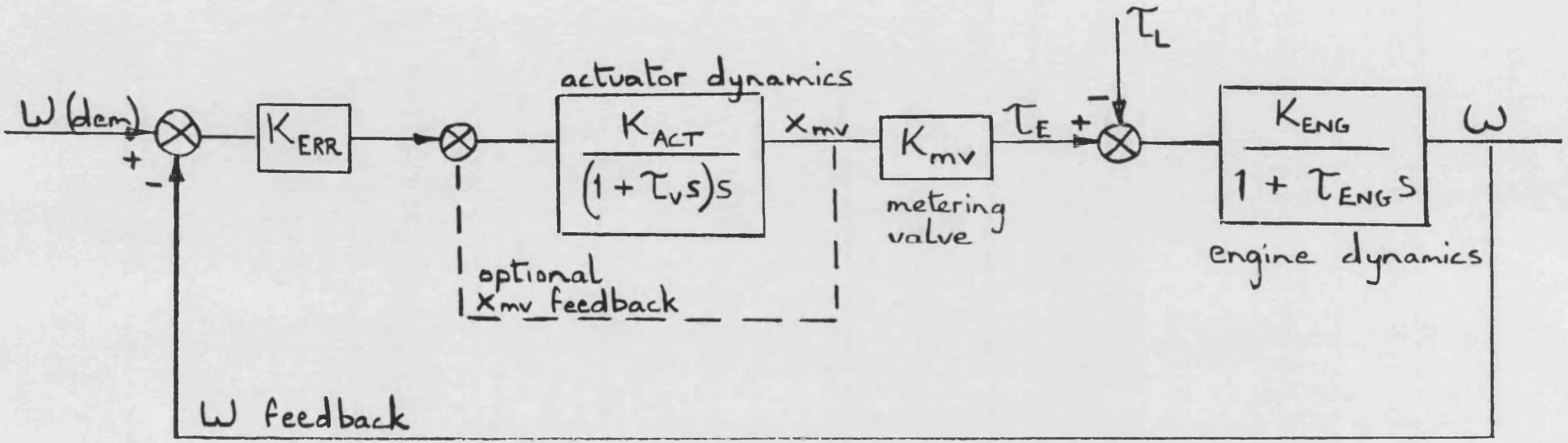

FIG. 7.16 SPEED CONTROL DYNAMICS

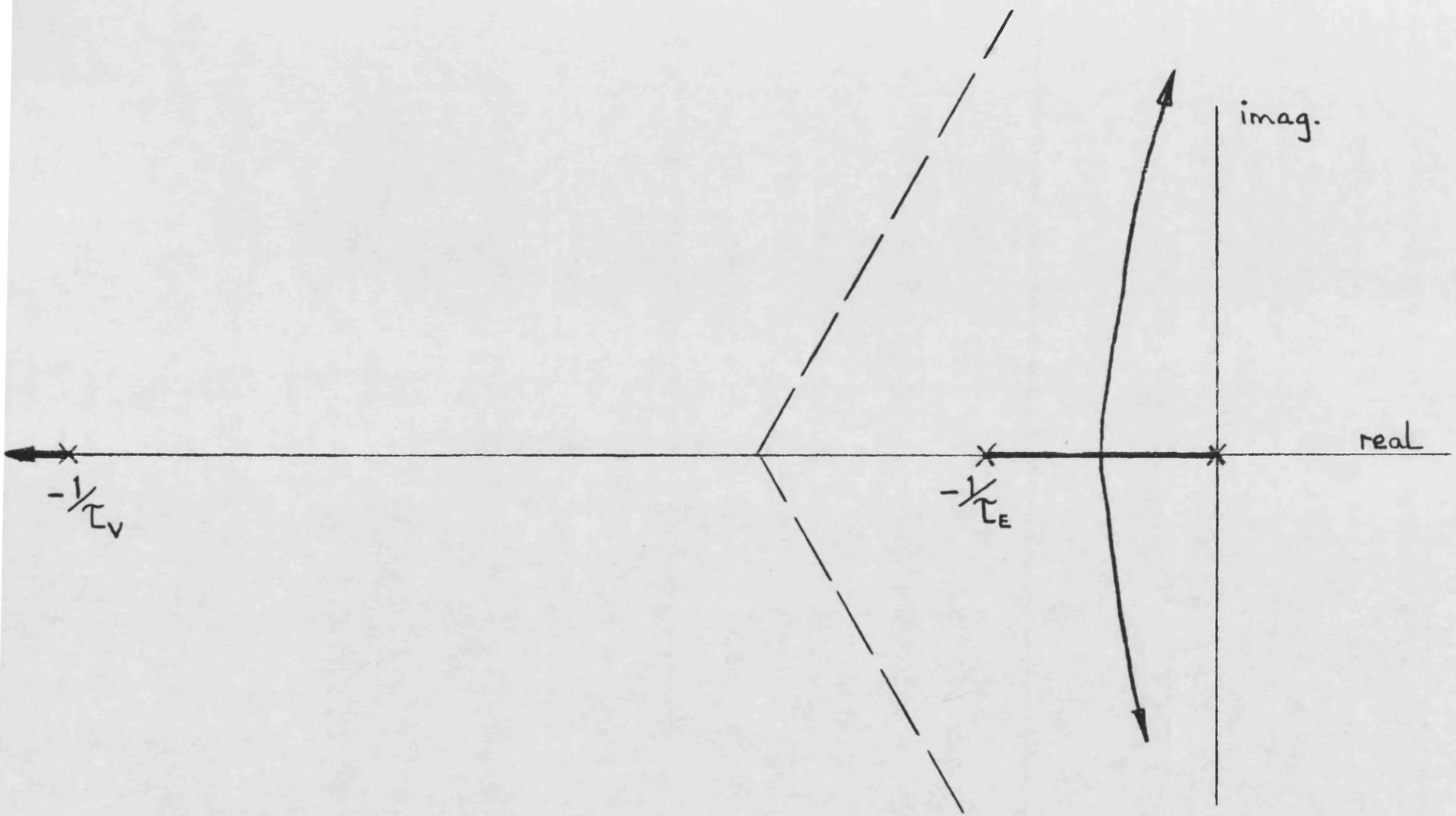

FIG. 7.17 ENGINE SPEED CONTROL WITHOUT AN INNER POSITION LOOP

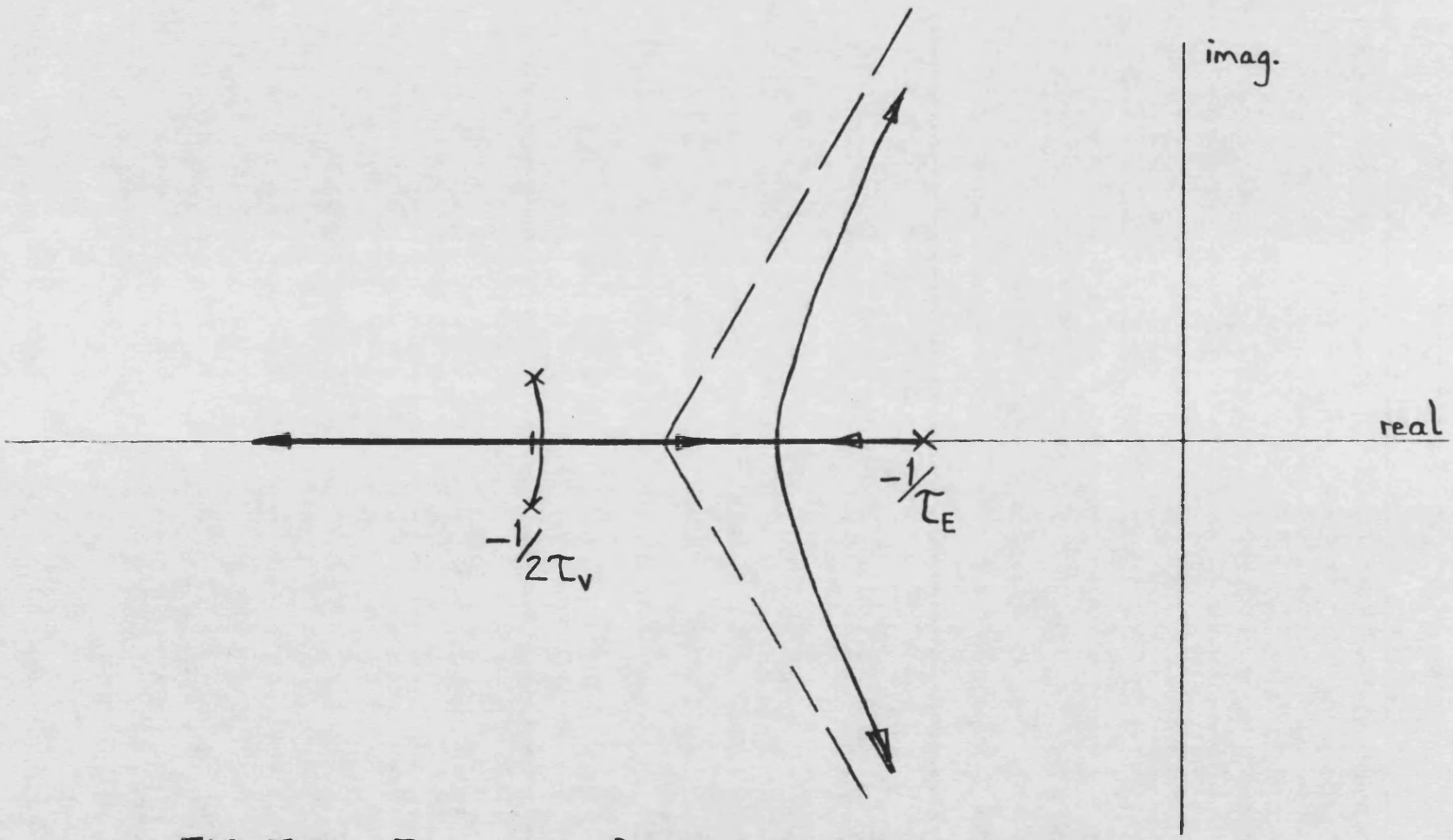

FIG. 7.18 ENGINE SPEED CONTROL WITH AN INNER POSITION LOOP

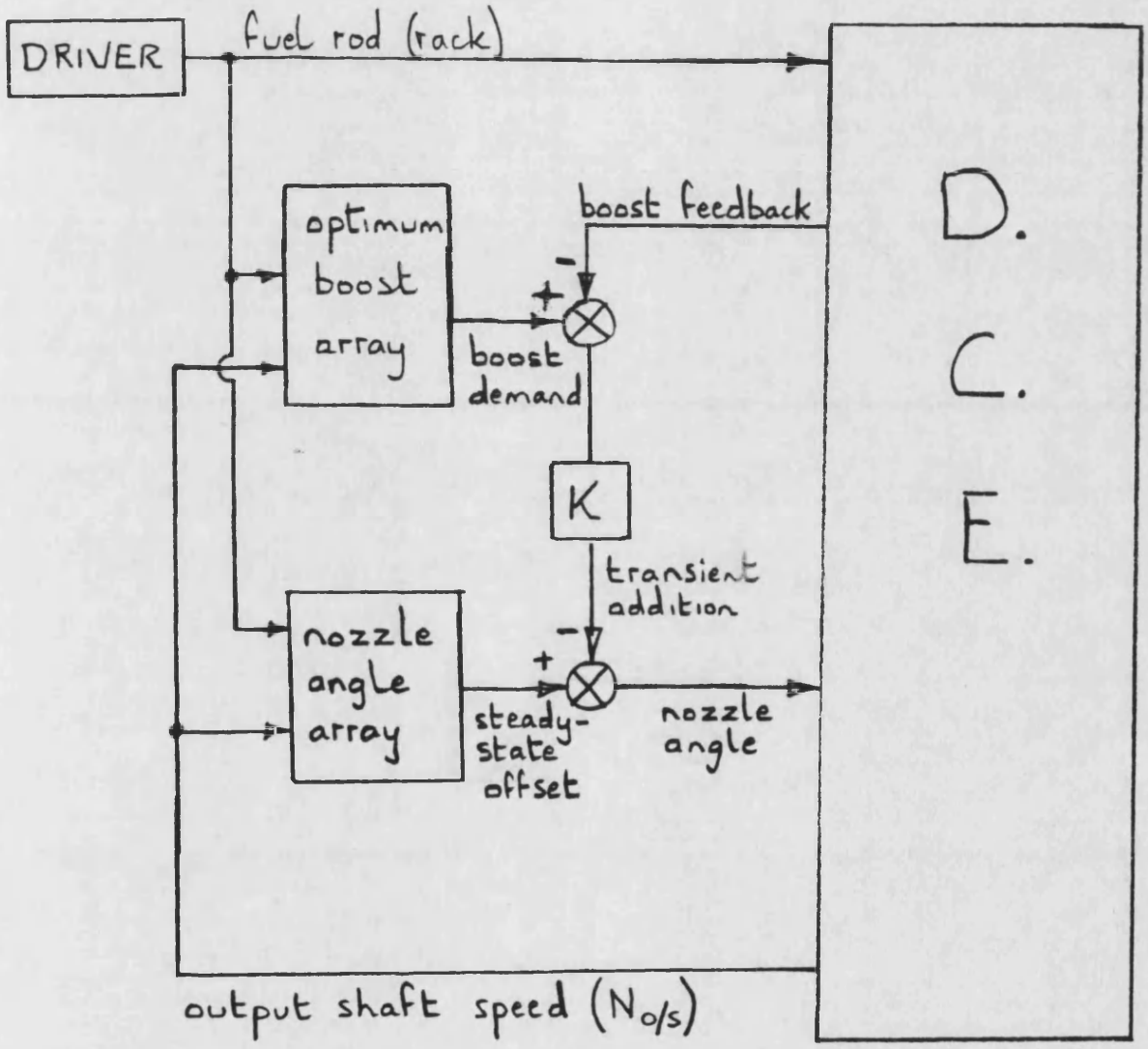

FIG. 7.19 CONTROL SCHEME A

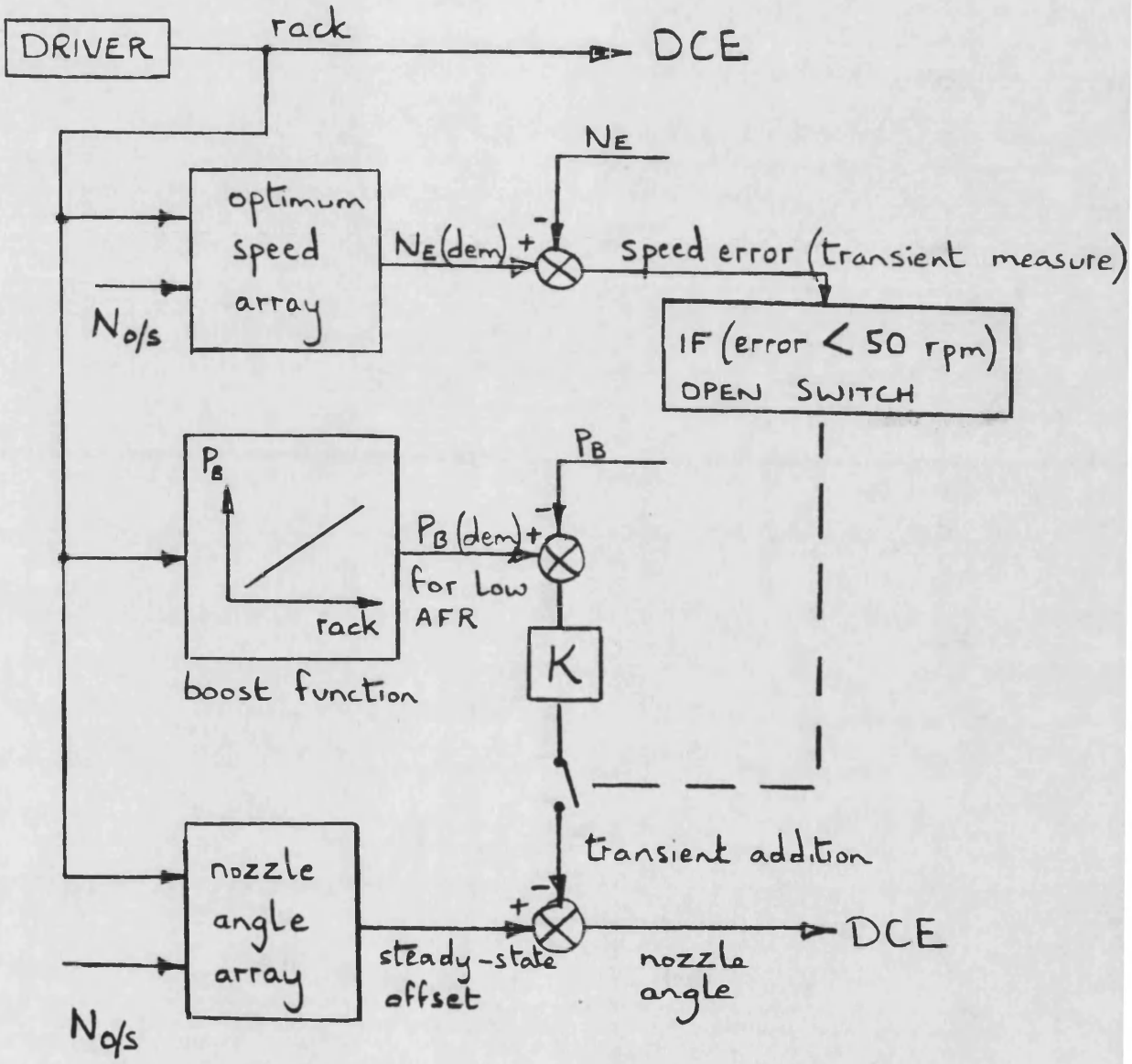

FIG. 7.20 CONTROL SCHEME B

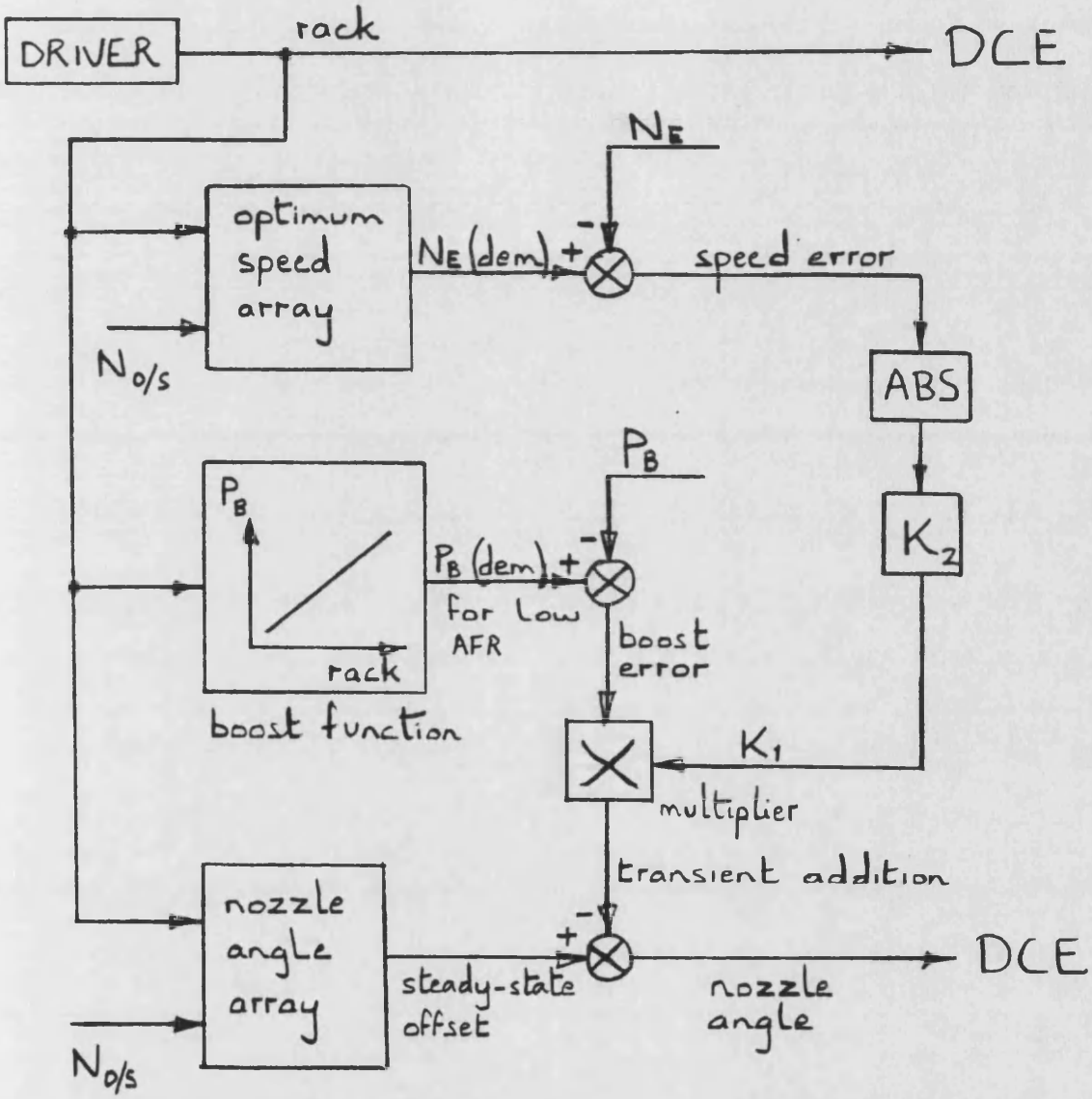

FIG. 7.21 CONTROL SCHEME C

FIG. 7.22 FUEL PER REV. VS. TIME SCHEMES A, B AND C

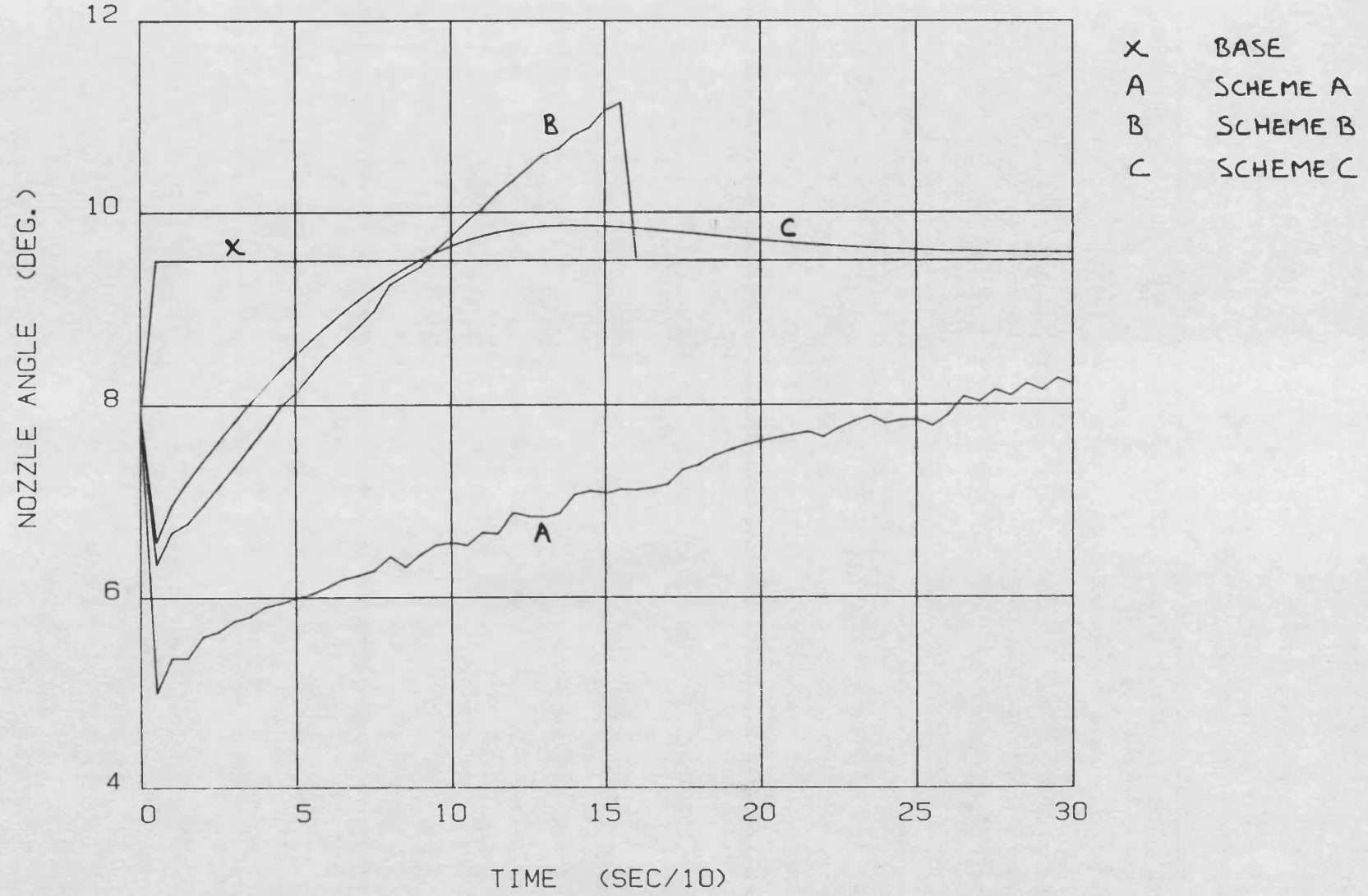

FIG. 7.23 NOZZLE ANGLE VS. TIME SCHEMES A, B AND C

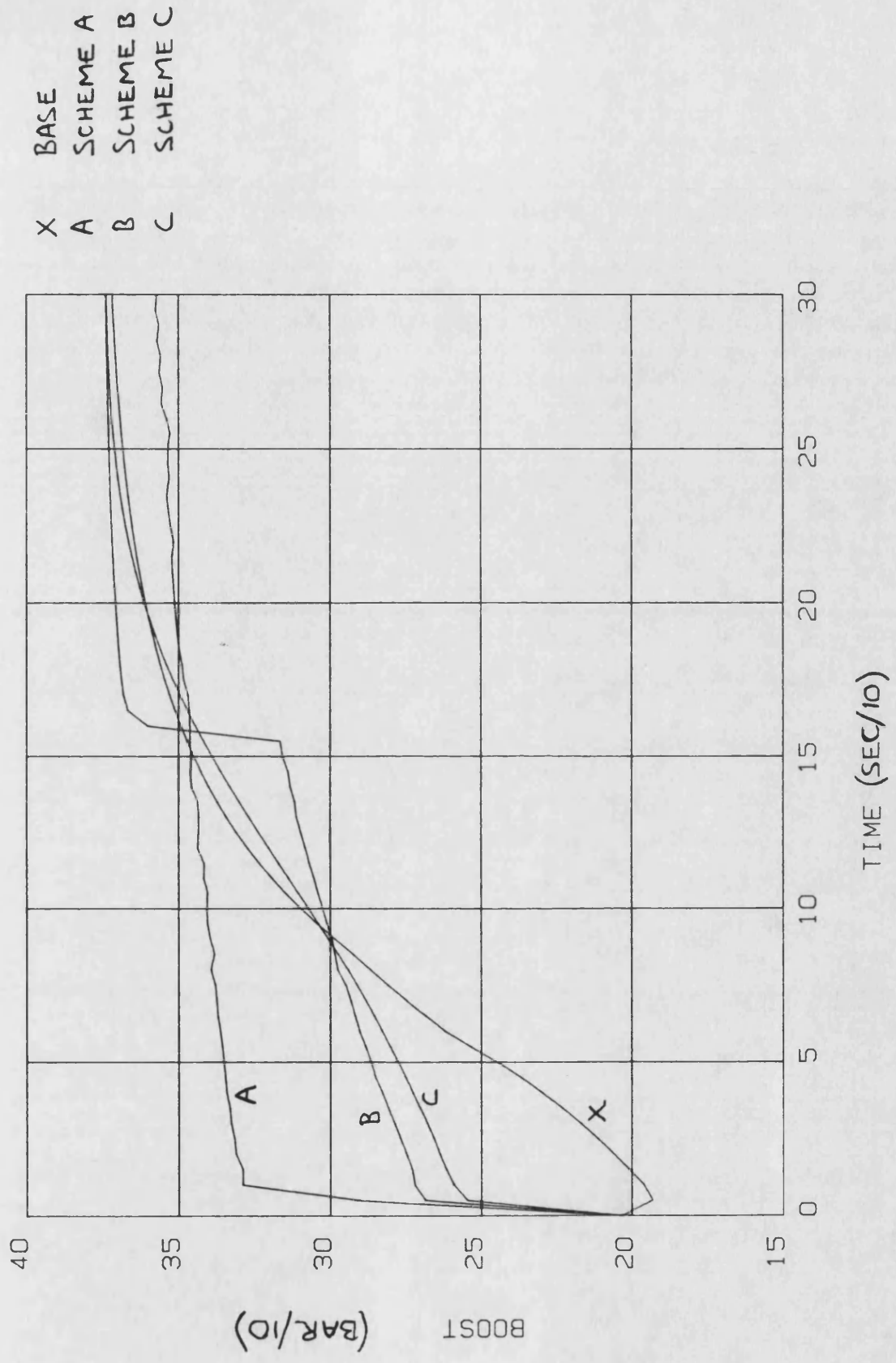

FIG. 7.24 BOOST PRESSURE VS. TIME. SCHEMES A, B AND C

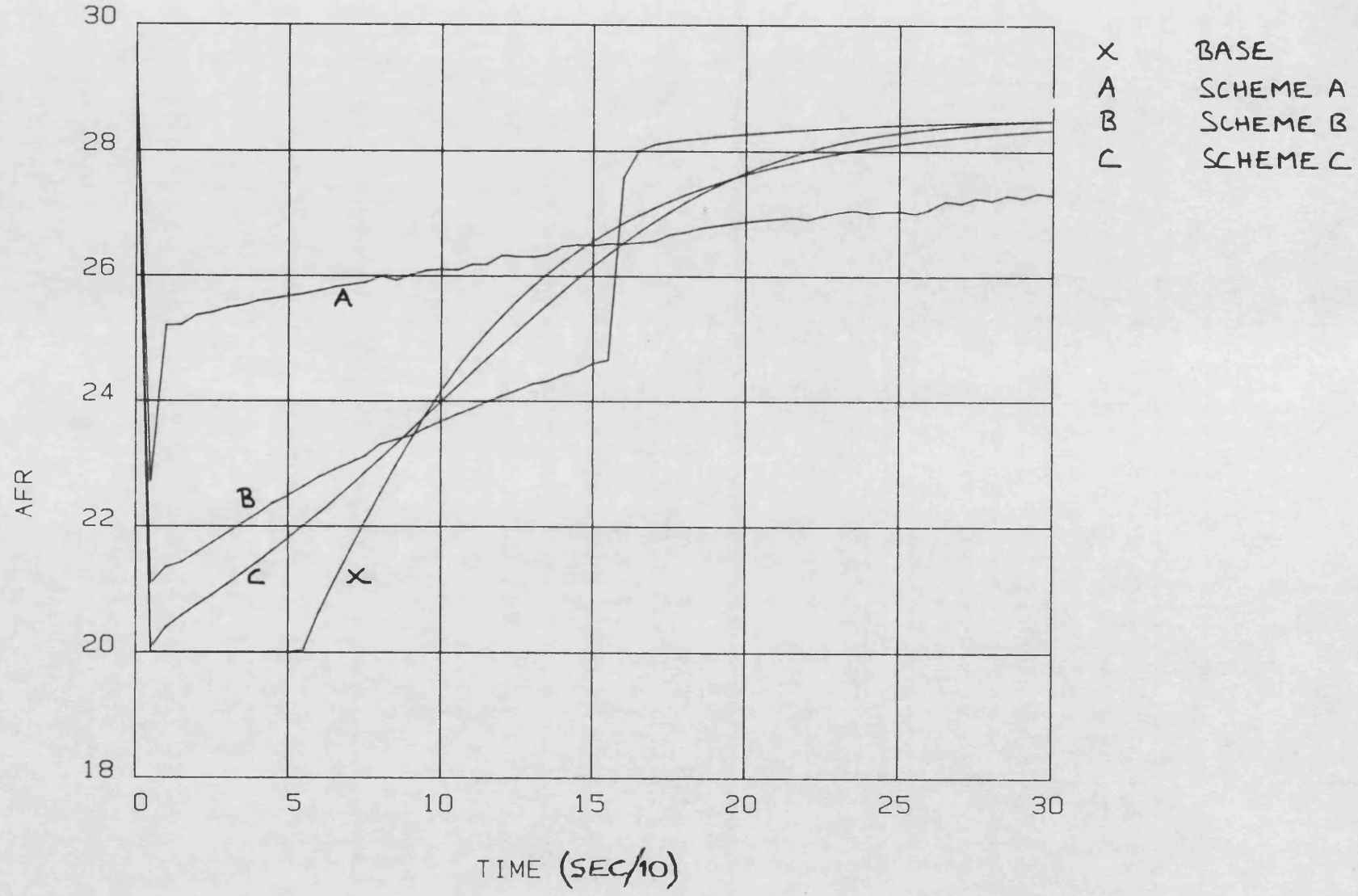

FIG. 7.25 AIR-FUEL RATIO VS. TIME SCHEMES A, B AND C

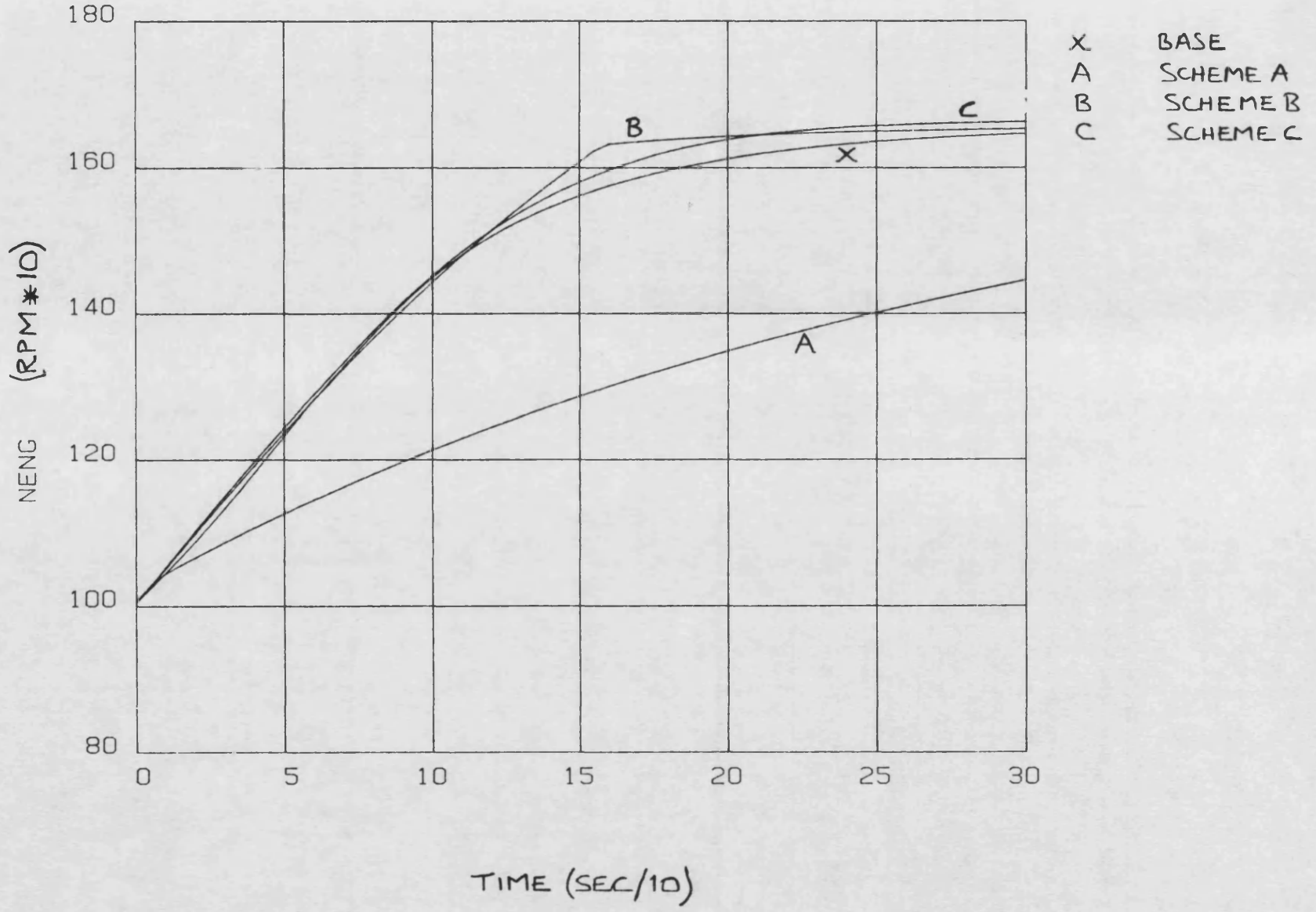

FIG. 7.26 ENGINE SPEED VS. TIME
SCHEMES A, B AND C

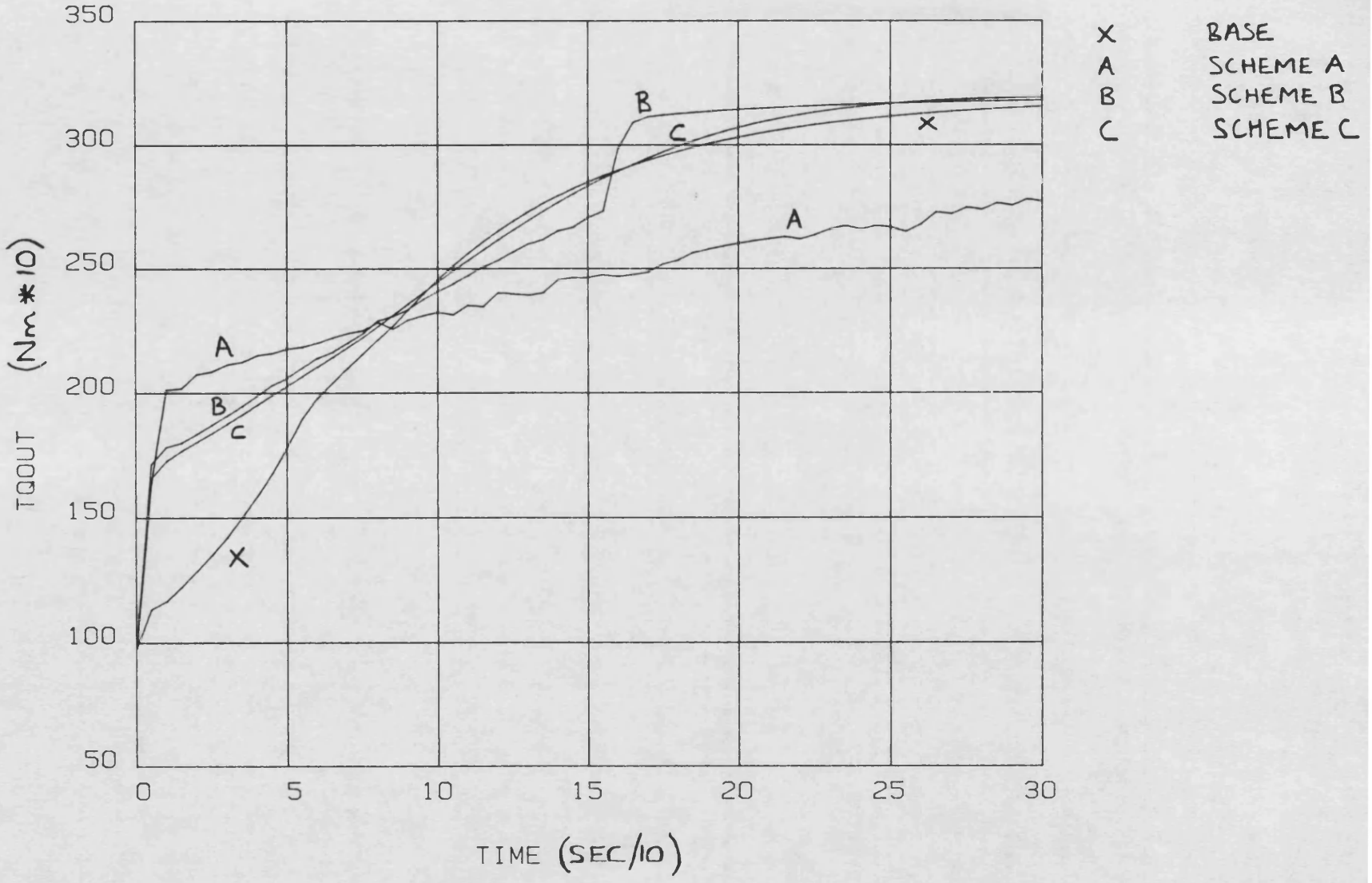

FIG. 7.27 OUTPUT TORQUE VS. TIME SCHEMES A, B AND C

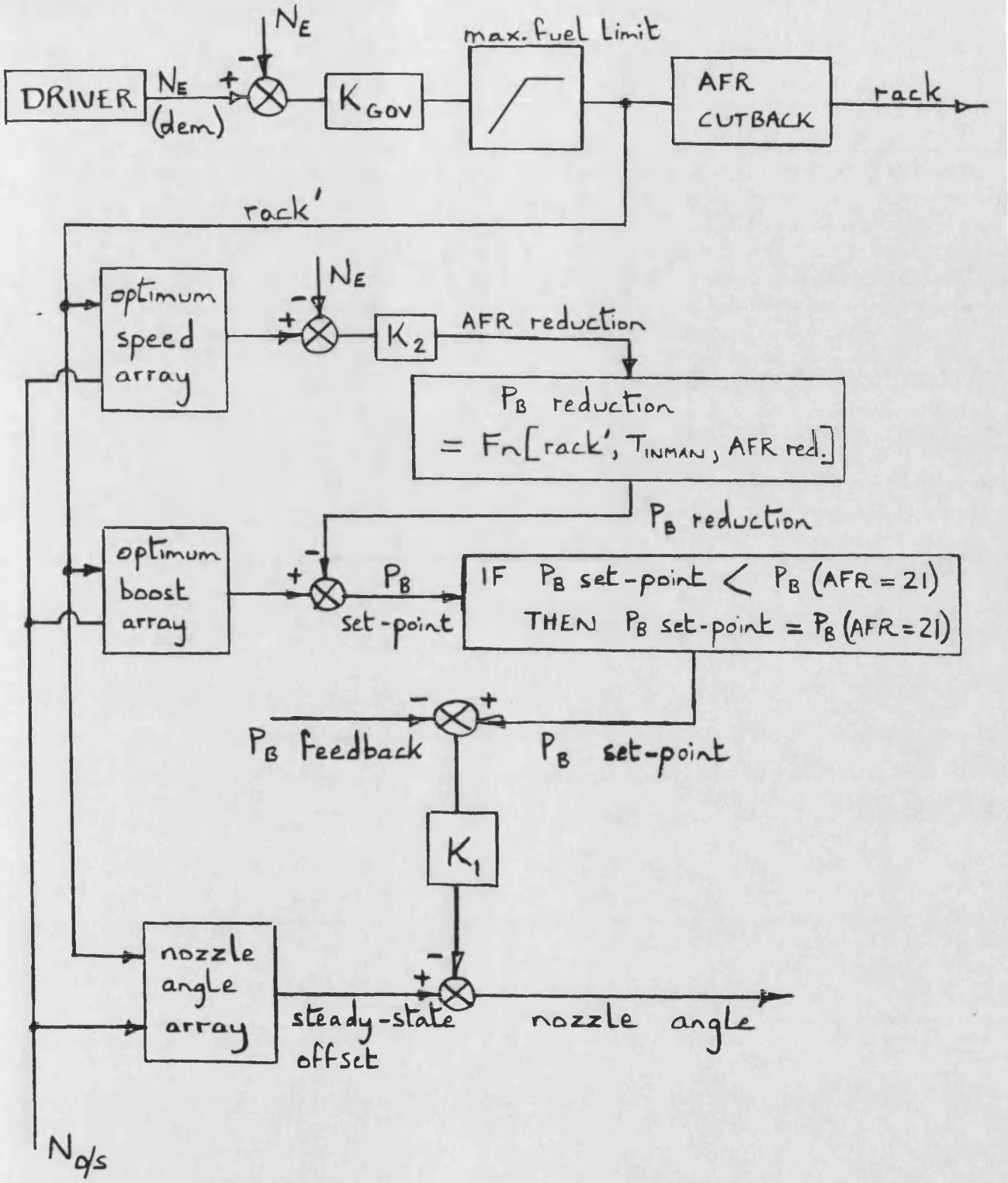

FIG. 7.28 CONTROL SCHEME D

FIG. 7.29 FUEL PER REVOLUTION VS. TIME
SCHEME D

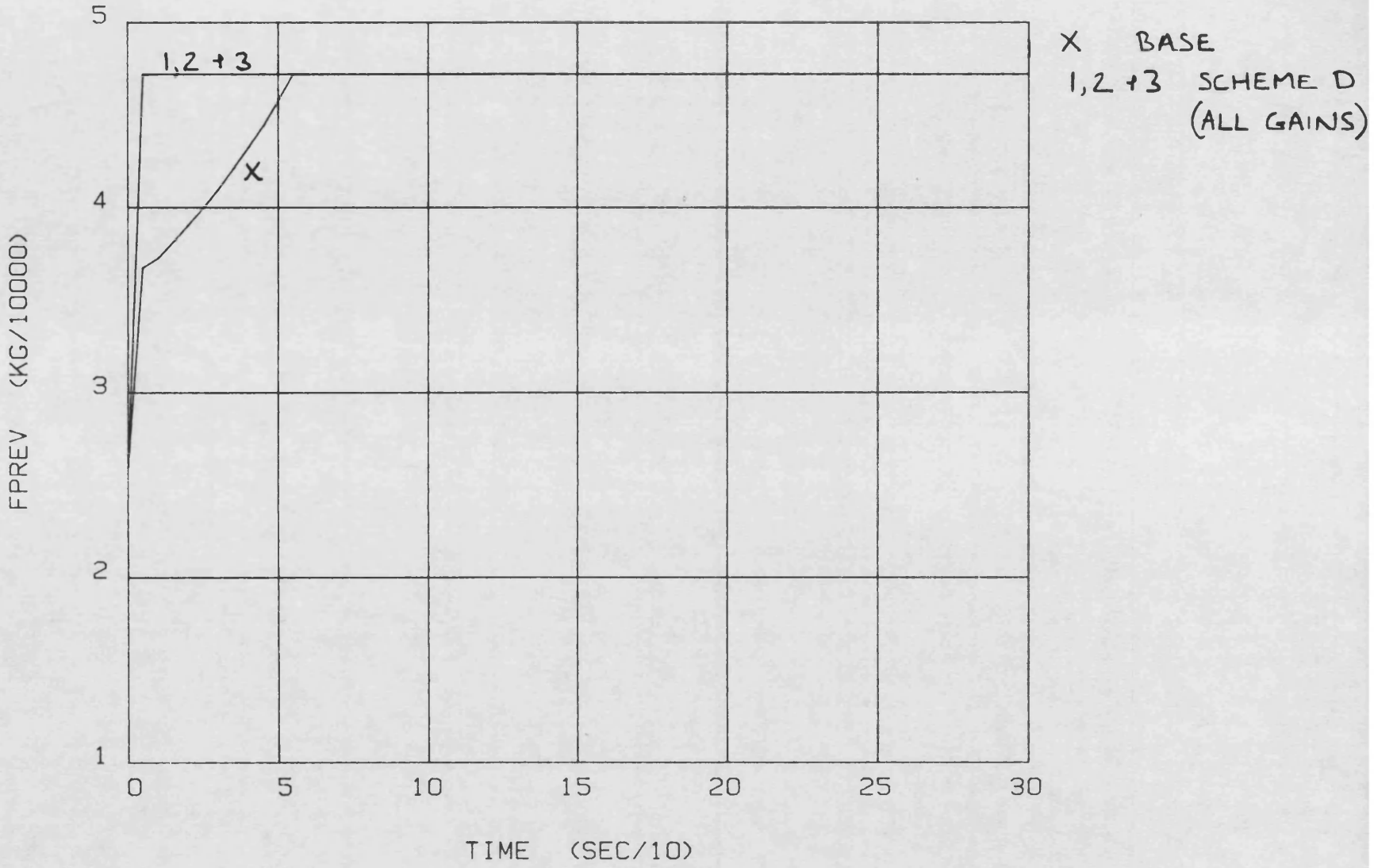

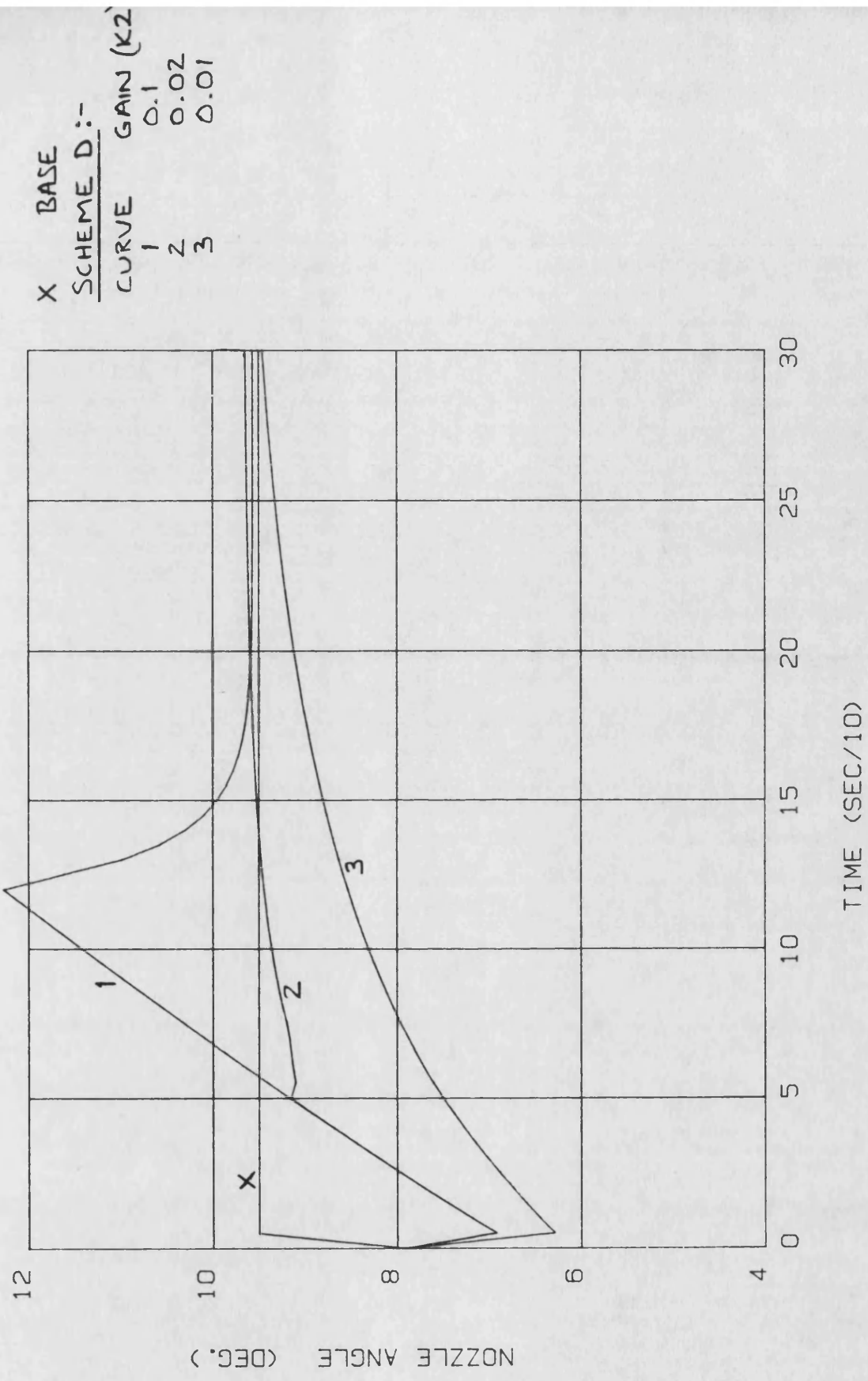

FIG. 7.30 NOZZLE ANGLE VS. SPEED SCHEME D

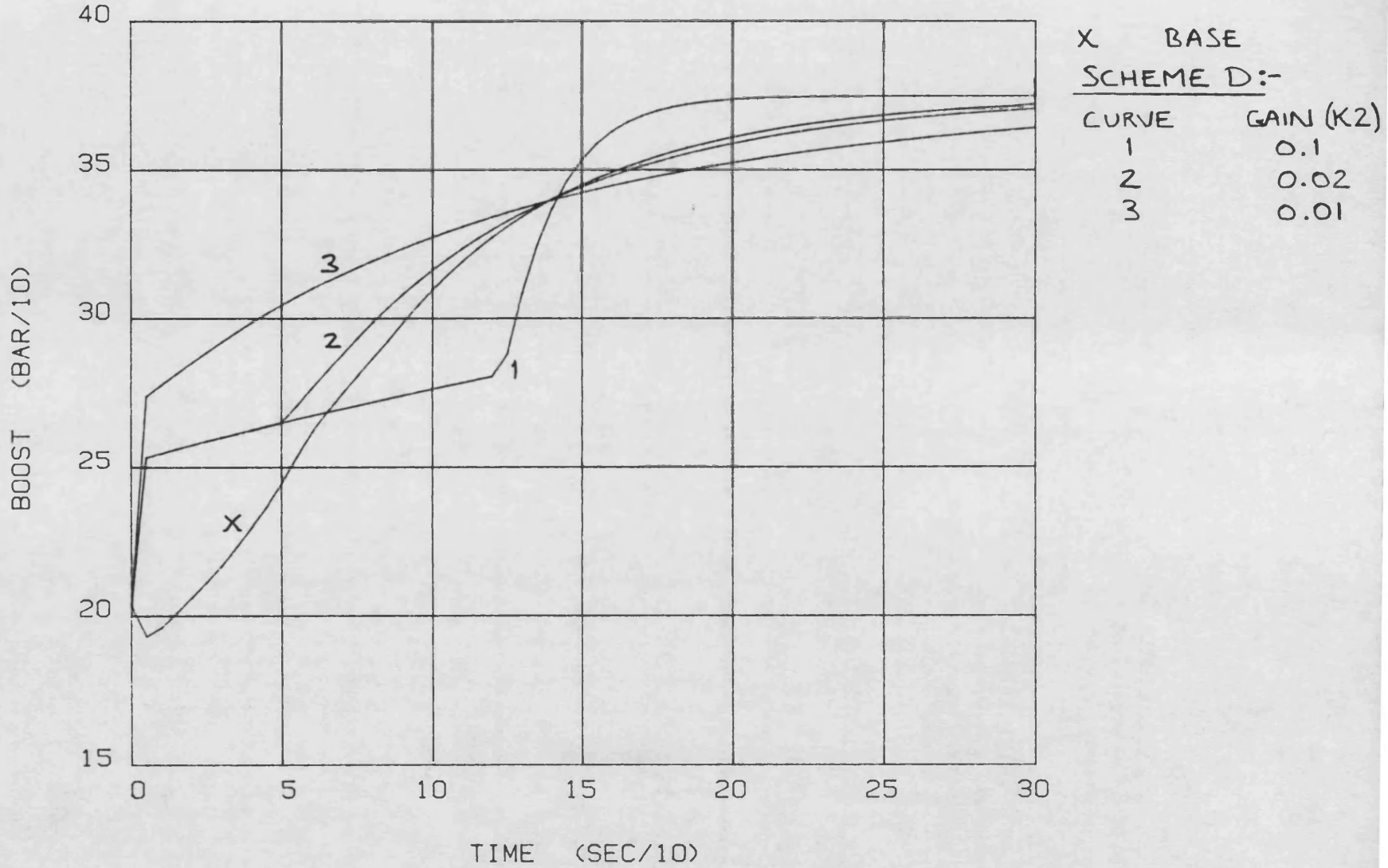

FIG. 7.31 BOOST PRESSURE VS. TIME SCHEME D

FIG. 7.32 AIR-FUEL RATIO VS. TIME

SCHEME D

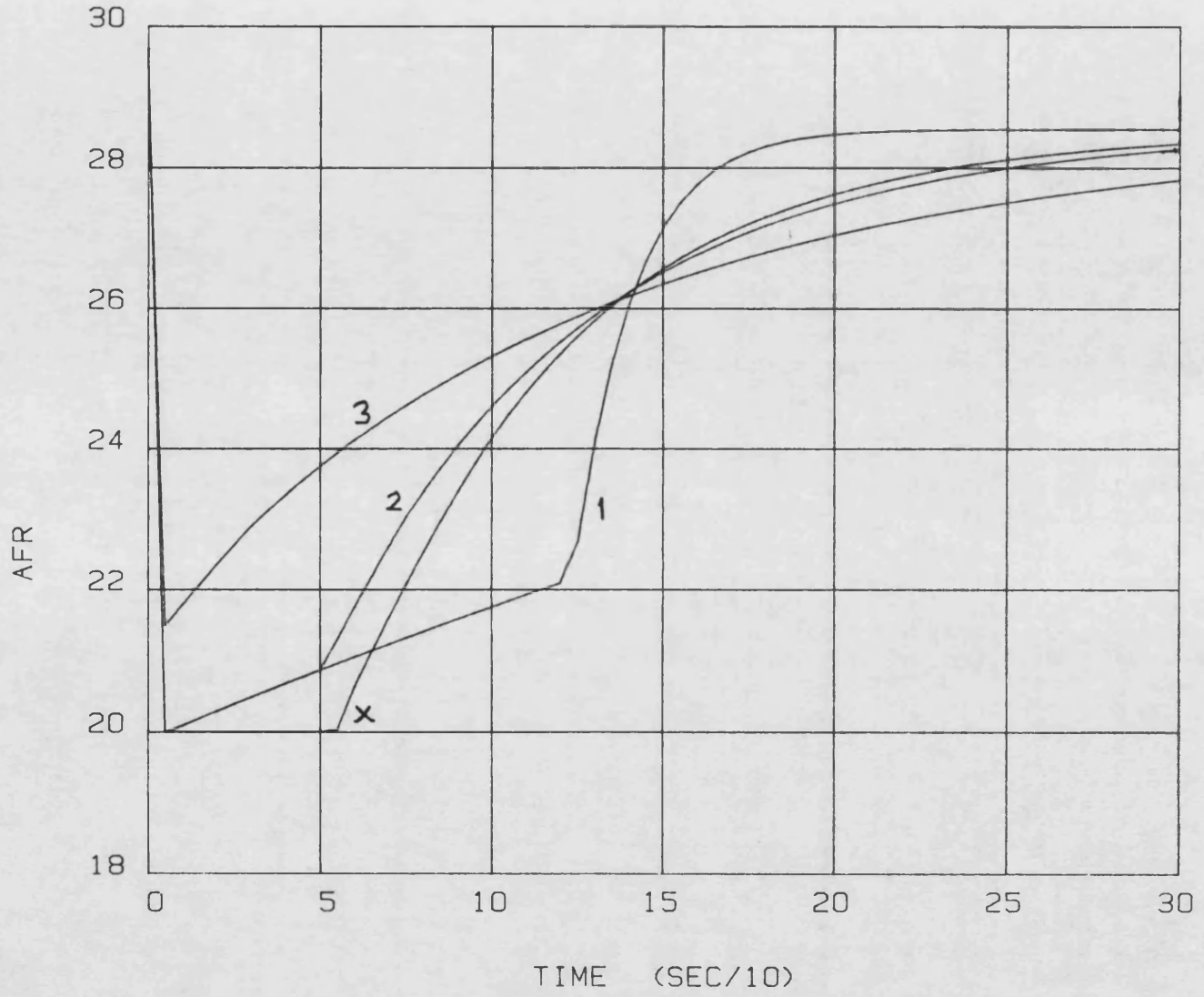

X BASE

SCHEME D:-

CURVE	GAIN(K2)
1	0.1
2	0.02
3	0.01

FIG. 7.33 ENGINE SPEED VS. TIME
SCHEME D

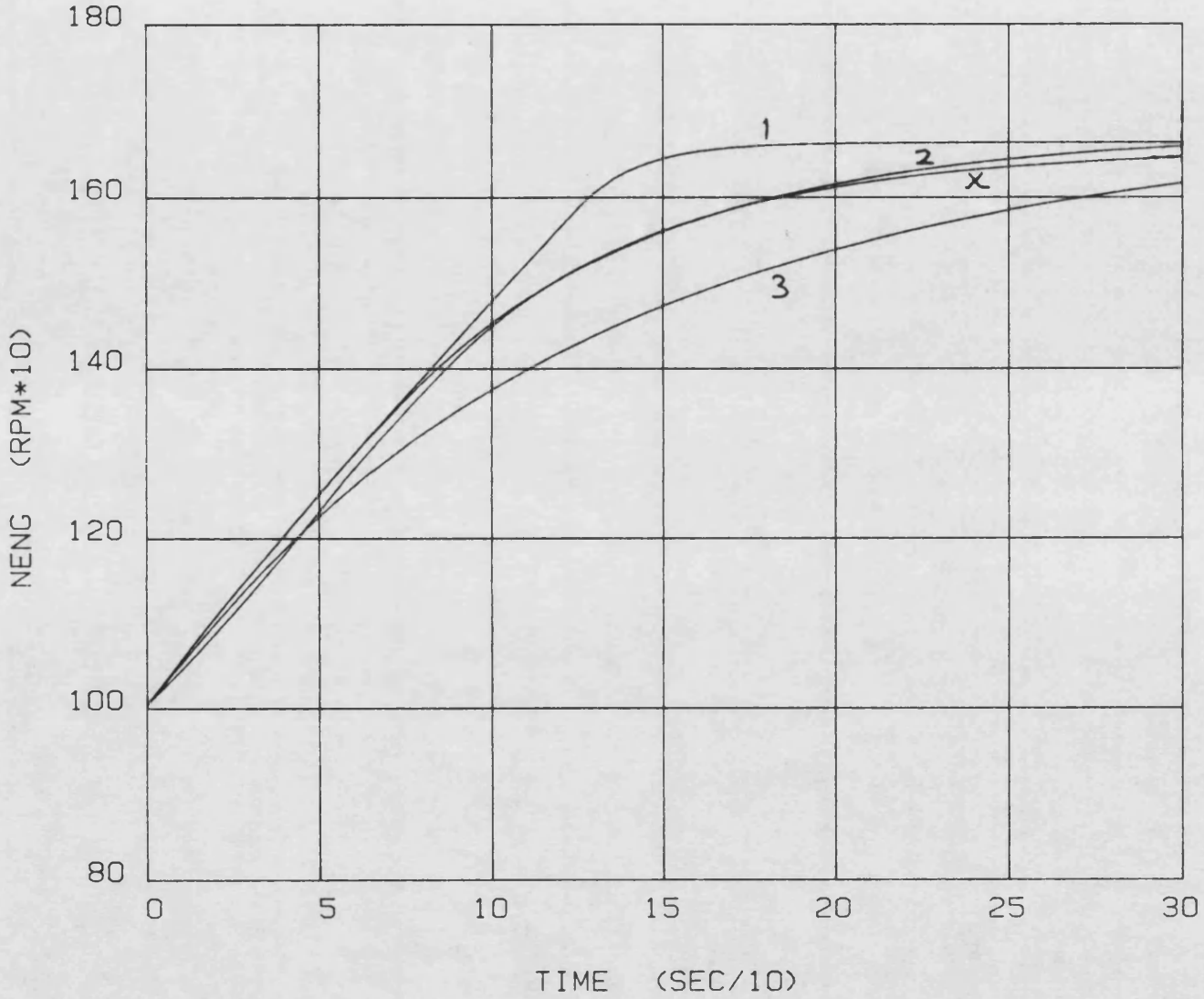

X BASE

SCHEME D:-

CURVE	GAIN (KZ
1	0.1
2	0.02
3	0.01

FIG. 7.34 OUTPUT TORQUE VS. TIME
SCHEME D

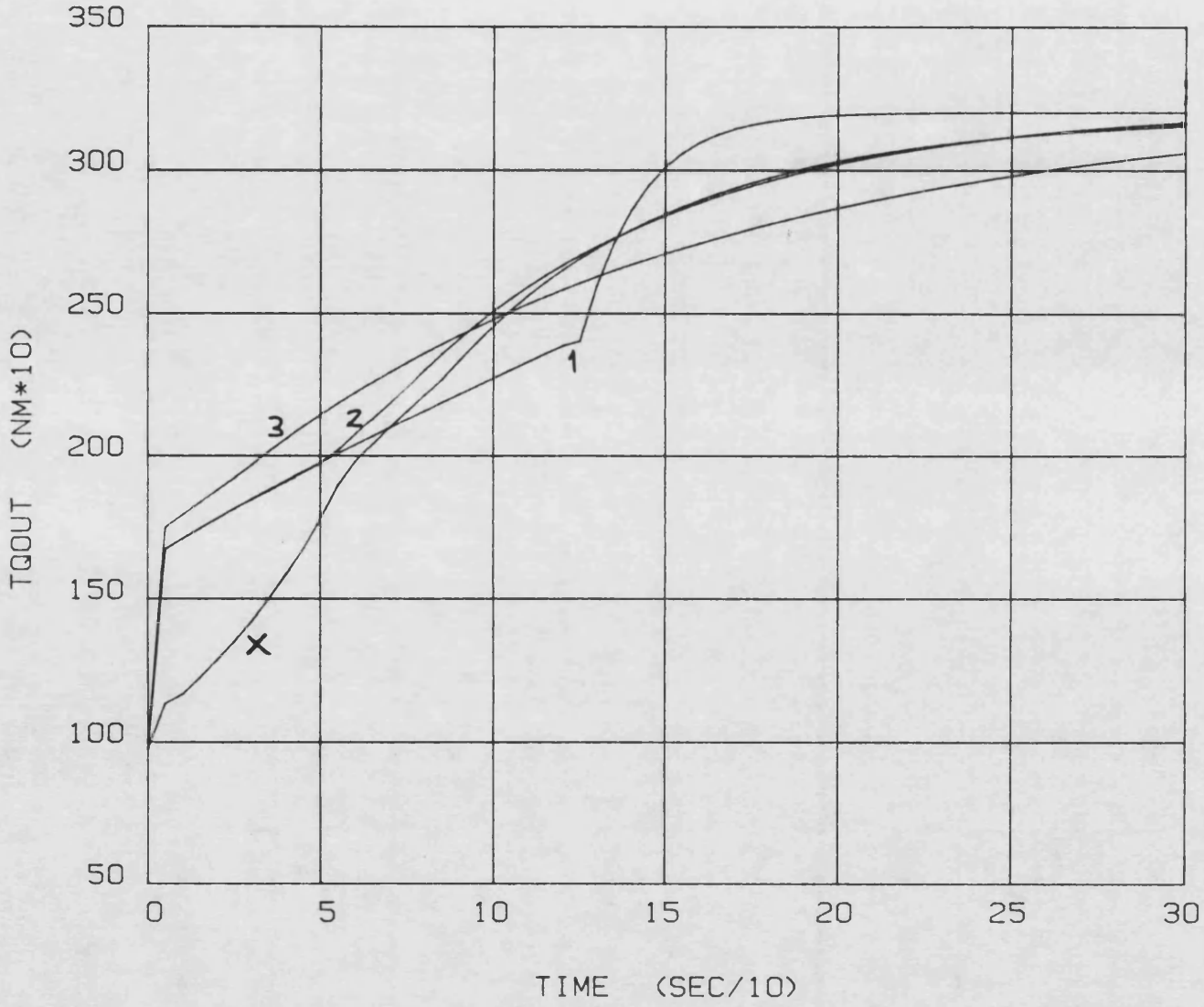

X BASE

SCHEME D:-

CURVE	GAIN (K2
1	0.1
2	0.02
3	0.01

CHAPTER 8

DISCUSSION AND CONCLUSIONS

8.1 DIESEL CONTROL SYSTEM DEVELOPMENT

8.2 THE CONTROL OF A VARIABLE GEOMETRY TURBOCHARGED DIESEL ENGINE

8.3 DIFFERENTIAL COMPOUND ENGINE CONTROLS

8.1 DIESEL CONTROL SYSTEM DEVELOPMENT

The research and development described in this thesis has been on the subject of Automotive Diesel control. The work has been on two Diesel systems in particular: a variable geometry turbocharged Diesel; and the Differential Compound Engine. These projects are summarised and conclusions drawn in the following two sections. There are several common themes to the work which are discussed in this section.

Fuel system control is common to both projects and has been approached in a similar manner (section 4.2.2). Electro-hydraulic governors have been implemented which provide alternative modes of control for testing and allow limiting torque fuelling (the fuel rack limit) to be scheduled. The latter can be adjusted either manually or by a micro' based controller.

Scheduling the fuel rack limit overcomes the need to match fuel pump characteristics to the engine's fuelling requirements. Future fuel pump governors will probably need only a simple ROM change to match a new engine. This should cut fuel system costs by allowing more standardisation.

Variable fuel injection timing has also been implemented on both engines. The devices used are based on Gardner spares fitted in a unit which replaces the automotive compressor (section 4.2.3). A helically splined shaft and sliding collar arrangement rotates the fuel pump drive relative to the crank-shaft. Variable timing is not yet standard on large in-line fuel pumps, however it will almost certainly be introduced in the not too distant future because of its direct effect on fuel economy.

Retarding timing reduces cylinder pressure and therefore allows increased fuelling (torque) if the air is available for complete combustion. The use of retard to increase torque may be limited to transient conditions if specific fuel consumption is significantly increased.

Fuel rack and injection timing actuation is likely to be either pneumatic, electric or electro-hydraulic (using engine oil as the working fluid). A small torque motor or linear solenoid could be used to move the spool of a hydraulic follower arrangement. A position sensor is not required for this form of hydraulic actuation.

Variable turbine geometry (VG) is another feature which is common to both prototype systems. Putting boost pressure feedback around the VG mechanism has proved to be a useful technique which gives the following advantages:-

i) Long term VG drift would be caused by such things as soot build-up, mechanical wear, changes in mechanism stiction etc. A boost feedback loop overcomes this problem by adjusting geometry until the correct pressure is obtained.

ii) In a commercial system an absolute pressure transducer could be used. This would compensate for changes in altitude within the capabilities of the turbocharger.

iii) A boost loop will fully close the VG mechanism during transients in an attempt to raise boost to the new set-point. This should improve pressure response as compared with a simple geometry change.

Variable geometry turbocharging is set to become the next major improvement to the commercial Diesel (ref. 63). Actuation is likely to be pneumatic, electric or by engine oil servo. Pneumatic actuation has the advantage of being reasonably well suited to high temperature operation. It can provide cooling if necessary and does not present a fire risk if leaks occur. The automotive compressor provides a supply of high pressure air ideal for this application.

Prototype engine management systems have been implemented on both Diesel drives (chapter 4 and section 7.2). Under steady-state conditions the control parameters are automatically adjusted to minimise fuel consumption and produce the best torque curve possible

within operational constaints. During transients this form of control may be overidden to improve response and drivability.

Microprocessor based supervisory controllers adjust control loop set-points using the pre-determined schedule method (section 3.2 discusses alternative approaches to steady-state performance optimisation). The set-points are functions of engine speed (output speed in the case of the DCE) and load. Ambient conditions were neglected to simplify the test work, but would have to be included in a commercial system.

Fuel rack is used as the measure of load, in preference to torque, because it is more likely to be accepted as a commercially viable measurement. Fuel per revolution is roughly proportional to rack position which therefore provides a good load indicator. Future fuel governors are likely to be driven by electronics which means a signal representing rack position will be readily available. This need not be a transducer output, it could be the actuator driving signal.

Alternative transient control algorithms have been investigated, experimentally for the VG (chapter 5), and using a computer model of the DCE (section 7.3). In both cases the response to rapid changes in fuelling can be improved by the incorporation of suitable transient algorithms. Boost pressure feedback is an inherant part of these algorithms, turbine geometry being manipulated to improve boost response.

Some aspects of Diesel control system performance will benefit from the use of adaptive algorithms. This involves varying control loop gains to suit the engine operating regime. Gains could be scheduled by the supervisory controller in much the same way as steady-state set-points. This is particularly relevant to boost pressure control and is discussed in sections 4.3.3 and 7.3.6. The inherent gain of the VG turbine depends on exhaust enthalpy and massflow which vary with fuelling and engine speed (compressor speed in the case of the DCE).

8.2 THE CONTROL OF A VARIABLE GEOMETRY TURBOCHARGED DIESEL ENGINE

The turbocharger and automotive diesel are not normally well matched, the former has an orifice like flow characteristic whereas the latter is a positive displacement machine. For road use a constant, if not rising, inlet pressure (boost) with falling engine speed is preferable. Turbocharger boost falls with engine speed thus limiting the torque rise and useful speed range of the engine.

The waste-gate as used on many turbocharged petrol engines is one solution. This operates by bypassing exhaust gas around the turbine, which is smaller than could otherwise be used without over-boosting the engine at max. speed. This method is inherently inefficient and is not used on large commercial diesels where low fuel consumption is a primary requirement.

The variable geometry (VG) turbocharger has a turbine stage with adjustable geometry so that the swallowing capacity (effective orifice size) can be altered to suit the engine operating conditions. As engine speed falls the turbine's effective size is reduced thus increasing low speed boost and hence engine torque. As long as turbine efficiency can be maintained with VG there should be no efficiency penalty, in fact fuel consumption should improve because engine air supply can be better matched to road conditions.

Variable geometry turbocharger development at the University of Bath has been sufficiently successful for Holset Engineering to produce their own prototypes. The project reported in chapters 4 & 5 was initiated to do engine test work and control system development aimed at:-

i) Determining the best Holset prototype.
ii) Examining the performance improvements, both steady-state and transient, made possible with that device.

iii) Implementing a prototype control system to demonstate that these improvements can be realised in a real installation.

The engine tested was a Leyland TL11 fitted with the following non-standard controls: variable turbine geometry; electronic fuel governing; and variable fuel injection timing. The mechanisms, their associated actuation and analogue controls are described in section 4.2.

Electronic governing was implemented to give remote control over the limiting torque curve (LTC) fuel rack limit. This is necessary if the LTC fuelling schedule is to be automatically taylored to suit the additional air provided by the VG turbocharger.

Variable fuel injection timing was included so that cylinder pressure limitations would not prevent full utilisation of the VG turbocharger. Retarding timing reduces cylinder pressure and therefore allows further up-fuelling if the air is available. Variable timing also improves part load efficiencies by providing further scope for optimisation.

A steady-state control system (fig. 4.9) has been implemented using the DEC LSI-11/23 development computer described in section 3.4. Boost pressure (or turbine geometry) and injection timing are scheduled as functions of engine speed and fuel rack position. The latter is used in preference to torque as a measure of engine load. Position measurement is simpler and less costly than torque measurement and therefore a better choice for any commercial system. The LTC rack limit is a function of engine speed allowing any desired LTC fuelling schedule. The set-points are output via DAC channels to the analogue controls (fig. 4.3).

An interesting instability was discovered when the scheduling system was used in conjunction with all-speed governing and a windage load characteristic. At high loads boost and engine speed oscillated in harmony. This was attributed to the effect of boost on efficiency and

hence engine speed. A change in speed causes the governor to move the rack which in turn leads to the scheduling system altering the boost pressure set-point. This has the effect of closing an unwanted feedback loop around the system (see section 4.3.3). In a real installation the inertia of the vehicle should prevent engine speed oscillating when in gear. Micro-switches could be used to detect clutch depression or neutral selected and the boost set-point held constant.

Optimal adjustment of boost pressure, injection timing and LTC fuelling gave the following performance improvements when compared with the standard engine (fixed geometry turbo' and fixed timing):-

PERFORMANCE CRITERIA	BASE ENGINE	OPTIMISED (with controls)
Rated power	191 Kw @ 2100 rpm	191 Kw @ 2300 rpm
Peak torque	1057 Nm @ 1300 rpm	1155 Nm @ 1360 rpm
Torque back-up	21%	46%
Useful speed range	800 rpm	940 rpm
Consumption loop area (@ 210 gm/KW.Hr)	100	161

The VG prototype proved to have a rather limited control range (fig 4.24), a larger turn-down ratio would be necessary to cover the engine speed range. In particular a larger turbine stage, which could be opened still further, would allow the control range to cover higher engine speeds.

Linearised schedules were tested to assess the loss in performance caused by schedule simplification. Such schedules could be implemented with simple analogue controls. The results were not conclusive, however, this avenue of investigation is only worth pursuing further if a commercial system is being considered.

A performance comparison of three alternative VG schedules has been undertaken. The optimum boost pressure schedule was compared with two compromise strategies which have transient performance advantages. As expected there were significant fuel consumption penalties for using the compromise stategies.

Transient performance with VG has been investigated by conducting fuel step tests under both constant speed and acceleration conditions (chapter 5). The aim was restricted to reducing turbo' lag and thus improving load acceptance and smoke emissions. Three alternative transient VG control strategies have been tested. Zero restriction tests were also performed to provide a base for comparison.

The constant speed tests mimic high gear fuel steps where vehicle inertia prevents rapid engine acceleration. The turbocharger response occurs at nominally constant engine speed. These tests were performed using the dynamometer in speed control mode.

The acceleration tests are necessary to assess turbocharger response in low gears. In this case governor runout is reached before the turbocharger has fully responded to the fuel increase. As a result engine acceleration has a direct effect on turbo' lag and load acceptance. These tests were performed by using the dynamometer to simulate vehicle inertia in the relevant gears (section 5.4.1).

Boost pressure scheduling and a compromise restriction vs. speed schedule gave the best transient turbocharger response. The latter sets optimum LTC. restriction at all loads. This has the effect of over restricting the turbocharger at part load so that boost pressure is higher at the beginning of a transient. However part load fuel consumption is no longer minimised. Boost pressure scheduling improves transient response by over restricting during the transient. There is no fuel consumption penalty under steady-state conditions as both LTC and part load boost settings are optimum.

In conclusion comprehensive engine testing and control system development has led to a prototype Diesel engine controller (fig. 4.9). This system optimises steady-state performance and provides a transient VG over-restriction to reduce the turbo' lag phenomenum. A boost pressure feedback loop was used to drive the VG mechanism as this provides the following benefits:-

i) Reduced turbo' lag as compared with a simple geometry change, with no part load fuel consumption penalty.
ii) Automatic compensation for long term changes such as soot build up and mechanical wear.
iii) Some degree of automatic altitude compensation if an absolute pressure transducer is used.

In addition to the ideas tested other functions could easily be included in a microprocessor based system. These might include: transient over-fuelling during vehicle acceleration; holding boost pressure up during gear changes in anticipation of clutch engagement; engine condition monitoring and fault diagnosis; and a cold start strategy.

8.3 DIFFERENTIAL COMPOUND ENGINE CONTROLS

The term compound engine refers to an arrangement where the supercharging compressor and exhaust turbine are geared to the engine. This allows excess exhaust energy, over that required to supercharge, to be recovered as useful work output. In the case of the Differential Compound Engine (DCE) the engine drives a fully floating epicyclic gearbox (fig. 6.5). The two epicyclic outputs drive a supercharging compressor and the vehicle drive-shaft respectively. The turbine is geared directly to the drive-shaft.

This arrangement allows engine speed to be held constant whilst drive-shaft speed falls. The compressor increases speed and therefore air delivery. The excess air, over that required by the engine, is fed to the exhaust turbine via an engine bypass. The combination of compressor, bypass and turbine provide a torque conversion effect. If the engine is run at maximum power the resulting torque curve resembles a constant power hyperbola. In actual fact the losses in the bypass torque conversion process are considerable, however, the recovery of exhaust energy compensates for this. In practice a torque back-up of around 3.5:1 at 20% of rated output speed is achievable.

The DCE has been under development for approximately twenty-four years. The author has been involved for the last five and has been responsible for control system development and the construction of the new Leyland 500 based prototype. The principles of DCE operation, a brief development history, and the latest prototype build are discussed in chapter 6. The control work is described in chapter 7, two areas of research are covered: the implementation of a steady-state controller; and computer simulation studies to determine suitable transient control algorithms.

The DCE has two fundamental controls which determine its basic operation and several secondary controls which improve performance. The fundamental variables are fuel input per revolution (rack position) and turbine nozzle angle. Together they establish the

epicyclic torque and speed conditions which in turn determine compressor boost and massflow respectively. If single input-output controls are implemented then rack and nozzle angle can be used to control engine speed and boost pressure. For this purpose they are interchangeable ie. nozzle angle can control either boost or speed so long as rack is used for the other.

Section 7.2 describes the implementation of a simple steady-state controller aimed at running the DCB at optimum efficiency. It was shown that so long as boost pressure is scheduled as a function of two variables, defining output load and speed, optimum efficiency results. This corrected a previous misconception that both engine speed and boost should be scheduled.

The resulting system design is shown in fig. 7.3, the driver provides the engine speed demand, which approximates to a power demand, and the micro' schedules the boost demand. Boost is a function of output speed and torque simply because the optimum schedules were available in this form. For a commercial system fuel rack position would be a more viable measure of load.

Alternative boost and engine speed control loop configurations were analysed using the root-locus technique (ref. 39). This method gives a qualitative measure of loop performance which is useful for comparison purposes. The resulting control loop algorithms were implemented with analogue electronics.

The boost loop set-point was generated by a "PET" micro-computer from the stored optimum schedule. This machine proved to be rather slow confirming the requirement for a more powerful development computer (see section 3.4). Despite this, under steady-state conditions boost pressure followed the scheduled demand accurately, thus proving the viability of the suggested control scheme.

A steady-state controller may not produce a rapid response to changes in demand without an additional transient algorithm. The design of

algorithms to improve DCE transient response has been investigated using a dynamic computer model (section 7.3). The algorithms tried are described by figs. 7.19-7.21 & 7.28. The response to a fuel step at the stall condition (20% of rated speed) was used as the means of comparison.

A simple nozzle angle step, to the new steady-state optimum, gives an unacceptably low initial torque rise. This is because initial boost pressure is far too low resulting in smoke limiting fuel reduction (AFR is smoke limited to 20:1). Drivability would be poor because of the driver anticipation required.

A boost feedback loop can be used to raise boost rapidly to its new steady-state optimum (scheme A). This gives a good initial torque but the final rise time is much longer. This was attributed to the reduced compressor torque available for acceleration resulting in a slower increase in massflow and thus turbine torque.

The solution (scheme C or D) is to control transient boost at a level just high enough to avoid AFR limiting fuel reduction. This gives a reasonable initial torque with the same final rise time as the simple nozzle step. Although initial boost is higher than that produced by a simple nozzle step so is engine torque and as a result the compressor torque available for acceleration is the same. Higher initial boost (scheme A) carries an acceleration time penalty.

In conclusion a transient control scheme can avoid smoke limiting fuel reduction and the associated low initial torque. However any improvement in final rise time is at the expense of torque earlier in the transient. The major limitation on transient response is engine, compressor and gear-train inertia. Pipe-work volumes are too small to have any effect on transient performance ie. boost pressure can be altered rapidly. This may not be the case with the experimental prototype because of its unrealistic pipe-work volume.

The simplified dynamic model (Appendix 2) used in this work proved to be a very useful tool for control algorithm design and comparison. If improved accuracy is required the non-dynamic elements (engine, compressor, turbine and gearbox losses) should be modelled by empirical arrays and accurate inertia and pipe volume data used. Transient test work with the experimental proto-type can be used to verify the model. However optimum control algorithm designs may differ because of the prototype's unrealistic pipe volumes.

Optimum controller gains are likely to vary with operating conditions and an adaptive system (see section 3.3.2) may be necessary. Future work is likely to include comprehensive transient studies to determine suitable controller gains for all conditions. The DCE's deceleration characteristics and control algorithms to enhance them require some study (scheme D should provide increased DCE braking).

The true test of transient algorithms is drivability which can only be properly assessed in a vehicle prototype.

REFERENCES

1. TAYLOR, C.F.
"The Internal-Combustion Engine in Theory and Practice"
M.I.T. Press, 1980

2. TARABAD, M
"Transmissions for passenger cars and commercial vehicles"
M.Sc. course notes (Diesel Engine Technology), Univ. of Bath, 1984

3. WATSON, N & JANOTA, M.S.
"Turbocharging the Internal Combustion Engine"
Macmillan, 1984

4. ZINNER, K.
"Supercharging of Internal Combustion Engines"
Springer-Verlag, 1978

5. WURM, J. et al
"Assessment of Positive Displacement Supercharging and Compounding of Adiabatic Diesels"
SAE 840430

6. KLARHOEFER, C. & WINKLER, G.
"Compounding a passenger car diesel with a positive displacement expander"
I.Mech.E. C96/86

7. KAMO, R. & BRYZIK, W.
"Adiabatic Turbocompound Engine Performance Prediction"
SAE 780068

8. KAMO, R. & BRYZIK, W.
"Cummins-TARADCOM Adiabatic Turbocompound Engine Program"
SAE 810070

9. TOYAMA, K. et al
"Heat Insulated Turbocompound Engine"
SAE 831345

10. BICKING, R.E.
"A piezoresistive integrated pressure transducer"
I.Mech.E. C164/81

11. OAKES, J.A.
"A pressure sensor for automotive application"
I.Mech.E. C181/81

12. SWARTZ, C.S. et al
"Advances in automotive silicon pressure transducer tehnology"
I.Mech.E. C182/81

13. WALZ, L. et al
"Progress in Electronic Diesel Control"
SAE 840442

14. GERSTENMEIER, J.
"Electronic control unit for passenger car antiskid (ABS)"
I.Mech.E. C186/81

15. BLOOMFIELD, E.J. & PENMAN, F.S.
"Rotational speed sensor/bearing assemblies"
I.Mech.E. C172/81

16. "Automotive Handbook"
Robert Bosch GmbH, 1978 translation

17. MACKIE, C.
"Vehicle condition monitoring and electronic instrument displays"
I.Mech.E. C175/81

18. GORILLE, I.
"Electronic Engine Management at Bosch"
SAE 840541

19. SCHULTE, E.
"Electronically controlled carburetter systems with dynamic adaption"
I.Mech.E. C165/81

20. RYDQVIST, J.E. et al
"A Turbocharged Engine with Microprocessor Controlled Boost Pressure"
SAE 810060

21. FLAXINGTON, D. & SZCZUPAK, D.T.
"Variable area radial-inflow turbines"
I.Mech.E. C36/82

22. DECKER, H. et al
"New Digital Engine Control Systems"
Robert Bosch GmbH

23. SCHWAB, M.
"Electronic control of a 4-speed automatic transmission with lock-up clutch"
SAE 840448

24. IRONSIDE, J.M. & STUBBS, P.W.R.
"Microcomputer control of an automotive perbury transmission"
I.Mech.E. C200/81

25. CROSS, M.
"Computers put a new spring in cars"
'New Scientist' journal, 22 May'86

26. DIMMOCK, N.A.
"A Compressor Routine Test Code"
Ministry of Aviation R.& M. No. 3337, 1963

27. PREST, P.H.
"Selection of Pressure Transducers"
School of Engineering, Univ. of Bath

28. "Temperature Handbook"
Calex Instrumentation, 1st edition

29. "Flow Measurement"
B.S. 1042

30. BEALE, E.S.L.
"Measurement of flow of fluids by orifices, nozzles, venturis and pitot tubes"
George Kent Ltd.

31. "Smokemeter Working Instructions"
Robert Bosch Ltd.

32. "Model 107 - User's Manual
In-line Diesel Exhaust Smokemeter"
Berkeley Controls Inc.

33. ANDERSON, U.A.
"Acceleration Response of a Variable Geometry Turbocharged 32 Tonne Truck"
M.Sc. thesis, Univ. of Bath, 1984

34. "Instrumentation Handbook for the Leyland TL11 test rig"
School of Engineering, Univ. of Bath

35. "Instrumentation Handbook for the Leyland 500 DCE test rig"
School of Engineering, Univ. of Bath

36. "Procedure for measuring basic highway vehicle engine performance and fuel consumption - spark ignition and diesel"
1983 SAE Handbook, SAE J1312, Sep'80

37. DEAL, M.H.
"Optimisation of engine-transmission systems in heavy commercial vehicles"
Ph.d. thesis, Univ. of Bath, 1980

38. BANISOLEIMAN, K.
"Performance assessment of continuously variable vehicle transmissions by computer simulation"
Ph.d. thesis, Univ. of Bath, 1983

39. HEALEY, M.
"Principles of Automatic Control"
Hodder & Stoughton, 1977

40. WELLSTEAD, P.E.
"Frequency Response Analysis"
Solartron Instruments, technical report 010/83

41. WILLIAM, B.J. & CLARKE, D.W.
"Plant Modelling from P.R.B.S. experiments"
'CONTROL' journal, Oct'68

42. WELLSTEAD, P.E.
"Self-Tuning Control"
course notes (Control of Mechanical Systems), UMIST, Oct'84

43. WIBERG, D.M.
"State Space and Linear Systems"
McGraw Hill, 1971

44. ROSENBROCK, H.H.
"Computer Aided Control System Design"
Academic Press, 1974

45. JUNG, W.G.
"IC Op-Amp Cookbook"
Howard W. Sams & Co., 1980

46. "LSI-11 Analog System User's Guide"
Digital Equipment Corporation, 1982

47. OKAZAKI, Y et al
"A case of variable geometry turbocharger development"
I.Mech.E. C111/86

48. McCUTCHEON, A.R.S. & BROWN M.W.G.
"Evaluation of a variable geometry turbocharger turbine on a commercial diesel engine"
I.Mech.E. C104/86

49. WALLACE, F.J. et al
"Variable Geometry Turbocharging - The Realistic Way Forward"
SAE 810336

50. BAGHERY, A.
"Variable Geometry Turbocharging of Transport Diesel Engines"
Ph.d. thesis, Univ. of Bath, 1975

51. ROBERTS, E.W.
"Variable Geometry Turbocharging; Optimisation and Control"
Ph.d. thesis, Univ. of Bath, 1984

52. BACKHOUSE, R.J.
"The dynamic behaviour and feedback control of a turbocharged automotive diesel engine with variable geometry turbine"
Ph.d. thesis, UMIST, 1986

53. WALLACE, F.J.
"Operating characteristics of compound engine schemes for traction purposes based on opposed piston two-stroke engines and differential gearing"
I.Mech.E., 1962

54. DAWSON, J.G. et al
"Some experiences with a Differentially Supercharged Diesel Engine"
I.Mech.E., 1964

55. WALLACE, F.J.
"Differential Compound Engine"
I.Mech.E., 1973

56. WALLACE, F.J.
"The Differential Compound Engine as an advanced integrated engine-transmission system for Trucks and off-highway applications"
School of Engineering, Univ. of Bath

57. "Mechanical Handbook for the Leyland 500 DCE test rig"
School of Engineering, Univ. of Bath

58. PRINCE, D.
"Torsional Oscillations"
Appendix A2, transfer report, School of Engineering, Univ. of Bath

59. TARABAD, M.
"Internal notes on Leyland 500 DCE design data obtained by simulation"
School of Engineering, Univ. of Bath

60. TRIVELLAS, D.
"Microprocessor aided control of the Differential Compound Engine"
M.Sc. thesis, Univ. of Bath, 1980

61. WALLACE, F.J. & KIMBER, R.M.
"Optimisation of the Differential Compound Engine using microprocessor control"
SAE 810256

62. WALLACE, F.J. et al
"Design and performance studies for a 1000 h.p. military version of the Differential Compound Engine"
I.Mech.E. C194/86

63. "Turbocharging and Turbochargers"
I.Mech.E. Conference proceedings, 1986

APPENDIX 1 -- SUPERVISORY CONTROL SOFTWARE

A set-point scheduling program has been written for the LSI-11/23 development computer. A program description can be found in section 4.3.2. This appendix provides additional details and software listings.

Two versions have been written: one (TL11) to implement the linearised schedules discussed in section 4.4.2; and another (TL11VG) for the VG. acceleration transients described in section 5.4. The latter does not include bumpless transfer as this was not considered necessary for the VG. mechanism alone. A listing of TL11 is included here. A listing of TL11VG can be found in ref. 33. The main program uses the following subroutines:-

1. SETPTS

This routine calculates the control loop set-points output to the DAC channels. It is compiled with the main routine as a single object file. Set-point calculation is separated from the rest of the code to increase program readability.

2. ADCONV (CHANNEL,VALUE)

This is an analogue to digital conversion (ADC) routine written in assembler. It is set up as a FORTRAN callable subroutine and controls the ADC module described in ref. 46.
CHANNEL is the ADC channel that is to be read and must be an integer between 0 and 7 inclusive.
VALUE is the result of the conversion, it is an integer between 0 and 4095 which corresponds to a voltage range of 0 to 10 volts.

3. IPOKE

This is a system subroutine which loads an address with the given 16 bit integer. It is used for loading the DAC registers and is described in the RT-11 Programmers Reference Manual. The required output voltage

(0-10V only) is multiplied by 409.5 to give a 12 bit integer. This is exclusive-ored (XOR) with hex FFF (ie. 0 corresponds to 10V, 4095 corresponds to 0V) before being poked to the DAC.

4. IY=INTRP1(XNORM,IYARR,ISIZE)

This is an integer function for fast 1-D linear interpolation. Given XNORM it returns a value for IY from the array IYARR (of dimension ISIZE). IY and IYARR are integers and are intended to be DAC words.

XNORM is X normalised to a real number on the same scale as the array index ie. if XNORM is 2.5 then IY is half way between IYARR(2) and IYARR(3). XNORM should be >1 and <ISIZE (eg. 9.999 rather than 10). Calculating XNORM before calling the interpolation function greatly simplifies the algorithm and, along with the use of integer arithmetic, results in rapid execution.

A real version of this function (RITRP1) is used by the dynamic model DCESIM described in the next appendix.

5. IZ=INTRP2(XNORM,YNORM,IZARR,IXSIZE,IYSIZE)

This is an integer function for fast 2-D linear interpolation. Given XNORM and YNORM it returns a value for IZ from the 2-D array IZARR (of dimensions IXSIZE and IYSIZE). XNORM and YNORM are normalised values of X and Y, this concept has already been explained for INTRP1.

2-D linear interpolation is achieved by doing three 1-D interpolations. The first in the X direction keeping Y constant at INT(YNORM), a second in the X direction with Y constant at INT(YNORM)+1, and the third in the Y direction with X constant at XNORM.

A real version of this function (RITRP2) is used by the dynamic model DCESIM described in the next appendix.

6. ITTINR

This is a system subroutine (see RT-11 programmers reference) which gets a character from the keyboard buffer. It is used to check for an exit request (space bar pressed) when the main scheduling loop is running. The terminal is put into "special terminal mode" (by setting bit 12 in the job status word) so that key presses are not echoed on the screen.

```
C LEYLAND TL11 SUPERVISORY CONTROL SYSTEM
C ****************************************
C
C D. Howard     May 1983
C version 1: simplified formulae for setpoints
C            bumpless start-up & shut-down
C
C this routine provides set-points for the following
C engine variables, which are controlled by analogue
C feedback loops:
C
C 1 inlet manifold pressure
C 2 injection timing
C 3 max. fuelling limit (max. rack posn.)
C
C START UP ROUTINE
C
C 1 read data & initialise variables/arrays
C
C 2 set up display
C
C 3 execute start-up procedure for bumpless transfer
C
C 4 enter MAIN LOOP
C
C MAIN LOOP OPERATIONS
C
C 1 read rack posn. and engine speed via ADC.
C   this determines the engines operating point.
C
C 2 obtain set-points from digitised optimisation
C   maps or optimum formulae as appropriate
C
C 3 output set-points to DACs.
C
C 4 check for exit request.
C
C 5 goto start of loop
C
C EXIT ROUTINE
C
C 1 execute shut-down procedure for bumpless transfer
C
C 2 return to start-up procedure
C
C
C*************************************************************
C START-UP ROUTINE
C*************************************************************
C
C READ DATA & INITIALISE
C read digitised optimisation data and store in arrays.
C convert array data & formulae constants from eng. units
C to normalised units for ADC & DAC channels.
C
      COMMON IMRACK(17),ISPEED,IRACK,IMAXRK,ITIM,IBOOST,IATMAD
      LOGICAL*1 ESC
      DATA ESC/27/
      OPEN(UNIT=3,TYPE='OLD',NAME='TL11.DAT')
C read in max. rack array
C values at 100rpm steps from 700 to 2300
      READ(3,3000)                        !skip one record
 3000 FORMAT(9HDUMMYDATA)
      DO 10 I=1,17                        !no. of points
      READ(3,3001) RMRACK                 !max. rack in mm
 3001 FORMAT(6X,F6.2)
 10   IMRACK(I)=RMRACK*0.4752*409.6       !convert mm to DAC word
      CLOSE(UNIT=3)
C DAC addresses
      IDAC0="170440
      IDAC1="170442
      IDAC2="170444
      IDAC3="170446
```

TL11.FOR (1 OF 3)

```
C SET UP DISPLAY
C set up the top half of the display which does not
C alter whilst the program is running.
C

        TYPE 7000, ESC,ESC
 7000   FORMAT(1X,1A1,'[2J',1A1,'[1;1H',              !VDU control
     &  5X,'TL-11 SUPERVISORY CONTROL SYSTEM'//
     &  6X,'set-points are output for the following engine variables:'//
     &  6x,'i)   inlet manifold pressure'/
     &  6x,'ii)  injection timing'/
     &  6x,'iii) max. fuelling limit (max. rack)'//
     &  6x,'these are, in turn, controlled by analogue feedback loops'/
     &  ///' OPERATOR COMMUNICATIONS:')
C
C START-UP PROCEDURE
C ask for atmos. pressure, initialise DACs & give instructions to
C operator for bumpless transfer to computer control.
C
C set atmos. pressure and calculate adjustment (IATMAD)
        TYPE 7005, ESC,ESC
 7005   FORMAT(1X,1A1,'[14;1H',1A1,'[J',              !VDU control
     &  'enter atmospheric pressure in mbar  ',$)
        READ (5,*) ATMPR
        IATMAD=ATMPR*2.048-2048
 20     TYPE 7001, ESC,ESC
 7001   FORMAT(1X,1A1,'[14;1H',1A1,'[J',              !VDU control
     &  'with engine at part load & under manual control'
     &  ,' enter S to start  ',$)
        READ (5,5000) REPLY
 5000   FORMAT(A1)
        IF (REPLY.NE.'S') GOTO 20
C read rack & speed from ADC channels
        CALL ADCONV(0,IRACK)
        CALL ADCONV(1,ISPEED)
C obtain set-points
        CALL SETPTS
C output set-points to DACs
        CALL IPOKE(IDAC0,IMAXRK.XOR."7777)
        CALL IPOKE(IDAC1,ITIM.XOR."7777)
        CALL IPOKE(IDAC2,IBOOST.XOR."7777)
C operators instuctions for bumpless transfer
        TIM=ITIM/409.6                              !convert to volts
        BOOST=IBOOST/409.6
        TYPE 7002, TIM,BOOST
 7002   FORMAT(/' set pots. as follows for bumpless transfer '
     &  ,'to computer control'/
     &  ' TIMING:  ',F6.2/
     &  ' BOOST:   ',F6.2/
     &  ' switch all 3 controls to computer input and enter C  ',$)
        READ (5,5000) REPLY
        IF (REPLY.NE.'C') GOTO 20
C set display & terminal mode for entering MAIN LOOP
        TYPE 7003, ESC,ESC

 7003   FORMAT(1X,1A1,'[14;1H',1A1,'[J',
     &  'press SPACE BAR to jump out of main program loop'/)
        CALL IPOKE("44,"10000.OR.IPEEK("44))  !set JSW bit 12 for...
C                                              special terminal mode
C*****************************************************************
C MAIN LOOP
C*****************************************************************
C
C read rack & speed from ADC channels
 100    CALL ADCONV(0,IRACK)
        CALL ADCONV(1,ISPEED)
C obtain set-points
        CALL SETPTS
C output set-points to DACs
        CALL IPOKE(IDAC0,IMAXRK.XOR."7777)
        CALL IPOKE(IDAC1,ITIM.XOR."7777)
        CALL IPOKE(IDAC2,IBOOST.XOR."7777)
C test for exit request (SPACE BAR pressed)
        ICHAR=ITTINR()
        IF (ICHAR.EQ."40) GOTO 200
        GOTO 100
```

TL11.FOR (2 OF 3)

```
C
C*************************************************************************
C EXIT ROUTINE
C*************************************************************************
C
C reset normal terminal mode & give operator instructions
C for bumpless transfer to manual operation
C
 200    CALL IPOKE("44,"167777.AND.IPEEK("44))          !clear JSW bit 12
        TIM=ITIM/409.6                                  !convert to volts
        BOOST=IBOOST/409.6
 210    TYPE 7004, ESC,ESC,TIM,BOOST
 7004   FORMAT(1X,1A1,'[14;1H',1A1,'[J',                !VDU control
     &  'set pots. as follows for bumpless transfer '
     &  ,'to manual control'/
     &  ' TIMING:  ',F6.2/
     &  ' BOOST:   ',F6.2/
     &  ' switch all 3 controls to manual input and enter C  ',$)
        READ (5,5000) REPLY
        IF (REPLY.NE.'C') GOTO 210
        GOTO 20
        STOP
        END


C*************************************************************************
C SETPOINTS CALCULATION SUBROUTINE
C*************************************************************************
C
C this routine calculates the optimum set points from rack & speed
C
        SUBROUTINE SETPTS


        COMMON IMRACK(17),ISPEED,IRACK,IMAXRK,ITIM,IBOOST,IATMAD
        IF (ISPEED.LT.1147) ISPEED=1147         !input speed limits
        IF (ISPEED.GT.3771) ISPEED=3771
        SPNORM=(ISPEED-983)/164.0               !normalised speed
        IMAXRK=INTRP1(SPNORM,IMRACK,17)         !interp for max rack
        ITIM=ISPEED-819+(IRACK-973)*0.6734      !calc. opt. timing
        IBOOST=(IRACK-1830)*2.876-IATMAD        !calc. opt. boost
        IF (ITIM.GT.4095) ITIM=4095             !timing dem. limits
        IF (ITIM.LT.0) ITIM=0
        IF (IBOOST.GT.4095) IBOOST=4095         !boost dem. limits
        IF (IBOOST.LT.0) IBOOST=0
        RETURN
        END
```

TL11.FOR (3 OF 3)

```
        .MACRO  ADC     CHANNEL,VALUE
        .GLOBL  ADCONV
ADCONV: MOV     £170400,R1      ;R1 < CSR ADDR.
        MOVB    CHANNEL,1(R1)   ;CSR < MULTIPLEXER CHANNEL
        BISB    £1,(R1)         ;SET A/D START BIT IN CSR
TEST:   TSTB    (R1)            ;TEST A/D DONE BIT IN CSR
        BPL     TEST
        MOV     2(R1),VALUE     ;VALUE < DBR
        RTS     PC              ;RETURN FROM SUBROUTINE
        .ENDM

        ADC     @2(R5),@4(R5)   ;CALL MACRO AS FORTRAN SUB.

        .END
```

```
C  1-D INTERPOLATION FUNCTION
C  given XNORM this routine returns a value for IY from the
C  array IYARR. XNORM is X normalised to a real number on
C  the same scale as the array indices. IY and IYARR are of
C  type INTEGER and are intended to be 200 words.

       FUNCTION INTRP1(XNORM,IYARR,ISIZE)

       DIMENSION IYARR(ISIZE)
       IXINT=INT(XNORM)            ! integer part of XNORM
       XFRAC=ABS(XNORM-IXINT)      ! fractional part of XNORM
       IY1=IYARR(IXINT)
       IY2=IYARR(IXINT+1)
       INTRP1=IY1+(IY2-IY1)*XFRAC          ! linear interpolation

       RETURN
       END
```

```
C  2-D INTERPOLATION FUNCTION
C  given X and Y values this routine returns a value for Z from
C  the 2-D array ZARRAY. X and Y must be normalised to real
C  numbers on the same scale as the array indices.
C  2-D interpolation is achieved by doing three 1-D interpolations

       FUNCTION  INTRP2(XNORM,YNORM,IZARR,IXSIZE,IYSIZE)

       DIMENSION IZARR(IXSIZE,IYSIZE)
       IXINT=INT(XNORM)              ! integer part of XNORM
       XFRAC=ABS(XNORM-IXINT)        ! fractional part of XNORM
       IYINT=INT(YNORM)
       YFRAC=ABS(YNORM-IYINT)

C  first 1-D interpolation, keeping Y constant

       IZ1=IZARR(IXINT,IYINT)
       IZ2=IZARR(IXINT+1,IYINT)
       Z3=IZ1+(IZ2-IZ1)*XFRAC          ! linear interpolation

C  second 1-D interpolation, keeping Y constant

       IZ1=IZARR(IXINT,IYINT+1)
       IZ2=IZARR(IXINT+1,IYINT+1)
       Z4=IZ1+(IZ2-IZ1)*XFRAC

C  final 1-D interpolation, keeping X constant

       INTRP2=Z3+(Z4-Z3)*YFRAC

       RETURN
```

ADC ROUTINE AND INTERPOLATION ROUTINES

APPENDIX 2 DYNAMIC DCE MODEL (DCESIM)

A dynamic model of the DCE was required for the transient control studies described in Section 7.3. Although a model was already available (DCETRAN) the author decided to write his own simplified model for the following reasons :

1. The numerous mistakes discovered in the DCETRAN code along with the total lack of comments destroyed all trust in that program.

2. It is easier to gain a conceptual grasp of a simple model.

3. The model is easier to modify and/or debug.

4. The model needs fewer parameters to define the particular DCE build.

5. The model runs more quickly and uses less memory space; this is particularly useful if long vehicle transients or frequency response tests are simulated.

This Appendix describes the resulting dynamic model for the DCE (DCESIM). The purpose is to provide a tool for transient modelling and transient control algorithm design. Unlike complex steady-state models the requirement is for the correct dynamic behaviour (form of response) rather than accurate thermodynamic data.

The principle dynamic and non-linear effects must be modelled fairly accurately. Individual components are modelled with arrays or simple equations representing empirically obtained characteristics. These include the principle non-linearities inherent in the DCE. The dynamics of the DCE are relatively simple comprising 2 inertial (acceleration) equations and 1 volume filling equation.

The program is designed to be easily understandable and hence straightforward to modify and debug. This is of prime importance for control algorithm development where many program modifications are likely. The code is split into three primary routines which interact with one another, and also call several secondary service routines (fig. 1). A main controlling routine handles all the terminal and disc

communications and runs the transient by successively calling the numerical integration subroutine (EULER). The integration routine in turn calls the model subroutine (DCEMOD) to obtain the rates of change of the DCE's three dynamic (state) variables. The state variables and their rates of change are held in two arrays : DCE and DCEDOT. These are passed between the main, integration, and model routines through CALL statements. The remainder of the non-dynamic variables calculated (or required) by the model subroutine are passed to (or from) the main routine via a COMMON block.

This arrangement has the advantage of separating the code for program control, numerical integration, and DCE modelling. A change of numerical method or modelling technique becomes a relatively simple task.

1. THE MAIN ROUTINE

The "main" routine is described by the flow-chart in fig. 2, and the attached program listing. Comprehensive comments are included within the code.

Data which is constant from one program run to the next is held in a data file on disc (DCEMOD.DAT). This includes empirical component characteristics, inertias, volumes, physical constants etc. Inputs which can vary for each transient are entered through the keyboard. These include control parameter settings, initial conditions, transient time etc.

The initial steady-state condition is obtained by repetitively calling EULER until a stable condition is converged upon. The transient is then run by calling EULER for the number of integration time steps (DT) making up a record interval, storing the transient data for that record interval, and then repeating the procedure until the transient is over.

After the transient is completed the user can request print and plot files on disc. Print-files are generated by the subroutine PROUT.

2. THE INTEGRATION SUBROUTINE

The numerical integration subroutine (EULER) is written in a standard fashion such that it may be used, without modification, for any simulation program. The predictor-corrector algorithm is employed, the

logic is shown by the flowchart in fig. 3. The dynamic "state vector" (X) or simply "state" is defined as those variables which describe the dynamic condition of the DCE, i.e. the variables which are the result of numerical integration.

First an initial estimate of the state at the next step (X_{n+1}) is calculated using the simple euler equation. Next the dynamic model (MODEL) is called to calculate the rate of change of state at the next time step ($\dot{X}_{n+1}$). Then the state at the next time step (X_{n+1}) is estimated using an average of $\dot{X}_n$ and $\dot{X}_{n+1}$. The last two steps are repeated until X_{n+1} converges. Finally, the old state is updated ($X_n = X_{n+1}$) in readiness for the next integration step.

3. THE MODEL SUBROUTINE

The dynamic model of the DCE is defined in subroutine DCEMOD. Given the DCE's dynamic state (DCE) this subroutine returns the rate of change of state (DCEDOT) for the numerical integration routine. The state vector DCE is an array containing the three dynamic variables : compressor speed, load speed and turbine inlet (volume) pressure. Other non-dynamic variables are passed between this routine and the main routine via a COMMON block.

The model is described by the diagram in fig 4 and the attached listing. Being a sequential set of calculations there is no particular advantage to be gained by providing a flow-chart.

1-D and 2-D interpolation functions are used by the DCEMOD subroutine, these are described in Appendix I .

Wherever empirical data is required, it has been obtained from DCETRAN for want of a better source. For the same reason, all empirical coefficients were chosen to match the program output with DCETRAN.

Engine airflow and, therefore, compressor and intercooler characteristics, have a first order effect on the match because of air-fuel ratio limiting fuel reduction. When suitable experimental results become available (including some transient response characteristics) the program should be re-matched.

The sub-models used for each component, including the assumptions made, are discussed below. The models are described in the same order as they occur in the calculations.

Compressor (Compair screw compressor)

Empirical data obtained from Compair has already been digitised for DCETRAN and other DCE programs on the mainframe. The same data is used for DCESIM. Compressor volume flow and work are stored in 2-D arrays as functions of pressure ratio and speed. The 2-D interpolation function RITRP2 is used to extract values. Compressor massflow and torque can then be calculated. Isentropic efficiency is obtained by first calculating isentropic outlet temperature and work. Actual outlet temperature can then be calculated.

Intercooler

The simple equations used by DCETRAN have been used. Until experimental results are available this will have to suffice.

Engine

Airflow through the engine is calculated from engine speed and inlet conditions using the perfect gas equation. Fuel per revolution (FPREV) and engine speed give fuel mass flow and hence overall air fuel ratio (AFR). If necessary FPREV is adjusted to limit AFR to a minimum of 20. Engine torque is split into three separate components : indicated torque, which is proportional to FPREV; speed proportional friction losses; and a fixed torque offset (TQENG = TQIND - TQFRIC - TQSTAT). Below an AFR of 30, indicated torque is also reduced linearly with AFR to model reducing combustion efficiency. The equation coefficients were chosen to match the program output with DCETRAN.

Exhaust temperature is calculated assuming that exhaust energy is 90% of engine output.

Bypass

The pressure drop through the bypass is assumed to be proportional to the square of bypass air velocity. Hence compressor delivery pressure is calculated from volume (turbine inlet) pressure.

Volume (Turbine Inlet) Temperature

The bulk volume temperature is assumed to be equal to the volume inlet temperature (fig. 4). This is calculated assuming perfect mixing of exhaust and bypass flows. In fact volume temperature will lag slightly behind inlet temperature during a transient because of the volume's energy storage capacity. Strictly speaking, the rate of volume temperature change should be calculated from the energy storage equation and numerically integrated. This approach requires more computation and is unlikely to increase accuracy because the volume entry and exit are not representative of the pipework boundaries where energy transfer actually occurs. For energy storage equations to be representative separate volumes should be used for each major change in gas temperature, i.e. four volumes should be used : post compressor, inlet manifold, exhaust manifold and turbine plenum (i.e. after mixing).

Turbine

The turbine is modelled by a single swallowing curve stored in a 1-D array. The pressure ratio axis is shifted vertically with non-dimensional turbine speed. Pressure ratios in the data-file are 1.3 below actual values. Given pressure ratio the 1-D interpolation function RITRP1 is used to obtain massflow. The figure extracted from the curve is a massflow per degree of nozzle angle which is then multiplied by the nozzle angle setting.

Volume Dynamics (Volume pressure)

Rate of change of volume pressure is derived from the perfect gas equation:-

$$\frac{dP}{dt} = \left(\frac{dM}{dt} RT + MR \frac{dT}{dt}\right) \frac{1}{V}$$

The rates of change of volume mass and temperature are calculated using the mass storage and energy storage equations respectively.

For constant Cp the energy storage equation can be written :-

$$\frac{dT_{VOL}}{dt} = \frac{\dot{M}_{IN} T_{IN} - \dot{M}_{OUT} T_{OUT}}{M_{VOL}}$$

However, in this case $T_{IN} = T_{OUT} = T_{VOL}$ (see vol. temp. calculation) so the equation reduces to :-

$$\frac{dT_{VOL}}{dt} = \frac{\left(\dot{M}_{IN} - \dot{M}_{OUT}\right) T_{VOL}}{M_{VOL}}$$

Inertia dynamics (compressor and load speed)

Load and compressor acceleration are calculated from their respective acceleration torques and inertias. Engine, compressor and turbine torque are available from previous calculations, load torque is a user input.

Annulus torque is obtained by subtracting engine acceleration torque (A_{ENG} * J_{ENG}) from developed torque. Hence planet carrier and sun torques are calculated using the epicyclic torque relationship.

Engine speed and acceleration are calculated from the epicyclic speed relationship.

4. USING THE PROGRAM

The data-file DCEMOD.DAT contains data which does not change for every program run. Variable descriptions are contained within the data-file, units that are not given can be determined by inspection of the variable notation and equations in the model subroutine (DCEMOD.FOR). To run the program simply type RUN DCESIM and then answer the questions that appear on the screen. Variable names displayed on the screen are defined in the variable notations at the beginning of DCESIM.FOR and DCEMOD.FOR.

The program asks the user for two control loop demands (PINDEM and NEDEM) and four control loop gains (K1,K2,K3,K4). Not all of these may be required depending on the control scheme modelled, any value may be entered for the redundant inputs.

Printout files are output to the printer using the PRINT command. Plot-files are output to the plotter using the DCEPLT program.

The data-file and FORTRAN source files can be changed using the editor utility. After editing and re-compiling a FORTRAN source file the program is linked using the command:-

LINK DCESIM, DCEMOD, EULER, RITRP1, RITRP2
(N.B. the subroutine PROUT is compiled with the main routine as 1 object file).

The program layout is such that the model can easily be changed by altering or replacing the subroutine DCEMOD. If the COMMON block variables are changed or added to, then corresponding modifications will be required in the main routine (DCESIM) (i.e. check all references to COMMON block variables including array DCEOUT).

The modifications made to DCEMOD to simulate control schemes A to D (see Section 7.3) have been included in the attached listings.

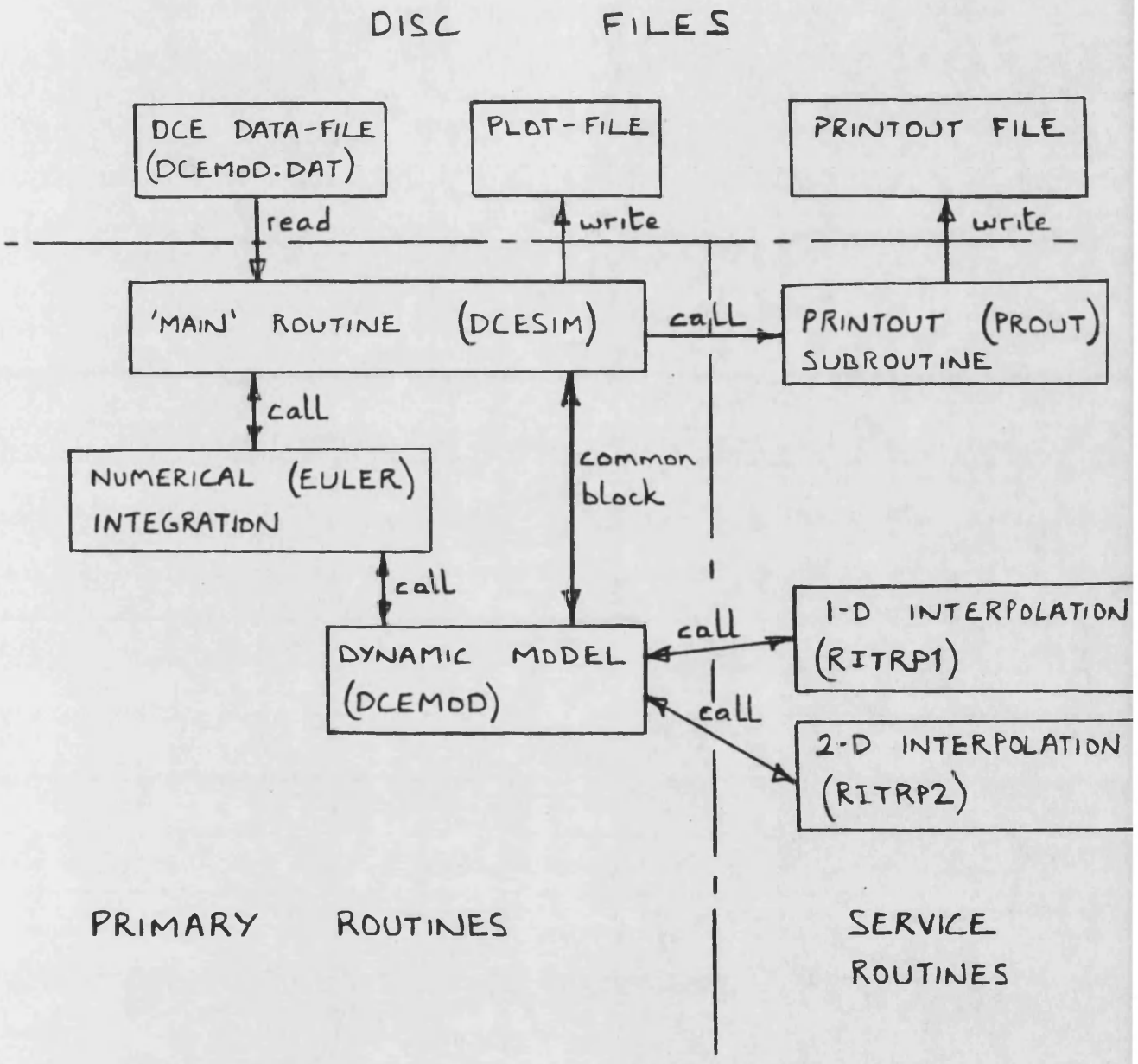

FIG 1. PROGRAM STRUCTURE

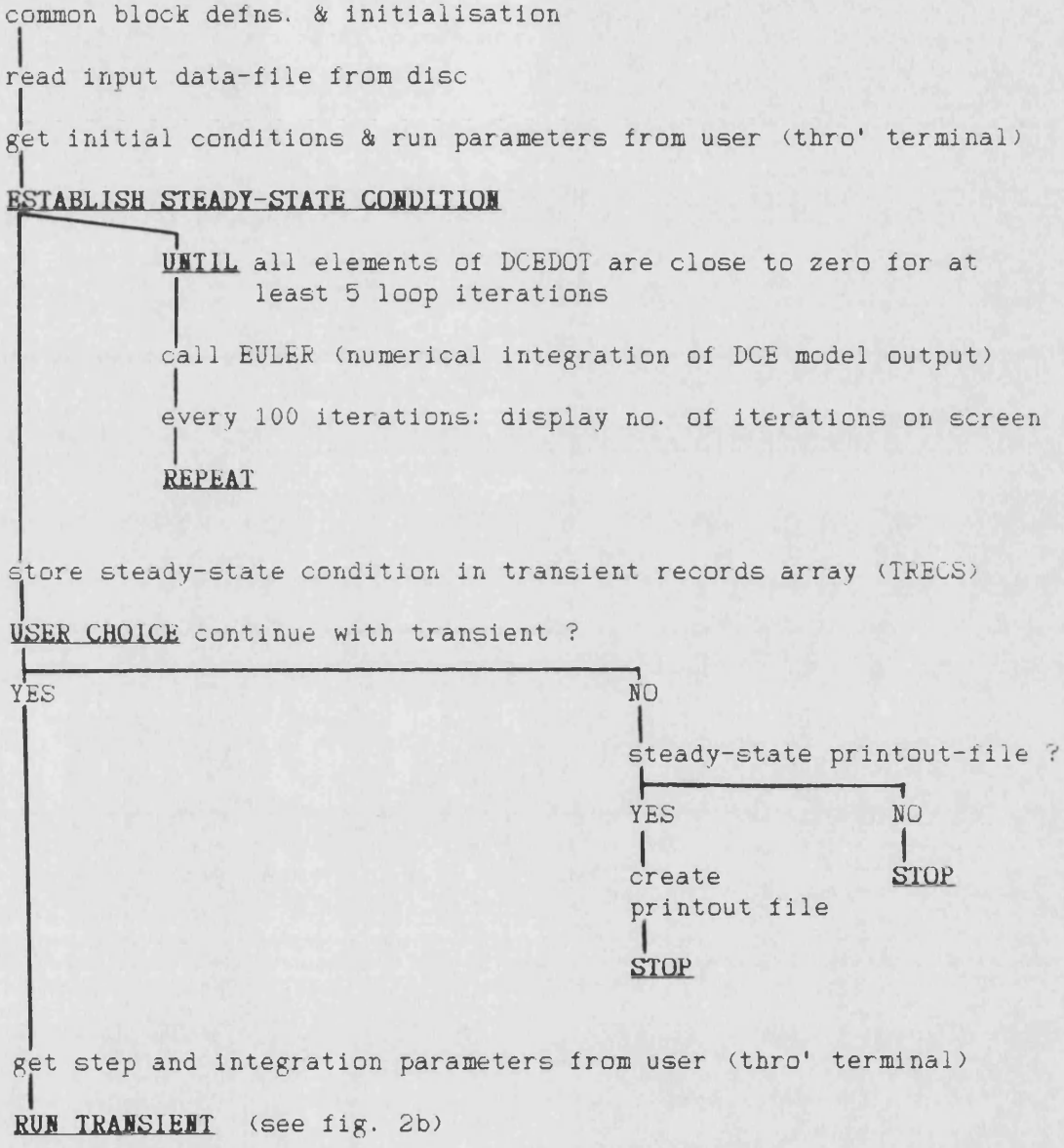

FIG. 2a **MAIN ROUTINE (DCESIM) FLOWCHART**

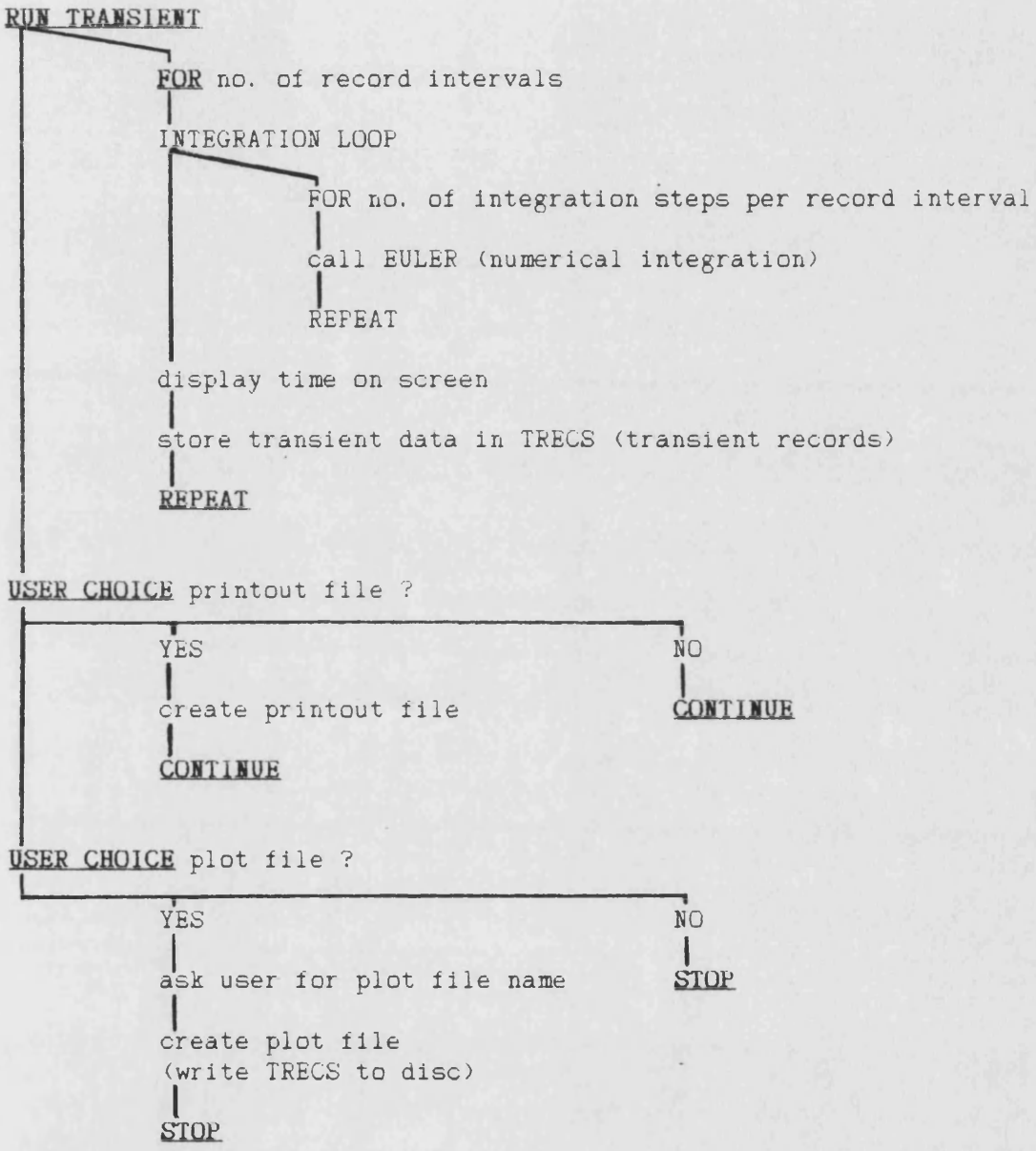

FIG. 2b **MAIN ROUTINE (DCESIM) FLOWCHART**

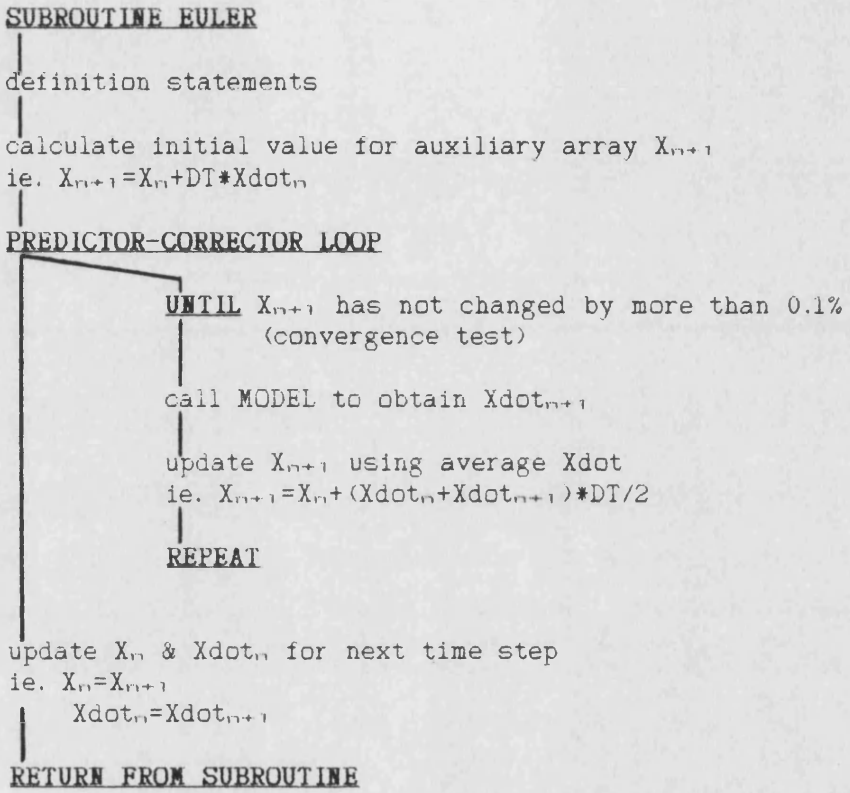

NB. X & Xdot are both arrays and Xdot=d/dt(X)

FIG. 3 NUMERICAL INTEGRATION ROUTINE (EULER) FLOWCHART

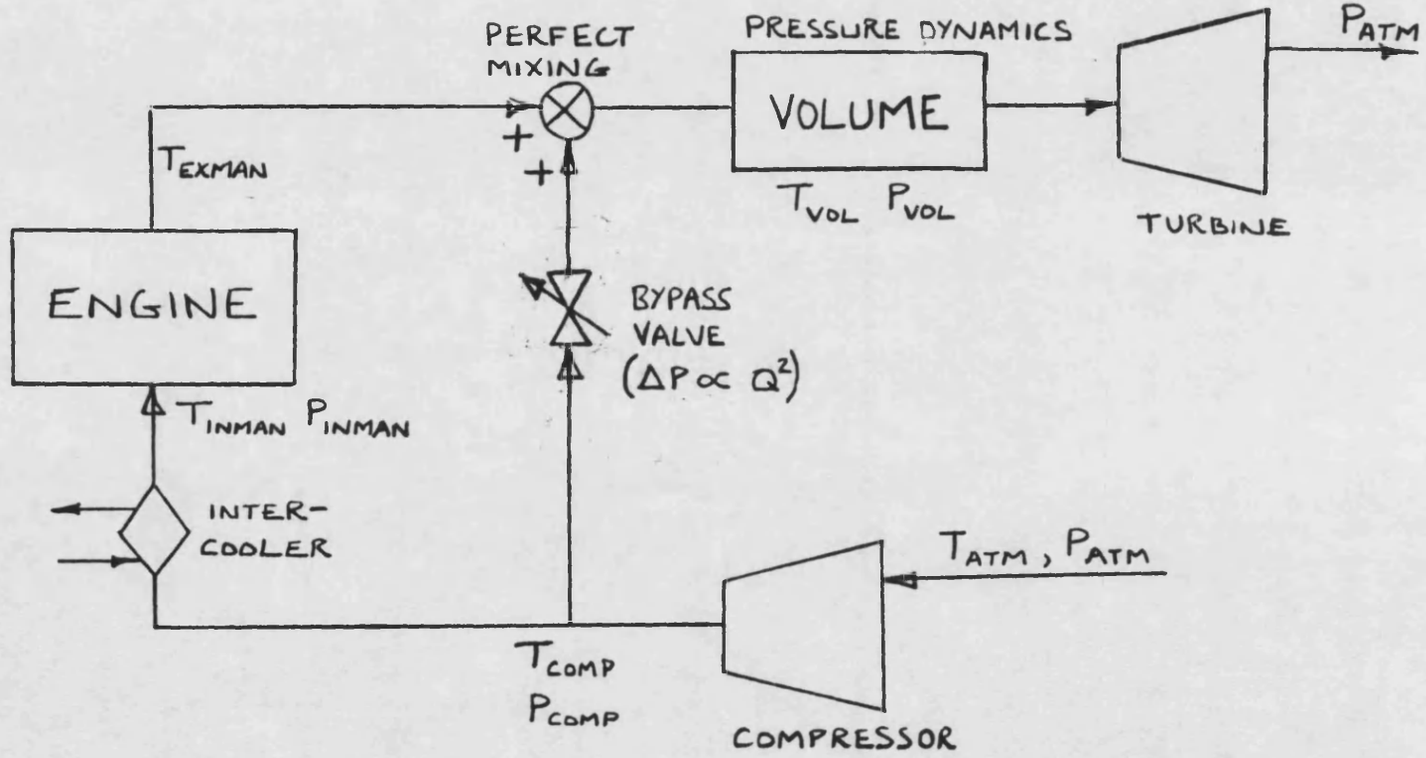

FIG 4. GAS PROPERTIES MODEL

```
C  TRANSIENT SIMULATION OF THE DCE (DCESIM)
C  ****************************************
C
C  written by D.Howard Nov'84
C  modified & matched to DCETRAN by D. Howard Apr'86
C
C  This program uses a simplified dynamic model of the DCE.
C
C  It is intended for transient control studies where the
C  speed and form of response (stability, overshoot etc.)
C  are more important than absolute thermodynamic accuracy.
C
C  The advantages of a simple model include:
C
C  1. It is easy to have a conceptual grasp of the model
C     as a whole, unlike a large complicated model.
C
C  2. The model is easier to modify and/or debug.
C
C  3. The model needs fewer parameters to define the particular
C     DCE build.
C
C  4. The model runs more quickly and uses less memory space,
C     this is particularly useful if long vehicle transients or
C     frequency response tests are simulated.
C
C  PROGRAM DESCRIPTION
C  -------------------
C
C  This program is the main controlling routine and performs the
C  following functions:
C
C  1. read fixed parameters from data file
C  2. read initial conditions from keyboard
C  3. establish steady-state by calling EULER and store in array
C  4. output steady-state results or proceed with transient
C  5. read transient parameters from keyboard
C  6. simulate transient by calling EULER and store data in array
C  7. output data to disc in form of printout or plot files
C
C  The following subroutines are used:
C
C  1. EULER   a numerical integration routine
C  2. DCEMOD  simple dynamic DCE model (called by EULER)
C  3. PROUT   writes a printout file to disc
C             (compiled with this main routine as one object file)
C  4. RITRP1  1-D linear interpolation routine
C  5. RITRP2  2-D linear interpolation routine
C
C  To link object files type:
C
C  LINK DCESIM,DCEMOD,EULER,RITRP1,RITRP2
C
C  VARIABLE NOTATION
C  -----------------
C
C  all model (DCE) variables are described in DCEMOD subroutine
C
C  DCE(3)          array describing dynamic state of DCE
C  DCEDOT(3)       rates of change of array 'DCE'
C  DCEOUT(30)      array containing non-dynamic output from DCEMOD
C  TRECS(40,100) transient records (one record every RECINT)...
C                  ..up to 40 variables, up to 100 records
C  DT              integration timestep
C  RECINT          recording interval
C  RUNTIM          transient run time
C  INREC           number of transient records stored in TRECS
C
C-------------------------------------------------------------------------
C
C
```

MAIN ROUTINE — DCESIM (1 OF 5)

```
      IMPLICIT REAL (A-H,J-Z)
      IMPLICIT INTEGER (I)
      BYTE FILE(11)                    !disc filename temporary store
      DIMENSION DCE(10),DCEDOT(10)     !only 10 to satisfy EULER dimensions
      VIRTUAL TRECS(40,100)
      EXTERNAL DCEMOD
C
C  common block variables which change with time
C  array DCEOUT is common with individual variables in DCEMOD subroutine
      COMMON DCEOUT(30)
C  common block variables which are constant whilst program is running
C  ie. can only be changed by editing data-file
      COMMON PATM,TATM,TCOOL
      COMMON JENG,JCOMP,JLOAD
      COMMON KTQC,KMC,KMINMA,KMF,KTQE,KFRIC,KBYPAS
      COMMON EFCOMP,EFTURB,EFCOOL
      COMMON CP,R,GAMMA
      COMMON CGR,OGR
      COMMON VOLUME,AREABY,TQSTAT
      COMMON MTARR(6),VFCARR(4,13),WCARR(4,13)
      COMMON K1,K2,K3,K4                                  !control gains
C  initial conditions
      DATA DCEDOT(1),DCEDOT(2),DCEDOT(3)/1.,1.,0./
      DATA FILE/11*0/
C
C-----------------------------------------------------------------------
C  READ INPUT DATA FILE
C-----------------------------------------------------------------------
C
      OPEN(UNIT=4,TYPE='OLD',NAME='DCEMOD.DAT')

      READ (4,401)
  401 FORMAT(//////)
      READ (4,*) (MTARR(I),I=1,6)
      READ (4,403)
  403 FORMAT(//////)
      DO 5 I=1,13
    5 READ (4,*) DUMMY,(VFCARR(I1,I),I1=1,4)
      READ (4,402)
  402 FORMAT(///)
      DO 6 I=1,13
    6 READ (4,*) DUMMY,(WCARR(I1,I),I1=1,4)
      READ (4,402)
      READ (4,*) KTQC,KMC,KMINMA,KMF,KTQE,KFRIC,KBYPAS
      READ (4,402)
      READ (4,*) EFCOMP,EFTURB,EFCOOL
      READ (4,402)
      READ (4,*) CGR,OGR,TGR
      READ (4,402)
      READ (4,*) JENG,JCOMP,JLOAD
      READ (4,402)
      READ (4,*) CP,R,GAMMA
      READ (4,402)
      READ (4,*) TCOOL,TATM,PATM,VOLUME,AREABY,TQSTAT

      CLOSE(UNIT=4)
```

MAIN ROUTINE — DCESIM (2 OF 5)

```
C
C-----------------------------------------------------------------
C  READ INITIAL CONDITIONS AND RUN PARAMETERS FROM TERMINAL
C-----------------------------------------------------------------
C
      TYPE 700
  700 FORMAT(//' integration step:'//' DT')
      ACCEPT *,DT
      TYPE 701
  701 FORMAT(//' enter initial conditions:'//' NCOMP,NLOAD,PVOL
     &,PCOMP')
      ACCEPT *,(DCE(I),I=1,3),DCEOUT(5)
      TYPE 702
  702 FORMAT(//' enter run parameters:'//' EPREV,NOZ,TGR,TQLOAD')
      ACCEPT *,DCEOUT(24),DCEOUT(26),DCEOUT(28),DCEOUT(13)
      TYPE 706
  706 FORMAT(//' enter control demands:'//' PINDEM,NEDEM')
      ACCEPT *,DCEOUT(29),DCEOUT(30)
      TYPE 709
  709 FORMAT(//' enter control gains:'//' K1,K2,K3,K4')
      ACCEPT *,K1,K2,K3,K4
C
C-----------------------------------------------------------------
C  ESTABLISH STEADY-STATE CONDITION
C  defined by DCEDOT elements being close to zero for five
C  integration periods DT; flag is zero when steady-state reached
C-----------------------------------------------------------------
C
      ICOUNT=0                                  !itteration counter
      ISFLAG=5                                  !convergence flag
   10 CALL EULER(DCE,DCEDOT,3,DT,DCEMOD)
      ICOUNT=ICOUNT+1
      ITYPE=ICOUNT/100                          !type every 100
      IF (ITYPE*100.EQ.ICOUNT) TYPE 730, ICOUNT
  730 FORMAT('+',I4,' itterations')
      IF (ABS(DCEDOT(1)).GT.5) GOTO 10
      IF (ABS(DCEDOT(2)).GT.5) GOTO 10
      IF (ABS(DCEDOT(3)).GT.0.1) GOTO 10
      ISFLAG=ISFLAG-1
      IF (ISFLAG.GT.0) GOTO 10
C
C-----------------------------------------------------------------
C  STORE STEADY-STATE DATA IN 'TRECS' ARRAY
C-----------------------------------------------------------------
C
      TRECS(1,1)=0            !time = zero
      DO 15 I=1,3             !DCE & DCEDOT arrays
      TRECS(I*2,1)=DCE(I)
   15 TRECS(I*2+1,1)=DCEDOT(I)
      DO 16 I=8,37            !data passed thro' COMMON
   16 TRECS(I,1)=DCEOUT(I-7)
C
C-----------------------------------------------------------------
C  OUTPUT STEADY-STATE RESULTS OR PROCEED WITH TRANSIENT
C-----------------------------------------------------------------
C
      TYPE 703
  703 FORMAT(//' run transient Y or N  ',$)
      ACCEPT 500,ANS
  500 FORMAT(A1)
      IF (ANS.EQ.'Y') GOTO 20
      TYPE 707                          !printout file ??
      ACCEPT 500,ANS
      IF (ANS.NE.'Y') GOTO 18
      CALL PROUT(1,TRECS,DT,0.,K1,K2,K3,K4)   !call printout routine
   18 STOP 'program halted after reaching steady-state condition'
C
C-----------------------------------------------------------------
C  READ STEP AND INTEGRATION PARAMETERS FROM TERMINAL
C-----------------------------------------------------------------
C
   20 TYPE 704
  704 FORMAT(//' enter transient parameters:'//' RECINT,RUNTIM')
      ACCEPT *,RECINT,RUNTIM
      TYPE 705
  705 FORMAT(//' enter step parameters:'//' EPREV,NOZ,TGR,TQLOAD')
      ACCEPT *,DCEOUT(24),DCEOUT(26),DCEOUT(28),DCEOUT(13)
      TYPE 710
  710 FORMAT(//' enter NEW control demands:'//' PINDEM,NEDEM')
      ACCEPT *,DCEOUT(29),DCEOUT(30)
```

MAIN ROUTINE — DCESIM (3 OF 5)

```
C
C-----------------------------------------------------------------
C  RUN TRANSIENT
C-----------------------------------------------------------------
C
      INREC=RUNTIM/RECINT+1    !no. of records of transient data
      INSTEP=RECINT/DT         !no. of integration steps per record
C
C  execute transient loop every record interval
C  ---------------------------------------------
C
      DO 40 IREC=2,INREC
C  integrate over recording interval
C  ie. call EULER
      DO 30 I=1,INSTEP
   30 CALL EULER(DCE,DCEDOT,3,DT,DCEMOD)
C  store transient data in 'TRECS' array
      TIME=(IREC-1)*RECINT
      TYPE 731, TIME                    !type time
  731 FORMAT('+TIME = ',G11.4)
      TRECS(1,IREC)=TIME                !record time
      DO 35 I=1,3                       !DCE & DCEDOT arrays
      TRECS(I*2,IREC)=DCE(I)
   35 TRECS(I*2+1,IREC)=DCEDOT(I)
      DO 40 I=8,37                      !data in COMMON block
   40 TRECS(I,IREC)=DCEOUT(I-7)
C
C
C-----------------------------------------------------------------
C  DATA PRINTOUT OR GRAPH PLOTS
C-----------------------------------------------------------------
C
      TYPE 707
  707 FORMAT(//' printout file Y or N  ',$)
      ACCEPT 500,ANS
      IF (ANS.NE.'Y') GOTO 50
      CALL PROUT(INREC,TRECS,DT,RUNTIM,K1,K2,K3,K4)
   50 TYPE 708
  708 FORMAT(//' plot file Y or N  ',$)
      ACCEPT 500,ANS
      IF (ANS.NE.'Y') GOTO 100
      TYPE 721
  721 FORMAT(//' enter plot file name')
      ACCEPT 510, (FILE(I),I=1,10)
  510 FORMAT(10A1)
      OPEN(UNIT=4,TYPE='NEW',NAME=FILE)
      DO 60 IREC=1,INREC
   60 WRITE(4,*) (TRECS(I,IREC),I=1,37)
      CLOSE (UNIT=4)
  100 STOP 'program halted after running transient'

      END

C
C-----------------------------------------------------------------
C  PRINTOUT SUBROUTINE
C-----------------------------------------------------------------
C
C  input variables:
C  INREC        no. of records to be printed
C  TRECS        array of records
C  DT           integration time step
C  RUNTIM       simulation run time
C  K1,K2,K3,K4  control algorithm gains
C

      SUBROUTINE PROUT(INREC,TRECS,DT,RUNTIM,K1,K2,K3,K4)

      IMPLICIT REAL (A-H,J-Z)
      IMPLICIT INTEGER (I)
      VIRTUAL TRECS(40,100)
      BYTE FILE(11)                     !disc filename temporary store
      DATA FILE/11*0/

      TYPE 720
  720 FORMAT(//' enter printout file name')
      ACCEPT 510, (FILE(I),I=1,10)
  510 FORMAT(10A1)
      OPEN(UNIT=4,TYPE='NEW',NAME=FILE)
      TYPE 725
  725 FORMAT(//' enter printout frequency')
      ACCEPT *,IFREQ
      INPRT=(INREC-1)/IFREQ+1           !no. of printed records
      INPAGE=INPRT/5+1                  !number of pages
      IF ((INPAGE-1)*5.EQ.INPRT) INPAGE=INPAGE-1   !all pages full
      DO 10 IPAGE=1,INPAGE              !one loop iteration per page
      IFCOL=(IPAGE-1)*5*IFREQ+1         !record no. in first column
      ILCOL=INPRT*IFREQ                 !record no. in last column
      IF (INPRT.GT.5*IPAGE) ILCOL=5*IPAGE*IFREQ
```

MAIN ROUTINE – DCESIM (4 OF 5)

```
C
C  Print one page
C
      WRITE(4,600) IPAGE,DT,RUNTIM,INREC,K1,K2,K3,K4
  600 FORMAT(//' PAGE ',I2,': TRANSIENT RESULTS
     & FROM DCESIM PROGRAM'/' DT=',G11.4,' RUNTIM=',G11.4,
     &' INREC=',I4/' K1=',G11.4,' K2=',G11.4,' K3=',G11.4,
     &' K4=',G11.4//)
      WRITE(4,601) (TRECS(1,I),I=IFCOL,ILCOL,IFREQ)   !Print one row
  601 FORMAT(' time (sec.)      ',5(1x,G11.4))
      WRITE(4,602)(TRECS(2,I),I=IFCOL,ILCOL,IFREQ)    !Print one row
  602 FORMAT(' Ncomp (rpm)      ',5(1x,G11.4))
      WRITE(4,603)(TRECS(3,I),I=IFCOL,ILCOL,IFREQ)    !Print one row
  603 FORMAT(' Acomp (rpm/sec)  ',5(1x,G11.4))
      WRITE(4,604)(TRECS(4,I),I=IFCOL,ILCOL,IFREQ)    !Print one row
  604 FORMAT(' Nload (rpm))     ',5(1x,G11.4))
      WRITE(4,605)(TRECS(5,I),I=IFCOL,ILCOL,IFREQ)    !Print one row
  605 FORMAT(' Aload (rpm/sec.) ',5(1x,G11.4))
      WRITE(4,606)(TRECS(6,I),I=IFCOL,ILCOL,IFREQ)    !Print one row
  606 FORMAT(' Pvol (Bar)       ',5(1x,G11.4))
      WRITE(4,607)(TRECS(7,I),I=IFCOL,ILCOL,IFREQ)    !Print one row
  607 FORMAT(' Pvodot (Bar/sec.)',5(1x,G11.4))
      WRITE(4,608)(TRECS(8,I),I=IFCOL,ILCOL,IFREQ)    !Print one row
  608 FORMAT(' Neng  (rpm)      ',5(1x,G11.4))
      WRITE(4,609)(TRECS(9,I),I=IFCOL,ILCOL,IFREQ)    !Print one row
  609 FORMAT(' Aeng  (rpm/sec.) ',5(1x,G11.4))
      WRITE(4,610)(TRECS(10,I),I=IFCOL,ILCOL,IFREQ)   !Print one row
  610 FORMAT(' Ntrb(rpm/sqrt(T))',5(1x,G11.4))
      WRITE(4,611)(TRECS(11,I),I=IFCOL,ILCOL,IFREQ)   !Print one row
  611 FORMAT(' Air/fuel ratio   ',5(1x,G11.4))
      WRITE(4,612)(TRECS(12,I),I=IFCOL,ILCOL,IFREQ)   !Print one row
  612 FORMAT(' Pcomp  (Bar)     ',5(1x,G11.4))
      WRITE(4,613)(TRECS(13,I),I=IFCOL,ILCOL,IFREQ)   !Print one row
  613 FORMAT(' Pinman (Bar)     ',5(1x,G11.4))
      WRITE(4,614)(TRECS(14,I),I=IFCOL,ILCOL,IFREQ)   !Print one row
  614 FORMAT(' TQeng (Nm)       ',5(1x,G11.4))
      WRITE(4,615)(TRECS(15,I),I=IFCOL,ILCOL,IFREQ)   !Print one row
  615 FORMAT(' TQann (Nm)       ',5(1x,G11.4))
      WRITE(4,616)(TRECS(16,I),I=IFCOL,ILCOL,IFREQ)   !Print one row
  616 FORMAT(' TQsun (Nm)       ',5(1x,G11.4))
      WRITE(4,617)(TRECS(17,I),I=IFCOL,ILCOL,IFREQ)   !Print one row
  617 FORMAT(' TQpc  (Nm)       ',5(1x,G11.4))
      WRITE(4,618)(TRECS(18,I),I=IFCOL,ILCOL,IFREQ)   !Print one row
  618 FORMAT(' TQcomp (Nm)      ',5(1x,G11.4))
      WRITE(4,619)(TRECS(19,I),I=IFCOL,ILCOL,IFREQ)   !Print one row
  619 FORMAT(' TQturb (Nm)      ',5(1x,G11.4))
      WRITE(4,620)(TRECS(20,I),I=IFCOL,ILCOL,IFREQ)   !Print one row
  620 FORMAT(' TQload (Nm)      ',5(1x,G11.4))
      WRITE(4,621)(TRECS(21,I),I=IFCOL,ILCOL,IFREQ)   !Print one row
  621 FORMAT(' TQout (Nm)       ',5(1x,G11.4))
      WRITE(4,622)(TRECS(22,I),I=IFCOL,ILCOL,IFREQ)   !Print one row
  622 FORMAT(' Mcomp (Kg/min)   ',5(1x,G11.4))
      WRITE(4,623)(TRECS(23,I),I=IFCOL,ILCOL,IFREQ)   !Print one row
  623 FORMAT(' Minman  (Kg/min) ',5(1x,G11.4))
      WRITE(4,624)(TRECS(24,I),I=IFCOL,ILCOL,IFREQ)   !Print one row
  624 FORMAT(' Mfuel (kg/min)   ',5(1x,G11.4))
      WRITE(4,625)(TRECS(25,I),I=IFCOL,ILCOL,IFREQ)   !Print one row
  625 FORMAT(' Mturb (kg/min)   ',5(1x,G11.4))
      WRITE(4,626)(TRECS(26,I),I=IFCOL,ILCOL,IFREQ)   !Print one row
  626 FORMAT(' Tinman (deg.K)   ',5(1x,G11.4))
      WRITE(4,627)(TRECS(27,I),I=IFCOL,ILCOL,IFREQ)   !Print one row
  627 FORMAT(' Texman (deg.K)   ',5(1x,G11.4))
      WRITE(4,628)(TRECS(28,I),I=IFCOL,ILCOL,IFREQ)   !Print one row
  628 FORMAT(' Tcomp  (deg.K)   ',5(1x,G11.4))
      WRITE(4,629)(TRECS(29,I),I=IFCOL,ILCOL,IFREQ)   !Print one row
  629 FORMAT(' Tvol   (deg.K)   ',5(1x,G11.4))
      WRITE(4,630)(TRECS(30,I),I=IFCOL,ILCOL,IFREQ)   !Print one row
  630 FORMAT(' Tvodot(deg.K/min)',5(1x,G11.4))
      WRITE(4,631)(TRECS(31,I),I=IFCOL,ILCOL,IFREQ)   !Print one row
  631 FORMAT(' FPREV  (         ',5(1x,G11.4))
      WRITE(4,632)(TRECS(32,I),I=IFCOL,ILCOL,IFREQ)   !Print one row
  632 FORMAT(' FPREVA (         ',5(1x,G11.4))
      WRITE(4,633)(TRECS(33,I),I=IFCOL,ILCOL,IFREQ)   !Print one row
  633 FORMAT(' NOZ (deg.)       ',5(1x,G11.4))
      WRITE(4,634)(TRECS(34,I),I=IFCOL,ILCOL,IFREQ)   !Print one row
  634 FORMAT(' NOZA (deg.)      ',5(1x,G11.4))
      WRITE(4,635)(TRECS(35,I),I=IFCOL,ILCOL,IFREQ)   !Print one row
  635 FORMAT(' turb. gear ratio ',5(1x,G11.4))
      WRITE(4,636)(TRECS(36,I),I=IFCOL,ILCOL,IFREQ)   !Print one row
  636 FORMAT(' PINDEM (Bar)     ',5(1x,G11.4))
      WRITE(4,637)(TRECS(37,I),I=IFCOL,ILCOL,IFREQ)   !Print one row
  637 FORMAT(' NEDEM (rpm)      ',5(1x,G11.4))

  10  CONTINUE
      CLOSE (UNIT=4)
      RETURN

      END
```

MAIN ROUTINE — DCESIM (5 OF 5)

```
C
C*************************************************************************
C  NUMERICAL INTEGRATION OF ARRAY 'XDOT' UPDATING ARRAY 'X'
C  XDOT is obtained from subroutine MODEL and
C  integrated using the predictor-corrector method
C*************************************************************************
C
C  VARIABLE LIST:
C  X             state-vector (array representing models dynamic state)
C  XDOT          rates of change of X with time
C  X1            X at step n+1
C  XDOT1         XDOT at step n+1
C  ISIZE         size of above arrays
C  DT            time step used for integration
C  MODEL         subroutine used to obtain XDOT at state X
C
      SUBROUTINE EULER(X,XDOT,ISIZE,DT,MODEL)

      IMPLICIT REAL (A-H,J-Z)
      IMPLICIT INTEGER (I)
      DIMENSION X(10),XDOT(10),X1(10),XDOT1(10),X1NEW(10)
      EXTERNAL MODEL
C
C-------------------------------------------------------------------------
C  using X and XDOT at step n
C  calculate auxiliary array X1 at step n+1
C-------------------------------------------------------------------------
C
      DO 10 I=1,ISIZE
 10   X1(I)=X(I)+DT*XDOT(I)
C
C-------------------------------------------------------------------------
C  PREDICTOR-CORRECTOR LOOP
C  Call MODEL to obtain auxiliary array XDOT1 at step n+1.
C  Recalculate auxiliary array X1 at step n+1 using average XDOT
C  Repeat process until convergence obtained.
C-------------------------------------------------------------------------
C
 15   CALL MODEL(X1,XDOT1)
      DO 20 I=1,ISIZE                !update X1 using average XDOT
 20   X1NEW(I)=X(I)+(DT/2)*(XDOT(I)+XDOT1(I))

C-------------------------------------------------------------------------
C  test for convergence
      DO 22 I=1,ISIZE
      ERROR=ABS((X1NEW(I)-X1(I))/X1(I))       !convergence error
 22   IF (ERROR.GT.0.001) GOTO 25             !continue itterating
      GOTO 35                                 !leave pred-corr loop
C-------------------------------------------------------------------------
 25   DO 30 I=1,ISIZE                !reset X1 array for next itteration
 30   X1(I)=X1NEW(I)
      GOTO 15
C
C-------------------------------------------------------------------------
C  update X and XDOT for next time step
C-------------------------------------------------------------------------
C
 35   DO 40 I=1,ISIZE
      X(I)=X1NEW(I)
 40   XDOT(I)=XDOT1(I)

      RETURN
      END
```

INTEGRATION SUBROUTINE (EULER)

```
C  SIMPLE DYNAMIC MODEL FOR DCE
C  ****************************
C
C  written by D.Howard Nov'84
C  modified & matched to DCETRAN by D.Howard Apr'86
C
C  version 1:
C  *********
C
C  This subroutine is a simplified dynamic model of the DCE.
C  It is designed to be called by a numerical integration routine
C  which then integrates the calculated rates of change.
C
C  dynamic equations give :
C  ----------------------
C  1. compressor acceleration
C  2. output acceleration
C  3. rate of pressure change in volume
C
C  all other variables are calculated using simple approximations
C  which assume no dynamics ie. no time lag between inputs and
C  outputs.
C
C  assumptions:
C  -----------
C  single volume (turbine plenum)
C  perfect mixing at junction before volume (exhaust with bypass)
C  volume bulk temp. = volume inlet temp.
C  planet inertias neglected
C  planet losses neglected
C
C  variable notation:
C  -----------------
C  DCE(3)        array describing dynamic state of DCE.
C  DCEDOT(3)     rates of change of array 'DCE'
C    array elements:
C                  1   NCOMP & ACOMP
C                  2   NLOAD & ALOAD
C                  3   PVOL  & PVODOT
C  TQ            torques (Nm)
C  W             powers (usually KW/60)
C  N             speeds (rpm)
C  A             acceleration (rpm/sec)
C  P             absolute pressures (Bar)
C  PR            pressure ratio
C  M             massflows (kg/min)
C  VF            volume flow (cubic ft./min)
C  VEL           air velocity (m/sec)
C  T             temperatures (deg.K)
C  R             perfect gas constant (KJ/kg degK)
C  CP            specific heat (KJ/kg degK)
C  GAMMA         CP/CV
C  J             inertias (Nm.sec/rpm)
C  K             linear gains (output/input)
C  EF            efficiency
C  RO            density (kg/m**3)
C  AREA          area (m**2)
C  VOLUME        volume capacity (litres)
C  VOMASS        mass stored in volume
C  FPREV         fuel per rev. (kg./10000)
C  FPREVA        adjusted FPREV (to limit AFR)
C  NOZ           user defined (fixed) nozzle angle (degrees)
C  NOZA          actual nozzle angle (when adjusted by control scheme)
C
C  suffix notation:
C  ---------------
C  ENG           engine
C  ANN           annulus
C  SUN           sun
C  PC            planet carrier
C  COMP          compressor
C  TURB          turbine
C  LOAD          load parameters
C  OUT           output-shaft conditions
C  BYPAS         bypass conditions
C  ATM           atmospheric conditions
C  VOL           conditions in volume
C  FUEL          fuel
C  INMAN         conditions in inlet manifold
C  EXMAN         conditions in exhaust manifold
C  COOL          intercooler cooling medium
C  IND           indicated
C  FRIC          friction
C  STAT          static (fixed) offset
C  DOT           rate of change w.r.t. time
C  ARR           signifies array name
C
```

SUBROUTINE DCEMOD (1 OF 3)

```
C-----------------------------------------------------------------------
C SPECIFICATION STATEMENTS, COMMONS, INITIALISATION
C-----------------------------------------------------------------------
C
      SUBROUTINE DCEMOD(DCE,DCEDOT)
C
      IMPLICIT REAL (A-H,J-Z)
      IMPLICIT INTEGER (I)
      INTEGER MTSIZE
      DIMENSION DCE(3),DCEDOT(3)
C
C  common block variables which change with time
      COMMON NENG,AENG,NTURB,AFR,PCOMP,PINMAN
      COMMON TQENG,TQANN,TQSUN,TQPC,TQCOMP,TQTURB,TQLOAD,TQOUT
      COMMON MCOMP,MINMAN,MFUEL,MTURB
      COMMON TINMAN,TEXMAN,TCOMP,TVOL,TVODOT
      COMMON FPREV,FPREVA,NOZ,NOZA,TGR
      COMMON PINDEM,NEDEM
C
C  common block variables which are constant for each run
      COMMON PATM,TATM,TCOOL
      COMMON JENG,JCOMP,JLOAD
      COMMON KTQC,KMC,KMINMA,KMF,KTQE,KFRIC,KBYPAS
      COMMON EFCOMP,EFTURB,EFCOOL
      COMMON CP,R,GAMMA
      COMMON CGR,QGR
      COMMON VOLUME,AREABY,TQSTAT
      COMMON MTARR(6),VFCARR(4,13),WCARR(4,13)
      COMMON K1,K2,K3,K4
C
      DATA MTSIZE,AENG/6,1./          !initialise: size of MTARR
C                                                  engine accl.
C-----------------------------------------------------------------------
C  RENAME DYNAMIC STATE VARIABLES (TO HELP PROGRAM READABILITY)
C-----------------------------------------------------------------------
C
      NCOMP=DCE(1)
      NLOAD=DCE(2)
      PVOL=DCE(3)
C
C-----------------------------------------------------------------------
C  COMPRESSOR CALCULATIONS -- EMPIRICAL DATA PULLED FROM 2-D ARRAYS
C-----------------------------------------------------------------------
C
      PRCOMP=PCOMP/PATM
C  check array indices are within limits and normalise for
C  2-D interpolation subroutine
      IF (NCOMP.LT.-200.) STOP 'program halted -- NCOMP too low'
      IF (NCOMP.GE.14200.) STOP 'program halted -- NCOMP too high'
      IF (PRCOMP.LT.-0.0343) STOP 'program halted -- PRCOMP too low'
      IF (PRCOMP.GE.4.1033) STOP 'program halted --PRCOMP too high'
      NCNORM=(NCOMP+200.)/4800.+1.
      PRNORM=(PRCOMP+0.0343)/0.3448+1.
C  calculate compressor massflow
      VFCOMP=RITRP2(NCNORM,PRNORM,VFCARR,4,13)        !cubic ft./min
      RO=PATM*100/(R*TATM)                            !density
      MCOMP=VFCOMP*0.02832*RO                         !Kg/min
C  compressor work and hence torque
      WCOMP=0.7457*60*RITRP2(NCNORM,PRNORM,WCARR,4,13)       !KW/60
      TQCOMP=WCOMP*1000/(NCOMP*2*3.1412)              !comp. torque Nm
C  isentropic outlet temp., comp. work and hence efficiency
      TCOMP=TATM*(PRCOMP)**((GAMMA-1)/GAMMA)    !isentropic outlet temp.
      WCISEN=MCOMP*CP*(TCOMP-TATM)              !isentropic work
      EFCOMP=WCISEN/WCOMP                       !isentropic efficiency
C  calculate actual outlet temp. using isentropic efficiency
      TCOMP=TATM+(TCOMP-TATM)/EFCOMP
C
C-----------------------------------------------------------------------
C  INTERCOOLER
C-----------------------------------------------------------------------
C
      PINMAN=0.95*PCOMP                         !DCETRAN equation
      TINMAN=TCOMP-EFCOOL*(TCOMP-TCOOL)         !DCETRAN equation
C
C-----------------------------------------------------------------------
C  ENGINE EQUATIONS
C-----------------------------------------------------------------------
C
      NENG=NCOMP/CGR+NLOAD/QGR          !speed from epicyclic equation
C  airflow thro' engine from perfect gas equation
      MINMAN=KMINMA*PINMAN*NENG/TINMAN
      FPREVA=FPREV                      !adjusted FPREV
      MFUEL=KMF*FPREVA*NENG             !fuel masssflow
      AFR=MINMAN/MFUEL                  !air-fuel ratio (NOT TRAPPED)
C  adjust fuelling to limit air-fuel ratio to a minimum of 20
```

SUBROUTINE DCEMOD (2 OF 3)

```
C  adjust fuelling to limit air-fuel ratio to a minimum of 20
        IF (AFR.GE.20.) GOTO 5
        AFR=20.
        MFUEL=MINMAN/20.
        EPREVA=MFUEL/(KMF*NENG)
C  relative efficiency drops linearly with AFR below AFR=30
  5     IF (AFR.LT.30.) EFREL=1-0.003*(30.-AFR)
C  engine torque proportional to EPREV and relative efficiency EFREL
        TQIND=KTQE*EPREVA*EFREL          !indicated torque
        TQFRIC=KFRIC*NENG                !friction torque
        TQENG=TQIND-TQFRIC-TQSTAT        !brake torque
        WENG=TQENG*NENG*2*3.142/1000.    !engine power in  KW/60
        MEXMAN=MINMAN+MFUEL
        TEXMAN=0.9*WENG/(CP*MEXMAN)+TINMAN !power to exh.=0.9*engine power
C
C-------------------------------------------------------------------------
C  BYPASS CALCULATIONS
C-------------------------------------------------------------------------
C
        MBYPAS=MCOMP-MINMAN                      !bypass mass flow
        RO=PCOMP*100/(R*TCOMP)                   !density of air in bypass
        VELBYP=MBYPAS/(AREABY*RO*60)             !air velocity in bypass
        PCOMP=PVOL+KBYPAS*VELBYP**2              !PVOL + pr. drop in bypass
C
C-------------------------------------------------------------------------
C  VOLUME TEMPERATURE ASSUMING CONSTANT Cp
C  AND PERFECT MIXING OF EXHAUST & BYPASS FLOW
C-------------------------------------------------------------------------
C
        TVOL=(MEXMAN*TEXMAN+MBYPAS*TCOMP)/(MCOMP+MFUEL)
C
C-------------------------------------------------------------------------
C  TURBINE CALCULATIONS
C-------------------------------------------------------------------------
C
C  no transient control
        NOZA=NOZ
        NTURB=NLOAD*TGR/SQRT(TVOL)       !non-dimensional turbine speed
C  shift pressure ratio axis linearly with speed
        PTURB=PVOL/PATM-1.3-(NTURB-1675)*0.05/100.
        MTURB=37.4*NOZA                  !chokes when PTURB is over 1.25
        IF (PTURB.GE.1.25) GOTO 10
        IF (PTURB.LT.0) PTURB=0
        PTNORM=PTURB/0.25+1.
C  massflow from turbine swallowing capacity curve
        MTURB=RITRP1(PTNORM,MTARR,MTSIZE)*NOZA  !non-dimensional massflow
 10     MTURB=MTURB*PVOL/SQRT(TVOL)             !Kg/min
C  turbine work (KW/60) were EFTURB=isetropic efficiency
        WTURB=MTURB*CP*TVOL*(1-PATM/PVOL**((GAMMA-1)/GAMMA))*EFTURB
        TQTURB=WTURB*1000/(NLOAD*2*3.1412)       !turbine torque in Nm
C
C-------------------------------------------------------------------------
C  RATE OF CHANGE OF PRESSURE WITH TIME (VOLUME DYNAMICS)
C-------------------------------------------------------------------------
C
C  mass stored in volume from perfect gas equation
        VOMASS=(PVOL*VOLUME)/(R*TVOL*10.)                        !kg
C  rate of change of VOMASS (mass storage equation)
        VOMDOT=(MCOMP+MFUEL-MTURB)                               !Kg/min
C  rate of change of TVOL (energy storage equation)
        TVODOT=(MEXMAN*TEXMAN+MBYPAS*TCOMP-MTURB*TVOL)/VOMASS    !deg.K/min
C  rate of change of PVOL from VOMDOT and TVODOT..
C  ..combined with perfect gas equation
        PVODOT=(VOMDOT*R*TVOL+TVODOT*R*VOMASS)/(VOLUME*6)    !Bar/sec
C
C-------------------------------------------------------------------------
C  TORQUE AND ACCELERATION EQUATIONS (INERTIA DYNAMICS)
C-------------------------------------------------------------------------
C
        TQANN=TQENG-AENG*JENG    !developed torque - acceleration torque
        TQSUN=0.96*TQANN/CGR     !epicyclic equations
        TQPC=TQANN/CGR
        TQOUT=TQPC*0.96+TQTURB*0.92      !developed output torque
C  acceleration equations (inertia dynamics)
        ACOMP=(TQSUN-TQCOMP)/JCOMP               !RPM/sec
        ALOAD=(TQOUT-TQLOAD)/JLOAD
        AENG=ACOMP/CGR+ALOAD/OGR         !acc. from epicyclic equation
C
C-------------------------------------------------------------------------
C  ASSIGN RATES OF CHANGE TO ARRAY DCEDOT
C-------------------------------------------------------------------------
C
        DCEDOT(1)=ACOMP
        DCEDOT(2)=ALOAD
        DCEDOT(3)=PVODOT

        RETURN
        END
```

SUBROUTINE DCEMDD (3 OF 3)

```
1) DK:DCEMOD.FOR
2) DK:DCECSA.FOR
**********
1)1      C  no transient control
1)               NOZA=NOZ
1)               NTURB=NLOAD*TGR/SQRT(TVOL)       !non-dimensional turbine speed
****
2)1      C  control scheme A
2)               NOZA=NOZ-K1*(PINDEM-PINMAN)      !transient nozzle angle
2)               IF (NOZA.LT.5.) NOZA=5.          !minimum nozzle angle
2)       C
2)               NTURB=NLOAD*TGR/SQRT(TVOL)       !non-dimensional turbine speed
```

```
1) DK:DCEMOD.FOR
2) DK:DCECSB.FOR
**********
1)1      C  no transient control
1)               NOZA=NOZ
1)               NTURB=NLOAD*TGR/SQRT(TVOL)       !non-dimensional turbine speed
****
2)1      C  control scheme B
2)               NOZA=NOZ                                  !transient nozzle angle
2)               NERR=ABS(NEDEM-NENG)                      !transient measure
2)               IF (NERR.GT.50.) NOZA=NOZ-K1*(PINDEM-PINMAN)
2)               IF (NOZA.LT.5.) NOZA=5.                   !minimum nozzle angle
2)       C
2)               NTURB=NLOAD*TGR/SQRT(TVOL)       !non-dimensional turbine speed
```

MODIFICATIONS FOR CONTROL SCHEMES A + B

```
1) DK:DCEMOD.FOR
2) DK:DCECSC.FOR

**********
1)1      C  no transient control
1)                NOZA=NOZ
1)                NTURB=NLOAD*TGR/SQRT(TVOL)       !non-dimensional turbine speed
****
2)1      C  control scheme C
2)                K1=K2*ABS(NEDEM-NENG)                    !transient gain
2)                NOZA=NOZ-K1*(PINDEM-PINMAN)              !transient nozzle angle
2)                IF (NOZA.LT.5.) NOZA=5.                  !minimum nozzle angle
2)                TYPE *,NOZA,K1
2)       C
2)                NTURB=NLOAD*TGR/SQRT(TVOL)       !non-dimensional turbine speed
```

MODIFICATIONS FOR CONTROL SCHEME C

```
1) DK:DCEMOD.FOR
2) DK:DCECSD.FOR
**********
1)1      C  airflow thro' engine from perfect gas equation
1)               MINMAN=KMINMA*PINMAN*NENG/TINMAN
1)               FPREVA=FPREV                          !adjusted FPREV
****
2)1      C  control scheme  D
2)       C  ****FPREV is borrowed for governor demand input****
2)               FPREVG=K3*(FPREV-NENG)                !governor droop equation
2)               IF (FPREVG.GT.4.718) FPREVG=4.718     !FPREV limits
2)               IF (FPREVG.LT.0.) FPREVG=0.
2)       C  airflow thro' engine from perfect gas equation
2)               MINMAN=KMINMA*PINMAN*NENG/TINMAN
2)               FPREVA=FPREVG                         !adjusted FPREV
```

```
**********
1)1      C  no transient control
1)               NOZA=NOZ
1)               NTURB=NLOAD*TGR/SQRT(TVOL)            !non-dimensional turbine speed
****
2)1      C  control scheme  D
2)       C-------------------------------------------------------------------
--
2)       C  calculate transient AFR reduction
2)               AFRRED=K2*(NEDEM-NENG)
2)       C  inlet manifold pressure reduction which will reduce AFR by AFRRED
2)               PINRED=AFRRED*KMF*FPREVG*TINMAN/KMINMA
2)               PINLOW=K4*KMF*FPREVG*TINMAN/KMINMA    !demand for minimum AFR
2)               PINSET=PINDEM-PINRED                  !optimum - reduction
2)               IF (PINSET.LT.PINLOW) PINSET=PINLOW   !limit pressure demand
2)       C  boost control loop implementation
2)               NOZA=NOZ-K1*(PINSET-PINMAN)
2)       C  limit nozzle angle
2)               IF (NOZA.GT.20.) NOZA=20.
2)               IF (NOZA.LT.5.) NOZA=5.
2)       C-------------------------------------------------------------------
2)               NTURB=NLOAD*TGR/SQRT(TVOL)            !non-dimensional turbine speed
```

MODIFICATIONS FOR CONTROL SCHEME D

```
C  1-D INTERPOLATION FUNCTION
C  given XNORM this routine returns a value for Y from the
C  array YARR. XNORM is X normalised to a real number on
C  the same scale as the array indices. Y and YARR are of
C  type REAL.

      REAL FUNCTION RITRP1(XNORM,YARR,ISIZE)

      IMPLICIT REAL (A-H,J-Z)
      IMPLICIT INTEGER (I)

      DIMENSION YARR(ISIZE)
      IXINT=INT(XNORM)           ! integer part of XNORM
      XFRAC=ABS(XNORM-IXINT)     ! fractional part of XNORM
      Y1=YARR(IXINT)
      Y2=YARR(IXINT+1)
      RITRP1=Y1+(Y2-Y1)*XFRAC          ! linear interpolation

      RETURN
      END
```

```
C  2-D INTERPOLATION FUNCTION
C  given X and Y values this routine returns a value for Z from
C  the 2-D array ZARRAY. X and Y must be normalised to real
C  numbers on the same scale as the array indices.
C  2-D interpolation is achieved by doing three 1-D interpolations

      FUNCTION  RITRP2(XNORM,YNORM,ZARR,IXSIZE,IYSIZE)

      IMPLICIT REAL (A-H,J-Z)
      IMPLICIT INTEGER (I)
      DIMENSION ZARR(IXSIZE,IYSIZE)
      IXINT=INT(XNORM)              ! integer part of XNORM
      XFRAC=ABS(XNORM-IXINT)        ! fractional part of XNORM
      IYINT=INT(YNORM)
      YFRAC=ABS(YNORM-IYINT)

C  first 1-D interpolation, keeping Y constant

      Z1=ZARR(IXINT,IYINT)
      Z2=ZARR(IXINT+1,IYINT)
      Z3=Z1+(Z2-Z1)*XFRAC          ! linear interpolation

C  second 1-D interpolation, keeping Y constant

      Z1=ZARR(IXINT,IYINT+1)
      Z2=ZARR(IXINT+1,IYINT+1)
      Z4=Z1+(Z2-Z1)*XFRAC

C  final 1-D interpolation, keeping X constant

      RITRP2=Z3+(Z4-Z3)*YFRAC

      RETURN
      END
```

REAL INTERPOLATION FUNCTIONS

(RITRP1 AND RITRP2)

DCEMOD DATA FILE
****
TURBINE CHARACTERISTIC :- non-dimensional massflow vs. pressure ratio
---

pressure ratio
0.0 .25 .50 .75 1.0 1.25
massflow (kg/min)*(deg.K**.5)/(bar)
0.0 23.1 31.0 34.4 36.4 37.4

COMPRESSOR CHARACTERISTICS (NB. exact match with DCETRAN !!!)
(This is only for matching purposes)
volume flow in cubic ft. per min.

press. ratio	speed -200	4600	9400	14200
-.0343	-72.5	687.5	1447.5	2207.5
.3105	-82.5	670.	1422.5	2175.
.6553	-92.5	652.5	1397.5	2142.5
1.0001	-102.5	635.	1372.5	2110.
1.3449	-112.5	617.5	1347.5	2077.5
1.6897	-122.5	600.	1322.5	2045.
2.0345	-132.5	582.5	1297.5	2012.5
2.3793	-127.5	580.	1287.5	1995.
2.7241	-145.	570.	1285.	2000.
3.0689	-140.	567.5	1275.	1982.5
3.4137	-152.5	557.5	1267.5	1977.5
3.7585	-165.	547.5	1260.	1972.5
4.1033	-177.5	537.5	1252.5	1967.5

compressor power consumption in horse power

press. ratio	speed -200	4600	9400	14200
-.0343	-11.	-15.	-19.	-23.
.3105	-10.	-5.	0.	5.
.6553	-9.	5.	19.	33.
1.0001	-8.	15.	38.	61.
1.3449	-7.	25.	57.	89.
1.6897	-6.	35.	76.	117.
2.0345	-5.	45.	95.	145.
2.3793	-3.5	52.5	108.5	164.5
2.7241	-7.	62.	131.	200.
3.0689	-4.5	66.	136.5	207.
3.4137	2.5	80.5	158.5	236.5
3.7585	9.5	95.	180.5	266.
4.1033	16.5	109.5	202.5	295.5

gains 'K' (coeffs. of proportionality)

KTQC	KMC	KMINMA	KMF	KTQE	KFRIC	KBYPAS
32.	0.0045	1.21	1.E-4	320.	0.05	12.E-6

efficiencies

EFCOMP	EFTURB	EFCOOL
0.90	0.70	0.80

gear ratios

CGR	OGR	TGR
8.83	1.35	60.

inertias

JENG	JCOMP	JLOAD
0.32	0.0063	10000.

gas properties

CP	R	GAMMA
1.03	0.287	1.39

general data

TCOOL	TATM	PATM	VOLUME	AREABY	TQSTAT
300.	293.	1.	20.0	0.0015	100.

DATA-FILE (DCEMOD.DAT)

```
C-------------------------------------------------------------
C PROGRAM TO PLOT DCESIM OUTPUT
C ****************************
C
C written by D. Howard, Feb. 1985
C
C this program reads the appropriate plot files created
C by the transient simulation program (DCESIM), and then
C calls the H.P. plotting subroutine (HPLOT).
C the graph axes are scaled to give I3 format labels
C thus avoiding untidy axes.
C
C-------------------------------------------------------------
C
      LOGICAL*1 STRERR,FILE(11,5),XTITLE(30),YTITLE(30)
      DIMENSION X(100,5),Y(100,5)      !data point arrays
      DATA FILE/11*0,                  !1st name
     &          11*0,                  !2nd name
     &          11*0,                  !3rd name
     &          11*0,                  !4th name
     &          11*0/                  !5th name
      DATA XTITLE/30*0/
      DATA YTITLE/30*0/
C
C-------------------------------------------------------------
C set plot parameters from keyboard :-
C   no. of curves
C   no. of points per curve
C   point spacing (dt)
C   filename for each curve
C   x-axis title
C   y-axis title
C   xscale,yscale
C   xmin,xmax,xgrid     (for graph grid)
C   ymin,ymax,ygrid
C-------------------------------------------------------------
C
C user instructions
C
      TYPE 750
 750  FORMAT(' DCESIM plotting program'/' graph axes must be scaled
     & so that labels are I3 format'/' no. of points includes first
     & point !!'/' variable position in records is counted from left'/
     &' HAVE YOU "SET-UP" 150 BAUD AND "SET LP: CTRL" ??'/
     &' if not then leave program and do so'//)
C
C no. of curves, no. of points, dt
C
      TYPE 700
 700  FORMAT(' ENTER: no. curves, no. points,
     & point spacing dt (secs)')
      ACCEPT *, NCURV,NPTS,DT
C number of variables in plot records
C
      TYPE 760
 760  FORMAT(' ENTER: number of variables in plot records')
      ACCEPT *,NVAR
C variable position reading from left of records
C
      TYPE 740
 740  FORMAT(' ENTER: variable position from left')
      ACCEPT *,IVAR
C filenames
C
      DO 5 J=1,NCURV                   !get NCURV filenames
      TYPE 701, J
 701  FORMAT(' ENTER: filename ',I2)
      ACCEPT 500, (FILE(I,J),I=1,10)
 500  FORMAT(10A1)
   5  CONTINUE
C xscale,yscale (scale data to suit graph axes-- I3 axis labels)
```

DCEPLT.FOR (1 OF 2)

```
C xscale,yscale (scale data to suit graph axes-- I3 axis labels)
C
      TYPE 725
 725  FORMAT(' ENTER: xscale,yscale (for integer (I3) graph axes)'/
     & ' nb. x=xscale*x and y=yscale*y')
      ACCEPT *, XSCALE,YSCALE
      DT=DT*XSCALE                    'scale to suit axis
C xmin,xmax,xgrid
C
      TYPE 704
 704  FORMAT(' ENTER: xmin,xmax,xgrid (I3 format only)')
      ACCEPT *, IXMIN,IXMAX,IXGRID
C x-axis title
C
      TYPE 702
 702  FORMAT(' ENTER: x-axis title')
      CALL GETSTR(5,XTITLE,29,STRERR)
C ymin,ymax,ygrid
C
      TYPE 705
 705  FORMAT(' ENTER: ymin,ymax,ygrid (I3 format only)')
      ACCEPT *, IYMIN,IYMAX,IYGRID
C y-axis title
C
      TYPE 703
 703  FORMAT(' ENTER: y-axis title')
      CALL GETSTR(5,YTITLE,29,STRERR)
C report GETSTR error flag set
C
      IF (STRERR) TYPE 720, STRERR
 720  FORMAT(/' GETSTR ERROR: STRERR=',I2)
C
C-------------------------------------------------------------
C read data points from files and store in 2-D array Y,
C the variable IVAR determines which field in the plot
C records is being read, NVAR is the number of fields.
C-------------------------------------------------------------
C
      DO 20 J=1,NCURV                 'no. of curves
C open plot file J ie. filename FILE(1,J)
      OPEN(UNIT=3,TYPE='OLD',NAME=FILE(1,J))
      REWIND 3
      DO 10 I=1,NPTS                              'no. of points
C read data from plot record (all data is read to keep in synch'.)
      IF (IVAR.GT.1) GOTO 15
      READ (3,*) DATA,(DUMMY,K=2,NVAR)
      GOTO 17
 15   IF (IVAR.LT.NVAR) GOTO 16
      READ (3,*) (DUMMY,K=1,NVAR-1),DATA
      GOTO 17
 16   READ (3,*) (DUMMY,K=1,IVAR-1),DATA,(DUMMY,K=IVAR+1,NVAR)
 17   Y(I,J)=DATA*YSCALE                          'scale to suit axis
      X(I,J)=DT*(I-1)+IXMIN                       'time
 10   CONTINUE
      CLOSE(UNIT=3)
 20   CONTINUE
C
C-------------------------------------------------------------
C call graph plotting subroutine for H.P. plotter
C-------------------------------------------------------------
C
      CALL HPLOT(NCURV,NPTS,X,Y,IYMIN,IYMAX,IYGRID,YTITLE,
     & IXMIN,IXMAX,IXGRID,XTITLE)

      STOP
      END
```

DCEPLT.FOR (2 OF 2)

```
C-----------------------------------------------------------------------
C PLOTTING SUBROUTINE FOR HP PLOTTER (HPLOT1)
C ****************************************
C
C written by D. Howard, March 1986
C
C This subroutine plots a set of curves against common axes.
C X & Y axis data is stored in the 2-D arrays XDATA & YDATA.
C The axes must be scaled so that axis labels are integer I3 format,
C thus producing tidy axes. The plot data must be scaled likewise.
C
C VARIABLE LIST:
C
C INCURV  no. of curves (5 max.)
C INPTS   no. of points per curve, incl. first point!! (100 max)
C XDATA   2-D array containing x-axis data
C YDATA   2-D array containing y-axis data
C IYMIN   Y at origin, scaled for I3 format ie. min. Y
C IYMAX   max. Y for graph axis, after scaling
C IYGRID  y-axis grid spacing, scaled
C YTITLE  y-axis title, incl. scaled units
C IXMIN   X at origin, scaled for I3 format
C IXMAX   max. X for graph axis, scaled
C IXGRID  x-axis grid spacing, scaled
C XTITLE  x-axis title, incl. scaled units
C ETX     label terminator
C ESC     RS232 set up command prefix
C INGRID  no. of grid lines on an axis
C ILABEL  axis grid labels
C IJOIN   Join flag   =0: do not join points   =1: Join points
C-----------------------------------------------------------------------
C

      SUBROUTINE HPLOT(INCURV,INPTS,XDATA,YDATA,IYMIN,IYMAX,IYGRID,
     &  YTITLE,IXMIN,IXMAX,IXGRID,XTITLE)

      IMPLICIT REAL (A-H,J-Z)
      IMPLICIT INTEGER (I)
      INTEGER LEN
      DIMENSION YDATA(100,5),XDATA(100,5)
      LOGICAL*1 ETX,ESC,XTITLE(30),YTITLE(30)
      DATA ETX,ESC/3,27/
C-----------------------------------------------------------------
C PLOTTER INITIALISATION:-
C set pen speed from operator, set up RS232 handshaking,
C define various plotter parameters, and move pen to origin.
C-----------------------------------------------------------------
      TYPE 710                          !set pen speed from operator
 710  FORMAT(/' ENTER PEN SPEED (0.38-38.1 cm/sec) '$)
      ACCEPT *, PVEL                    !pen velocity
      WRITE (6,600) ESC,ESC, IXMIN,IXMAX,IYMIN,IYMAX, PVEL,
     &              IXMIN,IYMIN
 600  FORMAT(' IN;',                    !initialise plotter
     &  1A1,'.I81;17:',                 !RS232 (ESC.) commands to...
     &  1A1,'.N19:',                    !..enable Xon-Xoff handshake
     &  'IP 2700,1500,8700,6500;',      !input P1 and P2
     &  'SC',4I4,';',                   !set scaling
     &  'TL 100;',                      !tick length
     &  'SI 0.19,0.27;',                !character size
     &  'VS',F8.3,';',                  !set pen velocity
     &  'SP 1;',                        !select pen 1
     &  'PU',2I4,';',                   !move pen to origin
     &  'PD;')                          !pen down
```

HPLOT.FOR (1 OF 3)

```
C
C*********************************************************************
C DRAW VERTICAL GRID LINES AND LABEL X-AXIS
C*********************************************************************
C
      INGRID=(IXMAX-IXMIN)/IXGRID      !number of vertical...
C                                      !...grids along x-axis
C---------------------------------------------------------------------
C draw vertical grid lines
C---------------------------------------------------------------------
      DO 10 I=1,INGRID
      WRITE (6,605) IXGRID
 605  FORMAT(' PR',I4,',0;',           !move one grid to right
     & 'XT;')                         !draw one vertical grid
 10   CONTINUE
C---------------------------------------------------------------------
C label x-axis at origin
C---------------------------------------------------------------------
      WRITE (6,610) IXMIN,IYMIN, IXMIN,ETX
 610  FORMAT(' PU;',                   !pen up
     & 'PA',2I4,';',                  !move to origin
     & 'CP -3,-1;',                   !3 char. left, 1 down
     & 'LB',I4,1A1)                   !label x-axis at origin
C---------------------------------------------------------------------
C label x-axis below each vertical grid line
C---------------------------------------------------------------------
      DO 20 I=1,INGRID
      ILABEL=IXGRID*I+IXMIN
      WRITE (6,615) IXGRID,ILABEL,ETX
 615  FORMAT('PR',I4,',0;',            !move one grid to right
     & 'CP -4,0;',                    !back 4 characters to left
     & 'LB',I4,1A1)                   !label x-axis below grid
 20   CONTINUE
C
C*********************************************************************
C DRAW HORIZONTAL GRID LINES AND LABEL Y-AXIS
C*********************************************************************
C
      INGRID=(IYMAX-IYMIN)/IYGRID      !number of horizontal...
C                                      !...grids along y-axis
C---------------------------------------------------------------------
C move to origin to do y-axis
C---------------------------------------------------------------------
      WRITE (6,617) IXMIN,IYMIN
 617  FORMAT('PU;',                    !pen up
     & 'PA',2I4,';',                  !move to origin
     & 'PD;')                         !pen down
C---------------------------------------------------------------------
C draw horizontal grid lines
C---------------------------------------------------------------------
      DO 25 I=1,INGRID
      WRITE (6,620) IYGRID
 620  FORMAT(' PR','0,',I4,';',        !move one grid up
     & 'YT;')                         !draw one horizontal grid
 25   CONTINUE
C---------------------------------------------------------------------
C label y-axis at origin
C---------------------------------------------------------------------
      WRITE (6,625) IXMIN,IYMIN, IXMIN,ETX
 625  FORMAT(' PU;',                   !pen up
     & 'PA',2I4,';',                  !move to origin
     & 'CP -5,0;',                    !move 5 characters left
     & 'LB',I4,1A1)                   !label y-axis at origin
C---------------------------------------------------------------------
C label y-axis beside each horizontal grid line
C---------------------------------------------------------------------
      DO 30 I=1,INGRID
      ILABEL=IYGRID*I+IYMIN
      WRITE (6,630) IYGRID,ILABEL,ETX
 630  FORMAT('PR','0,',I4,';',         !move one grid up
     & 'CP -4,0;',                    !back 4 characters to left
     & 'LB',I4,1A1)                   !label y-axis beside grid
 30   CONTINUE
```

HPLOT.FOR (2 OF 3)

```
C
C*********************************************************************
C WRITE AXIS TITLES
C*********************************************************************
C
C x-axis title
C---------------------------------------------------------------------
      WRITE (6,640) IXMIN,IYMIN
 640  FORMAT('PA',2I4,';',                  !move to origin
     & 'CP 20,-3;')                         !20 char. right, 3 down
      ILEN=LEN(XTITLE)                      !length of x-axis title
      DO 40 I=1,ILEN                        !write x-axis title
      WRITE (6,645) XTITLE(I),ETX
 645  FORMAT('LB',2A1)                      !draw one character
 40   CONTINUE
C---------------------------------------------------------------------
C y-axis title
C---------------------------------------------------------------------
      WRITE (6,650) IXMIN,IYMIN
 650  FORMAT('PA',2I4,';',                  !move to origin
     & 'CP -6,8;',                          !6 char. left, 8 up
     & 'DI 0,1;')                           !char. direction vertical
      ILEN=LEN(YTITLE)                      !length of y-axis title
      DO 50 I=1,ILEN                        !write y-axis title
      WRITE (6,655) YTITLE(I),ETX
 655  FORMAT('LB',2A1)                      !draw one character
 50   CONTINUE
C
C*********************************************************************
C ASK OPERATOR IF POINTS SHOULD BE JOINED
C*********************************************************************
C
      IJOIN=0                  !Join flag=0 (do not join points)
      TYPE 700
 700  FORMAT(/' JOIN POINTS ? (Y or N)  ',$)
      ACCEPT 500, ANS
 500  FORMAT (A1)
      IF (ANS.EQ.'Y') IJOIN=1               !Join flag=1 (Join points)
C
C*********************************************************************
C PLOT CURVES STORED IN ARRAYS XDATA AND YDATA
C*********************************************************************
C
      DO 70 I1=1,INCURV                     !for no. of curves
C---------------------------------------------------------------------
C points joined or not ?
C---------------------------------------------------------------------
      IF (IJOIN.EQ.0) GOTO 55               !points not joined
      WRITE (6,660) XDATA(1,I1),YDATA(1,I1)   !points joined
 660  FORMAT(
     & 'PU;',                               !pen up
     & 'PA',2F8.3,';',                      !move to first point
     & 'PD;')                               !pen down
      GOTO 56
 55   WRITE (6,661) XDATA(1,I1),YDATA(1,I1)   !points not joined
 661  FORMAT('SM+;',                         !set symbol mode for +
     & 'PU;',                               !pen up
     & 'PA',2F8.3,';')                      !move to first point
C---------------------------------------------------------------------
C plot one curve
C---------------------------------------------------------------------
 56   DO 60 I2=2,INPTS                      !for 2nd to last point
      WRITE (6,665) XDATA(I2,I1),YDATA(I2,I1)
 665  FORMAT('PA',2F8.3,';')                !move to next point
 60   CONTINUE
      WRITE (6,670) I1,ETX                  !label curve
 670  FORMAT('LB',I2,1A1)
 70   CONTINUE
      RETURN
      END
```

HPLOT.FOR (3 OF 3)

PAGE 1: TRANSIENT RESULTS FROM DIESIM PROGRAM
DT= 0.1000E-01 RUNTIM= 3.000 INREC= 61
K1= 0.0000 K2= 0.0000 K3= 0.0000 K4= 0.0000

time (sec.)	0.0000	0.2000	0.4000	0.6000	0.8000
Ncomp (rpm)	5608.	6337.	7169.	8046.	8845.
Acomp (rpm/sec)	4.807	3901.	4387.	4141.	3847.
Nload (rpm))	500.0	500.0	499.9	499.9	499.9
Aload (rpm/sec.)	0.1047E-01	-0.1714	-0.1415	-0.1021	-0.7873E-01
Pvol (Bar)	2.021	2.020	2.264	2.601	2.865
Pvodot (Bar/sec.)	0.1330E-02	1.030	1.393	1.479	1.249
Neng (rpm)	1005.	1088.	1182.	1282.	1372.
Aeng (rpm/sec.)	0.5521	441.6	496.7	468.9	435.6
Ntrb(rpm/sqrt(T))	1313.	1233.	1212.	1187.	1192.
Air/fuel ratio	29.68	20.00	20.00	20.63	22.53
Pcomp (Bar)	2.140	2.178	2.431	2.769	3.028
Pinman (Bar)	2.033	2.059	2.296	2.617	2.865
TQeng (Nm)	680.0	1057.	1183.	1303.	1307.
TQann (Nm)	679.8	916.8	1024.	1152.	1167.
TQsun (Nm)	73.91	99.68	111.4	125.2	126.9
TQpc (Nm)	503.5	679.1	758.7	853.1	864.8
TQcomp (Nm)	73.88	75.10	83.72	99.13	102.7
TQturb (Nm)	534.0	689.0	931.0	1261.	1503.
TQload (Nm)	870.0	3000.	3000.	3000.	3000.
TQout (Nm)	974.7	1286.	1585.	1979.	2213.
Mcomp (Kg/min)	24.63	28.26	32.26	36.46	40.23
Minman (Kg/min)	7.750	8.495	10.22	12.48	14.58
Mfuel (kg/min)	0.2611	0.4247	0.5112	0.6046	0.6473
Mturb (kg/min)	24.89	28.33	32.30	36.58	40.47
Tinman (deg.K)	319.1	319.1	321.3	325.3	326.1
Texman (deg.K)	787.7	1027.	1037.	1026.	972.7
Tcomp (deg.K)	395.6	395.7	406.5	426.4	430.7
Tvol (deg.K)	521.8	592.1	612.9	638.2	632.7
Tvodot(deg.K/min)	10.31	9062.	0.1131E+05	0.1089E+05	8276.
FPREV (	2.597	4.718	4.718	4.718	4.718
FPREVA (	2.597	3.904	4.324	4.718	4.718
NOZ (deg.)	7.900	9.500	9.500	9.500	9.500
NOZA (deg.)	7.900	9.500	9.500	9.500	9.500
turb. gear ratio	60.00	60.00	60.00	60.00	60.00
PINDEM (Bar)	0.0000	0.0000	0.0000	0.0000	0.0000
NEDEM (rpm)	0.0000	0.0000	0.0000	0.0000	0.0000

PAGE 2: TRANSIENT RESULTS FROM DIESIM PROGRAM
DT= 0.1000E-01 RUNTIM= 3.000 INREC= 61
K1= 0.0000 K2= 0.0000 K3= 0.0000 K4= 0.0000

time (sec.)	1.000	1.200	1.400	1.600	1.800
Ncomp (rpm)	9531.	0.1003E+05	0.1038E+05	0.1064E+05	0.1083E+05
Acomp (rpm/sec)	2904.	2087.	1512.	1100.	803.7
Nload (rpm))	499.9	499.9	499.9	499.9	499.9
Aload (rpm/sec.)	-0.5439E-01	-0.3496E-01	-0.2073E-01	-0.1028E-01	-0.2603E-02
Pvol (Bar)	3.106	3.289	3.421	3.517	3.588
Pvodot (Bar/sec.)	1.071	0.7737	0.5622	0.4101	0.3001
Neng (rpm)	1450.	1506.	1546.	1575.	1597.
Aeng (rpm/sec.)	328.8	236.3	171.2	124.6	91.01
Ntrb(rpm/sqrt(T))	1190.	1187.	1185.	1183.	1182.
Air/fuel ratio	24.15	25.36	26.22	26.84	27.30
Pcomp (Bar)	3.270	3.453	3.585	3.681	3.751
Pinman (Bar)	3.096	3.273	3.400	3.493	3.561
TQeng (Nm)	1311.	1313.	1315.	1317.	1318.
TQann (Nm)	1204.	1237.	1260.	1276.	1288.
TQsun (Nm)	130.9	134.4	137.0	138.7	140.0
TQpc (Nm)	891.7	916.0	933.1	945.3	954.1
TQcomp (Nm)	112.6	121.3	127.4	131.8	135.0
TQturb (Nm)	1739.	1925.	2062.	2163.	2237.
TQload (Nm)	3000.	3000.	3000.	3000.	3000.
TQout (Nm)	2456.	2650.	2793.	2897.	2974.
Mcomp (Kg/min)	43.45	45.78	47.46	48.69	49.59
Minman (Kg/min)	16.52	18.01	19.13	19.95	20.56
Mfuel (kg/min)	0.6840	0.7104	0.7294	0.7432	0.7533
Mturb (kg/min)	43.78	46.24	48.01	49.30	50.24
Tinman (deg.K)	328.7	331.0	332.6	333.7	334.6
Texman (deg.K)	935.2	911.0	895.0	884.1	876.5
Tcomp (deg.K)	443.6	455.0	463.0	468.7	472.8
Tvol (deg.K)	635.2	638.6	641.0	642.6	643.8
Tvodot(deg.K/min)	6573.	4508.	3160.	2248.	1615.
FPREV (	4.718	4.718	4.718	4.718	4.718
FPREVA (	4.718	4.718	4.718	4.718	4.718
NOZ (deg.)	9.500	9.500	9.500	9.500	9.500
NOZA (deg.)	9.500	9.500	9.500	9.500	9.500
turb. gear ratio	60.00	60.00	60.00	60.00	60.00
PINDEM (Bar)	0.0000	0.0000	0.0000	0.0000	0.0000
NEDEM (rpm)	0.0000	0.0000	0.0000	0.0000	0.0000

TYPICAL PRINTOUT FILE (BASE RESPONSE)

PAGE 3: TRANSIENT RESULTS FROM DCESIM PROGRAM
DT= 0.1000E-01 RUNTIM= 3.000 INREC= 61
K1= 0.0000 K2= 0.0000 K3= 0.0000 K4= 0.0000

time (sec.)	2.000	2.200	2.400	2.600	2.800
Ncomp (rpm)	0.1097E+05	0.1107E+05	0.1114E+05	0.1120E+05	0.1124E+05
Acomp (rpm/sec)	588.3	431.4	316.7	232.7	171.0
Nload (rpm))	499.9	499.9	499.9	499.9	499.9
Aload (rpm/sec.)	0.3041E-02	0.7191E-02	0.1024E-01	0.1249E-01	0.1414E-01
Pvol (Bar)	3.639	3.677	3.705	3.725	3.740
Pvodot (Bar/sec.)	0.2199	0.1614	0.1186	0.8713E-01	0.6406E-01
Neng (rpm)	1612.	1624.	1632.	1638.	1643.
Aeng (rpm/sec.)	66.63	48.86	35.87	26.36	19.38
Ntrb(rpm/sqrt(T))	1181.	1181.	1180.	1180.	1180.
Air/fuel ratio	27.63	27.87	28.05	28.18	28.27
Pcomp (Bar)	3.803	3.840	3.868	3.888	3.903
Pinman (Bar)	3.611	3.647	3.674	3.693	3.708
TQeng (Nm)	1318.	1319.	1319.	1320.	1320.
TQann (Nm)	1297.	1303.	1308.	1311.	1313.
TQsun (Nm)	141.0	141.7	142.2	142.5	142.8
TQpc (Nm)	960.6	965.2	968.6	971.1	973.0
TQcomp (Nm)	137.3	138.9	140.2	141.1	141.7
TQturb (Nm)	2292.	2332.	2361.	2383.	2399.
TQload (Nm)	3000.	3000.	3000.	3000.	3000.
TQout (Nm)	3030.	3072.	3102.	3125.	3141.
Mcomp (Kg/min)	50.24	50.72	51.08	51.34	51.53
Minman (Kg/min)	21.02	21.35	21.60	21.78	21.92
Mfuel (kg/min)	0.7607	0.7661	0.7701	0.7730	0.7751
Mturb (kg/min)	50.93	51.44	51.81	52.08	52.28
Tinman (deg.K)	335.2	335.6	335.9	336.1	336.3
Texman (deg.K)	871.1	867.3	864.5	862.5	861.0
Tcomp (deg.K)	475.8	477.9	479.5	480.7	481.5
Tvol (deg.K)	644.6	645.2	645.6	645.9	646.2
Tvodot(deg.K/min)	1169.	849.3	619.8	453.2	332.0
FPREV (	4.718	4.718	4.718	4.718	4.718
FPREVA (	4.718	4.718	4.718	4.718	4.718
NOZ (deg.)	9.500	9.500	9.500	9.500	9.500
NOZA (deg.)	9.500	9.500	9.500	9.500	9.500
turb. gear ratio	60.00	60.00	60.00	60.00	60.00
PINDEM (Bar)	0.0000	0.0000	0.0000	0.0000	0.0000
NEDEM (rpm)	0.0000	0.0000	0.0000	0.0000	0.0000

PAGE 4: TRANSIENT RESULTS FROM DCE PROGRAM
DT= 0.1000E-01 RUNTIM= 3.000 INREC= 61
K1= 0.0000 K2= 0.0000 K3= 0.0000 K4= 0.0000

time (sec.)	3.000
Ncomp (rpm)	0.1127E+05
Acomp (rpm/sec)	125.8
Nload (rpm))	499.9
Aload (rpm/sec.)	0.1536E-01
Pvol (Bar)	3.751
Pvodot (Bar/sec.)	0.4714E-01
Neng (rpm)	1646.
Aeng (rpm/sec.)	14.26
Ntrb(rpm/sqrt(T))	1180.
Air/fuel ratio	28.34
Pcomp (Bar)	3.914
Pinman (Bar)	3.718
TQeng (Nm)	1320.
TQann (Nm)	1315.
TQsun (Nm)	143.0
TQpc (Nm)	974.3
TQcomp (Nm)	142.2
TQturb (Nm)	2411.
TQload (Nm)	3000.
TQout (Nm)	3154.
Mcomp (Kg/min)	51.67
Minman (Kg/min)	22.01
Mfuel (kg/min)	0.7767
Mturb (kg/min)	52.43
Tinman (deg.K)	336.4
Texman (deg.K)	859.9
Tcomp (deg.K)	482.1
Tvol (deg.K)	646.3
Tvodot(deg.K/min)	243.7
FPREV (	4.718
FPREVA (	4.718
NOZ (deg.)	9.500
NOZA (deg.)	9.500
turb. gear ratio	60.00
PINDEM (Bar)	0.0000
NEDEM (rpm)	0.0000

TYPICAL PRINTOUT FILE (BASE RESPONSE)

2 OF 2

PAGE 1: TRANSIENT RESULTS FROM DCETM PROGRAM
DT= 0.1000E-01 RUNTIM= 3.000 INREC= 61
K1= 10.00 K2= 0.0000 K3= 0.0000 K4= 0.0000

time (sec.)	0.0000	0.2000	0.4000	0.6000	0.8000
Ncomp (rpm)	5619.	6149.	6510.	6846.	7158.
Acomp (rpm/sec)	4.861	1841.	1702.	1614.	1467.
Nload (rpm))	500.0	500.0	500.0	500.0	499.9
Aload (rpm/sec.)	0.7521E-02	-0.9261E-01	-0.8493E-01	-0.7995E-01	-0.7175E-01
Pvol (Bar)	2.020	3.434	3.460	3.473	3.500
Pvodot (Bar/sec.)	0.6130E-04	-1.152	-1.296	-0.4878E-01	-1.160
Neng (rpm)	1007.	1067.	1108.	1146.	1181.
Aeng (rpm/sec.)	0.5561	208.4	192.7	182.8	166.0
Ntrb(rpm/sqrt(T))	1314.	1138.	1143.	1148.	1151.
Air/fuel ratio	29.67	25.38	25.60	25.77	25.99
Pcomp (Bar)	2.139	3.478	3.510	3.531	3.564
Pinman (Bar)	2.032	3.309	3.340	3.361	3.392
TQeng (Nm)	679.9	1335.	1334.	1333.	1333.
TQann (Nm)	679.7	1269.	1273.	1275.	1279.
TQsun (Nm)	73.90	138.0	138.4	138.6	139.1
TQpc (Nm)	503.5	940.0	943.1	944.6	947.6
TQcomp (Nm)	73.87	126.4	127.7	128.5	129.8
TQturb (Nm)	534.6	1273.	1354.	1406.	1492.
TQload (Nm)	900.0	3000.	3000.	3000.	3000.
TQout (Nm)	975.2	2074.	2151.	2201.	2283.
Mcomp (Kg/min)	24.69	26.43	28.20	29.85	31.38
Minman (Kg/min)	7.758	12.77	13.38	13.93	14.48
Mfuel (kg/min)	0.2614	0.5083	0.5226	0.5405	0.5572
Mturb (kg/min)	24.95	27.28	29.12	30.41	32.30
Tinman (deg.K)	319.1	334.5	334.6	334.5	334.7
Texman (deg.K)	787.8	923.7	918.3	914.2	909.3
Tcomp (deg.K)	395.5	472.3	472.8	472.7	473.6
Tvol (deg.K)	521.6	694.8	688.4	682.9	678.7
Tvodot(deg.K/min)	0.4705	-6991.	-7735.	-287.5	-6740.
FPREV (	2.597	4.718	4.718	4.718	4.718
FPREVA (	2.597	4.718	4.718	4.718	4.718
NOZ (deg.)	7.900	9.500	9.500	9.500	9.500
NOZA (deg.)	7.923	5.595	5.902	6.113	6.423
turb. gear ratio	60.00	60.00	60.00	60.00	60.00
PINDEM (Bar)	2.030	3.700	3.700	3.700	3.700
NEDEM (rpm)	0.0000	0.0000	0.0000	0.0000	0.0000

PAGE 2: TRANSIENT RESULTS FROM DCETM PROGRAM
DT= 0.1000E-01 RUNTIM= 3.000 INREC= 61
K1= 10.00 K2= 0.0000 K3= 0.0000 K4= 0.0000

time (sec.)	1.000	1.200	1.400	1.600	1.800
Ncomp (rpm)	7449.	7720.	7974.	8211.	8432.
Acomp (rpm/sec)	1408.	1276.	1195.	1177.	1071.
Nload (rpm))	499.9	499.9	499.9	499.9	499.9
Aload (rpm/sec.)	-0.6745E-01	-0.5973E-01	-0.5460E-01	-0.5311E-01	-0.4669E-01
Pvol (Bar)	3.528	3.539	3.554	3.568	3.573
Pvodot (Bar/sec.)	0.1395	-1.285	-1.146	1.199	-0.5631E-01
Neng (rpm)	1214.	1245.	1273.	1300.	1325.
Aeng (rpm/sec.)	159.4	144.5	135.3	133.2	121.2
Ntrb(rpm/sqrt(T))	1155.	1157.	1160.	1162.	1164.
Air/fuel ratio	26.11	26.33	26.47	26.52	26.70
Pcomp (Bar)	3.594	3.613	3.634	3.652	3.664
Pinman (Bar)	3.407	3.438	3.457	3.462	3.489
TQeng (Nm)	1331.	1331.	1330.	1329.	1329.
TQann (Nm)	1280.	1285.	1287.	1286.	1291.
TQsun (Nm)	139.2	139.7	139.9	139.8	140.3
TQpc (Nm)	948.2	951.9	953.5	952.7	956.0
TQcomp (Nm)	130.3	131.7	132.4	132.4	133.6
TQturb (Nm)	1538.	1618.	1672.	1689.	1756.
TQload (Nm)	3000.	3000.	3000.	3000.	3000.
TQout (Nm)	2325.	2403.	2454.	2469.	2533.
Mcomp (Kg/min)	32.82	34.15	35.40	36.58	37.66
Minman (Kg/min)	14.95	15.46	15.90	16.27	16.70
Mfuel (kg/min)	0.5727	0.5872	0.6008	0.6134	0.6253
Mturb (kg/min)	33.35	35.14	36.36	36.82	38.31
Tinman (deg.K)	334.7	334.9	335.0	334.9	335.1
Texman (deg.K)	906.3	901.7	898.5	896.9	893.2
Tcomp (deg.K)	473.4	474.6	474.9	474.3	475.4
Tvol (deg.K)	674.6	671.9	669.1	666.1	664.4
Tvodot(deg.K/min)	800.7	-7316.	-6472.	6719.	-314.0
FPREV (	4.718	4.718	4.718	4.718	4.718
FPREVA (	4.718	4.718	4.718	4.718	4.718
NOZ (deg.)	9.500	9.500	9.500	9.500	9.500
NOZA (deg.)	6.570	6.880	7.074	7.124	7.386
turb. gear ratio	60.00	60.00	60.00	60.00	60.00
PINDEM (Bar)	3.700	3.700	3.700	3.700	3.700
NEDEM (rpm)	0.0000	0.0000	0.0000	0.0000	0.0000

SCHEME 'A' RESPONSE (1 OF 2)

PAGE 3: TRANSIENT RESULTS FROM DCETM PROGRAM
DT= 0.1000E-01 RUNTIM= 3.000 INREC= 61
K1= 10.00 K2= 0.0000 K3= 0.0000 K4= 0.0000

time (sec.)	2.000	2.200	2.400	2.600	2.800
Ncomp (rpm)	8640.	8835.	9017.	9188.	9349.
Acomp (rpm/sec)	972.6	944.9	884.9	839.2	769.4
Nload (rpm))	499.9	499.9	499.9	499.9	499.8
Aload (rpm/sec.)	-0.3982E-01	-0.3810E-01	-0.3416E-01	-0.3226E-01	-0.2627E-01
Pvol (Bar)	3.595	3.613	3.624	3.621	3.643
Pvodot (Bar/sec.)	-1.585	0.9392E-01	0.7007E-01	1.113	-0.4269
Neng (rpm)	1349.	1371.	1391.	1411.	1429.
Aeng (rpm/sec.)	110.1	107.0	100.2	95.01	87.12
Ntrb(rpm/sqrt(T))	1165.	1167.	1168.	1169.	1170.
Air/fuel ratio	26.87	26.91	27.01	27.08	27.21
Pcomp (Bar)	3.688	3.709	3.725	3.733	3.753
Pinman (Bar)	3.513	3.517	3.531	3.539	3.559
TQeng (Nm)	1328.	1327.	1327.	1326.	1326.
TQann (Nm)	1294.	1293.	1294.	1294.	1298.
TQsun (Nm)	140.7	140.5	140.7	140.7	141.1
TQpc (Nm)	958.8	957.6	958.7	958.4	961.2
TQcomp (Nm)	134.6	134.6	135.1	135.4	136.2
TQturb (Nm)	1828.	1847.	1889.	1910.	1972.
TQload (Nm)	3000.	3000.	3000.	3000.	3000.
TQout (Nm)	2602.	2619.	2658.	2677.	2737.
Mcomp (Kg/min)	38.68	39.65	40.55	41.40	42.19
Minman (Kg/min)	17.10	17.40	17.73	18.02	18.35
Mfuel (kg/min)	0.6364	0.6468	0.6565	0.6656	0.6742
Mturb (kg/min)	39.82	40.27	41.19	41.71	43.00
Tinman (deg.K)	335.3	335.2	335.3	335.3	335.4
Texman (deg.K)	889.9	888.6	886.4	884.9	882.3
Tcomp (deg.K)	476.4	475.9	476.3	476.3	477.1
Tvol (deg.K)	662.9	660.8	659.3	657.8	656.9
Tvodot(deg.K/min)	-8770.	515.8	382.8	6062.	-2311.
FPREV (	4.718	4.718	4.718	4.718	4.718
FPREVA (	4.718	4.718	4.718	4.718	4.718
NOZ (deg.)	9.500	9.500	9.500	9.500	9.500
NOZA (deg.)	7.627	7.669	7.810	7.893	8.094
turb. gear ratio	60.00	60.00	60.00	60.00	60.00
PINDEM (Bar)	3.700	3.700	3.700	3.700	3.700
NEDEM (rpm)	0.0000	0.0000	0.0000	0.0000	0.0000

PAGE 4: TRANSIENT RESULTS FROM DCETM PROGRAM
DT= 0.1000E-01 RUNTIM= 3.000 INREC= 61
K1= 10.00 K2= 0.0000 K3= 0.0000 K4= 0.0000

time (sec.)	3.000
Ncomp (rpm)	9500.
Acomp (rpm/sec)	721.4
Nload (rpm))	499.8
Aload (rpm/sec.)	-0.2310E-01
Pvol (Bar)	3.651
Pvodot (Bar/sec.)	-0.3855
Neng (rpm)	1446.
Aeng (rpm/sec.)	81.69
Ntrb(rpm/sqrt(T))	1171.
Air/fuel ratio	27.30
Pcomp (Bar)	3.765
Pinman (Bar)	3.571
TQeng (Nm)	1325.
TQann (Nm)	1299.
TQsun (Nm)	141.2
TQpc (Nm)	962.1
TQcomp (Nm)	136.7
TQturb (Nm)	2006.
TQload (Nm)	3000.
TQout (Nm)	2769.
Mcomp (Kg/min)	42.93
Minman (Kg/min)	18.62
Mfuel (kg/min)	0.6823
Mturb (kg/min)	43.74
Tinman (deg.K)	335.5
Texman (deg.K)	880.5
Tcomp (deg.K)	477.4
Tvol (deg.K)	655.9
Tvodot(deg.K/min)	-2078.
FPREV (	4.718
FPREVA (	4.718
NOZ (deg.)	9.500
NOZA (deg.)	8.208
turb. gear ratio	60.00
PINDEM (Bar)	3.700
NEDEM (rpm)	0.0000

SCHEME 'A' RESPONSE (2 OF 2)

PAGE 1: TRANSIENT RESULTS FROM DCETM PROGRAM
DT= 0.1000E-01 RUNTIM= 3.000 INREC= 61
K1= 10.00 K2= 0.0000 K3= 0.0000 K4= 0.0000

time (sec.)	0.0000	0.2000	0.4000	0.6000	0.8000
Ncomp (rpm)	5608.	6442.	7261.	8050.	8798.
Acomp (rpm/sec)	4.809	4193.	4019.	3873.	3532.
Nload (rpm))	500.0	500.0	500.0	499.9	499.9
Aload (rpm/sec.)	0.7469E-02	-0.1165	-0.1013	-0.8602E-01	-0.7094E-01
Pvol (Bar)	2.021	2.821	2.881	2.935	2.978
Pvodot (Bar/sec.)	0.1332E-02	1.344	0.7100	-0.2436	-0.8969
Neng (rpm)	1005.	1100.	1193.	1282.	1367.
Aeng (rpm/sec.)	0.5501	474.8	455.1	438.6	399.9
Ntrb(rpm/sqrt(T))	1313.	1164.	1175.	1184.	1189.
Air/fuel ratio	29.68	21.58	22.20	22.79	23.32
Pcomp (Bar)	2.140	2.898	2.981	3.060	3.125
Pinman (Bar)	2.033	2.746	2.826	2.902	2.975
TQeng (Nm)	680.0	1317.	1315.	1313.	1311.
TQann (Nm)	679.8	1165.	1169.	1172.	1184.
TQsun (Nm)	73.91	126.7	127.1	127.4	128.7
TQpc (Nm)	503.5	863.0	865.9	868.3	876.8
TQcomp (Nm)	73.88	100.3	101.8	103.0	106.4
TQturb (Nm)	534.0	1094.	1256.	1420.	1575.
TQload (Nm)	900.0	3000.	3000.	3000.	3000.
TQout (Nm)	974.7	1835.	1987.	2140.	2291.
Mcomp (Kg/min)	24.63	28.35	32.38	36.25	39.91
Minman (Kg/min)	7.750	11.20	12.49	13.79	15.04
Mfuel (kg/min)	0.2611	0.5189	0.5627	0.6049	0.6448
Mturb (kg/min)	24.89	28.44	32.72	36.93	40.84
Tinman (deg.K)	319.1	326.4	326.4	326.5	327.2
Texman (deg.K)	787.7	1005.	986.0	968.7	954.8
Tcomp (deg.K)	395.6	432.0	432.2	432.6	436.1
Tvol (deg.K)	521.8	664.6	651.6	641.9	636.7
Tvodot(deg.K/min)	10.31	9511.	4821.	-1598.	-5750.
FPREV (	2.597	4.718	4.718	4.718	4.718
FPREVA (	2.597	4.718	4.718	4.718	4.718
NOZ (deg.)	7.900	9.500	9.500	9.500	9.500
NOZA (deg.)	7.900	6.958	7.757	8.520	9.250
turb. gear ratio	60.00	60.00	60.00	60.00	60.00
PINDEM (Bar)	2.030	3.000	3.000	3.000	3.000
NEDEM (rpm)	1005.	1673.	1673.	1673.	1673.

PAGE 2: TRANSIENT RESULTS FROM DCETM PROGRAM
DT= 0.1000E-01 RUNTIM= 3.000 INREC= 61
K1= 10.00 K2= 0.0000 K3= 0.0000 K4= 0.0000

time (sec.)	1.000	1.200	1.400	1.600	1.800
Ncomp (rpm)	9478.	0.1010E+05	0.1067E+05	0.1114E+05	0.1120E+05
Acomp (rpm/sec)	3238.	2959.	2706.	527.5	232.3
Nload (rpm))	499.9	499.9	499.9	499.9	499.9
Aload (rpm/sec.)	-0.5910E-01	-0.4672E-01	-0.3483E-01	-0.1438E-02	0.1250E-01
Pvol (Bar)	3.020	3.053	3.087	3.605	3.726
Pvodot (Bar/sec.)	0.2530	0.5090E-01	-0.2055	4.374	0.8869E-01
Neng (rpm)	1444.	1514.	1578.	1632.	1638.
Aeng (rpm/sec.)	366.7	335.0	306.4	59.74	26.32
Ntrb(rpm/sqrt(T))	1193.	1195.	1197.	1183.	1180.
Air/fuel ratio	23.67	24.08	24.42	27.58	28.18
Pcomp (Bar)	3.193	3.243	3.301	3.773	3.889
Pinman (Bar)	3.025	3.083	3.131	3.602	3.693
TQeng (Nm)	1309.	1307.	1306.	1317.	1320.
TQann (Nm)	1190.	1200.	1206.	1288.	1311.
TQsun (Nm)	129.4	130.5	131.2	140.0	142.5
TQpc (Nm)	881.6	888.9	893.6	954.0	971.2
TQcomp (Nm)	109.0	111.8	114.1	136.7	141.1
TQturb (Nm)	1698.	1826.	1950.	2250.	2383.
TQload (Nm)	3000.	3000.	3000.	3000.	3000.
TQout (Nm)	2409.	2533.	2652.	2986.	3125.
Mcomp (Kg/min)	43.24	46.28	49.07	51.12	51.34
Minman (Kg/min)	16.12	17.20	18.18	21.24	21.78
Mfuel (kg/min)	0.6811	0.7142	0.7446	0.7700	0.7730
Mturb (kg/min)	43.84	46.98	49.88	50.47	52.08
Tinman (deg.K)	327.7	328.4	328.9	334.9	336.1
Texman (deg.K)	945.1	935.0	926.6	871.4	862.5
Tcomp (deg.K)	438.7	441.8	444.3	474.7	480.7
Tvol (deg.K)	632.5	629.8	627.5	642.9	645.9
Tvodot(deg.K/min)	1588.	315.1	-1252.	0.2342E+05	461.3
FPREV (	4.718	4.718	4.718	4.718	4.718
FPREVA (	4.718	4.718	4.718	4.718	4.718
NOZ (deg.)	9.500	9.500	9.500	9.500	9.500
NOZA (deg.)	9.753	10.33	10.81	9.500	9.500
turb. gear ratio	60.00	60.00	60.00	60.00	60.00
PINDEM (Bar)	3.000	3.000	3.000	3.000	3.000
NEDEM (rpm)	1673.	1673.	1673.	1673.	1673.

SCHEME 'B' RESPONSE (1 OF 2)

PAGE 3: TRANSIENT RESULTS FROM DCETM PROGRAM
DT= 0.1000E-01 RUNTIM= 3.000 INREC= 61
K1= 10.00 K2= 0.0000 K3= 0.0000 K4= 0.0000

time (sec.)	2.000	2.200	2.400	2.600	2.800
Ncomp (rpm)	0.1124E+05	0.1127E+05	0.1129E+05	0.1130E+05	0.1132E+05
Acomp (rpm/sec)	170.4	125.3	92.17	67.82	49.91
Nload (rpm))	499.9	499.9	499.9	499.9	499.9
Aload (rpm/sec.)	0.1416E-01	0.1537E-01	0.1626E-01	0.1691E-01	0.1740E-01
Pvol (Bar)	3.741	3.752	3.760	3.766	3.770
Pvodot (Bar/sec.)	0.6385E-01	0.4695E-01	0.3456E-01	0.2542E-01	0.1870E-01
Neng (rpm)	1643.	1646.	1649.	1651.	1652.
Aeng (rpm/sec.)	19.30	14.20	10.45	7.693	5.666
Ntrb(rpm/sqrt(T))	1180.	1180.	1180.	1180.	1180.
Air/fuel ratio	28.27	28.34	28.40	28.43	28.46
Pcomp (Bar)	3.903	3.914	3.922	3.928	3.933
Pinman (Bar)	3.708	3.718	3.726	3.732	3.736
TQeng (Nm)	1320.	1320.	1320.	1320.	1320.
TQann (Nm)	1314.	1315.	1317.	1318.	1318.
TQsun (Nm)	142.8	143.0	143.1	143.3	143.3
TQpc (Nm)	973.0	974.3	975.3	976.0	976.6
TQcomp (Nm)	141.7	142.2	142.6	142.8	143.0
TQturb (Nm)	2399.	2411.	2420.	2426.	2431.
TQload (Nm)	3000.	3000.	3000.	3000.	3000.
TQout (Nm)	3142.	3154.	3163.	3169.	3174.
Mcomp (Kg/min)	51.53	51.67	51.77	51.85	51.90
Minman (Kg/min)	21.92	22.02	22.09	22.14	22.18
Mfuel (kg/min)	0.7752	0.7767	0.7779	0.7787	0.7794
Mturb (kg/min)	52.28	52.43	52.54	52.62	52.68
Tinman (deg.K)	336.3	336.4	336.5	336.6	336.6
Texman (deg.K)	861.0	859.9	859.1	858.6	858.2
Tcomp (deg.K)	481.5	482.2	482.6	482.9	483.2
Tvol (deg.K)	646.2	646.3	646.5	646.5	646.6
Tvodot(deg.K/min)	330.9	242.7	178.2	130.9	96.24
FPREV (	4.718	4.718	4.718	4.718	4.718
FPREVA (	4.718	4.718	4.718	4.718	4.718
NOZ (deg.)	9.500	9.500	9.500	9.500	9.500
NOZA (deg.)	9.500	9.500	9.500	9.500	9.500
turb. gear ratio	60.00	60.00	60.00	60.00	60.00
PINDEM (Bar)	3.000	3.000	3.000	3.000	3.000
NEDEM (rpm)	1673.	1673.	1673.	1673.	1673.

PAGE 4: TRANSIENT RESULTS FROM DCETM PROGRAM
DT= 0.1000E-01 RUNTIM= 3.000 INREC= 61
K1= 10.00 K2= 0.0000 K3= 0.0000 K4= 0.0000

time (sec.)	3.000
Ncomp (rpm)	0.1132E+05
Acomp (rpm/sec)	36.73
Nload (rpm))	499.9
Aload (rpm/sec.)	0.1775E-01
Pvol (Bar)	3.773
Pvodot (Bar/sec.)	0.1374E-01
Neng (rpm)	1653.
Aeng (rpm/sec.)	4.173
Ntrb(rpm/sqrt(T))	1180.
Air/fuel ratio	28.48
Pcomp (Bar)	3.936
Pinman (Bar)	3.739
TQeng (Nm)	1320.
TQann (Nm)	1319.
TQsun (Nm)	143.4
TQpc (Nm)	977.0
TQcomp (Nm)	143.2
TQturb (Nm)	2434.
TQload (Nm)	3000.
TQout (Nm)	3178.
Mcomp (Kg/min)	51.94
Minman (Kg/min)	22.21
Mfuel (kg/min)	0.7798
Mturb (kg/min)	52.72
Tinman (deg.K)	336.7
Texman (deg.K)	857.8
Tcomp (deg.K)	483.4
Tvol (deg.K)	646.7
Tvodot(deg.K/min)	70.61
FPREV (	4.718
FPREVA (	4.718
NOZ (deg.)	9.500
NOZA (deg.)	9.500
turb. gear ratio	60.00
PINDEM (Bar)	3.000
NEDEM (rpm)	1673.

SCHEME 'B' RESPONSE (2 OF 2)

PAGE 1: TRANSIENT RESULTS FROM DCETM PROGRAM
DT= 0.1000E-01 RUNTIM= 3.000 INREC= 61
K1= 0.1064 K2= 0.1000E-01 K3= 0.0000 K4= 0.0000

time (sec.)	0.0000	0.2000	0.4000	0.6000	0.8000
Ncomp (rpm)	5608.	6467.	7310.	8116.	8886.
Acomp (rpm/sec)	4.813	4307.	4119.	3945.	3674.
Nload (rpm))	500.0	500.0	500.0	499.9	499.9
Aload (rpm/sec.)	0.7469E-02	-0.1196	-0.1049	-0.8963E-01	-0.7336E-01
Pvol (Bar)	2.021	2.686	2.757	2.842	2.948
Pvodot (Bar/sec.)	0.1339E-02	0.2445	0.3888	0.4729	0.5904
Neng (rpm)	1005.	1103.	1198.	1289.	1377.
Aeng (rpm/sec.)	0.5506	487.7	466.4	446.7	416.0
Ntrb(rpm/sqrt(T))	1313.	1165.	1177.	1186.	1191.
Air/fuel ratio	29.68	20.75	21.44	22.21	23.08
Pcomp (Bar)	2.140	2.778	2.873	2.979	3.102
Pinman (Bar)	2.033	2.636	2.724	2.825	2.941
TQeng (Nm)	680.0	1313.	1311.	1310.	1310.
TQann (Nm)	679.8	1156.	1161.	1167.	1175.
TQsun (Nm)	73.91	125.7	126.3	126.8	127.8
TQpc (Nm)	503.5	856.5	860.4	864.3	870.7
TQcomp (Nm)	73.88	98.58	100.3	102.0	104.7
TQturb (Nm)	534.0	1067.	1223.	1385.	1555.
TQload (Nm)	900.0	3000.	3000.	3000.	3000.
TQout (Nm)	974.7	1804.	1951.	2104.	2266.
Mcomp (Kg/min)	24.63	28.54	32.69	36.64	40.37
Minman (Kg/min)	7.750	10.80	12.12	13.51	14.99
Mfuel (kg/min)	0.2611	0.5203	0.5653	0.6084	0.6495
Mturb (kg/min)	24.89	28.98	33.14	37.09	40.82
Tinman (deg.K)	319.1	325.9	326.0	326.2	326.7
Texman (deg.K)	787.7	1028.	1006.	983.0	959.5
Tcomp (deg.K)	395.6	429.3	429.8	430.8	433.5
Tvol (deg.K)	521.8	662.6	649.5	640.1	634.1
Tvodot(deg.K/min)	10.38	1809.	2748.	3195.	3810.
FPREV (	2.597	4.718	4.718	4.718	4.718
FPREVA (	2.597	4.718	4.718	4.718	4.718
NOZ (deg.)	7.900	9.500	9.500	9.500	9.500
NOZA (deg.)	7.900	7.426	8.191	8.829	9.324
turb. gear ratio	60.00	60.00	60.00	60.00	60.00
PINDEM (Bar)	2.030	3.000	3.000	3.000	3.000
NEDEM (rpm)	1005.	1673.	1673.	1673.	1673.

PAGE 2: TRANSIENT RESULTS FROM DCETM PROGRAM
DT= 0.1000E-01 RUNTIM= 3.000 INREC= 61
K1= 0.1064 K2= 0.1000E-01 K3= 0.0000 K4= 0.0000

time (sec.)	1.000	1.200	1.400	1.600	1.800
Ncomp (rpm)	9555.	0.1010E+05	0.1052E+05	0.1083E+05	0.1105E+05
Acomp (rpm/sec)	3024.	2405.	1828.	1319.	898.3
Nload (rpm))	499.9	499.9	499.9	499.9	499.9
Aload (rpm/sec.)	-0.5537E-01	-0.3858E-01	-0.2352E-01	-0.1073E-01	-0.5570E-03
Pvol (Bar)	3.072	3.203	3.333	3.454	3.556
Pvodot (Bar/sec.)	0.6419	0.6603	0.6355	0.5636	0.4554
Neng (rpm)	1452.	1514.	1562.	1597.	1622.
Aeng (rpm/sec.)	342.5	272.3	207.0	149.3	101.7
Ntrb(rpm/sqrt(T))	1191.	1190.	1188.	1186.	1184.
Air/fuel ratio	23.99	24.89	25.75	26.52	27.17
Pcomp (Bar)	3.240	3.378	3.511	3.631	3.731
Pinman (Bar)	3.071	3.203	3.329	3.444	3.540
TQeng (Nm)	1310.	1311.	1312.	1314.	1316.
TQann (Nm)	1199.	1223.	1245.	1266.	1283.
TQsun (Nm)	130.4	132.9	135.4	137.6	139.4
TQpc (Nm)	888.3	905.7	922.4	937.4	950.1
TQcomp (Nm)	111.3	117.8	123.9	129.3	133.8
TQturb (Nm)	1732.	1896.	2043.	2166.	2263.
TQload (Nm)	3000.	3000.	3000.	3000.	3000.
TQout (Nm)	2446.	2614.	2765.	2893.	2994.
Mcomp (Kg/min)	43.59	46.19	48.20	49.69	50.72
Minman (Kg/min)	16.44	17.78	18.97	19.99	20.79
Mfuel (kg/min)	0.6853	0.7142	0.7368	0.7535	0.7653
Mturb (kg/min)	44.06	46.69	48.73	50.26	51.34
Tinman (deg.K)	328.4	330.0	331.6	333.0	334.2
Texman (deg.K)	938.5	919.3	902.5	888.6	877.8
Tcomp (deg.K)	441.8	450.0	457.9	464.9	470.8
Tvol (deg.K)	633.9	635.0	637.0	639.2	641.2
Tvodot(deg.K/min)	3974.	3928.	3643.	3129.	2464.
FPREV (	4.718	4.718	4.718	4.718	4.718
FPREVA (	4.718	4.718	4.718	4.718	4.718
NOZ (deg.)	9.500	9.500	9.500	9.500	9.500
NOZA (deg.)	9.657	9.823	9.867	9.837	9.775
turb. gear ratio	60.00	60.00	60.00	60.00	60.00
PINDEM (Bar)	3.000	3.000	3.000	3.000	3.000
NEDEM (rpm)	1673.	1673.	1673.	1673.	1673.

SCHEME 'C' RESPONSE (1 OF 2)

PAGE 3: TRANSIENT RESULTS FROM DCETM PROGRAM
DT= 0.1000E-01 RUNTIM= 3.000 INREC= 61
K1= 0.1064 K2= 0.1000E-01 K3= 0.0000 K4= 0.0000

time (sec.)	2.000	2.200	2.400	2.600	2.800
Ncomp (rpm)	0.1120E+05	0.1129E+05	0.1135E+05	0.1138E+05	0.1140E+05
Acomp (rpm/sec)	579.1	356.1	211.2	122.2	69.57
Nload (rpm))	499.9	499.9	499.9	499.9	499.9
Aload (rpm/sec.)	0.6936E-02	0.1206E-01	0.1534E-01	0.1733E-01	0.1851E-01
Pvol (Bar)	3.635	3.691	3.727	3.749	3.763
Pvodot (Bar/sec.)	0.3347	0.2258	0.1424	0.8563E-01	0.4991E-01
Neng (rpm)	1639.	1649.	1655.	1659.	1661.
Aeng (rpm/sec.)	65.59	40.34	23.93	13.85	7.892
Ntrb(rpm/sqrt(T))	1183.	1182.	1181.	1181.	1180.
Air/fuel ratio	27.66	28.00	28.22	28.36	28.44
Pcomp (Bar)	3.807	3.860	3.895	3.916	3.929
Pinman (Bar)	3.613	3.665	3.699	3.720	3.732
TQeng (Nm)	1317.	1318.	1319.	1319.	1320.
TQann (Nm)	1296.	1305.	1311.	1315.	1317.
TQsun (Nm)	140.9	141.9	142.5	142.9	143.2
TQpc (Nm)	959.8	966.7	971.2	973.9	975.6
TQcomp (Nm)	137.2	139.6	141.2	142.2	142.8
TQturb (Nm)	2335.	2383.	2414.	2433.	2444.
TQload (Nm)	3000.	3000.	3000.	3000.	3000.
TQout (Nm)	3069.	3121.	3153.	3173.	3185.
Mcomp (Kg/min)	51.40	51.83	52.08	52.23	52.32
Minman (Kg/min)	21.38	21.78	22.04	22.20	22.29
Mfuel (kg/min)	0.7731	0.7780	0.7810	0.7827	0.7837
Mturb (kg/min)	52.06	52.53	52.82	52.99	53.08
Tinman (deg.K)	335.1	335.7	336.1	336.4	336.5
Texman (deg.K)	870.0	864.8	861.4	859.4	858.2
Tcomp (deg.K)	475.4	478.6	480.7	481.9	482.7
Tvol (deg.K)	643.0	644.2	645.0	645.6	645.9
Tvodot(deg.K/min)	1776.	1183.	739.4	442.3	257.0
FPREV (	4.718	4.718	4.718	4.718	4.718
FPREVA (	4.718	4.718	4.718	4.718	4.718
NOZ (deg.)	9.500	9.500	9.500	9.500	9.500
NOZA (deg.)	9.711	9.659	9.623	9.600	9.587
turb. gear ratio	60.00	60.00	60.00	60.00	60.00
PINDEM (Bar)	3.000	3.000	3.000	3.000	3.000
NEDEM (rpm)	1673.	1673.	1673.	1673.	1673.

PAGE 4: TRANSIENT RESULTS FROM DCETM PROGRAM
DT= 0.1000E-01 RUNTIM= 3.000 INREC= 61
K1= 0.1064 K2= 0.1000E-01 K3= 0.0000 K4= 0.0000

time (sec.)	3.000
Ncomp (rpm)	0.1141E+05
Acomp (rpm/sec)	39.22
Nload (rpm))	499.9
Aload (rpm/sec.)	0.1918E-01
Pvol (Bar)	3.770
Pvodot (Bar/sec.)	0.2851E-01
Neng (rpm)	1662.
Aeng (rpm/sec.)	4.456
Ntrb(rpm/sqrt(T))	1180.
Air/fuel ratio	28.49
Pcomp (Bar)	3.936
Pinman (Bar)	3.739
TQeng (Nm)	1320.
TQann (Nm)	1318.
TQsun (Nm)	143.3
TQpc (Nm)	976.5
TQcomp (Nm)	143.1
TQturb (Nm)	2450.
TQload (Nm)	3000.
TQout (Nm)	3192.
Mcomp (Kg/min)	52.36
Minman (Kg/min)	22.34
Mfuel (kg/min)	0.7843
Mturb (kg/min)	53.14
Tinman (deg.K)	336.6
Texman (deg.K)	857.5
Tcomp (deg.K)	483.1
Tvol (deg.K)	646.0
Tvodot(deg.K/min)	146.6
FPREV (	4.718
FPREVA (	4.718
NOZ (deg.)	9.500
NOZA (deg.)	9.579
turb. gear ratio	60.00
PINDEM (Bar)	3.000
NEDEM (rpm)	1673.

SCHEME 'C' RESPONSE (2 OF 2)

PAGE 1: TRANSIENT RESULTS FROM DCETM PROGRAM
DT= 0.1000E-02 RUNTIM= 3.000 INREC= 61
K1= 20.00 K2= 0.1000 K3= 0.2500E-01 K4= 21.00

time (sec.)	0.0000	0.2000	0.4000	0.6000	0.8000
Ncomp (rpm)	5605.	6512.	7372.	8202.	9008.
Acomp (rpm/sec)	4.767	4417.	4220.	4088.	3973.
Nload (rpm))	500.0	500.0	500.0	499.9	499.9
Aload (rpm/sec.)	0.7359E-02	-0.1218	-0.1087	-0.9630E-01	-0.8432E-01
Pvol (Bar)	2.019	2.611	2.631	2.646	2.660
Pvodot (Bar/sec.)	0.3345E-02	0.1245	0.8682E-01	0.7294E-01	0.6229E-01
Neng (rpm)	1005.	1108.	1205.	1299.	1390.
Aeng (rpm/sec.)	0.5453	500.2	477.8	462.9	449.9
Ntrb(rpm/sqrt(T))	1313.	1167.	1179.	1188.	1196.
Air/fuel ratio	29.68	20.29	20.68	21.05	21.41
Pcomp (Bar)	2.138	2.711	2.763	2.813	2.861
Pinman (Bar)	2.031	2.575	2.625	2.672	2.717
TQeng (Nm)	679.5	1310.	1307.	1304.	1301.
TQann (Nm)	679.4	1150.	1154.	1156.	1157.
TQsun (Nm)	73.86	125.1	125.5	125.7	125.8
TQpc (Nm)	503.2	852.1	855.1	856.4	857.3
TQcomp (Nm)	73.83	97.23	98.92	99.94	100.8
TQturb (Nm)	533.1	1048.	1187.	1320.	1450.
TQload (Nm)	900.0	3000.	3000.	3000.	3000.
TQout (Nm)	973.6	1782.	1913.	2037.	2157.
Mcomp (Kg/min)	24.62	28.80	33.08	37.20	41.19
Minman (Kg/min)	7.748	10.61	11.76	12.91	14.05
Mfuel (kg/min)	0.2609	0.5227	0.5686	0.6130	0.6560
Mturb (kg/min)	24.88	29.26	33.62	37.79	41.82
Tinman (deg.K)	319.1	325.4	325.5	325.5	325.5
Texman (deg.K)	787.7	1042.	1027.	1014.	1001.
Tcomp (deg.K)	395.5	427.1	427.5	427.4	427.5
Tvol (deg.K)	521.7	660.4	647.2	637.1	629.1
Tvodot(deg.K/min)	25.92	944.5	640.8	526.8	442.0
FPREV (	1109.	2000.	2000.	2000.	2000.
FPREVA (	2.596	4.718	4.718	4.718	4.718
NOZ (deg.)	7.900	9.500	9.500	9.500	9.500
NOZA (deg.)	7.904	7.707	8.693	9.636	10.54
turb. gear ratio	60.00	60.00	60.00	60.00	60.00
PINDEM (Bar)	2.030	3.700	3.700	3.700	3.700
NEDEM (rpm)	1005.	1660.	1660.	1660.	1660.

PAGE 2: TRANSIENT RESULTS FROM DCETM PROGRAM
DT= 0.1000E-02 RUNTIM= 3.000 INREC= 61
K1= 20.00 K2= 0.1000 K3= 0.2500E-01 K4= 21.00

time (sec.)	1.000	1.200	1.400	1.600	1.800
Ncomp (rpm)	9792.	0.1056E+05	0.1113E+05	0.1138E+05	0.1139E+05
Acomp (rpm/sec)	3870.	3775.	1658.	517.7	158.7
Nload (rpm))	499.9	499.9	499.9	499.9	499.9
Aload (rpm/sec.)	-0.7270E-01	-0.6140E-01	-0.1403E-01	0.9474E-02	0.1678E-01
Pvol (Bar)	2.672	2.682	3.348	3.646	3.739
Pvodot (Bar/sec.)	0.5395E-01	0.4737E-01	2.483	0.7926	0.2453
Neng (rpm)	1479.	1566.	1631.	1654.	1660.
Aeng (rpm/sec.)	438.2	427.5	187.7	58.64	17.99
Ntrb(rpm/sqrt(T))	1202.	1207.	1191.	1183.	1181.
Air/fuel ratio	21.76	22.09	26.03	27.76	28.31
Pcomp (Bar)	2.907	2.952	3.547	3.821	3.907
Pinman (Bar)	2.762	2.804	3.368	3.629	3.712
TQeng (Nm)	1298.	1296.	1310.	1317.	1319.
TQann (Nm)	1158.	1159.	1250.	1298.	1313.
TQsun (Nm)	125.9	126.0	135.9	141.1	142.8
TQpc (Nm)	857.9	858.4	925.8	961.5	972.8
TQcomp (Nm)	101.5	102.2	125.4	137.9	141.8
TQturb (Nm)	1575.	1698.	2142.	2361.	2428.
TQload (Nm)	3000.	3000.	3000.	3000.	3000.
TQout (Nm)	2273.	2386.	2860.	3095.	3168.
Mcomp (Kg/min)	45.05	48.82	51.24	52.05	52.30
Minman (Kg/min)	15.18	16.32	20.03	21.66	22.17
Mfuel (kg/min)	0.6979	0.7388	0.7696	0.7801	0.7834
Mturb (kg/min)	45.73	49.54	51.19	52.57	53.00
Tinman (deg.K)	325.5	325.6	331.8	335.2	336.3
Texman (deg.K)	989.6	978.6	896.0	868.1	860.1
Tcomp (deg.K)	427.6	427.8	459.2	476.1	481.4
Tvol (deg.K)	622.7	617.4	633.9	642.6	645.2
Tvodot(deg.K/min)	377.3	327.2	0.1411E+05	4191.	1270.
FPREV (	2000.	2000.	2000.	2000.	2000.
FPREVA (	4.718	4.718	4.718	4.718	4.718
NOZ (deg.)	9.500	9.500	9.500	9.500	9.500
NOZA (deg.)	11.42	12.27	10.29	9.774	9.627
turb. gear ratio	60.00	60.00	60.00	60.00	60.00
PINDEM (Bar)	3.700	3.700	3.700	3.700	3.700
NEDEM (rpm)	1660.	1660.	1660.	1660.	1660.

SCHEME 'D' RESPONSE (1 OF 2)

PAGE 3: TRANSIENT RESULTS FROM DCETM PROGRAM
DT= 0.1000E-02 RUNTIM= 3.000 INREC= 61
K1= 20.00 K2= 0.1000 K3= 0.2500E-01 K4= 21.00

time (sec.)	2.000	2.200	2.400	2.600	2.800
Ncomp (rpm)	0.1141E+05	0.1142E+05	0.1142E+05	0.1142E+05	0.1142E+05
Acomp (rpm/sec)	48.29	14.57	4.285	1.209	0.3585
Nload (rpm))	499.9	499.9	499.9	499.9	499.9
Aload (rpm/sec.)	0.1901E-01	0.1969E-01	0.1990E-01	0.1996E-01	0.1997E-01
Pvol (Bar)	3.768	3.777	3.779	3.780	3.780
Pvodot (Bar/sec.)	0.7524E-01	0.2308E-01	0.6318E-02	0.1945E-02	0.1878E-03
Neng (rpm)	1663.	1663.	1663.	1663.	1663.
Aeng (rpm/sec.)	5.483	1.665	0.5000	0.1517	0.5539E-01
Ntrb(rpm/sqrt(T))	1180.	1180.	1180.	1180.	1180.
Air/fuel ratio	28.47	28.52	28.54	28.54	28.55
Pcomp (Bar)	3.934	3.942	3.944	3.945	3.945
Pinman (Bar)	3.737	3.745	3.747	3.748	3.748
TQeng (Nm)	1320.	1320.	1320.	1320.	1320.
TQann (Nm)	1318.	1319.	1320.	1320.	1320.
TQsun (Nm)	143.3	143.4	143.5	143.5	143.5
TQpc (Nm)	976.3	977.3	977.6	977.7	977.8
TQcomp (Nm)	143.0	143.4	143.5	143.5	143.5
TQturb (Nm)	2449.	2455.	2457.	2458.	2458.
TQload (Nm)	3000.	3000.	3000.	3000.	3000.
TQout (Nm)	3190.	3197.	3199.	3200.	3200.
Mcomp (Kg/min)	52.37	52.40	52.40	52.41	52.41
Minman (Kg/min)	22.33	22.38	22.40	22.40	22.40
Mfuel (kg/min)	0.7844	0.7847	0.7848	0.7848	0.7848
Mturb (kg/min)	53.13	53.17	53.19	53.19	53.19
Tinman (deg.K)	336.6	336.7	336.7	336.7	336.7
Texman (deg.K)	857.7	857.0	856.8	856.7	856.7
Tcomp (deg.K)	483.0	483.5	483.7	483.7	483.7
Tvol (deg.K)	646.0	646.2	646.3	646.3	646.3
Tvodot(deg.K/min)	387.0	118.5	32.40	9.968	0.9584
FPREV (	2000.	2000.	2000.	2000.	2000.
FPREVA (	4.718	4.718	4.718	4.718	4.718
NOZ (deg.)	9.500	9.500	9.500	9.500	9.500
NOZA (deg.)	9.583	9.570	9.566	9.565	9.564
turb. gear ratio	60.00	60.00	60.00	60.00	60.00
PINDEM (Bar)	3.700	3.700	3.700	3.700	3.700
NEDEM (rpm)	1660.	1660.	1660.	1660.	1660.

PAGE 4: TRANSIENT RESULTS FROM DCETM PROGRAM
DT= 0.1000E-02 RUNTIM= 3.000 INREC= 61
K1= 20.00 K2= 0.1000 K3= 0.2500E-01 K4= 21.00

time (sec.)	3.000
Ncomp (rpm)	0.1142E+05
Acomp (rpm/sec)	0.1284
Nload (rpm))	499.9
Aload (rpm/sec.)	0.1997E-01
Pvol (Bar)	3.780
Pvodot (Bar/sec.)	0.2089E-03
Neng (rpm)	1663.
Aeng (rpm/sec.)	0.2933E-01
Ntrb(rpm/sqrt(T))	1180.
Air/fuel ratio	28.55
Pcomp (Bar)	3.945
Pinman (Bar)	3.748
TQeng (Nm)	1320.
TQann (Nm)	1320.
TQsun (Nm)	143.5
TQpc (Nm)	977.8
TQcomp (Nm)	143.5
TQturb (Nm)	2458.
TQload (Nm)	3000.
TQout (Nm)	3200.
Mcomp (Kg/min)	52.41
Minman (Kg/min)	22.40
Mfuel (kg/min)	0.7848
Mturb (kg/min)	53.19
Tinman (deg.K)	336.7
Texman (deg.K)	856.7
Tcomp (deg.K)	483.7
Tvol (deg.K)	646.3
Tvodot(deg.K/min)	1.054
FPREV (	2000.
FPREVA (	4.718
NOZ (deg.)	9.500
NOZA (deg.)	9.564
turb. gear ratio	60.00
PINDEM (Bar)	3.700
NEDEM (rpm)	1660.

SCHEME 'D' RESPONSE (2 OF 2)